Vol. 17. No 2, 2015

ISSN 1507-2711
Cena: 25 zł (w tym 5% VAT)

EKSPLOATACJA I NIEZAWODNOŚĆ
MAINTENANCE AND RELIABILITY

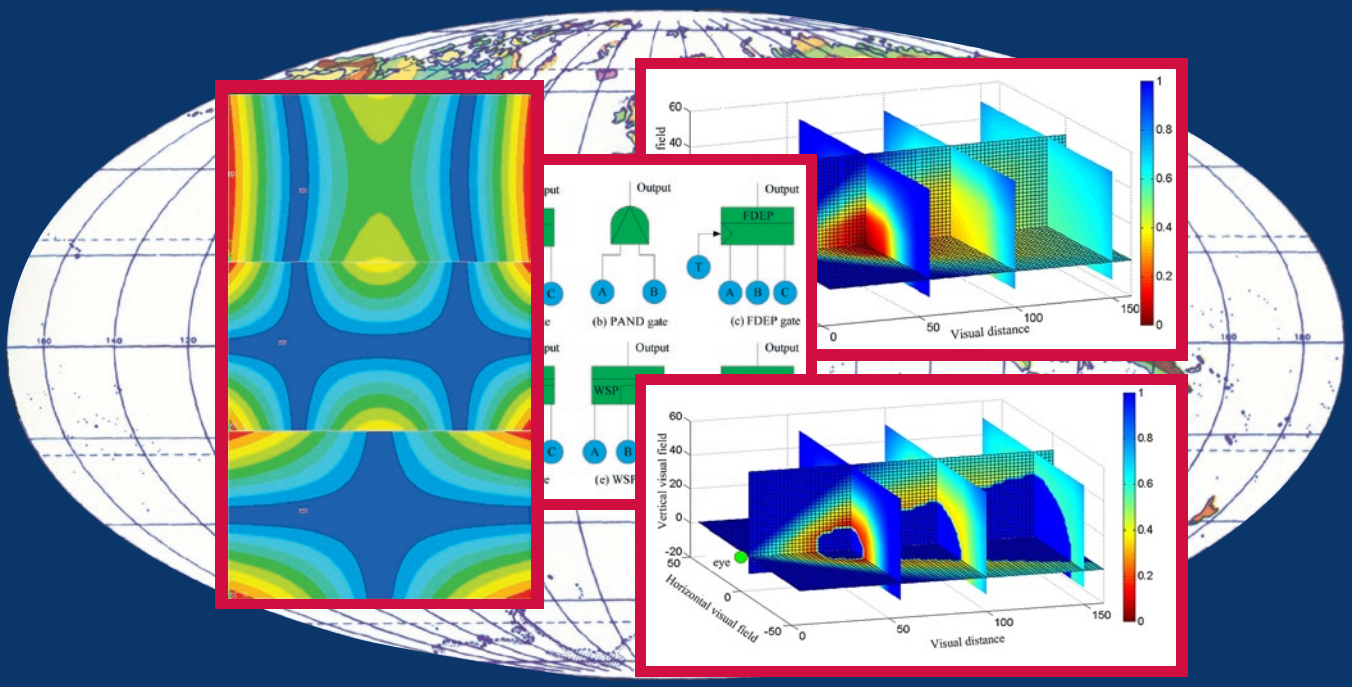

Polskie Naukowo Techniczne Towarzystwo Eksploatacyjne
Warszawa

Polish Maintenance Society
Warsaw

Co-financed by the Minister of Science and Higher Education

The Journal is indexed and abstracted in the Journal Citation Reports (JCR Science Edition), Scopus, Science Citation Index Expanded (SciSearch®) and Index Copernicus International.

The Quarterly appears on the list of journals credited with a high impact factor by the Polish Ministry of Science and Higher Education and is indexed in the Polish Technical Journal Contents database – BAZTECH and the database of the Digital Library Federation.

All the scientific articles have received two positive reviews from independent reviewers.

Our IF is 0.505

Editorial staff:	Dariusz Mazurkiewicz, PhD, DSc (Eng), Associate Professor (Editor-in-Chief, Secretary of the Scientific Board) Tomasz Klepka, PhD, DSc (Eng), Associate Professor (Deputy Editor-in-Chief) Teresa Błachnio-Krolopp, MSc (Eng) (Editorial secretary) Andrzej Koma (Typesetting and text makeup) Krzysztof Olszewski, PhD (Eng) (Webmaster)
Publisher:	Polish Maintenance Society, Warsaw
Scientific patronage:	Polish Academy of Sciences Branch in Lublin
Address for correspondence:	"Eksploatacja i Niezawodność" – Editorial Office ul. Nadbystrzycka 36, 20-618 Lublin, Poland e-mail: office@ein.org.pl http://www.ein.org.pl/
Circulation:	550 copies

Science and Technology

YANG R, ZHAO F, KANG J, LI H, TENG H. **Inspection optimization model with imperfect maintenance based on a three-stage failure process**. Eksploatacja i Niezawodnosc – Maintenance and Reliability 2015; 17 (2): 165–173, http://dx.doi.org/10.17531/ein.2015.2.1.

Rolling element bearings are one of the most widely used and vulnerable components in complex systems. The condition monitoring work is very critical for sustaining the system's availability and reducing the maintenance cost. Shock pulse method (SPM) is a common technique to measure the operating condition of rolling bearings as a three color scheme, e.g., green, yellow and red. This paper proposes an inspection model based on a three-stage failure process which aims to optimize the inspection interval of bearings by minimizing the expected cost per unit time. The three-stage failure process divides the bearings life into three stages before failure: good, minor defective and severe defective stages, corresponding to the three color scheme of SPM. Considering the need to lubricate bearings when the minor defective stage is identified by inspection in industrial applications, we assume that maintenance at the time of inspection identifying the minor defective stage is imperfect. The concept of proportional age reduction is used to model the effect of imperfect maintenance on the instantaneous rates of the minor defective stage, the severe defective stage and failure. Perfect maintenance however is carried out if inspection detects bearings being in the severe defective stage. Failure can be found once it occurs and replacement has to be implemented immediately. Finally, a numerical example is presented to illustrate the effectiveness of the proposed model.

YANG R, ZHAO F, KANG J, LI H, TENG H. **Model optymalizacji przeglądów w warunkach niepełnej konserwacji oparty o trójfazowy proces uszkodzenia**. Eksploatacja i Niezawodnosc – Maintenance and Reliability 2015; 17 (2): 165–173, http://dx.doi.org/10.17531/ein.2015.2.1.

Łożyska toczne są jednymi z najczęściej stosowanych i jednocześnie najbardziej narażonych na uszkodzenia części składowych układów złożonych. Monitorowanie stanu odgrywa bardzo istotną rolę w utrzymaniu dostępności układów i zmniejszeniu kosztów ich obsługi. Metoda impulsów uderzeniowych (SPM) jest powszechnie stosowaną techniką służącą do pomiaru stanu pracy łożysk tocznych, który reprezentowany jest za pomocą kodu trzech kolorów, na przykład, zielonego, żółtego i czerwonego. W artykule zaproponowano model przeglądów oparty na trójfazowym procesie uszkodzenia, który ma na celu optymalizację częstotliwości przeglądów łożysk poprzez minimalizację oczekiwanych kosztów przypadających na jednostkę czasu. Pojęcie trójfazowego procesu uszkodzenia pozwala podzielić żywotność łożyska na trzy fazy przed wystąpieniem uszkodzenia: fazę dobrego stanu, fazę drobnych defektów i fazę poważnych defektów. Podział ten odpowiada kodowi trzech kolorów SPM. Biorąc pod uwagę konieczność smarowania łożysk po zdiagnozowaniu, podczas przeglądu w warunkach przemysłowych, wystąpienia fazy drobnych defektów, zakładamy, że konserwacja w czasie takiego przeglądu jest konserwacją niepełną. Koncepcja proporcjonalnego obniżenia wieku służy do modelowania wpływu niepełnej konserwacji na chwilowe wartości intensywności fazy drobnych defektów, fazy poważnych defektów oraz uszkodzeń. Gdy podczas przeglądu stwierdzi się, że łożysko jest w fazie poważnych defektów, przeprowadza się pełną konserwację. Uszkodzenie zostaje wykryte zaraz po jego wystąpieniu, i wtedy należy dokonać natychmiastowej wymiany łożyska. Pod koniec artykułu, przedstawiono przykład numeryczny, który ilustruje wydajność proponowanego modelu.

WERBIŃSKA-WOJCIECHOWSKA S, ZAJĄC P. **Use of delay-time concept in modelling process of technical and logistics systems maintenance performance. Case study**. Eksploatacja i Niezawodnosc – Maintenance and Reliability 2015; 17 (2): 174–185, http://dx.doi.org/10.17531/ein.2015.2.2.

Article presents an overview of some recent developments in the area of modelling of technical systems' maintenance decisions with the use of delay-time concept. Thus, the literature overview from 1984-2012 in the analysed research area is given. Next, there is characterised the implementation algorithm for delay time analysis use in the area of logistic systems maintenance performance. Later, the example of methodology of using delay-time analysis implementation in the area of logistic system of ten forklifts performance analysis is investigated.

WERBIŃSKA-WOJCIECHOWSKA S, ZAJĄC P. **Zastosowanie koncepcji opóźnień czasowych w procesie modelowania utrzymania w stanie zdatności systemów technicznych i logistycznych. Studium przypadku**. Eksploatacja i Niezawodnosc – Maintenance and Reliability 2015; 17 (2): 174–185, http://dx.doi.org/10.17531/ein.2015.2.2.

W artykule przedstawiono zagadnienia związane z modelowaniem utrzymania systemów logistycznych w stanie zdatności z wykorzystaniem koncepcji opóźnień czasowych. Przedstawiono przegląd literatury z badanego obszaru obejmujący okres 1984-2012. Następnie został omówiony algorytm postępowania w procesie implementacji koncepcji opóźnień czasowych w obszarze utrzymania w stanie zdatności systemów logistycznych. W ostatnim punkcie, został przedstawiony przykład zastosowania opracowanej metodyki do oceny niezawodności i oczekiwanych kosztów obsługiwania dziesięciu wózków widłowych funkcjonujących w wybranym systemie.

GAO J, WANG H. **Operation reliability analysis based on fuzzy support vector machine for aircraft engines**. Eksploatacja i Niezawodnosc – Maintenance and Reliability 2015; 17 (2): 186–193, http://dx.doi.org/10.17531/ein.2015.2.3.

The aircraft engine is a complex and repairable system, and the diversity of its failure modes increases the difficulty of operation reliability analysis. It is necessary to establish a dynamic relationship among monitoring information, failure mode and system reliability for achieving scientific reliability analysis for aircraft engines. This paper has used fuzzy support vector machine (FVSM) method to fuse condition monitoring information. The reliability analysis models including Gamma process model and Winner process model, respectively for different failure modes, have been presented. Furthermore, these two models have been integrated on the basis of competing failures' mechanism. Bayesian model averaging has been used to analyze the effects of different failure modes on aircraft engines' reliability. As a result of above, the goal of an accurate analysis of the reliability for aircraft engines has been achieved. Example shows the effectiveness of the proposed model.

GAO J, WANG H. **Analiza niezawodności eksploatacyjnej silników lotniczych w oparciu o metodę rozmytej maszyny wektorów nośnych (FSVM)**. Eksploatacja i Niezawodnosc – Maintenance and Reliability 2015; 17 (2): 186–193, http://dx.doi.org/10.17531/ein.2015.2.3.

Silnik samolotu to złożony system naprawialny, a różnorodność przyczyn jego uszkodzeń zwiększa trudność analizy niezawodności eksploatacyjnej. Istnieje konieczność ustalenia dynamicznych związków pomiędzy monitorowaniem informacji, przyczynami uszkodzeń i niezawodnością systemu, których znajomość pozwoliłaby przeprowadzać naukową analizę niezawodności silników lotniczych. Do integracji danych z monitorowania informacji, w pracy wykorzystano metodę rozmytej maszyny wektorów nośnych (FSVM). Dla różnych przyczyn uszkodzeń, przedstawiono odpowiednie modele analizy niezawodności – model procesu Gamma i model procesu Wienera. Przedstawione modele zintegrowano na podstawie mechanizmu uszkodzeń konkurujących. Do analizy wpływu różnych przyczyn uszkodzeń na niezawodność silników lotniczych wykorzystano procedurę bayesowskiego uśredniania modeli. Dzięki powyższym krokom, osiągnięto założony cel dokładnej analizy niezawodności silników samolotowych. Przykład pokazuje skuteczność proponowanego modelu.

BIENIAŚ J, SUROWSKA B, JAKUBCZAK P. **Influence of repeated impact on damage growth in fibre reinforced polymer composites**. Eksploatacja i Niezawodnosc – Maintenance and Reliability 2015; 17 (2): 194–198, http://dx.doi.org/10.17531/ein.2015.2.4.

The study presents the problems of the influence of repeated low velocity and low energy impacts on damage growth in carbon and glass fibre reinforced high strength polymer composite. The laminate response to impacts was analyzed, the types of damages and their interrelations were identified as well as damages mechanisms were described for tested laminates subjected to repeated impacts. The following conclusions have been drawn on the basis of completed tests: (1) composite materials with polymer matrix reinforced with continuous glass and carbon fibres demonstrate limited resistance to repeated impacts. The laminates resistance to impacts depends mainly on the properties and type of components, particularly in case of reinforcing fibres, orientation of layer under the influence of external impact; (2) tested laminates with carbon fibres are characterized by lower resistance to repeated impacts than laminates with glass fibres. This is proved by the curves of laminate response to impacts, wider damage area and tendency to laminate structure perforation as a result of repeated impacts; (3) repeated impacts lead to damage growth mainly

BIENIAŚ J, SUROWSKA B, JAKUBCZAK P. **Wpływ uderzeń wielokrotnych na rozwój uszkodzenia kompozytów polimerowych wzmacnianych włóknami** . Eksploatacja i Niezawodnosc – Maintenance and Reliability 2015; 17 (2): 194–198, http://dx.doi.org/10.17531/ein.2015.2.4.

W pracy przedstawiono problematykę wpływu powtarzających się uderzeń o niskiej prędkości i niskiej energii na rozwój uszkodzenia wysokowytrzymałych kompozytów polimerowych wzmacnianych włóknem węglowym oraz szklanym. Dokonano analizy odpowiedzi laminatu na uderzenia, zidentyfikowano rodzaj i relacje pomiędzy uszkodzeniami, a także przedstawiono mechanizmy uszkodzenia w badanych laminatach poddanych wielokrotnym uderzeniom. Na podstawie przeprowadzonych badań wykazano że: (1) materiały kompozytowe o osnowie polimerowej wzmacniane ciągłymi włóknami szklanymi i węglowymi wykazują ograniczoną odporność na wielokrotne uderzenia. O odporności laminatów na uderzenia decydują głównie właściwości i rodzaj komponentów, w szczególności włókien wzmacniających, orientacja warstw pod wpływem oddziaływania zewnętrznego; (2) badane laminaty z włóknami węglowymi charakteryzują się niższą odpornością na wielokrotne uderzenia w porównaniu do laminatów z włóknem szklanym. Świadczą o tym charakterystyki odpowiedzi laminatu na uderzenia, większy obszar uszkodzenia oraz skłonność do perforacji struktury laminatu w wyniku wielokrotnych uderzeń; (3) uderzenia

through propagation of damage initiated in initial impacts phase. Delaminations and matrix cracks belong to the basic mechanisms of damages in composite materials; (4) composite damage propagates with increasing number of impacts in fibres orientation direction, particularly in lower composite layers. Further impacts may result in higher stress concentration and higher initiation energy causing the damage growth in various areas of the material. Further impacts increase the damage leading to gradual growth of damages initiated before.

GE D, LI D, LIN M, YANG Y-H. **SFRs-Based Numerical Simulation for the Reliability of Highly-coupled DFTs**. Eksploatacja i Niezawodnosc – Maintenance and Reliability 2015; 17 (2): 199–206, http://dx.doi.org/10.17531/ein.2015.2.5.

The failure behaviors of many real-life systems are very complex and sequence-dependent, and can be modeled by highly-coupled dynamic fault trees (DFTs). Existing approaches for solving DFTs, such as Markov state-space-based or inclusion-exclusion based methods all have their disadvantages. They either suffer from the problem of state space explosion or are subjected to the combination explosion. Additionally, Markov-based approaches become unavailable when components follow non-exponential time-to-failure distributions which prevail in real-life systems. To overcome shortcomings of the methods mentioned above, SFRs (Sequence Failure Regions)-Based numerical simulation approach is first proposed. The proposed method is applicable for a generalized cut sequence as well as highly-coupled DFTs modeling non-repairable systems with arbitrary time-to-failure distributed components. The results of the validation example indicate the reasonability of our proposed approach.

WERESA E, SEWERYN A, SZUSTA J, RAK Z. **Fatigue testing of transmission gear**. Eksploatacja i Niezawodnosc – Maintenance and Reliability 2015; 17 (2): 207–214, http://dx.doi.org/10.17531/ein.2015.2.6.

This paper presents the results of experimental tests of fatigue life of selected gears, performed on a test stand equipped with a hydraulic universal testing machine. The tests were performed on skew and straight cylindrical gears, made of EN AW-2017A and EN AW-7057 aluminium, and 40HM steel. Moreover, fatigue life curves for selected gears were presented, and the mechanisms of the occurrence of damage were analysed. Relationships describing the maximum value of torque during a loading cycle in relation to the number loading of cycles until the gear is damaged were also proposed.

LIU X, WANG W, PENG R. **An integrated production and delay-time based preventive maintenance planning model for a multi-product production system**. Eksploatacja i Niezawodnosc – Maintenance and Reliability 2015; 17 (2): 215–221, http://dx.doi.org/10.17531/ein.2015.2.7.

This paper integrates preventive maintenance and medium-term tactical production planning in a multi-product production system. In such a system, a set of products needs to be produced in lots during a specified finite planning horizon. Preventive maintenance is carried out periodically at the end of some production periods and corrective maintenance is always performed at failures. The system's available production capacity can be affected by maintenance, since both planned preventive maintenance and unplanned corrective maintenance result in downtime loss during the planning horizon. In addition to the time used for preventive and corrective maintenance, our model considers the setup time and the product quality, as these are affected by the defects and failures of the system. Procedures are proposed to identify the optimal production plan and preventive maintenance policy simultaneously. Our objective is to minimize the sum of maintenance, production, inventory, setup, backorder costs and the costs of unqualified products within the planning horizon. A real case from a steel factory is presented to illustrate the model.

FALKOWICZ K, FERDYNUS M, DĘBSKI H. **Numerical analysis of compressed plates with a cut-out operating in the geometrically nonlinear range**. Eksploatacja i Niezawodnosc – Maintenance and Reliability 2015; 17 (2): 222–227, http://dx.doi.org/10.17531/ein.2015.2.8.

This paper presents the results of a numerical analysis conducted to investigate uniformly compressed rectangular plates with different cut-out sizes. Made of high strength steel, the plates are articulatedly supported on their shorter edges. The FEM

wielokrotne powodują rozwój uszkodzenia głównie przez propagację uszkodzenia inicjowanego w czasie początkowych uderzeń. Do podstawowych mechanizmów uszkodzenia materiałów kompozytowych należą rozwarstwienia oraz pęknięcia osnowy; (4) wraz ze wzrostem liczby uderzeń uszkodzenie kompozytu propaguje w kierunku ułożenia włókien, szczególnie dolnych warstw kompozytu. Kolejne uderzenia mogą powodować większą kumulację naprężeń oraz energii inicjacji odpowiedzialnej za rozwój uszkodzenia w różnych obszarach materiału. Kolejne uderzenia powodują zwiększanie uszkodzenia prowadząc do stopniowego rozwoju wcześniej zainicjowanych uszkodzeń.

GE D, LI D, LIN M, YANG Y-H. **Metoda symulacji numerycznej oparta na pojęciu zakresów uszkodzeń sekwencyjnych służąca do obliczania niezawodności układów modelowanych metodą silnie sprzężonych dynamicznych drzew błędów**. Eksploatacja i Niezawodnosc – Maintenance and Reliability 2015; 17 (2): 199–206, http://dx.doi.org/10.17531/ein.2015.2.5.

Zachowania uszkodzeniowe wielu działających w rzeczywistości układów są bardzo złożone i zależą od sekwencji w jakiej występują uszkodzenia. Zachowania takie można modelować za pomocą silnie sprzężonych dynamicznych drzew błędów (DFT). Istniejące podejścia do rozwiązywania DFT, takie jak metody markowowskie oparte na pojęciu przestrzeni stanów i metody oparte na zasadzie włączeń i wyłączeń mają swoje ograniczenia:albo borykają się z problemem eksplozji przestrzeni stanów albo są narażone na eksplozję kombinatoryczną. Dodatkowo, podejścia markowowskie stają się niedostępne, gdy elementy składowe mają niewykładnicze rozkłady czasu do uszkodzenia, co ma miejsce w przeważającej części układów spotykanych w rzeczywistości. Aby przezwyciężyć mankamenty powyższych metod, zaproponowano metodę symulacji numerycznej opartą na pojęciu zakresów uszkodzeń sekwencyjnych (sequence failure regions, SFR). Proponowana metoda znajduje zastosowanie w modelowaniu systemów nienaprawialnych o elementach, które charakteryzuje arbitralnie przyjęty rozkład czasu do uszkodzenia. Metodę można stosować w modelowaniu opartym zarówno na uogólnionej sekwencji niezdatności (generalizedcut sequence), jak również silnie sprzężonych DFT. Wyniki uzyskane w przedstawionym przykładzie potwierdzają zasadność proponowanego przez nas podejścia.

WERESA E, SEWERYN A, SZUSTA J, RAK Z. **Doświadczalne badania trwałości zmęczeniowej przekładni zębatych**. Eksploatacja i Niezawodnosc – Maintenance and Reliability 2015; 17 (2): 207–214, http://dx.doi.org/10.17531/ein.2015.2.6.

W pracy przedstawiono wyniki badań doświadczalnych trwałości zmęczeniowej wybranych przekładni zębatych, wykonanych na opracowanym stanowisku badawczym wyposażonym w hydrauliczną maszynę wytrzymałościową. Badania przeprowadzono na walcowych kołach o zębach prostych i skośnych, wykonanych ze stopów aluminium EN AW-2017A i EN AW-7057 oraz stali 40HM. Ponadto zaprezentowano wykresy trwałości zmęczeniowej wybranych przekładni zębatych oraz przeanalizowano mechanizmy powstawania uszkodzeń. Zaproponowano także zależności określające maksymalną wartość momentu skręcającego w cyklu obciążenia od liczby cykli obciążenia do uszkodzenia przekładni.

LIU X, WANG W, PENG R. **Model integrujący planowanie opartej na pojęciu czasu opóźnienia konserwacji zapobiegawczej oraz planowanie produkcji dla systemów produkcji wieloasortymentowej**. Eksploatacja i Niezawodnosc – Maintenance and Reliability 2015; 17 (2): 215–221, http://dx.doi.org/10.17531/ein.2015.2.7.

W niniejszej pracy zintegrowano proces konserwacji zapobiegawczej z procesem średnioterminowego taktycznego planowania produkcji w odniesieniu do systemu produkcji wieloasortymentowej. W takim systemie, zestaw wyrobów jest produkowany partiami w określonym, skończonym horyzoncie planowania. Konserwacja zapobiegawcza prowadzona jest okresowo pod koniec wybranych okresów produkcyjnych, natomiast w przypadku wystąpienia uszkodzenia wykonuje się konserwację korygującą. Konserwacja może mieć wpływ na dostępne moce produkcyjne systemu, jako że zarówno planowana konserwacja prewencyjna jak i nieplanowana konserwacja korygująca powodują straty związane z przestojem urządzeń w danym horyzoncie planowania. Oprócz czasu potrzebnego na konserwację zapobiegawczą i korygującą, nasz model uwzględnia czas konfiguracji urządzeń oraz jakość produktów, ponieważ one również zależą od defektów i awarii systemu. Zaproponowano procedury, które pozwalają na jednoczesne określenie optymalnego planu produkcji i optymalnej strategii konserwacji prewencyjnej. Naszym celem jest minimalizacja sumy kosztów konserwacji, produkcji, zapasów, konfiguracji urządzeń oraz zamówień oczekujących a także kosztów produktów, które nie zostały zakwalifikowane do wprowadzenia do obrotu w danym horyzoncie planowania. Model zilustrowano na przykładzie rzeczywistego przypadku z fabryki stali.

FALKOWICZ K, FERDYNUS M, DĘBSKI H. **Numeryczne badania pracy ściskanych elementów płytowych z wycięciem w zakresie geometrycznie nieliniowym**. Eksploatacja i Niezawodnosc – Maintenance and Reliability 2015; 17 (2): 222–227, http://dx.doi.org/10.17531/ein.2015.2.8.

Przedmiotem badań są prostokątne płyty z wycięciem o zmiennych parametrach geometrycznych poddane równomiernemu ściskaniu. Płyty podparte przegubowo na krótszych krawędziach wykonano ze stali o wysokich właściwościach wytrzymałościowych. Badania

analysis examines the nonlinear stability of these structures in the post-buckling state, where the mode of buckling is forced to ensure their stable behaviour. The numerical computations are performed within the geometrically nonlinear range until the yield point is reached. The investigation involves determining the effect of cut-out sizes on elastic properties of the plates with respect to service loads. The numerical analysis is conducted using the ABAQUS software.

TANG D, YU J. **Optimal Replacement Policy for a Periodically Inspected System Subject to the Competing Soft and Sudden Failures**. Eksploatacja i Niezawodnosc – Maintenance and Reliability 2015; 17 (2): 228–235, http://dx.doi.org/10.17531/ein.2015.2.9.

This paper analyzes a replacement problem for a continuously degrading system which is periodically inspected and subject to the competing risk of soft and sudden failures. The system should be correctively replaced by a new one upon failure, or it could be preventively replaced before failure due to safety and economic considerations. Dependent soft and sudden failures are considered. The degradation process of the system observed by inspections exhibits a monotone increasing pattern and is described by a gamma process. The failure rate of the sudden failure is characterized by its dependency on the system age and the degradation state. By formulating the optimization problem in a semi-Markov decision process framework, the specific form of the optimal replacement policy which minimizes the long-run expected average cost per unit time is found, considering a cost structure that includes the cost for inspections, the cost for preventive replacement, and the costs for different failure modes. The corresponding computational algorithm to obtain the optimal replacement policy is also developed. A real data set is utilized to illustrate the application of the optimal replacement policy.

GE Z, WU F, YANG Y, LUO X. **One cabin equipment location method based on the visibility human-factor potential field**. Eksploatacja i Niezawodnosc – Maintenance and Reliability 2015; 17 (2): 236–242, http://dx.doi.org/10.17531/ein.2015.2.10.

The visibility is the basic condition for cabin equipment location. For the description of human, object and obstacle, the human-factor potential field concept is proposed in this paper, concluding the visibility potential field, the reachability potential field. The cabin equipment layout problem is modeled based on the basic visibility potential field model. The optimal layout optimization method is studied based on the particle swarm optimization (PSO) algorithm by natural selection. Finally, the applicability of the proposed idea is illustrated by numerical studies.

SOBRAL J, FERREIRA L. **Establishment of optimal physical assets inspection frequency based on risk principles**. Eksploatacja i Niezawodnosc – Maintenance and Reliability 2015; 17 (2): 243–249, http://dx.doi.org/10.17531/ein.2015.2.11.

Risk Based Inspection (RBI) is a risk methodology used as the basis for prioritizing and managing the efforts for an inspection program allowing the allocation of resources to provide a higher level of coverage on physical assets with higher risk. The main goal of RBI is to increase equipment availability while improving or maintaining the accepted level of risk. This paper presents the concept of risk, risk analysis and RBI methodology and shows an approach to determine the optimal inspection frequency for physical assets based on the potential risk and mainly on the quantification of the probability of failure. It makes use of some assumptions in a structured decision making process. The proposed methodology allows an optimization of inspection intervals deciding when the first inspection must be performed as well as the subsequent intervals of inspection. A demonstrative example is also presented to illustrate the application of the proposed methodology.

JIAKAI C, YAN H, WEI W. **Reliability analysis and optimization of equal load-sharing k-out-of-n phased-mission systems**. Eksploatacja i Niezawodnosc – Maintenance and Reliability 2015; 17 (2): 250–259, http://dx.doi.org/10.17531/ein.2015.2.12.

There are many studies on k-out-of-n systems, load-sharing systems (LSS) and phased-mission systems (PMS); however, little attention has been given to load-sharing k-out-of-n systems with phased-mission requirements. This paper considers equal load-sharing k-out-of-n phased-mission systems with identical components. A method is proposed for the phased-mission reliability analysis of the studied systems based on the applicable failure path (AFP). A modified universal generating function (UGF) is used in the AFP-searching algorithm because of its efficiency. The tampered failure rate load-sharing model for the exactly k-out-of-n: F system is introduced and integrated into the method. With the TFR model, the systems with arbitrary load-dependent

dotyczyły numerycznej analizy MES nieliniowej stateczności konstrukcji znajdujących się w stanie pokrytycznym z wymuszoną postacią wyboczenia zapewniającą stateczny charakter pracy konstrukcji. Obliczenia prowadzono w zakresie geometrycznie nieliniowym do uzyskania poziomu granicy plastyczności materiału. Badano wpływ parametrów geometrycznych wycięcia na charakterystykę sprężystą płyty w zakresie obciążeń eksploatacyjnych. Zastosowanym narzędziem numerycznym był program ABAQUS.

TANG D, YU J. **Optymalna polityka wymiany do zastosowania w systemach poddawanych przeglądom okresowymnarażonych na konkurujące uszkodzenia parametryczne i nagłe**. Eksploatacja i Niezawodnosc – Maintenance and Reliability 2015; 17 (2): 228–235, http://dx.doi.org/10.17531/ein.2015.2.9.

W artykule przeanalizowano problem wymiany dotyczący poddawanego przeglądom okresowym systemu ulegającego ciągłej degradacji i narażonego na konkurujące zagrożenie uszkodzeniami parametrycznymi i nagłymi. System taki powinien zostać wymieniony na nowy w ramach konserwacji korygującej w przypadku wystąpienia uszkodzenia lub też, ze względów bezpieczeństwa i względów ekonomicznych, można dokonać wymiany profilaktycznej jeszcze przed wystąpieniem uszkodzenia. W artykule rozważono przypadek zależnych od siebie uszkodzeń parametrycznych i nagłych. Proces degradacji systemu obserwowany podczas przeglądów ma charakter monotonicznie rosnący i można go opisać za pomocą procesu gamma. Intensywność uszkodzeń nagłych zależy od wieku systemu i jego stanu degradacji. Formułując problem optymalizacyjny w ramach semi-markowskiego procesu decyzyjnego, można określić formę optymalnej polityki wymiany, która minimalizowałaby długookresowy średni koszt na jednostkę czasu, z uwzględnieniem struktury kosztów, która obejmuje koszty przeglądów, koszty wymiany profilaktycznej oraz koszty różnych przyczyn uszkodzeń. Opracowano odpowiedni algorytm obliczeniowy umożliwiający ustalenie optymalnej polityki wymiany. Zastosowanie proponowanej optymalnej polityki wymiany zilustrowano na przykładzie zbioru rzeczywistych danych.

GE Z, WU F, YANG Y, LUO X. **Metoda rozmieszczania przyrządów pokładowych oparta na pojęciach potencjałowego pola widoczności oraz potencjałowego pola czynnika ludzkiego**. Eksploatacja i Niezawodnosc – Maintenance and Reliability 2015; 17 (2): 236–242, http://dx.doi.org/10.17531/ein.2015.2.10.

Widoczność jest podstawowym warunkiem przy projektowaniu rozmieszczenia przyrządów pokładowych. W przedstawionej pracy zaproponowano pojęcie potencjałowego pola czynnika ludzkiego (human-factor potential field, HFPF), które służy do opisu czynnika ludzkiego, przedmiotów oraz przeszkód. HFPF obejmuje pojęcia potencjałowego pola widoczności oraz potencjałowego pola dostępu. Problem umiejscowienia elementów wyposażenia kabiny zamodelowano na podstawie podstawowego modelu potencjałowego pola widoczności. Metodę optymalizacji rozmieszczenia elementów wyposażenia badano w oparciu o algorytm optymalizacji rojem cząstek (PSO), metodą naturalnej selekcji. Zastosowanie proponowanej koncepcji zilustrowano na przykładzie badań numerycznych.

SOBRAL J, FERREIRA L. **Ustalanie optymalnej częstotliwości przeglądów obiektów technicznych w oparciu o zasady oceny ryzyka**. Eksploatacja i Niezawodnosc – Maintenance and Reliability 2015; 17 (2): 243–249, http://dx.doi.org/10.17531/ein.2015.2.11.

Risk Based Maintenance (RBI), to metody planowania inspekcji obiektów, w tym ustalania priorytetów i zarządzania czynnościami obsługowymi, wykorzystujące zasady oceny ryzyka. Pozwalają one na taką alokację zasobów, która zapewnia wyższy poziom zabezpieczenia obiektów technicznych obarczonych wyższym ryzykiem. Głównym celem RBI jest zwiększenie dostępności sprzętu przy jednoczesnym zwiększeniu lub utrzymaniu akceptowalnego poziomu ryzyka. W artykule omówiono pojęcie ryzyka i zasady analizy ryzyka oraz metodologię RBI, a także przedstawiono metodę pozwalającą na określenie optymalnej częstotliwości przeglądów obiektów technicznych na podstawie potencjalnego ryzyka, a przede wszystkim ilościowo określonego prawdopodobieństwa uszkodzenia. Podejście to wykorzystuje niektóre założenia stosowane w ustrukturyzowanym procesie podejmowania decyzji. Zaproponowana metodologia pozwala na optymalizację długości okresów między przeglądami,dając możliwość określenia czasu wykonania pierwszego oraz kolejnych przeglądów. Zastosowanie proponowanej metodologii zilustrowano przykładem numerycznym.

JIAKAI C, YAN H, WEI W. **Analiza niezawodności oraz optymalizacja systemów fazowych typu „k z n" o równym podziale obciążenia elementów składowych**. Eksploatacja i Niezawodnosc – Maintenance and Reliability 2015; 17 (2): 250–259, http://dx.doi.org/10.17531/ein.2015.2.12.

Istnieje wiele badań na temat systemów typu „k z n", systemów z podziałem obciążenia (load-sharing systems, LSS) oraz systemów fazowych (tj. systemów o zadaniach okresowych) (phased-missionsystems, PMS); jak dotąd mało uwagi poświęcono jednak systemom typu „k z n" z podziałem obciążenia wymagającym realizacji różnych zadań w różnych przedziałach czasowych. Niniejszy artykuł omawia systemy fazowe typu „k z n" o równym podziale obciążenia przypadającego na identyczne elementy składowe. Zaproponowano metodę analizy niezawodności badanych systemów w poszczególnych fazach ich eksploatacji opartą na pojęciu właściwej ścieżki uszkodzeń (applicablefailurepath, AFP). W algorytmie wyszukującym AFP zastosowano zmodyfikowaną uniwersalną funkcję tworzącą (universal generating function, UGF), która cechuje się dużą wydajnością. Wprowadzono model manipulowanej intensywności uszkodzeń (tamperedfailurerate, TFR)

component failure distributions can be analyzed. According to the time and space complexity analysis, this method is particularly suitable for systems with small k-values. Two applications of the method are introduced in this paper. 1) A genetic algorithm (GA) based on the method is presented to solve the operational scheduling problem of systems with independent submissions. Two theorems are provided to solve the problem under some special conditions. 2) The method is used to select the optimal number of components to make the system reliable and robust.

JUREVICIUS M, TURLA V, BUREIKA G, KILIKEVICIUS A. **Effect of external excitation on dynamic characteristics of vibration isolating table**. Eksploatacja i Niezawodnosc – Maintenance and Reliability 2015; 17 (2): 260–265, http://dx.doi.org/10.17531/ein.2015.2.13.

Scientific publications available on sandwich panels in evaluating fundamental frequency with a non-dimensional parameter have been discussed in this article. Effectiveness of optical table with pneumatic vibration insulation supports have been analysed in low (1-50) Hz and higher (500-1200) Hz frequency range. Experiments of vibration transmissibility performed using vibration excitation apparatus and other special test equipment. The dynamics characteristics and application ranges of a table as low frequency vibration damper have been defined. Theoretical and experimental modal analysis of the main part of the system – top surface of table – has been performed. This analysis enabled to determine four resonant eigen-frequencies at higher frequency range. Research results show the reliability of vibration table usage and the dangerous zones of its exploitation.

KUSZ A, MARCINIAK A, SKWARCZ J. **Implementation of computation process in a bayesian network on the example of unit operating costs determination**. Eksploatacja i Niezawodnosc – Maintenance and Reliability 2015; 17 (2): 266–272, http://dx.doi.org/10.17531/ein.2015.2.14.

In technical systems understood in terms of Agile Systems, the important elements are information flows between all phases of an object existence. Among these information streams computation processes play an important role and can be done automatically and also in a natural way should include consideration of uncertainty. This article presents a model of such a process implemented in a Bayesian network technology. The model allows the prediction of the unit costs of operation of a combine harvester based on the monitoring of dependent variables. The values of the decision variables representing the parameters of the machine's operation and the intensity and the conditions for its operation, are known to an accuracy, which is defined by a probability distribution. The study shows, using inference mechanisms built into the network, how cost simulation studies of various situational options can be carried out.

LI X-T, TAO L-M, JIA M. **A Bayesian networks approach for event tree time-dependency analysis on phased-mission system**. Eksploatacja i Niezawodnosc – Maintenance and Reliability 2015; 17 (2): 273–281, http://dx.doi.org/10.17531/ein.2015.2.15.

Abstract: Event tree/ fault tree (E/FT) method is the most recognized probabilistic risk assessment tool for complex large engineering systems, while its classical formalism most often only considers pivotal events (PEs) being independent or time-independent. However, the practical difficulty regarding phased-mission system (PMS) is that the PEs always modelled by fault trees (FTs) are explicit dependent caused by shared basic events, and phase-dependent when the time interval between PEs is not negligible. In this paper, we combine the Bayesian networks (BN) with the E/FT analysis to figure such types of PMS based on the conditional probability to give expression of the phase-dependency, and further expand it by the dynamic Bayesian networks (DBN) to cope with more complex time-dependency such as functional dependency and spares. Then, two detailed examples are used to demonstrate the application of the proposed approach in complex event tree time-dependency analysis.

GILL A, KADZIŃSKI A. **The determination procedure of the onset of the object wear-out period based on monitoring of the empirical failure intensity function**. Eksploatacja i Niezawodnosc – Maintenance and Reliability 2015; 17 (2): 282–287, http://dx.doi.org/10.17531/ein.2015.2.16.

The estimation of the number of failures of technical objects is of key importance throughout the object life cycle, particularly in the wear-out period when the number of failures begins to grow significantly. In the literature related to this problem, examples exist of solutions (mathematical models) that can assist the estimation of the number of failures. For the description of the life cycles of objects, functions are usually used of known forms of probability distribution of the number of object failures. The procedure presented in this paper assumes the use of statistical data related

elementów o równym podziale obciążenia dla systemu, w którym liczba uszkodzeń wynosi dokładnie k z n. Model ten włączono do proponowanej metody analizy niezawodności. Przy pomocy modelu TFR można analizować systemy o dowolnych rozkładach uszkodzeń części składowych, gdzie uszkodzenia są zależne od obciążenia. Zgodnie z analizą złożoności czasowej i przestrzennej, metoda ta jest szczególnie przydatna do modelowania układów o małych wartościach k. W pracy przedstawiono dwa zastosowania metody. 1) oparty o omawianą metodę algorytm genetyczny (GA) do rozwiązywania problemu harmonogramowania prac w systemach z niezależnymi podzadaniami. Sformułowano dwa twierdzenia pozwalające na rozwiązanie problemu w pewnych szczególnych warunkach. 2) Wybór optymalnej liczby elementów składowych pozwalającej na zachowanie niezawodności i odporności systemu.

JUREVICIUS M, TURLA V, BUREIKA G, KILIKEVICIUS A. **Wpływ wzbudzania zewnętrznego na właściwości dynamiczne stołu wibroizolacyjnego**. Eksploatacja i Niezawodnosc – Maintenance and Reliability 2015; 17 (2): 260–265, http://dx.doi.org/10.17531/ein.2015.2.13.

W artykule omówiono dostępne publikacje naukowe dotyczące oceny częstotliwości podstawowej paneli przekładkowych z wykorzystaniem parametru bezwymiarowego. Analizowano wydajność stołu optycznego wyposażonego w podpory wibroizolacyjne w niskim (1-50 Hz) i wyższym (500-1200 Hz) zakresie częstotliwości. Doświadczenia dotyczące charaketrystyk przenoszenia drgań prowadzono z zastosowaniem aparatury do wzbudzania drgań i innych specjalnych urządzeń badawczych. Określono właściwości dynamiczne i zakres wykorzystania stołu jako tłumika drgań o niskiej częstotliwości. Dokonano teoretycznej i eksperymentalnej analizy modalnej głównej części systemu – górnej powierzchni stołu. Analiza ta pozwoliła wyodrębnić cztery częstości drgań własnych z wyższego zakresu częstotliwości. Wyniki badań potwierdzają niezawodność stołu wibracyjnego oraz określają strefy jego eksploatacji wykazujące niekorzystne właściwości.

KUSZ A, MARCINIAK A, SKWARCZ J. **Implementacja procedury obliczeniowej w sieci bayesowskiej na przykładzie wyznaczania jednostkowych kosztów eksploatacji**. Eksploatacja i Niezawodnosc – Maintenance and Reliability 2015; 17 (2): 266–272, http://dx.doi.org/10.17531/ein.2015.2.14.

W systemach technicznych rozumianych w kategoriach Agile Systems istotnym elementem są przepływy informacyjne pomiędzy wszystkimi fazami istnienia obiektu. Pośród tych strumieni informacyjnych istotną rolę odgrywają procesy obliczeniowe, które mogą być realizowane automatycznie a ponadto w naturalny sposób powinny umożliwiać uwzględnienie niepewności. W artykule przedstawiono przykład takiego procesu realizowanego w technologii sieci bayesowskiej. Model umożliwia predykcję jednostkowych kosztów eksploatacji kombajnu zbożowego na podstawie monitorowania wielkości zmiennych od których one zależą. Wartości zmiennych decyzyjnych reprezentujących parametry pracy maszyny oraz intensywność i warunki jej eksploatacji są znane z dokładnością do rozkładu prawdopodobieństwa. W pracy pokazano w jaki sposób wykorzystując mechanizmy wnioskowania wbudowane w sieci można prowadzić symulacyjne badania kosztów w różnych wariantach sytuacyjnych.

LI X-T, TAO L-M, JIA M. **Oparte na sieciach bayesowskich podejście do analizy zależności czasowychw systemach o zadaniach okresowych wykorzystujące metodę drzewa zdarzeń**. Eksploatacja i Niezawodnosc – Maintenance and Reliability 2015; 17 (2): 273–281, http://dx.doi.org/10.17531/ein.2015.2.15.

Metoda drzewa zdarzeń/drzewa błędów jest najbardziej znanym narzędziem probabilistycznej oceny ryzyka w złożonych, dużych systemach inżynieryjnych; jednak jej klasyczny formalizm najczęściej uwzględnia jedynie niezależne lub niezależne od czasu zdarzenia kluczowe. Praktyczną trudnością występującą w systemach o zadaniach okresowych jest to, że zdarzenia kluczowe, które zazwyczaj przedstawiane są w modelach drzewa błędów jako powiązane zależnościami jawnymi, mającymi związek ze wspólnym zdarzeniem podstawowym, tutaj powiązane są zależnościami czasowymi, jako że przedział czasowy pomiędzy pojedynczymi zdarzeniami kluczowymi nie jest bez znaczenia. W niniejszej pracy, połączyliśmy metodologie sieci Bayesa i analizy drzewa zdarzeń/błędów aby opisać za pomocą pojęcia prawdopodobieństwa warunkowego, zależności czasowe w systemach o zadaniach okresowych, a następnie rozwinęliśmy tę metodę, wykorzystując dynamiczne sieci Bayesa, które pozwalają na analizę bardziej złożonych zależności czasowych, takich jak zależności funkcjonalne i związane z użyciem części zamiennych. W końcowej części pracy przedstawiliśmy dwa szczegółowe przykłady zastosowania proponowanej metody do analizy złożonych zależności czasowych w drzewach zdarzeń.

GILL A, KADZIŃSKI A. **Procedura wyznaczania początku starzenia się obiektów na podstawie monitorowania empirycznej funkcji intensywności uszkodzeń**. Eksploatacja i Niezawodnosc – Maintenance and Reliability 2015; 17 (2): 282–287, http://dx.doi.org/10.17531/ein.2015.2.16.

Oszacowanie liczby uszkodzeń obiektów technicznych ma kluczowe znaczenie we wszystkich okresach cyklu życia obiektów, szczególnie w okresie uszkodzeń starzeniowych, kiedy to liczba uszkodzeń zaczyna znacząco rosnąć. W bibliografii tego zagadnienia przytoczone są przykłady rozwiązań (modeli matematycznych), którymi można wspomagać m.in. szacowanie liczby uszkodzeń. Do opisu cyklu życia obiektów technicznych wykorzystuje się zwykle funkcje o znanych postaciach rozkładów prawdopodobieństwa liczb uszkodzeń tych obiektów. Przedstawiona w niniejszym artykule procedura, zakłada

to the failures of uniform population of nonrenewable technical objects, recorded in the form of empirical function of failure intensity. It specifically serves the purpose of determining the characteristic point of life of these objects i.e. the onset of the wear-out period. Within the procedure, a model of fuzzy inference has been applied that reflects the human reasoning (expert of the system) observing/investigating the objects. The results of the developed procedure may constitute a basis for forecasting of failures of mechanical nonrenewable technical objects.

korzystanie ze statystycznych danych o uszkodzeniach jednorodnej zbiorowości nieodnawianych obiektów technicznych, zapisanych w postaci empirycznej funkcji intensywności uszkodzeń. Służy ona w szczególności do wyznaczenia charakterystycznego punktu życia tych obiektów tj. chwili rozpoczynania się okresu uszkodzeń starzeniowych. W ramach procedury zastosowano model wnioskowania rozmytego, który odwzorowuje rozumowanie człowieka (eksperta systemu) obserwującego/badającego obiekty. Wyniki opracowanej procedury mogą stać się podstawą prognozowania uszkodzeń nieodnawianych obiektów technicznych typu mechanicznego.

WU Z, HUANG N, LI R, ZHANG Y. **A delay reliability estimation method for Avionics Full Duplex Switched Ethernet based on stochastic network calculus**. Eksploatacja i Niezawodnosc – Maintenance and Reliability 2015; 17 (2): 288–296, http://dx.doi.org/10.17531/ein.2015.2.17.

The delay reliability estimation is required in order to guarantee the real-time communication for avionics full duplex switched Ethernet (AFDX). Stochastic network calculus (SNC) can be applied to estimate the reliability with a delay upper bound. However, only linear deterministic traffic envelope function is used to bound its traffic, which cannot represent the traffic randomness and is far from practice. In this paper, a stochastic traffic envelope function, which randomizes the input of SNC, is proposed to solve the problem. A new probabilistic algorithm is derived to estimate the delay reliability based on stochastic envelope functions. A test was conducted to demonstrate our method on an AFDX testbed, and the test results verify that the estimation of delay reliability via our algorithm is much closer to the empirical estimation.

WU Z, HUANG N, LI R, ZHANG Y. **Oparta na stochastycznym rachunku sieciowym metoda estymacji niezawodności czasu transmisji dla przełączanej pokładowej sieci ethernetowej typu AFDX umożliwiającej równoczesną transmisję dwukierunkową**. Eksploatacja i Niezawodnosc – Maintenance and Reliability 2015; 17 (2): 288–296, http://dx.doi.org/10.17531/ein.2015.2.17.

Ocena niezawodności czasu transmisji (czasu opóźnienia) jest niezbędną procedurą gwarantującą komunikację w czasie rzeczywistym za pośrednictwem przełączanej pokładowej sieci ethernetowej typu AFDX (Avionics Full Duplex Switched Ethernet), która umożliwia równoczesną transmisję dwukierunkową. Stochastyczny rachunek sieciowy (SNC) można stosować do oceny niezawodności przy zadanej górnej granicy opóźnienia. Do tej pory jednak, do ograniczania ruchu telekomunikacyjnego stosowano tylko liniową deterministyczną funkcję obwiedni (traffic envelope), która nie oddaje losowości ruchu telekomunikacyjnego i odbiega dalece od rzeczywistości. W niniejszej pracy zaproponowano rozwiązanie tego problemu wykorzystujące stochastyczną funkcję obwiedni ruchu telekomunikacyjnego. Wyprowadzono nowy algorytm probabilistyczny, który pozwala ocenić niezawodność czasu transmisji na podstawie funkcji obwiedni. Przeprowadzono badanie, w ramach którego testowano zaproponowaną metodę w środowisku testowym AFDX; wyniki testu pokazują, że ocena niezawodności czasu transmisji z wykorzystaniem zaproponowanego przez nas algorytmu jest znacznie bardziej zbliżona do estymacji empirycznej.

TU J, SUN C, ZHANG X, PAN H, CHENG R. **Maintenance strategy decision for avionics system based on cognitive uncertainty information processing**. Eksploatacja i Niezawodnosc – Maintenance and Reliability 2015; 17 (2): 297–305, http://dx.doi.org/10.17531/ein.2015.2.18.

Proper maintenance schedule is required to improve avionics systems reliability and safety. A decision approach to maintenance strategy remains a longstanding challenge in avionics system. With regard to fault diagnosis and equipment maintenance of avionics system, in which the equipment fault information are complex and uncertainty, a multi criteria of decision making method for avionics system based on cognitive uncertainty information processing is proposed to be used in the maintenance strategy decision. Firstly, vague set with three-parameters is introduced to make up for the shortage of the original vague set in expressing fuzzy information, a linguistic variables describing the qualitative indexes into three parameter vague of interval number is proposed. At the same time, due to risk psychological factors of maintenance policymakers that cause cognitive uncertainty are introduced into the maintenance decision process, and a prospect value function of three parameters vague interval value is defined based on prospect theory and the formula for measuring the distance between vague interval value, and a non-linear model of equipment maintenance policies can be established. The implementing process of maintenance policy decision for avionics system based on cognitive uncertainty information processing is given in this paper, and a ranking of the maintenance alternatives is determined. Finally, A specific example of decision of maintenance strategies in avionics system with the application of the proposed method is given, showing that the reliability centered maintenance strategy is the most suitable for avionics system.

TU J, SUN C, ZHANG X, PAN H, CHENG R. **Decyzja w zakresie strategii utrzymania ruchu układu elektroniki lotniczej w oparciu o przetwarzanie informacji związanych z niepewnością kognitywną**. Eksploatacja i Niezawodnosc – Maintenance and Reliability 2015; 17 (2): 297–305, http://dx.doi.org/10.17531/ein.2015.2.18.

Doskonalenie niezawodności i bezpieczeństwa układów elektroniki lotniczej wymaga odpowiedniego harmonogramu działań obsługowych. Podejście decyzyjne do strategii utrzymania ruchu od dawna pozostaje wyzwaniem w systemach awioniki. W odniesieniu do diagnozy uszkodzeń i konserwacji urządzeń systemów elektroniki lotniczej, w których informacje o usterkach urządzeń są złożone i obarczone niepewnością, zaproponowano metodę wielokryterialnego podejmowania decyzji opartą na przetwarzaniu informacji związanych z niepewnością kognitywną, którą można stosować przy podejmowaniu decyzji dotyczących strategii utrzymania ruchu. Po pierwsze, wprowadzono nieostry zbiór trzech parametrów, które pozwalają na wyrażenie wartości liczbowej zaproponowanych zmiennych lingwistycznych opisujących wskaźniki jakościowe, jako wartości z przedziału nieostrego. Jednocześnie, do pojęcia procesu decyzyjnego dotyczącego utrzymania ruchu wprowadzono pojęcie ryzyka związanego z powodującymi niepewność poznawczą czynnikami psychologicznymi kierującymi osobami podejmującymi decyzje obsługowe. Zdefiniowano także funkcję oceny dla wartości z przedziału nieostrego trzech parametrów na podstawie teorii perspektywy i wzór do pomiaru odległości między wartościami z przedziału nieostrego, oraz ustalono nieliniowy tryb polityki konserwacji sprzętu. W artykule zaprezentowano proces implementacji decyzji w zakresie polityki konserwacji układów elektroniki lotniczej w oparciu o przetwarzanie informacji związanych z niepewnością kognitywną, stworzono też ranking dostępnych alternatyw w zakresie utrzymania ruchu. Na koniec, zaprezentowano konkretny przykład decyzji w zakresie strategii konserwacji układów elektroniki lotniczej z zastosowaniem proponowanej metody, pokazując, że strategia utrzymania ruchu oparta na niezawodności jest najbardziej odpowiednia dla układów awioniki.

PENG W, LIU Y, ZHANG X, HUANG H-Z. **Sequential preventive maintenance policies with consideration of random adjustment-reduction features**. Eksploatacja i Niezawodnosc – Maintenance and Reliability 2015; 17 (2): 306–313, http://dx.doi.org/10.17531/ein.2015.2.19.

In existing literature, imperfect maintenance has been widely studied and many studies treat the effectiveness of imperfect maintenance as a fixed constant. In reality, it is more realistic to regard the maintenance efficiency as a random quantity as it may not be precise value due to the lack of sufficient data and/or the variation from system to system. In this paper, a hybrid imperfect maintenance model with random adjustment-reduction parameters is proposed, and a maintenance policy, namely the sequential preventive maintenance in periodic leisure interval, is studied based on the proposed hybrid random imperfect maintenance model, and the corresponding maintenance strategy is optimized by the genetic algorithm (GA). A numerical example and an example of the fuel injection pump of diesel engines are presented to illustrate the proposed method.

PENG W, LIU Y, ZHANG X, HUANG H-Z. **Strategia sekwencyjnej konserwacji zapobiegawczej z uwzględnieniem cech losowej korekcji i losowej redukcji wieku**. Eksploatacja i Niezawodnosc – Maintenance and Reliability 2015; 17 (2): 306–313, http://dx.doi.org/10.17531/ein.2015.2.19.

W literaturze, temat konserwacji niepełnej został szeroko zbadany i wiele z opisywanych badań traktuje wydajność konserwacji niepełnej jako wartość stałą. W rzeczywistości jednak wydajność konserwacji należy traktować jako wielkość losową, ponieważ nie można jej dokładnie określić ze względu na brak wystarczających danych i / lub różnice między poszczególnymi systemami. W niniejszej pracy zaproponowano model hybrydowy konserwacji niepełnej łączący pojęcia parametrów losowej korekcji i losowej redukcji wieku. Na podstawie proponowanego modelu hybrydowego losowej konserwacji niepełnej przebadano strategię sekwencyjnej konserwacji zapobiegawczej przeprowadzanej okresowo w czasie wolnym od pracy; omawianą strategię konserwacji zoptymalizowano za pomocą algorytmu genetycznego (GA). Proponowaną metodę zilustrowano przykładem liczbowym oraz omówiono na przykładzie pompy wtryskowej paliwa do silników wysokoprężnych.

ZHOU Y, ZHANG Z. **Optimal maintenance of a series production system with two multi-component subsystems and an intermediate buffer**. Eksploatacja i Niezawodnosc – Maintenance and Reliability 2015; 17 (2): 314–325, http://dx.doi.org/10.17531/ein.2015.2.20.

Intermediate buffers often exist in practical production systems to reduce the influence of the breakdown and maintenance ef subsystems on system production. At the same time, the effects of intermediate buffers also make the degradation process of the system more difficult to model. Some existing papers investigate the performance evaluation and maintenance optimisation of a production system with intermediate buffers under a predetermined maintenance strategy structure. However, only few papers pay attention to the property of the optimal maintenance strategy structure. This paper develops a method based on the Markov decision process to identify the optimal maintenance strategy for a series-parallel system with two multi-component subsystems and an intermediate buffer. The structure of the obtained optimal maintenance strategy is analysed, which shows that the optimal strategy structure cannot be modelled by a limited number of parameters. However, some useful properties of the strategy structure are obtained, which can simplify the maintenance optimisation. Another interesting finding is that a large buffer capacity cannot always bring about high average revenue even through the cost of holding an item in the buffer is much smaller than the production revenue per item.

ZHOU Y, ZHANG Z. **Optymalna strategia utrzymania ruchu dla seryjnego systemu produkcji złożonego z dwóch podsystemów wieloskładnikowych oraz buforu pośredniego**. Eksploatacja i Niezawodnosc – Maintenance and Reliability 2015; 17 (2): 314–325, http://dx.doi.org/10.17531/ein.2015.2.20.

W systemach produkcyjnych często stosuje się bufory pośrednie w celu zmniejszenia wpływu awarii i konserwacji podsystemów na system produkcji. Jednocześnie, oddziaływanie buforów pośrednich utrudnia modelowanie procesu degradacji systemu. Istnieją badania dotyczące oceny funkcjonowania i optymalizacji utrzymania systemów produkcyjnych wykorzystujących bufory pośrednie przy założeniu wcześniej określonej struktury strategii utrzymania ruchy. Jednak tylko nieliczne prace zwracają uwagę na własności optymalnej struktury strategii utrzymania ruchu. W przedstawionej pracy opracowano opartą na procesie decyzyjnym Markowa metodę określania optymalnej strategii utrzymania ruchu dla układu szeregowo-równoległego z dwoma podsystemami wieloskładnikowymi oraz buforem pośrednim. Przeanalizowano strukturę otrzymanej optymalnej strategii utrzymania i wykazano, że struktury takiej nie można zamodelować przy użyciu ograniczonej liczby parametrów. Jednak odkryto pewne przydatne właściwości struktury strategii, które mogą ułatwić optymalizację utrzymania ruchu. Innym interesującym odkryciem było to, że duża pojemność bufora nie zawsze daje wysoką średnią przychodów mimo iż koszty przechowywania obiektu w buforze są znacznie mniejsze niż przychody z produkcji w przeliczeniu na jeden obiekt.

Article citation info:
YANG R, ZHAO F, KANG J, LI H, TENG H. Inspection optimization model with imperfect maintenance based on a three-stage failure process. Eksploatacja i Niezawodnosc – Maintenance and Reliability 2015; 17 (2): 165–173, http://dx.doi.org/10.17531/ein.2015.2.1.

Ruifeng YANG
Fei ZHAO
Jianshe KANG
Haiping LI
Hongzhi TENG

INSPECTION OPTIMIZATION MODEL WITH IMPERFECT MAINTENANCE BASED ON A THREE-STAGE FAILURE PROCESS

MODEL OPTYMALIZACJI PRZEGLĄDÓW W WARUNKACH NIEPEŁNEJ KONSERWACJI OPARTY O TRÓJFAZOWY PROCES USZKODZENIA

Rolling element bearings are one of the most widely used and vulnerable components in complex systems. The condition monitoring work is very critical for sustaining the system's availability and reducing the maintenance cost. Shock pulse method (SPM) is a common technique to measure the operating condition of rolling bearings as a three color scheme, e.g., green, yellow and red. This paper proposes an inspection model based on a three-stage failure process which aims to optimize the inspection interval of bearings by minimizing the expected cost per unit time. The three-stage failure process divides the bearings life into three stages before failure: good, minor defective and severe defective stages, corresponding to the three color scheme of SPM. Considering the need to lubricate bearings when the minor defective stage is identified by inspection in industrial applications, we assume that maintenance at the time of inspection identifying the minor defective stage is imperfect. The concept of proportional age reduction is used to model the effect of imperfect maintenance on the instantaneous rates of the minor defective stage, the severe defective stage and failure. Perfect maintenance however is carried out if inspection detects bearings being in the severe defective stage. Failure can be found once it occurs and replacement has to be implemented immediately. Finally, a numerical example is presented to illustrate the effectiveness of the proposed model.

Keywords: *delay time modeling, three-stage failure process, inspection, imperfect maintenance, proportional age reduction.*

Łożyska toczne są jednymi z najczęściej stosowanych i jednocześnie najbardziej narażonych na uszkodzenia części składowych układów złożonych. Monitorowanie stanu odgrywa bardzo istotną rolę w utrzymaniu dostępności układów i zmniejszeniu kosztów ich obsługi. Metoda impulsów uderzeniowych (SPM) jest powszechnie stosowaną techniką służącą do pomiaru stanu pracy łożysk tocznych, który reprezentowany jest za pomocą kodu trzech kolorów, na przykład, zielonego, żółtego i czerwonego. W artykule zaproponowano model przeglądów oparty na trójfazowym procesie uszkodzenia, który ma na celu optymalizację częstotliwości przeglądów łożysk poprzez minimalizację oczekiwanych kosztów przypadających na jednostkę czasu. Pojęcie trójfazowego procesu uszkodzenia pozwala podzielić żywotność łożyska na trzy fazy przed wystąpieniem uszkodzenia: fazę dobrego stanu, fazę drobnych defektów i fazę poważnych defektów. Podział ten odpowiada kodowi trzech kolorów SPM. Biorąc pod uwagę konieczność smarowania łożysk po zdiagnozowaniu, podczas przeglądu w warunkach przemysłowych, wystąpienia fazy drobnych defektów, zakładamy, że konserwacja w czasie takiego przeglądu jest konserwacją niepełną. Koncepcja proporcjonalnego obniżenia wieku służy do modelowania wpływu niepełnej konserwacji na chwilowe wartości intensywności fazy drobnych defektów, fazy poważnych defektów oraz uszkodzeń. Gdy podczas przeglądu stwierdzi się, że łożysko jest w fazie poważnych defektów, przeprowadza się pełną konserwację. Uszkodzenie zostaje wykryte zaraz po jego wystąpieniu, i wtedy należy dokonać natychmiastowej wymiany łożyska. Pod koniec artykułu, przedstawiono przykład numeryczny, który ilustruje wydajność proponowanego modelu.

Słowa kluczowe: *Modelowanie metodą czasu zwłoki, trójfazowy proces uszkodzenia, przegląd, konserwacja niepełna, proporcjonalne obniżenie wieku.*

1. Introduction

Rolling element bearings are widely used in industrial rotating machinery, for example wind turbine and helicopter; and they are also considered as a type of critical components. Unexpected bearing faults are one of the most frequent reasons for machine breakdown and may result in significant economic losses. Therefore, taking appropriate and effective maintenance activities is required for achieving higher

availability and lower operational cost. Numerous maintenance policies have been implemented on the bearings to prevent the occurrence of failure [10]. Preventive maintenance (PM) is perhaps one of the most popular maintenance policies, by which maintenance activities are executed with a planned interval aiming at preventing potential failures from occurring [3, 13]. For most practical situations, PM is still a dominant maintenance policy due to its easy implementation.

Inspection as an important PM activity can or could reveal the status of the system being inspected, thus it helps maintenance engineers make decisions to avoid the occurrence of failure [20]. Inspections may be performed discretely with a periodic or aperiodic interval by using inspection instrument or continuously by modern condition monitoring devices. In industrial applications, inspectors carry out inspection activities on bearings mostly utilizing the inspection instrument, such as, SPM (Shock Pulse Method) instrument.

SPM, developed by SPM instrument AB Company in the early 1970s and originated in Sweden, is a patented technique and has achieved wide acceptance as a quantitative method for efficiently inspecting the condition of bearings [6, 12]. Through sampling the shock pulse amplitude of bearings over a period of time and displaying the maximum value dB_m and the carpet value dB_c, SPM provides a direct normalized shock value indicating the bearing operating state and lubrication condition [7]. Accordingly, maintenance engineers can make decisions in terms of the final shock value.

However, how often do engineers inspect the bearings or the determination of inspection interval is still a key issue. Traditionally in most industries, the inspection interval is usually determined by engineers' experience or by the manufacturer's recommendation [5]. However, such determination is conservative and undesired although it is easy to implement. Many researchers have developed numerous PM models to find the optimal inspection interval under various modeling assumptions [1, 8, 9]. However, in contrast with other PM models [3, 13], the models based on the delay-time concept have been proved to have the obvious advantages for optimizing the inspection interval since the delay-time technique can directly model the relationship between the inspection intervention and the system performance, see [15, 17, 22].

The delay time concept was first introduced by Christer in 1976 [2], which defines the failure process as a two-stage failure process, namely normal stage and delay time stage. The normal stage is from new to an initial point that a defect can be first identified by an inspection and the delay time stage from this initial point to failure [19]. By the definition of delay time concept, the plant can be in one of two states before failure, namely normal and defective. A defect can be identified if the inspection is carried out during the delay-time stage. Many inspection and PM models, especially successful case studies based on the two-stage failure process have been reported with actual applications in industry [18, 19].

However, some systems may be described more than two states before failure in industrial applications. For example, SPM indicates the bearing condition before failure as the condition scale (namely Green-Yellow-Red scale) depending on the shock value. Green with the shock value range 0-20 denotes bearing is normal, a minor defective bearing is represented by Yellow (20-35) and the shock value range 35-60 indicates a severe defective bearing, shown by Red. Then the state of bearing before failure may be in one of these three states, namely normal, minor defective, and severe defective. Considering this industrial scenario, Wang [16] firstly extended the two-stage failure process into a three-stage failure process, which is closer to the practical situation and provides more decision options for different states. In the work [16], the inspection interval is shortened to be half of the current interval to more frequently inspect the system when the minor defective stage is identified by inspection, but immediately replace the system if it is in the severe defective stage. Wang et al. [23] further extended the work [16] by considering a two-level inspection policy with PM and delaying the maintenance once the severe defective stage is identified and the time interval to the next PM is less than a threshold level. However, perfect maintenance for the defective system is assumed in the works [16, 23].

After the condition of bearing is measured utilizing the SPM instrument, maintenance engineers will carry out different decisions depending on the shock value. When the shock value is less than 20, namely the condition of bearing is good, do nothing and check the bearing until the next inspection. If the bearing is found to be in the minor defective stage, i. e., the shock value is within the interval (20, 35), lubrication is in need; however, replacement needs to be done immediately once the shock value exceeds 35 as replacement is generally a direct measure for bearings, where replacement can be viewed as renewing the bearing. However, when the bearing is found to be in the minor defective stage by inspection, being in yellow, lubrication is a common practice adopted in industry as a way to prolong the life of the system. The lubrication problem in PM models based on the delay time concept has been presented by Wang [21], which considered integratedly the routine service (RS), inspection, condition monitoring and preventive replacement. However, the lubrication is only implemented when the bearing is identified to be in the minor defective stage in the industry, rather than a part of inspection, or of repair or replacement. The lubrication aims at preventing the defects from arising, which will affect the instantaneous rates of defects and failure such that it can be regarded as imperfect maintenance. Wang et al. [14] have considered imperfect maintenance which is based on the two-stage failure process. However, the inspection model considering imperfect maintenance based on the three-stage failure process is closer to reality but not developed. To model the imperfect maintenance at the time of inspection identifying the minor defective stage, we borrow the concept of proportional age reduction (PAR), which has been widely utilized in imperfect maintenance optimization modeling [4].

The contributions of this work are as follows: (1) the system deterioration is subject to the three-stage failure process; (2) imperfect maintenance is considered after the system is found to be in the minor defective stage; (3) an inspection model with imperfect maintenance based on the three-stage failure process is presented.

The remaining parts of the paper are organized as follows: Section 2 presents the problem description and modeling assumptions. Section 3 formulates all possible renewal probabilistic models based on the three-stage failure process. The cost model is developed to find the optimal inspection interval by minimizing the expected cost per unit time in Section 4. Section 5 gives numerical examples and some discussions. Finally, Section 6 concludes the paper and the future researches are suggested.

2. Problem description and modeling assumptions

2.1. Problem description

The bearing is regarded as a single component system subject to a single failure mode and in the following part we refer to it simply as the system. The system is inspected periodically with the interval T to obtain the shock value and measure the operating condition. When the shock value of the system falls into green, namely less than 20, do nothing. If the shock value indicates that the system is in the minor defective stage, lubrication is carried out to prolong the system life, regarding as imperfect maintenance. However, the system needs to be replaced immediately once it is revealed by inspection to be in the severe defective stage with the shock value in the interval (35, 60). Failure can be found once it occurs such that replacement needs to be made immediately with an identical one. Replacement can restore the system to a new condition. However, imperfect maintenance at the time of inspection identifying the minor defective stage will affect the instantaneous rates of the minor defective stage, the severe defective

stage and failure at the next maintenance stage [14]. Fig.1 shows an illustration of the three-stage failure process based on SPM.

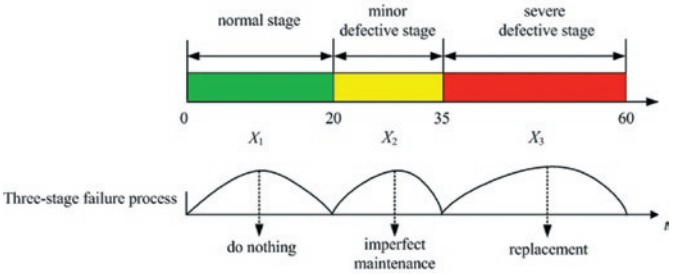

Fig. 1. Illustration of three-stage failure process based on SPM

2.2. Modeling assumptions

The following assumptions are proposed for a modeling purpose. Most assumptions have been explained in the previous section or problem description [14, 18, 19].

(1) The failure process of the system is divided into three stages, namely normal, minor and severe defective stages. These three stages are assumed to be independent.
(2) The system is inspected periodically with an interval T. There is no downtime caused by inspection since the system is checked online.
(3) Inspection is perfect such that the system condition can be identified with a probability 100%.
(4) When the inspection detects the system being in the normal stage, do nothing.
(5) If the system is found to be in the minor defective stage, we consider implementing lubrication, regarding as imperfect maintenance, which will affect the instantaneous rates of the minor defective stage, the severe defective stage and failure at the next maintenance stage.
(6) Once the system is found to be in the severe defective stage, replacing is always carried out immediately.
(7) The failure of the system can be observed immediately and replacement will be carried out at once.
(8) The system after replacement is viewed as new.

The following notation will be used in the subsequent modelling:

X_n random variable representing the duration of the *nth* stage, n=1, 2 and 3
T inspection interval
t_i time of the ith imperfect maintenance due to the minor defective stage identification
ρ improvement factor
Δi accumulated age
T_f time to failure
T_{pm} time to imperfect maintenance due to the minor defective stageidentification by an inspection
T_{ps} time to the severe defective stage identification
$\lambda_{i+1}(x)$ instantaneous rate of the minor defective stage after the ith imperfect maintenance
$\gamma_{i+1}(y)$ instantaneous rate of the severe defective stage after the ith imperfect maintenance
$h_{i+1}(z)$ failure rate after the ith imperfect maintenance
$f_{X_1,i+1}(x)$ probability density function (pdf) of the minor defective stage after the ith imperfect maintenance
$f_{X_2,i+1}(y)$ pdf of the severe defective stage after the ith imperfect maintenance
$f_{X_3,i+1}(z)$ pdf of failure after the ith imperfect maintenance
$F_{X_2,i+1}(y)$ cumulative distribution function (cdf) of the severe defective stage after the ith imperfect maintenance
$F_{X_3,i+1}(z)$ cdf of failure after the ith imperfect maintenance
$P_f((i\text{-}1)T,iT)$ probability of a failure renewal in $((i\text{-}1)T, iT)$
$P_m(iT)$ probability of imperfect maintenance of the minor defective stage at iT
$P_s(iT)$ probability of an inspection renewal due to the severe defective stage identification at iT
C_s average cost per inspection
C_f average cost per failure
C_{pm} average cost per imperfect maintenance
C_{ps} average cost caused by an inspection renewal due to identifying the severe defective stage
$C(T)$ expected cost per unit time
$EC(T)$ expected renewal cycle cost
$EC_f(T)$ expected cost caused by a failure renewal
$EC_s(T)$ expected cost caused by an inspection renewal
$EL(T)$ expected renewal cycle length
$EL_f(T)$ expected length caused by a failure renewal
$EL_s(T)$ expected length caused by an inspection renewal

3. Probabilistic models of a failure renewal and an inspection renewal considering imperfect maintenance

In order to establish the cost model using the renewal theorem, two renewal scenarios at the end of a renewal cycle, namely a failure renewal and an inspection renewal, should be considered. The probability models for both renewals need to be formulated as [16, 19] for a modelling purpose. Since it is assumed that imperfect maintenance is applied when the system is found to be in the minor defective stage, we introduce the PAR model firstly.

3.1. The PAR model

The PAR model assumes that the ith imperfect maintenance at t_i will shorten the length of the last operation time from t_i-t_{i-1} to $\rho(t_i-t_{i-1})$ [4]. The effective age after the ith imperfect maintenance is $t\text{-}\rho t_i$ ($t > t_i$) that indicates that it has no relationship with the maintenance history prior to t_i. So the difference between $t-\rho t_i$ and $t-t_i$, $\Delta i=(1-\rho)t_i$, is defined as the accumulative age which will affect the instantaneous rate of each stage for the $(i+1)$th maintenance stage [14].

If the ith imperfect maintenance for the minor defective stage is triggered at t_i, then the accumulative age is:

$$\Delta i = (1-\rho)t_i \tag{1}$$

The instantaneous rate of the minor defective stage after the ith imperfect maintenance can be defined as:

$$\lambda_{i+1}(x) = \lambda(x+\Delta_i) \tag{2}$$

where $x=t-t_i$.

The instantaneous rate of the severe defective stage after the ith imperfect maintenance can be defined as:

$$\gamma_{i+1}(y) = \gamma(y+\Delta_i) \tag{3}$$

where $y=t-t_i\text{-}x$.

Furthermore, the failure rate after the ith imperfect maintenance can be defined as:

$$h_{i+1}(z) = h(z + \Delta_i) \tag{4}$$

where $z=t-t_i-x-y$.

Here, $\rho=1$ corresponds to the maintenance at the minor defective stage is perfect and $\rho=0$ means the maintenance is minimal. However, the maintenance is imperfect if $0<\rho<1$.

Because the probability density function (pdf) of the system can be formulated as $f(t) = \lambda(t)e^{-\int_0^t \lambda(s)ds}$, the pdf of the minor defective stage after the ith imperfect maintenance is expressed as:

$$\begin{aligned} & f_{X_1,i+1}(x) \\ & = \lambda_{i+1}(x)\exp(-\int_0^x \lambda_{i+1}(s)ds) = \lambda(x+\Delta i)\exp(-\int_0^x \lambda(s+\Delta i)ds) \\ & = \lambda(x+\Delta i)\exp(-\int_{\Delta i}^{x+\Delta i} \lambda(s)ds) \end{aligned} \tag{5}$$

Using the similar way, the pdf of the severe defective stage after the ith imperfect maintenance is given as:

$$\begin{aligned} & f_{X_2,i+1}(y) \\ & = \gamma_{i+1}(y)\exp(-\int_0^y \gamma_{i+1}(s)ds) = \gamma(y+\Delta i)\exp(-\int_0^y \gamma(s+\Delta i)ds) \\ & = \gamma(y+\Delta i)\exp(-\int_{\Delta i}^{y+\Delta i} \gamma(s)ds) \end{aligned} \tag{6}$$

Moreover, the pdf of failure after the ith imperfect maintenance is formulated as:

$$\begin{aligned} & f_{X_3,i+1}(z) \\ & = h_{i+1}(z)\exp(-\int_0^z h_{i+1}(s)ds) = h(z+\Delta i)\exp(-\int_0^z h(s+\Delta i)ds) \\ & = h(z+\Delta i)\exp(-\int_{\Delta i}^{z+\Delta i} h(s)ds) \end{aligned} \tag{7}$$

The cumulative distribution function (cdf) of the severe defective stage and failure can be derived from Eqs. (6) and (7) as:

$$\begin{aligned} F_{X_2,i+1}(y) &= 1-\exp\left(-\int_{\Delta i}^{y+\Delta i}\gamma(s)ds\right) \\ F_{X_3,i+1}(z) &= 1-\exp\left(-\int_{\Delta i}^{z+\Delta i} h(s)ds\right) \end{aligned} \tag{8}$$

3.2. Probabilities of a failure renewal and an inspection renewal

Since the imperfect maintenance is done at the time of the minor defective stage identification by inspection and after the imperfect maintenance, the instantaneous rates of both defective stages and failure change, we should model the probability for a failure renewal and an inspection renewal based on the PAR model.

(1) Probability of imperfect maintenance due to the identification of the minor defective stage

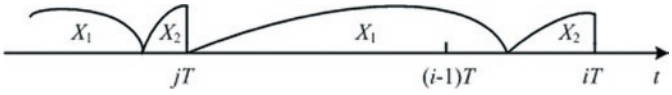

Fig. 2. An imperfect maintenance at iT since the minor defective stage is identified, and the last imperfect maintenance occurs at $t_j = jT$

The minor defective stage is identified at iT and the last imperfect maintenance at t_j when the system restarts the three-stage failure process, as shown in Fig. 2. It leads from assumption (3) that inspection is perfect, the duration of the normal stage is within $(i-j-1)T$ and $(i-j)T$. The minor defective stage is more than $(i-j)T-x$, where x is the duration of the normal stage. Accordingly, the probability of identifying the minor defective stage at iT since the last imperfect maintenance at jT is given as:

$$\begin{aligned} & P(T_{pm} = iT \,|\, \text{since the last imperfect maintenance at } jT) \\ & = P((i-j-1)T < x < (i-j)T, y > (i-j)T - x) \\ & = \int_{(i-j-1)T}^{(i-j)T} f_{X_1,j+1}(x)(1-F_{X_2,j+1}((i-j)T-x))dx \end{aligned} \tag{9}$$

Summing over all possibilities in Eq. (9) for the last imperfect maintenance, namely $j = 0,\ldots i-1$, we have the probability of the minor defective stage identified at iT, $P_m(iT)$, is given as:

$$\begin{aligned} & P_m(iT) \\ & = \sum_{j=0}^{i-1} P_m(jT)P(T_{pm} = iT \,|\, \text{since the lat imperfect maintenance at } jT) \\ & = \sum_{j=0}^{i-1} P_m(jT)\int_{(i-j-1)T}^{(i-j)T} f_{X_1,j+1}(x)(1-F_{X_2,j+1}((i-j)T-x))dx \end{aligned} \tag{10}$$

where $P_m(0)=1$, $j=0$ means there is no imperfect maintenance before renewal, $i=1,\ldots$.

(2) Probability of a failure renewal

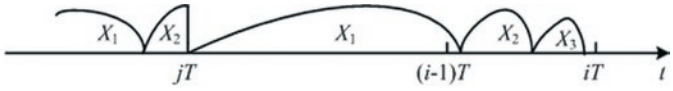

Fig. 3. The system fails in ((i-1)T, iT) since the last imperfect maintenance at jT

If a failure occurs at $T_f, T_f \in ((i-1)T, iT)$ since the last imperfect maintenance at jT, the system is renewed immediately according to assumption (7). Since it is assumed that inspection is perfect to identify the state of the system, the minor defective stage has been ended within $((i-1)T, iT)$ before a failure, as shown in Fig. 3. Similar to the derivation of Eq. (9), the probability of a failure renewal since the last imperfect maintenance at jT is given by:

$$\begin{aligned} & P((i-1)T < T_f < iT \,|\, \text{since the last imperfect maintenance at } jT) \\ & = P((i-j-1)T < x < (i-j)T, 0 < y < (i-j)T - x, 0 < z < (i-j)T - x - y) \\ & = \int_{(i-j-1)T}^{(i-j)T} f_{X_1,j+1}(x)\int_0^{(i-j)T-x} f_{X_2,j+1}(y)F_{X_3,j+1}((i-j)T-x-y)dydx \end{aligned} \tag{11}$$

Then the probability of a failure renewal in $((i-1)T, iT)$, $P_f((i-1)T, iT)$ is given as:

$$\begin{aligned} & P_f((i-1)T, iT) \\ & = \sum_{j=0}^{i-1} P_m(jT)P((i-1)T < T_f < iT \,|\, \text{since the last imperfect maintenance at } jT) \\ & = \sum_{j=0}^{i-1} P_m(jT)\int_{(i-j-1)T}^{(i-j)T} f_{X_1,j+1}(x)\int_0^{(i-j)T-x} f_{X_2,j+1}(y)F_{X_3,j+1}((i-j)T-x-y)dydx \end{aligned} \tag{12}$$

The pdf of a failure in $((i-1)T+z, (i-1)T+z+dz)$, $z \in (0,T)$ can be derived from Eq. (12) as:

$$
\begin{aligned}
&P_f((i-1)T+z,(i-1)T+z+dz)/dz \\
&=\sum_{j=0}^{i-1}P_m(jT)P((i-1)T+z<T_f<(i-1)T+z+dz)/dz \\
&=\sum_{j=0}^{i-1}P_m(jT)\int_{(i-j-1)T}^{(i-j-1)T+z}f_{X_1,j+1}(x)\int_0^{(i-j-1)T+z-x}f_{X_2,j+1}(y)f_{X_3}((i-j-1)T+z-x-y)dydx
\end{aligned}
\tag{13}
$$

(3) Probability of an inspection renewal

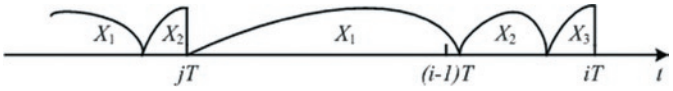

Fig. 4. The system is replaced at the time of the severe defective stage identification iT since the last imperfect maintenance at jT

If inspection detects the system being in the severe defective stage at iT since the last imperfect maintenance at jT, then from assumption (3), the minor defective stage must end within the interval $((i\text{-}1)T, iT)$, as shown in Fig. 4. Then we have the probability of an inspection renewal due to identifying the severe defective stage at iT under the condition that the last imperfect maintenance is carried out at jT.

$$
\begin{aligned}
&P(T_{ps}=iT\,|\,\text{since the last imperfect maintenance at } jT) \\
&=P((i-j-1)T<x<(i-j)T,0<y<(i-j)T-x,z>(i-j)T-x-y) \\
&=\int_{(i-j-1)T}^{(i-j)T}f_{X_1,j+1}(x)\int_0^{(i-j)T-x}f_{X_2,j+1}(y)(1-F_{X_3,j+1}((i-j)T-x-y))dydx
\end{aligned}
\tag{14}
$$

Since the time of the last imperfect maintenance jT may range from 0 to $(i\text{-}1)T$, using Eq. (14), the probability of an inspection renewal at iT, $P_s(iT)$, is formulated as:

$$
\begin{aligned}
&P_s(iT) \\
&=\sum_{j=0}^{i-1}P_m(jT)P(T_{ps}=iT\,|\,\text{since the last imperfect maintenance at } jT) \\
&=\sum_{j=0}^{i-1}P_m(jT)\int_{(i-j-1)T}^{(i-j)T}f_{X_1,j+1}(x)\int_0^{(i-j)T-x}f_{X_2,j+1}(y)(1-F_{X_3,j+1}((i-j)T-x-y))dydx
\end{aligned}
\tag{15}
$$

4. The Cost model

In order to calculate the expected cost per unit time using the renewal theorem, the expected renewal cycle cost and length need to be formulated based on the renewal probabilities, shown as Eqs. (12) and (15), and the cost parameters for inspection, imperfect maintenance and replacement.

4.1. The expected renewal cycle cost $EC(T)$

(1) If the system is renewed due to a failure at $T_f, T_f \in ((i-1)T, iT)$, the cost of a failure renewal cycle includes the cost of inspection, failure replacement and the imperfect maintenance previously and the cost caused by imperfect maintenance can be formulated by summing up all the possibilities before iT. Therefore, the cost of such an event is:

$$
(i-1)C_s+C_f+\sum_{j=1}^{i-1}P_m(jT)C_{pm} \tag{16}
$$

Considering a failure could fall into any of inspection intervals, according to Eqs. (12) and (16), the expected renewal cycle cost caused by a failure renewal by summing up all the possible realizations of i, $EC_f(T)$, is given as:

$$
\begin{aligned}
&EC_f(T) \\
&=\sum_{i=1}^{\infty}((i-1)C_s+C_f+\sum_{j=1}^{i-1}P_m(jT)C_{pm})P_f((i-1)T,iT) \\
&=\sum_{i=1}^{\infty}((i-1)C_s+C_f+\sum_{j=1}^{i-1}P_m(jT)C_{pm})(\sum_{j=1}^{i-1}P_m(jT)P((i-1)T<T_f<iT)) \\
&=\sum_{i=1}^{\infty}((i-1)C_s+C_f+\sum_{j=1}^{i-1}P_m(jT)C_{pm})\left[\sum_{j=1}^{i-1}P_m(jT)\int_{(i-j-1)T}^{(i-j)T}f_{X_1,j+1}(x)\int_0^{(i-j)T-x}f_{X_2,j+1}(y)\right. \\
&\qquad\left.F_{X_3,j+1}((i-j)T-x-y)dydx\right]
\end{aligned}
\tag{17}
$$

(2) If the severe defective stage is detected at an inspection iT, using the similar way as Eq. (16), the corresponding cost is given by:

$$iC_s + C_{ps} + \sum_{j=1}^{i-1} P_m(jT)C_{pm} \tag{18}$$

According to Eqs. (15) and (18), the expected renewal cycle cost caused by an inspection renewal by summing up all the possible realizations of i, $EC_s(T)$ is expressed as:

$$\begin{aligned} EC_s(T) &= \sum_{i=1}^{\infty}(iC_s + C_{ps} + \sum_{j=1}^{i-1} P_m(jT)C_{pm})P_s(iT) \\ &= \sum_{i=1}^{\infty}(iC_s + C_{ps} + \sum_{j=1}^{i-1} P_m(jT)C_{pm}) \\ &\left[\sum_{j=1}^{i-1} P_m(jT)P(T_{ps} = iT \,|\, \text{since the last imperfect maintenance at } jT)\right] \\ &= \sum_{i=1}^{\infty}(iC_s + C_{ps} + \sum_{j=1}^{i-1} P_m(jT)C_{pm})\left[\begin{array}{c}\sum_{j=1}^{i-1} P_m(jT)\int_{(i-j-1)T}^{(i-j)T} f_{X_1,j+1}(x)\int_0^{(i-j)T-x} f_{X_2,j+1}(y) \\ (1 - F_{X_3,j+1}((i-j)T - x - y))dydx\end{array}\right] \end{aligned} \tag{19}$$

4.2. The expected renewal cycle length *EL*(*T*)

Based on the pdf of a failure in ((*i*-1)*T*+z, (*i*-1)*T*+z+*dz*) shown in Eq. (13), the expected renewal cycle length caused by a failure renewal, $EL_f(T)$, is formulated as:

$$\begin{aligned} EL_f(T) &= \sum_{i=1}^{\infty}\int_0^T ((i-1)T + z)P_f((i-1)T + z, (i-1)T + z + dz) \\ &= \sum_{i=1}^{\infty}\int_0^T ((i-1)T + z)\sum_{j=1}^{i-1} P_m(jT)P((i-1)T + z < T_f < (i-1)T + z + dz) \\ &= \sum_{i=1}^{\infty}\int_0^T ((i-1)T + z)\left[\begin{array}{c}\sum_{j=1}^{i-1} P_m(jT)\int_{(i-j-1)T}^{(i-j-1)T+z} f_{X_1,j+1}(x)\int_0^{(i-j-1)T+z-x} f_{X_2,j+1}(y) \\ f_{X_3}((i-j-1)T + z - x - y)dydx\end{array}\right]dz \end{aligned} \tag{20}$$

The expected renewal cycle length caused by an inspection renewal, $EL_s(T)$, is given as:

$$\begin{aligned} EL_s(T) &= \sum_{i=1}^{\infty} iTP_s(iT) \\ &= \sum_{i=1}^{\infty} iT\sum_{j=1}^{i-1} P_m(jT)P(T_{ps} = iT \,|\, \text{since the last imperfect maintenance at } jT) \\ &= \sum_{i=1}^{\infty} iT\left[\begin{array}{c}\sum_{j=1}^{i-1} P_m(jT)\int_{(i-j-1)T}^{(i-j)T} f_{X_1,i+1}(x)\int_0^{(i-j)T-x} f_{X_2,i+1}(y) \\ (1 - F_{X_3,i+1}((i-j)T - x - y))dydx\end{array}\right] \end{aligned} \tag{21}$$

4.3. The expected cost per unit time

Based on the expected cycle cost and length for a failure renewal and an inspection renewal, the expected cost per unit time taking the inspection interval T as a decision variable can be calculated using the renewal reward theorem [11], shown as:

$$C(T) = \frac{EC(T)}{EL(T)} = \frac{EC_f(T) + EC_s(T)}{EL_f(T) + EL_s(T)} \tag{22}$$

5. Numerical example

In this section a numerical example is presented to show the application of the proposed model to minimize the expected cost per unit time and find the optimal inspection interval. Since the Weibull distribution is one of the most commonly used distributions in reliability [16], this paper assumes that these three stages in the failure process follow Weibull distributions with a non-decreasing failure rate. The occurrence rate of the minor defective stage, the severe defective stage and failure with Weibull distribution is given by:

$$\lambda(x;a,b)=\begin{Bmatrix} a\cdot b(b\cdot x)^{a-1} & x\geq 0 \\ 0 & x<0 \end{Bmatrix} \quad (23)$$

Since we cannot have the complete experimental data at present, the distribution parameters for these stages are assumed in Table 1. The cost parameters used in the cost model are shown in Table 2.

Table 1. Distribution parameters

a_1	b_1	a_2	b_2	a_3	b_3
2	0.5	2	0.333	2	0.25

Table 2. Cost parameters values

C_s	C_{pm}	C_{ps}	C_f
100	500	800	2000

Fig. 5 shows the expected renewal cycle cost with different values of T using Eqs. (17) and (19). It can be seen that the renewal cycle cost decreases firstly and then increases as T increases, finally turning to be relatively stable. It is due to that when the inspection interval is small, the expected renewal cycle cost is high because of the frequent inspection. However, once the inspection interval exceeds the expected failure time, failure occurs more easily and changing the inspection interval will not affect the failure process such that the expected renewal cycle cost will tend to be constant. Moreover, in order to study the effect of imperfect maintenance on the expected renewal cycle cost, three different values of ρ is selected. One is ρ=1 which means the maintenance at the minor defective stage identification is perfect and the other two values ρ=0.9 and ρ=0.8 imply the imperfect maintenance. From Fig. 5, it is noted that the expected renewal cycle cost rises with the increase of ρ which shows that imperfect maintenance will decrease the expected renewal cycle cost and the smaller the value of ρ, the smaller the expected renewal cycle cost.

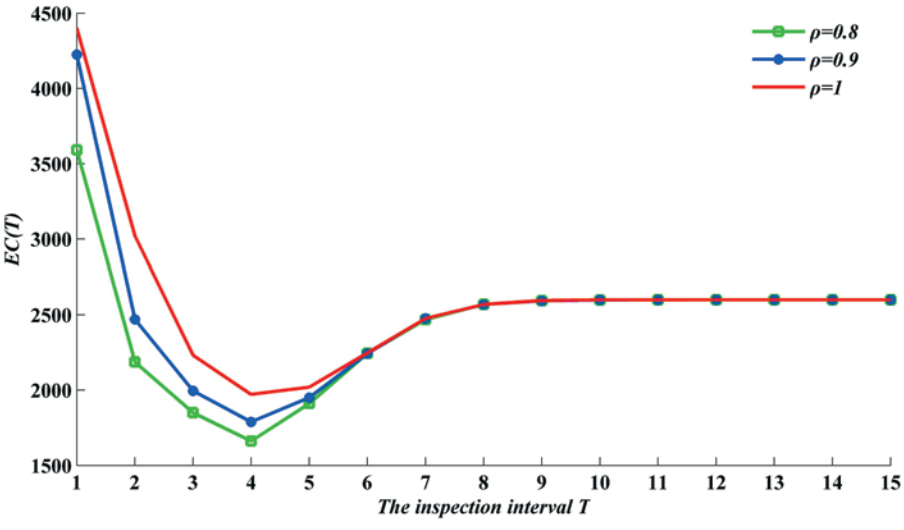

Fig. 5. The relationship between T and EC(T)

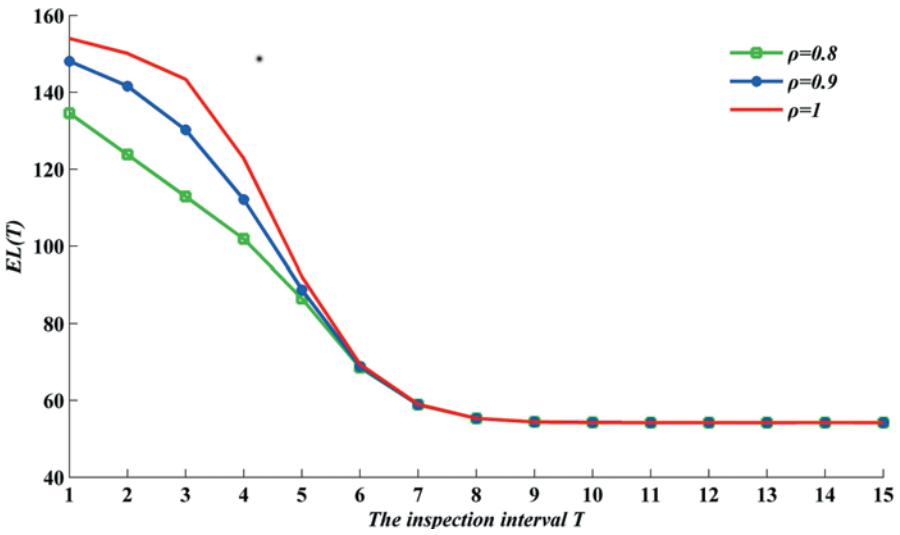

Fig.6. The relationship between T and EL(T)

Fig. 6 shows the expected renewal cycle length in terms of different values of T using Eqs. (20) and (21). We can see that the expected renewal cycle length decreases monotonically and finally turns to be relatively stable. It can be explained that once the inspection interval excesses the expected failure time, the failure must occur before inspection such that the expected renewal cycle length is constant. Moreover, the expected renewal cycle length also decreases with the reduction of ρ and the smaller value of ρ, the smaller the cycle length.

Fig.7 shows the expected cost per unit time in terms of the inspection interval under different values of ρ using Eq. (22). From the results in Fig.7, it can be seen that with the increase of the inspection interval, the expected cost per unit time firstly reduces and then increases. It is what we expected that the smaller inspection interval will lead to the frequent inspections with more inspection cost and if the inspection interval exceeds the expected failure time, a failure renewal is required such that the expected cost per unit time tends to be constant. Also for three scenarios of ρ in Fig.7, the trend of expected cost per unit time with different improve factors is same. It is confirmed that the smaller the value of ρ, the larger the expected cost per unit time. It is because that decreasing the value of ρ will decrease the expected cost and length simultaneously, but the expected renewal length falls faster. For the given parameters of distribution and cost, it can be seen from Fig.7 that the optimal inspection interval T^*=3 is same although the improve factor is different. The optimal expected cost per unit time is 12.9009, 14.9409 and 17.9949 respectively when the improve factor is 1, 0.9 and 0.8. Therefore, the optimal inspection interval T^*=3 with

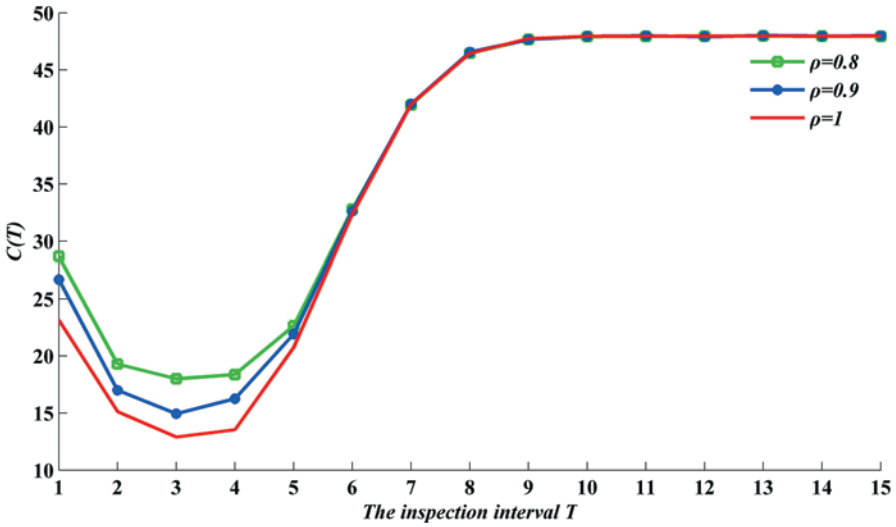

Fig. 7. The expected cost per unit time in terms of the inspection interval T

the minimal expected cost per unit time can be adopted to implement inspection and maintenance activities.

6. Conclusions

In this paper, an inspection optimization model is proposed based on a three-stage failure stage to optimize the inspection interval of bearings by minimizing the expected cost per unit time. The three states before failure using the concept of the three-stage failure process correspond to the three color scheme of bearings by SPM technique. The maintenance at the minor defective stage is regarded as imperfect maintenance, which will affect the instantaneous rates of the minor defective stage, the severe defective stage and failure. The maintenance at the severe defective stage and failure can be viewed as perfect maintenance. The proportional age reduction model is used to model the effect of imperfect maintenance at the minor defective stage identification. The results from the numerical example show that the optimal inspection interval can be found using the proposed model. Moreover, imperfect maintenance will decrease the expected renewal cycle cost and length but increase the expected cost per unit time.

Further research along this line can be developed such as: (1) considering a finite time horizon, (2) considering the availability of spare parts, and (3) case studies need to be implemented to validate the model. These issues will be researched in the future.

Acknowledgments

The research report here was partially supported by the NSFC under grant numbers 71420107023, 71231001 and 71301009, the Fundamental Research Funds for the Central Universities of China under grant numbers FRF-MP-13-009A and FRF-TP-13-026A, and by the MOE PhD supervisor fund, 20120006110025.

References

1. Bartholomew M, Christianson B, Zuo MJ. Optimizing preventive maintenance models. Computational Optimization and Applications 2006; 35(2): 261–279, http://dx.doi.org/10.1007/s10589-006-6449-x.
2. Christer AH. Innovative decision making. In Proceedings of the NATO Conference on the Role and Effectiveness of Theories of Decision in Practice. Hodder and Stoughton, 1976: 368–377.
3. Das AN, Sarmah SP. Preventive replacement models: an overview and their application in process industries. European Journal of Industrial Engineering 2010; 4(3):280–307, http://dx.doi.org/10.1504/EJIE.2010.033332.
4. Hu HJ, Cheng GX, Li Y, Tang YP. Risk-based maintenance strategy and its applications in a petrochemical reforming reaction system. Journal of Loss Prevention in the Process Industries 2009; 22: 392–397, http://dx.doi.org/10.1016/j.jlp.2009.02.001.
5. Jones B, Jenkinson I, Wang J. Methodology of using delay time analysis for a manufacturing industry. Reliability Engineering and System Safety 2009; 94: 111–24, http://dx.doi.org/10.1016/j.ress.2007.12.005,
6. Li Z, He ZJ, Zi YY, Chen XF. Bearing condition monitoring based on shock pulse method and improved redundant lifting scheme. Mathematics and Computers in Simulation 2008; 79: 318-338, http://dx.doi.org/10.1016/j.matcom.2007.12.004.
7. Masaru F, Minoru K. SPM shock pulse method for diagnostic system of rotating roll bearing. Japan Tappi Journal 2003; 57(4): 52-57.
8. Nicola RP and Dekker R. Optimal maintenance of multi-component systems: a review. In: Murthy DNP, Kobbacy AKS, editors. Complex system maintenance handbook. Amsterdam: Springer; 2008, http://dx.doi.org/10.1007/978-1-84800-011-7_11.
9. Pierskalla WP, Voelker JA. A survey of maintenance models: the control and surveillance of deteriorating systems. Naval Research Logistics Quarterly 2006; 23: 353–388, http://dx.doi.org/10.1002/nav.3800230302.
10. Robert BR, Jerome A. Rolling element bearing diagnostics—A tutorial. Mechanical Systems and Signal Processing 2011; 25: 485–520, http://dx.doi.org/10.1016/j.ymssp.2010.07.01.
11. Ross SM. Introduction to Probability Models. USA: Elsevier, 2007.
12. Tandon N, Yadava GS, Ramakrishna KM. A comparison of some condition monitoring techniques for the detection of defect in induction motor ball bearings. Mechanical Systems and Signal Processing 2007; 21: 244–256, http://dx.doi.org/10.1016/j.ymssp.2005.08.005.
13. Wang HZ. A survey of maintenance policies of deteriorating systems. European Journal of Operational Research 2002; 139: 469–489, http://dx.doi.org/10.1016/S0377-2217(01)00197-.
14. Wang L, Hu HJ, Wang YQ, Wu W, He PF. The availability model and parameters estimation method for the delay time model with imperfect maintenance at inspection. Applied mathematical modelling 2011; 35: 2855-2863, http://dx.doi.org/10.1016/j.apm.2010.11.070.
15. Wang W. A delay time based approach for risk analysis of maintenance activities. Journal of the Safety and Reliability Society 2003; 23(1): 103–113.
16. Wang W. An inspection model based on a three-stage failure process. Reliability Engineering and System Safety 2011; 96(7): 838–848, http://dx.doi.org/10.1016/j.ress.2011.03.003.

17. Wang W. An inspection model for a process with two types of inspections and repairs. Reliability Engineering and System Safety 2009; 94: 526–533, http://dx.doi.org/10.1016/j.ress.2008.06.010.
18. Wang W. An overview of the recent advances in delay-time-based maintenance modelling. Reliability Engineering and System Safety 2012; 106: 165–178, http://dx.doi.org/10.1016/j.ress.2012.04.004.
19. Wang W. Delay time modelling. In Complex System Maintenance Handbook. 2008; London, Springer: 345–370, http://dx.doi.org/10.1007/978-1-84800-011-7_1.
20. Wang W. Delay time modelling for optimized inspection intervals of production plant. Handbook of Maintenance Management and Engineering. 2009; London, Springer: 479–498.
21. Wang W. Models of inspection, routine service, and replacement for a serviceable one-component system. Reliability Engineering and System Safety 2013; 116: 57–63, http://dx.doi.org/10.1016/j.ress.2013.03.006.
22. Wang W, Banjevic D, Pecht MG. A multi-component and multi-failure mode inspection model based on the delay time concept. Reliability Engineering and System Safety 2010; 95(8): 912–920, http://dx.doi.org/10.1016/j.ress.2010.04.004.
23. Wang W, Zhao F, Peng R. A preventive maintenance model with a two-level inspection policy based on a three-stage failure process. Reliability Engineering and System Safety 2014; 121: 207–220, http://dx.doi.org/10.1016/j.ress.2013.08.007.

Ruifeng YANG
Mechanical Engineering College
Six xi, Heping West Road Number 97
Shijiazhuang, 050003, Hebei province, China

Fei ZHAO
Northeastern University at Qinhuangdao
No.143, Taishan Road, Economic and Technological Development Zone
Qinhhuangdao, 066004, Hebei province, China

Jianshe KANG
Haiping LI
Mechanical Engineering College
Six xi, Heping West Road Number 97
Shijiazhuang, 050003, Hebei province, China

Hongzhi TENG
Mechanical Engineering College
Six xi, Heping West Road Number 97
Shijiazhuang, 050003, Hebei province, China

E-mail: rfyangphm@163.com, Zhaofei.19841027@163.com,
jskang201206@126.com, hp_li0929@163.com, tenghzh@163.com

Article citation info:
WERBIŃSKA-WOJCIECHOWSKA S, ZAJĄC P. Use of delay-time concept in modelling process of technical and logistics systems maintenance performance. Case study. Eksploatacja i Niezawodnosc – Maintenance and Reliability 2015; 17 (2): 174–185, http://dx.doi.org/10.17531/ein.2015.2.2.

Sylwia WERBIŃSKA-WOJCIECHOWSKA
Paweł ZAJĄC

USE OF DELAY-TIME CONCEPT IN MODELLING PROCESS OF TECHNICAL AND LOGISTICS SYSTEMS MAINTENANCE PERFORMANCE. CASE STUDY

ZASTOSOWANIE KONCEPCJI OPÓŹNIEŃ CZASOWYCH W PROCESIE MODELOWANIA UTRZYMANIA W STANIE ZDATNOŚCI SYSTEMÓW TECHNICZNYCH I LOGISTYCZNYCH. STUDIUM PRZYPADKU*

Article presents an overview of some recent developments in the area of modelling of technical systems' maintenance decisions with the use of delay-time concept. Thus, the literature overview from 1984-2012 in the analysed research area is given. Next, there is characterised the implementation algorithm for delay time analysis use in the area of logistic systems maintenance performance. Later, the example of methodology of using delay-time analysis implementation in the area of logistic system of ten forklifts performance analysis is investigated.

***Keywords**: delay-time concept, maintenance, logistic system.*

W artykule przedstawiono zagadnienia związane z modelowaniem utrzymania systemów logistycznych w stanie zdatności z wykorzystaniem koncepcji opóźnień czasowych. Przedstawiono przegląd literatury z badanego obszaru obejmujący okres 1984-2012. Następnie został omówiony algorytm postępowania w procesie implementacji koncepcji opóźnień czasowych w obszarze utrzymania w stanie zdatności systemów logistycznych. W ostatnim punkcie, został przedstawiony przykład zastosowania opracowanej metodyki do oceny niezawodności i oczekiwanych kosztów obsługiwania dziesięciu wózków widłowych funkcjonujących w wybranym systemie.

***Słowa kluczowe**: koncepcja opóźnień czasowych, utrzymanie zdatności, system logistyczny.*

Symbols used in the paper

c_b – expected cost of repair
c_{con} – the expected consequence costs for the supported system and its environment caused by failure occurrence in logistics system
c_i – cost of inspection action performance
c_{ir} – expected repair costs during the implementation of inspections
$C(T)$ – function of the expected maintenance costs of a system
$C_C(T)$ – function of the expected consequences costs for the supported system and its environment
C_{utrz} – the total expected maintenance costs of a system in one inspection cycle
d – time of inspection action performance
d_b – random time of system downtime caused by its failure
$E_d(T)$ – function of system expected downtime
$\mathrm{E}(h)$ – expected value of delay time
$F(T)$ – cumulative distribution function of the time between failures of a system
$f(T)$ – probability density function of the time between failures of a system
$f_1(T)$ – probability density function of the time to the first failure
$F_h(h)$ – cumulative distribution function of the random variable delay time h
$f_h(h)$ – probability density function of the random variable delay time h
h – random variable for delay time
k – constant intensity of system failures occurrence
$MTBF$ – Mean Time Between Failures
$MTTR$ – Mean Time To Repair
$P_b(T)$ – function for system downstate probability
$R(T)$ – system reliability function
T – the time between system consecutive inspection actions performance
T_{opt} – the optimal time between system consecutive inspection actions performance

1. Introduction

Effective performance of logistics systems/networks and supply chains requires a proper definition of e.g. time relations which occur between the system's facilities and its processes. This issue has gained particular importance over the last 30 years. On the one hand, this is connected with the increased awareness of managers regarding the need to control the operating costs of technical systems and the logistics systems that support them. On the other hand, the increased availability of methods and tools to support the modelling process provides the opportunity to study and solve new problems within the analysed scientific area [87].

The problem of time delays is typical for many physical or technical systems, and has been raised e.g. in biology, mechanics and economics [38]. Time in logistic systems is traditionally seen with respect to [10]:

(*) Tekst artykułu w polskiej wersji językowej dostępny w elektronicznym wydaniu kwartalnika na stronie ***www.ein.org.pl***

- execution time of (internal and external) placed customer's order - specifying the time between the moment the order has been placed by the customer and its completion. In this case, the concept of time is relative to the level of supported enterprise performance as perceived by the customer,
- resource efficiency in the basic processes of the supported enterprise. For instance, in the case of manufacturing systems, the concept of time is directly related to minimizing downtime and optimizing capacity utilization,
- duration of various fundamental processes, covering the period from the time when all resources necessary to perform the process are ready for use, until the moment the result of the process has been achieved. The concept of time directly depends on the thorough identification of the process structure.

Therefore, accurate determination of the time relations in the logistic system will depend e.g. on the type of the modelled system (storage, transport, etc.), the type of operating task, the definition of the efficiency type that is essential in the system (e.g. whether one is interested in the system's efficiency within a certain time horizon), and the behaviour of the system during its downtime (whether a single failure should affect the reliability of the whole system). The basic classification of system models with a time resource, taking into account the above features, has been presented e.g. in [88, 89].

The article focuses on the issues associated with the maintenance modelling of logistics systems using *Delay Time Analysis* approach, with particular emphasis on the methodology applying the concept of delay time in practice. The second part of the article focuses on the analysis of an internal transport system of a manufacturing company in the metallurgical sector. The proposed methodology was used to assess the reliability and the expected maintenance costs of the operating forklifts.

2. Modelling of technical and logistical systems maintenance processes using delay time analysis

The papers published over the last 50 years cover a wide range of problems in the area of modelling and design of maintenance processes in technical facilities (maintenance theory). Issues often discussed in the literature regard the areas of reliability modelling or necessary supplies providing for operational processes performance of e.g. production and transportation systems (e.g. works [6, 46, 47, 65, 72, 75, 76]), or the uncertainty of operating data (e.g. works [7, 57, 93]). A basic overview of these research works was presented in one of the first articles – [62], and later developed and extended by the authors Valdez-Flores & Feldman in [74]. The importance of the tasks related to the analysed research area as well as its diversity is supported by many studies (e.g. [18, 52, 53, 54, 55, 61, 69, 77]), where the authors provide an overview of basic models of selecting an optimal maintenance strategy for both single- and multi-element systems. At the same time, papers focused to the issue of maintaining single-element systems have been analysed e.g. in [5, 36, 69, 77], and those focused on the optimization of operation processes of multi-element systems are given e.g. in [18, 34, 55, 59, 67, 71].

One of the basic tasks associated with technical systems maintenance involves inspection process implementation [18, 62]. In this area it is possible to use the delay-time concept, enabling the modelling of the consequences of the Inspection Policy implementation for technical facilities performance [23].

The presented approach, used to this day in the renewal processes theory in order to optimize the technical systems downtime caused by undetected failure (optimization of time period between consecutive inspection actions performance), has been the subject of analysis since the 1970s, e.g. by authors Christer, Waller and Whitelaw (e.g. [22, 23, 28, 29, 30, 32]). In this concept, it is assumed that the system/component failure does not occur suddenly, but is preceded by certain symptoms indicative of future damage [24]. The time between the moment u, where the first detectable signals of the forthcoming failure appear, and the moment the system is failed is called the time delay and is denoted by h [21, 24]. This issue has been investigated e.g. in the papers [43, 44, 58].

Known in the literature delay-time models can be classified into two main groups [81]:

- models for single-element systems and models for complex systems, treated as a single technical facility,
- models for multi-element systems.

This topic has been widely studied in literature, e.g. in [2, 8, 19, 20, 21, 24, 25, 48, 58, 64, 77, 78], where reviews of the literature in the area of applying the delay time concept are given, and in [43, 44, 58, 86], where attention was paid to the possibilities of using of delay time models in multi-element systems performance.

One of the first papers focused on modelling the time delay in single-element systems is [27]. In this paper, the author analyses the decision-making process of system maintenance (item replacement) based on a survey research implementation. Furthermore, in this area the authors analysed e.g. systems reliability issues (e.g. papers [4, 16, 22, 41, 94]), time delay parameter estimation problems (e.g. paper [9]), risk analyses (e.g. [82]), the implementation of semi-Markov processes (e.g. [31]), or system safety issues (e.g. [84]).

The basic delay time model for multi-element systems was presented e.g. in the papers [24, 29, 30, 82]. The basic assumptions of the model include a perfect inspection performance, independence of the operating system components, Poisson process of defects occurrence in the system, known $f_h(h)$ function, and a fixed period of inspection process d. For such assumptions, it is possible to determine the system failure probability $P_b(T)$, or a function of the expected system downtime $E_d(T)$.

Development of the mentioned model includes e.g. the assumption of a non-perfect inspection performance (e.g. [14, 21, 79, 80]) or a non-Poisson process of defect appearance in the system (e.g. [3]). Moreover, the problem of model parameters estimation has been presented (e.g. [21, 80, 81, 85]).

3. Methodology of delay time concept use in the modelling of technical and logistics systems maintenance processes performance

Literature provides many papers devoted to the application of the concept of time delays in the real-life systems performance. The main areas of model application include e.g. the production systems performance (e.g. [1, 45]), failure processes of gearboxes (e.g. [49]), modelling operation processes of: vehicle fleets (e.g. [28, 35, 40, 68]), fishing vessels (e.g. [63]) or medical equipment (e.g. [26]). An important area of potential application of the presented approach is the logistics systems performance.

The basic functions of logistics include effective and efficient management of: the flow of resources and storage of goods (raw materials, semi-finished and finished goods) and services, from their sources of origin to the place of consumption, and the information associated with the material flow in order to meet the needs and requirements of customers [91]. Therefore, in the area of business logistics, efficiency of logistics processes of actors participating in the logistics chain is based on maintaining a balance between: the increasing demand for basic and support resources, the shorter duration of the logistic tasks, and control of the costs throughout the entire chain [11, 90, 91], based on the three main logistics pillars given e.g. in [56].

At the same time, the problems of logistics can also be defined in the area of operation of technical systems [88]. Based on the basic literature on logistics engineering (e.g. [12, 13, 17]), using a systemic approach in logistics, there can be defined the logistical support sys-

tem, which according to [12, 17] is defined as *purposely organized technical system's subsystem to support its primary (operational) process performance through the integration of all activities associated with the effective and beneficial flows of material resources and the necessary information, and providing necessary for this process logistics resources (supporting equipment and control and measurement equipment)*. The presented definition refers on the one hand, to the life cycle of the system, on the other, includes both business logistics and military logistics characteristics.

The logistical considerations can be divided into two basic concepts of logistic support system reliability: upstate and its downstate, which can lead to e.g. [50]:

- disrupting or even preventing the execution of the current logistic task,
- inability to undertake new logistic tasks.

Taking into account the downstate of the support system, there should be defined a new perspective of the efficient and effective performance of the supported system, which requires analysing the logistics system inability for specific tasks performance, under certain conditions and at certain times, when a logistic request is randomly occurred in the system.

The available literature on reliability theory provides a number of papers on the subject of modelling and assessing the logistics systems performance, designed to support technical facilities that are subject to maintenance processes implementation. The developed models, however, are primarily limited to the analysis of the supply process providing the technical system with the necessary spare parts (e.g. [15]), taking into account the problem of ensuring the necessary number of repairmen and multi-echelon issues (e.g. [37, 66, 70]), without investigating the impact of the operation of other logistics elements on the supported system's reliability, dependability or availability.

Other aspects of the analysed research area, which require further analysis, regard to e.g. the area of assessment of the supply sources, inventory management problems, consideration of the storage limitations, and integration of logistic tasks with the objectives of the technical facilities maintenance strategy [51].

At the same time, over the last twenty years there has been observable an increase in interest in the issues of time management and analysis of the time relations observed in technical systems/facilities, including those involved in logistics. A review of the fundamental research issues related to the modelling of time relations in logistic chains are presented e.g. in [60].

Following this considerations and taking into account the complexity of the logistic support systems, proper modelling of their operation can be based on the delay time concept implementation. In this case, effective development of a logistics system performance model requires using appropriate methodology [45].

This problem is analysed e.g. in the paper [63], which presents an algorithm of applying the delay time concept in the operation of complex systems. Then, in [83], the authors proposed a modelling algorithm for inspection processes in multi-element systems performance, where the process of defects occurrence is of the NHPP type. Methodology of modelling time delays in production systems was discussed in [45]. The authors proposed an algorithm of maintenance optimization for the case of complex systems, which supplements the estimation of expected maintenance costs and model of expected period of downstate with the so-called model for assessing the consequences of failure (*environmental model*), which defines the effect of a malfunction of the production machine in a manufacturing company (e.g. production downtime).

The methodology of modelling the technical systems maintenance processes including the delay time concept when using the Monte Carlo simulation techniques were developed in [33]. The authors have proposed algorithms for the case of perfect/imperfect inspection and for the case of imperfect repair.

While developing the methodology for modelling the processes of technical systems maintenance, taking into account the delay time concept, it should be noted that the purpose of the model is usually to minimize the expected duration of system downtime $E_d(T)$, or the expected maintenance costs $C(T)$. At the same time, in the case of logistics systems performance, the impact of their components failures on the level of supported system performance and its environment is also important. The level of this impact can be expressed by the function of the expected logistic support system failure consequences costs $C_C(T)$. On the other hand, further considerations omit the possibility of performing a multi-criteria analysis.

The algorithm for the determination of the optimal time between the inspection actions performance T includes the following steps (Fig. 1) [33, 45, 83]:

- understanding the process of maintaining the selected system (e.g. determining the type of the involved maintenance operation, the relationship between the system's components),
- identifying the problems in the selected system operational process (e.g. long-term repair operations, frequent damage),
- preliminary definition of model assumptions (e.g. single-/multi-element system), specifying the type of operational and diagnostic data that can and should be collected in order to carry out the maintenance optimization,
- data collection and analysis – based on using subjective and objective methods,
- determining the assumptions of the model – based on the data and knowledge about the performed operational processes,
- estimating the basic parameters of the model – for example, functions $f_h(h)$ and $F_h(h)$ for the time delay parameter h, selecting the probability distribution for the time between failures or the repair time,
- defining optimization criteria – depending on the available operational data and model assumptions,
- estimating the function of the optimization criterion, designating the optimal period T,
- determining the relationship between the expected value of the time delay parameter h and the optimal period T – in order to determine whether the delay time concept implementation allows for optimum solution obtainment (more info e.g. in [43, 44]).

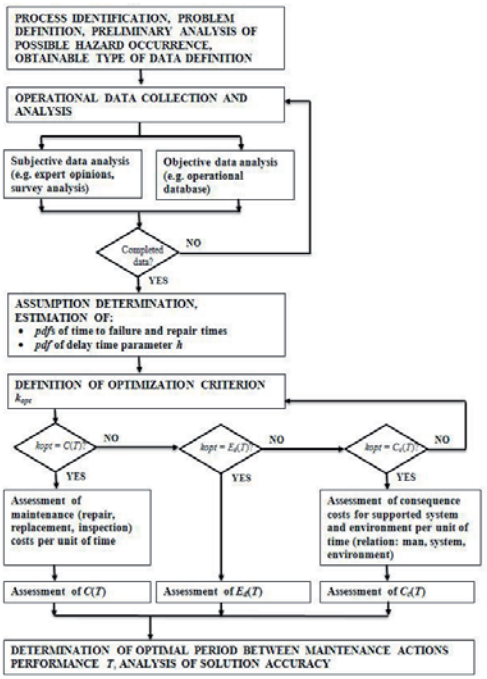

Fig. 1. The algorithm for assessment of optimal period T using the delay time concept. Own contribution based on [33, 45, 83]

One of the important issue is the method of determining the model's criterion functions. The form of the function will depend on the assumptions of the system. For example, in the case of a complex system, one of the basic models of the periodic inspection, based on the use of the delay time concept is the model of technical object periodic inspection presented in [30]. The basic assumptions of this model include:

a) inspections are held at a fixed time T and last d time units,
b) the cost of inspection action performance is c_i units,
c) inspection operations are perfect, which means that all defects that can be detected during the inspection are identified,
d) inspections are carried out independently of each other,
e) failures are independent and occur in the system with a constant intensity k,
f) all defects detected during the inspection operation are removed during the inspection process,
g) system failure lasts a short period of time d_b, compared to periods T and d,
h) the time delay h is independent of the failure intensity and has the known form of the functions $f_h(h)$ and $F_h(h)$.

With taking into account the assumptions defined as above, the function for system downtime probability $P_b(T)$ is given by [30]:

$$P_b(T) = \frac{1}{T}\int_0^T (T-h) f_h(h) dh \tag{1}$$

The expected downtime, defined by the function $E_d(T)$, can be described as follows [30]:

$$E_d(T) = \frac{kTd_b P_b(T) + d}{T + d} \tag{2}$$

At the same time, assuming the expected cost of repair c_b, the expected repair costs during the inspection actions performance c_{ir}, the expected maintenance cost within the period T can be described by the function $C(T)$ in the form [30. 45]:

$$C(T) = \frac{1}{(T+d)}\left\{kT\left[c_b P_b(T) + c_{ir}\left(1 - P_b(T)\right)\right] + c_i\right\} \tag{3}$$

Moreover, the expected consequences costs for the supported system and its environment caused by failure occurrence in logistics system can be presented as follows:

$$C_C(T) = \frac{1}{(T+d)}\left\{kTc_{con} P_b(T)\right\} \tag{4}$$

where: c_{con} – the expected consequence costs for the supported system and its environment caused by failure occurrence in logistics system (e.g. related to the loss of life, degree of damage to the supported system, the delay in the implementation of fundamental processes, etc.)

Simulation model for multi-element systems performance with taking into account delay time concept implementation was developed e.g. in the papers [42, 43, 44].

4. Case study

In order to demonstrate the applicability of the discussed methodology for using the concept of time delays in logistic systems performance, an analysis of a manufacturing company (non-ferrous metal smelter) was carried out. The study focused on the process of operation of forklift trucks, which are used in the manufacturing plant.

The analysed forklift trucks primarily support manufacturing processes performance, take deliveries of materials and support warehouses, where goods are stored after leaving the production line. The most important workplace for forklifts is the production line. A forklift is used in the smelter batch storehouse next to the elevator that supplies the furnace. The operator's task is to take the batch with a forklift from the ramp or the yard (according to the production requirements), insert it into the elevator, which takes the batch to the smelter. The work here is done continuously and remains uninterrupted under a three-shift work. Around 350 tons of feed material is melted during one shift. Two tracks directed to support the production work about 14 mth[1] per one shift. The working conditions are variable, as in the case of taking deliveries. Additionally, forklifts which support production often dispose of liquid material at high temperatures, reaching up to 900°C. In such instances, the temperature inside the cabin rises rapidly to about 65°C.

Another place of forklift work is the unloading ramp, where it takes batches of material delivered by rail and the yard, where supplies delivered by car fleet are stored. 4÷6 forklifts are simultaneously deployed at the railway platform to unload wagons with batches for production, which include 5÷24 metal sheets weighing about 1800 kg each. The daily delivery by rail consists of 19 wagons.

An equivalent workplace for operators working on the railway platform is the yard, where they unload trucks loaded with the same batches as railway wagons. This is where batch weighing about 2500 kg each are delivered. About 300 tons are delivered daily. Work in these areas takes place in variable and severe weather conditions. Forklifts must deal with huge overloads associated with heat, snow and frequent glaze when wheels lips are frequent. The plant is usually dusty. The situation is similar on the loading ramp, which is why forklifts have a triple filtration system and are inspected more frequently.

Apart from the main places of the work, which involve handling production and receiving supplies, forklifts carry out a number of other tasks related to the maintenance of other departments of the plant. For example, their work involves daily supply of departments with technical gases, salts and chemicals, technical materials delivered from storage, necessary for maintaining production, supplying the packing departments with steel tapes and stretch tapes, which are used to pack finished goods.

The data necessary for the reliability analysis performance include the operational and maintenance data of ten electric forklifts of the selected brand, covering the period of operation from January 2000 to February 2013. These data contain the exact information about operational performance of forklifts, durations of repairs and planned maintenance actions, identification of the items replaced and all defects that occurred during that time.

4.1. The operational process of forklifts and analysis of operational data

The routes of forklift movement are variable and depend in particular on the tasks that the forklift performs. The most frequent and regular operations include loading the furnace – production support and reception of supplies. After a short briefing at the beginning of each shift, the operator lists the equipment they collect in the so-called forklift work report. In this report, the operator makes the following entry (operator entry based on the example of forklift truck no. 4 dated

1) 1 motohour (pl. *motogodzina*) (mth) – according to the definition given by the Polish Language Dictionary PWN [39] – an hour of engine operating.
Standard unit of measurement used to assess operational time of lift pallet trucks; among others engine hours counter level is given for periodic maintenance and repair actions performance in the forklift's Maintenance Log, which according to e.g. the Act of Law of 21 December 2000 on technical supervision [73] is an obligatory for owners/users of forklifts since 18th of August, 2003.

29-10-2010): Date of collection: 29-10-2010 Shift: I, mileage at the beginning of shift: 3207 mth, condition of the truck: here, the operator inspects the equipment. If the truck is not failed, they sign the "*Forklift available*"; if not, they describe the malfunction or damage in the place of failure information. They then sign the report in "*Equipment in use*". After making such an entry in the report, the operator goes to their place of work, such as furnace loading place or unloading supplies place. The operator moves around the batch storehouse, the yard and the loading ramp, which are covered with asphalt and concrete. Work on the aforementioned date during first shift lasts from 7.00 a.m. to 3.00 p.m. The daily average limit of moto-hours worked by a forklift in these areas is approximately 7 mth. The operator, who drives back to the department at the end of their shift shall return the equipment, also making an entry in the report: they shall sign "*Equipment return*", enter the amount of work made – in this case 7 mth. At this stage, there should be any comments following the shift regarding the operation of the machine filled in, or if any failures were noted, the operator is required to make the entry in the "*Failure*" box as well. The abovementioned forklift which moves around the described routes and locations travels around 170 mth monthly. It covers as many as 2000 mth per year. During this time, the forklift truck undergoes 20 OT-1 maintenance procedures (every 100 mth), which involve the following steps:

1. purging the entire forklift truck (engine, oil coolers, water coolers),
2. inspection of all fluids,
3. replacing air filters – fuses,
4. lubricating all lubrication points in the forklift,
5. tire control,
6. control of the forklift truck's moving parts (suspension, steering system, elements of the mast and carriage),
7. checking the technical condition of the chains and carriage,
8. visual inspection of the equipment.

In addition, approximately every 500 mth, OT-2 maintenance procedures are performed. Apart from the activities performed within the framework of OT-1, these consist of the following additional steps:

1. replacement of engine oil with the oil filter,
2. replacement of all air filters.

In addition to carrying out the specified maintenance operation, at least once a year, after driving about 1700 mth, the forklift undergoes replacement of hydraulic oil (65 litres) and gear oil (15 litres). Furthermore, the truck uses two sets of front tires and four sets of rear tires. During this time, it also burns about 5500 litres of diesel.

Figures 2 and 3 illustrate the route of forklift trucks when handling the production – loading the smelter and unloading deliveries with melting batches.

Forklift truck working on the production (loading the furnace) works an average of about 6-7 mth within one shift. Maintenance staff who carry out the repair and warranty maintenance of equipment convert 1 moto hour to 100 kilometres.

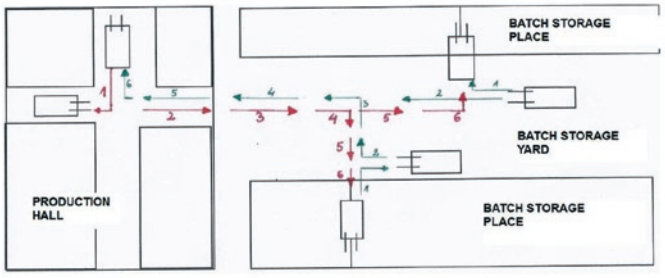

Fig. 2. Diagram of the route of the forklift loading the smelter (red line – driving of forklift for batch taken from batch storage yard, blue line – driving of forklift with batch to the melting furnace)

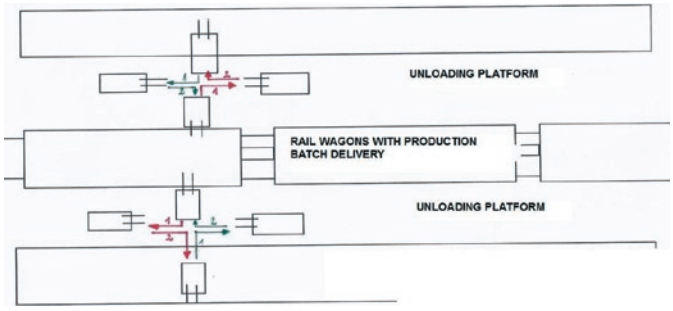

Fig. 3. Diagram of the route of the forklift working in unloading site (red line – driving of forklifts with batch taken from rail wagon to the place of batch storage, blue line – driving of forklifts for batch being on the rail wagon)

There are usually four forklifts working in the unloading site for deliveries on the unloading ramp and yard, and each of them runs approx. 5 mth during each shift.

The non-ferrous metal smelter currently has twelve 4-ton Komatsu forklifts (analysis covered ten trucks). The advantages of this type of forklift include their simple and compact design, easy handling, low failure rate, large, broad and specialized service facilities. In addition, minimal electronics in the trucks, a 5-cylinder drive unit, powered by a simple injection pump with injectors causes makes the truck extremely easy to operate and use, both for the operator and the mechanic.

The electric forklift is a repairable object, i.e. one that is subject to repair following a failure.[2] Reliability analysis of the test objects was carried out on the basis of the maintenance report containing information about mileage, the list of repairs and data of maintenance and repair times. Basic data obtained during the analysis of the forklift operation process has been presented in Table 1.

Table 1. Operational parameters of analysed forklifts

Forklift No.	Mileage (mth)	Number of defects	**MTBF**(h)	**MTTR**(h)
1	3685	97	38.0	5.6
2	3636	82	44.3	6.5
3	5513	100	55.1	6.3
4	7310	107	68.3	6.4
5	1876	26	72.2	5.5
7	3624	79	45.9	6.6
8	2684	51	52.6	7.3
9	4374	89	49.1	7.8
10	4990	50	99.8	6.6
11	5224	67	78.0	6.4

The study of the 10 trucks allowed for the determination of e.g. the time to first failure. The probability distribution of working time to the first failure can be described by the Weibull distribution (Fig. 4). It was also possible to determine the reliability function $R(t)$, Cumulative distribution function $F(t)$, or the probability density function of time to the truck's failure $f(t)$. The data analysis was based on the program Weibull++ v. 6 (ReliaSoft Co., USA) implementation, which allowed e.g. choosing the probability distribution of the random variable for the lifetime. It is a log-normal distribution (Fig. 5).

In the analysed time period, there were 748 defects observable in the systems of the frame and carriage body, electrical installations and equipment, hydraulic system, as well as lifting, drive, steering, and braking systems.

2 As defined in the PNTTE operation dictionary [92]

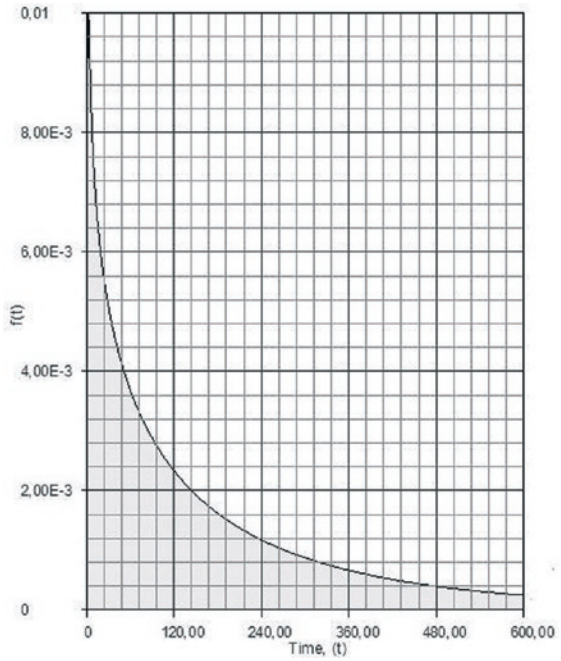

Fig. 4. Function f1(t) of the density of the probability distribution of the time to the first failure

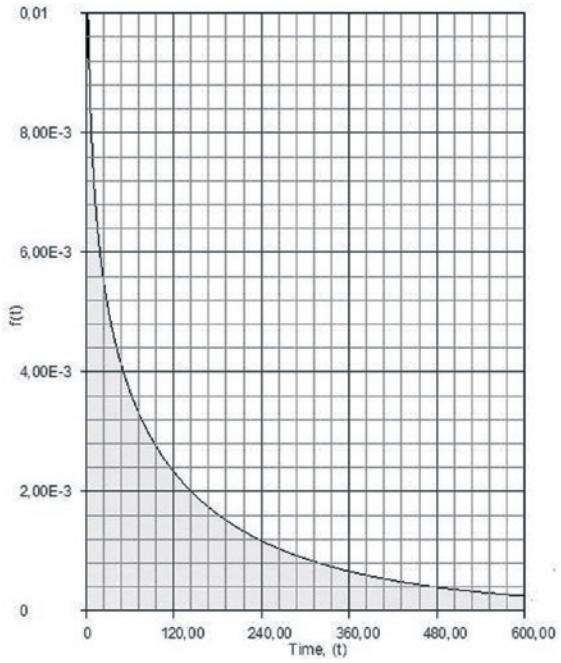

Fig. 5. Function f(t) of the density of the probability distribution of the time between failures

The weak link in the analysed forklift are the elements comprising the rear suspension of the truck. This is where elements of swivel connectors wear easily, as well as parts fastening crossovers between the rear wheel and the rear twist beam axle. The noticed problem concerned the rapid wear and tear of these elements without prior warning signs of future damage – no noticeable backlash occurs prior to failure. As a result, the rapid wear of these elements usually results in breakage and crumbling of connector bearings and swivel bolts, which leads to breakdowns and equipment downtime. Another drawback of the currently used forklift trucks is the fact that they do not have cabins fitted as standard. Cabins are fitted additionally in separate plants that deal with forklift facilities. These cabins also lack air conditioning and a suitable design to facilitate the work of the operator.

4.2. Maintenance costs for forklift trucks

The next step of research analysis covered an economic analysis of the forklifts. The obtained results are shown for the four trucks of the same type, equipped with a 4-cylinder engine with a displacement of 3200 cm3 and power of 63,000 KW, working in the same areas and performing the same operational tasks: warehouse work, production support and unloading supplies. Tables 2 and 3 summarize the total operating costs in 2010 and 2011. During this period, the unit cost of OT-1 and OT-2 maintenance amounted to 230 PLN and 750 PLN. The cost of testing made by Office of Technical Inspections allowing the truck to work amounted to another 520 PLN in 2010 and 560 PLN in 2011.

The average cost per man-hour for the service department employee was estimated at 20 PLN, which allows determining the average cost of labour for repair/replacement at 130 PLN. The average cost of repairing a forklift truck has been set at 2500 PLN, and the average cost of truck maintenance (repair/replacement) during inspection action performance including man labour - at the level of 1500 PLN.

Due to the lack of data, it is impossible to estimate the cost of the consequences of damage to a forklift truck for the supported system (production system) and its environment.

4.3. Analysis of the maintenance process of forklift trucks using the delay time concept

In order to use the algorithm shown in the Section 3, it is necessary to estimate a number of parameters. Due to the inability to estimate the cost parameters including the assessment of the impact of forklifts downstate on the production process, the process of selecting the optimal period T shall be analysed, using the criterion of the expected period of system downtime and the expected maintenance costs.

The analysed system is a multi-element system. The basic parameters were estimated as follows:

a) the inspection action performance time d was estimated at 2 h,
b) the time required to remove the failures d_b was 6.5h (mean time of all repairs registered for the ten forklifts),
c) the total operating time during the test period was (for 10 trucks) 42916 mth,

Table 2. General operating costs of a forklift truck in 2010

	The overall cost of maintaining forklift trucks in 2010 [PLN]					
Forklift:	**Cost of diesel consumption**	**Preventive maintenance costs**	**Tire replacement costs**	**The costs of handling operations***	**Salary of the mechanic / conservator**	**The average annual cost of maintenance:**
W-4	26 413.24	3 800.00	8 573.98	7 488.60	3 000.00 PLN	49 275.82
W-6	24 975.72	4 030.00	7 524.52	7 488.60	3 000.00 PLN	47 018.84
W-10	26 356.12	3 800.00	8 573.98	7 488.60	3 000.00 PLN	49 218.70
W-11	23 309.72	3 800.00	8 573.98	7 488.60	3 000.00 PLN	46 172.30
					Total:	191 685.66

** costs include e.g. periodic replacements of hydraulic oil and testing made by Office of Technical Inspections*

Table 3. General operating costs of a forklift truck in 2011

The overall cost of maintaining forklift trucks in 2011 [PLN]						
Forklift:	Cost of diesel consumption	Preventive maintenance costs	Tire replacement costs	The costs of handling operations*	Salary of the mechanic / conservator	The average annual cost of maintenance:
W-4	28 728.00	5 470.00	10 851.20	7 488.60	3 000.00	55 537.80
W-6	37 700.25	7 890.00	7 524.52	8 516.80	3 000.00	64 631.57
W-10	40 446.00	7 140.00	11 900.66	10 991.80	3 000.00	73 478.46
W-11	32 382.00	6 680.00	10 851.20	8 338.60	3 000.00	61 251.80
					Total:	254 899.63

**** costs include e.g. periodic replacements of hydraulic oil and testing made by Office of Technical Inspections***

d) the fixed intensity k of system failures occurrence has been set at $k = 0.017155$ per moto hour,
e) MTBF at 58.29 mth, with standard variation of 88.24 mth.

In the present case, it is assumed that the process of the system failures is a Poisson process with a constant intensity k at 0.017155 failure/mth.

After estimating the parameter data, there should be also specified the time delay h, which is assumed to be independent of the failure intensity and has a well-known form of the function $f_h(h)$ and $F_h(h)$. In the case of the operation of the analysed technical facilities, there is no historical data about the u time moments of the occurrence of symptoms of forthcoming failures. Therefore, there is no reliable information as to which probability distribution should be used to model the time delay parameter to obtain the best results. On the other hand, based on the paper [42] it is crucial to know the expected time delay period of E(h), while the probability distributions of the variable have a lesser impact on the model results. Therefore, the article focuses on the case, in which the time delay parameter is described by exponential distribution, and the probability density function is as follows:

$$f_h(h) = \lambda e^{-\lambda h} \tag{5}$$

Using the designated parameters and substituting function (1) in the equation (2), the expected system downtime $E_d(T)$ can be described as follows:

$$E_d(T) = \frac{kT\left[\frac{1}{T}\int_0^T (T-h) f_h(h)dh\right] d_b + d}{T+d} \tag{6}$$

Substituting the system parameters and the formula (5) to equation (6) will give the following:

$$E_d(T) = \frac{(0{,}017155T)\left[\frac{1}{T}\int_0^T (T-h)\lambda e^{-\lambda h}dh\right] 6{,}5 + 2}{T+2} \tag{7}$$

Taking into account the average failure rate of λ in the equation (7) (in the analysed case, λ = k = 0.017155) the results are presented in the graph shown in Fig. 6. For this particular case, the optimal time between the consecutive inspection actions performance is 61 mth.

Then, substituting functions (1) and (5) to the formula (3), the expected maintenance costs of forklifts per time unit in the operating cycle can be described by the following formula:

$$C(T) = \frac{1}{(T+d)}\left\{kT\left[c_{ir} + \frac{1}{T}(c_b + c_{ir})\int_0^T (T-h) f_h(h)dh\right] + c_i\right\} \tag{8}$$

which allows reaching the following:

$$C(T) = \frac{1}{(T+2)}\left\{0{,}017155 \cdot T\left[1500 + \frac{1}{T}(2500+1500)\int_0^T (T-h)\lambda e^{-\lambda h}dh\right] + 250\right\} \tag{9}$$

Figure 7 shows the cost results of the system performance. In the present case, the optimal time period T_{opt} is 45 mth, with the total expected costs of system maintenance at the level of 1 602 PLN per operating cycle (C(45) equal to 35.60 PLN). In the case of leaving the optimal time period T_{opt} at 61 mth (according to the formula (7)) - the total expected maintenance costs amounted to approximately 2 531 PLN per operating cycle, which gives a nominal increase of 929 PLN (costs C(61) = 35.88 PLN).

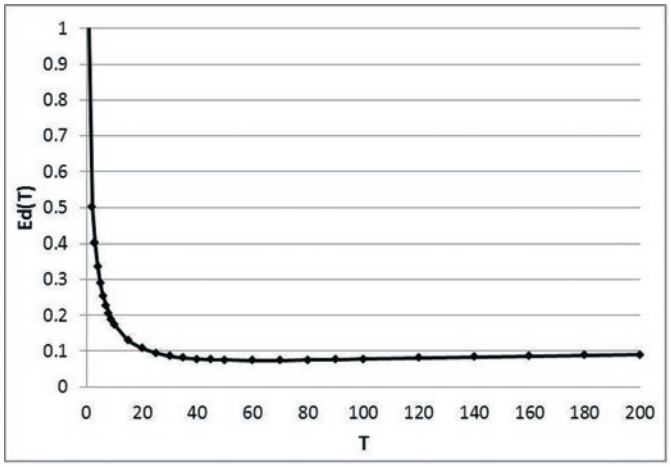

Fig. 6. Function Ed(T) when the time delay parameter is described exponentially

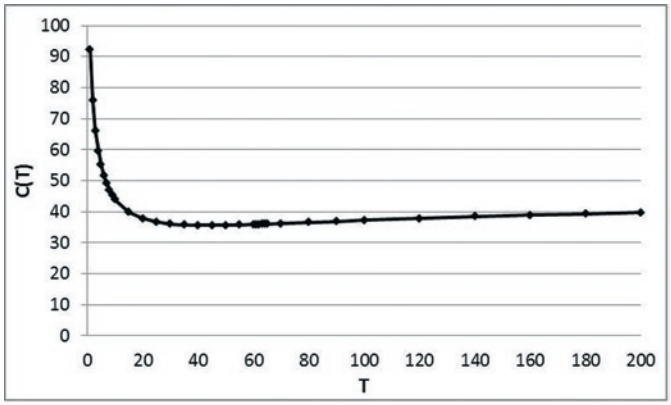

Fig. 7. Function C(T) when the time delay parameter is described exponentially

4.4. Maintenance costs for forklift trucks

In order to analyse the influence of model parameters' levels changes on the level of the analysed functions $E_d(T)$ and $C(T)$, a sensitivity analysis has been conducted. In the first step, the effect of time parameters on the level of the expected period of operating forklifts downtime has been explored. One of the parameters that can affect the results of the model is the average time of system inspection d. Prolonging the period d will affect the extension of period T_{opt} and result in a higher expected period of system downtime, as shown in Table 4 and Figure 8.

The second parameter, whose effect on the level of function $E_d(T)$ was analysed, is the mean repair time d_b. The results of the analysis are shown in Table 5 and Figure 9. As expected, the shorter mean system repair time, the longer the period T_{opt} and the lower the expected period of downtime. A similar effect is obtained when extending the mean time between failures, but in this case the changes are almost imperceptible – extending MTBF by nearly 100% extends the T_{opt} by only 9 mth (Table 6).

Table 4. The sensitivity analysis of function $E_d(T)$ to changes in the mean period of system inspection d

d [h]	T_{opt}[mth]	$E_d(T_{opt})$
1	40	0.055939
2	**61**	**0.074431**
3	80	0.086954
4	100	0.096334
5	140	0.103483
6	180	0.109056

Table 5. The sensitivity analysis of function $E_d(T)$ to changes in the mean repair time d_b

db[h]	Topt[mth]	Ed(Topt)
3	120	0.046513
4	90	0.055834
5	80	0.063951
6	65	0.071084
6.5	**61**	**0.074431**
7	60	0.077679
8	52	0.083695
9	50	0.089396
10	45	0.094662

Table 6. The sensitivity analysis of function $E_d(T)$ to changes in the mean time between failures

MTBF [h]	Topt[h]	Ed(Topt)
40	55	0.086446
45	58	0.082585
50	58	0079197
58.29	**61**	**0.074431**
65	63	0.071165
70	64	0.069003
80	65	0.065251
100	70	0.059305

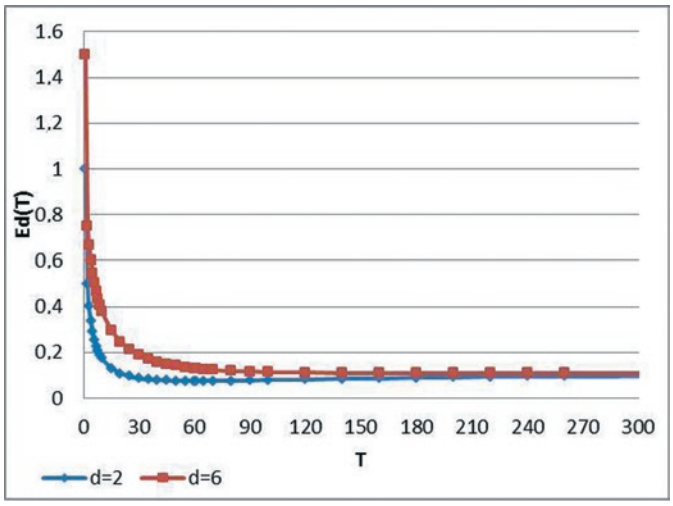

Fig. 8. Function $E_d(T)$ upon changing the mean duration of system inspection d

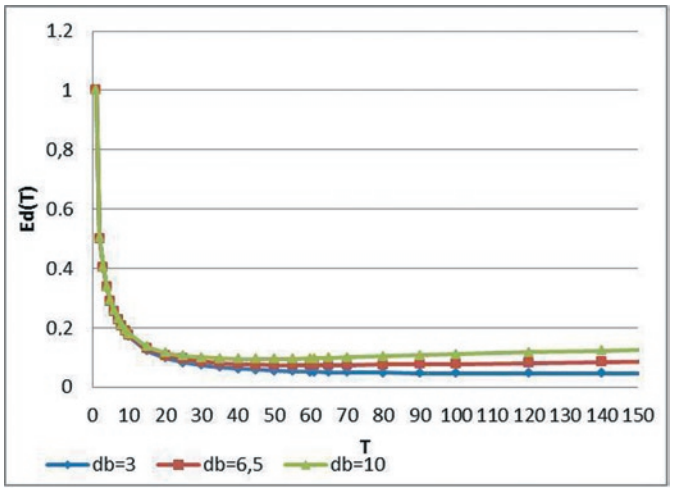

Fig. 9. Function $E_d(T)$ upon changing the mean repair time d_b

In the second part of the analysis, the effect of economic parameters on the level of the expected system maintenance costs per time unit $C(T)$ has been explored. The evaluation analysis includes the change in the mean cost c_i, mean cost c_{ir}, and mean cost c_b.

As shown in Table 7 and in Figure 10, the increase of mean cost c_i to the level of costs of preventive inspections allowing forklift operation, the optimal period T_{opt} has been increased by 100% while changing the expected maintenance costs per time unit by approximately 5 PLN (and changing the total expected cost of system maintenance per operating cycle by more than 2 000 PLN).

In accordance with the opinion of experts, in the case of assessing the change in the average cost c_{ir}, the mean value of this cost in the long term is rather expected to decrease. This in turn will result in shortening an optimal of the period T_{opt} (Table 8, Figure 11).

The last analysed parameter is the average cost of system repair c_b. In the event of forklift trucks failure occurrence, the operations involve the replacement/repair of items such as rod ends, actuators, or computers, where the repair costs far outweigh the amount of 2 500 PLN. On the other hand, there are many repairs whose cost does not exceed 1 000 PLN. Therefore, the change in the cost has been estimated at −500 PLN to +1 000 PLN relative to the base level of this input parameter (Table 9, Figure 12). As expected, the more expensive the repair operation, the shorter the period T should be. If the expected cost of repair increase to 3 500 PLN, there is a noticeable shortening of the optimal period T_{opt} by 33%, which will reduce the total expected costs of maintaining the system in the operational cycle

to around 1 200 PLN with an expected cost per time unit at 39.97 PLN (an increase by 4.17 PLN/mth).

Table 7. The sensitivity analysis of function C(T) to changes in the mean cost of system inspection ci

c_i [PLN]	T_{opt}[mth]	$C(T_{opt})$ [PLN]	C_{utrz}[PLN]
130	25	32.21	805.32
250	45	35.59	1601.77
400	70	38.24	2677.08
560	90	40.22	3619.85

Table 8. The sensitivity analysis of function C(T) to changes in the mean cost of system repair performed during inspection action c_{ir}

c_{ir}[PLN]	T_{opt}[mth]	$C(T_{opt})$ [PLN]	C_{utrz}[PLN]
1000	35	29.62	1036.88
1500	45	35.59	1601.78
2000	70	41.03	2871.84

Table 9. The sensitivity analysis of function C(T) to changes in the mean cost of system repair c_b

c_b[PLN]	T_{opt}[mth]	$C(T_{opt})$ [PLN]	C_{utrz}[PLN]
2000	70	32.54	2277.96
2500	45	35.59	1601.78
3000	35	37.88	1325.80
3500	30	39.78	1193.46

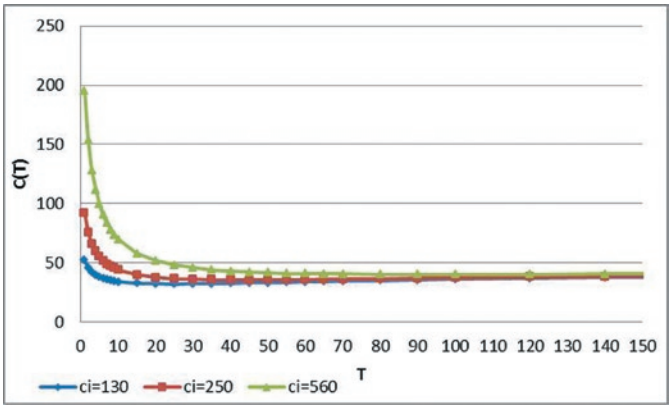

Fig. 10. Function C(T) upon changing the mean cost of system inspection c_i

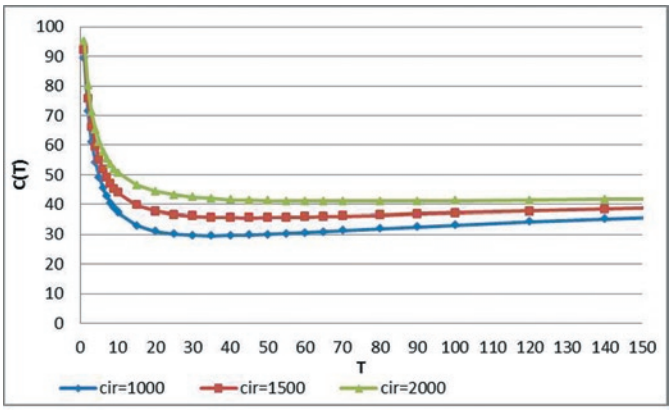

Fig. 11. Function C(T) upon changing the mean cost of repair made during system inspection action performance c_{ir}

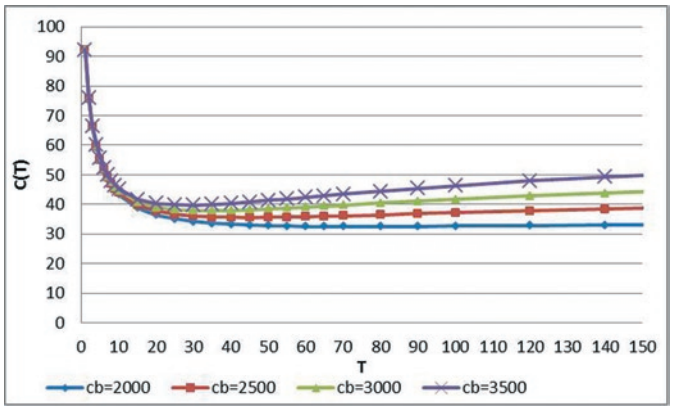

Fig. 12. Function C(T) upon changing the mean cost of facility repairs c_b

5. Summary

Analysis and proper selection of maintenance strategies for logistic support systems is one of the most important aspects discussed in literature. In the present case, the lack of reliability in the forklifts' operational tasks performance would have prevented the proper performance of the metallurgical plant, which would expose the company to significant financial losses due to e.g. production downtime.

In the present case, there have been applied the algorithm for the selection of the optimal period T_{opt} for the operation of forklift trucks in the selected production system. Under the adopted assumptions the optimal period T_{opt} has been determined at 61 mth, taking into account the criterion of expected period of downtime $E_d(T)$, and at 45 mth when considering the economic criterion $C(T)$. However, the lack of data made it impossible to analyse the optimization of the period T with consideration of the criterion of the expected consequence costs of the forklift failure. Therefore, future research directions should expand the presented analysis by a third evaluation process following the collection of the necessary operational and economic data.

Meanwhile, in the present case, the optimal period T_{opt}, equal to 61 mth, assuming a three-shift work system, and an average of 7 mth worked per shift, means that the period of inspection is approximately 3 days. Taking into account the working conditions of forklift trucks, this approximation appears to be credible.

The article focuses on presenting the applicability of the delay time concept to determine the optimal interval between inspections performance. The proposed methodology can be supportive for managers in their decision-making process, including determining the proper operational time of technical objects. This article is a continuation of work on the issue related to delay time modelling for multi-element systems, as presented in the papers [20, 30, 31, 38]. In their research work, the authors will focus in subsequent steps on identifying the opportunities for the application of delay time models to assess the performance of real-life technical systems (e.g. consideration of imperfect inspections), or the development of mathematical models for multi-element systems with time delays. This will allow defining the fundamental principles of selecting a preventive maintenance policy from the point of view of the person managing the operation of the technical system.

Acknowledgments

Authors are appreciate reviewer for his valuable comments that have helped us to improve the paper.

References

1. Akbarov A., Christer A. 1. H., H., Wang W. Problem identification in maintenance modelling: a case study. International Journal of Production Research 2008; 46(4): 1031-1046, http://dx.doi.org/10.1080/00207540600960708.
2. Alzubaidi H. J. Maintenance modelling of a major hospital complex. PhD thesis. Salford: University of Salford, 1993.
3. Ascher H. E., Kobbacy K. A. H. Modelling preventive maintenance for deteriorating repairable systems. IMA Journal of Mathematics Applied in Business & Industry 1995; 6: 85-99.
4. Attia A. F. Estimation of the reliability function using the delay-time models. Microelectronics Reliability 1997; 37(2): 323-327, http://dx.doi.org/10.1016/S0026-2714(96)00012-1.
5. Aven T., Dekker, R. A useful framework for optimal replacement models. Reliability Engineering and System Safety 1997; 58(1): 61-67, http://dx.doi.org/10.1016/S0951-8320(97)00055-0.
6. Babiarz B. An introduction to the assessment of reliability of the heat supply systems. International Journal of Pressure Vessels and Piping 2006; 83(4): 230-235, http://dx.doi.org/10.1016/j.ijpvp.2006.02.002.
7. Bajda A., Wrażeń M., Laskowski D. Diagnostics the quality of data transfer in the management of crisis situation. Electrical Review 2011;87(9A): 72-78.
8. Baker R. D., Christer A. H. Review of delay-time OR modelling of engineering aspects of maintenance. European Journal of Operational Research 1994; 73: 407-422, http://dx.doi.org/10.1016/0377-2217(94)90234-8.
9. Baker R. D., Wang W. Estimating the delay-time distribution of faults in repairable machinery from failure data. IMA Journal of Mathematics Applied in Business & Industry 1992; 3: 259-281.
10. Bartezzaghi E., Spina G., Verganti R. Lead-time models of business processes. International Journal of Operations and Production Management 1994; 14(5): 5-20, http://dx.doi.org/10.1108/01443579410056768.
11. Beamon B. M. Supply chain Design and Analysis: Models and Methods. International Journal of Production Economics 1998; 55(3): 281-294, http://dx.doi.org/10.1016/S0925-5273(98)00079-6.
12. Blanchard B. S. Logistics engineering and management. Pearson Prentice Hall: Upper Saddle River, 2004.
13. Blanchard B. S. Logistics Requirements: Established From The Beginning. SOLETech 2002; 5.1: 1-6.
14. Cai J., Zhu L. A delay-time model with imperfect inspection for aircraft structure subject to a finite time horizon. Proc. of IEEE International Conference on Grey Systems and Intelligent Services 2011. 15-8 Sept. 2011, Nanjing, China, http://dx.doi.org/10.1109/GSIS.2011.6044102.
15. Catuneanu V. M., Moldovan C., Popentin, Fl., Gheorghin M. Optimum system availability and spare allocation. Microelectronic Reliability 1988; 28(3): 353-357, http://dx.doi.org/10.1016/0026-2714(88)90388-5.
16. Cerone P. On a simplified delay time model of reliability of equipment subject to inspection monitoring. Journal of the Operational Research Society 1991; 42(6): 505-511, http://dx.doi.org/10.1038/sj/jors/0420607, http://dx.doi.org/10.1057/jors.1991.98, http://dx.doi.org/10.2307/2583457.
17. Chaberek M. Makro- i mikroekonomiczne aspekty wsparcia logistycznego. Wyd. U.G.: Gdańsk, 2002.
18. Cho I. D., Parlar M. A survey of maintenance models for multi-unit systems. European Journal of Operational Research 1991; 51: 1-23, http://dx.doi.org/10.1016/0377-2217(91)90141-H.
19. Choi K-M. Semi-Markov and Delay Time Models of Maintenance. PhD thesis. Salford: University of Salford, 1997.
20. Christer A. H. A Review of Delay Time Analysis for Modelling Plant Maintenance. in: Stochastic Models in Reliability and Maintenance, Osaki S. (ed.), Berlin Heidelberg: Springer, 2002, http://dx.doi.org/10.1007/978-3-540-24808-8_4.
21. Christer A. H. Developments in delay time analysis for modelling plant maintenance. Journal of the Operational Research Society 1999; 50: 1120-1137, http://dx.doi.org/10.2307/3010083, http://dx.doi.org/10.1057/palgrave.jors.2600837.
22. Christer A. H. Delay-time model of reliability of equipment subject to inspection monitoring. Journal of the Operational Research Society 1987; 38(4): 329-334, http://dx.doi.org/10.2307/2582056, http://dx.doi.org/10.1057/jors.1987.54.
23. Christer A. H. Modelling inspection policies for building maintenance. Journal of the Operational Research Society 1982; 33: 723-732, http://dx.doi.org/10.2307/2634320, http://dx.doi.org/10.1057/jors.1982.161.
24. Christer A. H., Redmond D. F. Revising models of maintenance and inspection. International Journal of Production Economics 1992; 24: 227-234, http://dx.doi.org/10.1016/0925-5273(92)90134-S.
25. Christer A. H., Redmond D. F. A recent mathematical development in maintenance theory. IMA Journal of Mathematics Applied in Business and Industry 1990; 2: 97-108.
26. Christer A. H., Scarf P. A. A robust replacement model with applications to medical equipment. Journal of the Operational Research Society 1994; 45(3): 261-275, http://dx.doi.org/10.2307/2584160, http://dx.doi.org/10.1057/jors.1994.39.
27. Christer A. H., Waller W. M. A Descriptive model of capital plant replacement, Journal of the Operational Research Society 1987; 38(6): 473-477, http://dx.doi.org/10.1057/jors.1987.84, http://dx.doi.org/10.2307/2582760.
28. Christer A. H., Waller W. M. An operational research approach to planned maintenance: modelling P.M. for a vehicle fleet. Journal of the Operational Research Society 1984; 35(11): 967-984, http://dx.doi.org/10.1057/jors.1984.193, http://dx.doi.org/10.2307/2582454.
29. Christer A. H., Waller W. M. Reducing production downtime using delay-time analysis. Journal of the Operational Research Society 1984; 35(6): 499-512, http://dx.doi.org/10.1057/jors.1984.103, http://dx.doi.org/10.2307/2581797.
30. Christer A. H., Waller W. M. Delay Time Models of Industrial Inspection Maintenance Problems. Journal of the Operational Research Society 1984; 35(5): 401-406, http://dx.doi.org/10.1057/jors.1984.80, http://dx.doi.org/10.2307/2581368.
31. Christer A.H., Wang W., Choi K., Van der Duyn Schouten F. A. The robustness of the semi-Markov and delay time single-component inspection models to the Markov assumption. IMA Journal of Management Mathematics 2001; 12: 75-88, http://dx.doi.org/10.1093/imaman/12.1.75.
32. Christer A. H., Whitelaw J. An operational research approach to breakdown maintenance: problem recognition. Journal of the Operational Research Society 1983; 34(11): 1041-1052, http://dx.doi.org/10.2307/2581013, http://dx.doi.org/10.1057/jors.1983.235.
33. Cunningham A., Wang W., Zio E., Allanson D., Wall A., Wang J. Application of Delay-time Analysis via Monte Carlo Simulation. Journal of Marine Engineering and Technology 2011; 10(3): 57-72.

34. Dekker R., Roelvink I. F. K. Marginal cost criteria for preventive replacement of a group of components. European Journal of Operational Research 1995; 84: 467-480, http://dx.doi.org/10.1016/0377-2217(93)E0346-Y.
35. Desa M. I., Christer A. H. Modelling in the absence of data: a case study of fleet maintenance in a developing country. Journal of the Operational Research Society 2001; 52: 247-260, http://dx.doi.org/10.1057/palgrave.jors.2601107.
36. Frostig E. Comparison of maintenance policies with monotone failure rate distributions. Applied Stochastic Models in Business and Industry 2003; 19: 51-65, http://dx.doi.org/10.1002/asmb.485.
37. Gross D., Pinkus C. E. Designing a support system for repairable items. Computers & Operations Research 1979; 6: 59-68, http://dx.doi.org/10.1016/0305-0548(79)90017-0.
38. Hennet J-C., Tarbouriech S. Stability conditions of constrained delay systems via positive invariance. International Journal of Robust and Nonlinear Control 1998; 8: 265-278, http://dx.doi.org/10.1002/(SICI)1099-1239(199803)8:3<265::AID-RNC311>3.3.CO;2-#, http://dx.doi.org/10.1002/(SICI)1099-1239(199803)8:3<265::AID-RNC311>3.0.CO;2-8, http://sjp.pwn.pl/sjp/motogodzina;2484786 (dostęp: 15.12.2014r.).
39. Jardine A. K. S., Hassounah M. I. An optimal vehicle-fleet inspection schedule. Journal of the Operational Research Society 1990; 41(9): 791-799, http://dx.doi.org/10.1057/jors.1990.116, http://dx.doi.org/10.2307/2583494.
40. Jia X., Christer A. H. A periodic testing model for a preparedness system with a defective state. IMA Journal of Management Mathematics 2002; 13: 39-49, http://dx.doi.org/10.1093/imaman/13.1.39.
41. Jodejko-Pietruczuk A., Werbińska-Wojciechowska S. Analysis of maintenance models' parameters estimation for technical systems with delay time. Eksploatacja i Niezawodnosc - Maintenance and Reliability 2014; 16(2): 288-294.
42. Jodejko-Pietruczuk A., Werbińska-Wojciechowska S. Economical effectiveness of Delay Time approach using in Time-Based maintenance modelling. Proc. of PSAM 11 & ESREL 2012 Conference, 25-29 June 2012, Helsinki, Finland.
43. Jodejko-Pietruczuk A., Werbińska-Wojciechowska S. Analysis of Block-Inspection Policy parameters from economical and availability point of view. Proc. of PSAM 11 & ESREL 2012 Conference, 25-29 June 2012, Helsinki, Finland.
44. Jones B., Jenkinson I., Wang J. Methodology of using delay-time analysis for a manufacturing industry. Reliability Engineering and System Safety 2009; 94: 111-124, http://dx.doi.org/10.1016/j.ress.2007.12.005.
45. Kierzkowski A. Reliability models of transportation system of low cost airlines. In: Reliability, risk and safety: back to the future. Ale B. J. M., Papazoglou J. A., Zio E., Raton, B (eds). CRC Press: London 2010.
46. Kierzkowski A., Kowalski M., Magott J., Nowakowski T. Maintenance process optimization for low-cost airlines. Proc. of PSAM 11 & ESREL 2012 Conference, 25-29 June 2012, Helsinki, Finland.
47. Lee C. Applications of delay time theory to maintenance practice of complex plant. PhD work. T.I.M.E. Research Institute. Salford: University of Salford, 1999.
48. Leung F., Kit-leung M. Using delay-time analysis to study the maintenance problem of gearboxes. International Journal of Operations & Production Management 1996; 16(12): 98-105, http://dx.doi.org/10.1108/01443579610151779.
49. Lewitowicz J. Risk in logistics (in Polish). Logistyka 2007; 5: 1-6.
50. Melo M. T., Nikel S., Saldanha da Gama F.: Dynamic multi-commodity capacitated facility location: a mathematical modeling framework for strategic supply chain planning. Computers & Operations Research 2005; 33(1): 181-208, http://dx.doi.org/10.1016/j.cor.2004.07.005.
51. Młyńczak M., Nowakowski T., Werbińska-Wojciechowska S. Technical systems maintenance models classification (in Polish). In: Technical systems maintenance problems, monograph (in Polish). Siergiejczyk M. (ed.) Warsaw: Warsaw University of Technology Publishing House, 2014.
52. Nakagawa T. A summary of discrete replacement policies. European Journal of Operational Research 1984; 17: 382-392, http://dx.doi.org/10.1016/0377-2217(84)90134-6.
53. Nicolai R. P., Dekker R. A review of multi-component maintenance models. Proc. of European Safety and Reliability Conference ESREL 2007, eds. Aven, T. & Vinnem, J.E., Leiden: CRC Press/Balkema: 289-296.
54. Nicolai R. P., Dekker R. Optimal maintenance of multicomponent systems: a review. Economic Institute Report 2006.
55. Nowakowski T. Analysis of modern trends of logistics technology development. Archives of Civil and Mechanical Engineering 2011; 11(3):699-706, http://dx.doi.org/10.1016/S1644-9665(12)60110-1.
56. Nowakowski T. Problems with analyzing operational data uncertainty. Archives of Civil and Mechanical Engineering 2010; 10(3): 95-109. http://dx.doi.org/10.1016/S1644-9665(12)60139-3,
57. Nowakowski T., Werbińska-Wojciechowska S. Developments of time dependencies modeling concepts, Advances in safety, reliability and risk management. Proc. of the European Safety and Reliability Conference, ESREL 2011, Troyes, France, 18-22 September 2011. Leiden: CRC Press/Balkema: 832-838.
58. Nowakowski T., Werbińska S. On problems of multicomponent system maintenance modeling. International Journal of Automation and Computing 2009; 6(4): 364-378, http://dx.doi.org/10.1007/s11633-009-0364-4.
59. Nowakowski T., Werbińska S. Chosen problems of logistic chain performance assessment (in Polish). In: Chosen issues of applied logistics (in Polish). Bukowski L. (ed). Krakow: Publ. House of AGH University Science of Technology, 2009.
60. Pham H., Wang H. Imperfect maintenance. European Journal of Operational Research 1996; 94: 425-438, http://dx.doi.org/10.1016/0377-2217(96)00099-9, http://dx.doi.org/10.1016/S0377-2217(96)00099-9.
61. Pierskalla W. P., Voelker J. A. A survey of maintenance models: the control and surveillance of deteriorating systems. Naval Research Logistics Quarterly 1976; 23: 353-388, http://dx.doi.org/10.1002/nav.3800230302.
62. Pillay A., Wang J., Wall A. D., Ruxton T. A maintenance study of fishing vessel equipment using delay-time analysis. Journal of Quality in Maintenance Engineering 2001; 7(2): 118-127, http://dx.doi.org/10.1108/13552510110397421.
63. Redmond D. F. Delay Time Analysis in Maintenance. PhD thesis. Salford: University of Salford, 1997.
64. Restel F. J. Train punctuality model for a selected part of railway transportation system. Proc. of 22nd Annual Conference on European Safety and Reliability ESREL 2013. 29 September-02 October 2013, Amsterdam, the Netherlands, 2014.
65. Sarkar J. Li F. Limiting average availability of a system supported by several spares and several repair facilities. Statistics and Probability Letters 2006; 76: 1965-1974, http://dx.doi.org/10.1016/j.spl.2006.04.046.
66. Scarf P. A. On the application of mathematical models in maintenance. European Journal of Operational Research 1997; 99: 493-506, http://

dx.doi.org/10.1016/S0377-2217(96)00316-5.
67. Scarf P. A., Bouamra O. On the application of a capital replacement model for a mixed fleet. IMA Journal of Mathematics Applied in Business & Industry 1995; 6: 39-52.
68. Sherif Y. S. Reliability analysis: Optimal inspection & maintenance schedules of failing equipment. Microelectronics and Reliability 1982; 22(1): 59-115, http://dx.doi.org/10.1016/0026-2714(82)90051-8.
69. Subramanian R., Natarajan R. An n-unit standby redundant system with r repair facilities and preventive maintenance. Microelectronics Reliability 1982; 22(3): 367-377, http://dx.doi.org/10.1016/0026-2714(82)90011-7.
70. Thomas L. C. A survey of maintenance and replacement models for maintainability and reliability of multi-item systems. Reliability Engineering 1986; 16: 297-309, http://dx.doi.org/10.1016/0143-8174(86)90099-5.
71. Tomaszek H., Jasztal M., Zieja M. Application of the Paris formula with M=2 and the variable load spectrum to a simplified method for evaluation of reliability and fatigue life demonstrated by aircraft components. Eksploatacja i Niezawodnosc – Maintenance and Reliability 2013; 15(4): 297-303.
72. Ustawa z dnia 21 grudnia 2000 r. o dozorze technicznym (the Act of Law of 21 December 2000 on technical supervision).
73. Valdez-Flores C., Feldman R. A survey of preventive maintenance models for stochastically deteriorating single-unit systems. Naval Research Logistics 1989; 36: 419-446, http://dx.doi.org/10.1002/1520-6750(198908)36:4<419::AID-NAV3220360407>3.0.CO;2-5.
74. 75. Valis D., Koucky M., Zak L. On approaches for non-direct determination of system deterioration. Eksploatacja i Niezawodnosc - Maintenance and Reliability 2012; 14(1): 33-41.
75. Valis D., Zak L., Pokora O. Engine residual technical life estimation based on tribo data. Eksploatacja i Niezawodnosc – Maintenance and Reliability 2014; 16(2): 203-210.
76. Wang H. A survey of maintenance policies of deteriorating systems. European Journal of Operational Research 2002; 139: 469-489, http://dx.doi.org/10.1016/S0377-2217(01)00197-7.
77. Wang W. An overview of the recent advances in delay-time-based maintenance modeling. Reliability Engineering and System Safety 2012; 106: 165-178, http://dx.doi.org/10.1016/j.ress.2012.04.004.
78. Wang W. Modeling planned maintenance with non-homogeneous defect arrivals and variable probability of defect identification. Eksploatacja i Niezawodnosc - Maintenance and Reliability 2010; 2: 73-78.
79. Wang W. Delay time modelling for optimized inspection intervals of production plant. In: Handbook of Maintenance Management and Engineering. Ben-Daya, M., Duffuaa, S. O., Raouf, A., Knezevic, J., Ait-Kadi, D. (eds.). London: Springer, 2009, http://dx.doi.org/10.1007/978-1-84882-472-0_19.
80. Wang W. Delay time modelling. In: Complex system maintenance handbook. Kobbacy, A. H., Prabhakar Murthy, D. N. (eds.). London: Springer, 2008, http://dx.doi.org/10.1007/978-1-84800-011-7_14.
81. Wang W. A delay time based approach for risk analysis of maintenance activities. Journal of the Safety and Reliability Society 2003; 23(1): 103-113.
82. Wang W., Christer A. H. Solution algorithms for a nonhomogeneous multi-component inspection model. Computers & Operations Research 2003; 30: 19-34, http://dx.doi.org/10.1016/S0305-0548(01)00074-0.
83. Wang W., Christer A. H. A modelling procedure to optimize component safety inspection over a finite time horizon. International Quality and Reliability Engineering 1997; 13: 217-224, http://dx.doi.org/10.1002/(SICI)1099-1638(199707)13:4<217::AID-QRE107>3.3.CO;2-G, http://dx.doi.org/10.1002/(SICI)1099-1638(199707)13:4<217::AID-QRE107>3.0.CO;2-P.
84. Wen-yua LV, Wang W. Modelling preventive maintenance of production plant given estimated PM data and actual failure times. Proc. of International Conference on Management Science and Engineering 2006, 5-7 October 2006, Lille.
85. Werbińska-Wojciechowska S. Problems of logistics systems modelling with the use of DTA approach. Logistics and Transport 2012; 2: 63-74.
86. Werbińska-Wojciechowska S. Modelling of time relations in production systems (in Polish). Logistyka 2010; 2: 1-10.
87. Werbińska S. Model of logistic support for means of transport operational system performance (in Polish). PhD. Thesis. Wroclaw: Wroclaw University of Technology, 2008.
88. Werbińska S. Reliability model for logistic support system with time relations (in Polish). Logistyka 2007; 3: 1-12.
89. Witkowski K., Kiba-Janiak M., Seniuk S. Map of Logistics processes as a part of creating an enterprise supply chain in the metallurgical company. Proc. of 21st International Conference on Metallurgy and Materials, 23-25 May, 2012, Brno Czech Republic.
90. www.cscmp.org (dostęp: 20.10.2014r.).
91. www.eksploatacja.waw.pl/indexphp.php?s=4000 (dostęp: 20.10.2014r.).
92. Zajac M., Kierzkowski A. Uncertainty assessment in semi Markov methods for Weibull functions distributions. In: Advances in Safety,Reliability and Risk Management – Proc. of the European Safety and Reliability Conference, ESREL 2011. 18-22 September 2011, Troyes France.
93. Zhao J., Chan A. H. C., Roberts C., Madelin K. B. Reliability evaluation and optimisation of imperfect inspections for a component with multi-defects. Reliability Engineering and Systems Safety 2007; 92: 65-73, http://dx.doi.org/10.1016/j.ress.2005.11.003.

Sylwia WERBIŃSKA-WOJCIECHOWSKA
Paweł ZAJĄC
Faculty of Mechanical Engineering
Department of Operation of Logistic Systems, Transportation Systems and Hydraulic Systems
Wroclaw University of Technology
ul. Wybrzeze Wyspianskiego 27, 50-370, Wrocław, Poland
e-mail: sylwia.werbinska@pwr.edu.pl, pawel.zajac@pwr.edu.pl

Article citation info:
GAO J, Wang H. Operation reliability analysis based on fuzzy support vector machine for aircraft engines. Eksploatacja i Niezawodnosc – Maintenance and Reliability 2015; 17 (2): 186–193, http://dx.doi.org/10.17531/ein.2015.2.3.

Jun GAO
Huawei WANG

OPERATION RELIABILITY ANALYSIS BASED ON FUZZY SUPPORT VECTOR MACHINE FOR AIRCRAFT ENGINES

ANALIZA NIEZAWODNOŚCI EKSPLOATACYJNEJ SILNIKÓW LOTNICZYCH W OPARCIU O METODĘ ROZMYTEJ MASZYNY WEKTORÓW NOŚNYCH (FSVM)

The aircraft engine is a complex and repairable system, and the diversity of its failure modes increases the difficulty of operation reliability analysis. It is necessary to establish a dynamic relationship among monitoring information, failure mode and system reliability for achieving scientific reliability analysis for aircraft engines. This paper has used fuzzy support vector machine (FVSM) method to fuse condition monitoring information. The reliability analysis models including Gamma process model and Winner process model, respectively for different failure modes, have been presented. Furthermore, these two models have been integrated on the basis of competing failures' mechanism. Bayesian model averaging has been used to analyze the effects of different failure modes on aircraft engines' reliability. As a result of above, the goal of an accurate analysis of the reliability for aircraft engines has been achieved. Example shows the effectiveness of the proposed model.

Keywords: *aircraft engine, reliability analysis, competing failure, Bayesian model averaging, data fusion.*

Silnik samolotu to złożony system naprawialny, a różnorodność przyczyn jego uszkodzeń zwiększa trudność analizy niezawodności eksploatacyjnej. Istnieje konieczność ustalenia dynamicznych związków pomiędzy monitorowaniem informacji, przyczynami uszkodzeń i niezawodnością systemu, których znajomość pozwoliłaby przeprowadzać naukową analizę niezawodności silników lotniczych. Do integracji danych z monitorowania informacji, w pracy wykorzystano metodę rozmytej maszyny wektorów nośnych (FSVM). Dla różnych przyczyn uszkodzeń, przedstawiono odpowiednie modele analizy niezawodności – model procesu Gamma i model procesu Wienera. Przedstawione modele zintegrowano na podstawie mechanizmu uszkodzeń konkurujących. Do analizy wpływu różnych przyczyn uszkodzeń na niezawodność silników lotniczych wykorzystano procedurę bayesowskiego uśredniania modeli. Dzięki powyższym krokom, osiągnięto założony cel dokładnej analizy niezawodności silników samolotowych. Przykład pokazuje skuteczność proponowanego modelu.

Słowa kluczowe: *silnik samolotu, analiza niezawodności, uszkodzenie konkurujące, bayesowskie uśrednianie modeli, fuzja danych.*

1. Introduction

The level of the aircraft engines' reliability affects flight safety directly. Estimating the reliability level scientifically and objectively is the foundation of reliability management and decision-making of maintenance for aircraft engines. The difficulties of operation reliability analysis for aircraft engines lie in three aspects. First, there are less failure data and rich condition monitoring data. Second, there is a problem of competing failures caused by the diversity of failure modes arising from the complexity of the system. Third, the operational reliability is dynamic change.

Extracting reliability information from a large amount of monitoring information is a common concern issue in the current theoretical and engineering field. Researchers in the United States, Britain, Australia and other countries promote using HUMS(health and usage monitoring systems) to monitor the health and use of engines, structure, etc, which can provide full-time health information and on-line monitoring, in order to make the diagnosis and prediction of the remaining life of the equipment, structure and operation [10]. HP Engine Company has developed an advanced life prediction system for gas turbine engines, which integrates fault prognostics and health management capacity [22]. Sugier J, Anders GJ [24] described the deterioration process by a Markov model, developed the equipment life curve using its various characteristics and quantified other reliability parameters. Cobel proposed using data fusion method, which fuses condition monitoring data and fault data effectively, to predict the remaining life, used genetic algorithm to select optimal monitoring parameters, applied GPM (General path model, GPM) to achieve that transform the traditional reliability analysis based on failure time to analysis based on failure process [7]. For the operation reliability or on-line reliability analyisis, Lu H et al. presented a evaluation model of real-time performance based on time series method, and researched the reliability prediction of the bit excessive wear failure by regarding drill thrust as a performance monitoring parameters [15]. Elwany and Gebraeel presented a model for predicting system performance reliability based on Bayesian, and applied to parts replacement and inventory decisions [8]. Li et al. discussed the multi-state coherent system composed of multi-state components [14]. Chinnam made use of the reliability condition of some parts which performance degenerate signals were monitored and adopted a general polynomial regression model to describe performance change [6].

For complex systems, the reliability evaluation of single failure mode or single point of failure is an ideal assumption. But in terms of practical situation of aircraft engines, the failure modes are various and multi-failure modes often coexist. The failure modes can be divided into degradation failure and sudden failure only on the basis

of major categories of classification. Different failure modes interact each other, constantly change their forms of expression and mechanism of action in different stages of the running system. It is a problem of competing failures in essence, increasing the complexity of the reliability evaluation. The problem of competing failures has drawn a lot of concern in the field of reliability engineering. Lehmann surveyed some approaches to model the relationship between failure time data and covariate data like internal degradation and external environment models [13]. Bagdonavičius et al. made use of the half updating process of the linear degradation model to study the non-parameter estimation method of competing failure model, and to simplify the calculation, the model used decomposition method [1]. Pareek et al. studied the problem of censored data processing for competing failures [16]. Bedford et al. presented a competing risks reliability model for a system that releases signals each time of its condition deteriorates and provided a framework for the determination of the underlying system time from right-censored data [2]. Su et al. regarded the incidence of sudden failure as the function of performance degradation amount, made use of Wiener process to describe the degradation process, and proposed a reliability evaluation model for competing failures [23]. Bocchetti et al. proposed a competing risk model to describe the reliability of the cylinder liners of a marine Diesel engine, in which the wear process is described by a stochastic process and the failure time due to the thermal cracking is described by the Weibull distribution [3]. Park et al.[17] and Kundu et al. [12] considered the analysis of incomplete data in the presence of competing risks among several groups. Chen et al. developed methods for competing risks when individual events are correlated with clusters [4]. Wang et al. used Bivariate exponential models to analyze competing risks data involving two correlated risk components [26]. Xing et al. presented a combinatorial method for the reliability analysis of system subject to competing propagated failures and failure isolation effect [27]. Salinas-Torres et al. [20] and Polpo et al. [19] proposed the Bayesian nonparametric estimator of the reliability of a series system under a competing risk scenario. Peng et al. developed reliability models and preventive maintenance policies for systems subject to multiple Dependent Competing Failure Process (MDCFP) [18].

For the characteristics of aircraft engines' opertion reliability, the information fusion technology will be referenced to the aircraft engines' reliability modeling and the input parameters of the reliability model will be determined by information fusion. The impacts of competing failure modes on system reliability will be analyzed through data. The paper will use fuzzy support vector machine to fuse online condition monotoring data. Further, Bayesian model averaging method are used to study the data, to select the optimal model, and to propose a reliability analysis model for aircraft engines based on competing failures.

2. The modeling framework of operation reliability analysis for aircraft engines

The paper intends to combine the recent research results concerning operation reliability analysis and competing failures, and to propose operation reliability analysis methods based on competing failures for aircraft engines. The monitoring information characteristics of aircraft engines are reflected in the following aspects. First, there are multi-source monitoring information to monitor aircraft engines operation reliability. Second, there are insufficient monitoring information because of monitoring cost consideration. Third, the monitoring infomation often has some noise because of operation environment change and sensor reliability. Therefore, it can be concluded that for the analysis and prediction of aircraft engines performance, the problem consists in the data analysis of small sample and high noise. Fuzzy support vector machine has been selected to model operation condition of aircraft engines. Failure mechanism of aircraft engines should be considered, establishing the reliability anaylysis models respectively for the different failure modes. In the case of different failure modes coexist, the reliability analysis model based on competing failures is established. The modelling process is shown in Fig.1.

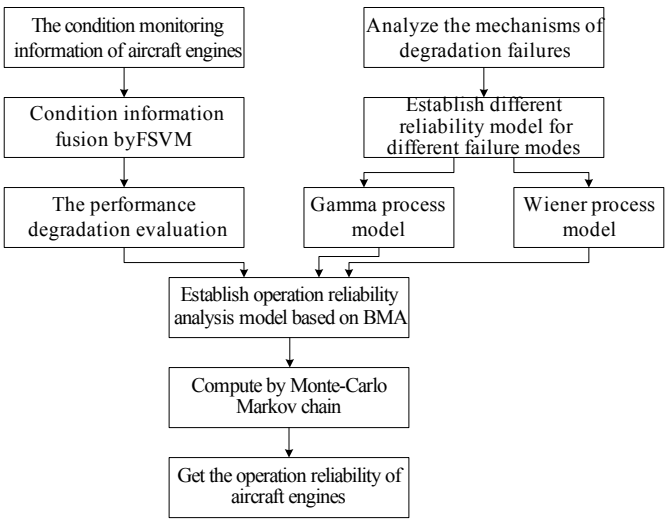

Fig. 1. The flow diagram of operation reliability analysis for aircraft engines based on FSVM

3. Performance degradation analysis of aircraft engines

In the aircraft engine operation process, performance degradation is the main reason leading to reliability decrease. So, it is necessary to evaluate performance degradation. By evaluating the performance degradation level, performance degradation reliability of aircraft engines can be evaluated. The performance degradation evaluation is based on condition monitoring information, through processing and fusion condition monitoring information of aircraft engines.

3.1. Condition monitoring information of aircraft engines

The performance monitoring of aircraft engines includes three categories, namely, gas path monitoring, oil monitoring and vibration monitoring. The engines' performance degradation (or reduced efficiency) will usually be reflected in changes of monitoring parameters.

I Gas path monitoring. Gas path system is the key composition of aircraft engines, which includes air-compressor, combustor and turbine, etc. Gas path monitoring consists of some subsets of inter-stage pressure and temperatures, spool speeds and fuel flow. The main monitoring parameters of gas path are exhaust gas temperature and fuel flow.

II Oil monitoring. Oil monitoring includes various oil system temperature, pressures, fuel temperature, and delivery pressure. Oil monitoring are the auxiliary instruments for aircraft engines, which can be used for monitoring components of lubrication system and its sealing. The main oil monitoring parameters are oil pressure, oil temperature, and oil consumption rate.

III Vibration measurements. High and low spools of aircraft engines are composed of blades, plates, axis and bearings. There are some vibration signals while wear and damage occur during rotation. The key parameters of vibration measurements include low pressure vibration and high pressure vibration.

The performance degradation is usually reflected on the change of condition monitoring parameters. For example, if exhaust gas temperature exceeds the standard, oil consumption rate will increase, or

high pressure rotor speed deviation will occur, and a conclusion can be drawn that the aircraft engine is deteriorating.

3.2. Performance degradation evaluation based on fuzzy support vector machine

Comprehensively using above parameters to reflect the performance degradation of aircraft engines from the multi-dimensional perspective will be more realistic. In the paper, the problem can be solved by using fuzzy support vector machine. The advantages of fuzzy support vector machine method are shown as followed:

First, support vector machine (SVM) is presented as the study system of supposed linear function space which is used in high-dimension feature space by Vapnik and others [25] according to principles of structure risk minimization in study theory of statistics; it finds the best compromise between complexity of method and study ability according to limited sample information; it takes advantage of supporting vector machine in dealing with small sample and prediction to make it come true that it can be a highly effective conducting inference from training data sample to prediction sample, and to solve the reality problems of small sample, nonlinear, high dimension and local minimum point more sufficiently [21].

Second, fuzzy support vector machine can excellently handle samples with noise and outlier rejecting. It can achieve the goal of eliminating the influence of noise and outlier rejecting samples by applying fuzzy technology to support vector machine, using different punishment weight coefficients for different samples, giving smaller weight to samples with noise and outlier rejecting [9, 11]. There are a lot of applications by FSVM prediction. For example, Cheng et al utilized weighted SVM, fuzzy logic and fast messy Genetic Algorithm (fmGA) to handle distinct characteristics in Estimate at Completion (EAC) prediction [5].

3.3. Fuzzy support vector machine algorithm

(1) Method of support vector machine

Note that training sample is denoted by $\{(x_i, y_i) | i = 1,2,\cdots,l\}$. In the sample, $x_i \in R^n$ is input variables, $y_i \in R$ is output variables. Nonlinear mapping $\phi(\cdot)$ is to input the sample from late space mapping to high-dimension feature space, and construct best decision function in this feature space: $f(x) = (\omega \cdot \phi(x) + b)$,where $\omega \cdot \phi(x)$ is set as the scalar product of vector and mapping function , b is the bias. Thus, the corresponding constraint optimization problem can be shown as:

$$\min_{\omega,b,\xi,\xi^*} \frac{1}{2}\|\omega\|^2 + C\sum_{i=1}^{l}(\xi_i + \xi_i^*) \tag{1}$$

$$\text{s.t.} \begin{cases} y_i - \omega^T \cdot \varphi(x_i) - b \le \varepsilon + \xi_i \\ \omega^T \cdot \varphi(x_i) + b - y_i \le \varepsilon + \xi_i^* \\ \xi_i, \xi_i^* \ge 0 \end{cases}, \quad i = 1,2,\cdots,l$$

In Eq.(1), C is s a penalty factor, it has made a compromise between empirical risk and trust scope, ξ_i, ξ_i^* is relax quantum, each of them shows the upper and low limit of training error $\left(\left|y_i - \left[\omega^T \cdot \varphi(x_i + b)\right]\right| < \varepsilon\right)$ in the constraint of error ε; ε is the defined error of insensitive pricing function Vapnik-ε. Eq.(1) has set the optimization problem which is a typical convex quadratic programming problem. According to Lagrange theory, weight vector equals to the linear combination of training data:

$$\omega = \sum_{i=1}^{l}(a_i - a_i^*)\phi(x_i) \tag{2}$$

Putting Eq.(2) in Eq.(1), the prediction values of the unknown point can be got as followed.

$$f(x) = \sum_{i=1}^{l}(\alpha_i - \alpha_i^*)K(x_i, x) + b \tag{3}$$

Where $K(x_i, x) = \phi(x_i) \cdot \phi(x)$ is denoted as kernel function.

(2) Model of fuzzy support vector machine

Fuzzy support vector machine introduces fuzzy theory into support vector, and adds a membership attribute $\mu(\delta \le s \le 1)$ to every sample (x, y) ,where δ is arbitrarily small positive to show the subordination degree between sample *x* and type *y*.

Denoting the training sample as:

$$U = \{(x_i, y_i, u_i) | x_i \in R^n, \varepsilon \le u_i \le 1\}, \quad i = 1,2,\cdots,l \tag{4}$$

Thus, its corresponding optimization problem is:

$$\min_{\omega,b,\xi,\xi^*} \frac{1}{2}\|\omega\|^2 + C\sum_{i=1}^{l}(\mu_i \xi_i) \tag{5}$$

As is known from Eq. (5), this kind of fuzzy support vector machine, which makes samples with different membership, plays different roles in point training just by fussing the penalty factor C . The bigger μ_i is, the more important the sample is, and the less possible the classification mistake is. When it is noise or outlier rejecting, the sample will reduce the effort on training by giving very small value to its membership so that it can widely reduce the influence of noise or outlier rejecting to support vector machine.

(3) Method of determining membership

In order to determine the relationship between effective sample with outlier rejecting or noise, the paper uses affinity to determine membership function. After having found the smallest hyper-sphere of the sample set in feature space, marking the core and radius of the smallest hyper-sphere with a and r , thus the membership of the sample can be described as followed:

$$\mu(x_i) = \begin{cases} 0.6 \times \left[\dfrac{1 - \|\phi(x_i) - a\|/r}{1 + \|\phi(x_i) - a\|/r}\right] + 0.4, \|\phi(x_i) - a\| \le r \\ 0.4 \times \left[\dfrac{1}{1 + (1 + \|\phi(x_i) - a\|/r)}\right], \|\phi(x_i) - a\| > r \end{cases} \tag{6}$$

This method makes a distinction between effective sample from noise or outlier rejecting more effectively and takes different calculation method of membership to effective sample and noise or outlier rejecting, and under the situation of maintaining support vector and membership big enough, it also can reduces the membership of noise and outlier rejecting so that it reduces the sensitivity of fuzzy support vector machine for noise. The calculation of membership is achieved by determining the radius of the smallest hyper-sphere.

4. Performance degradation analysis of aircraft engines

Considered the multi-failure mode, sole reliability model is difficult to analyze aircraft engines reliability. The paper chooses Gamma process and Wiener process to describe aircraft engines operation reliability. Gamma process model mainly applied in the gradual performance degradation and reliability monotone decreasing. Wiener process model mainly applied in the structural reliability analysis, which has the function of describing multi-factors random disturbance effect on reliability. Using above two reliability analysis model, the reliability change law can be described comprehensively.

4.1. Gamma process reliability analysis model

Let $y(t)$ be the amount of performance degradation failures at time t and l be the failures threshold. When $y(t) \geq l$, aircraft engines will come up with performance degradation failures. Aircraft engines' performance degradation is irreversible, that is, the performance gradually decreases and the amount of performance degradation is constantly increasing with the use of time. Therefore, the Gamma process can be applied to describe the degradation process. Assume that y_0 is aircraft engines' initial performance, so $w(t) = y(t) - y(t_0)$ represents the accumulated deterioration at time t. Because degradation amount increases monotonically, for any t_i, t_j, if $t_j > t_i$, there must be $w(t_j) - w(t_i) > 0$. Assume that degradation amount $w(t)$ obey $Ga(\mu(t), \lambda)$, its density function can be expressed as follows:

$$f_g(\xi, \alpha(t), \lambda) = \frac{\lambda^{\alpha(t)}}{\Gamma(\alpha(t))} \zeta^{\mu(t)-1} e^{-\lambda\zeta} \tag{7}$$

where, α and λ represent shape parameter and scale parameter respectively; $\Gamma(\alpha) = \int_0^\infty t^{\alpha-1} e^{-t} dt$ is Gamma function.

Generally assume that the scale parameter does not change in a performance monitoring process. Shape parameter changes with the change of the degradation process, because the extent and rate of the performance degradation experience an increasing trend, so we assume that shape parameter is proportional with expected degradation degree and time power, that is:

$$\alpha(t) = kt^v \tag{8}$$

Further, Eq.(7) can be transformed as following:

$$f_g(\xi, \alpha(t), \lambda) = \frac{\lambda^{kt^v}}{\Gamma(kt^v)} \zeta^{kt^v-1} e^{-\lambda x} I_{(0,\infty)}(\zeta) \tag{9}$$

Based on the theory of system reliability, the reliability for degradation failures can be depicted as following:

$$R_g(t) = P\{T > t\} \Rightarrow P\{w(t) < \varepsilon\} \tag{10}$$

where, ε is the failure threshold for performance degradation of an aircraft engine.

Then, the reliability evaluation for performance degradation of an aircraft engine can be depicted as following:

$$R_g(t) = \int_0^\varepsilon f_w(\zeta) d\zeta = \int_0^\varepsilon \frac{\lambda^{kt^v}}{\Gamma(kt^v)} \xi^{kt^v-1} e^{-\lambda\xi} d\xi \tag{11}$$

4.2. Wiener reliability analysis model

The Wiener process from Brown motion in the physics. Denoted degradation amout $w(t)$ as the following:

$$w(t) = \eta t + \delta B(t), \quad t \geq 0 \tag{12}$$

The stochastic process is defined as $\{W(t)\}$,If $t > 0$, $\{W(t)\}$ is defined as Wiener process and satisfy the following assumptions:

I $w(0) = 0$;

II $\{w(t)\}$; $t > 0$ with a stationary independent increments;

III For any $t > 0$, $\{w(t)\}$ is normal random variable, whose mean is 0, the variance is $\delta^2 t$;

For any $0 \leq s < \infty$, $[W(t) - W(s)]$ follow Gaussian distributions $N[\eta(t-s), \delta^2(t-s)]$.

Assuming that the aircraft engine failure threshold is, the failure time of aircraft engine is described as the following:

$$T = \inf\{t; w(t) > w\} \tag{13}$$

Accordingly, at this time aircraft engine opertaion reliability is:

$$R_{wi}(t) = P\{T. > t\} = 1 - F(t) = \Phi\left(\frac{\eta t - \varepsilon}{\delta\sqrt{t}}\right) - \exp\left(\frac{2\eta\varepsilon}{\delta^2}\right)\Phi\left(\frac{-\eta t - \varepsilon}{\delta\sqrt{t}}\right), \; t > 0 \tag{14}$$

The probability distribution function is described as the following:

$$f_{wi}(t) = \frac{1}{\sqrt{2\pi\delta^2 t^3}} \exp\left(-\frac{(\varepsilon - \eta t)^2}{2\delta^2 t}\right) \tag{15}$$

Distribution form for the above is Inverse Gaussian, denoted as $t \sim IG(\mu, \beta)$.

4.3. Reliability analysis of aircraft engines using Bayesian model averaging(BMA)

For the complex system like aircraft engines, single reliability model is difficult to objectively describe the reliability change process. It is necessary to use multi-model technology to comprehensively analysis multi-modes of aircraft engines, which will improve the accuracy of reliability analysis and prediction. To study the mechanism of different reliability models, this paper will use Bayesian model averaging method. Bayesian model averaging (Bayesian model averaging, BMA) is a probability forecast approach that is proposed recently and is used in multi-mode collection. The forecast probability density function (PDF) of a particular variable in BMA, is a weighted average of a single model forecast probability distribution after deviation correction, and the weight is the corresponding model's posterior probability which represents each model's relative forecast skill in the model training phase. The secondary use of condition monitoring data and event data can be achieved through BMA technology. And this not only solves the problem of reliability analysis based on a single failures mode, but also solves the problem of interaction of multiple failures modes. Based on the data re-learning, the goal of an accurate analysis of civil aircraft system reliability can be achieved.

The multi-model is described as the following:

$$p(X,\theta_k,M_k)=P(M_k)\,p(\theta_k|M_k)\,p(X|\theta_k,M_k) \tag{16}$$

$k\in\kappa$ represents the index of model, $P(M_k)$ represents the prior density function of M_k, $p(\theta_k|M_k)$ represents the conditional probability of θ_k under the model M_k, $p(X|\theta_k,M_k)$ represents the conditional probability function of event X under the model M_k and the parameter θ_k.

The probability of event X under the model M_k can be computed as following:

$$P(X|M_k)=\int_{\Theta_k} p(,_k|M_k)\,p(X|\theta_k,M_k)\,d\theta_k \tag{17}$$

Using Bayes theorem, the posterior density can be described as following:

$$P(M_k|X)=\frac{P(M_k)P(X|M_k)}{P(X)} \tag{18}$$

The prediction effect is compared the actual value with the prediction value. The weight can be assigned by the Monte-Carlo Markov chain method.

For the aircraft engines, $M=\{M_1,M_2\}$ represents the reliability analysis models M_1 represents the gamma reliability analysis model, M_2 represents the Wiener process reliability analysis model. Operation reliability analysis model for aircraft engines can be described as following:

$$p\left[R|\left(M_1,M_2,R^T\right)\right]=\sum_{j=1}^{2}\rho_j p_j\left(R|\left(M_j,R^T\right)\right) \tag{19}$$

$M_j(j=1,2)$ represents the reliability analysis model which should be averaged, $p_j\left(R|\left(f_j,R^T\right)\right)$ represents the probability density function of single failure model, which is the probabiliy density fuction of failure mode $j(j=1,2)$ under known reliability R. ρ_j represents the posterior probability of failur mode j being best failure mode, which is negative and $\sum_{j=1}^{2}\rho_j=1$, which reflect the contribution degree of each falure mode on reliability analysis.

The posterior expection and variance of reliability by BMA can be described as following:

$$E(R|D)=\sum_{j=1}^{2}p(M_j|D)\cdot E\left[R|M_j,D\right]=\sum_{j=1}^{2}\rho_j M_j \tag{20}$$

$$Var(R|D)=\sum_{j=1}^{2}\rho_j\left(M_j-\sum_{i=1}^{2}\rho_i M_i\right)^2+\sum_{j=1}^{2}\rho_j\sigma_j^2 \tag{21}$$

Where, σ_j^2 is the prediction error of model M_j under data set D. From eq. (21) the prediction variance of BMA include two intem, the first is the dispersion degree in the set, the second is the variance of prediction model itself.

In the paper, we use Markov Monte-Carlo (Markov Chain Monte Carlo, MCMC) simulation algorithm to calculate the failure mode weighting model in BMA model. MCMC is an important method to deal with complex statistical problems, especially for high dimensional integrals by Monte Carlo to compute the posterior distribution density. MCMC algorithm uses a number of different Markov chain, random sampling got based on BMA weights and variance in the likelihood function of weight variables. Considering the model weight itself is random, we assumes the weight is normal distribution. Using Metropolis-Hastings sampling technique, for the probability density function $\pi(\rho_i)$ for the unknown parameters $\rho_i(i=1,2)$. Choose start point $\rho_i^{(0)}$, meet $\pi\left(\rho_i^{(0)}\right)>0$, produce Markov chain according to the following steps iteration:

A. Suppose condition value $\rho_i^{(m-1)}$ at time $m-1$ and get a candidate from suggested density $\pi\left(\rho_i^*\left|\rho_i^{(m-1)}\right.\right)$;

B. Compute acceptance probability of candidate point θ^*,

$$\pi\left(\rho_i^{(m-1)},\rho_i^*\right)=\min\left\{1,\frac{\pi\left(\rho_i^*\right)p\left(\rho_i^{(m-1)}\left|\rho_i^*\right.\right)}{\pi\left(\rho_i^{(m-1)}\right)p\left(\rho_i^*\left|\rho_i^{(m-1)}\right.\right)}\right\} \tag{22}$$

C. Get a random u from $U(0,1)$, if $u<\pi\left(\rho_i^{(m-1)},\rho_i^*\right)$, the candidate point is accepted, and $\rho_i^{(m)}=\rho_i^*$. Otherwise, $\rho_i^{(m)}=\rho_i^{(m-1)}$.

After enough iterations, M-H algorithm makes the Markov chain converges to the target distribution.

5. Example

Table 1 shows the 36 samples which have repaired and replaced engines. There are six parameters have been monitored, which are DEGT (the deviation exhaust gas tempreture), DWF (the deviation of fuel flow), DOP (the deviation of oil pressure), DHPRS (the deviation of high pressure rotor speed), DLPRV (the deviation of the low pressure rotor vibration value) and DHPRV (the deviation of high-pressure rotor vibration value). The engines' TSI (Time Since Installation) and FH (Fight Hour) from the beginning of the monitoring moment can be obtained. From the data of Table 1, the relationship between PDD (Performance Degradation Degree) and the various monitoring parameters can be extracted by the FVSM. In Table 1, the former 24 samples are as training samples and the latter 12 samples are as test samples.

The training samples comparison between predictive values and real values are shown in Fig. 2 and the test samples comparison between predictive values and real values are shown in Fig. 3. As far as the comparison between the real value and predictive value by Fig. 2 and Fig. 3, there are good effectiveness of prediction. By computation, the total predictive error is below 10% , and the result satisfy the basic demand of performance degradation evaluation of aircraft engines.

By collecting 9 samples condition monitoring parameters of some on-wing aircraft engines, the performance degradation degree can be calculated . Then, the performance degradation degree can be used as input variable, the gamma reliability model and the Wiener reliability model are used to analyze reliability of aircraft engine, respectively.

Table 1. Key performance monitoring parameters for some aircraft engines

Monitoring point	DEGT	DWF	DOP	FHPRS	DLPRV	ZVB2R	TSI(FH)	PDD
1	7.51	2.54	1.89	-7.27	1.06	0.32	4055	0.1192
2	-4.74	3.52	1.92	-5.16	0.52	0.55	7095	0.0459
3	-0.03	2.03	1.19	-8.33	0.57	0.37	7801	0.0378
4	8.04	5.16	1.69	-7.74	0.24	0.57	3331	0.1176
5	7.77	7.80	2.12	-6.81	0.86	0.46	3832	0.1207
6	4.69	2.66	1.83	-3.76	0.31	0.51	3282	0.1028
⋮	⋮	⋮	⋮	⋮	⋮	⋮	⋮	⋮
32	4.23	4.83	1.96	-58.92	0.17	0.62	3397	0.096
33	14.28	5.25	1.63	-2.03	0.78	0.94	1422	0.1572
34	11.38	3.14	1.63	4.19	0.23	0.74	3330	0.1465
35	8.24	3.17	2.18	9.78	1.05	0.76	1954	0.1185
36	9.12	3.37	1.78	6.89	0.31	0.46	6752	0.1290

Table 2. The reliability parameters and reliability analysis results by different reliability models

No	Running time t_i(FH)	Gamma reliability model				Wiener reliability model				R_{BMA}
		a_i	b_i	ρ_G	R_G	η_i	δ_i	ρ_W	R_W	
1	493	1.31	36815	0.179	0.9970	1.042×10^{-5}	1.556×10^{-3}	0.821	0.9970	0.9970
2	1052	1.28	34921	0.358	0.9904	1.711×10^{-5}	1.163×10^{-3}	0.642	0.9909	0.9907
3	1707	1.26	33028	0.419	0.9796	1.757×10^{-5}	8.823×10^{-4}	0.581	0.9726	0.9755
4	2109	1.25	32392	0.525	0.9720	1.660×10^{-5}	7.608×10^{-4}	0.475	0.9686	0.9704
5	2805	1.23	36053	0.576	0.9630	1426×10^{-5}	6.432×10^{-4}	0.424	0.9608	0.9621
6	3206	1.22	35216	0.647	0.9541	1.560×10^{-5}	5.289×10^{-4}	0.353	0.9525	0.9535
7	3924	1.19	36893	0.751	0.9401	1.626×10^{-5}	3.777×10^{-4}	0.249	0.9370	0.9393
8	4740	1.18	37029	0.415	0.9243	1.688×10^{-5}	2.060×10^{-4}	0.585	0.9207	0.9222
9	5595	1.16	38351	0.392	0.9080	1.698×10^{-5}	5.142×10^{-5}	0.608	0.9030	0.9050

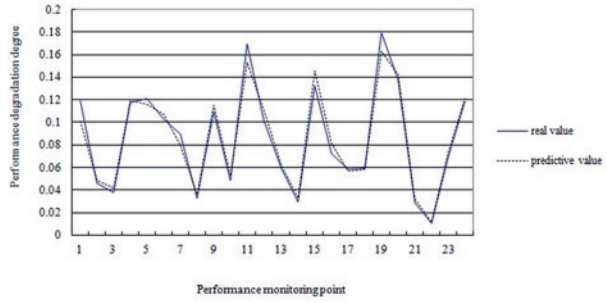

Fig. 2. Performance degradation degree comparison between predictive values and real values on tranning samples

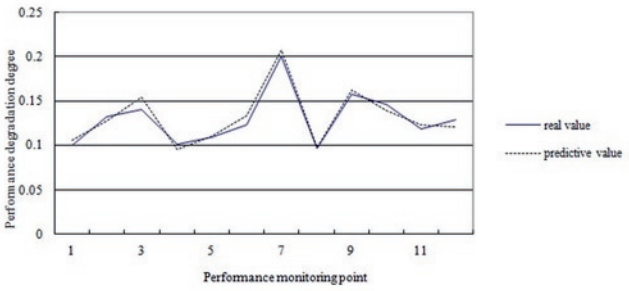

Fig. 3. Performance degradation degree comparison between predictive values and real values on test samples

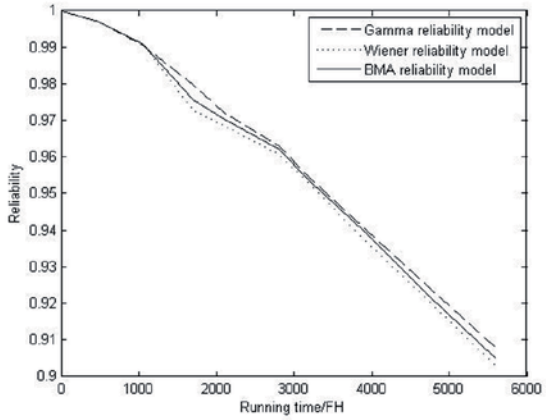

Fig. 4. Reliability curve of different reliability model s on aircraft engines

The parameters of Gamma reliability model and Wiener reliability model are shown in Table 2.

At the same time, BMA are used to calculated the each model weight, then the reliability model of aircraft engine can be calculated integrated Gamma reliability model and Wiener reliability model into one framework. The computation results by different reliability model are also shown in Table 2. The reliability comparison among Gamma reliability model, Wiener reliability model and BMA reliability model are shown in Fig. 4. From Fig. 4, BMA reliability model are averaged by Gamma reliability model and Wiener reliability model. Fig. 5 gives the probability density function of Gamma reliability model

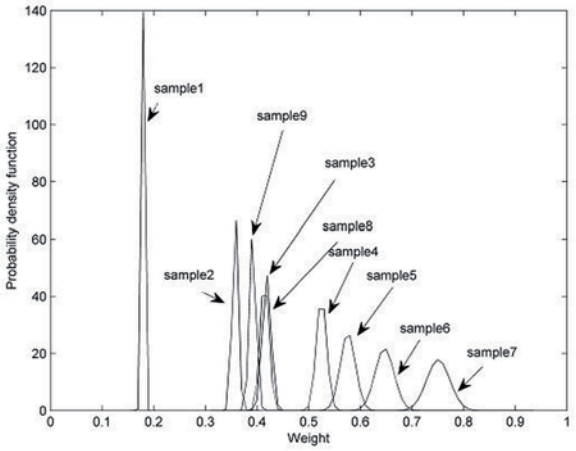

Fig. 5. Probability density function of weight on Gamma reliability model

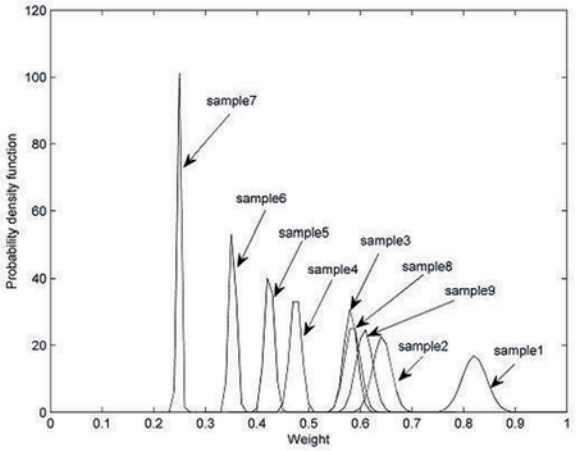

Fig. 6. Probability density function of weight on Wiener reliability model

weight. Fig. 6 gives the probability density function of Wiener reliability model weight.

For the three alternative models, the Gamma reliability model and Wiener reliability model represent the different failure mode. BMA reliability model represent the different failure modes into one framework by computing the different reliability model weight. So, BMA can really analyze the mechanism of action between the different failure modes through learning different data. The advantages of the model are that it has higher forecast accuracy and it can effectively avoid the reliability overestimate or underestimate.

6. Conclusion

In this paper, the mechanism of different failure modes aircraft engines has been analyzed. Fuzzy support vector machine (FVSM) method are used to fuse condition monitoring information. The reliability analysis models including Gamma process model and Wiener process model, respectively for different failure modes, have been presented. Furthermore, these two models have been integrated on the basis of competing failures' mechanism. BMA has been used to analyze the impacts of different failure modes on aircraft engines' reliability. A reliability evaluation model for competing failures has been proposed, and the traditional model of competing failures has been transformed. This method not only can make full use of condition monitoring information, but also can analyze the mechanism and transforming relationship between different failure modes through data learning. The method should be studied further.

Acknowledgement

The research work was supported by National Natural Science Fund of China(U1233115, 71401073).

References

1. Bagdonavičius V, Bikelis A & Kazakevičius V et al. Analysis of joint multiple failure mode and linear degradation data with renewals. Journal of Statistical Plaaning and Inference 2007;137(7): 2191-2207, http://dx.doi.org/10.1016/j.jspi.2006.07.002.
2. Bedford T, Dewan I , Meileijson I. The signal model: A model for competing risks of opportunistic maintenance. European Journal of Operational Research 2011; 214(3):665-673, http://dx.doi.org/10.1016/j.ejor.2011.05.01.
3. Bocchetti D, Giorgio M & Guida M et al. A competing risk model for the reliability of cylinder lines in marine Diesel engines. Reliability Engineering and System Safety 2009; 94(8):1299-1307, http://dx.doi.org/10.1016/j.ress.2009.01.010.
4. Chen B E, Lramer J L & Greene M H. Competing risk analysis of correlated failure time data. Biometrics 2008; 64(1):172-179, http://dx.doi.org/10.1111/j.1541-0420.2007.00868.x.
5. Cheng M Y, Hoang N D, et al. A novel time-dependent evolutionary fuzzy SVM inference model for estimating construction project at completion. Engineering Application of Artificial Intelligence 2012; 25(3):744-752, http://dx.doi.org/10.1016/j.engappai.2011.09.02.
6. Chinnam RB. On-line reliability estimation for individual components using statistical degradation signal models. Quality and Reliability Engineering International 2002; 18(1): 53–73, http://dx.doi.org/10.1002/qre.45.
7. Cobel J B. Merging data sources to predict remaining useful life-An automated method to identify prognostic parameters. University of Teenessee, Knoxville 2010.
8. Elwany A H , Gebraeel N Z. Sensor driven prognostic models for equipment replacement and spare part s inventory. IIE Transactions 2008; 40(7) : 629-639, http://dx.doi.org/10.1080/0740817070173081.
9. Hong D H, Hwang C. Support vector fuzzy regression machines. Fuzzy sets and systems 2003 ; 138 (2-1):271-281.
10. Kenneth P. Measuring the Performance of a HUM System - the Features that Count. Proceeding of Third International Conference on Health and Usage Monitoring - HUMS2003 . Australia: DSTO Platforms Sciences Laboratory; 2003.
11. Kikuchi T, Abe S. Comparison between error correcting output codes and fuzzy vector machines. Pattern Recognition Letters 2005; 26(12): 1937-1945, http://dx.doi.org/10.1016/j.patrec.2005.03.014.
12. Kundu D& Sarhan A M. Analysis of incomplete data in presence of competing risks among several groups. IEEE Transactions on Reliability 2006 ;55(2):262 – 269, http://dx.doi.org/10.1109/TR.2006.874919.
13. Lehmann A. Joint modeling of degradation and failure time data. Journal of Statistical Planning and Inference 2009;139(5):1693–1706, http://dx.doi.org/10.1016/j.jspi.2008.05.02.

14. Li J A, Wu Y, Keung Lai K, et al. Reliability estimation and prediction of multi-state components and coherent systems. Reliability Engineering & System Safety 2005; 88(1): 93-98, http://dx.doi.org/10.1016/j.ress.2004.07.010.
15. Lu H, Kolarik WJ& Lu S. Real time performance reliability prediction. IEEE Transactions on Reliability 2001; 50 (4) : 353-357, http://dx.doi.org/10.1109/24.983393.
16. Pareek B, Kundu D, Kumar S. On progressively competing risks data for Weibull distributions. Computational ststistics and data analysis 2009; 53(12-1):4083-4094.
17. Park C, Kulasekera K B. Parametric inference of incomplete data with competing risks among several groups. IEEE Transactions on Reliability 2004; 53(1):11–21, http://dx.doi.org/10.1109/TR.2003.821946.
18. Peng H, Feng Q M, Coit D W. Reliability and maintenance modeling for systems subject to multiple dependent competing failure process. IIE Transactions 2011; 43(5):12-22.
19. Polpo A, Sinha D. Correction in Bayesian nonparametric estimation in a series system or a competing-risk model. Statistics and Probability Letters 2011; 81(12):1756-1759, http://dx.doi.org/10.1016/j.spl.2011.07.023.
20. Salinas-Torres V, Pereira C , Tiwari R. Bayesian nonparametric estimation in a series system or a competing risks model. Journal of Nonparametric Statistics 2002; 14(4):449-458, http://dx.doi.org/10.1080/10485250213114.
21. Sapankevych N, Sankar R. Time series prediction using support vector machines: a survey. Computation Intelligence Magazine, IEEE 2009; 4(2):24-38, http://dx.doi.org/10.1109/MCI.2009.932254.
22. Suarez E L, Duffy M I, Gamache R N et al. Jet engine life prediction systems integrated with prognostics health management. Proceeding of IEEE Aerospace Conference;2004.
23. Su C, Zhang Y. System reliability assessment based on Wiener process and competing failure analysis. Journal of Southeast University2010; 26(4):554-557.
24. Sugier J, AnderS gJ. Modelling and evaluation of deterioration process with maintenance activities. Eksploatacja i Niezawodnosc – Maintenance and Reliability 2013; 15 (4): 305–311.
25. Vapnik, V. The nature of statistical learning theory. Springer-Berlag, New York, 1995, http://dx.doi.org/10.1007/978-1-4757-2440-0.
26. Wang C P, Ghosh M. Bayesian analysis of bivariate competing risks model with covariates. Journal of Statistical Planning and Inference2003; 115(2-1):441-459.
27. Xing L D, Levitin G. Combinatorial analysis of systems with competing failures subject to failure isolation and propagation effects. Reliability Engineering and System Safety 2010 ; 95(11):1210-1215, http://dx.doi.org/10.1016/j.ress.2010.06.014.

Jun GAO
Department of Management
Shijiazhuang Mechanical Engineering College
Shijiazhuang, Hebei 050003, China

Huawei WANG
College of Civil Aviation
Nanjing University of Aeronautics and Astronautics
Nanjing, Jiangsu210016, China

E-mails: guaguaguagua@163.com, huawei@nuaa.edu.cn

Article citation info:
BIENIAŚ J, SUROWSKA B, JAKUBCZAK P. Influence of repeated impact on damage growth in fibre reinforced polymer composites. Eksploatacja i Niezawodnosc – Maintenance and Reliability 2015; 17 (2): 194–198, http://dx.doi.org/10.17531/ein.2015.2.4.

Jarosław BIENIAŚ
Barbara SUROWSKA
Patryk JAKUBCZAK

INFLUENCE OF REPEATED IMPACT ON DAMAGE GROWTH IN FIBRE REINFORCED POLYMER COMPOSITES

WPŁYW UDERZEŃ WIELOKROTNYCH NA ROZWÓJ USZKODZENIA KOMPOZYTÓW POLIMEROWYCH WZMACNIANYCH WŁÓKNAMI*

The study presents the problems of the influence of repeated low velocity and low energy impacts on damage growth in carbon and glass fibre reinforced high strength polymer composite. The laminate response to impacts was analyzed, the types of damages and their interrelations were identified as well as damages mechanisms were described for tested laminates subjected to repeated impacts. The following conclusions have been drawn on the basis of completed tests: (1) composite materials with polymer matrix reinforced with continuous glass and carbon fibres demonstrate limited resistance to repeated impacts. The laminates resistance to impacts depends mainly on the properties and type of components, particularly in case of reinforcing fibres, orientation of layer under the influence of external impact; (2) tested laminates with carbon fibres are characterized by lower resistance to repeated impacts than laminates with glass fibres. This is proved by the curves of laminate response to impacts, wider damage area and tendency to laminate structure perforation as a result of repeated impacts; (3) repeated impacts lead to damage growth mainly through propagation of damage initiated in initial impacts phase. Delaminations and matrix cracks belong to the basic mechanisms of damages in composite materials; (4) composite damage propagates with increasing number of impacts in fibres orientation direction, particularly in lower composite layers. Further impacts may result in higher stress concentration and higher initiation energy causing the damage growth in various areas of the material. Further impacts increase the damage leading to gradual growth of damages initiated before.

***Keywords**: composites, repeated impact, NDT, damage.*

W pracy przedstawiono problematykę wpływu powtarzających się uderzeń o niskiej prędkości i niskiej energii na rozwój uszkodzenia wysokowytrzymałych kompozytów polimerowych wzmacnianych włóknem węglowym oraz szklanym. Dokonano analizy odpowiedzi laminatu na uderzenia, zidentyfikowano rodzaj i relacje pomiędzy uszkodzeniami, a także przedstawiono mechanizmy uszkodzenia w badanych laminatach poddanych wielokrotnym uderzeniom. Na podstawie przeprowadzonych badań wykazano że: (1) materiały kompozytowe o osnowie polimerowej wzmacniane ciągłymi włóknami szklanymi i węglowymi wykazują ograniczoną odporność na wielokrotne uderzenia. O odporności laminatów na uderzenia decydują głównie właściwości i rodzaj komponentów, w szczególności włókien wzmacniających, orientacja warstw pod wpływem oddziaływania zewnętrznego; (2) badane laminaty z włóknami węglowymi charakteryzują się niższą odpornością na wielokrotne uderzenia w porównaniu do laminatów z włóknem szklanym. Świadczą o tym charakterystyki odpowiedzi laminatu na uderzenia, większy obszar uszkodzenia oraz skłonność do perforacji struktury laminatu w wyniku wielokrotnych uderzeń; (3) uderzenia wielokrotne powodują rozwój uszkodzenia głównie przez propagację uszkodzenia inicjowanego w czasie początkowych uderzeń. Do podstawowych mechanizmów uszkodzenia materiałów kompozytowych należą rozwarstwienia oraz pęknięcia osnowy; (4) wraz ze wzrostem liczby uderzeń uszkodzenie kompozytu propaguje w kierunku ułożenia włókien, szczególnie dolnych warstw kompozytu. Kolejne uderzenia mogą powodować większą kumulację naprężeń oraz energii inicjacji odpowiedzialnej za rozwój uszkodzenia w różnych obszarach materiału. Kolejne uderzenia powodują zwiększanie uszkodzenia prowadząc do stopniowego rozwoju wcześniej zainicjowanych uszkodzeń.

***Słowa kluczowe**: kompozyt, uderzenia, badania nieniszczące, uszkodzenie.*

1. Introduction

Fibre reinforced polymer composites (FRP) are widely used in many sectors, mainly in aeronautical engineering for the elements of aircraft, including the skins. Due to the trends towards maintenance costs reduction and towards the reduction of aircraft structure weight, the demand level for durable and damage resistance materials is high [25]. These requirements are met by the composite structures characterized i.a. by high level of static and fatigue strength, low density and corrosion resistance. However they are characterized by limited resistance to impacts with concentrated force [19].

The resistance to impacts is particularly important in the scope of aircraft operation and their reliability. The aircraft are required to perform determined functions at determined time and operation conditions. The impacts may lead to degradation of individual structural elements and consequently to the reduction of their service life and finally affecting the safety level [21].

The dynamic loads may be generated in course of flight and ground handling of aircrafts e.g. by falling tools, collisions with load-

(*) Tekst artykułu w polskiej wersji językowej dostępny w elektronicznym wydaniu kwartalnika na stronie ***www.ein.org.pl***

ing and technical support trucks, foreign bodiesthrust by the engine and aircraft wheels and tyres damage [22, 25]. As can be drawn from technical literature [25], completed repairs of critical elements of airframes in passenger aircrafts (Boeing 747) in course of their scheduled service life were caused by three types of damages i.e. mainly fatigue cracks, corrosion processes and damages caused by impacts; the latter encompassed about 13%. The impacts may lead to complete perforation of composite structure and to generation of invisible damages with numerous delaminations, cracks in composite matrix and in reinforcing fibres [1, 8, 11, 24].

At the moment several published research papers relate to the evaluation of the influence of the impacts on damage growth in composite aircraft structures. Richardson et al. [19] described the influence of low velocity impacts on fibre composites damage degree vs. impact velocity and energy. From the conclusions presented by the authors it appears that the damages of composite structures caused by the impacts can be subdivided into damages propagating inside the structure and external damages e.g. in the form of perforations. The type of matrix and reinforcement material belong to the factors determining the character of damage as well as the damage initiation and propagation mechanisms at the impact. The carbon fibres, due to their higher brittleness and lower deformation in comparison with glass fibres or aramid fibres, are characterized by the lowest resistance to impacts [19]. The composites reinforced with carbon fibres are characterized by degradation of fibres as prevailing form of damage. But fibre glass reinforced composites are characterized by extensive delaminations in composite structure [3]. Other authors [11, 20, 21, 23, 26] evaluated the influence of fibres orientation in the form of reinforcement on composites damage growth, the influence of damage on their static and fatigue strength as well as the influence of environment conditions on the resistance of composite materials to impacts.

There are only a few studies describing the evaluation of the influence of repeated impact on damage growth in composite materials which may be found in the literature [10, 17, 18]. The authors indicate that repeated impact may contribute to significant damage growth in composite structures through the cyclical growth of originally initiated damages [9]. The influence of repeated impact is tested mainly in the low energy range in order to evaluate the damage growth progress from insignificant material degradation level [23]. It is justified in case of airspace materials exposed to this type of damages and difficult diagnostics thereof. Aymerich et al. [5] demonstrated that even an insignificant internal structure degradation after single impact may lead to the reduction of composite strength even by several tens of percent. However in case of repeated impact, the influence of damage growth on the reduction of mechanical properties has been not evaluated yet.

The article presents the problem of the influence of repeated impact with low – velocity and low energy on damage growth in high strength polymer composites reinforced with carbon and glass fibres. The laminate response to impacts was analyzed, the types of damages and their interrelations were identified as well as damages mechanisms were described for tested laminates subjected to repeated impacts.

2. Materials and methods

Two types of composites were tested. Carbon fibre reinforced composites (CFRP) and glass fibre reinforced composites (GFRP). The FRP panels examined in this study were made of AS7J carbon/epoxy prepreg (0.13 mm of thickness, Hexcel, USA) and R-glass fibres with epoxy resin prepreg (0.25 mm of thickness, Hexcel, USA). The nominal fibre content was about 60 vol.%. The lay-up scheme of both laminates was $(0_6/90_6)$ for CFRP and $(0_3/90_3)$ for GFRP. Total thickness of laminates was 1.5 mm.

The composite laminates were produced in the Department of Materials Engineering - Lublin University of Technology by using autoclave method (Scholz Maschinenbau, Germany). The cure cycle was carried out at a heating rate of 2°C/min up to 135°C and held at this temperature for two hours. The pressure and the vacuum used were 0.4 and 0.08 MPa, respectively.

The low-energy impact test were performed at room temperature using a drop-weight impact tester (InstronDynatup 9340) with possibility of recording force-time curves. Impact tests were carried out according to ASTM D7136 standard [17]. Samples dimension was 150x100 mm. A hemispherical impactor tip with a diameter of 38.1 mm and mass of 1.4 kg was used. Impact with 5 J energy were conducted one, three and five times in the same point.

Laminates after one, three and five impacts were tested with macroscopic observations and NDT methods for damage area evaluation. As NDT the ultrasonic pulse-echo method were used (OmniScan MX, Olympus, Japan).

3. Results and discussion

The typical force-time (*f-t*) and force-deflection (*f-d*) curves recorded during impact are shown in Figure 1.

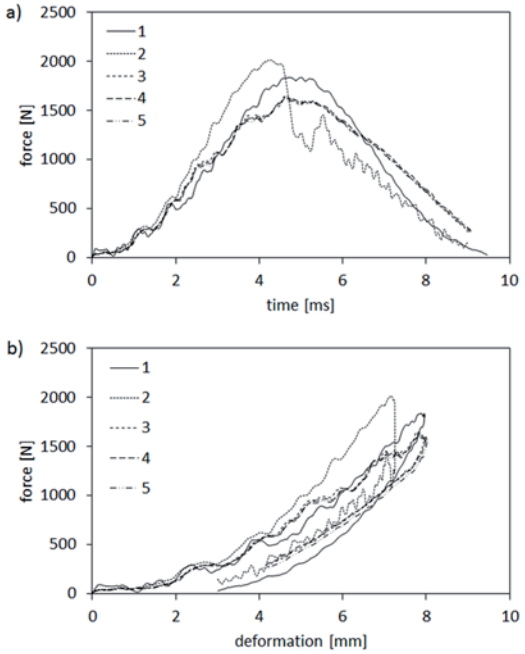

Fig. 1. Force - time (a,c) and force - deflection (b,d) curves of fibre reinforced polymer composites after multiple impact

There are four specific phases of force change on force vs. time curves as a result of impact: the initial stage of system stabilization, force increase stage, time of reaching the maximum force, *Fm* (Fig. 1a,c) and force decrease stage thereafter. Described force-time stages gradually represent the material reaction to the influence of the impactor, regardless of the successive impact number. The first stage of the force value variations is responsible for the system stabilization. The force fluctuations in this stage represent the vibration of the material – impactor system [16]. The force fluctuations observed in the next force increase stage are insignificant and mainly associated with local degradation of composite structure [16]. The matrix degradation and propagation of delaminations, particularly on the boundaries of layers with different orientation of reinforcing fibres occur in case of low impact energies [11]. The smoothest force curve is observed at the first impact. Therefore it can be found that an insignificant and local damage is observed. Such circumstances are observed in case of glass

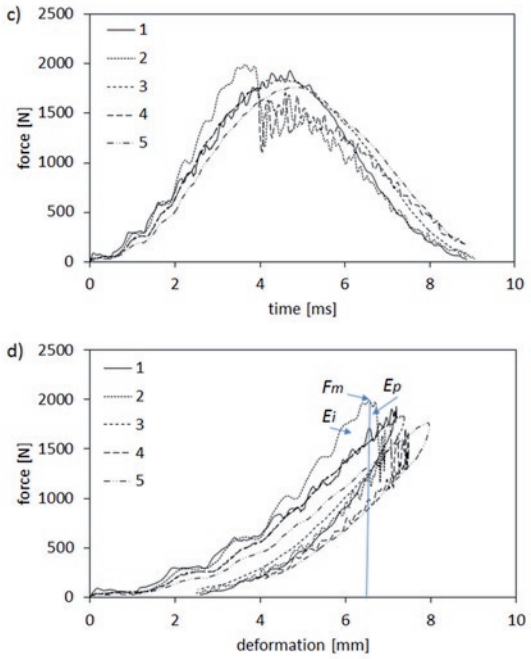

Fig. 1. (continued) Force - time (a,c) and force - deflection (b,d) curvesof fibre reinforced polymer composites after multiple impact

and carbon composite.The local damages are initiated in the material without significantly reducing the composite rigidity but simultaneously reducing the whole energy of initial impacts. However the successive impacts lead to the occurrence of higher force fluctuations at the time of impact. Particularly the second and the third impact lead to the sudden reduction of force after *Fm* is reached (Fig. 1a,c). The sudden reductions of force after the achievement of the maximum value of force have been also observed by other authors [16, 21, 22]. They concluding that such variations of the force values rather indicate to more extensive and advanced material damage, finally reducing the rigidity and strength of the material. The reduction of force was higher after the second impact in glass composite (about 50%) (Fig. 1a).The reduction in carbon composite (force reduction by about 40% after *Fm* is reached) was lower but characterized by greater number of fluctuations (Fig. 1c). Probably observed difference was caused by various degradation mechanisms in these composites under the influence of impact.The next impacts (i.e. fourth and fifth impact) are not characterized by intensive force fluctuations at the time of impact (Fig. 1a,c). It may mean that the next impacts do not initiate any new areas of significant structure degradation any more. However the damages initiated before are gradually growing and absorbing most energy in course of the next impacts. Simultaneously the measured time of material – impactor contact is similar for all the impacts. Chakraborty [9] found that the nucleation of the new delamination locations occurs in carbon composites as a result of repeated impacts. However the area damage previously is also an intensively growing area. Nevertheless the shape of force curve in course of further impacts indicates that the damage growth is rather stable and relatively uniform without any further drastic loss of material cohesion. Morais et al. [17] and Found et al. [10] obtained similar results in their evaluations of the damage growth vs. number of impacts, indicating the stable growth of composite damage vs. increased number of impacts. The interrelations between the successive *f-t* curves are similar in the both types of materials, which indicates their similar trends in the scope of damage propagation as a result of repeated impacts.

The analysis of relationship between the initiation energy (E_i) and degradation propagation energy (E_p) is possible on the basis of the force – deflection (*f-d*) curves for the material in course of successive impacts [2, 13, 22]. Among others Sohn et al. [22] described that the point of reaching maximum force (F_m) determines the areas of damage initiation energy until the maximum force point is reached, as well as the area of damage propagation energy after reaching the maximum force point (Fig. 1d). All absorbed energy during impact (E_a) is the sum of initiation energy (E_i) and propagation energy (E_p). The aggregate energy absorbed (E_a) by the material during the dynamic impact is the sum of the initiation (E_i) and propagation energy (E_p). Similar energy relationships have been found in these curves *(f-d)* for glass and carbon composites (Fig. 1b,d). From among all the impacts, the second and third impacts maintain noticeably different relationships between E_i and E_p. The value of force which may be observed in these cases is slightly higher at similar deflection and the value of propagation energy field is lower. It can be caused by the significant damage growth at these impacts. The shape of the force – deflection (*f-d*) curves does not indicate to any laminates perforations. It has been denoted that the value of the impactor deflection at the total force reduction after the impact is close to the initial value of the deflection observed for the force stage (after the system stabilization stage). This relationship is similar for the both materials cases. Similar values of the deflections after each next impact indicate to the lack of permanent deformation of composites. Higher values of the material deflections in case of impact have been recorded for fibre glass composites because, among others, the elongation to break for glass fibres (R type) is about two times higher than in case of high strength carbon fibres. Brittle and highly durable materials will be characterized by higher initiation energy and lower propagation energy. Carbon fibre reinforced composites can be matched to this group. On the other hand, more plastic but less durable materials will have lower initiation energy and higher propagation energy. This may also concern composites containing glass fibres [6]. Higher deformation may result in higher interlayer delaminations in composites due to higher values of lateral shear stresses [11]. Higher susceptibility to bending strains in case of impact is associated with lower rigidity characterizing GFRP composites in comparison to CFRP composites.

In order to distinguish responses to repeated impacts in CFRP and GFRP composites, the analysis of their damage was carried out after the successive impact. The macroscopic image of tested samples is shown in Figure 2, where invisible macroscopic damages (BVID), cracks and delaminations were found.

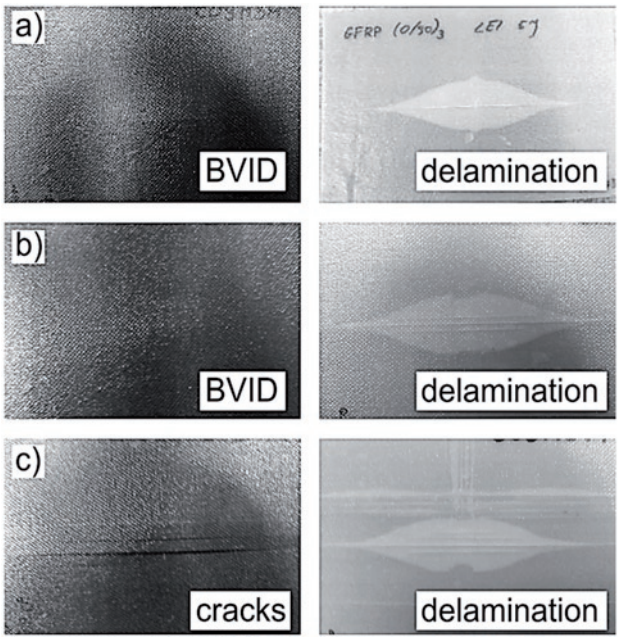

Fig. 2. Macroscopic image of composites plates (CFRP left side and GFRP right side) after one (a), three (b) and five (c) impacts

The damage zone in case of an epoxy carbon composite is characterized by an invisible internal damage. The macroscopic observation of damage propagating in the material is not possible after the first and third impact (Fig. 2a,b). It indicates that occurred damage is an internal damage and may initiate and propagate in the form of delaminations and matrix cracks. This type of damage area after low energy impacts was described in many published testing results [17, 19, 26]. Richardson et al. [19], in his overview study referred to many studies describing this type of damage as Non-Visible Impact Damage (NVID) or Barely Visible Impact Damage (BVID), which nevertheless severely reduces the structural integrity of the component. Barely Visible Impact Damages (BVID) propagate in composite structures mainly in case of low energy impacts [17, 26]. On the basis of executed tests it has been denoted that the damage propagates in external layers at the fifth impact. The breaking of external layer (bottom layer on impact end) is observable along the fibres direction in this layer (Fig. 2c). Longitudinal matrix crack propagated practically through the entire length of sample. Such type of damage is caused by bending strain at impact point but any fibres crack has been not observed in CFRP composite.

In case of the transparent epoxy carbon composite, the macroscopic observation makes it possible to identify the damage after the next impacts (Fig. 2). Extensive delaminations have been detected within the structure after the first impact. The growth of delaminations is conforming with the direction of composite layers in its bottom layers. Bidirectional composite layers system (0/90) caused prevailing delaminations propagation. Delaminations in the laminates subjected to dynamic impact observed on the interface layer with various fibre orientation. Delamination shape is quite oval with the major axis aligned with fibre orientation in the lower layer. According to Richardson et al. [19] delaminations occur in the areas with higher resin content between layers with various orientations. The shape of the delamination results from shear stress distribution around the area surrounding the impactor, low interlayer shear resistance alongside or close to the fibre orientation direction as well as from matrix cracking caused by bending stress [11].

The system 0/90 is characterized by the highest anisotropy of stiffness with prevailing shear stresses in composite.The third and fifth impacts in GFRP composite result in the growth of delaminations and in the occurrence of the matrix cracks also in the external layers of composite. The third impact causes the ignition of the matrix cracks also in 0 direction. The fifth impact causes further propagation ofthese cracks (Fig. 2c). In order to determine the trends in the scope of the damage growth as a result of multiple impacts, the surface area has been determined for composites after the first, third and fifth impact. The damage area growth versus impact number is presented in Figure 3.

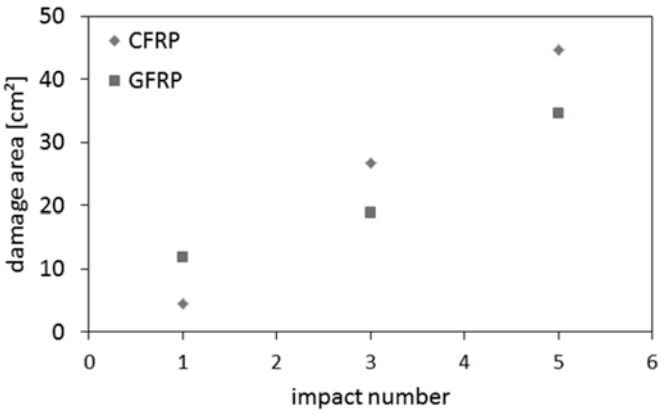

Fig. 3. Damage area growth vs. number of impacts

The analysed damage surface area is one of the most frequently used evaluation criteria for the influence of low velocity impacts on the condition of composite materials structure [4, 14, 22]. The damage surface area determined by means of NDT methods encompasses all detectable types of damage which may occur in the composite structures. Mainly delaminations and cracks belong to this group. The calculations of damage surface areas after the impacts presented in the literature determine the surface area for the largest delamination. In case of systems consisting of fibres with many interface layers with different fibres orientation, the damages occurring in individual layers are not added together [14, 15]. In case of materials under test, the delamination propagates mainly at the boundary between 0 and 90 layers. On the basis of completed measurements it may be concluded that the damage surface area increases after the next impact. In case of CFRP composite a stable growth of damage is noticeable after the next impacts. The damage surface area increases with increasing number of impacts (Fig. 3). In case of CFRP composite, the growth is more dynamic after later impacts. The larger values of surface areas of the damage in carbon composite in case of repeated impacts indicate its lower resistance to this type of loads than in case of glass composites. This trend is caused among others by higher stiffness of CFRP composite (E~131 GPa in 0° direction, E~8 GPa in 90° direction) [25] than GFRP composite (E~56 GPa 0° direction, E~16 GPa in 90° direction) [7]. The greater part of energy can be absorbed by initiation and propagation in carbon composites. But in glass composites, the part of absorbed energy is associated with larger deformation achievable in course of impact. In accordance with data accessible in literature [10], at sufficiently high number of impacts, the growth of damage surface area is characterized by more and more decreasing growth dynamics. Increasing number of impacts leads to fibres degradation and trend to perforations.

4. Conclusions

The following conclusions can be drawn on the basis of executed tests consisting in repeated impacts by means of concentrated force for polymer fibre composite materials:

1. Composite materials with polymer matrix reinforced with continuous glass and carbon fibres demonstrate limited resistance to repeated impacts. The laminates resistance to impacts depends mainly on the properties and type of components, particularly in case of reinforcing fibres and orientation of layers in composite.
2. Tested laminates with carbon fibres are characterized by lower resistance to repeated impacts than laminates with glass fibres. This is proved by the curves of laminate response to impacts, wider damage area and tendency to laminate structure perforation as a result of repeated impacts.
3. Repeated impacts lead to damage growth mainly through the propagation of damage initiated at the time of initial impacts. Delaminations and matrix cracks belong to the basic mechanisms of damage in composite materials.
4. With the increasing number of impacts, the composite damage propagates in fibres orientation direction, particularly in lower layers of composite. Further impacts may lead to increased concentration of stresses and initiation energy responsible for damage growth in various areas of material. The next impacts increase the damage leading to gradual growth of damages initiated previously.

Acknowledgments

The project was financed by the National Science Centre allocated on the basis of the decision No DEC-2012/05/N/ST8/03788.

References

1. Abrate S. Impact on composite structures. Cambridge University Press 1998. Chaper 4, Low-Velocity impact damage; 135-160.
2. Atas C., Sayman O. An overall view on impact response of woven fabric composite plates. Composite Structures 2008; 82: 336-345, http://dx.doi.org/10.1016/j.compstruct.2007.01.014.
3. Aktas M., Atas C., Icten B.M., Karakuzu R. An experimental investigation of the impact response of composite laminates. Composites Structures 2009; 87: 307-313, http://dx.doi.org/10.1016/j.compstruct.2008.02.003.
4. ASTM D7136. Standard test metod for measuring the damage resistance of a fiber-reinforced-polymer matrix composites to a drop-weight impact event. Book of Standards, Volume 15.03, (2005).
5. Aymerich F., Priolo P. Characterization of fracture modes in stiched and unstiched cross-ply laminates subjected to low-velocity impact and compression after impact loading. International Journal of impact Engineering 2008; 35: 591-608, http://dx.doi.org/10.1016/j.ijimpeng.2007.02.009.
6. Beaumont P.W.R., Riewald P.G., Zweben C. Methods for improving the impact resistance of composite materials, in Foreign object impact damage to composites. ASTM STP 568, American Society for Testing and Materials 1974; 134-158.
7. Bieniaś J., Dębski H. Numeryczna analiza tarcz kompozytowych zbrojonych włóknami szklanymi i węglowymi w warunkach złożonego stanu obciążenia. Kompozyty (Composites) 2010; 10:2: 127-132.
8. Cantwell W.J., Curtis P., Morton J. An assessment of the impact performance of CFRP reinforced with high strain carbon fibres. Composite Science and Technology 1986; 25: 133–148, http://dx.doi.org/10.1016/0266-3538(86)90039-4.
9. Chakraborty D. Delamination of laminated fibre reinforced plastic composites under multiple cylindrical impact. Materials and Design 2007; 28: 1142-1153, http://dx.doi.org/10.1016/j.matdes.2006.01.029.
10. Found M.S., Howard I.C. Signle and multiple impact behavior of a CFRP laminate. Composite Structures 1995; 32: 159-163, http://dx.doi.org/10.1016/0263-8223(95)00024-0.
11. González E.V., Maimí P., Camanho P.P., Lopes C.S., Blanco N. Effects of ply clustering in laminated composite plates under low-velocity impact loading. Composites Science and Technology 2011; 71: 805–817, http://dx.doi.org/10.1016/j.compscitech.2010.12.018.
12. Guan Z., Yang Ch. Low-velocity impact and damage process of composite laminates. Journal of Composite Materials 2002; 36: 851-871, http://dx.doi.org/10.1177/0021998302036007512.
13. Hyla I., Lizurek A. Zastosowanie badań dynamicznych do analizy mechanizmu pękania udarowego kompozytów warstwowych. Kompozyty (Composites) 2002; 2: 374-377.
14. Karakuzu R., Erbil E., Aktas M. Damage prediction in glass/epoxy laminates subjected to impact loading. Indian Journal of Engineering and Materials Sciences 2010; 17: 186-198.
15. Kim G., Hong S., Jhang K.Y., Kim G.H. NDE of low-velocity impact damage in composite laminates using ESPI, digital shearography and ultrasound C-scan techniques. International Journal of Precision Engineering and Manufacturing 2012; 13: 869-876, http://dx.doi.org/10.1007/s12541-012-0113-4.
16. Liu D., Raju B.B., Dang X. Impact perforation resistance of laminated and assemled composite plates. International Journal of impact Engineering 2000; 24: 733-746, http://dx.doi.org/10.1016/S0734-743X(00)00021-X.
17. Morais W.A., Monteiro S.N., d'Almeida J.R.M. Evaluation of repeated low energy impact damage in carbon–epoxy composite materials. Composite Structures 2005; 67: 307–315, http://dx.doi.org/10.1016/j.compstruct.2004.01.012.
18. Rajkumar G.R., Krishana M., Narasimha Murthy H.N., Sharma S.C., Vishnu Mahesh K.R. Investigation of repeated low-velocity impact behaviour of GFRP/Aluminium and CFRP/Aluminium laminates. International Journal of Soft Computung and Engineering 2012; 1(6): 50-58.
19. Richardson M.O.W., Wisheart M.J. Review of low-velocity impact properties of composite materials. Composites Part A 1996; 27: 1123-1131, http://dx.doi.org/10.1016/1359-835X(96)00074-7.
20. Sánchez-Sáez S., Barbero E., Navarro C. Compressive residual strength at low temperatures of composite laminates subjected to low-velocity impacts. Composite Structures 2008; 85: 226–232, http://dx.doi.org/10.1016/j.compstruct.2007.10.026.
21. Shyr T.W., Pan Y.H. Impact resistance and damage characteristics of composite laminates. Composite Structures 2003; 62: 193-203, http://dx.doi.org/10.1016/S0263-8223(03)00114-4.
22. Sohn M.S., Hu X.Z., Kim J.K., Walker L. Impact damage characterisation of carbon fibre/epoxy composites with multi-layer reinforcement. Composites: Part B 2000; 31: 681-691, http://dx.doi.org/10.1016/S1359-8368(00)00028-7.
23. Tai N.H., Yipa M.C., Lin J.L. Effects of low-energy impact on the fatigue behavior of carbon/epoxy composites. Composite Science and Technology 1998; 58: 1-8, http://dx.doi.org/10.1016/S0266-3538(97)00075-4.
24. Yang F.J., Cantwell W.J. Impact damage initiation in composite materials. Composite Science and Technology 2010; 70: 336–342, http://dx.doi.org/10.1016/j.compscitech.2009.11.004.
25. Vogelesang L.B., Vlot A.. Development of fibre metal laminates for advanced aerospace structures. Journal of Materials Processing Technology 2000; 103: 1-5. http://dx.doi.org/10.1016/S0924-0136(00)00411-8.
26. Wang S.X., Wu L.Z., Ma L. Low-velocity impact and residual tensile strength analysis to carbon fiber composite laminates. Materials Design 2010; 31: 118–125, http://dx.doi.org/10.1016/j.matdes.2009.07.003.

Jarosław BIENIAŚ
Barbara SUROWSKA
Patryk JAKUBCZAK
Department of Materials Engineering
Mechanical Faculty
Lublin University of Technology
ul. Nadbystrzycka 36, 20-618 Lublin, Poland
E-mail: j.bienias@pollub.pl

Article citation info:
GE D, LI D, LIN M, YANG Y-H. SFRs-Based Numerical Simulation for the Reliability of Highly-coupled DFTs. Eksploatacja i Niezawodnosc – Maintenance and Reliability 2015; 17 (2): 199–206, http://dx.doi.org/10.17531/ein.2015.2.5.

Daochuan GE
Dong LI
Meng LIN
Yan-Hua YANG

SFRS-BASED NUMERICAL SIMULATION FOR THE RELIABILITY OF HIGHLY-COUPLED DFTS

METODA SYMULACJI NUMERYCZNEJ OPARTA NA POJĘCIU ZAKRESÓW USZKODZEŃ SEKWENCYJNYCH SŁUŻĄCA DO OBLICZANIA NIEZAWODNOŚCI UKŁADÓW MODELOWANYCH METODĄ SILNIE SPRZĘŻONYCH DYNAMICZNYCH DRZEW BŁĘDÓW

The failure behaviors of many real-life systems are very complex and sequence-dependent, and can be modeled by highly-coupled dynamic fault trees (DFTs). Existing approaches for solving DFTs, such as Markov state-space-based or inclusion-exclusion based methods all have their disadvantages. They either suffer from the problem of state space explosion or are subjected to the combination explosion. Additionally, Markov-based approaches become unavailable when components follow non-exponential time-to-failure distributions which prevail in real-life systems. To overcome shortcomings of the methods mentioned above, SFRs (Sequence Failure Regions)-Based numerical simulation approach is first proposed. The proposed method is applicable for a generalized cut sequence as well as highly-coupled DFTs modeling non-repairable systems with arbitrary time-to-failure distributed components. The results of the validation example indicate the reasonability of our proposed approach.

Keywords: *highly-coupled DFTs, sequence failure region, arbitrary distributions, numerical simulation.*

Zachowania uszkodzeniowe wielu działających w rzeczywistości układów są bardzo złożone i zależą od sekwencji w jakiej występują uszkodzenia. Zachowania takie można modelować za pomocą silnie sprzężonych dynamicznych drzew błędów (DFT). Istniejące podejścia do rozwiązywania DFT, takie jak metody markowowskie oparte na pojęciu przestrzeni stanów i metody oparte na zasadzie włączeń i wyłączeń mają swoje ograniczenia:albo borykają się z problemem eksplozji przestrzeni stanów albo są narażone na eksplozję kombinatoryczną. Dodatkowo, podejścia markowowskie stają się niedostępne, gdy elementy składowe mają niewykładnicze rozkłady czasu do uszkodzenia, co ma miejsce w przeważającej części układów spotykanych w rzeczywistości. Aby przezwyciężyć mankamenty powyższych metod, zaproponowano metodę symulacji numerycznej opartą na pojęciu zakresów uszkodzeń sekwencyjnych (sequence failure regions, SFR). Proponowana metoda znajduje zastosowanie w modelowaniu systemów nienaprawialnych o elementach, które charakteryzuje arbitralnie przyjęty rozkład czasu do uszkodzenia. Metodę można stosować w modelowaniu opartym zarówno na uogólnionej sekwencji niezdatności (generalizedcut sequence), jak również silnie sprzężonych DFT. Wyniki uzyskane w przedstawionym przykładzie potwierdzają zasadność proponowanego przez nas podejścia.

Słowa kluczowe: *silnie sprzężone dynamiczne drzewo błędów, zakres uszkodzeń sekwencyjnych, arbitralnie przyjęty rozkład, symulacja numeryczna.*

1. Introduction

Dynamic fault trees have been presented [6, 7, 8] as an extension of traditional static fault trees with the aim to model complex systems having sequence- and function-dependent failure behaviors. Such modeling techniques are widely used in Nuclear Power Plant (NPP) industry, space mission systems and chemical process plant where systems safety is emphatically focused. The problem is how to quantify the reliability index of complex systems modeled by highly-coupled DFTs. Markov-based methods [1, 15, 19] have been proved to be efficient and versatile. But these approaches are subjected to the problem of "state space explosion". To mitigate the scale of the system state space to be considered, some hierarchical methods [11, 23, 24] (i.e., modularization techniques) are developed. Such hierarchical approaches can greatly reduce the Markov state space using a "divide and conquer" strategy under some circumstances. Yet these techniques become unfeasible when the independent sub-modules are placed under a dynamic gate. The IE-based approach [14, 18] is a combinatorial method based on enumerating the complete minimal cut sequences/sets (MCSs) of a considered DFT. In contrast to Markov-based methods, the IE-based approach is efficient since it does not require highly-coupled DFTs converted to state space forms. To calculate the reliability of a considered DFT, the complete minimal cut sequences/sets would be rewritten using the inclusion-exclusion principle. Given that a DFT has n MCSs, the IE formula would generate 2^n-1 logic products. Hence the IE-based approach is vulnerable to the problem of combinatorial explosion.

To overcome the shortcomings of existing methods mentioned above, sequence failure regions (SFR)-based numerical simulation

approach is first proposed. This method relies on the complete MCSs, i.e., minimal cut sequence set (MCSS), of a considered DFT. Some achievements for finding the MCSS have been made as: Liu et al [13] proposed a series of inference rules to generate the MCSS of a given DFT; Shrestha et al [20] put forward a sorting algorithm to enumerate the MCSS; Merle et al [17] presented several temporal operators and related operation rules to deduce the structure function of a DFT which finally can be reduced to the MCSS. Actually, as to numerical simulation for reliability of a system modeled by DFT, some researchers [2, 9, 12, 25] have made prospective studies and applications. Unfortunately, such simulation-based methods are just based on different dynamic gates. To the author's knowledge, no articles have presented a numerical simulation approach for a generalized minimal cut sequence (GMCS) as well as a highly-coupled DFT. By contrast, the proposed method is considered to be a universal numerical simulation tool for non-repairable DFTs with arbitrary distributions, including a GMCS. Results of the validation example indicate the proposed method is reasonable.

2. Basic Concepts

2.1. Dynamic Logic Gates

To characterize sequence- and function-dependent failure behaviors existing in many real-life systems, Dugan et al [5, 6] introduced several new dynamic gates, such as Sequence Enforcing (SEQ) gate, Priority AND (PAND) gate, Function Dependent (FDEP) gate, Cold Spare (CSP) gate, Warm Spare (WSP) gate, and Hot Spare (HSP) gate. Such dynamic gates are integrated into static fault trees to form DFTs. Hence, the occurrence of a considered DFT not only depends on the combinations of basic events, but also depends on their failure orders. Figure 1 shows the commonly-used dynamic gates for a DFT.

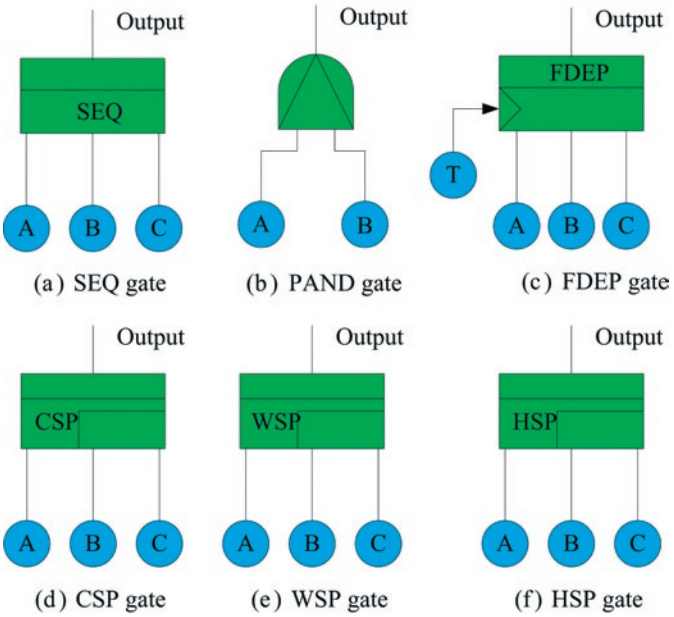

Fig. 1 Dynamic gates used in DFT

(a) SEQ gate: SEQ gate forces the input events to fail in a left to right order. That is to say an input event never fails before all the input ones to its left hand have already failed. As to the SEQ gate in Fig.1 (a), the only failure sequence is that A fails first, then B fails, and C fails last.

(b) PAND gate: PAND gate is used to detect certain failure sequences of input events [7]. In a PAND gate, different failure orders are permitted, but only a specific failure sequence (from left to right) leads to the fire of the gate. For the PAND gate in Fig.1 (b), there exist two failure sequences: A fails first, then B fails; B fails first, the A fails. But only the former failure order can lead to the firing of the gate.

(c) FDEP gate: FDEP gate characterizes a situation where the occurrence of a trigger event may cause other dependent components unusable, but the occurrence of dependent events does not have any effect on the trigger event. As to the FDEP gate in Fig.1 (c), T is a trigger event of which the occurrence would cause dependent components A, B, and C unusable.

(d) CSP gate: CSP gate allows modeling of the case where the spares stay at an unpowered state when the primary event operates normally, That is to say cold spares never fail before the ones to its left. Hence, the failure behavior of CSP gate is similar to SEQ gate. For the CSP gate in Fig.1 (d), A as the primary event fails first, then the first cold spare B fails, at last the second cold spare C fails.

(e) WSP gate: Unlike CSP gate, the spares in WSP gate operate at a reduced power when the primary event operates successfully. It means that warm spares can fail independently in standby state and all of the possible failure sequences may occur.

(f) HSP gate: In a HSP gate, the spares run at a full power when the primary event operates normally. Its failure behaviors are logically equivalent to static AND gate.

2.2. Minimal Cut Sequence Set

In DFTs, the occurrence of the top event not only relies on the combinations of basic events, but also relies on their failure sequences. Apparently, traditional minimal cut set is unable to express such failure behaviors. To solve this problem, the concept of a minimal cut sequence (MCS) is first proposed by Tang and Dugan [21] to express the minimal failure sequence that leads to an occurrence of a DFT's top event. As to a general MCS, it can be written as $A_1 \rightarrow A_2 \rightarrow \cdots \rightarrow A_n$ where the capital letter A_i represents a basic event denoting an occurrence of a failure, and the symbol "$\rightarrow$" indicates the order of failure precedence, i.e., the left event failing before the right one. Hence, a specific MCS expresses what events and in what ways of failing sequences that leads to an occurrence of a DFT or a module. As mentioned in section 1.1, the failure of the spares always depends on the primary event. To reflect such dependence in a MCS expression, three special symbols are introduced as: ${}^{0}_{A_i}A_j$, ${}^{\alpha}_{A_i}A_j$ and ${}^{1}_{A_i}A_j$. The symbol ${}^{0}_{A_i}A_j$ represents A_j fails as a cold spare of A_i and means A_j fails after A_i, ${}^{\alpha}_{A_i}A_j$ denotes A_j fails as a warm spare of A_i in standby state and implies A_j fails before A_i fails, and ${}^{1}_{A_i}A_j$ indicates A_j fails as a warm spare of A_i after replacing the faulty primary unit and implies A_j fails after A_i. Obviously, as to a non-repairable DFT, the complete MCSs, i.e., minimal cut sequence set (MCSS), can characterize its failure logic. Supposing that a DFT has n MCSs, the system failure logic (SFL) can be expressed by:

$$\begin{aligned} \mathrm{SFL}_{\mathrm{MCSS}} &= \mathrm{MCS}_1 \cup \mathrm{MCS}_2 \cup \cdots \cup \mathrm{MCS}_n \\ &= \bigcup_{i=1}^{n} \mathrm{MCS}_i \end{aligned} \tag{1}$$

where, MCS_i represents the i_{th} MCS. Hence, for the WSP gate in Fig.1 (e), the SFL can be written as:

$$\begin{aligned} \mathrm{SFL}_{\mathrm{MCSS}} = &\left(\mathrm{A} \rightarrow {}^{1}_{\mathrm{A}}\mathrm{B} \rightarrow {}^{1}_{\mathrm{B}}\mathrm{C}\right) \cup \left(\mathrm{A} \rightarrow {}^{\alpha}_{\mathrm{B}}\mathrm{C} \rightarrow {}^{1}_{\mathrm{A}}\mathrm{B}\right) \cup \left({}^{\alpha}_{\mathrm{A}}\mathrm{B} \rightarrow \mathrm{A} \rightarrow {}^{1}_{\mathrm{A}}\mathrm{C}\right) \\ &\cup \left({}^{\alpha}_{\mathrm{A}}\mathrm{B} \rightarrow {}^{\alpha}_{\mathrm{A}}\mathrm{C} \rightarrow \mathrm{A}\right) \cup \left({}^{\alpha}_{\mathrm{B}}\mathrm{C} \rightarrow \mathrm{A} \rightarrow {}^{1}_{\mathrm{A}}\mathrm{B}\right) \cup \left({}^{\alpha}_{\mathrm{B}}\mathrm{C} \rightarrow {}^{\alpha}_{\mathrm{A}}\mathrm{B} \rightarrow \mathrm{A}\right) \end{aligned} \tag{2}$$

3. SFLD and SFR

3.1. Sequence Failure Logic Diagram

A specific MCS is just a logic relationship and only provide qualitative information. To reflect the inner failure mechanisms of a MCS, a sequence failure logic diagram (SFLD) is introduced which is a graphical description of a MCS. In a SFLD, the failure behavior of an event is expressed by its time to failure, the vertical axis represents the failure sequence of a specific MCS where each event is placed according to its position located in the considered MCS, and the horizontal axis indicates time. To illustrate such SFLD, a complex DFT is introduced in Fig. 2, where three typical dynamic gates are highly-coupled together.

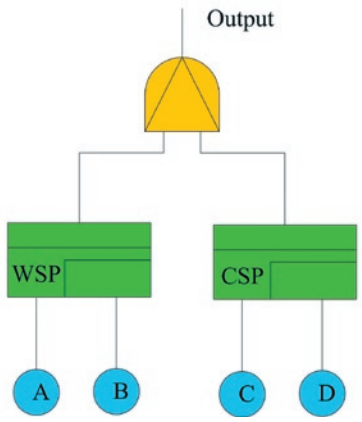

Fig. 2. An illustrative example

Applying the inference rules presented in Ref. [13], the SFL of the considered DFT can be expressed as:

$$\begin{aligned}\mathrm{SFL_{MCSS}} = &\left(\mathrm{A}\to {}_{\mathrm{A}}^{1}\mathrm{B}\to\mathrm{C}\to {}_{C}^{0}\mathrm{D}\right)\cup\left(\mathrm{A}\to\mathrm{C}\to {}_{\mathrm{A}}^{1}\mathrm{B}\to {}_{C}^{0}\mathrm{D}\right)\\ &\cup\left(\mathrm{C}\to\mathrm{A}\to {}_{\mathrm{A}}^{1}\mathrm{B}\to {}_{C}^{0}\mathrm{D}\right)\cup\left({}_{\mathrm{A}}^{\alpha}\mathrm{B}\to\mathrm{A}\to\mathrm{C}\to {}_{C}^{0}\mathrm{D}\right)\\ &\cup\left({}_{\mathrm{A}}^{\alpha}\mathrm{B}\to\mathrm{C}\to\mathrm{A}\to {}_{C}^{0}\mathrm{D}\right)\cup\left(\mathrm{C}\to {}_{\mathrm{A}}^{\alpha}\mathrm{B}\to\mathrm{A}\to {}_{C}^{0}\mathrm{D}\right)\end{aligned} \quad (3)$$

In this article, we use τ_{X} to represent the time-to-failure of X in a working state at full power, and use $\overline{\tau_{\mathrm{X}}}$ to express the time-to-failure of X in a standby state at a reduced power. Assume the system starts at t=0, and mission time is t_m. Take the first MCS $\mathrm{A}\to {}_{\mathrm{A}}^{1}\mathrm{B}\to\mathrm{C}\to {}_{C}^{0}\mathrm{D}$ for example: A starts at t=0, and then fails in the region (0, t_m); B also starts at t=0, first it must survive the primary A, and then fails after A in working state; C starts at t=0 as well, and then fails after B; D starts after C fails, and then fails before t_m. And its SFLD is drawn in Fig. 3.

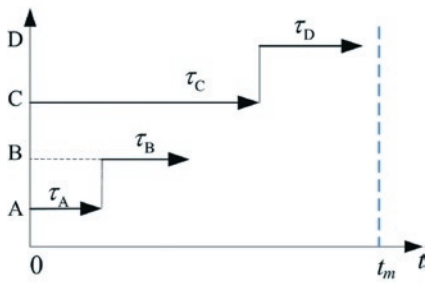

Fig. 3. SFLD for $A\to {}_{A}^{1}B\to C\to {}_{C}^{0}D$

3.2. Sequence Failure Region

In our previous paper [10], we put forward probabilistic model-based multi-integration formulas to quantify a GMCS and pointed out that the occurrence probability of a GMCS can be obtained by doing integration of the random variables over the valid sequential intervals referring to time to failure of components involved in a GMCS. That is, if and only if the events occur in their valid intervals that leads to occurrence of the considered GMCS. Hence, for a GMCS, such valid sequential intervals can be considered as a sequence failure region (SFR). As to a GMCS: $\mathrm{A}_1\to\mathrm{A}_2\to\cdots\to\mathrm{A}_n$, the SFLD with a SFR is shown in Fig. 4.

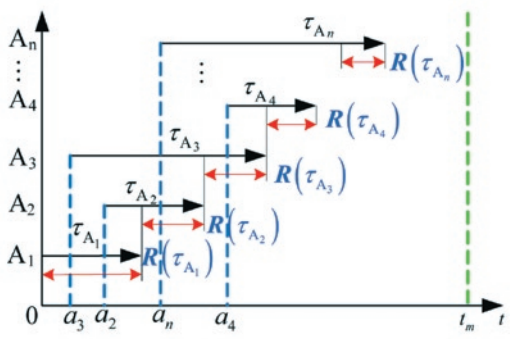

Fig. 4. SFLD for a GMCS with a SFR

The $R(\tau_{\mathrm{A}_i})$ represents the valid failure region of τ_{A_i} ; $a_i(1<i\le n)$ denotes the start point of A_i considering some components do not need to start at t=0, such as cold spares, and $0\le a_i\le t_m$. As discussed in Ref. [10], the $R(\tau_{\mathrm{A}_i})$ can be always expressed by:

$$\begin{aligned}&R\left(\tau_{\mathrm{A}_1}\right)=\left\{\tau_{\mathrm{A}_1}\mid\ 0<\tau_{\mathrm{A}_1}<t_m\right\}\\ &R\left(\tau_{\mathrm{A}_2}\right)=\left\{\tau_{\mathrm{A}_2}\mid\ \phi_2\left(\tau_{\mathrm{A}_1},a_2,t_m\right)<\tau_{\mathrm{A}_2}<\varphi_2\left(\tau_{\mathrm{A}_1},a_2,t_m\right)\right\}\\ &\quad\vdots\\ &R\left(\tau_{\mathrm{A}_i}\right)=\left\{\tau_{\mathrm{A}_i}\mid\ \phi_i\left(\tau_{\mathrm{A}_1},\tau_{\mathrm{A}_2},\cdots,\tau_{\mathrm{A}_{i-1}},a_2,a_3,\cdots,a_{i1},t_m\right)<\tau_{\mathrm{A}_i}\right.\\ &\qquad\left.<\varphi_i\left(\tau_{\mathrm{A}_1},\tau_{\mathrm{A}_2},\cdots,\tau_{\mathrm{A}_{i-1}},a_2,a_3,\cdots,a_{i1},t_m\right)\right\}\qquad 1<i\le n,\end{aligned} \quad (4)$$

where ϕ_i/φ_i is a linear expression representing the lower/upper boundary of $R(\tau_{\mathrm{A}_i})$, and the explicit expressions of ϕ_i and φ_i are defined by the specific MCS. Note that the Eq. (4) never considers the cases where some warm spares fail after replacing the faulty primary units. For such cases, the reference [10] points out that it is okay to add prerequisites that the warm spares survive the faulty ones in a standby state. Supposing that A_2 is a warm spare of A_1, then the Eq. (4) should be rewritten as:

$$\begin{aligned}&R\left(\tau_{\mathrm{A}_1}\right)=\left\{\ \tau_{\mathrm{A}_1}\mid\ 0<\tau_{\mathrm{A}_1}<t_m\right\}\\ &R\left(\overline{\tau_{\mathrm{A}_2}}\right)=\left\{\ \overline{\tau_{\mathrm{A}}}\mid\ \tau_{\mathrm{A}_1}<\overline{\tau_{\mathrm{A}}}<\infty\right\}\\ &R\left(\tau_{\mathrm{A}_2}\right)=\left\{\ \tau_{\mathrm{A}_2}\mid\ \phi_2\left(\tau_{\mathrm{A}_1},a_2,t_m\right)<\tau_{\mathrm{A}_2}<\varphi_2\left(\tau_{\mathrm{A}_1},a_2,t_m\right)\right\}\\ &\quad\vdots\\ &R\left(\tau_{\mathrm{A}_i}\right)=\left\{\ \tau_{\mathrm{A}_i}\mid\ \phi_i\left(\tau_{\mathrm{A}_1},\tau_{\mathrm{A}_2},\cdots,\tau_{\mathrm{A}_{i-1}},a_2,a_3,\cdots,a_{i1},t_m\right)\right.\\ &\qquad\left.<\tau_{\mathrm{A}_i}<\varphi_i\left(\tau_{\mathrm{A}_1},\tau_{\mathrm{A}_2},\cdots,\tau_{\mathrm{A}_{i-1}},a_2,a_3,\cdots,a_{i1},t_m\right)\right\}\quad 1<i\le n\end{aligned} \quad (5)$$

As to the MCS expressed by Eq. (4), the corresponding SFR can be expressed as:

$$\mathrm{SFR}_{\mathrm{A}_1\to\mathrm{A}_2\cdots\to\mathrm{A}_n}=\left\{\boldsymbol{\Omega}_f \mid \bigcap_{i=1}^{n} R\left(\tau_{\mathrm{A}_i}\right)\right\}, \tag{6}$$

where the $\boldsymbol{\Omega}_f$ indicates the failure region of the considered MCS. And for the MCS expressed by Eq. (5), the failure region can be represented by:

$$\mathrm{SFR}_{\mathrm{A}_1\to{}_{\mathrm{A}_1}{}^{1}\mathrm{A}_2\cdots\to\mathrm{A}_n}=\left\{\boldsymbol{\Omega}_f \mid R\left(\overline{\tau_{\mathrm{A}_2}}\right)\bigcap_{i=1}^{n} R\left(\tau_{\mathrm{A}_i}\right)\right\}. \tag{7}$$

For a general MCS with k ($k<n$) warm spares failing in a working state at full power, its failure region can be also obtained inferentially from the Eq. (5). Here, we assume that a DFT has m MCSs, and the sequence failure region of the j_{th} MCS can be expressed as $\boldsymbol{\Omega}_{f-j}$. According to the Eq. (1), the system sequence failure regions (SFRs) can be expressed as:

$$\mathrm{SFRs}_{system}=\left\{\boldsymbol{\Omega}_{sys} \mid \bigcup_{j=1}^{m}\boldsymbol{\Omega}_{f-j}\right\}, \tag{8}$$

where the $\boldsymbol{\Omega}_{sys}$ represents the failure region of a system.

4. SFRs-based Numerical Simulation Approach

4.1. Theoretical Foundation-CMC

The crude Monte Carlo (CMC) method is often used to study a probability problem with a statistical simulation through converting the analytical model under study into a probabilistic model. Given a set of variables sector $\mathbf{X}=\{x_1, x_2, \ldots, x_n\}$, and $\mathbf{X}\subseteq R^{(n)}$ where $R^{(n)}$ represents a n-dimensional real space, the failure probability of which the $\mathbf{X}$ occur in the failure region $\boldsymbol{\Omega}_f=\{\mathbf{X}\mid g(\mathbf{X})<0\}$ can be calculated by:

$$P_f=\int_{-\infty}^{+\infty} I\left[g(\mathbf{X})\right]f(\mathbf{X})d(\mathbf{X}), \tag{9}$$

where $f(\mathbf{X})$ is the joint probability density function (PDF), and $I[g(\mathbf{X})]$ is an indicator function which is defined as:

$$I\left[g(\mathbf{X})\right]=\begin{cases}1 & g(\mathbf{X})<0\\ 0 & others\end{cases} \tag{10}$$

However, the Eq. (9) cannot be solved analytically when the explicit inverse function of $f(\mathbf{X})$ does not exist. Thanks to the rule of large numbers, the P_f can be evaluated approximately by a statistical simulation approach, i.e., CMC method, using the following statistical expression:

$$\widehat{P_f}=\frac{1}{N}\sum_{i=1}^{N} I\left[g(\mathbf{X})\right] \tag{11}$$

Based on the Central Limit Theorem, the following equation must hold for any nonnegative number x:

$$\lim_{N\to\infty} P\left(\frac{\left|P_f-\widehat{P_f}\right|}{\sigma^2_{\widehat{P_f}}}<x\right)=\frac{1}{\sqrt{2\pi}}\int_{-x}^{x} e^{-\frac{t^2}{2}}dt, \tag{12}$$

where $\sigma^2_{\widehat{P_f}}$ is the variance of the $\widehat{P_f}$, and $\sigma^2_{\widehat{P_f}}=\frac{1}{\mathrm{N}}\widehat{P_f}\times\left(1-\widehat{P_f}\right)$. As N is chosen large enough, we can get the approximate equation as:

$$\lim_{N\to\infty} P\left(\left|P_f-\widehat{P_f}\right|<x\sqrt{\widehat{P_f}\cdot\left(1-\widehat{P_f}\right)\cdot 1/N}\right)=1-\alpha, \tag{13}$$

where $(1-\alpha)$ is the confidence level. Then, the absolute error for the $\widehat{P_f}$ can be evaluated by:

$$\varepsilon_a=\left|P_f-\widehat{P_f}\right|\le z_{\alpha/2}\cdot\sqrt{\widehat{P_f}\cdot\left(1-\widehat{P_f}\right)\cdot 1/N}, \tag{14}$$

where the $z_{\alpha/2}$ is the quantile of the $\alpha/2$. And the relative error for the $\widehat{P_f}$ can be also expressed by:

$$\varepsilon_r=\frac{\left|P_f-\widehat{P_f}\right|}{P_f}\le z_{\alpha/2}\cdot\sqrt{\frac{1-\widehat{P_f}}{N\widehat{P_f}}} \tag{15}$$

Considering $\widehat{P_f}$ is a small amount, the simulation number N is approximately expressed as:

$$N\approx\frac{z^2_{\alpha/2}}{\widehat{P_f}\cdot\varepsilon_r^2} \tag{16}$$

Obviously, given a relative error ε_r and a confidence level $(1-\alpha)$, the simulation number N is inversely proportional to $\widehat{P_f}$. In general, the value of ε_r is set as 0.1 and the confidence level is defined as 0.95, then the simulation number N should be chosen as: $N=384/\widehat{P_f}$.

4.2. SFRs-based CMC for a highly coupled DFT

To explain the proposed method, the GMCS indicated by Eq. (4) is considered once again. The analytical solution to the considered GMCS can be obtained using a sequential multi-integration by:

$$\begin{aligned}P_{GMCS\_f}&=\int_{R^{+(\mathrm{n})}} I\left[h(\boldsymbol{\tau})\right]f(\boldsymbol{\tau})d\boldsymbol{\tau}\\&=\int_{R\left(\tau_{A_1}\right)}d\tau_{A_1}\int_{R\left(\tau_{A_2}\right)}d\tau_{A_2}\cdots\int_{R\left(\tau_{A_2}\right)}\prod_{i=1}^{n} f_i(\tau_{\mathrm{A}_i})d\tau_{A_n}\end{aligned} \tag{17}$$

Where $R^{+(n)}$ represents a n-dimensional positive real space; $f(\boldsymbol{\tau})$ is the joint PDF; $f_i(\tau_{\mathrm{A}_i})$ is the PDF of τ_{A_i}; $I[h(\boldsymbol{\tau})]$ is the indicator function, and $I[h(\boldsymbol{\tau})]=1$ given $\boldsymbol{\tau}\subseteq\boldsymbol{\Omega}_f$ (SFR), otherwise, $I[h(\boldsymbol{\tau})]=0$. Yet the primitive function $f_i(\tau_{\mathrm{A}_i})$ cannot be found explicitly in some cases, and the Eq. (17) is calculated numerically. Note that the numerical computation complexity would reach up $\mathrm{O}(\mathrm{M}^n)$, where the M is the number of equal slices of dividing $R_i(\tau_{\mathrm{A}_i})$. Hence, solving such n-embedded integral by numerical integration method is very time consuming, especially a result with a high accuracy is needed.

In this section, a SFRs-based CMC for simulating the occurrence probability of GMCS is proposed. Suppose that the simulated sample

point for $\tau=\{\tau_{A_1},\tau_{A_2},\cdots,\tau_{A_n}\}$ is denoted as: $\hat{\tau}=\{\widehat{\tau_{A_1}},\widehat{\tau_{A_2}},\cdots,\widehat{\tau_{A_n}}\}$.

Then, the P_{GMCS_f} can be evaluated using the CMC method as:

$$\hat{P}_{GMCS\_f}=\frac{1}{N}\sum_{i=1}^{N}I\left[h\left(\hat{\tau}\right)\right] \tag{18}$$

where the statistical indicator function (SIF) $I[h(\hat{\tau})]$ is defined as:

$$I\left[h\left(\hat{\tau}\right)\right]=\begin{cases}1 & \left(\widehat{\tau_{A_1}}\in R\left(\tau_{A_1}\right),\widehat{\tau_{A_2}}\in R\left(\tau_{A_2}\right),\cdots,\widehat{\tau_{A_n}}\in R\left(\tau_{A_n}\right)\right)\\ 0 & others\end{cases} \tag{19}$$

The simulated sample point $\hat{\tau}$ can be obtained using a random sampling approach. Given that the cumulative distribution function (CDF) of τ_{A_i} is $F(\tau_{A_i})$, then the τ_{A_i} can be always expressed as:

$$\tau_{A_i}=G\left(F\left(\tau_{A_i}\right)\right) \tag{20}$$

And the sample point can be sampled by

$$\widehat{\tau_{A_i}}=G\left(\varepsilon\right) \tag{21}$$

where ε is a uniform random number used to replace $F(\tau_{A_i})$ in Eq. (20), and ε can be obtained in [0,1] by any standard random number generator.

Suppose that τ_{A_i} follows the exponential distribution with a failure rate parameter λ, and the $f(\tau_{A_i})$, $F(\tau_{A_i})$ of τ_{A_i} provided by the following expressions:

$$f\left(\tau_{A_i}\right)=\lambda e^{-\lambda\cdot\tau_{A_i}},$$
$$F\left(\tau_{A_i}\right)=1-e^{-\lambda\cdot\tau_{A_i}}.$$

Then the τ_{A_i} is expressed as a function of $F(\tau_{A_i})$, i.e., G(F(τ_{A_i})).

$$\tau_{A_1}=G\left(F\left(\tau_{A_i}\right)\right)=\frac{1}{\lambda}\ln\left(\frac{1}{1-F\left(\tau_{A_1}\right)}\right). \tag{22}$$

The simulation procedures for the SFRs-based CMC for a GMCS are shown in ***Algorithm 1***.

Algorithm 1.

Step 1. Let the failure number N_{GMCS_f}=0.

Step 2. Generate the sample point $\hat{\tau}=\{\widehat{\tau_{A_1}},\widehat{\tau_{A_2}},\cdots,\widehat{\tau_{A_n}}\}$.

Step 3. Calculate $I\left[h(\hat{\tau})\right]$.

Step 4. If the $I\left[h(\hat{\tau})\right]$=1, then $N_{GMCS\_f}=N_{GMCS\_f}+1$.

Step 5. Transfer to Step 2 in case that the total simulated number does not equal a given N.

Step 6. Output the occurrence probability of a given GMCS:

$$P_{GMCS\_f}=\frac{N_{GMCS\_f}}{N}.$$

Now we will discuss how to simulate a highly coupled DFT. As mentioned in section 3.2, an occurrence of any MCS can lead to the failure of a considered highly coupled DFT, and system failure region can be expressed as: $SFRs_{system}=\left\{\Omega_{sys}\,|\bigcap_{j=1}^{m}\Omega_j\right\}$. Given that the DFT under study is non-repairable, the system fails only once in its lifespan. That is to say at most one MCS occurs in a simulation. Given that a DFT has m MCSs and n input events. Then referring to the ***Algorithm 1*** for a GMCS, the complete SFRs-based numerical simulation procedures for a highly coupled DFT are shown in Fig. 5, where the P_{syst_f} is the simulated unreliability of a considered system.

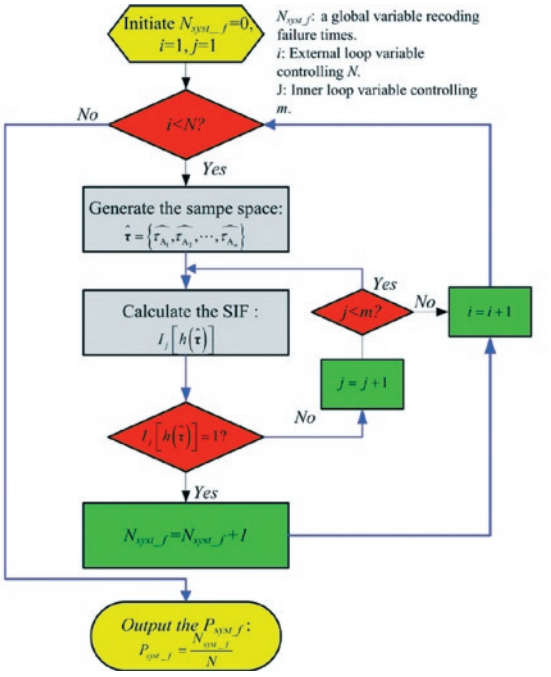

Fig. 5. Flow chart of SFRs-based CMC method for a highly coupled DFT

4.3. Validation Example

In this section, the illustrative example in Fig. 2 is considered for a validation purpose. In the first case, suppose that all of the components are exponentially time-to-failure distributed, and their failure parameters are listed in Table 1.

Table 1. failure parameters of components in Fig. 2

Component	A	B	C	D
Failure rate (/h)	5.5e-3	1.0e-3(s*) 7.0e-3(a*)	3.5e-3	5.0e-3

s*: the failure rate in a standby state.

a*: the failure rate in a working state.

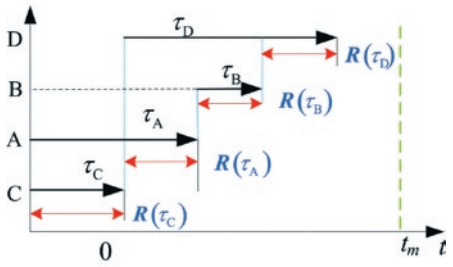

Fig. 6. SFLD of $C\rightarrow A\rightarrow {}^{1}_{A}B\rightarrow {}^{0}_{C}D$

Given the MCSS expressed by Eq. (3), the SFLD of each MCS with its SFR can be drawn. As an illustration, we present the specific SFLD of the third MCS with its SFR (Fig. 6), which represents the

most complex failure behavior. Note that the component B failing in working state means that the B must survive the primary A. That is to say $\overline{\tau_B} > \tau_A$. Hence, the SFR of the MCS can be expressed as $\Omega_f = R(\tau_C) \cap R(\tau_A) \cap R(\overline{\tau_B}) \cap R(\tau_B) \cap R(\tau_D)$, where,

$$R(\tau_C) = (0,\ t_m),$$
$$R(\tau_A) = (\tau_C,\ t_m),\ R(\overline{\tau_B}) = (\tau_A, +\infty),$$
$$R(\tau_B) = (0, t_m - \tau_A),\ R(\tau_D) = (\tau_A + \tau_B - \tau_C, t_m - \tau_C).$$

Similarly, the specific SFRs for other MCSs are also obtained. Now we use the SFRs-based simulation method to evaluate the reliability of the considered example system. For a comparison purpose, the Markov-based approach is adopted as a benchmark. The results obtained by the two methods are shown in Fig. 7.

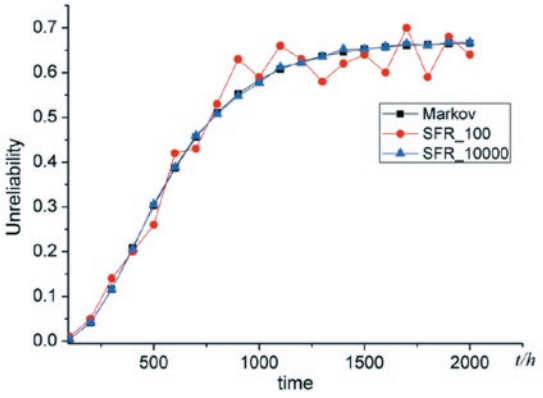

Fig. 7. Comparisons of the results under exponential distributions

With the simulation sample size N=100, the ε_r (relative error) of the results obtained by SFRs-based simulation and Markov-based approaches is notable. Yet with the increasing of N, ε_r becomes smaller and smaller. As the simulation sample size reaches up 1.0e+4, the results derived from the two methods are matched.

Without loss of generality, the case with general distributions is also considered, where A follows the Weibull distribution with arguments (shape: m=2, scale: η=80), B is the exponential distribution (s*=4.0e-3/h, a*=2.0e-2/h), C follows the lognormal distributions with parameters (μ=15, δ=10) and D is the exponential distribution with failure rate 1.5e-2/h. Given that the Markov approach is not applicable for non-exponential distribution situations, we adopt the IE-based method as a benchmark where each cut sequence is solved numerically. The results obtained at different mission times are listed in Table 2.

Table 2 comparisons of results for general distributions

Mission time (h)	SFRs-based simulation method	IE- based method
100	0.014566	0.014932
200	0.046863	0.047943
300	0.064775	0.065541
400	0.075933	0.076180
500	0.083211	0.083529

Obviously, the results obtained by the SFRs-based simulation method are in good agreement with those derived by the IE-based method. For the computational efficiency, the average computing time for SFRs-based approach (N=1.0e+6) is about 3.09 *mins*, yet the average computing time for IE-based method (M=100) reaches up 324.7 *mins*. Hence compared with the IE-based method, the SFRs-based simulation approach is more efficient.

5. A case study

The WPS (water pumping system) is a critical-safety system for PWR (Pressurized Water Reactor) and it is used to carry of the reaction heat of reactor core by pumping coolant from the water source. If the system loses its function, it will cause a severe consequence. Hence, it is quite significant to analyze the reliability of the system.

The system is operational requiring at least two pumps to be successful. The system consists of three pumps among which pump A and B are operating under normal circumstances, and C as a cold spare stays at an unpowered state. Once some pump fails, the pump C will be started by a switch D to replace the faulty one. The switch is controlled by a sensor system E which is used to detect the failure signal of the active pumps. As soon as a failure signal is received, the sensor system E will activate the cold spare C through controlling the switch D. Hence, the WSP fails if pump A or B fails after D or E fails. In addition, the sensor system E is dependent on the power suppliers P_1 and P_2 among which P_1 is the primary supplier and P_2 is a cold spare as P_1. The simplified DFT model of the system is shown in Fig. 8.

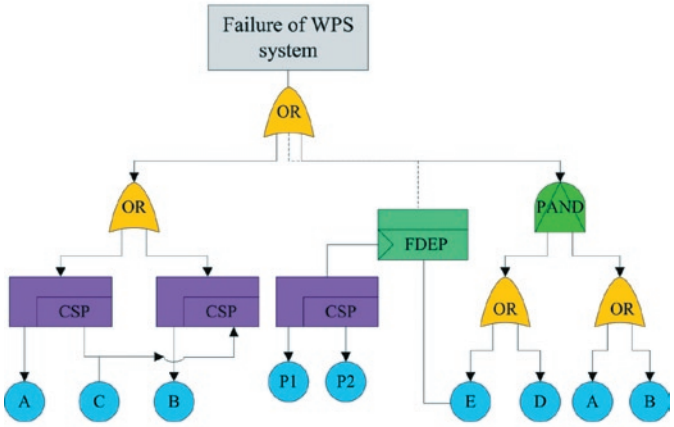

Fig. 8. Simplified DFT model of WPS system

Given that the time to failure of pumps follows the lognormal distributions, the failure parameters are: mean: $\mu_{A,B,C}$=15, variances: σ_A=25, σ_B=30, σ_C=35. The switch D follows the uniform distribution in the lifespan [0, 10^4 h]. Power suppliers P_1 and P_2 are the Weibull distributions with the arguments: m_{P_1}=2 (shape), η_{P_1}=80 (scale); m_{P_2}=2 (shape), η_{P_2}=100 (scale), and the sensor system E is exponentially distributed with failure rate λ_E=1.0e-4. The system failure logic can be expressed using its MCSS by:

$$\begin{aligned} SFL_{MCSS} = P_1 \rightarrow {}^{0}_{P_1}P_2 \rightarrow A + P_1 \rightarrow {}^{0}_{P_1}P_2 \rightarrow B + D \rightarrow A + D \rightarrow B \\ + A \rightarrow {}^{0}_{A}C + B \rightarrow {}^{0}_{B}C + E \rightarrow A + E \rightarrow B + A \rightarrow B + B \rightarrow A \end{aligned} \quad (23)$$

Considering that there exist non-exponential distributions in the considered system, Markov-based approaches are not longer applicable. The IE-based method is suitable for such case, yet the IE (inclusion-exclusion) formula would generates 2^{10}-1 (1023) logic terms,

Table 3. the results obtained by SFR simulation

Mission time	N_1=1.0e+4		N_2=1.0e+5		N_3=1.0e+6	
	Unreliability	Comp. time	Unreliability	Comp. time	Unreliability	Comp. time
500 (h)	0.3843	2.4s	0.3846	26.3s	0.3851	277.4s
1000 (h)	0.3938	2.2s	0.3935	20.5s	0.3932	274.5s
1500 (h)	0.3991	2.4s	0.3979	27.4s	0.3982	291.8s

and the logic terms should be further expanded into disjoint cut sequences as the repeated events appearing in different MCSs. Hence, to calculate the unreliability of the WPS system, the IE-based approach would produce tens of thousands cut sequences. It is a very tedious and error-prone process, and furthermore, as mentioned in section 4.2, the computational complexity to solve a cut sequence would reach up O (M^n). Hence, it is very time-consuming by applying the IE-based method. To make an efficient analysis of the system reliability, the SFRs-based simulation approach is applied. The results at different sampling sizes are listed in Table 3. Obviously, the SFRs-based simulation method can offer reasonable solutions efficiently.

6. Conclusion

In this paper, the SFRs-based numerical simulation approach is proposed to analyze a highly coupled DFT on its MCSS. This method is not only applicable for a DFT, but also applicable for a GMCS which is a significant contribution of this paper. The complete simulation procedures are provided. The results of the case study indicate the proposed method can offer reasonable solutions with an affordable computing time.

As to low probability events, the proposed method is time-consuming, which can be viewed as a disadvantage of this approach. In the feature work, we are focused on advanced sampling techniques to improve its efficiency, such as importance sampling [4, 22], adaptive importance sampling [16, 3], and etc.

Acknowledgment

The Authors would like to acknowledge the financial support by the National Science and Technology Major Project (2011ZX06004-024).

References

1. Alam M, Al-Sagaf UM. Quantitative reliability evaluation of repairable phased-mission systems using Markov approach. IEEE Transactions on Reliability 1986; R-35(5):498-503, http://dx.doi.org/10.1109/TR.1986.4335529.
2. Alireza Ejlali, Seyed Ghassem Miremadi. FPGA-based Monte Carlo simulation for fault tree analysis. Microelectronic Reliability 2004; 44(6): 1017-1028, http://dx.doi.org/10.1016/j.microrel.2004.01.016.
3. Au SK, Beck JL. A new adaptive importance sampling scheme for reliability calculations. Structural Safety 1999; 21(2): 135-158, http://dx.doi.org/10.1016/S0167-4730(99)00014-.
4. Au SK, Beck JL. Important sampling in high Dimensions. Structural Safety, 2003; 25(2): 139-163, http://dx.doi.org/10.1016/S0167-4730(02)00047-4
5. Coppit D, Sullivan KJ, Dugan JB. Formal semantics of models for computational engineering: a case study on dynamic fault tree. Proceeding of the 11th International Symposium on Software Reliability Engineering 2000; 270-282.
6. Dugan JB, Bavuso SJ, Boyd MA. Dynamic fault-tree models for fault-tolerant computer systems. IEEE Transactions on Reliability 1992; 41(3): 363-377, http://dx.doi.org/10.1109/24.159800.
7. Dugan JB, Bavuso SJ, Boyd MA. Fault Trees and Sequence Dependencies. Proceedings of Annual Reliability and Maintenance Symposium 1990; 286-293, http://dx.doi.org/10.1109/ARMS.1990.67971.
8. Dugan JB, Sullivan KJ, Coppit D. Developing a low-cost high-quality software tool for dynamic fault-tree analysis. IEEE Transactions on Reliability 2000; 49(1): 49-59, http://dx.doi.org/10.1109/24.855536.
9. Dugra Rao K, Gopika V, Sanyasi Rao VVS, Kushwaha HS, Verma AK, Srividya A. Dynamic fault tree analysis using Monte Carlo simulation in probabilistic safety assessment. Reliability Engineering and System Safety 2009; 94(4): 872–883, http://dx.doi.org/10.1016/j.ress.2008.09.007.
10. Ge D, Zhang R, Chou Q, Yang Y. Probabilistic model-based multi-integration formulas for quantifying a generalized minimal cut sequence. Proceedings of the institution of Mechanical Engineers, Part O: Journal of Risk and Reliability 2014 (in press); DOI: 10.1177/1748006X14552004.
11. Gulati R, Dugan JB. A Modular Approach for Analyzing Static and Dynamic Fault Trees. Proceedings of Annual Reliability & Maintenance Symposium 1997; 57-63.
12. Liang X, Yi H, Zhang Y, Feng Z. Numerical simulation to reliability analysis of fault-tolerant repairable system. Journal of Shanghai Jiaotong University (Science) 2010; 15(5): 526-534, http://dx.doi.org/10.1007/s12204-010-1044-9.
13. Liu D, Xing W, Zhang C, et al. Cut sequence generation for fault tree analysis. Proceeding of the 4th International Conference on Embedded Software and Systems, 2007; 592–603, http://dx.doi.org/10.1007/978-3-540-72685-2_55.
14. Long W, Sato Y, Horigome M. Quantification of sequential failure logic for fault tree analysis. Reliability Engineering and System Safety 2000; 67(3): 269-274, http://dx.doi.org/10.1016/S0951-8320(99)00075-7.
15. Manian R, Dugan JB, Coppit D, Sullivan KJ. Combining various solution techniques for dynamic fault tree analysis of computer systems. Proceeding of the Third IEEE International High-Assurance System Engineering Symposium 1998; 21-28.
16. Oh M-S, Berger JO. Adaptive importance sampling in Monte Carlo integration. Journal of Statistical Computation and Simulation 1992; 4: 143-168, http://dx.doi.org/10.1080/00949659208810398.
17. Merle G, Roussel J-M, Lesage J-J. Algebraic determination of the structure functions of Dynamic Fault Trees. Reliability Engineering and

System Safety 2011; 96(2): 267–277, http://dx.doi.org/10.1016/j.ress.2010.10.001.
18. Merle G, Roussel J-M, Lesage J-J. Quantitative Analysis of Dynamic Fault Trees Based on the Structure Function, Quality and Reliability Engineering International 2014; 30(1): 143-156, http://dx.doi.org/10.1002/qre.1487.
19. Misra KB (Editor). Handbook of performability engineering. London: Springer-Verlag, 2008, http://dx.doi.org/10.1007/978-1-84800-131-2.
20. Shrestha M, Xing L, Xu H. Complete sequence set generation algorithm for reliability analysis of dynamic systems with sequence-dependent failures. Proceeding of the 16th ISSAT International Conference on Reliability and Quality in Design 2010; 382–386.
21. Tang Z, Dugan JB. Minimal cut set/sequence generation for dynamic fault trees. Proceedings of Annual Reliability and Maintenance Symposium 2004; 1-5.
22. Tokdar ST, Kass RE. Importance sampling: a review. Computational statistics 2010; 2(1): 54-60, http://dx.doi.org/10.1002/wics.56.
23. Xing L, Shrestha A, Meshkat L, Wang W. Incorporating Common-Cause Failures into the Modular Hierarchical Systems Analysis. Reliability, IEEE Transactions on 2009; 58(1):10-19, http://dx.doi.org/10.1109/TR.2008.2011855.
24. Yevkin O. An improved modular approach for dynamic fault tree analysis. Proceedings of Annual Reliability and Maintenance Symposium 2011; 1-5.
25. Yevkin O. An improved Monte Carlo method in fault tree analysis. Proceedings of Annual Reliability and Maintenance Symposium 2010; 1-5.

Daochuan GE
Dong LI
Meng LIN
Yan-hua YANG
School of Nuclear Science and Engineering
Shanghai Jiao Tong University
Shanghai 200240, China

Emails: gdch-2008@163.com, lidonghzkd1@126.com,
linmeng@sjtu.edu.cn, yangyh@sjtu.edu.cn

Article citation info:
WERESA E, SEWERYN A, SZUSTA J, RAK Z. Fatigue testing of transmission gear. Eksploatacja i Niezawodnosc – Maintenance and Reliability 2015; 17 (2): 207–214, http://dx.doi.org/10.17531/ein.2015.2.6.

Emil WERESA
Andrzej SEWERYN
Jarosław SZUSTA
Zdzisław RAK

FATIGUE TESTING OF TRANSMISSION GEAR

DOŚWIADCZALNE BADANIA TRWAŁOŚCI ZMĘCZENIOWEJ PRZEKŁADNI ZĘBATYCH*

This paper presents the results of experimental tests of fatigue life of selected gears, performed on a test stand equipped with a hydraulic universal testing machine. The tests were performed on skew and straight cylindrical gears, made of EN AW-2017A and EN AW-7057 aluminium, and 40HM steel. Moreover, fatigue life curves for selected gears were presented, and the mechanisms of the occurrence of damage were analysed. Relationships describing the maximum value of torque during a loading cycle in relation to the number loading of cycles until the gear is damaged were also proposed.

***Keywords**: Life cycle fatigue, gear box, experiment, cracking, damage.*

W pracy przedstawiono wyniki badań doświadczalnych trwałości zmęczeniowej wybranych przekładni zębatych, wykonanych na opracowanym stanowisku badawczym wyposażonym w hydrauliczną maszynę wytrzymałościową. Badania przeprowadzono na walcowych kołach o zębach prostych i skośnych, wykonanych ze stopów aluminium EN AW-2017A i EN AW-7057 oraz stali 40HM. Ponadto zaprezentowano wykresy trwałości zmęczeniowej wybranych przekładni zębatych oraz przeanalizowano mechanizmy powstawania uszkodzeń. Zaproponowano także zależności określające maksymalną wartość momentu skręcającego w cyklu obciążenia od liczby cykli obciążenia do uszkodzenia przekładni.

***Słowa kluczowe**: Trwałość zmęczeniowa, przekładnia zębata, eksperyment, pęknięcia, uszkodzenia.*

1. INTRODUCTION

Working loads of construction elements, especially cyclically changing loads, cause nucleation and the development of damage in the material, which often leads to fatigue destruction of the whole element [9, 10]. In the case of uniaxial or proportional biaxial loads, the damage cumulates on privileged surfaces; the life of material is determined on the basis of the results of standard tests presented in the form of fatigue curves [14, 15]. The prediction of fatigue life of construction elements that operate in conditions of nonproportionate loads (which occurs in the case of cylindrical gears) is a huge computational problem [5, 12]. The difficulties are connected with the necessity to formulate and experimentally verify general criteria descriptions allowing for the cumulation of damage on different physical surfaces, and to establish the surface of crack initiation and the crack criterion [10, 19].

The development of damage, and then the initiation of fatigue cracking in gears is particularly intensive in two areas: in the area of contact of gear teeth (from contact pressures) and at the base of the loaded tooth (from twisting and shearing).

In the former case, gear damage is the result of local crumbling on the surfaces of the mating teeth (mainly pitting wear caused by high values of contact, normal, and tangential stresses) [18]. In the latter case, damage to the element is the result of fracture to the teeth base (propagation of fatigue cracking until the whole of the tooth breaks off). It should be added that fatigue cracking in mating gears may appear both in the outer layer of the tooth, and inside the material - near the border between the outer layer and the core [4].

Prediction of the development of fatigue damage in gears as early as at the stage of their design allows to determine the lifespan of a given gear in conditions of normal operation, and avoid serious damage to the whole device. Fatigue calculations for gears usually consist in determining the fatigue life of the tooth base [7]. The computational procedure consists in determining the infinite fatigue life of a gear, which is expressed as the value of the normal stress at tooth base which the rim material can transfer without breaking it during at least 3x106 loading cycles [3]. This value is too small, as gears often work in such manner that the number of loading cycles is considerably higher. For comparative calculations, the values of infinite fatigue life obtained in tests of smooth samples at uniaxial tension-compression or uniaxial pulsation from-zero bending are used [17]. Another method for the determination of fatigue life of gear teeth requires the creation of a fatigue life curve on the basis of experimental tests of real gear pairs in operating conditions [10]. Most of the available papers connected with fatigue tests of gears are based on calculations with the use of the finite element method. There are fewer papers devoted to experimental verification and fatigue tests of real life gears.

This paper proposes an own design of a test stand that differs significantly from the solutions currently in use. Employing a hydraulic universal testing machine and a torsion torque sensor resulted in an accurate representation of mating of individual contact pairs [20]. The stand allows to determine the fatigue life of gears, i.e. the relationship between the maximum torsion torque during a cycle and the number of loading cycles causing the initiation of fatigue cracking on the contact surface or at the base of the tooth, using only one gear for the tests.

2. STANDS FOR FATIGUE TESTING OF GEARS

Up to now, the most commonly used stand for experimental testing of the fatigue life of gears has been the power-closed-loop test stand, often called the circulating power stand [11]. A scheme of the "power-closed-loop" gears is shown in Fig. 1. It consists of two one-

(*) Tekst artykułu w polskiej wersji językowej dostępny w elektronicznym wydaniu kwartalnika na stronie ***www.ein.org.pl***

step gears with the same transmission ratios, the so-called test gears 1 and closing gears 2, two torsion bars 3 and 4, tightening clutch 5 and medium-power electric motor (generally 6 to 12 kW) 6. In the test gears there are the two tested gears, while in the closing gears – the gears closing the circuit whose life is much higher in comparison with the test gears. One of the key elements of the power-closed-loop stand is the loading unit. For this purpose, tightening clutch 5 is used the most commonly, enabling the turning of bars 3 of the gears with the appropriate torque.

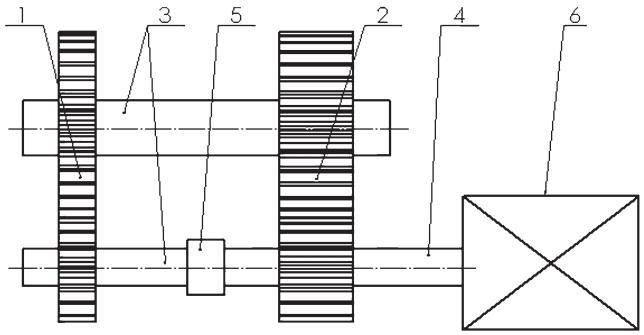

Fig. 1. Power-closed-loop stand 1 – test gears, 2 – closing gears, 3 – torsion bars, 4 – bar plug for the connection with the motor, 5 – tightening clutch, 6 – motor [11]

The scheme of the construction of the classic stand is shown in Figure 2. It consists of test gears 1, clutch or loading brake 3 mounted on one of the gear shafts, and motor 2 (e.g. electric), which forces the load torque of the gears. Classic stands find their use in dimensionally small gears, which yield small load torques.

In the latest version of the stand for testing toothed gears, a hydraulic method of loading is used. This allows to load the tested gears with a constant torque, similarly to the classic stand with mechanical tightening pre-set before commencing the test (Fig. 2). This solution allows to apply torsion torque in a changeable (programmed) manner, automatically during the performance of a test (without stopping the stand). This change may occur in a continuous, discrete, or even random manner.

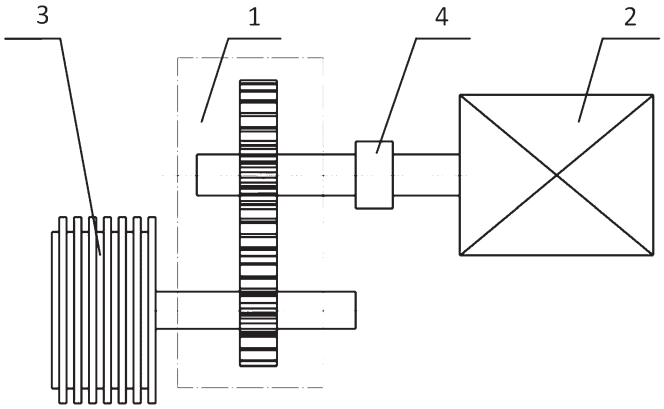

Fig. 2. Classic stand for toothed gears testing, 1 – body of the tested toothed gears, 2 – motor, 3 – loading clutch or electromechanical brake, 4 – clutch [3]

Stands for tests in the gigacycle range usually consist of: a computer, an analogue-to-digital converter, a device inducing oscillations (e.g. inductor), with a frequency of 20 kHz or more, and the tested toothed gears. A block scheme of this kind of stand is presented in Figure 3 [8].

Fig.3. Block scheme of a stand for testing gigacycle fatigue life [8]

The results of the experimental tests on the described stands are, above all, the relationships between the maximum value of torsion (propulsive) torque during a loading cycle and the number of loading cycles until the destruction, obtained on the discussed stand.

Example fatigue characteristics are presented in Fig. 4. Line 1 represents infinite fatigue life. In the case of curve 2 the necessity for determining fatigue life also in the range of a very high number of cycles can be easily observed [13].

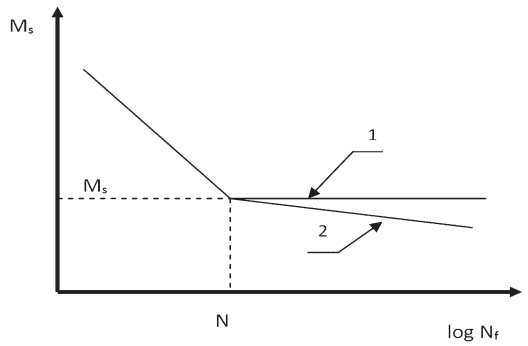

Fig. 4. Fatigue life curve of toothed gears; 1 – infinite fatigue life, 2 – gigacycle fatigue life [13]

3. METHODOLOGY OF TOOTHED GEARS TESTING

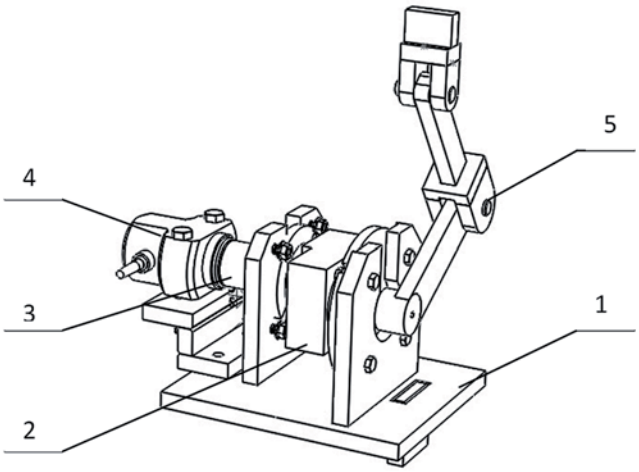

Fig. 5. Test stand device for the determination of the fatigue life of gears; 1 – mounting base, 2 – gears, 3 – clutch, 4 – torque sensor, 5 – crankshaft mechanism.

The paper presents an original stand for the determination of the fatigue life of gears. When designing it, the authors' aim was to reflect the operating and technical conditions of the tested pair of gears as accurately as possible. The presented test stand consists of base 1 mounted to the holder of the universal testing machine (MTS 322 Test Frame), which allows to apply a programmable load curve. To the base, by means of adequately profiled flanges, gears body 2 is mounted, inside which the tested pair of gears is located. The output shaft of the gears is mounted by means of clutch 3 with torque sensor 4 that collects data during the test. The drive shaft of the gears is connected through crankshaft mechanism 5 with a second holder of the

universal testing machine, thus closing the kinematic chain of the load [20].

In the presented solution, in order to apply load, crankshaft mechanism 5 is used, which changes programmed reciprocating motion of the inductive actuator of the universal testing machine into rotational motion of the drive shaft of tested gears 2. The torsion torque at the output shaft is recorded in real time by means of strain torque sensor 4. The measurement circuit enables acquisition of the value of the measurement signal from the torque sensor and the value of the respective forcing load.

The presented stand allows to determine the fatigue life of toothed gears representing real operating conditions, i.e. the susceptibility of shafts, bearing nodes, and elements of torque transfer. Moreover, a single pair of mating gears allows to determine the whole fatigue characteristic of the gears. Each point on the fatigue curve is determined on a single pair of mating teeth, or two at most in the case of two pairs of teeth intermeshing. After finishing the test at a given load level, the gear shaft rotates, so that the next undamaged pair of teeth intermeshes, then the process of cyclic loading is repeated. Owing to this approach it is possible to reduce the cost of fatigue tests by lowering the number of test samples (gears).

The initial parameters in the presented stand model are: maximum torque $M_{s\max}$ applied by maximum linear displacement of the actuator of the universal testing machine to the drive shaft of the gears, and the frequency of load application *f*. The initial angle of rotation of shaft α_g is determined indirectly from the geometry of the crank mechanism. The influence of the following parameters on the fatigue life of the gears can be determined on the described stand: gear ratio, type of cooling and lubricating fluid, material properties, teeth shape, and processing technology. During the tests recorded are the torsion torque of the gears' output shaft versus time curve, the number of loading cycles, and the angle of rotation of α_g.

The scheme of the method for the determination of the fatigue life of wheels of the tested gears on the presented stand are shown in Figure 6. The view of the test stand is shown in Figure 7.

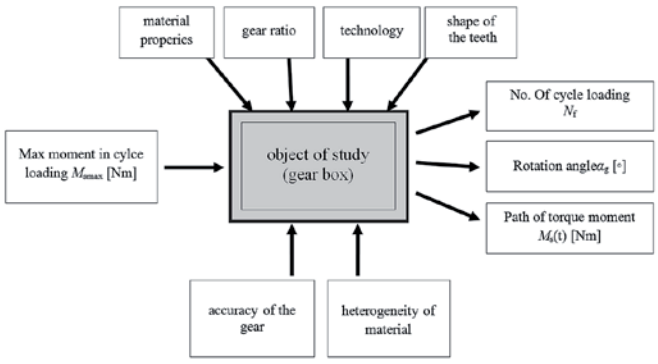

Fig. 6. Scheme of fatigue tests of gears

The testing process may be disrupted by imperfections in the workmanship of the tested gears, material inhomogeneity, and play in bearing nodes.

Figure 8 shows example curves of the from-zero torque loading the tested gears and the respective curves of force and displacement of the actuator of the universal testing machine. The character of the torque curve is similar to one occurring in real life operating conditions. Initiation and development of fatigue cracks causes an increase of the susceptibility of the mating gear teeth, and thus an increase of the angle of shaft rotation α_g. On its basis, the moment of gear damage caused by initiation and propagation of fatigue cracks in the tooth base or on the contact surface of teeth is determined.

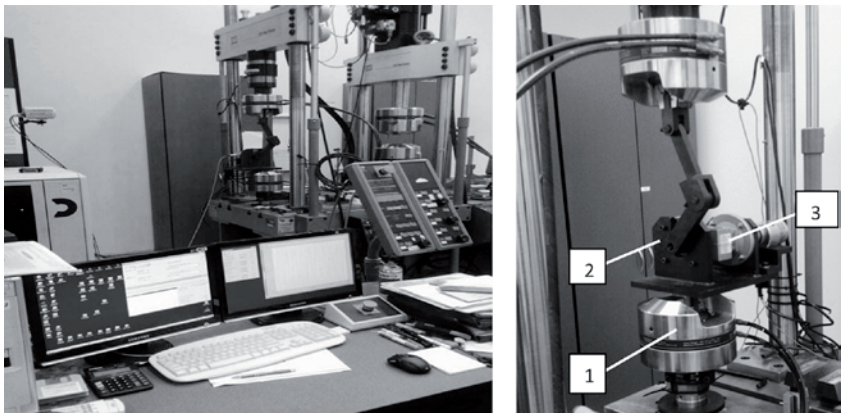

Fig. 7. View of the test stand; 1 – universal testing machine, 2 – body of the stand, 3 – tested gears

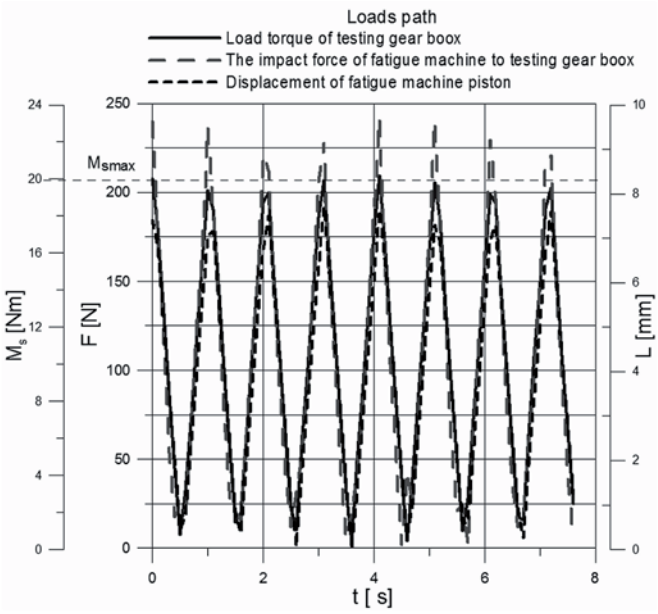

Fig. 8. Example load curves implemented in the performed tests

4. EXPERIMENTAL TESTS OF FATIGUE LIFE OF GEARS

The experimental tests were carried out on both straight and skew cylindrical gears. The gears made of EN AW-2017A and EN AW-7057 aluminium alloys had straight teeth with a normal module of 1.5 mm, while the gears made of 40HM steel had skew teeth and a module of 1 mm.

The fatigue tests were carried out in the laboratory of the Department of Mechanics and Applied Computer Science at Faculty of Mechanical Engineering of Białystok University of Technology. For each of the load levels, three repetitions were performed. The value of the determined loading cycles until fatigue cracking is initiated is shown in table 2 and Figure 10.

The next stage of the experiment were tests of skew gears. The results of the tests are presented in Figure 13 and table 6.

On the basis of the performed tests, two different mechanisms of fatigue damage to gears were observed. In the first one, cracking of the tooth base occurred. Fatigue cracks occurred above the bottom land of tooth. This mechanism occurred in the case of loads caused by torsion torque M_s with higher amplitudes. In this mechanism, the dominant stresses are those caused by teeth bending.

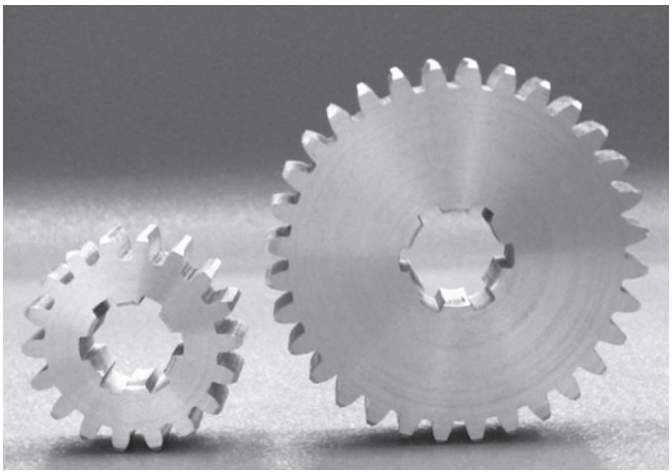

Fig. 9. View of straight-tooth samples used for the tests – gears no. 1 (Tab. 1)

Table 1. Parameters of straight gears – gears no. 1

Parameters	Gears I	Gears II
No. of teeth – Z	32	18
Tooth module – m	1.5 mm	1.5 mm
Pitch diameter – d_p	48 mm	27 mm
Extremal diameter – d_z	51 mm	30 mm
Surface roughness – R_a	0.63	0.63
Angle of intermeshing – α	20°	20°
Material	EN AW-2017A	
Technology of execution	boundary	
Lubrication	SAE 75W90	

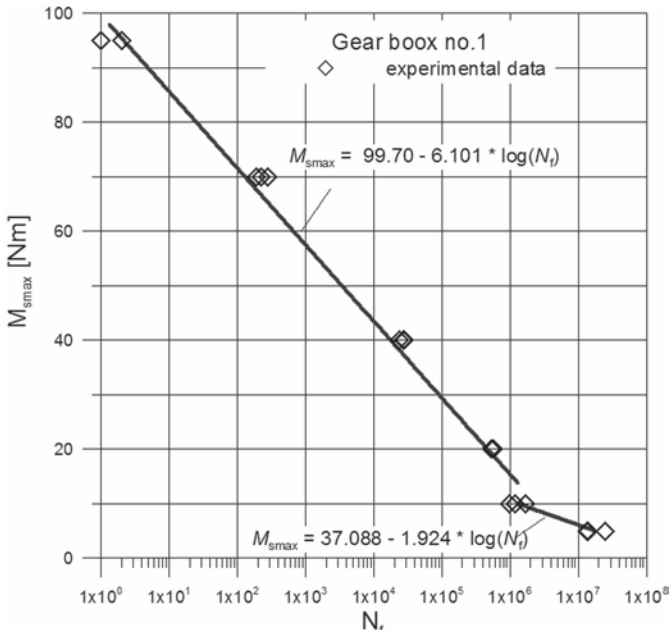

Fig. 10. Gears fatigue life curve – gears no. 1 (Tab. 1)

Figure 14 presents the trajectories of cracks observed in the tests and the respective values of maximum load. The curves of the trajectories of fatigue cracks at gear tooth base observed in the tests corroborate the results obtained on the basis of numerical calculations [2, 6, 13, 16].

Table 2. Results of tests of fatigue life of gears no. 1

Loading M_{smax} [Nm]	Number of loading cycles until the gear are damaged Nf		
	Sample1	Sample 2	Sample 3
95	1	1	2
70	190	280	226
40	24238	26854	27736
20	533304	524200	568112
10	1200542	986735	1699242
5	24523101	14121002	13569321

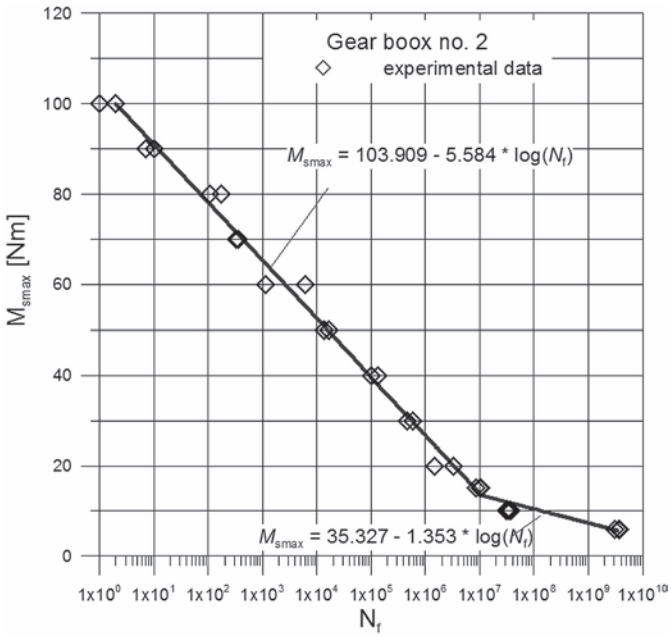

Fig. 11. Gears fatigue life curve – gears no. 2 (Tab. 3)

Table 3. Parameters of straight gears – gears no. 2.

Parameters	Gears I	Gears II
No. of teeth – Z	32	18
Tooth module – m	1.5 mm	1.5 mm
Pitch diameter – d_p	48 mm	27 mm
Extremal diameter – d_z	51 mm	30 mm
Surface roughness – R_a	0.63	0.63
Angle of intermesching – α	20°	20°
Material	EN AW-7075	
Technology of execution	boundary	
Lubrication	SAE 75W90	

Figures 15–16 present example fatigue cracks of tooth base (the first mechanism of damage to the toothed gear); both in the case of straight gears (Fig. 15), and skew gears (Fig. 16).

The second observed mechanism of gear damage is wear of the contact surface of a tooth. In this case wear to the gear is determined by the values of surface stresses. This type of damage was connected with the action of torsion torque with relatively small amplitudes on the gears.

Table 4. Results of tests of fatigue life of gears no. 2

Loading M_{smax} [Nm]	Number of loading cycles until the gear are damaged N_f		
	Sample 1	Sample 2	Sample 3
100	1	2	3
90	7	10	4
80	106	177	164
70	327	361	411
60	1154	6032	3456
50	16384	13880	10154
40	134104	100088	95860
30	576543	469870	720365
20	1448130	3214827	1148100
15	10050301	10456321	8451111
10	37267451	31267045	35409245
6	726745000	126745966	549245877

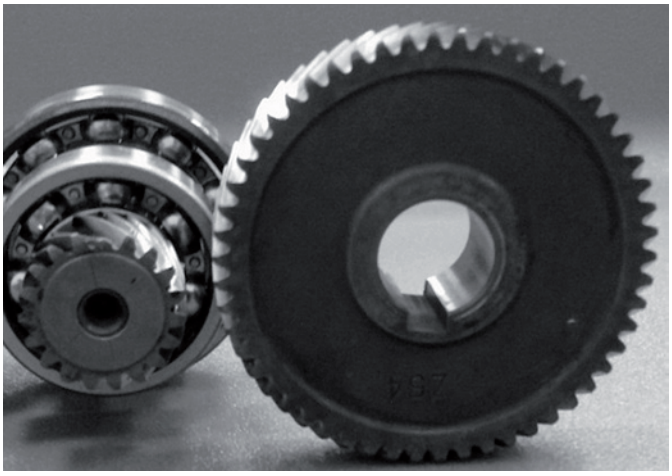

Fig. 12. View of the tested samples of cylindrical skew gears – gears no. 3 (Tab. 5)

Table 5. Parameters of skew gears – gears no. 3.

Parameters	Gears I	Gears II
No. of teeth – Z	54	19
Tooth module – m	1 mm	1 mm
Pitch diameter – d_p	55 mm	19 mm
Extremal diameter – d_z	57 mm	21 mm
Surface roughness – R_a	0.32	0.32
The angle of inclination of the teeth – β	10°	10°
Material	40HM	
Technology of execution	boundary	
Lubrication	SAE 75W90	

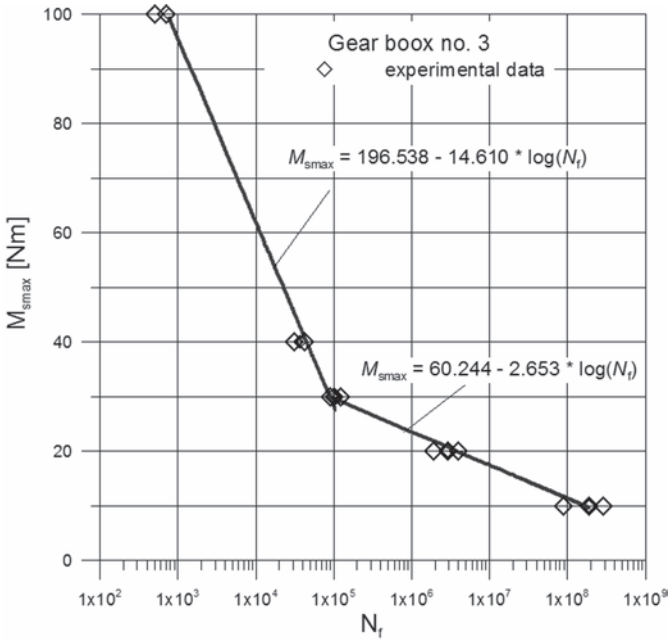

Fig. 13. Curve of fatigue life of gears – gears no. 3 (Tab. 5)

Table 6. Results of tests of fatigue life of gears no. 3

Loading M_{smax} [Nm]	Number of loading cycles until the gear are damaged N_f		
	Sample 1	Sample 2	Sample 3
100	702	511	1102
40	31007	42500	37607
30	90053	121653	100356
20	2915190	3913330	1915190
10	188407160	89466122	289221100

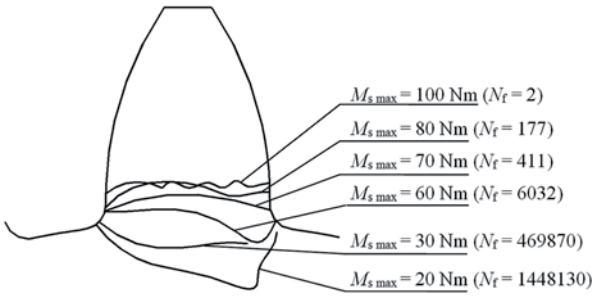

Fig. 14 Scheme of trajectories of fatigue cracks at tooth base in gears no. 2 (tab. 3)

During the tests typical mechanisms of wear of the surfaces of the pair of wheels in contact (pitting and adhesion) were observed [3]. In the case of the pitting mechanism of wear of teeth contact surface, micro-cracks progressing towards the inside of the wheel material were observed (Fig. 17a), while for the adhesive mechanism of wear, fragments of material were torn off without apparent additional micro-cracks (Fig. 17b).

5. PREDICTION OF FATIGUE LIFE OF GEARS

On the basis of the relationships between the maximum torsion torque in a loading cycle and the number of loading cycles causing gears damage obtained in fatigue test, and the performed analysis of the mechanisms of cracking and wear of gears, an attempt at preparing

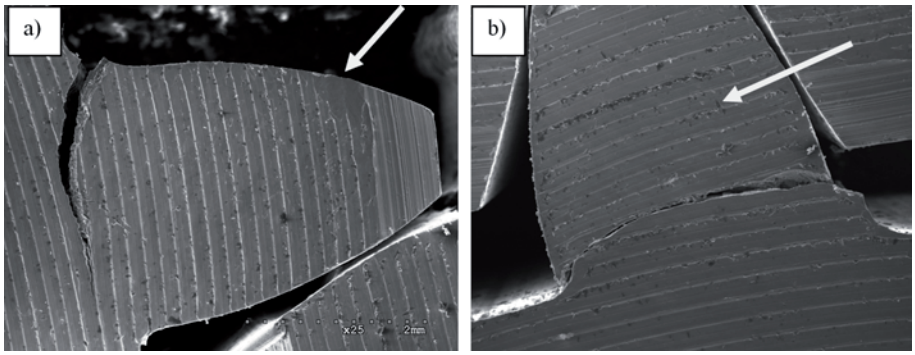

Fig. 15. Cracking in a tooth in gears no. 2 (tab. 3) that occurred as a result of the action of fatigue loads a) maximum torsion torque in a loading cycle M_{smax} = 30 Nm, number of loading cycles N_f = 469870, b) M_{smax} = 70 Nm, number of cycles N_f = 361 in 25× magnification

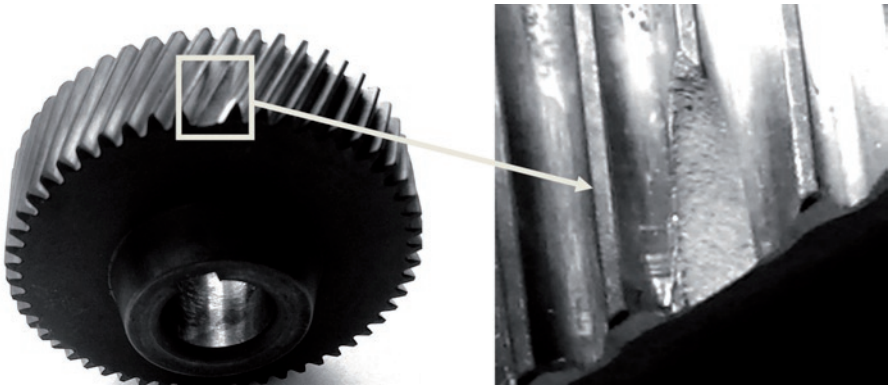

Fig. 16. Cracking of skew gear tooth caused by a cyclically changing load (from-zero pulsating cycle) a) maximum value of torsion torque in a loading cycle M_{smax} = 100 Nm, number of loading cycles N_f= 702

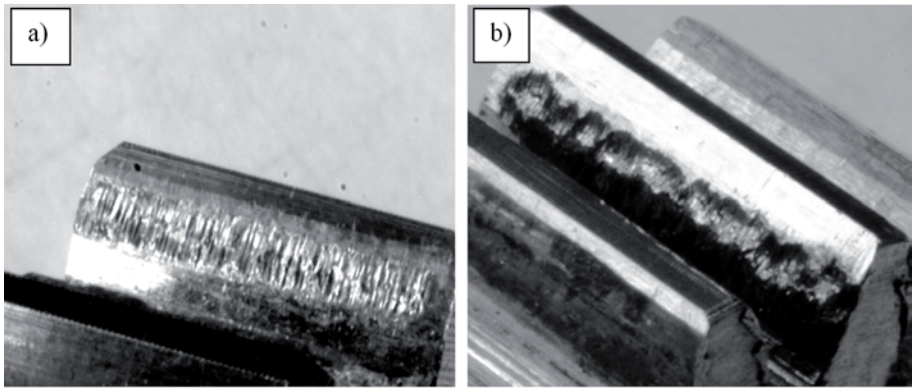

Fig. 17. Damage to tooth surface caused by a cyclically changing load, maximum value of torsion torque in a loading cycle M_{smax} = 20 Nm, number of loading cycles N_f = 3214827, b) M_{smax} = 10212 Nm, N_f= 35409245

semi-empirical relationships describing the fatigue life of gears was made. Figure 18 presents schematic curves of the fatigue life for both mechanisms of gears damage.

Fatigue life in the case in question can be described with the following equations:

$$\begin{aligned} M_{\mathrm{smax}}\left(N_{\mathrm{f}}\right) &= M_{\mathrm{fc}} - \eta_{\mathrm{f}} \log\left(N_{\mathrm{f}}\right) && \text{dla } M_{\mathrm{smax}} \geq M_{\mathrm{p}}, \\ M_{\mathrm{smax}}\left(N_{\mathrm{f}}\right) &= M_{\mathrm{wc}} - \eta_{\mathrm{w}} \log\left(N_{\mathrm{f}}\right) && \text{dla } M_{\mathrm{smax}} < M_{\mathrm{p}}, \end{aligned} \quad (1)$$

where: M_{smax} – maximum torsion torque in a gear loading cycle, N_{f} number of loading cycles until the gears are damaged, M_{fc} – critical value of torsion torque in the gears (causing tooth base cracking), M_{wc}– computational value of torsion torque connected with the second mechanism of damage (wear of teeth contact surfaces), η_{f}, η_{w} – coefficients determined experimentally depending on the parameters of the tested gears for the first (fatigue cracking of tooth base) and the second (wear of tooth contact surface) mechanism of gears damage, respectively.

Table 7 compares the values of the parameters obtained in the tests in relationships describing fatigue life of the tested gears.

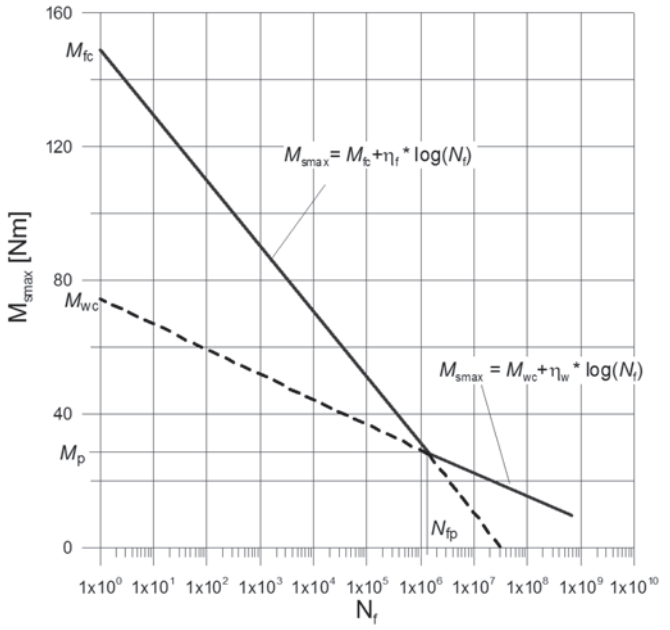

Fig. 18. Schematic formulation of the relationship between the maximum value of torsion torque in gears during a loading cycle and the number of loading cycles for two gears damage mechanisms: cracking of tooth base and wear of contact surface

6. SUMMARY

The paper presents a new stand for the determination of the relationship between the maximum torsion torque during a loading cycle and the number of cycles until gears are damaged, in which cyclically changing loads were applied by means of a hydraulic universal testing machine. On the presented stand it is possible to determine the fatigue life of gears reflecting real life operating conditions, i.e. the susceptibility of shafts, bearing nodes, and elements of torque transfer. Moreover, a single pair of mating gears allows to determine the whole fatigue characteristics of gears. Owing to this approach it is possible to reduce the costs of fatigue tests through lowering the number of test samples (gears).

The designed stand made it possible to perform fatigue tests of straight and skew cylindrical gears, in which the wheels were made from three different materials. The tests yielded information about the mechanisms of initiation and propagation of fatigue cracks, and the mechanisms of wear in gears. An analysis of the obtained results allowed to create semi-empirical relationships describing fatigue life of gears taking into consideration two mechanisms of damage: fatigue cracking of tooth base and wear of the contact surface of teeth.

It should be added that it is necessary to perform additional experimental tests of fatigue life of gears with other construction parameters and made from other materials, in order to verify the presented computational relationships. Recommended are also fatigue tests in the gigacycle range so as to determine the character of computational relationships in this range.

The obtained results of experimental fatigue tests (the relationship between the maximum value of load and the number of cycles until the gears are damaged, trajectories of fatigue cracking) may be used by other researchers to verify computational models, especially those employing the finite element method.

Table. 7. Comparison of the values of parameters in relationships describing the fatigue life of the tested gears

Gear boox	Value of parameters in eq (1)			
	η_f [Nm]	M_{cf} [Nm]	η_w [Nm]	M_{cw} [Nm]
Gear boox no 1 (tab. 1)	-6,101	99,695	-1,924	37,088
Gear boox no 2 (tab. 3)	-5,584	103,909	-1,353	35,327
Gear boox no 3 (tab. 5)	-14,610	196,538	-2,653	60,244

Acknowledgements

The investigation described in this paper in part of the research project no. N504 340336 Sponsored by the Polish State Committee for Scientific Research and realized in Silesian University of Technology.

References

1. Aberšek B, Flašker J, Glodež S. Review of mathematical and experimental models for determination of service life of gears. Engineering Fracture Mechanics, 2004; 71(4–6): 439–453, http://dx.doi.org/10.1016/S0013-7944(03)00050-X.
2. Bathias C, Paris PC. Gigacycle Fatigue in Mechanical Practice. Marcel Dekker, New York, 2005.
3. Drewniak J. Laboratory research of toothed gears. (in Polish) Wyd. ATH Bielsko-Biała, 2000.
4. Fajdiga G, Sraml M. Fatigue crack initiation and propagation under cyclic contact loading. Engineering Fracture Mechanics, 2009; 76: 1320–1335, http://dx.doi.org/10.1016/j.engfracmech.2009.02.005.
5. Feng P-E, Qi Y, Qiu Q. Pinion Assembly Strategies for Planetary Gear Sets. Journal of Mechanical Design, Des 2013; 135(5): 051007, http://dx.doi.org/10.1115/1.4023965.
6. Glodež S, M. Šraml, J. Kramberger A computional model for determination of serwice life of gears. International Journal of Fatigue. 2002; 24: 1013 – 1020, http://dx.doi.org/10.1016/S0142-1123(02)00024-5.
7. ISO 6336 Calculation of load capacitiy of spur and helical gears, International Standard, Genewe, 2006.
8. Jasiński, M. Radkowski, S. Diagnosis of the gigacycle fatigue processes in the gear. Diagnostics, (in Polish) 2005; 36: 13 – 24.
9. Kocańda S. Fatigue Failure of Metals, Springer; 1978, http://dx.doi.org/10.1007/978-94-009-9914-5.
10. Li S, Kahraman A, Klein M. A fatigue model for spur gear contacts operating under mixed elastohydrodynamic lubrication conditions. Journal of Mechanical Design, 2012; 134(4): 041007, http://dx.doi.org/10.1115/1.4005655.
11. Lewicki, D. Effect of Speed (Centrifugal Load) on Gear Crack Propagation Direction. U.S. Army Research Laboratory, Glenn Research Center, Cleveland, Ohio Aug 2001.
12. Marines I, Bin X, Bathias C. An understanding of very high cycle fatigue of metals. International Journal of Fatigue, 2003; 25: 1101-1107, http://dx.doi.org/10.1016/S0142-1123(03)00147-6.
13. Podrug S, Srecko Glodež S, Jelaska D. Numerical Modelling of Crack Growth in a Gear Tooth Root. Journal of Mechanical Engineering,

2011; 577-8: 579-586, http://dx.doi.org/10.5545/sv-jme.2009.127.
14. Seweryn A, Buczyński A, Szusta J. Damage accumulation model for low cycle fatigue, International Journal of Fatigue, 2008; 30: 756-765, http://dx.doi.org/10.1016/j.ijfatigue.2007.03.019.
15. Szusta J, Seweryn A. Fatigue damage accumulation modelling in the range of complex low-cycle loadings – The strain approach and its experimental verification on the basis of EN AW 2007 aluminum alloy, International Journal of Fatigue, 2011; 33: 255-264, http://dx.doi.org/10.1016/j.ijfatigue.2010.08.013.
16. Stahl K, Hohl BR, Tobie T. Tooth Flank Breakage: Influences on Subsurface Initiated Fatigue Failures of Case Hardened Gears. 25th International Conference on Design Theory and Methodology; ASME Power Transmission and Gearing Conference Portland, Oregon, USA, August 4–7. 2013; 5.
17. Szusta J. Seweryn A. Low-cycle fatigue model of damage accumulation – The strain approach. Engineering Fracture Mechanics, 2010; 77: 1604-1616, http://dx.doi.org/10.1016/j.engfracmech.2010.04.014.
18. Townsend DP. Zaretsky EV, Scibbe HW. Lubricant and Additives Effects on Spur Gear Fatigue Life Transactions of the ASME. Journal of Tribology, 1986; 108: 468–477, http://dx.doi.org/10.1115/1.3261243.
19. Ural A, Heber G, Wawrzynek P, Ingraffea A, Lewicki D, Neto J Three-dimensional, parallel, finite element simulation of fatigue crack growth in a spiral bevel pinion gear. Engineering Fracture Mechanics. 2005; 72: 1148–1170, http://dx.doi.org/10.1016/j.engfracmech.2004.08.004.
20. Weresa E. Szusta J. Test stand to determined fatigue propertin of gear boxes. Patent Application no. W.121171, 2012.

Emil WERESA
Andrzej SEWERYN
Jarosław SZUSTA
Faculty of Mechanical Engineering
Bialystok University of Technology
ul. Wiejska 45C, 15-351 Białystok, Poland

Zdzisław RAK
Faculty of Mechanical Engineering
Silesian University of Technology
ul. Konarskiego 18A, 44-100 Gliwice, Poland

E-mails: e.weresa@pb.edu.pl, zdzislaw.rak@polsl.pl

Article citation info:
LIU X, WANG W, PENG R. An integrated production and delay-time based preventive maintenance planning model for a multi-product production system. Eksploatacja i Niezawodnosc – Maintenance and Reliability 2015; 17 (2): 215–221, http://dx.doi.org/10.17531/ein.2015.2.7.

Xuejuan LIU
Wenbin WANG
Rui PENG

AN INTEGRATED PRODUCTION AND DELAY-TIME BASED PREVENTIVE MAINTENANCE PLANNING MODEL FOR A MULTI-PRODUCT PRODUCTION SYSTEM

MODEL INTEGRUJĄCY PLANOWANIE OPARTEJ NA POJĘCIU CZASU OPÓŹNIENIA KONSERWACJI ZAPOBIEGAWCZEJ ORAZ PLANOWANIE PRODUKCJI DLA SYSTEMÓW PRODUKCJI WIELOASORTYMENTOWEJ

This paper integrates preventive maintenance and medium-term tactical production planning in a multi-product production system. In such a system, a set of products needs to be produced in lots during a specified finite planning horizon. Preventive maintenance is carried out periodically at the end of some production periods and corrective maintenance is always performed at failures. The system's available production capacity can be affected by maintenance, since both planned preventive maintenance and unplanned corrective maintenance result in downtime loss during the planning horizon. In addition to the time used for preventive and corrective maintenance, our model considers the setup time and the product quality, as these are affected by the defects and failures of the system. Procedures are proposed to identify the optimal production plan and preventive maintenance policy simultaneously. Our objective is to minimize the sum of maintenance, production, inventory, setup, backorder costs and the costs of unqualified products within the planning horizon. A real case from a steel factory is presented to illustrate the model.

***Keywords**: Production planning, preventive maintenance, delay-time, integration, multi-product.*

W niniejszej pracy zintegrowano proces konserwacji zapobiegawczej z procesem średnioterminowego taktycznego planowania produkcji w odniesieniu do systemu produkcji wieloasortymentowej. W takim systemie, zestaw wyrobów jest produkowany partiami w określonym, skończonym horyzoncie planowania. Konserwacja zapobiegawcza prowadzona jest okresowo pod koniec wybranych okresów produkcyjnych, natomiast w przypadku wystąpienia uszkodzenia wykonuje się konserwację korygującą. Konserwacja może mieć wpływ na dostępne moce produkcyjne systemu, jako że zarówno planowana konserwacja prewencyjna jak i nieplanowana konserwacja korygująca powodują straty związane z przestojem urządzeń w danym horyzoncie planowania. Oprócz czasu potrzebnego na konserwację zapobiegawczą i korygującą, nasz model uwzględnia czas konfiguracji urządzeń oraz jakość produktów, ponieważ one również zależą od defektów i awarii systemu. Zaproponowano procedury, które pozwalają na jednoczesne określenie optymalnego planu produkcji i optymalnej strategii konserwacji prewencyjnej. Naszym celem jest minimalizacja sumy kosztów konserwacji, produkcji, zapasów, konfiguracji urządzeń oraz zamówień oczekujących a także kosztów produktów, które nie zostały zakwalifikowane do wprowadzenia do obrotu w danym horyzoncie planowania. Model zilustrowano na przykładzie rzeczywistego przypadku z fabryki stali.

***Słowa kluczowe**: Planowanie produkcji, konserwacja zapobiegawcza, czas opóźnienia, integracja, wieloasortymentowy.*

1. Introduction

Production planning is an activity that considers the best use of production capacity in order to satisfy customer demand during a specified finite planning horizon. There are three types of production planning, based on the different lengths of the planning horizon: the strategic planning level (long-term), the tactical planning level (medium-term) and the operational planning level (short-term) [11]. In general, the length of the long-term planning is about one year or more. In this stage, the aggregate demands need to be forecasted, and some strategic decisions, such as product category, equipment and resource planning, need to be made. The length of the medium-term planning is about one month or more. This stage often involves making decisions on production quantities or lot sizing and on the maintenance policy over the planning horizon. The length of the short-term planning is about one week or less, and this stage involves making decisions on the day-to-day scheduling of production operations based on customer orders and tactical planning. In this paper, our focus is on the medium-term tactical production planning, since at this level the production quantities or lot sizing should be determined, and the preventive maintenance (PM) decisions should be scheduled. Throughout this paper, we will use the term 'production planning' instead of 'tactical production planning', for simplicity.

Production and maintenance departments are usually located separately in modern companies. The production department has to make production planning based on the maximum production capacity, and to satisfy customers' demands, whereas the maintenance department has to ensure the proper functioning of the production system through maintenance actions. Conflict is inevitably generated since the two departments share the same system. If the production department ignores the occupation of maintenance time, or just considers it subjectively or empirically, the system may experience idle time, production delays and even shortages. On the other hand, if the maintenance department schedules the maintenance without considering the produc-

tion planning, excessive maintenance or inadequate maintenance may occur, so that the productive capacity cannot be fully used. Thus, it is necessary to find an integrated model to optimize the production and maintenance planning simultaneously.

There are only a few related researches at the tactical level in this integrated area. Weinstein and Chung [22] studied the integration of production and maintenance decisions in a hierarchical planning environment, and evaluated an organization's maintenance policy using a three-part model, where an aggregate planning model was described using a mixed-integer linear programming in stage one, a master production scheduling model was proposed to minimize the weighted deviations from the goals given at the aggregate level in stage two, and the master production schedule and the maintenance plan were simulated in stage three, which is the only stage studying the system failures. Their work was further researched by Aghezzaf et al. [1], which considered the reliability parameters of the production system at the early stage of the planning process, and developed a multi-item capacitated lot-sizing problem based on a system that was subjected to random failures, to minimize the expected total costs of production and maintenance. This work was extended by Aghezzaf and Najid [2], which discussed the issue of integrating production planning and PM in a production system composed of parallel failure-prone production lines. Two mathematical programming models for the problem were proposed, where the first model assumed that each production line of the system implements a cyclic preventive maintenance policy, the second model relaxed the cyclic restriction, but the backorder cost was not considered both in [1] and [2]. Fitouhi and Nourelfath [8] developed an integrated model for planning production and non-cyclical PM for a single machine. The backorder cost is considered and an enumeration method is used to get all of the PM solutions in the model, which was later extended in [9] to multi-state systems. Nourelfath et al. [15] also developed an integrated model for production and PM planning in multi-stage systems, where the preventive maintenance selection task in the integrated planning model is solved using a genetic algorithm. This work was then extended by Nourelfath and Chatelet [14] to a parallel system with dependent components, and a simulated annealing algorithm was developed. These works were well studied about the integrated problem, but some assumptions can be relaxed. For example, they did not consider the production quality influenced by the system, that is, they implicitly assumed that all of the products were qualified whereas unqualified products are common in reality. Besides, the setup time was ignored in the model, and the downtime caused by failures was not formulated by real production time. These gaps are filled in this paper.

The purpose of this paper is to develop an integrated production and PM model at the tactical level. The objective of the model is to determine the production and maintenance plan that minimizes the expected total cost over a finite planning horizon, which includes several equal-length periods. A set of products must be produced in lots during this planning horizon, and the demand for the same product may vary from one period to another. For example, the length of the planning horizon may be half a year, which may be thought of as six separate monthly periods, and the demand of the same product may vary from month to month. Since the production capacity is influenced by both PM and failures – and is therefore random – the production quantity of each product in each period will be calculated with consideration of the inventory and backorder. Since the system is subject to random failures, the PM is carried out periodically at the end of some production planning periods, whereas the corrective maintenance is always performed at a failure. The innovative points of this paper are 1) Previous works usually assume that the downtime caused by failures can be ignored, whereas our model considers this type of downtime when formulating the expected number of system failures over each period, 2) the downtime caused by setup is also studied, whereas no other literature has attempted, to our best knowledge, 3) we also consider how the product quality is affected by the defects and failures in system, and this was also not studied in previous works, 4) to model the PM decision for the system, we use the delay-time concept.

The concept of the delay-time has been widely applied in maintenance modeling and optimization; see [17] for a detailed review. The failure process of a component is regarded as a two-stage process: the period from new to the initial point of the defect, usually referred to as the normal stage or time-to-defect; and the period from the initial point to the component failure, referred to as the delay-time stage [3], as shown in Fig. 1. If the PM, which is considered to be perfect, is carried out during the delay-time, the defect can be identified and removed by repair or replacement. The delay-time models have been applied to single-component systems [4, 16, 24] and complex systems with many components [5, 6, 18–21]. In this paper, we use the complex system delay-time model since typical production systems are equipped with many components. For complex systems, multiple defects can be present at one time, and the arrival process of the defects can be approximated by a Homogenous Poisson Process (HPP) – see [17]. Fig. 2 illustrates the defect arrival and failure processes of a complex system where PM interventions were carried out at points A and B. It is clear from Fig. 2 that three defects could be identified and removed if the defect identification and removal are perfect. The delay-time-based PM models differ from other PM models in that they directly model the relationship between the PM and the number of system failures. Many case studies have shown the validity of the delay-time-based models [10, 13, 23].

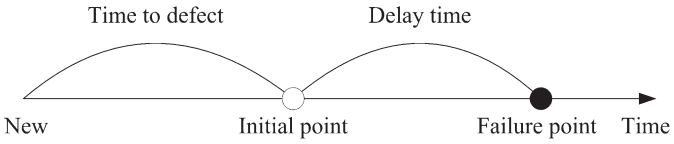

Fig. 1. The delay-time for a defect. '○' initial point, '●' failure point

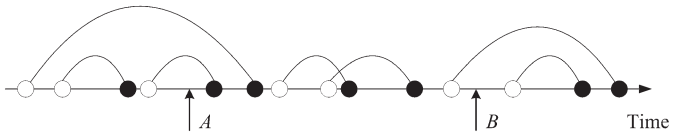

Fig. 2. The defect arrival and failure processes of a complex system

This paper is organized as follows. The model assumptions and notations are given in Section 2. Section 3 formulates the problem. Numerical examples are presented in Section 4. Section 5 concludes the paper.

2. Assumptions and notations

2.1. Assumptions

(1) The defects of the system arrive independently according to an HPP.
(2) The delay-time of all defects is independent and identically distributed.
(3) The PM is perfect and renews the system.
(4) A corrective maintenance is always performed at a failure, which is minimal in the sense that it will only repair the failed component while the defect arrival rate of the system is unaffected.
(5) The setup structure is sequence-independent.
(6) The PM may be carried out at the end of some production periods.

(7) The percentage of unqualified products is proportional to the number of failures.

Assumptions (1) and (2) have been used in previous delay-time models. Assumption (3) is for modeling simplification. Assumption (4) is commonly used in maintenance modeling, such as in [12], where – due to the time constraint and the need to resume the production as soon as possible – only the failed component is repaired or replaced, while the defect and failure rates of the system are unchanged after the repair. Assumption (5) is one of the two setup structures. Usually, production changeover between different products can incur setup time and setup costs. If the setup time and cost in a period are independent of the sequence, it is termed as a sequence-independent structure. Alternatively, the sequence-dependent structure refers to the case where the setup time and cost depend on the sequence of the products, and is more complex than the sequence-independent situation – see [11]. In this paper, we consider the simpler situation, and the more complex situation will be studied in a separate paper. Assumption (6) is practice-based since periodic PM is still the main form of preventive maintenance used in factories throughout the world. The rationale in assumption (7) lies in the fact that more failures mean more defective components within the system, which furthermore leads to the production of more unqualified products, given that the failure arrival process is a Non-Homogeneous Poisson Process (NHPP) [17].

2.2. Notations

(1) Model parameters

H The length of the planning horizon.
Z The number of periods during H.
T The length of each period.
n The number of different products.
d_{ij} The demand for product i in period j, i=1,2,⋯,n, j=1,2,⋯,Z.
t_i Production time for each unit of product i.
ξ_j The actual production time for all products needed to be produced in period j.
u The defect arrival point.
$f(\cdot)$ The probability density function (pdf) of the delay-time.
$F(\cdot)$ The cumulative distribution function (cdf) of the delay-time.
λ The rate of the occurrence of defects.
d_s^i The average time per setup for product i.
d_d The average time to repair per defect identified at a PM.
d_f The average time to repair per failure.
d_p The average time per inspection at a PM.
C_s^i The average setup cost of producing product i.
C_d The average cost of repairing a defective component that is identified at a PM.
C_f The average cost of repairing a failure, which contains the cost of repairing or replacing the failed component and the additional cost of unavailability.
C_p The average cost of an inspection at a PM.
C_{dp} The average cost of one unit of unqualified product.
p_i The cost of producing one unit of product i.
h_i Inventory holding cost per unit of product i per unit time.
b_i Backorder cost per unit of product i.
$E_N(dp)$ The expected number of unqualified products.
$E_C(dp)$ The expected total cost of unqualified products.
$E_C(m)$ The expected total cost of maintenance.

(2) Model variables

x_{ij} Quantity of product i produced in period j.
I_{ij} Inventory of product i at the end of period j; I_{i0} denotes the inventory of product i at the beginning of period 1.
y_{ij} Binary variable, which is equal to 1 if product i is produced in period j, and 0 otherwise.
B_{ij} Backorder level of product i at the end of period j; B_{i0} denotes the backorder of product i at the beginning of period 1.
T_{PM} The length of the PM interval, $T_{PM}=kT$, k is a positive integer, $1\le k\le Z$

3. The models

In this section, we first describe the research problem, then we evaluate the production time constraint in each period, the expected total cost of maintenance and the expected total cost of unqualified products, at last the integrated model is derived.

3.1. Problem description

The integrated production and maintenance strategy is illustrated in Fig. 3. The length of the planning horizon is H, including Z periods of fixed length T, and a set of products need to be produced during this planning horizon. For each period j, the demand for product i, d_{ij}, needs to be satisfied either by production in this period or by carrying inventories from earlier periods, but the backorder may happen due to setup and PM times, so we consider not only inventory holding cost but also backorder cost in our model. The number of PMs during the planning horizon is $\lfloor Z/k \rfloor$, since the length of PM interval T_{PM} is equal to kT, where $\lfloor Z/k \rfloor$ is the largest integer smaller than or equal to Z/k. The planning horizon can be divided into two parts, with the first part $\left[0,(\lfloor Z/k \rfloor k)T\right]$ including $\lfloor Z/k \rfloor$ equal PM intervals $\left[\hat{z}kT,(\hat{z}+1)kT\right]$, where $\hat{z}=0,1,\cdots,\lfloor Z/k \rfloor-1$, and the second part $\left[(\lfloor Z/k \rfloor k)T,ZT\right]$, the length of which is shorter than T_{PM}. We must decide which products to produce in which periods, the exact production quantities, and PM interval, in order to minimize the sum of PM, production, unqualified products, setup, backorder and inventory holding costs.

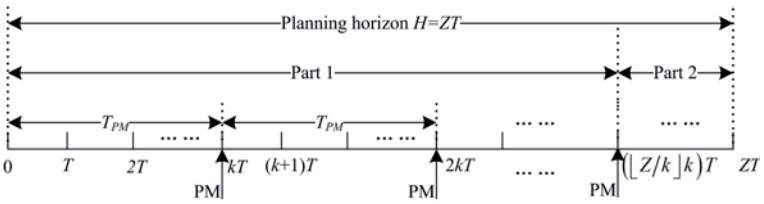

Fig. 3. Integrated production and maintenance strategy.

3.2. The production time constraint

(1) The production time constraint in $\left[0,(\lfloor Z/k \rfloor k)T\right]$

As the quantity of product i produced in period j is x_{ij}, the actual total production time in period j is $\xi_j=\sum_{i=1}^{n} t_i x_{ij}$. Specifically, in PM interval $\left[\hat{z}kT,(\hat{z}+1)kT\right]$, the period number j ranges from $\hat{z}k+1$ to $\hat{z}k+k$. We use $L_j\left(x_{ij},y_{ij},T_{PM}\right)$ to denote the production time constraint in period j, that is, $\sum_{i=1}^{n} t_i x_{ij} \le L_j\left(x_{ij},y_{ij},T_{PM}\right)$.

The first period in PM interval $\left[\hat{z}kT,(\hat{z}+1)kT\right]$ is $\left[\hat{z}kT,(\hat{z}k+1)T\right]$. In this period, $j=\hat{z}k+1$, the expected number of failures is $\int_0^{\xi_{\hat{z}k+1}}\lambda\int_0^t f(t-u)dudt=\int_0^{\xi_{\hat{z}k+1}}\lambda F(t)dt$, the expected downtime

caused by failures is $d_f\int_0^{\xi_{\hat{z}k+1}}\lambda F(t)dt$, [13], and the downtime caused by setup in this period is $\sum_{i=1}^{n}d_s^i y_{i,\hat{z}k+1}$. Thus, we have $\xi_{\hat{z}k+1}+d_f\int_0^{\xi_{\hat{z}k+1}}\lambda F(t)dt+\sum_{i=1}^{n}d_s^i y_{i,\hat{z}k+1}\le T$, that is,

$$L_{\hat{z}k+1}\left(x_{i,\hat{z}k+1},y_{i,\hat{z}k+1},T_{PM}\right)=T-d_f\int_0^{\xi_{\hat{z}k+1}}\lambda F(t)dt-\sum_{i=1}^{n}d_s^i y_{i,\hat{z}k+1}. \quad (1)$$

Similarly, the time constraint in the subsequent periods until the penultimate period can be expressed as

$$L_{\hat{z}k+k'}\left(x_{i,\hat{z}k+k'},y_{i,\hat{z}k+k'},T_{PM}\right)=T-d_f\int_{\sum_{a=1}^{k'-1}\xi_{\hat{z}k+a}}^{\sum_{a=1}^{k'}\xi_{\hat{z}k+a}}\lambda F(t)dt-\sum_{i=1}^{n}d_s^i y_{i,\hat{z}k+k'}, \quad (2)$$

where $k'=2,\cdots,k-1$.

The PM is carried out in the last period, where $j=\hat{z}k+k$; the number of defects identified at PM is $\int_0^{\sum_{a=1}^{k}\xi_{\hat{z}k+a}}\lambda\left[1-F(t)\right]dt$, so the expected downtime caused by PM is $d_p+d_d\int_0^{\sum_{a=1}^{k}\xi_{\hat{z}k+a}}\lambda\left[1-F(t)\right]dt$. The time constraint in this period can be given by:

$$L_{\hat{z}k+k}\left(x_{i,\hat{z}k+k},y_{i,\hat{z}k+k},T_{PM}\right)=T-d_f\int_{\sum_{a=1}^{k-1}\xi_{\hat{z}k+a}}^{\sum_{a=1}^{k}\xi_{\hat{z}k+a}}\lambda F(t)dt-d_p-d_d\int_0^{\sum_{a=1}^{k}\xi_{\hat{z}k+a}}\lambda\left[1-F(t)\right]dt-\sum_{i=1}^{n}d_s^i y_{i,\hat{z}k+k}. \quad (3)$$

(2) The production time constraint in $\left[\left(\lfloor Z/k\rfloor k\right)T,ZT\right]$

In $\left[\left(\lfloor Z/k\rfloor k\right)T,ZT\right]$, j can be denoted as $\lfloor Z/k\rfloor k+1,\cdots,Z$ orderly, in each period. We only consider the downtime caused by failures and setup, since PM is not carried out during this interval. The model of the production time constraint is similar to Equations (1) and (2), so we will not express it here.

3.3. The cost model of maintenance and unqualified products

(1) The expected maintenance cost

Based on Section 3.2, during each PM interval $\left[\hat{z}kT,\left(\hat{z}+1\right)kT\right]$, the actual production time is $\xi^{\hat{z}}=\sum_{j=\hat{z}k+1}^{\hat{z}k+k}\xi_j=\sum_{j=\hat{z}k+1}^{\hat{z}k+k}\sum_{i=1}^{n}t_i x_{ij}$, the expected number of failures is $\int_0^{\xi^{\hat{z}}}\lambda F(t)dt$, and the expected number of defects identified at PM is $\int_0^{\xi^{\hat{z}}}\lambda\left[1-F(t)\right]dt$. The failure and the repair cost of the defects are $C_f\int_0^{\xi^{\hat{z}}}\lambda F(t)dt$ and $C_d\int_0^{\xi^{\hat{z}}}\lambda\left[1-F(t)\right]dt$, respectively. The PM cost is C_p.

The actual production time during $\left[\left(\lfloor Z/k\rfloor k\right)T,ZT\right]$ can be expressed as $\xi'=\sum_{j=\lfloor Z/k\rfloor k+1}^{Z}\xi_j=\sum_{j=\lfloor Z/k\rfloor k+1}^{Z}\sum_{i=1}^{n}t_i x_{ij}$, and the expected failure repair cost is $C_f\int_0^{\xi'}\lambda F(t)dt$.

Then, the total maintenance costs during the planning horizon can be expressed as:

$$E_C(m)=\sum_{\hat{z}=0}^{\lfloor Z/k\rfloor-1}\left\{C_f\int_0^{\xi^{\hat{z}}}\lambda F(t)\,\mathrm{d}t+C_d\int_0^{\xi^{\hat{z}}}\lambda\left[1-F(t)\right]\mathrm{d}t+C_p\right\}+C_f\int_0^{\xi'}\lambda F(t)\,\mathrm{d}t. \quad (4)$$

(2) The expected cost of unqualified products

We then consider the quality of products affected by the defects and failures in the system. Based on Assumption (7), a coefficient β will be used to construct the relationship between the expected number of unqualified products, $E_N(dp)$, and the number of failures: we have $E_N(dp)=\beta\left[\sum_{\hat{z}=0}^{\lfloor Z/k\rfloor-1}\int_0^{\xi^{\hat{z}}}\lambda F(t)\,\mathrm{d}t+\int_0^{\xi'}\lambda F(t)\,\mathrm{d}t\right]$. The expected cost incurred due to unqualified products in the planning horizon can be given as:

$$E_C(dp)=C_{dp}E_N(dp). \quad (5)$$

3.4. The integrated model

Based on the models proposed in Section 3.2 and Section 3.3, the integrated cost model can be expressed as follows:

$$\text{Minimize}\ \sum_{i=1}^{n}\sum_{j=1}^{Z}\left(p_i x_{ij}+b_i B_{ij}+h_i I_{ij}+C_s^i y_{ij}\right)+E_C(m)+E_C(dp) \quad (6)$$

$$\text{Subject to:}\ I_{ij}-B_{ij}=I_{i,j-1}-B_{i,j-1}+x_{ij}-d_{ij}, \quad (7)$$

$$x_{ij}\le\left(\sum_{j^*\ge j}d_{ij^*}+B_{i,j-1}\right)y_{ij}, \quad (8)$$

$$\sum_{i=1}^{n}t_i x_{ij}\le L_j\left(x_{ij},y_{ij},T_{PM}\right), \quad (9)$$

$$y_{ij}\in\{0,1\}, \quad (10)$$

$$x_{ij},\ I_{ij},\ B_{ij}\ge 0. \quad (11)$$

The objective function (6) consists of the total production cost, the total backorder cost, the total inventory cost, the total setup cost,

the expected total maintenance cost as given by Equation (4) and the total expected cost of unqualified products as given by Equation (5) during the planning horizon. Equation (7) relates backorder or inventory at the start and the end of period j to the production quantity and the demand in that period; clearly $I_{ij} > 0$ and $B_{ij} > 0$ cannot hold simultaneously. Equation (8) sets the upper limit of x_{ij}, and if $y_{ij} = 0$ then $x_{ij} = 0$, and if $y_{ij} = 1$ then $x_{ij} \geq 0$. Equation (9) corresponds to the available production time constraint in period j, the detail of which was proposed in Section 3.1. Equation (10) indicates that y_{ij} is a binary variable. Equation (11) indicates that x_{ij}, I_{ij} and B_{ij} are all non-negative numbers.

The integrated cost model, Equations (6)–(11), can be solved by some mathematical programming software (e.g., LINGO or MATLAB). In our paper, we use MATLAB to solve it.

3.5. Validation

The integrated cost model is composed of two parts, the linear function $\sum_{i=1}^{n}\sum_{j=1}^{Z}\left(p_i x_{ij} + b_i B_{ij} + h_i I_{ij} + C_s^i y_{ij}\right)$, and the nonlinear function $E_C(m)$ and $E_C(dp)$. The linear part is commonly used in literature so we pay attention to validate $E_C(m)$ and $E_C(dp)$. Both $E_C(m)$ and $E_C(dp)$ were derived based on assumptions (1) and (2). Here we explain the rationale of the two assumptions. For complex systems, an approximation was made based on the delay-time concept: defect arrivals from all components are grouped and modelled by a stochastic point process, such as an HPP, and the delay times of all defects follow one identical distribution. This HPP approximation has been justified mathematically in [7], and the grouped delay time case was verified by simulation studies and a case study in [6].

4. Numerical example

In this Section, the pdf of the delay-time is assumed to follow an exponential distribution with parameter α. Previous delay-time-based case studies have used an exponential distribution as the delay-time [4], and this was chosen based on the best fit to the actual data. Subsequently, a simulation test was carried out to confirm that, for a complex system with many components, the pooled delay-time followed an exponential distribution approximately [6].

We now present a real case to demonstrate the integrated cost model proposed in Section 3. The data in this section was collected from our recent visit to a factory producing steel gratings. There are several production systems in this factory, and we chose a system that produces two types of steel gratings, that is, n=2. The production unit is 'ton', and the demands of products are as shown in Table 1. The planning horizon is Z=6 months with T=30 days (the time unit is 'day'). Table 2 shows the time and cost parameters, and the other parameters are λ=0.0462, α=0.0833 and β=0.5.

Table 1. Demands of products in every period.

	j=1	j=2	j=3	j=4	j=5	j=6
d_{1j}	700	1050	1000	880	1300	600
d_{2j}	1100	700	800	900	580	1200

Table 2. The time and the cost parameters

	t_i	d_s^i	C_s^i	p_i	h_i	b_i
i=1	0.0167	0.0139	55	1200	50	1400
i=2	0.0165	0.0135	50	1000	40	1200
d_d	d_f	d_p	C_p	C_d	C_f	C_{dp}
0.012	0.0417	0.0174	20	200	800	25

Table 3. The optimal total cost with different PM intervals.

T_{PM}	1 month	2 months	3 months	4 months	5 months	6 months
Total cost	1.1936e+07	***1.1934e+07***	1.1935e+07	1.1935e+07	1.1936e+07	1.1935e+07

Table 4. The optimal production plan with T_{PM}=2 months.

Period	Product 1				Product 2			
	x_{1j}	I_{1j}	B_{1j}	y_{1j}	x_{2j}	I_{2j}	B_{2j}	y_{2j}
1	700	0	0	1	1105.8	5.8	0	1
2	1050	0	0	1	749	54.8	0	1
3	1000	0	0	1	802.2	57	0	1
4	880	0	0	1	921	78	0	1
5	1300	0	0	1	498.5	0	3.5	1
6	600	0	0	1	1203.5	0	0	1

Table 5. The optimal production plan with h_1=50, h_2=60 and T_{PM}=2 months.

Period	Product 1				Product 2			
	x_{1j}	I_{1j}	B_{1j}	y_{1j}	x_{2j}	I_{2j}	B_{2j}	y_{2j}
1	705.8	5.8	0	1	1100	0	0	1
2	1098.3	54.1	0	1	700	0	0	1
3	1002.2	56.3	0	1	800	0	0	1
4	900.8	77.1	0	1	900	0	0	1
5	1222.9	0	0	1	576.5	0	3.5	1
6	600	0	0	1	1203.5	0	0	1

Using Equations (1)–(11) and the parameters given above, we can calculate all of the optimal results corresponding to different PM intervals, as shown in Table 3. It can be seen that the minimum total cost is 1.1934e+07 when the PM interval is 2 months, that is, carrying out the PM bi-monthly is the best choice for this system.

Table 4 shows the detailed results with the optimal PM policy, and we can see that I_{1j}=0, B_{1j}=0, $I_{2j} \neq 0$ (j=1~4) and $B_{25} \neq 0$. Both the inventory and backorder occur for product 2, but neither occur for product 1. This is because $h_1 > h_2$ and $b_1 > b_2$. To confirm this, changing the inventory cost parameters to h_1=50 and h_2=60, we can get the optimal production plan as shown in Table 5, where $I_{1j} \neq 0$ (j=1~4) and I_{2j}=0. Table 4 also shows the production planning in every period. The factory can arrange its production and maintenance according to our model and results.

5. Conclusion

An integrated production and periodic PM planning model was proposed at the tactical level for a complex system, with the delay-time concept used to model the PM decision for the system. A real case was studied as a numerical example. Using this integrated model, we can decide which products need to be produced and their exact production quantities in each period, and the optimal PM interval can be calculated simultaneously. From the example, we can see that the production quantities were also influenced by the inventory cost and backorder cost of different products. Of course, this study has certain limitations, which leads to the need for further research: 1) considering the integrated production and PM planning with a sequence-dependent setup structure; 2) considering non-periodic PM policies; and 3) considering several types of defects and failures that may have different impacts on the cost and downtime of the production systems.

Acknowledgement

The research report here is partially supported by the NSFC under grant number 71231001, 71301009 and 71420107023, the Fundamental Research Funds for the Central Universities of China, FRF-SD-12-020A, and by the MOE PhD supervisor fund, 20120006110025.

References

1. Aghezzaf EH, Jamali MA, Ait-Kadi D. An integrated production and preventive maintenance planning model. European Journal of Operational Research 2007; 181(2): 679–685, http://dx.doi.org/10.1016/j.ejor.2006.06.032.
2. Aghezzaf EH, Najid NM. Integrated production planning and preventive maintenance in deteriorating production systems. Information Sciences 2008; 178: 3382–3392, http://dx.doi.org/10.1016/j.ins.2008.05.007.
3. Anna JP, Sylwia WW. Analysis of maintenance models' parameters estimation for technical systems with delay time. Eksploatacja i Niezawodnosc – Maintenance and Reliability 2014; 16(2): 288–294.
4. Baker R, Wang W. Developing and testing the delay-time model. Journal of the Operational Research Society 1993; 44(4): 361–374, http://dx.doi.org/10.1057/jors.1993.66, http://dx.doi.org/10.2307/2584414.
5. Christer AH, Wang W. A delay-time-based maintenance model of a multi-component system. IMA Journal of Management Mathematics 1995; 6(2): 205–222, http://dx.doi.org/10.1093/imaman/6.2.205.
6. Christer AH, Wang W, Baker RD, Sharp J. Modelling maintenance practice of production plant using the delay-time concept. IMA Journal of Management Mathematics 1995; 6(1): 67–83, http://dx.doi.org/10.1093/imaman/6.1.67.
7. Cox DR. Renewal theory. London: Chapman and Hall; 1962.
8. Fitouhi MC, Nourelfath M. Integrating noncyclical preventive maintenance scheduling and production planning for a single machine. International Journal of Production Economics 2012; 136 (2): 344–351, http://dx.doi.org/10.1016/j.ijpe.2011.12.021.
9. Fitouhi MC, Nourelfath M. Integrating noncyclical preventive maintenance scheduling and production planning for multi-state systems. Reliability Engineering and System Safety 2014; 121: 175–186, http://dx.doi.org/10.1016/j.ress.2013.07.009.
10. Fu B, Wang W, Shi X. A risk analysis based on a two-stage delayed diagnosis regression model with application to chronic disease progression. European Journal of Operational Research 2012; 218(3): 847–855, http://dx.doi.org/10.1016/j.ejor.2011.12.013.
11. Karimi B, Fatemi-Ghomi SMT, Wilson JM. The capacitated lot sizing problem: a review of models and algorithms. Omega 2003; 31: 365–378, http://dx.doi.org/10.1016/S0305-0483(03)00059-8.
12. Liao G. Optimal ecnomic production quantity policy for randomly failing processes with minimal repair, backorder and preventive maintenance. International Journal of Systems Science 2012; 44(9): 1602–1612, http://dx.doi.org/10.1080/00207721.2012.659702.
13. Lv W, Wang W. Modelling Preventive maintenance based on the delay time concept in the context of a case study. Eksploatacja i Niezawodnosc – Maintenance and Reliability 2011; 3: 4–10.
14. Nourelfath M, Chatelet E. Integrating production, inventory and maintenance planning for a parallel system with dependent components. Reliability Engineering and System Safety 2012; 101: 59–66, http://dx.doi.org/10.1016/j.ress.2012.02.001.
15. Nourelfath M, Fitouhi MC, Machani M. An integrated model for production and preventive maintenance planning in multi-state systems. IEEE Transactions on Reliability 2010; 59 (3): 496–506, http://dx.doi.org/10.1109/TR.2010.2056412.
16. Okumura S, Jardine AKS, Yamashina H. Inspection policy for a deteriorating single-unit system characterized by a delay-time model. International Journal of Production Research 1996; 34(9): 2441–2460, http://dx.doi.org/10.1080/00207549608905037.
17. Wang W. An overview of the recent advances in delay-time-based maintenance modeling. Reliability Engineering and System Safety 2012; 106: 165–178, http://dx.doi.org/10.1016/j.ress.2012.04.004.
18. Wang W. Modeling planned maintenance with non-homogeneous defect arrivals and variable probability of defect identification. Eksploatacja i Niezawodnosc – Maintenance and Reliability 2010; 2: 73–78.
19. Wang W, Banjevic D. Ergodicity of forward times of the renewal process in a block-based inspection model using the delay-time concept. Reliability Engineering and System Safety 2012; 100: 1–7, http://dx.doi.org/10.1016/j.ress.2011.12.011.
20. Wang W, Banjevic D, Pecht M. A multi-component and multi-failure mode inspection model based on the delay-time concept. Reliability Engineering and System Safety 2010; 95: 912–920, http://dx.doi.org/10.1016/j.ress.2010.04.004.
21. Wang W, Christer AH. Solution algorithms for a nonhomogeneous multi-component inspection model. Computers and Operations Research 2003; 30(1): 19–34, http://dx.doi.org/10.1016/S0305-0548(01)00074-0.
22. Weinstein L, Chung CH. Integrating maintenance and production decisions in a hierarchical production planning environment. Computers and Operations Research 1999; 26(10–11): 1059–1074, http://dx.doi.org/10.1016/S0305-0548(99)00022-2.
23. Wu S, Wang W. Optimal inspection policy for three-state systems monitored by control charts. Applied Mathematics and Computation 2011; 217(23): 9810–9819, http://dx.doi.org/10.1016/j.amc.2011.04.075.
24. Zhao J, Jia X. An optimal policy of inspection for a component with delayed repair. Eksploatacja i Niezawodnosc – Maintenance and Reliability 2009; 3: 20–23.

Xuejuan LIU
Donlinks School of Economics and Management,
University of Science and Technology Beijing, Beijing
100083, China

Wenbin WANG
Donlinks School of Economics and Management,
University of Science and Technology Beijing
Beijing 100083, China

Faculty of Business and Law
Manchester Metropolitan University
United Kingdom

Rui PENG
Donlinks School of Economics and Management,
University of Science and Technology Beijing, Beijing
100083, China.

E-mails: xjliu0903@163.com, wangwb@ustb.edu.cn,
pengrui1988@ustb.edu.cn

Article citation info:
FALKOWICZ K, FERDYNUS M, DĘBSKI H. Numerical analysis of compressed plates with a cut-out operating in the geometrically nonlinear range. Eksploatacja i Niezawodnosc – Maintenance and Reliability 2015; 17 (2): 222–227, http://dx.doi.org/10.17531/ein.2015.2.8.

Katarzyna FALKOWICZ
Mirosław FERDYNUS
Hubert DĘBSKI

NUMERICAL ANALYSIS OF COMPRESSED PLATES WITH A CUT-OUT OPERATING IN THE GEOMETRICALLY NONLINEAR RANGE

NUMERYCZNE BADANIA PRACY ŚCISKANYCH ELEMENTÓW PŁYTOWYCH Z WYCIĘCIEM W ZAKRESIE GEOMETRYCZNIE NIELINIOWYM*

This paper presents the results of a numerical analysis conducted to investigate uniformly compressed rectangular plates with different cut-out sizes. Made of high strength steel, the plates are articulatedly supported on their shorter edges. The FEM analysis examines the nonlinear stability of these structures in the post-buckling state, where the mode of buckling is forced to ensure their stable behaviour. The numerical computations are performed within the geometrically nonlinear range until the yield point is reached. The investigation involves determining the effect of cut-out sizes on elastic properties of the plates with respect to service loads. The numerical analysis is conducted using the ABAQUS software.

Keywords: *thin-walled structures, finite element method, numerical analysis, thin-walled elastic elements, plate stability.*

Przedmiotem badań są prostokątne płyty z wycięciem o zmiennych parametrach geometrycznych poddane równomiernemu ściskaniu. Płyty podparte przegubowo na krótszych krawędziach wykonano ze stali o wysokich właściwościach wytrzymałościowych. Badania dotyczyły numerycznej analizy MES nieliniowej stateczności konstrukcji znajdujących się w stanie pokrytycznym z wymuszoną postacią wyboczenia zapewniającą stateczny charakter pracy konstrukcji. Obliczenia prowadzono w zakresie geometrycznie nieliniowym do uzyskania poziomu granicy plastyczności materiału. Badano wpływ parametrów geometrycznych wycięcia na charakterystykę sprężystą płyty w zakresie obciążeń eksploatacyjnych. Zastosowanym narzędziem numerycznym był program ABAQUS.

Słowa kluczowe: *konstrukcje cienkościenne, metoda elementów skończonych, analiza numeryczna, cienkościenne elementy sprężyste, stateczność konstrukcji płytowych.*

1. Introduction

Thin-walled load-carrying structures are characterized by high strength and rigidity as well as low weight. Given the above properties, these structures are widely applied not only in the aerospace and automotive sectors, but also in designs where low structure weight is crucial. A disadvantage of thin-walled structures is that they are prone to loss of stability under compressive or shearing loads [2, 3, 9, 13, 21–25, 28, 29]. Nonetheless, thin-walled structural elements can operate even after their stability loss provided that they do it in the elastic range [11, 14, 21, 27]. These structures are particularly sensitive to geometric inaccuracies, which is critical regarding their use. For this reason, they must be precisely manufactured to prevent premature loss of stability. Uniform thin-walled plates are relatively cheap to produce, yet they can carry relatively low loads due to their low flexural rigidity. When subjected to compression, these plates lose stability even under small loads. With common methods for improving load capacity such as the use of stiffeners or ribs, the form of a structure is not only considerably modified, but its weight can increase, too. However, there is a way in which load capacity of thin-walled structures can be greatly improved while the structures themselves can be used as both carrying structures and elastic elements. This can be done by forcing these structures to operate in a higher buckling mode (flexural and torsional). To do so, it is necessary to make a cut-out in the plate and slightly displace the vertical zone in the opposite direction. This displacement will be realized in a special frame - so that the jump on basic mode was impossible. In this way, the plate acquires the desired characteristics, i.e. stable operation in the post-buckling range.

Issues of the stability and post-buckling behaviors of plate structure with all sorts of holes was described in [19], where you can find a very comprehensive review of the literature on this issue. At that work as the author of the earliest elaboration, in numerical terms, is given Pennington Vanna [16], who as first considered the problem of the stability of elastic uniaxially compression plate with a cut-out. The article presents the results of FEM calculations and compared to the results of experimental studies. The earliest post-buckling behavior analysis of plate structures with cut-out are reported in [18]. A major contribution brings the works [15, 17, 20, 30], where are considered the postcritical states and limited carrying capacity of this type of structures. Not encountered of research, where was investigated plate structures with cut-out and in which attempted to force of the higher flexural and torsional mode deformation of the structure.

In the researched load-carrying structure, one can clearly distinguish a vertical zone where this thin-walled element undergoes compression and bending as well as a horizontal zone where it is mainly subjected to torsion. Plate characteristics vary depending on the area of these zones. This observation is critical with respect to plate opera-

(*) Tekst artykułu w polskiej wersji językowej dostępny w elektronicznym wydaniu kwartalnika na stronie ***www.ein.org.pl***

tion as it indicates that it is possible to produce elements with identical dimensions yet totally different rigidity.

The design of machines and devices sometimes requires the use of elements that will protect them from damage. Such elements should have low weight and specific operating characteristics. Apart from that, machine design often requires the use of elastic elements that need to be built in a rectangular space. In either cases, plates with a cut-out can be applied.

The investigation involved examining a thin-walled plate with a cut-out to be used as an elastic or carrying element. We investigated the effect of cut-out sizes on the characteristics of plate operation with respect to service loads. The numerical analysis was performed by the finite element method.

2. Research object and scope

The analysis was performed on rectangular plates with different cut-out sizes. The plates were made of spring steel 50HS and had the following material properties: a Young's modulus, E, of 210000MPa, a Poisson's ratio, v, of 0.3, a yield point, R_e, of 1180 MPa and a strength limit, R_m, of 1320 MPa. In all examined cases, the plates had the same overall dimensions: a height, H, of 250 mm, a width, B, of 150 mm and a thickness, g, of 1 mm (Fig. 1). The investigated plates had a centrally located, symmetric cut-out, the geometric variables of which, i.e. height a and width b, exerted a significant effect on the structure's behaviour under load. The investigated range of the cut-out geometric variables was respectively: a = 80÷200 mm and b = 10÷50 mm, which meant examining 35 cases of cut-out geometry.

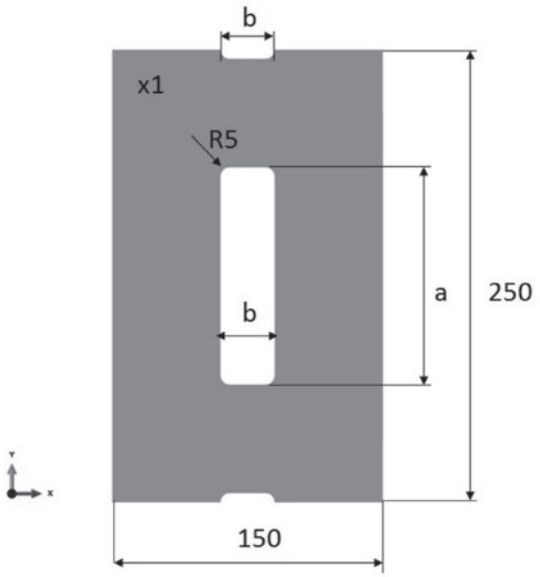

Fig. 1. Geometric dimensions of a plate with a cut-out

The investigation involved performing a numerical analysis of non-linear stability of a uniformly compressed plate, where a higher mode of buckling was forced to ensure stable operation of this structure in the post-buckling state. In order to examine the desired buckling mode, the plate had a central cut-out, the geometric dimensions of which had a direct effect on the plate's stability and operation in the post-buckling state. As a result, they affected the characteristics of the plate's post-buckling equilibrium path in the elastic state. This way of shaping elastic properties of plates is particularly important if such structures are to be used for various designs. Owing to considerable displacements that occurred when the plate was under load, the numerical analysis also involved solving the problem of geometric nonlinearity using the Newton-Raphson method [1, 4, 5]. The numerical analysis was performed using the FE-based commercial software ABAQUS® [1].

3. Numerical analysis

The discretization of the tested plate was made using the eight-node reduced integration shell elements (S8R), each element having six degrees of freedom at every node. In these thin-walled shell elements, the strains corresponding to the membrane state are determined based on linear displacements, while the flexural strains are defined based on the angular displacements [1, 8]. In the analysis, we used elements with the second order shape function**.** Fig. 2 shows the general view of the numerical model of the structure.

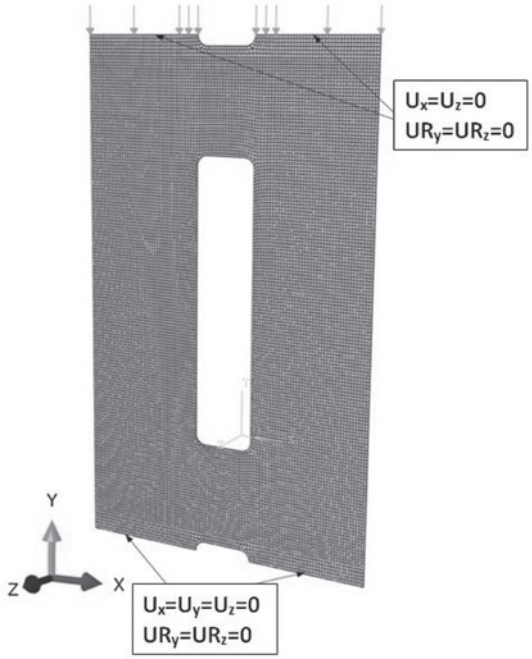

Fig. 2. Discrete model of a plate with a central cut-out

The boundary conditions of the numerical model which plotted the articulated support of the plate were defined by blocking the kinematic degrees of freedom of the nodes located on the upper and lower edges of the plate. The FEM model was loaded by applying uniform load to the upper edge of the plate.

The numerical analysis assumed that the operating range of the elastic element is set below the yield point and it does not alter the original rigidity of this element. Thus, the computations were continued until reaching the yield point, i.e., R_e=1180 MPa. The operational range of the structure was defined by the linear and elastic material model.

The numerical computations were run in two stages. The first stage involved examining the buckling state of the structure. The solving of this problem consisted in determining the buckling load and the corresponding mode of stability loss. For every case, we determined 3 lowest buckling modes, which allowed us to determine the flexural and torsional buckling mode that would ensure stable operation of the structure after buckling. The second stage of the computations involved solving the problem of nonlinear stability. The computations were made using models with initiated geometric imperfection which corresponded to the flexural and torsional buckling mode [10, 12]. In the computations, the amplitude of initial imperfections was set to 0.1 of the plate thickness.

4. Discussion of the numerical results

The numerical analysis enabled the determination of post-buckling equilibrium paths of compressed rectangular plates depending on the cut-out geometric variables: height *a* and width *b*. The numerical calculations were conducted for the buckling mode that ensured stable operation of the structure in the post-buckling range (Fig. 3).

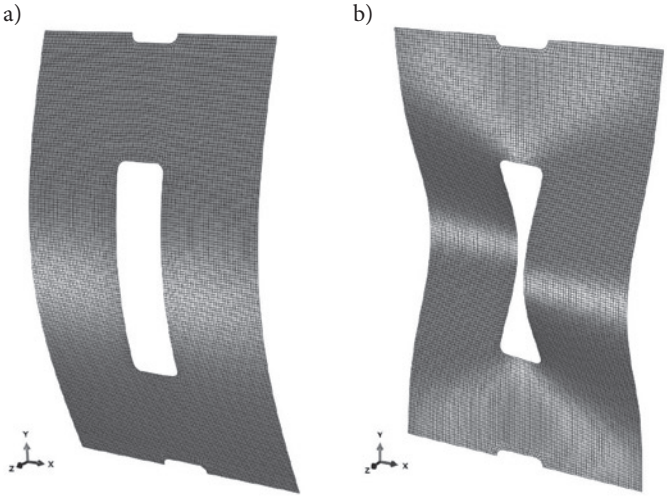

Fig. 3. Modes of stability loss in a plate with a cut-out: a) initial mode, b) higher mode

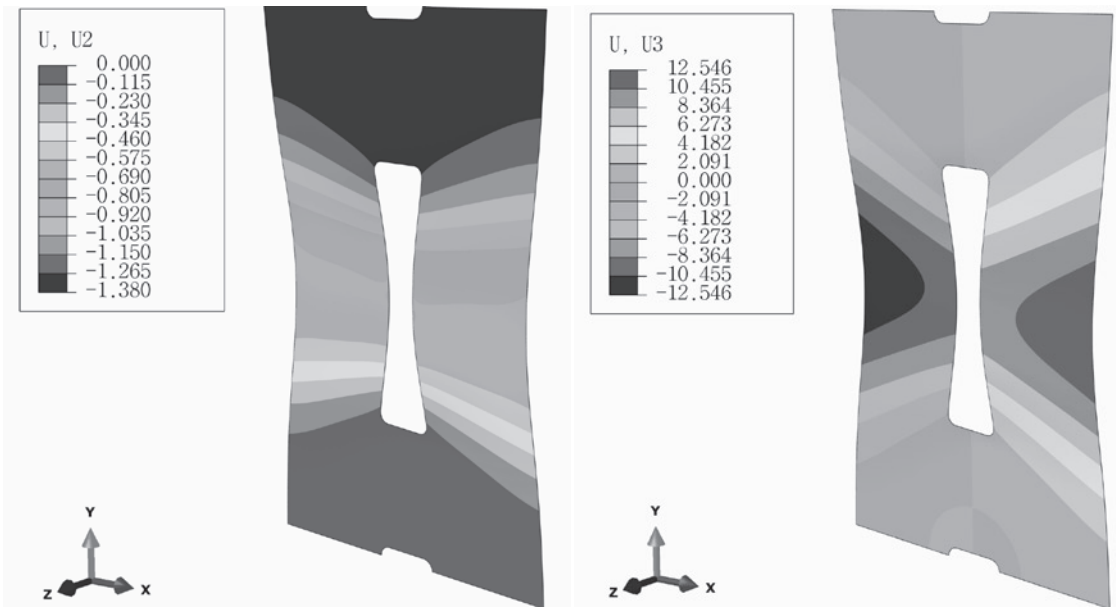

Fig. 4. Plate deformation in the post-buckling state: a) vertical deflection, b) lateral deflections

The buckling mode applied in the non-linear stability analysis constituted a higher eigenvalue and it corresponded to the flexural and torsional mode, one that forced non-symmetric deflections of the plate opposite to the cut-out. In effect, the load-carrying capacity of the structure was greatly improved compared to the same-sized uniform plate wherein the loss of stability corresponded to the lowest eigenvalue (flexural buckling). An example of the distribution of displacements in the plate with the cut-out is shown in Fig. 4.

The numerical results allowed us to perform both qualitative and quantitative analysis of the structure's behaviour in the post-buckling range. In all investigated cases, the post-buckling modes were made to be higher forms of the implemented buckling mode until the yield point was reached when the structure began to deform plastically, only to fail in the end. For this range, we developed post-buckling equilibrium paths, *P-U2*, in order to illustrate the relationships between load and vertical deflection of the plate edge. Thereby determined characteristics allowed us to evaluate the structure's operation depending on the geometric variables *a* and *b*. Fig. 5 shows some of the structure's operating characteristics versus cut-out heights in the tested plates (variable *a*). The curves reveal that – with the plate overall dimensions maintained unchanged – one can obtain structures with totally different operating characteristics, depending on the cut-out sizes.

The quantitative analysis of the results revealed a high discrepancy regarding the load capacity at different cut-out heights, ranging from 1003.1 N for a 200 mm high cut-out (50×200 plate) to 5000 N for a 80 mm high cut-out (10×80 plate). The cut-out width had greatest effect on 100 mm high plates where the highest difference in load capacity amounted to 1637.4 N. The results confirm that the cut-out height *a* has a significant effect on the post-buckling characteristics of the tested plates. This is important from a practical point of view as it means that - when it comes to structures with elastic elements – we can produce thin-walled structures with the required operating characteristics. Detailed results concerning the allowable operating ranges of the plate in elastic state, depending on the cut-out dimensions, are listed in Table 1. A nearly fivefold difference in load capacity upon the reaching of the yield point proves that the characteristics of elastic elements designed thereby can, to a great extent, be shaped as desired.

The operational ranges of the tested structures are illustrated in Fig. 6. The results demonstrate that the cut-out variables are relatively easy to select so as to produce a plate with the required rigidity in a wide range of load.

Fig. 7 shows the plot of reduced stress determined using the Huber-Mises-Hencky (H-M-H) hypothesis for the load that causes reaching the stress level which corresponds to the yield point and fro individual stress state components (plate with a 30x120mm cut-out). The distributions of reduced stress indicate that the corner of the cut-out is the crucial region of the structure, since it determines this structure's

Table 1. Maximum load capacity the plate [N] depending on the cut-out variables a and b – loads causing plastic deformation of the plate

Cut-out width *b* [mm]	Cut-out height *a* [mm]						
	80	100	120	140	160	180	200
10	5000.0	4600.0	3529.3	2854.1	2318.1	1909.6	1558.9
20	5000.0	4017.9	3166.9	2560.6	2106.5	1721.4	1405.2
30	4707.6	3613.4	2861.6	2313.7	1905.4	1558.4	1250.0
40	4252.4	3267.7	2605.0	2107.5	1720.0	1400.0	1113.5
50	3851.5	2962.6	2316.0	1907.7	1558.1	1261.0	1003.1

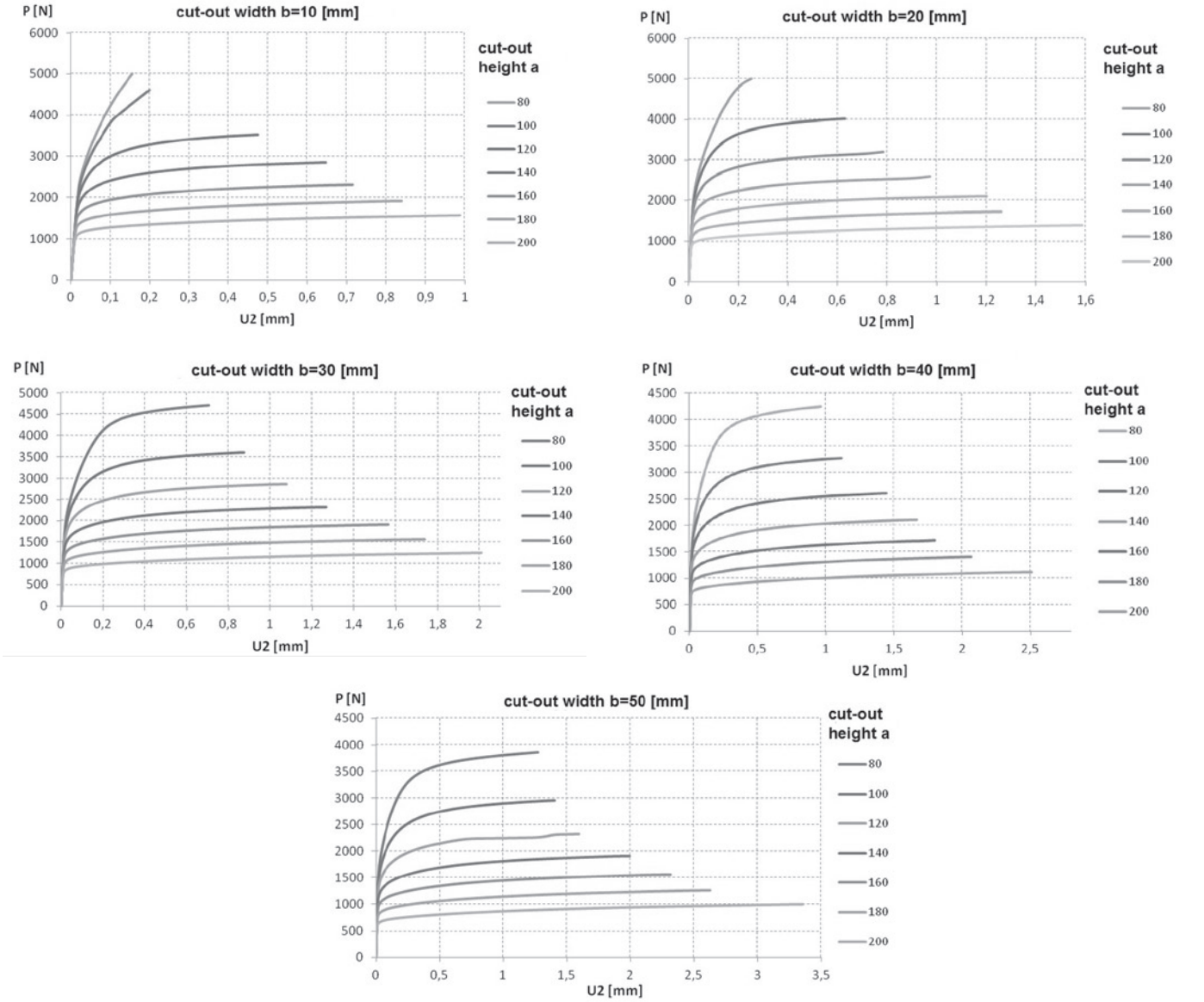

Fig. 5. Post-buckling equilibrium paths P-U2 versus height of the cut-out

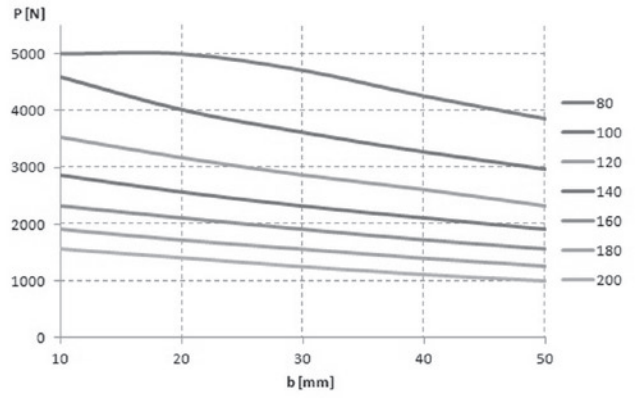

Fig. 6. Maximum load capacity of the plate [N] versus the cut-out variables a and b

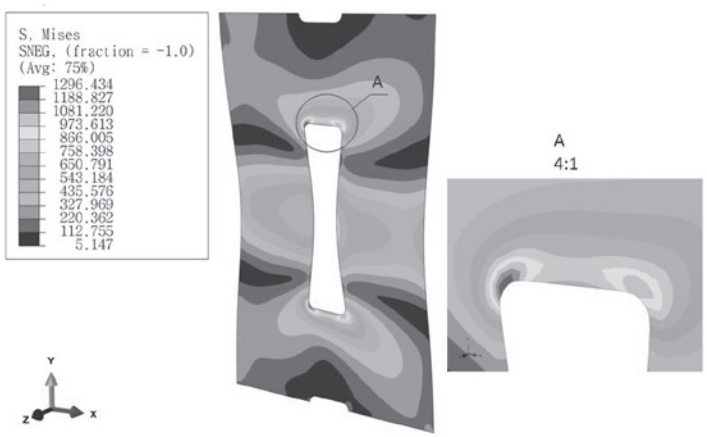

Fig. 7. Distribution of the H-M-H reduced stress in a plate with a 30x120mm cut-out, including the corners

operation in the elastic range. It is in this region that the material begins to deform plastically; therefore – as assumed – the deforming load is defined as the limit service load.

An analysis of the plate's deformation reveals significant differences in the behaviour of particular regions of this structure. The vertical strips of the plate undergo bending, while the horizontal ones are subjected to

torsion. Given such effort state of the plate, it is to be noted that structures made of isotropic materials will operate within a limited and, thus, unfavorable range due to exceeding the flow stress level in the cut-out corners. It seems highly probable that this undesired effect can be considerably reduced by the application of the material with orthotropic properties as it enables tailoring the material's operating characteristics as desired, depending on a region. Such properties are possessed, among others, by fibrous composites whose strength properties and rigidity can be shaped as required**,** hence they can be used to produce structures with improved load carrying capacity [4–7,26]. This problem will be investigated in further research.

6. Conclusions

The paper presented the numerical analysis of non-linear stability of composite plates subjected to compression. The results demonstrate that elastic properties of the investigated structures can be shaped to a great extent in the post-buckling state. The proposed solution regarding non-linear and elastic plates operating in a forced, higher buckling mode offers a broad spectrum of applications due to a relatively simple selection of the required parameters of the structure**,** such as its rigidity or the range of service loads. This is confirmed by the quantitative analysis of the results, particularly with regard to the maximum loads which range from 1003.1 to 5000 N depending on the cut-out size. We obtained an almost fivefold increase in load capacity in the elastic range for the plates with overall dimensions maintained identical. This observation is vital from the operating point of view, as it means that the structure's properties can be adjusted, while its designed structural features (dimensions) are retained and the weight is only slightly changed.

The findings are useful for examining structure deformation and effort in the full load range. As a result, it is possible to identify regions that are particularly prone to plastic deformation, which leads to loss of elastic properties of the structure. The numerical results reveal that these regions are located in the corners of the plate cut-out and that they determine the plate's load capacity in the elastic range. The analysis of the post-buckling equilibrium paths makes it possible to estimate the structure's behaviour after stability loss, which – in turn – enables the estimation of rigidity of the elastic element depending on cut-out sizes. Given the above, the results provide vital information for the forming process and optimization of the investigated structure's operating characteristics in terms of service loads.

References

1. Abaqus. HTML Documentation.
2. Bazant ZP, Cedolin L.: Stability of structures. Elastic, inelastic, fracture and damage theories. Oxford University Press 1991.
3. Coan JM. Large-Deflection Theory for Plates With Small Initial Curvature Loaded in Edge Compression, ASME. Journal of Applied Mechanics 1951; 18:143-151.
4. Dębski H, Kubiak T, Teter A. Buckling and postbuckling behavior of thin-walled composite channel section beam. Composite Structures 2013; 100: 195-204, http://dx.doi.org/10.1016/j.compstruct.2012.12.033
5. Dębski H. Experimental investigation post-buckling behaviour of composite column with top-hat cross section. Eksploatacja i Niezawodnosc Maintenance and Reliability 2013; 2: 105-109.
6. Dębski H, Kubiak T, Teter A. Experimental investigation of channel-section composite profiles behavior with various sequences of plies subjected to static. Thin-Walled Structures 2013; 71: 147-154, http://dx.doi.org/10.1016/j.tws.2013.07.008.
7. Dębski H, Kubiak T, Teter A. Numerical and experimental studies of compressed composite columns with complex open cross-sections. Composite Structures 2014; 118: 28-36, http://dx.doi.org/10.1016/j.compstruct.2014.07.033.
8. Dębski H, Koszałka G, Ferdynus M. Application of FEM in the analysis of the structure of a trailer supporting frame with variable operation parameters. Eksploatacja i Niezawodnosc – Maintenance and Reliability 2012; 14(2): 107-113.
9. Koiter WT. Elastic stability and post-buckling behavior. In Proceedings of the Symposium on Non-linear Problems. Wisconsin: Univ. of Wisconsin Press 1963; 257-275.
10. Kolakowski Z, Mania RJ. Semi-analytical method versus the FEM for analyzing of the local post-buckling of thin-walled composite structures. Composite Structures 2013; 97:99–106, http://dx.doi.org/10.1016/j.compstruct.2012.10.035.
11. Kopecki T, Mazurek P. Problems of numerical bifurcation reproducing in postcritical deformation states of aircraft structures. Journal of Theoretical and Applied Mechanics 2013; 51(4): 969-977.
12. Kopecki T, Mazurek P. Numerical representation of post-critical deformations in the processes of determining stress distributions in closed multi-segment thin-walled aircraft load-bearing structures. Eksploatacja i Niezawodnosc – Maintenance and Reliability 2014; 16(1): 164-169.
13. Królak M. and Mania R.J., (eds.), Statics, dynamics and stability of structures. Stability of thin-walled plate structures. Series of monographs. Łodz: Technical University of Lodz, 2011.
14. Kubiak T, Static and Dynamic Buckling of Thin-Walled Plate Structures. Springer 2013; 1-25, http://dx.doi.org/10.1007/978-3-319-00654-3_1, http://dx.doi.org/10.1007/978-3-319-00654-3.
15. Narayanan R, Chow FY. Ultimate capacity of uniaxially compressed perforated plates. Thin-Walled Structures 1984; 2(2): 241-264, http://dx.doi.org/10.1016/0263-8231(84)90021-.
16. Pennington Vann W. Compressive buckling of perforated plate elements. Proceedings of the First Specialty Conference on Cold-Formed Structures. University of Missouri-Rolla 1971; 51-57.
17. Prabhakara DL, Datta PK. Vibration, Buckling and Parametric Instability Behaviour of Plates with Centally Located Cutouts Subjected to In-Plane Edge Loading (Tension or Compression). Thin-Walled Structures 1997; 27(4): 287-310, http://dx.doi.org/10.1016/S0263-8231(96)00033-X.
18. Ritchie D, Rhodes J. Buckling and post-buckling behaviour of plates with holes. The Aeronautical Quarterly 1975; 26(4): 281-296.
19. Shanmugam NE. Openings in Thin-walled Steel Structures. Thin-Walled Structures 1997; 28(3/4): 355-372, http://dx.doi.org/10.1016/S0263-8231(97)00053-0.
20. Shanmugam NE, Thevendran V, Tan YH. Design formula for axially compressed perforated plates. Thin-Walled Structures 1999; 34(1): 1-20, http://dx.doi.org/10.1016/S0263-8231(98)00052-4.
21. Simitses GJ, Hodges DH. Fundamentals of structural stability . Amsterdam: Elsevier/Butterworth-Heinemann, 2006.
22. Singer J, Arbocz J, Weller T. Buckling Experiments. Experimental methods in buckling of thin-walled structure. Basic concepts, columns,

beams, and plates. New York: John Wiley & Sons Inc., 1998.
23. Singer J, Arbocz J, Weller T, Buckling Experiments. Experimental methods in buckling of thin-walled structure. Shells built-up structures, composites and additional topics. New York: John Wiley & Sons Inc., 2002, http://dx.doi.org/10.1002/9780470172995.
24. Spencer HH. Walker AC. Techniques for Measuring The Critical Loads of Column and Plates. SESA Spring Meeting, 1974.
25. Tereszkowski Z. An experimental method for determining critical loads of plates. Archive of mechanical engineering 1970; 3: 485-493.
26. Teter A, Dębski H, Samborski S. On buckling collapse and failure analysis of thin-walled composite lipped-channel columns subjected to uniaxial compression. Thin-Walled Structures 2014; 85: 324-331, http://dx.doi.org/10.1016/j.tws.2014.09.010.
27. Thompson JMT, Hunt GW. General theory of elastic stability. New York: Wiley, 1973.
28. Van der Heijden AMA (red.). W.T. Koiter's Elastic Stability of Solids and Structures. Cambridge University Press, 2009.
29. Venkataramaiah KR, Roorda J. Analysis of local plate buckling experimental data. Sixth international specialty conference on cold-formed steel structures. St. Louis: Missouri S&T: formerly the University of Missouri-Rolla 1982; 45-74.
30. Yu WW, Davies ChS. Cold-formed steel members with perforated elements. Proceedings of the American Society of Civil Engineers 1973; 99: 2061-2077.

Katarzyna FALKOWICZ
Mirosław FERDYNUS
Hubert DĘBSKI
Faculty of Mechanical Engineering
Lublin University of Technology
ul. Nadbystrzycka 36, 20-816 Lublin, Poland
E-mails: k.falkowicz@pollub.pl, m.ferdynus@pollub.pl,
h.debski@pollub.pl

Article citation info:
TANG D, YU J. Optimal Replacement Policy for a Periodically Inspected System Subject to the Competing Soft and Sudden Failures. Eksploatacja i Niezawodnosc – Maintenance and Reliability 2015; 17 (2): 228–235, http://dx.doi.org/10.17531/ein.2015.2.9.

Diyin TANG
Jinsong YU

OPTIMAL REPLACEMENT POLICY FOR A PERIODICALLY INSPECTED SYSTEM SUBJECT TO THE COMPETING SOFT AND SUDDEN FAILURES

OPTYMALNA POLITYKA WYMIANY DO ZASTOSOWANIA W SYSTEMACH PODDAWANYCH PRZEGLĄDOM OKRESOWYMNARAŻONYCH NA KONKURUJĄCE USZKODZENIA PARAMETRYCZNE I NAGŁE

This paper analyzes a replacement problem for a continuously degrading system which is periodically inspected and subject to the competing risk of soft and sudden failures. The system should be correctively replaced by a new one upon failure, or it could be preventively replaced before failure due to safety and economic considerations. Dependent soft and sudden failures are considered. The degradation process of the system observed by inspections exhibits a monotone increasing pattern and is described by a gamma process. The failure rate of the sudden failure is characterized by its dependency on the system age and the degradation state. By formulating the optimization problem in a semi-Markov decision process framework, the specific form of the optimal replacement policy which minimizes the long-run expected average cost per unit time is found, considering a cost structure that includes the cost for inspections, the cost for preventive replacement, and the costs for different failure modes. The corresponding computational algorithm to obtain the optimal replacement policy is also developed. A real data set is utilized to illustrate the application of the optimal replacement policy.

Keywords: *condition-based maintenance, periodic inspections, competing risk, soft failure, sudden failure.*

W artykule przeanalizowano problem wymiany dotyczący poddawanego przeglądom okresowym systemu ulegającego ciągłej degradacji i narażonego na konkurujące zagrożenie uszkodzeniami parametrycznymi i nagłymi. System taki powinien zostać wymieniony na nowy w ramach konserwacji korygującej w przypadku wystąpienia uszkodzenia lub też, ze względów bezpieczeństwa i względów ekonomicznych, można dokonać wymiany profilaktycznej jeszcze przed wystąpieniem uszkodzenia. W artykule rozważono przypadek zależnych od siebie uszkodzeń parametrycznych i nagłych. Proces degradacji systemu obserwowany podczas przeglądów ma charakter monotonicznie rosnący i można go opisać za pomocą procesu gamma. Intensywność uszkodzeń nagłych zależy od wieku systemu i jego stanu degradacji. Formułując problem optymalizacyjny w ramach semi-markowskiego procesu decyzyjnego, można określić formę optymalnej polityki wymiany, która minimalizowałaby długookresowy średni koszt na jednostkę czasu, z uwzględnieniem struktury kosztów, która obejmuje koszty przeglądów, koszty wymiany profilaktycznej oraz koszty różnych przyczyn uszkodzeń. Opracowano odpowiedni algorytm obliczeniowy umożliwiający ustalenie optymalnej polityki wymiany. Zastosowanie proponowanej optymalnej polityki wymiany zilustrowano na przykładzie zbioru rzeczywistych danych.

Słowa kluczowe: *utrzymanie ruchu zależne od stanu technicznego urządzeń, przegląd okresowy, zagrożenie konkurujące, uszkodzenie parametryczne, uszkodzenie nagłe.*

1. Introduction

Pressure from the market spurs the advancement of maintenance strategies. Traditional maintenance strategies such as corrective maintenance, which only takes place when the failure is observed, and age-based or length-of-usage-based policy, which are merely performed at scheduled intervals, are not always able to meet the ever-growing demand for high level of system reliability while balancing the operating costs. In recent years, the advance of instrumentation & measurement technology has brought about the idea of condition-based maintenance (CBM). In contrast with any pre-determined maintenance strategy, CBM enables maintenance actions based on the condition monitoring information collected at real-time. Some successful examples of implementing CBM in real systems have demonstrated its efficiency and effectiveness in preventing catastrophic failures and improving maintenance performance (e.g. [1, 4, 6, 11, 12, 14]).

The interest of most CBM policies has chiefly focused on a single failure mode, and the failure mode being mostly considered is the failure due to degradation, which is usually referred to as the soft failure. Soft failure is identified when the system state defined by the degradation level exceeds a predetermined threshold, and when it happens, the system is no longer assumed to be able to function satisfactorily or safely and it should be stopped and replaced, even if no physical failure is observed. The most frequently used CBM strategy for a continuous-state degrading system subject to the soft failure is the control-limit policy. Wang [19] jointly optimized the inspection interval and a control limit of preventive maintenance for a degradation process described by a linear growth model with random coefficients. Liao *et al.* [13] investigated a condition-based availability limit policy for a gamma-process-based degrading system, considering imperfect maintenance and an availability constraint. Policies with multiple control limits have also been proposed with the aim to improve CBM effectiveness and to satisfy different requirements. In [7], a CBM policy using multi-level control limits was proposed and optimized. The degrading system was modeled by a gamma process, and multiple control limits were used to determine the current maintenance actions and future inspection times. Elwanly *et al.* [6] analyzed a replacement problem for the exponentially increasing degradation system. They

demonstrated that the optimal replacement policy was a multi-level control-limit policy with monotonically increasing control limits.

However, considering only the soft failure seems to be inadequate for the degrading systems that are also subject to the sudden failures. In many practical situations, sudden failures are very likely to interrupt the graceful degradation and then result in more serious consequences. Therefore, in this paper, we consider a competing risk maintenance situation. The system is regarded as failed when the degradation process reaches a critical threshold or when the sudden failure occurs although the degradation process has not reached the threshold. Most of the present papers that deal with such failure scenario assume that the degradation process and the sudden failure are independent with each other. Nevertheless, even if independence is demonstrated to be appropriate for certain types of competing risks, e.g. [2, 8, 20, 21], in many situations the dependent structure between the two failure modes is of importance and should not be neglected. We consider the dependence is described by the failure rate of the sudden failure, which is influenced by both the age and the degradation state of the system. Similar assumptions were also found in Huynh *et al.* [9], Liu *et al.* [15], Castro *et al.* [3] and Huynh *et al.* [10] to deal with competing risk maintenance situation. A preventive threshold in terms of the degradation state was optimized in Huynh *et al.* [9] and Liu *et al.* [15] with different monitoring strategies. The former focused on periodically inspected systems and the latter dealt with continuously monitored ones. Castro *et al.* [13] also considered a degradation state - based control limit as the alarm of preventive maintenance, but multiple degradation processes were involved in the failure mechanism. In Huynh *et al.* [10], a novel CBM strategy was proposed using the mean residual life as the control limit. The effectiveness and potential of condition indices that are not strictly limited to failure mechanism in CBM decision-making problems was firstly investigated.

In this paper, we will focus on analyzing the optimal replacement policy for a periodically inspected system subject to the competing soft and sudden failures. This policy performs the preventive replacement only at inspection instants, and correctively replaces the system at the time of failure. We describe the degrading system using a gamma degradation process, which implies that the soft failure of the system results from a gradual and irreversible accumulation of deterioration. The failure rate corresponding to the sudden failure is described by a proportional hazards model, which means that it is influenced by both the age of the system and the state degradation of the system. Using the above models, we will show that for a certain group of maintenance situations the optimal replacement policy minimizing the average cost has a specific form, and it is also in fact a monotonically non-increasing multi-level control-limit policy. Computational algorithm to calculate the optimal multi-level control limits is developed as well, using a semi-Markov decision process framework. Finally, we will present a case study using a real laser data set from Meeker and Escorbar [16] to illustrate the proposed policy.

The paper is organized as follows. Section 2 describes the model for system degradation and sudden failures. In Section 3, we present the replacement problem. In Section 4, we examine the structure of the optimal replacement policy. The computational algorithm to calculate the optimal replacement policy is developed in Section 5. Section 6 gives an example based on a real data set. Conclusions are in Section 7.

2. Model of system degradation and sudden failure

2.1. Model of system degradation

We consider a continuously deteriorating system subject to periodic inspections. Due to limitations such as difficulty in placing sensors, the costs by condition monitoring, the internal structure of the system, and etc., not all systems can be continuously monitored. Therefore, the periodic monitoring strategy is a typical approach applied in many real applications. The degradation state of the system is hidden and can only be known by inspections. Generally, due to the physical nature of most degradation processes, the degradation state usually presents a monotonically increasing (or decreasing) trend. Even some fluctuations may occur due to measurement errors, self-recovering mechanism, etc., when the inspection interval is long enough, the observed increment between two inspections is still very likely to be non-negative. For degradation process involving s-independent and non-negative increments, gamma process is an appropriate stochastic model to describe it (see e.g. [18]). We assume that the system degradation process $\{Y(t), t \geq 0\}$ starts from a known initial state y_0 and follows a gamma process $Ga(\eta(t),\gamma)$. Let Y_n denote the degradation state observed at inspection time $t_n = nh$, $n = 1,2,3,...$, where h is the inspection interval. Then, the probability density function (pdf) of the increment $z_n = Y_n - Y_{n-1}$ in the inspection interval $[(n-1)h, nh)$ has the form:

$$f_{z_n}(z) = \frac{\gamma(\gamma z)^{\eta_n - \eta_{n-1} - 1} \exp(-\gamma z)}{\Gamma(\eta_n - \eta_{n-1})} \tag{1}$$

where $\eta(t)$ is a given, monotone increasing function and $\eta_n = \eta(nh)$.

If the soft failure threshold D_f is given, the probability of soft failure for the next inspection interval $(nh, (n+1)nh]$ conditioning on the current observation Y_n ($Y_n < D_f$) can be written as:

$$\Pr\left(T < t_{n+1} \mid Y_n, Y_n < D_f\right) = \int_{D_f - Y_n}^{+\infty} f_{z_{n+1}}(z)\,dz \tag{2}$$

In the following, we use homogeneous gamma process, i.e. $\eta(t)=\eta t$, at first for rigorous mathematical derivation of the optimal replacement policy. Extensions of the policy to cover a more general form of the gamma degradation model will be discussed as well.

2.2. Model of sudden failure

Sudden failure is a common failure mode which may interrupt a graceful degradation. In many practical situations, the sudden failure rate is very likely to be influenced by the degradation process. For example, the higher the degradation, the more the system is prone to sudden failures. Thus, it is reasonable to assume that the failure rate of sudden failures depends on the degradation process. In this paper, we assume that the failure rate of sudden failures is described by the proportional hazards (PH) model (see e.g. [5]), which explicitly includes both the effect of the age and the degradation state. It can be expressed by the following relation:

$$\lambda(t, Y_t) = \lambda_0(t;\boldsymbol{\alpha})\theta\left[Y(t);\boldsymbol{\beta}\right]. \tag{3}$$

where $\lambda_0(t;\boldsymbol{\alpha})$ denotes baseline failure rate at time t with unknown vector of parameters $\boldsymbol{\alpha}$, and $\theta[Y(t); \boldsymbol{\beta}]$with the unknown vector of parameters $\boldsymbol{\beta}$ is a positive function dependent only on the values of the degradation state $Y(t)$.

Due to the restraint of the periodic inspection policy, the values of $Y(t)$ are only known at some discrete points of time. Thus, we approximate the failure rate at time t as:

$$\lambda(t,Y_t)=\lambda_0(t;\alpha)\theta(Y_{n-1};\beta),\quad if\ t\in[(n-1)h,nh). \tag{4}$$

For the system which has not failed by time nh, if the latest observation is Y_n, the conditional reliability function of surviving beyond $nh+t$ for any $0<t<h$ can be approximated as:

$$R(Y_n,n,t)=\Pr(T>nh+t,t<h\mid T>nh,Y_n)$$
$$=\exp\left\{-\int_{nh}^{nh+t}\lambda_0(s;\alpha)\theta(Y_n;\beta)ds\right\}=\exp\left\{-\theta(Y_n;\beta)\int_{nh}^{nh+t}\lambda_0(s;\alpha)ds\right\}. \tag{5}$$

Then, the expected sojourn time for system to keep operating during interval $[nh,nh+a)$ ($0<a<h$) is given by

$$\tau(Y_n,n,a)=\int_0^a R(Y_n,n,t)dt=\int_0^a\exp\left\{-\theta(Y_n;\beta)\int_{nh}^{nh+t}\lambda_0(s;\alpha)ds\right\}dt. \tag{6}$$

3. The optimal replacement problem

Consider a non-repairable single-unit system described as in Section 2. The degradation state of the system is hidden and the soft failure is non-self-announcing. No indicator can exhibit the degradation state except to do an inspection. The system starts working at time $t=0$ and is inspected every h time units. The inspections are assumed to be perfect and incurred a cost C_0. Three kinds of replacement actions are available on the system:

1. If the system's degradation state identified by inspection exceeds its soft failure threshold D_f, a corrective replacement is performed with the expected cost C_2+C.
2. If sudden failure happens before the degradation state reaches the threshold D_f, the system is also correctively replaced, but with a possibly more expensive expected cost C_1+C ($C_1>C_2$).
3. At the time of inspection, if the system still operates and its degradation state observed by inspection is below the soft failure threshold D_f, a preventive replacement may exert on the system instantaneously at the expected cost C.

After the replacement, the system is back to as-good-as-new state. Even though both the preventive and the corrective maintenance actions bring the system back to the as-good-as-new state, they are generally different in practice because the unplanned maintenance actions (i.e. corrective replacements) may have to include a larger economic loss. Moreover, the corrective replacement for sudden failure is quite possible to be more expensive than that for soft failure because of its unexpected nature and the damage resulting from physical breakdown.

In addition, we introduce the following assumptions:

1. Any replacement, whether corrective or preventive, takes negligible time.
2. The baseline function $\lambda_0(t;\alpha)$ in the PH model is non-decreasing for $t\geq 0$.
3. The link function $\theta[Y(t);\beta]$ is a non-decreasing function of the degradation state $Y(t)$.
4. The inspection cost C_0 is very small compared to any replacement cost. It is reasonable because condition-monitoring loses its significance if the monitoring cost is too high.

The objective of our replacement policy is to minimize the long-run expected average cost per unit time g by performing appropriate preventive replacement. Denote the state space by $\Omega=(\mathbf{H},\mathbf{K})$, where $\mathbf{H}=\{nh;n=0,1,2,...\}$ represents the inspection times and $\mathbf{K}$ represents the possible states of observed Y_n. We note that discretization of the continuous degradation state is applied in the following proof procedure in order to guarantee a finite state space for the policy optimization model. We will explain the details of the discretization scheme in Section 5. Let $V(n,Y_n)$ be the relative value function (see e.g. [17]) that formulates the relative cost in the infinite-horizon decision process when the system is currently in state $(n,Y_n)\in\Omega$, and $F_{Y_{n+1}}(y\mid n,Y_n)$ be the conditional cumulative distribution function (cdf) of Y_{n+1}, then the optimality equations can be expressed as follows:

$$V(n,Y_n)=\begin{cases}C_2+C+V(0,Y_0), & if\ Y_n\geq D_f\\ \min\{C+V(0,Y_0),W(n,Y_n)\}, & if\ Y_n<D_f\end{cases} \tag{7}$$

where

$$W(n,Y_n)=[C_1+C+V(0,Y_0)][1-R(Y_n,n,h)]+R(Y_n,n,h)\int_{Y_n}^{D_f}V(n+1,y)F_{Y_{n+1}}(y\mid n,Y_n)$$
$$+R(Y_n,n,h)\Pr(T<t_{n+1}\mid Y_n,Y_n<D_f)[C_2+C+V(0,Y_0)]+C_0R(Y_n,n,h)-g\tau(Y_n,n,h) \tag{8}$$

The first line of Eq. (7) describes the situation that if the observed degradation state by current inspection exceeds the soft failure threshold D_f, we perform an immediate corrective replacement at the expected cost C_2+C and put the system back to as-good-as-new state. The second line of Eq. (7) proposes the maintenance rule that if the observed degradation state is below the soft failure threshold D_f, we can either choose to preventively replace the system, or do nothing and continue operation, depending on the relative costs of the two different maintenance actions.

4. Structure of the optimal replacement policy

In this section, we will examine the structure of the optimal replacement policy for the replacement problem defined in Section 3.

Theorem 1. If $C_1>C_2+C_0$, the relative value function $V(n,Y_n)$ defined by the second line of Eq. (7) is non-decreasing for $(n,Y_n)\in\Omega$ and for any positive constant g.

Proof. Following the second line of Eq. (7), since $V(n,Y_n)=\min\{C+V(0,Y_0),W(n,Y_n)\}$, $V(n,Y_n)\leq C+V(0,Y_0)$. Let $V^k(n,Y_n)$ denote the relative value function at the k th iteration of the value iteration algorithm. We start by defining the initial value:

$$V^0(n,Y_n)=0\ \text{ for any }\ n \tag{9}$$

$V^0(n,Y_n)$ is non-decreasing for $(n,Y_n)\in\Omega$. Next, assume that $V^k(n,Y_n)$ is non-decreasing for $Y_n<D_f$ and $V^k(n,Y_n)\leq C+V^k(0,Y_0)$ are true at the k th iteration, then from Eq. (7),

$$V^{k+1}(n,Y_n)=\min\left\{C+V^k(0,Y_0),W^k(n,Y_n)\right\} \tag{10}$$

where:

$$
\begin{aligned}
W^k(n,Y_n) &= \left[C_1 + C + V^k(0,Y_0)\right]\left[1 - R(Y_n,n,h)\right] + R(Y_n,n,h)\int_{Y_n}^{D_f} V^k(n+1,y) F_{Y_{n+1}}(y \mid n, Y_n) \\
&\quad + C_0 R(Y_n,n,h) + R(Y_n,n,h)\Pr\left(T < t_{n+1} \mid Y_n, Y_n < D_f\right)\left[C_2 + C + V^k(0,Y_0)\right] - g\tau(Y_n,n,h) \\
&= \left[C_1 + C + V^k(0,Y_0)\right] - R(Y_n,n,h)\int_{Y_n}^{D_f}\left[C + V^k(0,Y_0) - V^k(n+1,y)\right] F_{Y_{n+1}}(y \mid n, Y_n) \\
&\quad - R(Y_n,n,h)\left[C_1 - C_2 \Pr\left(T < t_{n+1} \mid Y_n, Y_n < D_f\right) - C_0\right] - g\tau(Y_n,n,h)
\end{aligned} \tag{11}
$$

By induction hypothesis, $V^k(n,Y_n)$ is non-decreasing for $(n,Y_n) \in \Omega$ if $Y_n < D_f$. $R(Y_n,n,h)$ and $\tau(Y_n,n,h)$ in Eq. (11) are also non-increasing functions for $(n,Y_n) \in \Omega$. Moreover, since we consider a homogeneous gamma process, $F_{Y_{n+1}}(y \mid n, Y_n)$ is non-increasing and $\Pr\left(T < t_{n+1} \mid Y_n, Y_n < D_f\right)$ defined by Eq. (2) is also non-decreasing for $(n,Y_n) \in \Omega$. Therefore, if $C_1 > C_2 + C_0$, $W^k(n,Y_n)$ is non-decreasing for any positive constant g. Since both $C + V^k(0,Y_0)$ and $W^k(n,Y_n)$ in Eq. (10) are non-decreasing, $V^{k+1}(n,Y_n)$ is non-decreasing as well, which completes the proof.

Based on Theorem 1, we are able to find the form of optimal replacement policy by analyzing the optimality equations Eq. (7) and Eq. (8).

Theorem 2. Let 0 represent the immediate preventive replacement upon observation of the system state, 1 represent the immediate corrective replacement for the soft failure, and $+\infty$ corresponds to no replacements. If $C_1 > C_2 + C_0$, the optimal replacement policy has the following form:

$$
\delta(n,Y_n) = \begin{cases} 0, \text{ if } C_1 - R(Y_n,n,h)\left[C_1 - C_2 \Pr\left(T < t_{n+1} \mid Y_n, Y_n < D_f\right) - C_0\right] \geq g\tau(Y_n,n,h) \\ 1, \text{ if } Y_n \geq D_f \\ +\infty, \text{ if } C_1 - R(Y_n,n,h)\left[C_1 - C_2 \Pr\left(T < t_{n+1} \mid Y_n, Y_n < D_f\right) - C_0\right] < g\tau(Y_n,n,h) \end{cases} \tag{12}
$$

Proof.

Consider the case if:

$$C_1 - R(Y_n,n,h)\left[C_1 - C_2 \Pr\left(T < t_{n+1} \mid Y_n, Y_n < D_f\right) - C_0\right] < g\tau(Y_n,n,h),$$

then:

$$
\begin{aligned}
&W(n,z) - C - V(0,Y_0) \\
&= C_0 R(Y_n,n,h) + C_1\left[1 - R(Y_n,n,h)\right] + R(Y_n,n,h)\int_{Y_n}^{D_f}\left[V(n+1,y) - C - V(0,Y_0)\right] F_{Y_{n+1}}(y \mid n, Y_n) \\
&+ R(Y_n,n,h)\Pr\left(T < t_{n+1} \mid Y_n, Y_n < D_f\right)\left[C_2 + C + V(0,Y_0)\right] \\
&- R(Y_n,n,h)\Pr\left(T < t_{n+1} \mid Y_n, Y_n < D_f\right)\left[C + V(0,Y_0)\right] - g\tau(Y_n,n,h) \\
&= C_1 - R(Y_n,n,h)\left[C_1 - C_2 \Pr\left(T < t_{n+1} \mid Y_n, Y_n < D_f\right) - C_0\right] \\
&+ R(Y_n,n,h)\int_{Y_n}^{D_f}\left[V(n+1,y) - C - V(0,Y_0)\right] F_{Y_{n+1}}(y \mid n, Y_n) - g\tau(Y_n,n,h) \\
&< 0
\end{aligned}
$$

So that in this case the optimal decision is no replacement.

Consider the case if:

$$C_1 - R(Y_n,n,h)\left[C_1 - C_2 \Pr\left(T < t_{n+1} \mid Y_n, Y_n < D_f\right) - C_0\right] \geq g\tau(Y_n,n,h)$$

and assume that $V(n,Y_n) = W(n,Y_n) < C + V(0,Y_0)$. For $Y_{n+1} < D_f$, we have:

$$
\begin{aligned}
&V(n+1,Y_{n+1}) - V(n,Y_n) \\
&= V(n+1,Y_{n+1}) - \left[C_1 + C + V(0,Y_0)\right]\left[1 - R(Y_n,n,h)\right] + R(Y_n,n,h)\int_{Y_n}^{D_f} V(n+1,y) F_{Y_{n+1}}(y \mid n, Y_n) \\
&+ R(Y_n,n,h)\Pr\left(T < t_{n+1} \mid Y_n, Y_n < D_f\right)\left[C_2 + C + V(0,Y_0)\right] - C_0 R(Y_n,n,h) - g\tau(Y_n,n,h) \\
&= V(n+1,Y_{n+1}) - \left[C + V(0,Y_0)\right] + R(Y_n,n,h)\int_{Y_n}^{D_f}\left[V(n+1,y) - C - V(0,Y_0)\right] F_{Y_{n+1}}(y \mid n, Y_n) \\
&+ C_1 - R(Y_n,n,h)\left[C_1 - C_2 \Pr\left(T < t_{n+1} \mid Y_n\right) - C_0\right] - g\tau(Y_n,n,h) \\
&< C_1 - R(Y_n,n,h)\left[C_1 - C_2 \Pr\left(T < t_{n+1} \mid Y_n\right) - C_0\right] - g\tau(Y_n,n,h) \leq 0
\end{aligned}
$$

which is a contradiction to Theorem 1.

So that if:

$$C_1 - R(Y_n,n,h)\left[C_1 - C_2 \Pr\left(T < t_{n+1} \mid Y_n, Y_n < D_f\right) - C_0\right] \geq g\tau(Y_n,n,h),$$

the optimal decision is an immediate preventive replacement. This establishes the result.

Next, we will show in Theorem 3 that for the replacement problem defined in Section 3, the optimal replacement policy is a monotonically non-increasing multi-level control-limit policy in terms of the degradation state.

Theorem 3. If $C_1 > C_2 + C_0$, for all inspection times $t_n = nh$, if the observed system state Y_n is below the soft failure threshold D_f, the optimal decision is to preventively replace the system if and only if $Y_n \geq w_n^*$, where w_n^* is the optimal control limit at $t_n = nh$. The control limit w_n^* is monotonically non-increasing in n.

Proof. By Theorem 2, consider the condition for the preventive replacement:

$$\frac{C_1 - R(Y_n,n,h)\left[C_1 - C_2 \Pr\left(T < t_{n+1} \mid Y_n, Y_n < D_f\right) - C_0\right]}{\tau(Y_n,n,h)} \geq g \tag{13}$$

For any $t_n = nh$, the left-hand side of Eq. (13) is non-decreasing in Y_n. Therefore, if $\exists w_n^* < D_f$ makes Eq. (13) holds for $Y_n = w_n^*$, then Eq. (13) still holds for any $Y_n \geq w_n^*$. In other words, given that the optimal decision for degradation state at $Y_n = w_n^*$ is to preventively replace, the optimal decision for degradation state $Y_n \geq w_n^*$ is also to preventively replace. Thus, the optimal replacement policy at time $t_n = nh$ is a control-limit policy with control limit w_n^*.

On the other hand, since the left-hand side of Eq. (13) is non-decreasing in n, so that for any Y_n, there exists a starting time n^*h such that for any $nh \geq n^*h$ the optimal decision is to preventively replace the system. By the existence of a control limit w_n^* for each inspection time and a starting time n^*h for each degradation state, the control limit is w_n^* monotonically non-increasing in n.

Remark. We only use the homogeneous gamma process to derive the above optimal replacement policy. However, the optimality still establishes using other degradation models, if that $\Pr\left(T < t_{n+1} \mid Y_n, Y_n < D_f\right)$ is non-decreasing for $(n,Y_n) \in \Omega$ can be validated. The non-decreasing $\Pr\left(T < t_{n+1} \mid Y_n, Y_n < D_f\right)$ for $(n,Y_n) \in \Omega$ indicates two characteristics of a degradation process. Firstly, at the same inspection time, the degradation process which has a more severe deterioration would have a larger probability of soft failure during next inspection interval; secondly, for the same degradation state, the system which is "older" would be more likely to confront soft failure for the next inspection

interval. These two phenomena can be found in many real situations. Even if $\Pr\left(T < t_{n+1} \mid Y_n, Y_n < D_f\right)$ is not strictly non-decreasing for $(n, Y_n) \in \Omega$, the above replacement policy still might be the optimal since $R(Y_n, n, h)$, the conditional reliability function of sudden failure, may dominate the trend of $W(n, Y_n)$. Similarly, $C_1 > C_2 + C_0$ is also a quite strong assumption in order to ensure the monotonicity; in fact, if $R(Y_n, n, h)$ decreases quickly enough as the system ages, the theorems still hold.

5. Computation of the Optimal Replacement Policy

We demonstrate in Section 4 that the optimal replacement policy has a specific form, and it is also a multi-level control-limit policy with non-increasing control limits w_n^*. To apply this policy, it is necessary to compute the minimum long-run expected average cost per unit time g. We thus develop a computational procedure using semi-Markov decision process (SMDP) to obtain g. The computation of SMDP requires discretizing the possible range of values of $Y_n \in [y_0, +\infty)$ into a finite set of states. Define $[D_f, +\infty)$ as the failure state $\mathbf{F}$. We can then divide the continuous state space of $[y_0, D_f]$ into L equidistant intervals with constant length $\Delta = (D_f - y_0)/L$. If for some fixed integer $0 < \bar{k}_n < L$, $\bar{k}_n\Delta$ is defined as the control limit $\bar{w}_n$ at inspection time $t_n = nh$, then the warning state $\mathbf{W}_n$ at inspection time $t_n = nh$ will be $[\bar{k}_n\Delta + y_0, L\Delta + y_0)$, and the healthy state $\mathbf{S}_n$ will be $[y_0, \bar{k}_n\Delta + y_0)$. Thus, we approximate the state space $\Omega = (\mathbf{H}, \mathbf{K})$ by a non-decreasing homogeneous Markov chain with countable state space considering states (k, n), $(\mathbf{W}_n, n)$, $(\mathbf{F}, n)$.

Based on the above discretization scheme, for the system which has not failed by time t_n, if Y_n is known, the conditional reliability function defined in Eq. (5) is calculated as follows:

$$R(Y_n, n, t) = R(k, n, t) = \begin{cases} \Pr(T > t, t < h \mid Y_0 = y_0), \text{ for } k = 0, n = 0 \\ \Pr(T > nh + t, t < h \mid T > nh, Y_n = (k + 0.5)\Delta + y_0), \text{ for } 0 \le k < \bar{k}_n, n = 1, 2, \ldots \end{cases}$$
$$= \begin{cases} \exp\left\{-\theta(y_0; \boldsymbol{\beta}) \int_0^t \gamma_0(s; \boldsymbol{\alpha}) ds\right\}, \text{ for } k = 0, n = 0 \\ \exp\left\{-\theta[(k + 0.5)\Delta + y_0; \boldsymbol{\beta}] \int_{nh}^{nh+t} \gamma_0(s; \boldsymbol{\alpha}) ds\right\}, \text{ for } 0 \le k < \bar{k}_n, n = 1, 2, \ldots \end{cases} \tag{14}$$

Then, the expected sojourn time defined in Eq. (6) is calculated by:

$$\tau(Y_n, n, a) = \tau(k, n, a) = \int_0^a R(k, n, t) dt$$
$$= \begin{cases} \int_0^a \exp\left\{-\theta(y_0; \boldsymbol{\beta}) \int_0^t \lambda_0(s; \boldsymbol{\alpha}) ds\right\} dt, \text{ for } k = 0, n = 0 \\ \int_0^a \exp\left\{-\theta[(k + 0.5)\Delta + y_0; \boldsymbol{\beta}] \int_{nh}^{nh+t} \lambda_0(s; \boldsymbol{\alpha}) ds\right\} dt, \text{ for } 0 \le k < \bar{k}_n, n = 1, 2, \ldots \end{cases} \tag{15}$$

Next, we will derive the one-step transition probabilities in the SMDP. Using homogeneous gamma process, the probability that the value of Y_{n+1} will be in state $[l\Delta + y_0, (l+1)\Delta + y_0]$ given the current value of Y_n is in the interval $[k\Delta + y_0, (k+1)\Delta + y_0]$, $0 \le k < \bar{k}_n, 0 \le l < L$, is calculated by:

$$p_{(k,n),(l,n+1)} =$$
$$\begin{cases} \Pr\left(Y_{n+1} \in [l\Delta + y_0, (l+1)\Delta + y_0] \mid Y_0 = y_0\right), \text{ for } k = 0, n = 0 \\ \Pr\left(Y_{n+1} \in [l\Delta + y_0, (l+1)\Delta + y_0] \mid Y_n = (k + 0.5)\Delta + y_0\right), \text{ for } 0 \le k < k_n, k \le l < L, n = 0, 1, \ldots \end{cases}$$
$$= R(k, n, h) \int_{(l-k-0.5)\Delta}^{(l-k+0.5)\Delta} \frac{\gamma(\gamma z)^{h-1} \exp(-\gamma z)}{\Gamma(h)} dz. \tag{16}$$

Similarly, the probability that the value of Y_{n+1} will be in the warning state $\mathbf{W}_{n+1}$ given the current value of Y_n is in the interval $[k\Delta + y_0, (k+1)\Delta + y_0]$, $0 \le k < \bar{k}_n$, is calculated by:

$$p_{(k,n),(\mathbf{W}_{n+1}, n+1)} = \begin{cases} \Pr\left(Y_{n+1} \in \mathbf{W}_{n+1} \mid Y_0 = y_0\right), \text{ for } k = 0, n = 0 \\ \Pr\left(Y_{n+1} \in \mathbf{W}_{n+1} \mid Y_n = (k + 0.5)\Delta + y_0\right), \text{ for } 0 \le k < k_n, n = 0, 1, \ldots \end{cases}$$
$$= R(k, n, h) \int_{k_{n+1}-k-0.5}^{(L-k+0.5)\Delta} \frac{\gamma(\gamma z)^{h-1} \exp(-\gamma z)}{\Gamma(h)} dz. \tag{17}$$

Moreover, the probability that the value of Y_{n+1} will be in the failure region determined by state $\mathbf{F}$ given the current value of Y_n is in the interval $[k\Delta + y_0, (k+1)\Delta + y_0]$, $0 \le k < \bar{k}_n$, is calculated by:

$$p_{(k,n),(\mathbf{F}, n+1)} = \begin{cases} \Pr\left(Y_{n+1} \in \mathbf{F} \mid Y_0 = y_0\right), \text{ for } k = 0, n = 0 \\ \Pr\left(Y_{n+1} \in \mathbf{F} \mid Y_n = (k + 0.5)\Delta + y_0\right), \text{ for } 0 \le k < k_n, n = 0, 1, \ldots \end{cases}$$
$$= R(k, n, h) \left(1 - \int_0^{(L-k+0.5)\Delta} \frac{\gamma(\gamma z)^{h-1} \exp(-\gamma z)}{\Gamma(h)} dz\right). \tag{18}$$

With the definition of the state space, for a fixed control limit χ, the warning state $\mathbf{W}_n$ at inspection time $t_n = nh$ will be $[\bar{k}_n\Delta + y_0, L\Delta + y_0)$, where $\bar{k}_n$ can be approximated by

$$\bar{k}_n = \min\left\{k; C_1 - R(k, n, h)\left(C_1 - C_2 \Pr\left(T < t_{n+1} \mid Y_n = k\Delta + y_0, k < L\right) - C_0\right) \ge \chi \tau(k, n, h)\right\} \tag{19}$$

If $\bar{k}_n \ge L$, only corrective replacement is allowed at inspection time $t_n = nh$; and if $\bar{k}_n \le 0$, the system should stop operating at inspection time $t_n = nh$ with an immediate preventive or corrective replacement. The smallest time to stop operating and enforce replacement is defined as $\tilde{t}_\chi = \tilde{n}_\chi h$. Thus, the determination of a control limit χ can be transformed into determining the $\tilde{n}_\chi$. For a fixed integer $\tilde{n}_\chi$, the corresponding control limit χ is given by:

$$\chi = \frac{C_1 - R(0, \tilde{n}_\chi, h)\left[C_1 - C_2 \Pr\left(T < t_{\tilde{n}_\chi + 1} \mid Y_n = y_0\right) - C_0\right]}{\tau(0, \tilde{n}_\chi, h)} \tag{20}$$

Once all of the quantities above are defined, for a fixed integer $\tilde{n}_\chi$, the long-run expected average cost per unit time $g(\chi)$ for the competing risk of soft and sudden failure can be obtained by solving the following systems of linear equations (see e.g. [17]):

$$
\begin{aligned}
&V(0,0) = C_0 + (C_1 + C)\left[1 - R(0,0,h)\right] - g(\chi)\tau(0,0,h) + \sum_{l=0}^{\bar{k}_1} p_{(0,0),(l,1)} V(1,l) + p_{(0,0),(\mathbf{W}_1,1)} V(1,\mathbf{W}_1) \\
&\quad + p_{(0,0),(\mathbf{F},1)} V(1,\mathbf{F}) + [1 - R(0,0,h)] V(0,0) \\
&V(n,k) = C_0 R(k,n,h) + (C_1 + C)\left[1 - R(k,n,h)\right] - g(\chi)\tau(k,n,\boldsymbol{h}) + \sum_{l=0}^{\bar{k}_{n+1}} p_{(k,n),(l,n+1)} V(n+1,l) \\
&\quad + p_{(k,n),(\mathbf{W}_{n+1},n+1)} V(n+1,\mathbf{W}_{n+1}) + p_{(k,n),(\mathbf{F},n+1)} V(n+1,\mathbf{F}) + \left[1 - R(k,n,h)\right] V(0,0), \\
&\quad \text{for } k = 0,1,\ldots,\bar{k}_{\tilde{n}_\chi} \text{ and } n = 1,2,\ldots,\tilde{n}_\chi - 1 \\
&V(n,\mathbf{W}_n) = C + V(0,0), \text{ for } n = 1,2,\ldots,\tilde{\boldsymbol{n}}_\chi \\
&V(n,\mathbf{F}) = C_2 + C + V(0,0), \text{ for } n = 1,2,\ldots,\tilde{n}_\chi \\
&V(\tilde{n}_\chi,k) = V(\tilde{n}_\chi,\mathbf{W}_{\tilde{n}_\chi}), \text{ for } k = 0,1,\ldots,\bar{k}_{\tilde{n}_\chi} \\
&V(p,q) = 0, \text{ for some } p = 0,1,\ldots,L \text{ and } q = 0,1,\ldots,\tilde{n}_\chi.
\end{aligned}
\tag{21}
$$

where $V(\bullet,\bullet)$ is the same relative value function as defined in Section 3, considering discretized degradation states.

So that the optimal control limit χ^* and corresponding minimum long-run expected average cost per unit time $g(\chi^*)$ can be found by:

$$
g(\chi^*) = \inf_{\tilde{n}_\chi} \{g(\chi)\}. \tag{22}
$$

A stopping rule for determining an appropriate L to partition the continuous state space $[y_0, D_f]$ is needed in this algorithm, which could be:

$$
g(\chi^* \mid L = 2^{U+1}) - g(\chi^* \mid L = 2^U) \le \delta. \tag{23}
$$

where U is positive integer and δ is the selected small number.

6. Case study

In this section, we use a real degradation data presented by Meeker and Escobar [16] (Chapter 13, Example 13.5) to illustrate the application of our proposed optimal replacement policy. This data set consists of 20 degradation histories, describing the degradation process of some GaAs lasers subject to the competing soft and sudden failures. During the life of GaAs lasers, the degradation causes an increase in the laser's operating current. The laser is considered to be failed if the operating current increases to D_f percent of its original value. On the other hand, physical breakdown due to the sudden failures may also occur and consequently interrupts the graceful degradation. For illustration purpose, we assume $D_f = 5$ as the soft failure threshold, and the operating currents were inspected every $h = 100$ hours up to $\tau = 2000$ hours or until the sudden failure happens. The degradation paths are plotted in Fig.1, in which 13 out of 20 degrade gradually till the censored time, while the other 7 samples show a sharp increase in operating current when the sudden failure occurs.

First, we fit the data using the model described in Section 2. We assume the baseline hazard function is Weibull hazard function denoted as $\lambda_0(t)=\rho t^{\rho-1}/\sigma^\rho$ and the function to quantify the effect of system degradation state on the failure rate is exponential having the form $\theta(Y_t) = \exp(cY_t)$, where c is a real coefficient. Using joint likelihood function and the interior-reflective Newton method, we obtain the ML estimates for the model parameters, as shown in Table 1.

In order to validate the fitted model, we use the probability plot to assess whether the increments of laser degradation follow the gamma process $Ga(\eta h, \gamma)$ and compare the ML estimates with non-parametric Kaplan-Meier estimates for the PH model. Fig. 2 and Fig. 3 show the results, demonstrating that the fitted model is well suited for the laser data. Note that in Fig. 3, we approximate the cumulative distribution function by:

Table 1. ML estimates for the model parameters

Parameters	η	γ	ρ	σ	c
ML estimates	4.7676	19.5353	1.3932	8.3859	0.3540

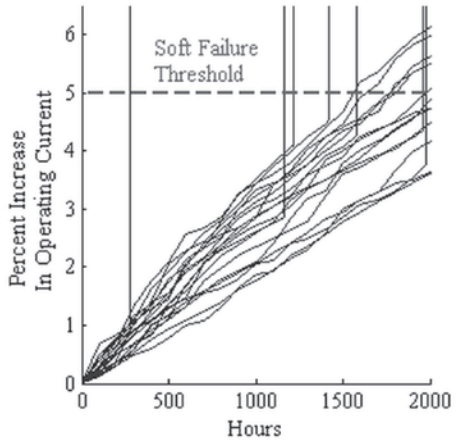

Fig. 1. Degradation paths for the laser data

$$
F(nh) = 1 - \exp\left(-\int_0^{nh} \lambda_0(t;\rho,\sigma)\theta[Y(t);c]dt\right) = 1 - \exp\left(-\sum_{k=0}^{n-1} \exp\left[cE(Y_k)\right] \int_{kh}^{(k+1)h} \rho t^{\rho-1}/\alpha^\rho dt\right). \tag{24}
$$

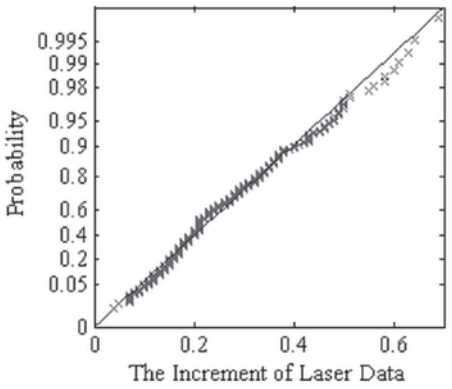

Fig.2. Probability plot of the increments for the laser data

Next, we consider the following replacement costs to illustrate our replacement policy: $C_0 = 100$, $C = 1000$, $C_1 = 4000$, $C_2 = 3000$. Since $C_1 > C_2 + C_0$, the optimal replacement policy proposed in Section 4 is applicable to this case. We partition the continuous state space of $[y_0 = 0, D_f = 5]$ into $L = 128$ intervals. The long-run expected average cost per thousand hours $g(\chi)$ for different control limits χ are plotted in Fig.4, in which we can find the minimum long-run expected average cost per thousand hours is $g(\chi^*) = 1586.052$ with the optimal control limit $\chi^* = 1587.573$. Using the control limit $\chi^* = 1587.573$, the optimal control limits w_n^* in terms of degradation level at each inspection time $t_n = nh$ presents a decreasing trend in time, as shown in Fig. 5. When the observed degradation level Y_n exceeds w_n^*, the optimal maintenance policy is to preventively replace the system. We demonstrate the appropriateness of $L = 128$ using the stopping rule of Eq. (23). The results are shown in Table 2.

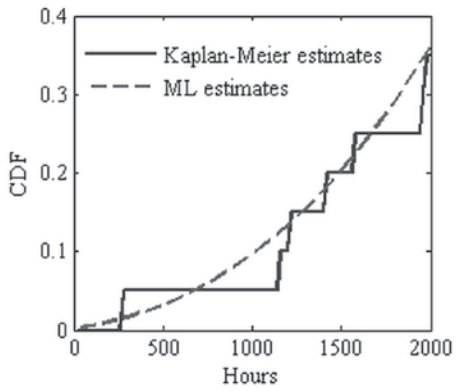

Fig. 3. ML estimates and the Kaplan-Meier estimates for the marginal CDF of sudden failure times

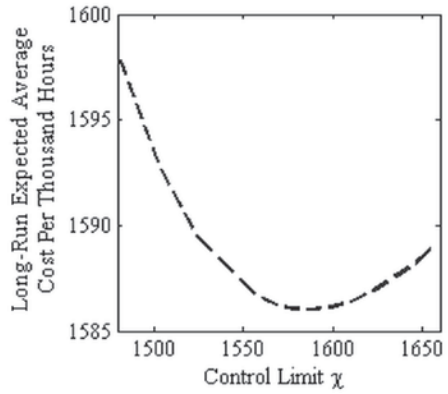

Fig. 4. The long-run expected average costs per thousand hours for different control limits

7. Conclusion

In this paper, we have investigated the optimal replacement policy for a periodically inspected system subject to the competing risk of soft and sudden failures. This policy focuses on the system whose degradation process can be described by a gamma process and sudden failure rate by a PH model. If the preventive replacement only performs at inspection times and the sudden failure dominates in the failure mechanism, it is demonstrated that the optimal replacement policy has a specific form and it is actually a multi-level control-limit policy with control limits in terms of the degradation level. A computational algorithm based on a SMDP framework has also been developed to obtain the optimal replacement policy. The entire procedure of applying this policy is illustrated by a real laser example.

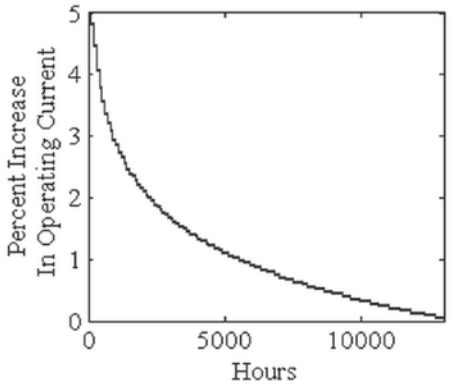

Fig. 5. The optimal control limits w_n^* at each inspection time

Table 2. χ^* and $g(\chi^*)$ under different combinations of L

L	16	32	64	128	256
χ^*	1521.154	1538.410	1570.134	1587.573	1590.965
$g(\chi^*)$	1520.362	1538.742	1569.721	1586.052	1590.750

References

1. Besnard F, Bertling L. An approach for condition-based maintenance optimization applied to wind turbine blades. IEEE Transactions on Sustainable Energy 2010; 1(2): 77-83, http://dx.doi.org/10.1109/TSTE.2010.2049452.
2. Bocchetti D, Giorgio M, Guida M, Pulcini G. A competing risk model for the reliability of cylinder liners in marine diesel engines. Reliability Engineering & System Safety 2009; 94(8): 1299-1307, http://dx.doi.org/10.1016/j.ress.2009.01.010.
3. Castro IT, Caballé NC, Pérez CJ. A condition-based maintenance for a system subject to multiple degradation processes and external shocks. International Journal of Systems Science 2013; ahead-of-print: 1-13, http://dx.doi.org/10.1080/00207721.2013.828796.
4. Coats D, Cho K, Shin YJ, Goodman N, Blechertas V, Bayoumi AE. Advanced time-frequency mutual information measures for condition based maintenance of helicopter drive trains. IEEE Transactions on Instrumentation and Measurement 2004; 60(8): 2984-2994, http://dx.doi.org/10.1109/TIM.2011.2122370.
5. Cox DR, Oakes D. Analysis of survival data. Chapman and Hall; 1984.
6. Elwany AH, Gebraeel NZ, Maillart LM. Structured replacement policies for components with complex degradation processes and dedicated sensors. Operations research 2011; 59(3): 684-695, http://dx.doi.org/10.1287/opre.1110.0912.
7. Grall A, Bérenguer C, and Dieulle L. A condition-based maintenance policy for stochastically deteriorating systems. Reliability Engineering & System Safety 2002; 76(2): 167-180, http://dx.doi.org/10.1016/S0951-8320(01)00148-X.
8. Huang W, Askin RG. Reliability analysis of electronic devices with multiple competing failure modes involving performance aging degradation. Quality and Reliability Engineering International 2003; 19(3): 241-254, http://dx.doi.org/10.1002/qre.524.
9. Huynh KT, Barros A, Bérenguer C, Castro IT. A periodic inspection and replacement policy for systems subject to competing failure modes due to degradation and traumatic events. Reliability Engineering & System Safety 2011; 96(4): 497-508, http://dx.doi.org/10.1016/j.ress.2010.12.018.
10. Huynh KT, Castro IT, Barros A, Bérenguer C. On the use of mean residual life as a condition index for condition-based maintenance decision making. IEEE Transactions on Systems, Man, and Cybernetics: Systems 2014; 44(7): 877-893, http://dx.doi.org/10.1109/TSMC.2013.2290772.
11. Jiang R, Yu J, Makis V. Optimal Bayesian estimation and control scheme for gear shaft fault detection. Computers & Industrial Engineering

2012; 63(4): 754-762, http://dx.doi.org/10.1016/j.cie.2012.04.015.
12. Kim MJ, Jiang R, Makis V, Lee CG. Optimal Bayesian fault prediction scheme for a partially observable system subject to random failure. European Journal of Operational Research 2011; 214(2): 331-339, http://dx.doi.org/10.1016/j.ejor.2011.04.023.
13. Liao H, Elsayed EA, Chan LY. Maintenance of continuously monitored degrading systems. European Journal of Operational Research 2006; 175(2): 821-835, http://dx.doi.org/10.1016/j.ejor.2005.05.017.
14. Lin D, Wiseman M, Banjevic D, Jardine, AK. An approach to signal processing and condition-based maintenance for gearboxes subject to tooth failure. Mechanical Systems and Signal Processing 2004; 18(5): 993-1007, http://dx.doi.org/10.1016/j.ymssp.2003.10.005.
15. Liu X, Li J, Al-Khalifa KN, Hamouda AS, Coit DW, and Elsayed E A. Condition-based maintenance for continuously monitored degrading systems with multiple failure modes. IIE Transactions 2013; 45(4): 422-435, http://dx.doi.org/10.1080/0740817X.2012.690930.
16. Meeker WQ, Escobar LA. Statistical methods for reliability data. John Wiley & Sons; 1998.
17. Tijms HC. Stochastic models: an algorithmic approach. John Wiley & Sons; 1994.
18. van Noortwijk JM. A survey of the application of gamma processes in maintenance. Reliability Engineering & System Safety 2009; 94(1): 2-21, http://dx.doi.org/10.1016/j.ress.2007.03.019.
19. Wang WB. A model to determine the optimal critical level and the monitoring intervals in condition-based maintenance. International Journal of Production Research 2000; 38(6): 1425-1436, http://dx.doi.org/10.1080/002075400188933.
20. Zhu Y, Elsayed EA, Liao H, Chan LY. Availability optimization of systems subject to competing risk. European Journal of Operational Research 2010; 202(3): 781-788, http://dx.doi.org/10.1016/j.ejor.2009.06.008.
21. Ye ZS, Xie M, Tang LC, Shen Y. Degradation-based burn-in planning under competing risks. Technometrics 2012; 54(2): 159-168, http://dx.doi.org/10.1080/00401706.2012.676946.

Diyin TANG
Jinsong YU
School of Automation Science and Electrical Engineering
Beihang University
No. 37 Xueyuan Road, Haidian District
Beijing, China, 100191
Collaborative Innovation Center of Advanced Aero-Engine
Beijing, China, 100191
E-mails: amytdy@asee.buaa.edu.cn, yujs@buaa.edu.cn

Article citation info:
GE Z, WU F, YANG Y, LUO X. One cabin equipment location method based on the visibility human-factor potential field. Eksploatacja i Niezawodnosc – Maintenance and Reliability 2015; 17 (2): 236–242, http://dx.doi.org/10.17531/ein.2015.2.10.

Zhexue GE
Fuzhang WU
Yongmin YANG
Xu LUO

ONE CABIN EQUIPMENT LOCATION METHOD BASED ON THE VISIBILITY HUMAN-FACTOR POTENTIAL FIELD

METODA ROZMIESZCZANIA PRZYRZĄDÓW POKŁADOWYCH OPARTA NA POJĘCIACH POTENCJAŁOWEGO POLA WIDOCZNOŚCI ORAZ POTENCJAŁOWEGO POLA CZYNNIKA LUDZKIEGO

The visibility is the basic condition for cabin equipment location. For the description of human, object and obstacle, the human-factor potential field concept is proposed in this paper, concluding the visibility potential field, the reachability potential field. The cabin equipment layout problem is modeled based on the basic visibility potential field model. The optimal layout optimization method is studied based on the particle swarm optimization (PSO) algorithm by natural selection. Finally, the applicability of the proposed idea is illustrated by numerical studies.

Keywords: *cabin equipment, the human-factor potential field (HFPF), visibility potential field(VPF), layout optimization, particle swarm optimization (PSO).*

Widoczność jest podstawowym warunkiem przy projektowaniu rozmieszczenia przyrządów pokładowych. W przedstawionej pracy zaproponowano pojęcie potencjałowego pola czynnika ludzkiego (human-factor potential field, HFPF), które służy do opisu czynnika ludzkiego, przedmiotów oraz przeszkód. HFPF obejmuje pojęcia potencjałowego pola widoczności oraz potencjałowego pola dostępu. Problem umiejscowienia elementów wyposażenia kabiny zamodelowano na podstawie podstawowego modelu potencjałowego pola widoczności. Metodę optymalizacji rozmieszczenia elementów wyposażenia badano w oparciu o algorytm optymalizacji rojem cząstek (PSO), metodą naturalnej selekcji. Zastosowanie proponowanej koncepcji zilustrowano na przykładzie badań numerycznych.

Słowa kluczowe: *przyrządy pokładowe, potencjałowe pole czynnika ludzkiego (HFPF), potencjałowe pole widoczności (VPF), optymalizacja rozmieszczenia, optymalizacja rojem cząstek (PSO).*

1. Introduction

Ships, aircraft, armored vehicle, etc. usually consist of cabin structure, and there are a lot of cabin equipment requires manual inspection, monitoring, maintenance and operation [10]. In the cabin design process, visibility is one very important design factor to ensure the monitored equipment within the visual scope [9]. All the equipment to be maintained need reasonable operation space, and the determination of the space distribution of the equipment is an important part of the product design.

There are a large number of studies analyzing the visibility of product. However, in most cases the process is based on the graphics method and needs manual participation. Yin adopts visual cone method to assess the visibility of manufacturing process [12]. Bidault combines the method of clipping plane and visual cone [3]. In order to increase the design and analysis efficiency of the space layout design, the model based on visibility optimization design method is indispensable, but there are very few relative studies at present.

This paper mainly studies the cabin equipment layout method from the field point of view. To describe the relationship between the human body, the obstacle and the object, the conception of the human-factor potential field is put forward in the paper, and the mathematical model of visibility potential field is established. Then the optimization design method of space layout based on the visibility target is studied so as to improve the spatial layout of visual design efficiency and design quality. The layout optimization design model is established and solved by the particle swarm optimization algorithm.

2. The Human-factor Potential Field Concept

2.1. The artificial potential field

The artificial potential field (APF) method originated in the physics field theory [5, 7], which is first proposed by Khatbi in 1986 [7].It is artificially built similar to the physics potential field and can be applied to the study on some non-physics problems. The basic principle of APF can be summarized as follows. The motion of the manipulator or mobile robots can be considered in an abstract artificial force field. Target point X_{goal} generates attractive force on the robot X , and obstacle X_{obs} generates repulsion to the robot, and finally the motion of the robot is determined according to the composition of the forces. The direction of non-collision path is gotten by the direction of the descent potential function. The method has been widely used for real-time obstacle avoidance and smooth trajectory control.

Since the artificial potential field is one scalar field and its characteristics are similar to the electric field. The artificial potential field method creates a potential field U in the motion space of moving object. The potential field is composed of two parts: one is the attractive force field $\dot{U}_{att}$, it increases monotonically with the distance of the moving object and target, and directs to the target point; another is the repulsive force field $\dot{U}_{rep}$, it decreases monotonically with the increasing of moving object and obstacle distance and has a maximum value when the moving object in the location of obstacle. $\dot{U}_{rep}$ points to the direction opposite to the target point.

The total potential field is the sum of attractive force part and repulsive force part. The force of one moving object in the artificial potential field is the negative gradient of U:

$$F(X)=\dot{U}_{att}(X)+\dot{U}_{rep}(X)=-\nabla U(X) \tag{1}$$

The attractive force field in the whole area is defined as:

$$\dot{U}_{att}(X)=\frac{1}{2}\xi\rho^{m}\left(X,X_{goal}\right) \tag{2}$$

Where, ξ is the proportional coefficient, $\rho\left(X,X_{goal}\right)$ is the distance of moving object X to the object X_{goal}, $m=2$.

The attractive force of the moving object is the negative gradient of attractive potential energy:

$$F_{att}(X)=-\nabla U_{att}(X)=\xi\left(X,X_{goal}\right) \tag{3}$$

The force linearly goes to zero when the moving object approaches the target.

One general formula for the repulsive force field is:

$$\dot{U}_{rep}(X)=\begin{cases}\frac{1}{2}\eta\frac{1}{\rho\left(X,X_{goal}\right)}\cdots\rho\left(X,X_{obs}\right)\le\rho_0\\ 0\cdots\rho\left(X,X_{obs}\right)>\rho_0\end{cases} \tag{4}$$

The resultant of force is the composition of attraction and repulsion forces, i.e.:

$$F_{total}=F_{att}+F_{rep} \tag{5}$$

The next movement of the moving object can be determined by the force magnitude and direction.

2.2. The Human-factor Potential Field concept

Based on the definition of artificial potential field, the human-factor potential field (HFPF) is an artificial field to describe the impact of operator to the product. It reflects the interaction mechanism between operator and product operability features, and it includes the independent and complex field of human visibility, accessibility and comfort, potential field.

In the HFPF, each design unit structure will have some human-factor potential energy, the body and optimal human performance region produce attractive force to the unit, while the repulsion forces are produced between the different structures. Thus the dynamic change of the product structure and layout can be driven, and the best location for the design unit can be found to maximize the attractive force.

Definition 1: The HFPF refers to the artificial field interaction between various human factors and environment subjects. It can be formulated as (6):

$$U(X)=u(h_i(X),e_j(X)) \tag{6}$$

Where, $h_i(X)$ is the human factor parameter of space point $X=(x,y,z)$, and $e_j(X)$ is the environmental parameter of X. According to the artificial potential concept, the HFPF can be divided into the gravitational potential field U_{att} and the repulsive potential field U_{rep}, and the former is produced by the target and operator, while the latter is produced by the interactions of obstacles and operator.

The human-factor ability includes a lot of factors. Visual, auditory, tactile, olfactory, proprioceptive, etc. are associated with the feeling, and working space, comfort, etc. are associated with exercise capacity. So the HFPF includes visibility potential field, auditory potential field, tactile potential field, olfactory potential field, accessibility and other potential field, etc. This paper mainly focuses on the visibility potential field.

Definition 2: The visibility potential field $U_C(X)$ describes the interaction of eyes and all space points. It represents the space observation ability of eyes and can be formulated as (7):

$$U_C(X)=u_c(h_{ci}(X),e_{cj}(X)) \tag{7}$$

Where, $h_{ci}(X)$ represents the parameters associated with visibility, such as visual acuity, visual field, visual range and visual fatigue [1, 2, 4, 8, 11]. $e_{ci}(X)$ represents the environment parameters associated with visibility, such as light environment, obstacles between the target point and the human eye.

3. The modeling of visibility potential field

3.1. The visibility potential model

The visibility potential field (VPF) can be expressed as the sum of the attractive filed function and repulsion field function as follows:

$$U_C(X_P)=U_{C\_att}(X_P)+U_{C\_rep}(X_P) \tag{8}$$

Where, $U_{C\_att}(X_P)$ is the attractive visibility potential field. The influence factor of the eye enginery includes the amount of visual field, the visual distance and so on. The influence factor of the environment concludes obstacle, light and so on[9]. For simplicity, the visual field and visual distance are to be considered in the paper.

$$U_{C\_att}(X_P)=u\left(C_\theta(X_P),C_l(X_P),C_{light}(X_P)\right)=1-C_\theta(X_P)\bullet C_l(X_P) \tag{9}$$

Where, $C_\theta(X_P)$, $C_l(X_P)$ are the eye visual function. They can denote the relationship of visibility with the visual field and visual distance respectively. $X_P=\{x_P,y_P,z_P\}$ is the coordinate of the point P.

$U_{C\_rep}(X_P)$ is the repulsion visibility potential field. It can be expressed as follows:

$$\begin{aligned}U_{C\_rep}(X_P)&=U\left(C_e(X_P),C_\theta(X_P),C_l(X_P),C_{obs}(X_P)\right)\\&=C_e(X_P)\bullet C_\theta(X_P)\bullet C_l(X_P)\bullet C_{obs}(X_P)\end{aligned} \tag{10}$$

Then ,the visibility potential energy function is formula (11):

$$\begin{aligned} U_C(X_P) &= U_{C\_cat}(X_P) + U_{C\_rep}(X_P) \\ &= 1 - C_e(X_Q) \bullet C_\theta(X_Q) \bullet C_l(X_Q) \bullet (1 - C_{obs}(X_P)) \end{aligned} \tag{11}$$

Where $C_{obs}(X_P)$ represents the effect function of the obstacle to visibility.

3.2. The visual field function

The visual field is the space that can be seen by eyes when the environment and head remain stationary. According to the relationship between visual field and visibility in literature 5, visual field function is defined as follows:

$$C_\theta(X) = C_{\theta y}(X) \bullet C_{\theta x}(X) \tag{12}$$

When the head remained stationary but eye in the rotation, vertical field of human normal sight direction is horizontal line of 15 degree down, which is the human natural angle of sight. The line of sight of the upper and lower 15° is the comfortable vertical visual field, and the maximum vertical field of view is the region of above the normal sight line of sight 40° to 20° below [9]. Some representative point values of vertical visual field can be gotten as Table 1.

Table 1. Some representative direction values of vertical visual field

Direction number	Angle (degree)	Visibility value
1	-20	0
2	-15	0.8
3	0	1
4	15	0.8
5	40	0

Based on Table 1, the relationship between $C_{\theta y}$ and vertical sight angles can be gotten by polynomial fitting. It can be formulated as follows:

$$C_{\theta y} = 2.8120\theta_y{}^3 - 4.9801\theta_y{}^2 + 0.5892\theta_y + 1.0495 \tag{13}$$

Similarly, the scope between 15° left and right of the center line is the best horizontal vision scope of both eyes, while the scope between 13° left and right of the center line is the maximum field of view. Some representative point values of horizontal visual field can be gotten as Table 2.

Table 2. Some representative direction values of horizontalvisual field

Direction number	Angle (degree)	Visibility value
1	-35	0
2	-15	0.8
3	0	1
4	15	0.8
5	35	0

The horizontal visual field C_{θ_x} can be formulated as(14):

$$C_{\theta x} = -0.2089\theta_x{}^3 - 2.7580\theta_x{}^2 + 0.1103\theta_x + 1.0596 \tag{14}$$

Where θ_x is the horizontal visual angle of sight.

3.3. Visual distance function

The visual distance in operation directly affects the reading speed and accuracy, it should be determined by the size and shape of observation object. Usually, the most suitable visual region is 38~76 cm, less than 38 cm can cause dizziness, more than 76 cm may lose details. Using 4 order polynomial fitting, visibility distance function ξ_j can be gotten as:

$$C_l = 9.9531\times10^{-8} \bullet l^4 - 2.0927\times10^{-5} \bullet l^3 + 0.0011\times10^{-2} \bullet l^2 - 2.7047\times10^{-4} \bullet l + 0.0038 \tag{15}$$

Where, n is the visual distance.

3.4. Obstacle influence function

Among the environmental factors, the impact of obstacles is mostly concerned. When people are watching the object, the obstacle blocked area cannot be seen. The obstacle influence function should be formulated according to the geometric relations of human, obstacle and space point. Suppose the eye locates at point O, and the obstacle locates at point O', the obstacle is simplified to a circular area of radius R_{obs}. $\overrightarrow{l_{\mathrm{obs}}} = \overrightarrow{OO'}$ is the distance between the obstacle and eye, θ_{R} is angel between obstacle edge and eyesight baseline. For space point P, the distance to eye is (x_i, y_i). Then the obstacle visibility function C_{obs} can be expressed as follows:

$$C_{obs} = \begin{cases} 0 & if \ \left|\overrightarrow{l_P}\right| > \left|\overrightarrow{l_{obs}}\right| \text{ and } \theta_{\mathrm{P}} \le \theta_{\mathrm{R}} \\ 1 & if \ \left|\overrightarrow{l_P}\right| > \left|\overrightarrow{l_{obs}}\right| \text{ and } \theta_{\mathrm{P}} > \theta_{\mathrm{R}} \\ 1 & if \ \left|\overrightarrow{l_P}\right| \le \left|\overrightarrow{l_{obs}}\right| \end{cases} \tag{16}$$

In order to ensure C_{obs} can be continuous and differentiable, the obstacle surrounding area is looked as the transition region. Suppose C_{obs} changes from 1to 0 between θ_{R} and θ_M. Then C_{obs} can be smoothed as formula (17).

$$C_{obs} = \begin{cases} 0 & \text{if } \left|\overrightarrow{l_P}\right| > \left|\overrightarrow{l_{obs}}\right| \text{ and } \theta_{\mathrm{P}} \le \theta_{\mathrm{R}} \\ a \bullet \left(\theta_P - \theta_R\right)^3 + b \bullet \left(\theta_P - \theta_R\right)^2 + c \bullet \left(\theta_P - \theta_R\right)^3 + d & \text{if } \left|\overrightarrow{l_P}\right| > \left|\overrightarrow{l_{obs}}\right| \text{ and } \theta_{\mathrm{R}} < \theta_{\mathrm{P}} \le \theta_{\mathrm{M}} \\ 1 & \text{if } \left|\overrightarrow{l_P}\right| > \left|\overrightarrow{l_{obs}}\right| \text{ and } \theta_{\mathrm{P}} > \theta_{\mathrm{M}} \\ 1 & \text{if } \left|\overrightarrow{l_P}\right| \le \left|\overrightarrow{l_{obs}}\right| \end{cases} \tag{17}$$

Where:

$$a = -1 \Big/ (\theta_M^3 - \theta_R^3 - 3\theta_R^2\theta_M^3 + 3\theta_R^4 - 3\theta_M^4\theta_R + 3\theta_M\theta_R^3 - 3\theta_M^5 + 3\theta_M^2\theta_R^2)$$

$$b = 3(-\theta_M^3 + \theta_R^2) \Big/ (-\theta_M + \theta_R)(\theta_M^3 - \theta_R^3 - 3\theta_R^2\theta_M^3 + 3\theta_R^4 - 3\theta_M^4\theta_R + 3\theta_M\theta_R^3 - 3\theta_M^5 + 3\theta_M^2\theta_R^2)$$

$$c = -\frac{-3\theta_M\theta_R(\theta_M - \theta_R^2)}{(-\theta_M + \theta_R)(\theta_M^3 - \theta_R^3 - 3\theta_R^2\theta_M^3 + 3\theta_R^4 - 3\theta_M^4\theta_R + 3\theta_M\theta_R^3 - 3\theta_M^5 + 3\theta_M^2\theta_R^2)}$$

$$d = -\frac{-\theta_M(3\theta_R^3 - 6\theta_M^2\theta_R^2 - \theta_M^3 + 3\theta_M^5 - \theta_R\theta_M^2)}{(-\theta_M + \theta_R)(\theta_M^3 - \theta_R^3 - 3\theta_R^2\theta_M^3 + 3\theta_R^4 - 3\theta_M^4\theta_R + 3\theta_M\theta_R^3 - 3\theta_M^5 + 3\theta_M^2\theta_R^2)}$$

Using MATLAB software, the space distribution of VPF can be drawn based on the VPF model. Different color can demonstrate the potential difference of every space point in the three-dimension map.

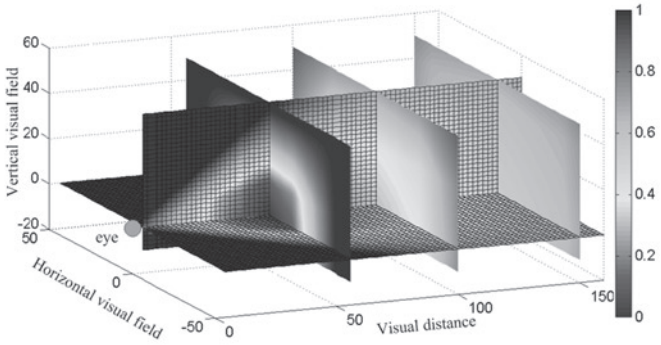

Fig. 1. Distribution of VPF without obstacle

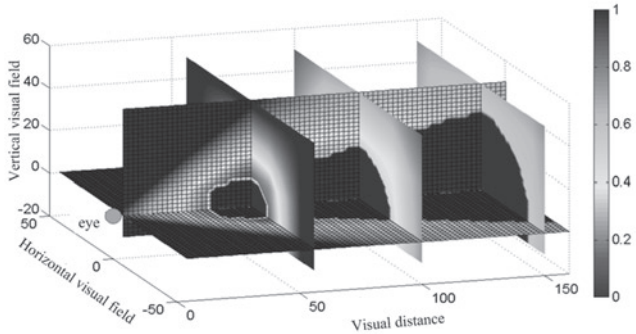

Fig. 2. Distribution of VPF with obstacle

Choose $\theta_M = 1.1\theta_R$. The lower potential ,the better visibility. The cross section perpendicular to the eyesight line can reflect the VPF of certain visual distance. Fig. 1. shows the VPF when the distance is 56 cm. When an obstacle exits at (0,0,50) with a radius of 10 cm, the VPF can be shown as Fig. 2., from which we can see that the VPF of blocked area is or close to 1, which means very poor visibility.

4. Space visibility optimizing layout

4.1. Modeling

Layout optimization modeling includes the determination of the optimization variables, objective function and the constraints.

(1) Objective function

It can be approximated considered that the visibility potential energy of one equipment is the sum of all the face points. Since not every point on the equipment has visibility requirement, the visibility potential energy can mainly concentrate on the highly required points that is the critical visual point. Then, the i-th object visibility function can be $U_C(i)=\sum_{j=1}^{m}\xi_{ij}U_C(X_{ij})$, where, m is the number of critical visual points on the target, ξ_{ij} represents the weight of the j-th key visual point, $0 \le \xi_{ij} \le 1$, and $\sum_{j=1}^{m}\xi_{ij}=1$. U_j represents the visibility potential energy of j -th critical visual point.

The comprehensive visibility potential energy represents the visibility of space layout design, which is the weighted sums of the visibility of all objects in the layout space, as $U_C=\sum_{i=1}^{n}\psi_i \bullet U_C(i)$, where, n expresses the number of layout objects, ψ_i is the weight of i-th object, $0 \le \psi_j \le 1$, and $\sum_{i=1}^{n}\psi_j=1$, $U_C(i)$ specifies the visibility potential energy of i-th object.

Therefore, the objective function can be expressed as follows:

$$\begin{cases} \max U_{com} = \max \sum_{i=1}^{n}\psi_i \sum_{j=1}^{m}\xi_{i,j} \bullet U_{i,j} \\ 0 \le \psi_i \le 1, 0 \le \xi_{i,j} \le 1, \sum_{i=1}^{n}\psi_i = 1, \sum_{j=1}^{m}\xi_{i,j} = 1 \end{cases} \tag{18}$$

(2) Representation of geometric objects

In this paper 2D plane layout problem is studied. Layout objects are simplified as rectangles or circles. The center coordinates (x_i, y_i), length l_i and width b_i size of rectangle is used to express geometric information of objects. The center coordinates (x_i, y_i) and radius R_i of rectangle are used to express geometric information of objects, which are showed in the Fig. 3.

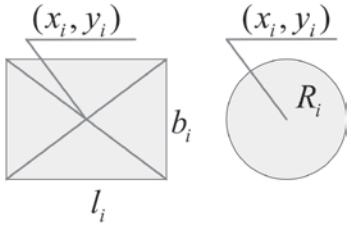

Fig. 3. Geometric information of object

(3) Constraint conditions

Constraint conditions mainly include the geometric constraint. Geometric constraint contains non-interference and boundary conditions. Non-interference conditions require that there is no overlapping part. Boundary conditions require that any object cannot beyond the given layout space.

The constraint conditions is defined as follows:

$$s.t. \begin{cases} g_i(x) > 0 \\ h_i(x) = 0 \end{cases} \tag{19}$$

Where, $g_i(x) > 0$ and $h_i(x) = 0$ respectively represent the inequalities and ebullition of the constraint conditions.

4.2. Algorithm of layout optimization

The model solution belongs to a NP problem, which could be solved by genetic algorithm, simulated annealing algorithm and particle swarm optimization. In this paper, the particle swarm optimization with advantage of simple structure and fast convergence speed has been adopted. The flow chart of layout optimization algorithm is shown in Fig. 4.

The first step is importing the information of layout. The second step is modeling the layout optimization. The third step is solving the layout optimization model. The last step is outputting the result of layout optimization [6]. Parameter setting includes the size, the number of key point and visibility weight of the objects. The position and speed updating method is defined as follows:

$$\begin{aligned} \mathrm{v}_{i,j}(t+1) &= w\mathrm{v}_{i,j}(t) + c_1 r_1[p_{i,j} - \mathrm{x}_{i,j}(t)] + c_2 r_2[p_{i,j} - \mathrm{x}_{i,j}(t)] \\ \mathrm{x}_{i,j}(t+1) &= \mathrm{x}_{i,j}(t) + \mathrm{v}_{i,j}(t+1), j = 1,2,\ldots,d \end{aligned} \tag{20}$$

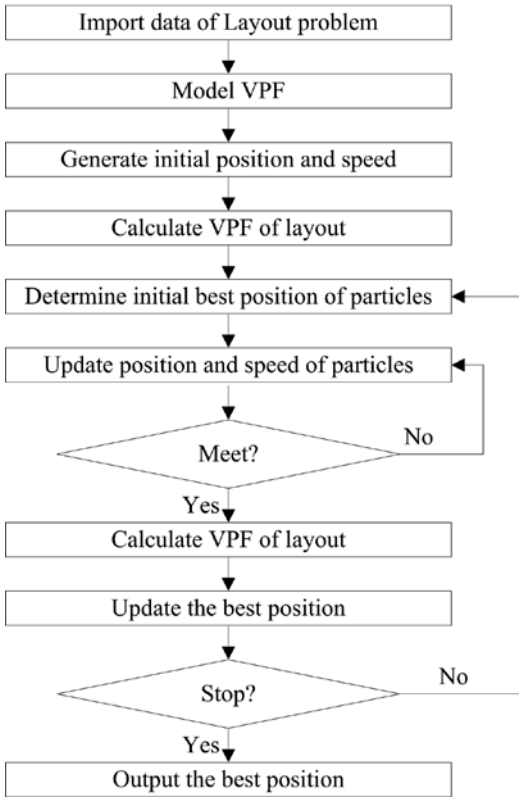

Fig. 4. Particle swarm optimization of layout optimization

Where, x and v respectively represent the position and speed of particles. c_1 and c_2 represent the learning factor. r_1 and r_2 represent the random numbers.

When updating the best particle position and speed, the particle swarm is sorted by the fitness value, the position and speed of the half of the poorest particles are replaced by half of the best particles. The stopping criterion is the iterative times and iterative accuracy.

5. Example and analysis

5.1. Problem Description

Assuming a certain type of cabin is circular with a radius of 50cm, there is a fixed internal obstacle. Within the spare space, the equipment (named A, B, C, D) layout problem is to be considered. The position to be monitored is at each geometric center of the equipment. The operator is parallel to the cabin plane with a distance of 60 cm, and the eyesight is perpendicular to the cabin plane. Between the operator and the cabin there is a circular visual obstacle, with a radius of 10 cm, and the distance from the cabin floor is 40 cm. The position relationship between each other is shown in Fig. 5. For simplicity, assume the body posture and eyesight are fixed. The initial layout is shown in Fig. 6. The size, initial position and weight of the key viewpoint are shown in Table 1.

Table 1. Parameters of object

Serial number	Length l_i(cm)	Width b_i(cm)	Initial Position
1	30	20	(0, 30)
2	R_2=10		(35, 0)
3	20	20	(0, −25)
4	16	16	(−20, 3)

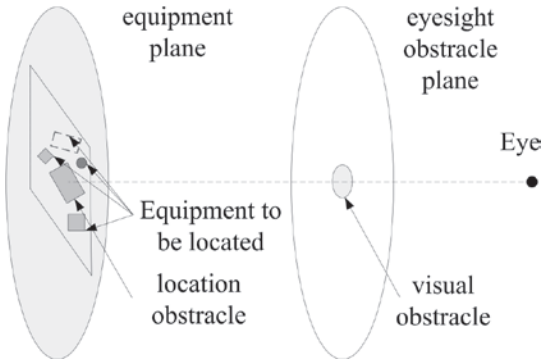

Fig. 5. The relationship of the equipment to be optimized

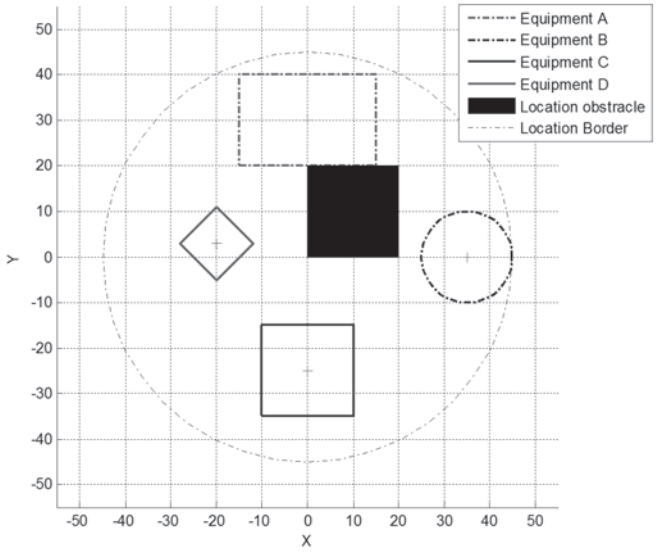

Fig. 6. Initial Position of all objects

The layout of the equipment must meet that there is no collision between each equipment and the barrier, and the visibility of the monitor points is the best. The HFPF method is applied for the optimal solution. It can be calculated that the VPF of the initial layout is 1.1348.

5.2. Modeling

According to the visibility model, the objective function is established as follows:

$$\min U_C = \min \sum_{i=1}^{4} c_i \bullet U_{Ci}$$

The constraint condition is determined as follows:

(1) Non-interference condition is determined as $|x_i - x_j| > \frac{l_i + l_j}{2}$

or $|y_i - y_j| > \frac{b_i + b_j}{2}$ $i = A,B,C,D,E$; $j = A,B,C,D,E$

(2) Boundary Conditions:
Boundary conditions are determined as follows:

$$\sqrt{x_i^2 + y_i^2} + \sqrt{l_i^2 + b_i^2}\,/2 < R \text{ (Rectangular)} \quad \sqrt{x_i^2 + y_i^2} + R_i < R \text{ (Circle)}$$

5.3. Simulation results and analysis

The MATLAB software is used to obtain the layout designed scheme with the best VPF index. Particle number, learning factor and the iterative times are respectively set at 40, 2 and 1000. Let $\theta_M = 1.1\theta_R$ in formula (17). Inertia weight uses adaptive weight method and the nonlinear dynamic inertia weight.

(1) When no visual obstacle exits, the layout result based on the particle swarm optimization method is showed in Fig. 7. Compared with the VPF of initial layout, the VPF of layout reduces greatly to 0.2452.

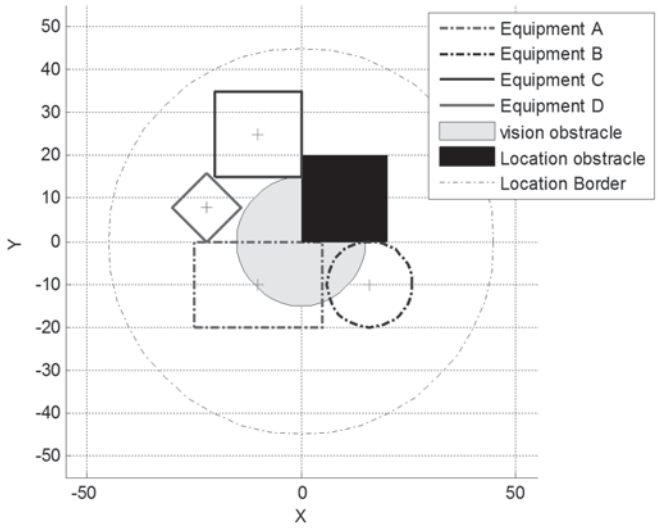

Fig. 7. The result of layout optimization without obstacles

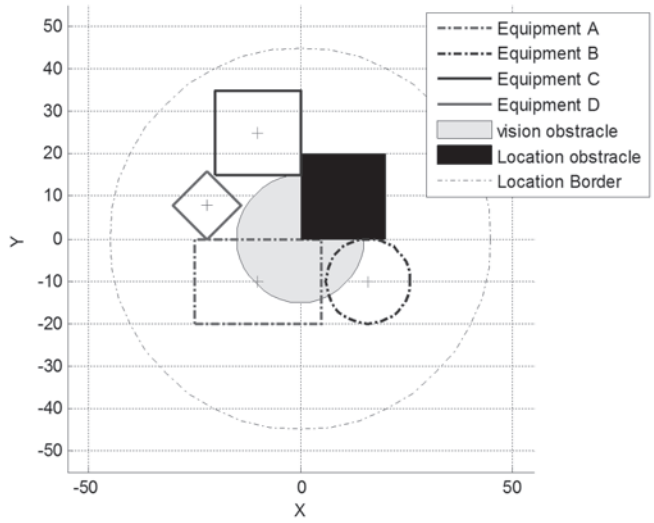

Fig. 8. The result of layout optimization with the obstacles

(2) When the visual obstacle located at point (0,0,60), the layout optimization result is shown in Fig.8. The VPF of layout is 0.4124, we can see that all the key visual points of objects can avoid the invisible area caused by the visual obstacle.

(3) The convergence speed of fitness value is shown in Figure 9. The VPF reaches 0.2452and become stable while iterative times are 252. It can also be demonstrated that PSO method with adaptive weight has strong convergence ability, which not only can avoid finding the local optimal value, but also has very fast convergence speed.

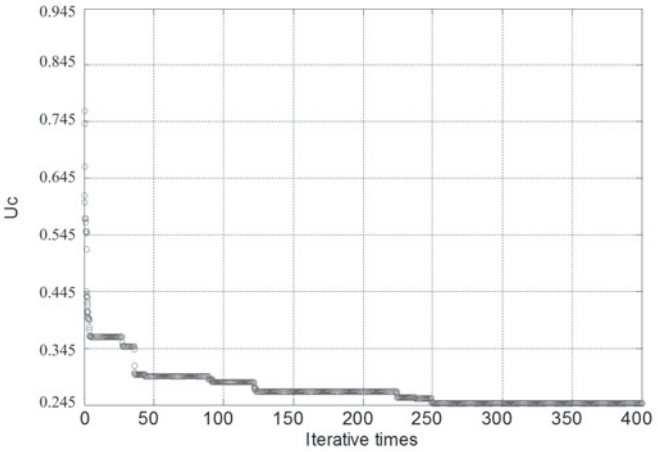

Fig. 9. Convergence speed of PSO

6. Conclusion

The human-factor potential field concept is proposed based on the traditional artificial field, concluding the visibility potential field, the reachability potential field and so on. It can describe the relationship of human, object and obstacle. The basic visibility potential field model is composed of vertical visual field, horizontal visual field, obstacle influence and so on. In order to realize optimization of visibility, the layout optimization method based on the VPF is put forward. The particle swarm optimization based method on natural selection is applied to solve the model, which can obtain the optimal solution with faster convergence speed. However only the plane layout is concerned in this paper, the complex three-dimensional layout should be studied in the future.

Acknowledgement

The research work is financed by the project of National Natural Science Foundation of China 51005238.

References

1. Abdel-Malek K, Yang J, Brand R, Tanbour E. Towards understanding the workspace of the upper extremities. SAE Transactions Journal of Passenger Cars: Mechanical Systems 2001; 6: 2198-2206.
2. Bendsoe MP, Sigmund O. Topology Optimization: theory, methods and applications. NewYork: Springer-Verlag Berlin Heidelberg 2003: 35-55.
3. Bidault F, Chablat D, Chedmail P, Pino L. A distributed approach for access and visibility task with a manikin and a robot in a virtual reality environment. IEEE Transactions on Industrial Electronics2003; 4: 692-698.

4. Blackmore D, Samulyak R, Leu MC. A singularity theory approach to swept volumes. International Journal of Shape Modeling 2000; 6: 105-129, http://dx.doi.org/10.1142/S0218654300000089.
5. Gilbert EG, Johnson D W. Distance functions and their application to robot path planning in the presence of obstacles. IEEE J Robotics and Automation 1985; 1: 21-30, http://dx.doi.org/10.1109/JRA.1985.1087003.
6. Ji Z; Liao HL, Wu QH. Particle swarm algorithm and its application. Beijing: Science Press; 2008.
7. Khatib O. Real-time obstacle avoidance for manipulators and mobile Robots[J]. The International Journal of Robotics Research 1986; 1:90-98, http://dx.doi.org/10.1177/027836498600500106.
8. Liu JL, Zen F M, Su QJ. Study on application of ergonomics based on CATIA in virtual design of marine power plant [J]. Journal of Wuhan university of technology social sciences edition 2008; 4: 657-660.
9. Sun YL. Human factors engineering [M]. Beijing: Science and Technology of China Publishing House; 2005.
10. Tjiparuro Z, Thompson G. Review of maintainability design principles and their application to conceptual design. Proceedings of the Institution of Mechanical Engineers, Part E: Journal of Process Mechanical Engineering 2004; 2:103-113, http://dx.doi.org/10.1243/095440804774134280.
11. Yang JZ, Sinokrot T, Abdel-Malek K. A general analytic approach for SantosTM upper extremity workspace. Computers & Industrial Engineering 2008; 54: 242-258, http://dx.doi.org/10.1016/j.cie.2007.07.008.
12. Yin ZP, Ding H, Xiong YL. Visibility theory and algorithms with application to manufacturing processes. International Journal of Production Research 2000; 13:2891-2909, http://dx.doi.org/10.1080/00207540050117350.

Zhexue GE
Laboratory of Science and Technology on Integrated Logistics Support
School of Mechatronics Engineering and Automation
National University of Defense Technology
De Ya Road, 109, Changsha, Hunan 410073, P. R. China

Fuzhang WU
China Aerodynamics Research and Development Center
Mian yang, Sichuan 621000, P. R. China

Yongmin YANG
Xu LUO
Laboratory of Science and Technology on Integrated Logistics Support
School of Mechatronics Engineering and Automation
National University of Defense Technology
De Ya Road, 109, Changsha, Hunan 410073, P. R. China

E-mails: gzx@nudt.edu.cn, lsai@cardc.cn, yangyongmin@163.com

Article citation info:
SOBRAL J, FERREIRA L. Establishment of optimal physical assets inspection frequency based on risk principles. Eksploatacja i Niezawodnosc – Maintenance and Reliability 2015; 17 (2): 243–249, http://dx.doi.org/10.17531/ein.2015.2.11.

José SOBRAL
Luís FERREIRA

ESTABLISHMENT OF OPTIMAL PHYSICAL ASSETS INSPECTION FREQUENCY BASED ON RISK PRINCIPLES

USTALANIE OPTYMALNEJ CZĘSTOTLIWOŚCI PRZEGLĄDÓW OBIEKTÓW TECHNICZNYCH W OPARCIU O ZASADY OCENY RYZYKA

Risk Based Inspection (RBI) is a risk methodology used as the basis for prioritizing and managing the efforts for an inspection program allowing the allocation of resources to provide a higher level of coverage on physical assets with higher risk. The main goal of RBI is to increase equipment availability while improving or maintaining the accepted level of risk. This paper presents the concept of risk, risk analysis and RBI methodology and shows an approach to determine the optimal inspection frequency for physical assets based on the potential risk and mainly on the quantification of the probability of failure. It makes use of some assumptions in a structured decision making process. The proposed methodology allows an optimization of inspection intervals deciding when the first inspection must be performed as well as the subsequent intervals of inspection. A demonstrative example is also presented to illustrate the application of the proposed methodology.

Keywords*: risk analysis, risk based inspection, inspection frequency.*

Risk Based Maintenance (RBI), to metody planowania inspekcji obiektów, w tym ustalania priorytetów i zarządzania czynnościami obsługowymi, wykorzystujące zasady oceny ryzyka. Pozwalają one na taką alokację zasobów, która zapewnia wyższy poziom zabezpieczenia obiektów technicznych obarczonych wyższym ryzykiem. Głównym celem RBI jest zwiększenie dostępności sprzętu przy jednoczesnym zwiększeniu lub utrzymaniu akceptowalnego poziomu ryzyka. W artykule omówiono pojęcie ryzyka i zasady analizy ryzyka oraz metodologię RBI, a także przedstawiono metodę pozwalającą na określenie optymalnej częstotliwości przeglądów obiektów technicznych na podstawie potencjalnego ryzyka, a przede wszystkim ilościowo określonego prawdopodobieństwa uszkodzenia. Podejście to wykorzystuje niektóre założenia stosowane w ustrukturyzowanym procesie podejmowania decyzji. Zaproponowana metodologia pozwala na optymalizację długości okresów między przeglądami,dając możliwość określenia czasu wykonania pierwszego oraz kolejnych przeglądów. Zastosowanie proponowanej metodologii zilustrowano przykładem numerycznym.

Słowa kluczowe*: analiza ryzyka, planowanie przeglądów warunkowane ryzykiem, częstość przeglądów.*

1. Introduction

In the last decades many strategies and methodologies were developed to help managers, engineers and technicians to make the best decisions in the maintenance field. Some of them are applicable for industry in general while others became a reference in a specific field or type of industry. In high risk industrial facilities there is a need for implementing a strategy that must combine safety and reliability with economy. Periodic inspections are usually performed as a maintenance activity to avoid unplanned plant shutdown, unsafe situations and consequent high costs due to unavailability.

To pursue this objective, in 1983 the American Petroleum Institute (API) initiated a project named Risk Based Inspection (RBI) as the result of a necessity to ensure acceptable levels of risk in the petrochemical facilities [3]. As a risk methodology, RBI can be used as the basis for prioritizing and managing the efforts of an inspection program. In the majority of industrial facilities a relatively high amount of risk is related with a small percentage of asset items. To apply maintenance efforts in a justified manner and inside a tolerable risk level, methodologies like RBI must be followed. A RBI program allows the allocation of resources for inspection activities to provide a higher level of coverage on the high risk items and an appropriate effort on the lower risk ones. The main goal of RBI is to increase equipment availability while improving or maintaining the accepted level of risk.

Usually the main difficulty is to determine the optimal inspection frequency. This is an important aspect once higher frequency corresponds to higher maintenance costs (but with lower risk) while lower frequency means an increasing risk although the inherent lower maintenance costs. To overcome this ambiguity it is necessary to create some kind of method to determine the appropriate asset inspection frequency.

The main objective of this paper is to present a methodology that can be used to determine and reach the optimal asset inspection frequency meaning that risk will be under a defined and desired level.

The paper is organized into four sections. Section 2 gives a brief description about the concept and principles of risk analysis, presents the RBI methodology and points out some applications of it. In Section 3 a methodology to determine the optimal inspection frequency is proposed, a demonstrative example of the methodology is shown and some discussion is performed. Finally, in Section 4 some conclusions are stated about the subject of the study.

2. Risk analysis and RBI methodology

As equipment will not remain safe or reliable if not properly maintained, the general goal of a maintenance process is to make use of the knowledge of failures and accidents to achieve the possible and accepted safety level with the lowest possible cost [4]. To this scope, process industry is increasingly making use of risk analysis techniques to develop cost and/or safety optimal inspection plans [14]. Sometimes risk management is based on safety standards but, as stated by Abrahamsen et al. [1], it does not give always the expected effect on safety due to budget constraints once it implies that other important measures to reduce risk are not applied. Risk methodologies generally define the risk of operating physical assets as the combination of the consequence of failure (CoF) and the likelihood or probability of failure (PoF), where the previous is related with the potential effects of an undesirable event for people, business and/or environment and the later one refers to the probability of occurrence of such event (failure).

2.1. Risk analysis

Most of times risk analysis is a complex task because it is a function of several factors. The way to perform it must be carefully selected taking into account the purpose of the analysis and the desired precision of the results.

While some failures frequently occur without significant adverse consequences, others are potentially dangerous although their low probability of occurrence. Organizations must focus on these two elements (PoF and CoF) together in a way to observe the risk and its acceptability. Acceptance can be based on some criteria such as ALARP (As Low As Reasonably Practicable), MEM (Minimum Endogenous Mortality) or GAMAB (Globalement Au Moins Aussi Bon). The ALARP criterion is the most used in practice because it is a flexible approach where the risk area is divided in three zones, which should be defined before the risk analysis [23].

In other situations, it is common to present a risk matrix where the acceptance criteria are established showing acceptable and unacceptable regions according to the achieved value of risk. These criteria may be a consequence of legislation or regulations or may derive from corporate safety and financial policies and constraints. If a particular risk is unacceptable, then some mitigation actions shall be considered such as decommission, inspection or condition monitoring, consequence mitigation or probability mitigation.

When performing a risk analysis the analyst looks at the available data and failure information regarding some equipment as a way to determine the PoF, which is usually based on statistical data. Most of time, to know the PoF for each situation is a hard job because several deteriorating mechanisms and failure modes can be present in a particular item at the same time or failure data can be given from a mixed population representing several failure modes. If statistical data is aggregate it is difficult to perform an accurate analysis and achieve objective results that can lead to the implementation of an effective inspection plan. The likelihood or PoF is often established on generic failure rate estimations, sometimes based on a compilation of available asset failure historic data from various industries, as for example Offshore Reliability Data [20]. These database failure frequencies must then be affected by specific field adjustment factors. Tien et al. [27] refer that these adjustment factors can be divided into equipment and management system factors. Others attempt to quantify the PoF with less subjectivity and model failures based on operational and organizational errors showing that direct causes of all accidents are combinations of human errors, hardware failures and external events [9]. Papazoglou and Aneziris [21] assess the effects of organisational and management factors linking the results of a safety management audit with the frequencies of basic events based on a quantified risk assessment (QRA). They apply this methodology on a chemical installation showing that it allows a reflection of the deficiencies or strengths of the safety management system. Also, Milazzo et al. [18] studied the organizational and management factors as variables that must be incorporated into the process of assessment of the frequency of failures, giving the example of a loss of containment due to a failure in piping and how to link its causes with the measures adopted by the company to prevent it.

If we are considering critical physical assets in a process industry, the CoF usually refer to the impact on safety, business and environmental issues. Kim et al. [16] present a study focusing on the status of risk management activities conducted by petrochemical plants in Korea and on the global trends in the area. In this work some interesting tables are shown referring major accidents in a period (1999-2001), insured loss, property loss and loss due to business suspension. This information can then be used to assess the CoF in a similar facility.

Risk analysis is a decision-oriented process consisting of risk assessment, risk management, and risk communication. Fig. 1 illustrates a logical process of a risk analysis.

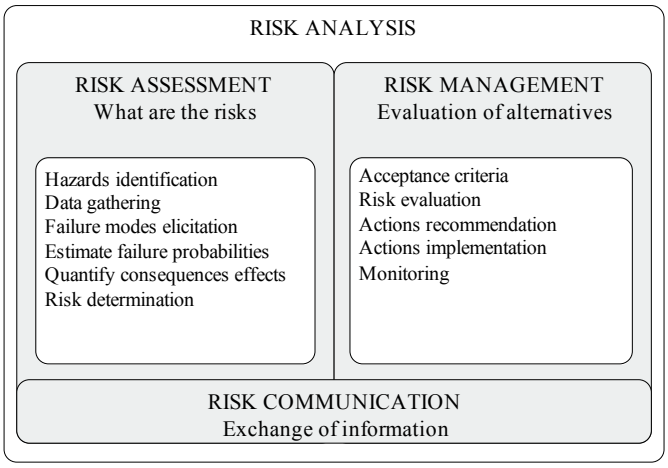

Fig. 1. Logical process of a risk analysis

From Fig. 1 it can be seen that a risk analysis process is a structured technique following a risk policy and ending on the implementation of actions leading to the reduction of the probability of failure and/or minimizing the effects of its consequences, if the achieved risk is considered as unacceptable. Risk analysis can be performed in a qualitative, semi-quantitative or in a quantitative way.

2.2. The RBI methodology

The main objective of RBI is basically to use the limited inspection and maintenance resources in coping with the really significant risks, once it is demonstrated and it is accepted that up to 20% of equipment items give rise to at least 80% of risk exposures [7]. Also, according to Lee and Teo [17] 10-20% of items give rise to 80-95% of equipment risk exposures. The same order of values is referred by Jovanovic [13] on his study about risk-based inspection and maintenance in power and process plants in Europe.

The purpose of RBI is to help the decision process, on prioritizing resources for inspection activities in a way to manage risk. Inspection does not directly reduce risk but it is a risk management activity that may lead to risk reduction. RBI complements other risk-based and safety initiatives such as RCM (Reliability Centred Maintenance), PHA (Preliminary Hazard Analysis), SIL (Safety Integrity Level), LOPA (Layer of Protection Analysis) or FMEA (Failure Mode and Effects Analysis).

An inspection strategy can be established taking into account the results of a risk assessment on the risk management process.

There are specific industrial areas where RBI methodology has been proposed in the last few years, which are basically referred to the oil and gas industry and nuclear power plants (NPP). In these industries the RBI methodology is usually focused on mechanical integrity of pressure equipment to minimize the risk of loss of containment due to deterioration. Pressure vessels, piping, storage tanks, rotating equipment, boilers and heaters or heat exchangers are examples of physical assets typically associated to a RBI process. The Section 2.3 shows some studies and examples of application of RBI methodology.

2.3. Typical applications of the RBI methodology

The current Section intends to demonstrate the potential capabilities of RBI methodology and the importance of inspection activity stating some examples of studies on different areas and involving distinct types of physical assets.

Singh and Markeset [26] tried to establish an RBI program for pipes, using a fuzzy logic framework estimating the rate of CO_2 corrosion in carbon steel pipes and taking into account the efficiency of inspection as a fuzzy variable where the goal is to estimate the rate of corrosion and use it to develop a risk-based inspection program.

Chang et al. [7] propose a RBI methodology aiming to optimize the inspection strategy of the piping at refinery and petrochemical plants in Taiwan. The goal of their work is to avoid under-inspection or over-inspection reducing risk and costs.

In the nuclear field, and still focusing in piping, a probabilistic failure analysis was done to find failures in piping segments, followed by a risk assessment [29]. At the end the risk levels corresponding to each pipe segment are ranked and an inspection program established.

A comparative study of two approaches was made by Simola et al. [25] to estimate pipe leak and rupture frequencies. The goal is to reduce inspection activities in some locations with low risk and concentrate efforts in higher risk zones. It is the risk-informed in-service inspection (RI-ISI). Some industrial applications of these approaches are referred in the paper.

Santosh et al. [22] refer a study where the goal is to obtain the failure probabilities for pipelines carrying H_2S (Hydrogen Sulphide) to establish a RBI program for heavy water plants. Corrosion due to H_2S is an important form of pipeline deterioration due to aggressive environments. It promotes metal loss reducing pipelines loading capacity.

In the same field Tien et al. [27] developed a risk based piping inspection guideline system built in accordance with international standards and local government regulations. The outcome of this work showed that most of the risk resulted from a small number of pipelines.

Noori and Price [19] present a risk approach to the management of boiler tube thinning based on inspection data, covering four boiler units of a power station over a period of five years. This data refers to the boiler regions where corrosion/erosion is the major cause of boiler tubes failure.

Chien et al. [8] propose a strategy for a semi-quantitative RBI applied to pressure safety valves installed in pressurized vessels. The authors present pressure safety valves characteristics from a practical point of view and its relationship to inspection and maintenance issues. Using statistical technique analysis the relationship of aging condition and some parameters was then performed and inspection intervals suggested.

Recently, the development of a two-stage inspection process for the assessment of deteriorating infrastructure was presented by Sheils et al. [24] based on the effect of the cost and quality of non-destructive testing tools to access the condition of infrastructure elements during their lifetime and where each stage of inspection is incorporated into a maintenance management model. According to the authors it was the first time that detection and sizing of an inspection were considered.

Bertolini et al. [6] present an application of a Risk Based Inspection and Maintenance process (RBI&M) which includes the work of a panel of experts composed by academic and refinery operators. The risk is analyzed assuming four impact categories (health and safety, environmental, economic and reputation). The results of such study reveal a clear necessity of improvement in maintenance quality indices.

RBI&M is also mentioned by Khan et al. [15] using in their work a fuzzy logic methodology to estimate risk by combining fuzzy likelihood of occurrence and its fuzzy consequence evaluation. The methodology is then based on aggregative risk analysis and multi attribute decision making.

Hulshof et al. [12] refer that RBI is an attractive method that had been applied at several Dutch power plants in the last ten years promoting a huge inspection interval extension.

Kallen and Noortwijk [14] present a decision making process using an adaptive Bayesian model to determine optimal inspection plans under uncertain deterioration corrosion damage mechanism. This model was exemplified for a pressurized steel vessel.

Another Bayesian approach is suggested by Giribone and Valette [11] computing the PoF assuming it as "the main driver for scheduling periodical inspections". This article describes the theoretical principles yielding the calculation of the PoF prior to conduct an inspection and after performing it. In this work is referred the EU project RIMAP (Risk Based Inspection and Maintenance Procedure) which includes PoF determination.

RIMAP is also mentioned in a work produced by Bareib et al. [5] referring an European Guideline for optimized risk based maintenance and inspection planning of industrial plants. The authors also refer that RIMAP application in piping systems of power plants gives transparency to the decision making process.

RBI methodology has also promoted the development of various computer applications in order to facilitate their application in the field. For example Vianello et al. [28] presented a RBI software tool that encloses all functionalities for an easier management of the technical data, the Inspection Manager software. It allows to create in a short time an item's list and the catalogue of items object of RBI study based on plant's P&ID, process data, specifications, reports and maintenance historical data.

The above examples show that RBI has proved to be a very useful methodology for risk analysis in high risk industries, allowing controlling risks at relatively low costs. As it can be seen from the above literature review it has been applied to many industries, especially to static physical assets submitted to pressure and temperature and where lack of containment represents dangerous consequences and high failure costs. However, the methodology is increasingly being applied to other type of assets and fields with the appropriate adequacy.

2.4. The problem

Risk analysis is usually used to develop an effective inspection plan for facilities and their physical assets. These inspection plans include the inspection methods and technologies to be used, the extension of inspection, the inspection intervals and other risk mitigation activities.

Most of the situations described in the previous section have the objective to establish the referred inspection plans for the inherent assets under analysis. In these plans an important decision to take is the inspection interval. The majority of the studies presented determine a static inspection frequency, meaning that time between inspections is always constant. Some of them follow the American Petroleum Institute - Recommended Practice 580 [2], where the inspection frequency should be scheduled at the half remaining life or established on the basis of fluid content, depending whichever is shorter. However, this recommendation can lead to under-inspection of some high risk items

or over-inspection with resources and cost waste on low risk items. In a recent study [10] referring the petroleum industry and regarding the determination of the frequency for testing safety instrumented systems (SIS) it was discussed whether the decision criteria of halving or doubling test intervals should be adopted for well barriers based on the comparison of the estimated failure rate and the failure rate in design. The authors suggested a new type of criterion incorporating the level of significance when deciding if the test interval should double or not.

Reality shows that risk is dynamic and thus inspection frequency must also be dynamic. This characteristic and premise is based on the constant change of the PoF once almost physical assets and their items had an increasingly probability of occurrence in time.

Therefore, the problem of establishing an inspection plan is to find a method to promote an adequacy of inspection intervals to the changing reality. Section 3 shows a methodology to determine the optimal physical assets inspection frequency based on risk principles.

3. Proposed methodology

The proposed methodology differentiates the period of time to first inspection (TTFI) from the subsequent inspection periods taking into account pre-established targets for PoF and tolerable or acceptable risk. This relatively new approach supports the main objective of the proposed methodology. Fig. 2 shows in a schematic way the framework of the proposal.

The main difficulty in risk analysis is concerned with the determination of each individual PoF. In this methodology the cumulative

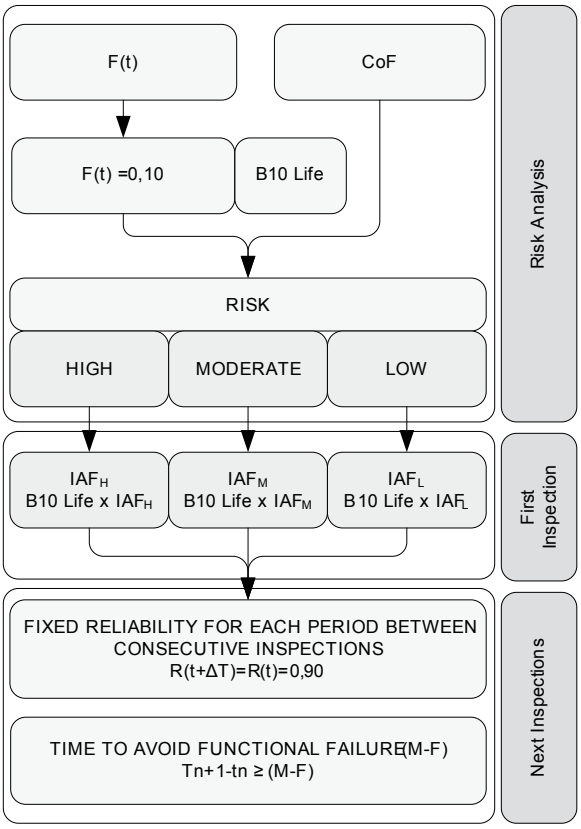

Fig. 2. Proposed methodology framework

failure probability function [F(t)] for each item is assumed to be calculated on reliability studies (life data analysis) or using generic failure frequency (GFF) from a reliable database, affected by modification factors, such as management factor, actual age, damage mechanism, environmental stress or inspection effectiveness.

After knowing the inherent F(t), a maximum value of probability of failure is then established. In this methodology it was stated a 10% maximum probability of failure, corresponding to the so-called B10 Life (the term was initially used to refer 10% of Bearings (B) life and later extended to other reliability studies, although remaining with the "B"). Then, calculating the severity of the consequence of failure (CoF) in a pre-defined scale (monetary, category or other qualitative measure) it is possible to localize the risk in a specific risk matrix.

The establishment of the acceptance criteria follows the API recommended practice 581 [3] where three regions are identified in the proposed risk matrix, namely:

- High risk zone;
- Moderate risk zone;
- Low risk zone.

Time to first inspection (TTFI) is applied to new items (for example after replacement or overall activities) and is established in accordance with risk category. In this case an Inspection Adjustment Factor (IAF) is applied to B10 Life distinguishing the potential risk from High (H), Moderate (M) and Low (L). In this methodology the IAF values were adopted as shown in Table 1. Each organisation is allowed to establish different IAF according to specific objectives.

Once determined the TTFI the following inspections should vary according to the potential failure mode under observation. The decision criteria used in the proposed methodology is based upon the principle that a constant conditional reliability should be maintained between two consecutive inspections and with a pre-defined value. Using this assumption and taking in consideration the conditional reliability expression

Table 1. Values adopted for Inspection Adjustment Factor (IAF)

Risk	Inspection Adjustment Factor (IAF)	Time To First Inspection (TTFI)
High	0.80	B10 Life x 0,80
Moderate	1.00	B10 Life x 1,00
Low	1.20	B10 Life x 1,20

$$R(\Delta t \mid T) = \frac{R(T+\Delta t)}{R(T)} \tag{1}$$

it can be stated that

$$R(T+\Delta t) = R(T) \tag{2}$$

This result can now be combined with any failure probability distribution based on available data. For example, due to its wide range of applicability on practical cases, if it is assumed a bi-parametric Weibull distribution with a probability density function expressed by:

$$f(t) = \frac{\beta}{\eta}.\left(\frac{t}{\eta}\right)^{\beta-1}.e^{-\left(\frac{t}{\eta}\right)^{\beta}} \tag{3}$$

Where β represents the shape parameter and η represents the characteristic life or scale parameter of Weibull distribution.

Reliability is given by:

$$R(t) = e^{-\left(\frac{t}{\eta}\right)^{\beta}} \tag{4}$$

In these circumstances the time for the n[th] inspection can be expressed by:

$$t_n = \eta.\left[-\ln\left(R(t)\right)^n\right]^{\frac{1}{\beta}} \quad (5)$$

In this scope, three scenarios can be presented:

- If $\beta < 1$, which means a decreasing failure rate, $(t_{n+1}-t_n) < (t_{n+2}-t_{n+1})$;
- If $\beta = 1$, which means a constant failure rate, $(t_{n+1}-t_n) = (t_{n+2}-t_{n+1})$;
- If $\beta > 1$, which means a increasing failure rate, $(t_{n+1}-t_n) > (t_{n+2}-t_{n+1})$;

3.1. Demonstrative example

In an industrial facility an important item presents two distinct failure modes (FM#1 and FM#2) which failure probabilities can be represented by Weibull function with the following parameters:

Table 2. Weibull parameters

Failure Mode	β (Shape parameter)	η (Scale parameter) [h]	h(t) (Hazard rate)
FM#1	0.50	1500	Decreasing
FM#2	1.50	1500	Increasing

In accordance to the proposed methodology and with a maximum acceptable cumulative probability of failure of 0.1 between consecutive inspections a preliminary inspection schedule can now be established for each failure mode.

Table 3. Inspection schedule for FM#1

Inspection (n)	$R(t)^n$	Inspection Moment (t_n)	Inspection Period [t_n-(t_{n-1})]	F(t)	Hazard Rate [h(t)]	$R(t_n+\Delta t\|t_n)$
1	0.9000	16.65	16.65	0.1000	0.003164	-
2	0.8100	66.61	49.95	0.1900	0.001582	0.9000
3	0.7290	149.86	83.26	0.2710	0.001055	0.9000
4	0.6561	266.42	116.56	0.3439	0.000791	0.9000
5	0.5905	416.28	149.86	0.4095	0.000633	0.9000
6	0.5314	599.45	183.16	0.4686	0.000527	0.9000
7	0.4783	815.91	216.47	0.5217	0.000452	0.9000
8	0.4305	1065.68	249.77	0.5695	0.000395	0.9000
9	0.3874	1348.75	283.07	0.6126	0.000352	0.9000
10	0.3487	1665.13	316.37	0.6513	0.000316	0.9000

Table 4. Inspection schedule for FM#2

Inspection (n)	$R(t)^n$	Inspection Moment (t_n)	Inspection Period [t_n-(t_{n-1})]	F(t)	Hazard Rate [h(t)]	$R(t_n+\Delta t\|t_n)$
1	0.9000	334.61	334.61	0.1000	0.000472	-
2	0.8100	531.17	196.55	0.1900	0.000595	0.9000
3	0.7290	696.02	164.86	0.2710	0.000681	0.9000
4	0.6561	843.17	147.15	0.3439	0.000750	0.9000
5	0.5905	978.42	135.24	0.4095	0.000808	0.9000
6	0.5314	1104.87	126.45	0.4686	0.000858	0.9000
7	0.4783	1224.45	119.58	0.5217	0.000903	0.9000
8	0.4305	1338.45	114.00	0.5695	0.000945	0.9000
9	0.3874	1447.79	109.33	0.6126	0.000982	0.9000
10	0.3487	1553.14	105.35	0.6513	0.001018	0.9000

The results show in a clear way the influence of failure mode in inspection intervals and it is also noticeable that:

- When failure rate decreases, inspection intervals increase;
- When failure rate increases, inspection intervals decrease.

3.2. Discussion

If there is a lead time to failure (P-F interval) between potential failure (P) and functional failure (F), the establishment of inspection intervals should also take this information into account. Usually technicians adopt a constant interval for inspections with a frequency of half period between "P" and "F".

However, if we assume that between these two points there is an instant "M" that will be the ultimate time to detect a failure progression and provide measures to avoid the occurrence of a functional failure at "F", its detection must be obtained between "P" and "M". The proposed methodology should be followed while $(t_{n+1}-t_n) \geq (M-F)$. If this condition is not fulfilled then all inspections should be done in periods not less than (M−F).

Taking into account the demonstrative example of FM#2 for a high risk zone and assuming 100 hours as the necessary time act in a way to avoid functional failure, the inspection schedule can be determined as shown in Table 5.

For the above reasons, it can be seen that from the 6[th] inspection on the inspection intervals cannot be less than 100 hours. Chronologically inspection schedule can be represented as shown in Fig. 3, where the white zone corresponds to (M−F) period and the darker one the remaining time or clearance between inspections.

However, if one follows this inspection schedule, it must be remembered that from the 6[th] inspection (where the frequency is maintained at a constant value of 100 hours) our initial premise of having a constant conditional reliability of 90% in each period between inspections will not be fulfilled, meaning a higher probability of failure and an inherent higher risk.

Based on this reflection it is then recommended to act preventively when $(t_{n+1}-t_n) \leq (M-F)$, avoiding the functional failure due to the increased probability of failure.

Considering the above example (FM#2) when the item reaches approximately 884 operating hours an overall must be performed and

from that a new inspection schedule must be implemented and followed.

Table 5. Inspection intervals

Inspection (n)	Initial Inspection Moment	Inspection Period (IP)	IP X IAF	**New Inspection Moment**
1	335	335	268	**268**
2	531	197	157	**425**
3	696	165	132	**557**
4	843	147	118	**675**
5	978	135	108	**783**
6	1105	126	101	**884**
7	1224	120	96 – 100	**984**
8	1338	114	91 – 100	**1084**
9	1448	109	87 – 100	**1184**
10	1553	105	84 – 100	**1284**

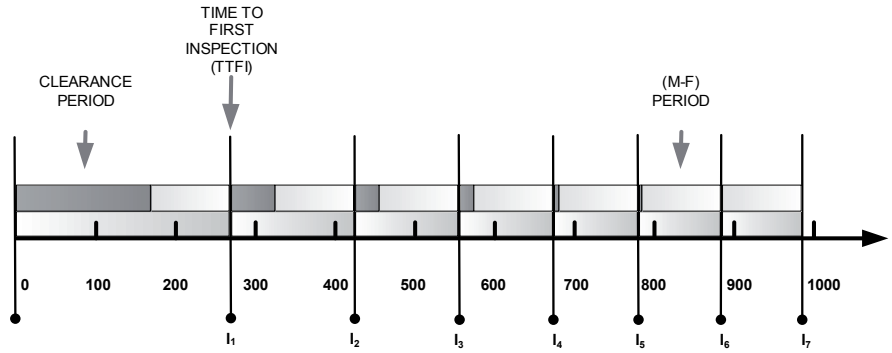

Fig. 3. Inspection schedule

4. Conclusions

Risk based inspection (RBI) methodology had been increasingly used in the last decade in risk assessment with great emphasis at petrochemical industry, power plants and nuclear plants. In this paper its importance was showed and some applications were referred. It is a method to manage risk reducing maintenance costs at the same time.

The great advantage of RBI methodology is based on the capability to determine different levels of risk in an installation and concentrate major efforts in inspection of items in accordance to these risks.

In this paper was proposed a methodology that accomplishes the API recommended practices and allows the establishment of different inspection periods taking into account an assumed constant probability of failure and putting emphasis on the separation of the first inspection and the subsequent ones. The methodology takes also into account the time period necessary to avoid a functional failure after an inspection.

Using this methodology one can create an inspection programme for each item or each failure mode and make decisions about preventive maintenance activities based on risk with an economic balance behind.

This methodology is flexible enough, being possible to change some values as the assumed probability of failure, the Inspection Adjustment Factor or the determination of subsequent times to inspect.

Future work will be focused on the harmonization of inspection programme with other maintenance activities and the evaluation of inherent costs.

References

1. Abrahamsen, E, Asche, F, Milazzo, M. An evaluation of the effects on safety of using safety standards in major hazard industries. Safety Science; 2013; 59: 173-178, http://dx.doi.org/10.1016/j.ssci.2013.05.011.
2. API RP 580. Risk-Based Inspection – API Recommended Practice 580. Second Edition. American Petroleum Institute; 2009.
3. API RP 581. Risk-Based Inspection – Base Resource Document. First Edition. American Petroleum Institute; 2000.
4. Arunraj N, Maiti J. Risk-based maintenance – Techniques and applications. Journal of Hazardous Materials; 2007; 142: 653-661, http://dx.doi.org/10.1016/j.jhazmat.2006.06.069.
5. Bareib J, Buck P, Matschecko B, Jovanovic A, Balos D, Perunicic M. RIMAP demonstration project. Risk-based life management of piping system in power plant Heilbronn. International Journal of Pressure Vessels and Piping; 2004; 81:807-813, http://dx.doi.org/10.1016/j.ijpvp.2004.07.004.
6. Bertolini M, Bevilacqua M, Ciarapica F, Giacchetta G. Development of risk-based inspection and maintenance procedures for an oil refinery. Journal of Loss Prevention in the Process Industries; 2009; 22:244-253, http://dx.doi.org/10.1016/j.jlp.2009.01.003.
7. Chang M, Chang R, Shu C, Lin K. Application of risk based inspection in refinery and processing piping. Journal of Loss Prevention in the Process Industries; 2005; 18:397-402, http://dx.doi.org/10.1016/j.jlp.2005.06.036.
8. Chien C, Chen C, Chao Y. A strategy for the risk-based inspection of pressure safety valves. Reliability Engineering & System Safety; 2009; 94:810-818, http://dx.doi.org/10.1016/j.ress.2008.09.002.
9. Embrey, D. Incorporating management and organisational factors into probabilistic safety assessment. Reliability Engineering & System Safety; 1992; 38:199-208, http://dx.doi.org/10.1016/0951-8320(92)90121-Z.
10. Gelyani, A, Selvik, J, Abrahamsen, E. Decision criteria for updating test intervals for well barriers. Journal of Risk Research; 2014: 1-11, http://dx.doi.org/10.1080/13669877.2014.961521.
11. Giribone R, Valette B. Principles of failure probability assessment (PoF). International Journal of Pressure Vessels and Piping; 2004; 81:797-806, http://dx.doi.org/10.1016/j.ijpvp.2004.07.010.
12. Hulshof H, Noteboom J, Welberg P, Bruijn L. Improved plant availability by advanced condition based inspections. International Journal of

Pressure Vessels and Piping; 2004; 81:491-497, http://dx.doi.org/10.1016/j.ijpvp.2003.12.022.
13. Jovanovic A. Risk-based inspection and maintenance in power and process plants in Europe. Nuclear Engineering and Design; 2003; 226:165-182, http://dx.doi.org/10.1016/j.nucengdes.2003.06.001.
14. Kallen M, Noortwijk J. Optimal maintenance decisions under imperfect inspection. Reliability Engineering & System Safety; 2005; 90:177-185, http://dx.doi.org/10.1016/j.ress.2004.10.004.
15. Khan F, Sadiq R, Haddara M. Risk-based inspection and maintenance (RBIM). Multi-attribute decision-making with aggregative risk analysis. Process Safety and Environmental Protection; 2004; 82:398-411, http://dx.doi.org/10.1205/psep.82.6.398.53209.
16. Kim T, Kim J, Kim Y, Kim K. Current risk management status of the Korean petrochemical industry. Journal of Loss Prevention in the Process Industries; 2002; 15:311-318, http://dx.doi.org/10.1016/S0950-4230(02)00014-1.
17. Lee C, Teo Y. Det Norske Veritas RBI study for the ammonia storage plant. ROC: Taiwan Fertilizer Kaohsiung Ammonia Terminal; 2001.
18. Milazzo, M, Maschio, G, Uguccioni G. The influence of risk prevention measures on the frequency of failure of piping. International Journal of Performability Engineering; 2010; 6:19-33.
19. Noori S, Price J. A risk approach to the management of boiler tube thinning. Nuclear Engineering and Design; 2006; 236:405-414, http://dx.doi.org/10.1016/j.nucengdes.2005.09.019.
20. OREDA. Offshore Reliability Data – 4th Edition, Prepared by SINTEF Industrial Management, Published by the OREDA Participants; 2002.
21. Papazoglou, I, Aneziris, O. On the quantification of the effects of organisational and management factors in chemical installations; Reliability Engineering & System Safety; 1999; 63:33-45, http://dx.doi.org/10.1016/S0951-8320(98)00013-1.
22. Santosh, Vinod G, Shrivastava O, Saraf R, Ghosh A, Kushwaha H. Reliability analysis of pipelines carrying H2S for risk based inspection of heavy water plants. Reliability Engineering & System Safety; 2006; 91:163-170, http://dx.doi.org/10.1016/j.ress.2004.11.021.
23. Schroder H, Kauer R. Regulatory requirements related to risk-based inspection and maintenance. International Journal of Pressure Vessels and Piping; 2004; 81:847-854, http://dx.doi.org/10.1016/j.ijpvp.2004.07.002.
24. Sheils E, O'Connor A, Breysse D, Schoefs F; Yotte S. Development of a two-stage inspection process for the assessment of deteriorating infrastructure. Reliability Engineering & System Safety; 2010; 95:182-194, http://dx.doi.org/10.1016/j.ress.2009.09.008.
25. Simola K, Pulkkinen U, Talja H, Roikonen P, Saarenheimo A. Comparison of approaches for estimating pipe rupture frequencies for risk-informed in-service inspections. Reliability Engineering & System Safety; 2004; 84:65-74, http://dx.doi.org/10.1016/j.ress.2003.10.008
26. Singh M, Markeset T. A methodology for risk-based inspection planning of oil and gas pipes based on fuzzy logic framework. Engineering Failure Analysis; 2009; 16:2098-2113, http://dx.doi.org/10.1016/j.engfailanal.2009.02.003.
27. Tien S, Hwang W, Tsai C. Study of a risk-based piping inspection guideline system. ISA Transactions; 2007; 46:119-126, http://dx.doi.org/10.1016/j.isatra.2006.06.006.
28. Vianello, C, Maschio, G, Mura, A, Babolin, D, Gambato, F, Attori, C. Development of a RBI tool for inspection management in chemical plants. Chemical Engineering Tansactions; 2013; 31:235-240.
29. You J, Kuo H, Wu W. Case studies of risk-informed in service inspection. Nuclear Engineering and Design; 2006; 236:35-46, http://dx.doi.org/10.1016/j.nucengdes.2005.06.014.

José SOBRAL
ISEL – Instituto Superior de Engenharia de Lisboa
Mechanical Engineering Department
Rua Conselheiro Emídio Navarro, 1
1959-007 Lisboa, Portugal

Centre for Marine Technology and Engineering (CENTEC)
Instituto Superior Técnico, Universidade de Lisboa
Av. Rovisco Pais
1049-001 Lisboa, Portugal

Luís FERREIRA
FEUP – Faculdade de Engenharia da Universidade do Porto
Mechanical Engineering Department
Rua Dr. Roberto Frias
4200-465 Porto, Portugal

Emails: jsobral@dem.isel.ipl.pt, lferreir@fe.up.pt

Article citation info:
JIAKAI C, YAN H, WEI W. Reliability analysis and optimization of equal load-sharing *k*-out-of-*n* phased-mission systems. Eksploatacja i Niezawodnosc – Maintenance and Reliability 2015; 17 (2): 250–259, http://dx.doi.org/10.17531/ein.2015.2.12.

Chen JIAKAI
He YAN
Wei WEI

RELIABILITY ANALYSIS AND OPTIMIZATION OF EQUAL LOAD-SHARING *K*-OUT-OF-*N* PHASED-MISSION SYSTEMS

ANALIZA NIEZAWODNOŚCI ORAZ OPTYMALIZACJA SYSTEMÓW FAZOWYCH TYPU „*K* Z *N*" O RÓWNYM PODZIALE OBCIĄŻENIA ELEMENTÓW SKŁADOWYCH

There are many studies on k-out-of-n systems, load-sharing systems (LSS) and phased-mission systems (PMS); however, little attention has been given to load-sharing k-out-of-n systems with phased-mission requirements. This paper considers equal load-sharing k-out-of-n phased-mission systems with identical components. A method is proposed for the phased-mission reliability analysis of the studied systems based on the applicable failure path (AFP). A modified universal generating function (UGF) is used in the AFP-searching algorithm because of its efficiency. The tampered failure rate load-sharing model for the exactly k-out-of-n: F system is introduced and integrated into the method. With the TFR model, the systems with arbitrary load-dependent component failure distributions can be analyzed. According to the time and space complexity analysis, this method is particularly suitable for systems with small k-values. Two applications of the method are introduced in this paper. 1) A genetic algorithm (GA) based on the method is presented to solve the operational scheduling problem of systems with independent submissions. Two theorems are provided to solve the problem under some special conditions. 2) The method is used to select the optimal number of components to make the system reliable and robust.

Keywords: *Applicable Failure Path (AFP), Genetic Algorithm (GA), Phased-mission System (PMS), Tampered Failure Rate (TFR) Model, Universal Generating Function (UGF).*

Istnieje wiele badań na temat systemów typu „k z n", systemów z podziałem obciążenia (load-sharing systems, LSS) oraz systemów fazowych (tj. systemów o zadaniach okresowych) (phased-missionsystems, PMS); jak dotąd mało uwagi poświęcono jednak systemom typu „k z n" z podziałem obciążenia wymagającym realizacji różnych zadań w różnych przedziałach czasowych. Niniejszy artykuł omawia systemy fazowe typu „k z n" o równym podziale obciążenia przypadającego na identyczne elementy składowe. Zaproponowano metodę analizy niezawodności badanych systemów w poszczególnych fazach ich eksploatacji opartą na pojęciu właściwej ścieżki uszkodzeń (applicablefailurepath, AFP). W algorytmie wyszukującym AFP zastosowano zmodyfikowaną uniwersalną funkcję tworzącą (universal generating function, UGF), która cechuje się dużą wydajnością. Wprowadzono model manipulowanej intensywności uszkodzeń (tamperedfailurerate, TFR) elementów o równym podziale obciążenia dla systemu, w którym liczba uszkodzeń wynosi dokładnie k z n. Model ten włączono do proponowanej metody analizy niezawodności. Przy pomocy modelu TFR można analizować systemy o dowolnych rozkładach uszkodzeń części składowych, gdzie uszkodzenia są zależne od obciążenia. Zgodnie z analizą złożoności czasowej i przestrzennej, metoda ta jest szczególnie przydatna do modelowania układów o małych wartościach k. W pracy przedstawiono dwa zastosowania metody. 1) oparty o omawianą metodę algorytm genetyczny (GA) do rozwiązywania problemu harmonogramowania prac w systemach z niezależnymi podzadaniami. Sformułowano dwa twierdzenia pozwalające na rozwiązanie problemu w pewnych szczególnych warunkach. 2) Wybór optymalnej liczby elementów składowych pozwalającej na zachowanie niezawodności i odporności systemu.

Słowa kluczowe: *Właściwa ścieżka uszkodzeń (AFP), algorytm genetyczny (GA), system fazowy (o zadaniach okresowych) (PMS), Model manipulowanej intensywności uszkodzeń (TFR), Uniwersalna funkcja tworząca (UGF).*

Acronyms

AFP	applicable failure path
GA	genetic algorithm
i.i.d.	independent identically distributed
LSS	load-sharing system
PMS	phased-mission system
TFR	tampered failure rate
UGF	universal generating function

Nomenclature

M	Number of phases
N	Number of components
k_i	k-value of the i_{th} phase
$\bar{\boldsymbol{K}}$	A set of k-values
K_s	An execution sequence vector
L_i	Load of the i_{th} phase
τ_i	Duration of the i_{th} phase
μ	Component capacity

k_{mi}	Minimum value of $\{k_i, k_{i+1},\ldots, k_M\}$, i.e., the maximum allowed number of failed components in the i_{th} phase
k_{mavr}	Average value of $\{k_{m1}, k_{m2},\ldots, k_{mM}\}$
K_m	Vector $[k_{m1}, k_{m2},\ldots, k_{mM}]$, the maximum allowed number of failed components in each phase
Δk_i	Number of newly failed components in the i_{th} phase
ΔK	A failure path
ΔK^{sub}	A failure subpath
ΔK^a	A applicable failure path
ΔK_l^a	The l_{th} applicable failure path in set V
V	Set of all applicable failure paths
$V(K_m)$	A set of all applicable failure paths related to a specified K_m
C	Cardinal number of AFP set V
$U(z)$	Universal generating function
$U_i(z)$	Universal generating function of the i_{th} phase
$\Omega_{\varphi,\phi,\varphi,\phi}$	Composition operators for the UGFs of two different phases
$h(t)$	Failure rate or hazard rate
α_i	Failure rate of the system when (i-1) components have failed
$\delta(L)$	Tampered factor at load L
R or $R(V)$	Phased-mission reliability of the studied system
$R(V(K_m))$	Phased-mission reliability of studied system related to a specified K_m
$R_e(k,n,t)$	Reliability of exactly k-out-n: F system
$R_e(m_i,n_i,\tau_i,L_i)$	Reliability of exactly m_i -out-n_i: F system under duration τ_i and load L_i
τ_{ei}	Effective age of first (i-1) phases
$F(\bar{\boldsymbol{K}})$	A set of all execution sequences
$R_a(k,n,t)$	Reliability of the load-sharing k-out-of-n: F system

1. Introduction

The operation life of phased-mission systems (PMSs) consists of consecutive and non-overlapping time periods (phases). The environmental or operational conditions, stresses and reliability requirements may vary with the phases. Practical phased-mission systems in the real world involve aerospace, nuclear power, airborne weapon systems and distributed computing systems. A classic example is an aircraft with the phases of taxi, takeoff, ascent, level-flight, descent, and landing [36]. Compared with single-phased systems, PMSs have much more complicated characteristics, such as dynamic behavior and dependence across phases. This dynamic behavior may require a distinct model for each phase, and the dependence across phases indicates that the state of a given component at the beginning of a new phase may be identical to the state at the end of the previous phase [34]. Various approaches, e.g., BDDs (binary decision diagrams) [38], recursive algorithms [20] and numerical methods with Markov chain [33], have been suggested for analyzing the reliability of PMSs. Xing *et al*. [35] analyzed a generalized phased mission system (GPMS) with combinatorial phase requirements (CPR), which have flexible failure criteria and outcomes. The latest review of different PMSs and analysis techniques was presented by Xing and Amari [34]. However, because of the complicated characteristics of PMSs and the computational complexity of the existing methods, only some small-scale PMS problems can be accurately solved [35].

An important characteristic of systems with high reliability is fault tolerance, which is often achieved by redundancy. A common realization of redundancy is the k-out-of-n system, which was introduced by Birnbaum *et al*. [8]. A system with n components that properly operates only when no fewer than k components are functioning is called a k-out-of-n: G system. Analogously, a system that fails if and only if at least k out of n components fail is named a k-out-of-n: F system. Hence, a k-out-of-n: G system is equivalent to a (n-k+1)-out-of-n: F system and vice versa. For example, a four-engined plane in which at least two engines must work for the plane to fly normally can be considered a two-out-of-four system [26]. Both parallel and series systems are special cases of the k-out-of-n system. The k-out-of-n redundancy widely applies in many military and industrial systems, e.g., space systems, airborne weapon systems, and distributed computing systems. However, these systems are also PMSs [35]. Load-sharing k-out-of-n systems are an important type of systems with k-out-of-n redundancy. The term load-sharing indicates that the remaining surviving components share a load that is imposed on the system; in other words, a failed component may increase the load on other surviving components. Subsequently, it may increase the failure rate of any surviving component; it is natural to assume that a heavier load indicates a higher failure rate. A typical load-sharing system (LSS) is the Daniels system [16], which has n fibers that are subject to a load process. Because the performance of both load-sharing systems and k-out-of-n systems depends on the number of functioning components, these two types of systems can be integrated together as a load-sharing k-out-of-n system in practical applications. An example is a long belt conveyor, which was studied by Yun *et al.* [37]. Because of the loading policy [30] and dependence between components, the reliability analysis of a load-sharing k-out-of-n system is more complex than that of a k-out-of-n system. Moreover, the performance of some load-sharing k-out-of-n systems is affected by load [9].

Most research on load-sharing k-out-of-n systems is single-phased. Little attention is paid to phased-mission requirements. Mohammad *et al*. [24] studied phased-mission systems with load-sharing components, but subsystems should be independent. Amari and Xing [4] proposed an efficient method to precisely evaluate the reliability of k-out-of-n systems with identical components that are subject to phased-mission requirements. Later, Xing *et al*. [35] used a similar method for the reliability analysis of phased-mission systems with imperfect fault coverage. However, the component failures are s-independent in the studies of Amari [4] and Xing *et al*. [35]. Hence, the method [35] is unsuitable for systems with load-sharing components.

In this paper, we propose a method to precisely evaluate the reliability of equal load-sharing k-out-of-n phased-mission systems with identical components. The method is based on the applicable failure path (AFP). A modified universal generating function (UGF [25]) is used in the AFP-searching procedure. The tampered failure rate (TFR) model is introduced to describe the load-dependent failure rate of each component. With the TFR load-sharing model for exactly k-out-of-n systems, the method can analyze systems with arbitrary load-dependent component failure distributions. Two different applications are introduced in this paper: 1) a genetic algorithm (GA) based on the method is offered to solve the operational scheduling problem of phased-mission systems with independent submissions and 2) the method is used to select the optimal number of components for systems.

The remainder of the paper is organized as follows. Section 2 provides an overview of the problem to be solved, including a system description, assumptions, and problem inputs. Section 3 describes the AFP-based method for the reliability evaluation of the studied phased-mission system. Section 4 presents the applications of the method with a genetic algorithm (GA) in the operational scheduling of phased-mission systems with independent submissions. The effectiveness of the method is verified using three examples in section 5. Finally, section 6 concludes the paper.

1. Problem statement

This paper considers the reliability evaluation of equal load-sharing k-out-of-n phased-mission systems and optimizes the operational scheduling of systems with independent submissions. The assumptions and inputs for the problem are listed in the following subsections.

2.1. System description and assumptions

1. The system mission consists of M consecutive, non-overlapping phases.
2. The system has N identical components. Each component has two states: failed and operational.
3. The system is a load-sharing k-out-of-n: F phased-mission system. The load and k-value may differ by phase.
4. The components share the total system load equally. The load is constant in each phase.
5. The failure rate of each component is affected by the load imposed on it.
6. The system is non-repairable during each phase, but at the end of each phase, all functional components are maintained. A maintained component is as reliable as a new component.
7. If the system fails in any phase, the overall mission is considered failed.

2.2. Input parameters

All required input parameters to solve the problem are listed as follows:

1. M: Number of phases.
2. $L_{i.}$ Total system load in each phase.
3. τ_i: Duration of each phase.
4. μ: Component capacity.
5. n: Number of components.
6. $k_{i.}$: Failure criterion for each phase.
7. Baseline failure time distribution of components and tampered factor of the TFR model.

This paper focuses on the system-level reliability evaluation with the above input parameters.

3. Phased-Mission Reliability Analysis

3.1. An AFP-based method for the reliability evaluation

Suppose that a system has n components and requires at least n-k_i+1 components under normal operation in the i_{th} phase with load L_i. It should be noted that the k-values of different phases are not independent. For example, because the system is non-repairable, if $k_i > k_j$ ($i < j$) and (k_i -1) components fail in the i_{th} phase, the system will certainly fail in the j_{th} phase (because k_i -1 $\geq k_j$). Therefore, if we want the system to be operational at the beginning of the j_{th} phase, the maximum allowed number of failed components in the i_{th} phase is $\min(k_i,k_j)$ - 1=k_j -1 ($i < j$). Thus, we have

$$k_{mi}=\min(k_i,k_{i+1},\ldots,k_M) \tag{1}$$

where k_{mi} is the actual k-value instead of k_i.

Define $K_m=[k_{m1}, k_{m2},\ldots, k_{m\text{M}}]$, where k_{mi} is non-decreasing w.r.t. i. To guarantee the normal operation in the i_{th} phase, the total number of failed components must be less than k_{mi}, which indicates:

$$\sum_{j=1}^{i}\Delta k_j < k_{mi} \tag{2}$$

where Δk_j is the number of newly failed components in the j_{th} phase.

Definition 3.1.1: A Failure Path is a sequence of the numbers of newly failed components in all phases:

$$\Delta K=[\Delta k_1,\Delta k_2,\ldots,\Delta k_M] \tag{3}$$

Definition 3.1.2: A Failure Subpath is a part of a failure path:

$$\Delta K^{sub}=[\Delta k_{d_1},\Delta k_{d_1+1},\ldots,\Delta k_{d_2}],1\le d_1<d_2\le M \tag{4}$$

Definition 3.1.3: An Applicable Failure Path (AFP) is a failure path that satisfies (2) for any $i \leq M$:

$$\Delta K^{a}=[\Delta k_1,\Delta k_2,\ldots,\Delta k_M],\forall i\le M,\sum_{j=1}^{i}\Delta k_j<k_{mi} \tag{5}$$

Theorem 3.1.1: The necessary and sufficient condition for the system under normal operation is that the numbers of newly failed components in each phase can comprise an AFP.

Theorem 3.1.1 clearly holds for the condition of AFP. Define a set of AFPs:

$$V=\{\Delta K_l^a, l=1,2,\ldots,C\} \tag{6}$$

where C is the cardinal number of the set V; in other words, C is the total number of AFPs. The phased-mission reliability can be evaluated as:

$$R=R(V)=\sum_{\Delta K_l^a\in V}R(\Delta K_l^a)=\sum_{\Delta K_l^a\in V}\prod_{i=1}^{M}R_e(\Delta k_{li},N-\sum_{j=0}^{i-1}\Delta k_{lj},\tau_i) \tag{7}$$

where Δk_{l0}=0, τ_i is the duration time of the i_{th} phase and $R_e(k,n,t)$ is the reliability of exactly k-out-n: F systems (or exactly (n-k+1)-out-of-n: G systems [19]). **An exactly k-out-n: F system is a system with exactly k failed components at time t**. The last equation in (7) is deduced from assumption 6 in section 2. Furthermore, according to assumption 5, $R_e(k,n,t)$ depends on the load in each phase.

$$R=\sum_{\Delta K_l^a\in V}\prod_{i=1}^{M}R_e(\Delta k_{li},N-\sum_{j=0}^{i-1}\Delta k_{li},\tau_i,L_i) \tag{8}$$

To compute the exact phased-mission reliability of a system using (8), we must obtain the AFP set V and the closed-form analytical solution of $R_e(k,n,t)$.

3.2. An AFP-Searching Algorithm Based on a Modified UGF

The AFP set V of a sequence of specified k-values is obtained using a modified UGF method. The universal generating function (UGF), which is a simple and rapid technique, was first introduced by Ushakov [29]. It is widely adopted in reliability analyses because of its efficiency. It is particularly useful in the reliability analysis of systems with multi-states and large numbers of components [12, 18, 19]. In the traditional UGF method, the UGF of a component i over state space G^i is written as a z-transformation polynomial:

$$U_i(z)=\sum\nolimits_{g_j^i\in G^i}p_j^i z^{g_j^i} \tag{9}$$

where g_j^i is the j_{th} state of the i_{th} component, and p_j^i is the probability of the i_{th} component in state g_j^i. Composition operators are used to obtain the UGF of a subset that is composed of a certain number of components. For example, the resulting UGF of component $i1$ and $i2$ is:

$$U(z)=\Omega_{\phi}(U_{i1}(z),U_{i2}(z))=\sum_{g_r^{i1}\in G^{i1}}\sum_{g_s^{i2}\in G^{i2}}p_r^{i1}p_s^{i2}z^{\phi(g_r^{i1},g_s^{i2})} \quad (10)$$

where $\phi(g_r^{i1},g_s^{i2})$ is the equivalent productivity of two components; it is $\phi(g_r^{i1},g_s^{i2})=\min(g_r^{i1},g_s^{i2})$ for series components or $\phi(g_r^{i1},g_s^{i2})=g_r^{i1}+g_s^{i2}$ for parallel components. Thus, we can evaluate the performance distribution of the entire system by repeatedly merging UGFs of all components.

In this paper, a modified UGF is provided to facilitate the expression and implementation of the AFP-searching algorithm.

Definition 3.2.1: A modified UGF (mUGF) of the i_{th} phase instead of the i_{th} component is defined as:

$$U_i(z)=\sum_{j=0}^{k_{mi}-1}j\bullet z^{[j]},i\in\{1,2,\ldots,M\} \quad (11)$$

where j is the j_{th} state of the i_{th} phase, which refers to the number of newly failed components. $[j]$ is a vector that records the number of newly failed components in each phase.

Definition 3.2.2: A composition operator for two different phases is defined as:

$$U(z)=\Omega_{\varphi,\phi}(U_{i1}(z),U_{i2}(z))=\sum_{r_1=0}^{k_{mi1}-1}\sum_{r_2=0}^{k_{mi2}-1}\varphi(r_1,r_2)z^{\phi([r_1],[r_2])}=\sum_{r_1}^{k_{mi1}-1}\sum_{r_2}^{k_{mi2}-1}(r_1+r_2)z^{[r_1,r_2]} \quad (12)$$

where $\varphi(r_1,r_2)=r_1+r_2$, and $\phi([r_1],[r_2])=[r_1,r_2]$. There are some remarks for (12):

Remark 1: $\varphi(\cdot)$ adds two elements together. $\phi(\cdot)$ merges two vectors together, its parameters are not exchangeable, $\phi([r_1],[r_2])\neq\phi([r_2],[r_1])$, because the result of $\phi(\cdot)$ indicates the execution sequence of phases.

Remark 2: We can repeatedly apply (12) to a sequence of phases to obtain a composite mUGF. In such a case, the term $r_1z^{r_1}$ in $U_{il}(z)$ must be rewritten as $r_1z^{s_1}$, where $\boldsymbol{s_1}$ is a combined vector. The length of $\boldsymbol{s_1}$ is the number of the processed phases; the sum of all elements in $\boldsymbol{s_1}$ is $\boldsymbol{r_1}$.

Remark 3: When (12) is repeatedly used for a sequence of phases, the vector s_1 in $r_lz^{s_l}$ represents a failure subpath. Therefore, for a sequence of phases, the final result from (12) contains all failure paths, including all AFPs and non-AFPs. If all failure subpaths related to the non-AFPs are removed after each calculation, then the AFP set V can be obtained.

Therefore, an AFP-searching algorithm is described as follows:

Algorithm 1: An AFP-Searching Algorithm:

1. $U(z)=U_1(z)$;
2. For $i=2,3,\ldots,M$;
   2.1 $U(z)=\Omega_{\varphi,\phi}(U(z),U_i(z))$;
   2.2 For each resulting term $r_lz^{s_l}$ in $U(z)$ from step 2.1;
      2.2.1 If $r_l\geq k_{mi}$, then remove the term from $U(z)$.

Finally, the AFP set is:

$$V=\{\Delta K_l^a=s_l:r_lz^{s_l}\text{ is a term in }U(z)\} \quad (13)$$

3.3. The time and space complexity of the method

Theorem 3.3.1: The cardinal number of the AFP set V in (5) satidfies:

$$C\leq\prod_{i=1}^{M}k_{mi}\leq(k_{mavr})^M \quad (14)$$

where k_{mavr}=mean$\{k_{mi}\}$.

Proof. The theorem can be proven using the inequality of arithmetic and geometric means.

For the reliability $R_e(m_i,n_i,\tau_i,L_i)$ of the i_{th} phase, we have $m_i\in\{0,1,\ldots,k_{mi}-1\}$ and $n_i\in\{n-k_{m(i-1)}+1,n-k_{m(i-1)}+2,\ldots,n\}$. Calculating and storing the values of all $R_e(m_i,n_i,\tau_i,L_i)$'s in advance are recommended to improve the computational efficiency.

The required storage space is mainly for storing the AFP set V and the values of all $R_e(m_i,n_i,\tau_i,L_i)$'s, whose space complexities are $O(C)$ and $O(\sum_{i=1}^{M}k_{mi(i-1)}k_{mi})$, respectively. According to (14) and the inequality of arithmetic and geometric means, the space complexity of the method is:

$$SC=O(C+\sum_{i=1}^{M}k_{m(i-1)}k_{mi})=O((k_{mavr})^M+Mk_{mavr}^2) \quad (15)$$

The computational time cost is mainly from three parts: the AFP-searching procedure, the calculations of all $R_e(m_i,n_i,\tau_i,L_i)$'s and (8), whose time complexities are, $O(\prod_{i=1}^{M}k_{mi})$ and $O(\sum_{i=1}^{M}k_{mi(i-1)}k_{mi})$ and $O(MC)$, respectively. Thus, the computational time complexity is:

$$TC=O(\prod_{i=1}^{M}k_{mi}+\sum_{i=1}^{M}k_{m(i-1)}k_{mi}+MC)=O(M(k_{mavr})^M+Mk_{mavr}^2) \quad (16)$$

By (15) and (16), the time and space complexity depends on the number of phases and k-values (the maximum allowed number of failed components) for the phases. Therefore, small k-values will decrease the time and space complexity of the method.

3.4. TFR model for an exactly *k*-out-*n*: F system

According to the regenerative process,

$$R_e(k,n,t)=R_a(k+1,n,t)-R_a(k,n,t) \quad (17)$$

where $R_a(k,n,t)$ is the reliability of load-sharing k-out-of-n: F systems. Here, the tampered failure rate (TFR) model is used to obtain a closed-form analytical expression of $R_e(k,n,t)$.

The TFR model was introduced by Bhattacharyya and Soejoeti [7] for the step-stress accelerated life test (ALT). Amari *et al*. [3] provided a closed-form analytical solution for the reliability of tampered failure rate load-sharing k-out-of-n: G systems with identical components, where all surviving components equally share the total system load. Several other models can be found in [1, 2, 23, 31]. Wang and Fei [31] studied the conditions for the coincidence of TFR, tampered random variable (TRV) and cumulative effect (CE) models.

According to the TFR model, if load L is imposed on a component, the failure rate (or hazard rate) of the component is:

$$h(t)=\delta(L)h_0(t) \quad (18)$$

where $h_0(t)$ is the baseline hazard rate and $\delta(L)$ is the tampered factor at load L.

For an equal load-sharing k-out-of-n system with identical components, let λ_i denote the failure rate of each surviving component when (i-1) (i=1,2,…,k) components have failed. We have:

$$\lambda_i = \delta(\frac{L}{n-i+1})h_0 \tag{19}$$

where L is the total load on the system and h_0 is a constant.

In particular, if the failure rate of each surviving component is directly proportional to the load imposed on it, then

$$\delta(\frac{L}{n-i+1}) = c\bullet\frac{L}{n-i+1} \tag{20}$$

where c is a constant. Therefore, the i_{th} failure of the system occurs at rate:

$$\alpha_i = (n-i+1)\lambda_i = (n-i+1)\delta(\frac{L}{n-i+1})h_0 = (n-i+1)c\frac{L}{n-i+1}h_0 = cLh_0 \tag{21}$$

In this case, all α_i's are equal. However, in other cases, the α_i's may be different. Amari *et al*. [3] have offered closed-form analytical expressions of $R_a(k,n,t)$ in three different cases. With (17) and the expressions of Amari *et al*. [3], the closed-form analytical expressions of the system reliability **of exactly tampered failure rate load-sharing k-out-of-n: F systems with i.i.d. components and the exponential failure time distributions** can be easily derived as follows.

Case (a): All α_i's are equal (say α).

$$R_e(k,n,t) = \frac{(\alpha t)^k \exp(-\alpha t)}{k!} \tag{22}$$

Case (b): All α_i's are distinct.

$$R_e(k,n,t) = \sum_{i=1}^{k}(A_i^{'} - A_i)\exp(-\alpha_i t) + A_{k+1}^{'}\exp(-\alpha_{k+1}t) \tag{23}$$

where:

$$A_i = \prod_{\substack{j=1\\ j\neq i}}^{k}\frac{\alpha_j}{\alpha_j-\alpha_i}, A_i^{'} = \begin{cases} A_i\dfrac{\alpha_{k+1}}{\alpha_{k+1}-\alpha_i}, i<k+1 \\ \displaystyle\prod_{j=1}^{k}\frac{\alpha_j}{\alpha_j-\alpha_{k+1}}, i=k+1 \end{cases}$$

Case(c): α_i's are neither equal nor distinct. Specifically, assume that these α_i's take a (1<a<k) distinct values, $\beta_1,\beta_2,\ldots,\beta_a$. With possibly some renumbering of these α_i values, assume:

$$\begin{aligned} &\alpha_1 = \cdots = \alpha_{r_1} = \beta_1 \\ &\alpha_{r_1+1} = \cdots = \alpha_{r_1+r_2} = \beta_2 \\ &\quad\vdots \\ &\alpha_{r_1+r_2+\cdots+r_{a-1}+1} = \cdots = \alpha_{r_1+r_2+\cdots+r_a} = \beta_a \end{aligned} \tag{24}$$

where the assumptions are:

1) $a \geq 1$ and an integer
2) All β_i's are distinct
3) Sum of r_i's is equal to k
4) Each $r_i \geq 1$ and an integer.

There are two different cases under **case (c)** regarding α_{k+1}:

Case (c-1): $\forall i \in \{1,2,..,k\}$, $\alpha_{k+1} \neq \alpha_i$.

$$R_e(k,m,t) = B\sum_{j=1}^{a}\sum_{l=1}^{r_j}\frac{\alpha_{k+1}\Phi_{jl}^{1}(-\beta_j) - \Phi_{jl}(-\beta_j)}{(l-1)!(\beta_j)^{r_j-l+1}}\bullet\text{poif}(r_j-l;\beta_j t) + \alpha_k B\frac{\Phi_{(a+1)l}^{1}(-\alpha_{k+1})}{\alpha_{k+1}}\bullet\text{poif}(1;\alpha_{k+1}t) \tag{25}$$

Case (c-2): $\exists i \in \{1,2,...,k\}$, $\alpha_{k+1}=\alpha_i$, assume $\alpha_{k+1}=\alpha_s$.

$$\begin{aligned} R_e(k,m,t) = {} & B\sum_{\substack{j=1\\ j\neq s}}^{a}\sum_{l=1}^{r_j}\frac{\alpha_{k+1}\Phi_{jl}^{2}(-\beta_j) - \Phi_{jl}(-\beta_j)}{(l-1)!(\beta_j)^{r_j-l+1}}\bullet\text{poif}(r_j-l;\beta_j t) \\ & + \sum_{l=1}^{r_s}\left(\frac{\dfrac{\Phi_{sl}^{2}(-\alpha_{k+1})\text{poif}(r_s+1-l;\alpha_{k+1}t) - \Phi_{sl}(-\alpha_{k+1})\text{poif}(r_s-l;\alpha_{k+1}t)}{\alpha_{k+1}}}{(l-1)!(\alpha_{k+1})^{r_s-l+1}}\right) \\ & + \frac{\Phi_{s(r_s+1)}^{2}(-\alpha_{k+1})}{r_s!\alpha_{k+1}}\bullet\text{poif}(1;\alpha_{k+1}t) \end{aligned} \tag{26}$$

where:

$$\begin{aligned} & B = \prod_{j=1}^{a}(\beta_j)^{r_j};\ \Phi_{jl}(t) \equiv D^{l-1}\left(\prod_{\substack{i=1\\ i\neq j}}^{a}(\beta_i+t)^{-r_i}\right) \\ & \Phi_{jl}^{1}(t) = \begin{cases} \Phi_{jl}^{2}(t), & j \leq a \\ D^{l-1}\left(\displaystyle\prod_{i=1}^{a}(\beta_i+t)^{-r_i}\right), & j = a+1 \end{cases} \\ & \Phi_{jl}^{2}(t) = D^{l-1}\left(\frac{\displaystyle\prod_{i=1}^{a}(\beta_i+t)^{-r_i}}{\alpha_{k+1}+t}\right) \\ & \text{poif}(r_j-l;\beta_j t) = \sum_{i=0}^{r_j-l}\frac{\exp(-\beta_j t)(\beta_j t)^i}{i!} \end{aligned} \tag{27}$$

For the TFR models with an arbitrary baseline failure distribution $F(t)$, we can perform the time transformation suggested by Amari *et al*.[3]:

$$t' = \text{H}(t) = -\ln[1-\text{F}(t)] \tag{28}$$

It can be proved that t'=H(t) follows an exponential distribution with a mean of 1 and a failure rate of 1. Thus, we can calculate $R_e(k,n,t)$ in the transformed scale by (25), (26) or (27), and the system failure rate α_i can be obtained by (18), (19) and (21) with $h_0(t')$=1. **Therefore, unless otherwise specified, only the TFR models with an exponential failure time baseline distribution are discussed in this paper.**

Moreover, the failure patterns of the same component may differ by phase, which means that the values of $R_e(k, n, t)$ may be different in two different phases for the same k, n and t. In such a case, (7) and (8) are still applicable, and we should calculate all possible $R_e(k, n, t)$'s for each phase.

If the functional components are never maintained at the end of each phase, meaning that the system failure rate depends on the pre-

vious phases, we can use the effective age of the systems [1] in the reliability evaluation. However, this evaluation is beyond the scope of this paper, and we will only provide a brief discussion.

For an AFP, the system reliability can be obtained through the effective age of the system at the end of the final phase; thus, the phased-mission reliability is evaluated by summing the reliabilities of all AFPs.

To obtain the effective age of the system at the beginning of the i_{th} phase, the following equation must be solved:

$$R_e(k_{m(i-1)}, n_{i-1}, \tau_{e(i-1)} + \tau_{i-1}, L_{i-1}) = R_e(k_{m(i-1)}, n_{i-1}, \tau_{ei}, L_i) \quad (29)$$

where $R_e(k_{m(i-1)},n_{i-1},\tau_{e(i-1)}+\tau_{i-1},L_{i-1})$ $(i \in \{2,3,\ldots,M\})$ is the reliability at the end of the $(i\text{-}1)_{\text{th}}$ phase and τ_{ei} is the effective age of the system at the beginning of the i_{th} phases. Solving (29) may be complicated.

The reliability at the end of the i_{th} phase can be expressed as $R_e(k_{mi},n_i,\tau_{ei}+\tau_i,L_i)$, where τ_i is the duration of the i_{th} phase. As a result, the phased-mission reliability is expressed as follows instead of (8):

$$R = \sum_{\Delta K_l^a \in V} R_e(\Delta k_{lM}, N - \sum_{i=0}^{M-1} \Delta k_{li}, \tau_{elM} + \tau_M, L_M) \quad (30)$$

where τ_{elM} is the effective age of the system at the beginning of the final phase for the l_{th} AFP.

4. Applications for operational scheduling optimization

Before further discussion, we apply a new assumption to the system:

Assumption A1. The submissions in different phases are independent, and the execution order of the submissions can change.

The system under assumption A1 can execute the submissions independently in random order. For example, a collection system collects different data at different places, and a computation/communication system selects tasks with different computation complexities and resource requirements from a waiting queue.

4.1. Two theorems to solve the problem under special conditions.

4.1.1. The durations of phases are constant.

Suppose $\bar{\boldsymbol{K}}$ is a set of k-values of M different phases for M different submissions. The vector is an execution sequence of phases, and k_{si} is the k-value of the i_{th} phase. $F(\bar{K})$ is defined as a set of execution sequences:

$$F(\bar{K}) = F(\{k_1,k_2,\ldots,k_M\}) = \{K_s = [k_{si}]_{1\times M} : \text{any sequence of } k_i\} \quad (31)$$

Lemma 4.1: Under assumption A1, for a specified $\bar{\boldsymbol{K}}$ and any, $K_s \in F(\bar{K})$ the AFP set on K_s is a subset of the AFP set on $K_* \in F(\bar{K})$, where $k_{*1} \le k_{*2} \le \ldots \le k_{*M}$. Therefore, the cardinal number of the AFP set V on K_s (Value of C) reaches the maximum value when K_s=K_*.

Proof. Consider an execution sequence K_{sc}=$[k_{sc1},k_{sc2},\ldots,k_{scM}]$ and k_r=min$\{k_{sci}\}$, r>1. According to the discussion in section 3.1, the corresponding actual k-values K_m can be expressed as $K_m = [\underbrace{k_r,k_r,\ldots,k_r}_{r},\underbrace{k_{m(r+1)},\ldots,k_{mM}}_{M-r}]$. If the positions of $k_{(r\text{-}1)}$ and k_r (note that $k_{(r\text{-}1)} \ge k_r$) are swapped, there is a new execution sequence K_{sc}'=$[k_{sc1},k_{sc2},\ldots,k_r,k_{r\text{-}1},\ldots,k_{scM}]$ and a new $K_m' = [\underbrace{k_r,k_r,\ldots,k_r}_{r-1},\underbrace{k_{m(r-1)},k_{m(r+1)}\ldots,k_{mM}}_{M-r+1}]$, where $k_{m(r\text{-}1)} \ge k_r$. Comparing $\boldsymbol{K'_m}$ with $\boldsymbol{K_m}$, we note the only difference is that the value at the r_{th} position of $\boldsymbol{K'_m}$ is no smaller than that of $\boldsymbol{K_m}$. Therefore, it can be easily argued that for $\forall \boldsymbol{\Delta K_l^a} \in V(\boldsymbol{K_m})$, $\boldsymbol{\Delta K_l^a} \in V(\boldsymbol{K'_m})$. In other words, $V(\boldsymbol{K_m})$ is a subset of $V(\boldsymbol{K'_m})$, $V(\boldsymbol{K_m}) \subseteq V(\boldsymbol{K'_m})$.

Repeat the above procedure until k_r is moved to the first position, and perform the same procedure with the left k-values (without k_r). Finally, all k_{sci}'s are ranked in ascending order.

Hence, any $\boldsymbol{K_s}$ can turn to $\boldsymbol{K_*}$, where $k_{*1} \le k_{*2} \le \ldots \le k_{*M}$. With the course of the proof, it can be asserted that the AFP set on $\boldsymbol{K_s}$ is a subset of the AFP set on $\boldsymbol{K_*}$.

Theorem 4.1: If all phase durations τ_i and loads L_i are equal, $R(V(\boldsymbol{K_m}))$ in (8) reaches the maximum value when $V(\boldsymbol{K_m})$ takes the largest cardinal number.

Proof. Because all phase durations and loads are equal, for any two different phases, they have the same value of $R_e(k,n,\tau_i,L_i)$ if they have the same k and n. In other words, for all phases, $R_e(k,n,\tau_i,L_i)$ only depends on k and n. Therefore, for any identical AFP $\boldsymbol{\Delta K_l^a}$ in different AFP sets, they have the same value of the term $\prod_{i=1}^{M} R_e(\Delta k_{li}, N - \sum_{j=0}^{i-1} \Delta k_{lj}, \tau_i, L_i)$ in (8). Thus, from (8), larger AFP set indicates higher reliability. Moreover, according to **Lemma 4.1**, the AFP set on $\boldsymbol{K_s}$ is a subset of that on $\boldsymbol{K_*}$ with k-values in ascending order. Hence, the AFP set on contains all other AFP sets and takes the largest cardinal number. Therefore, **Theorem 4.1** is proven.

According to the above lemmas and theorem, if the failure probability of components varies little with time or all phase durations and loads are equal, the maximum phased-mission reliability can be acquired by sorting all k-values in ascending order.

4.1.2. The durations of phases are affected by the load and component capacity.

The duration of a mission in many practical systems, such as communication network systems [15], computer systems [10] and control systems [11], depends on the component capacity. Similar to **Theorem 4.1**, there is **Theorem 4.2** under the following **Assumption A2**:

Assumption A2: Suppose all components have the same capacity and the duration of a phase (submission) depends on the component capacity, which indicates that the duration of the i_{th} phase is $\tau_i = \frac{L_i}{n_i \mu}$ if no component fails in the phase and that the maximum duration is $\frac{L_i}{(n_i - \Delta k_i)\mu}$, if Δk_i components fail at the end of the phase. Therefore:

$$\frac{L_i}{n_i \mu} \le \tau_i \le \frac{L_i}{(n_i - \Delta k_i)\mu} \quad (32)$$

Theorem 4.2: Under **Assumption A2**, if all loads L_i are equal, $R(V(\boldsymbol{K_m}))$ in (8) reaches the maximum value when $V(\boldsymbol{K_m})$ takes the largest cardinal number.

Proof. Because all components have the same capacity and all phases have the same load, duration τ_i is determined if k and n are specified. Therefore, similar to the proof procedure of **Theorem 4.1**, the above theorem is proven.

4.2. General optimization problem

In the real world, the phase duration and load may be different in different phases. Therefore, there is an optimization problem as follows:

Max

$$R(V(K_m))$$

s.t.

$$\begin{aligned} &\text{A specified } \bar{K} = \{k_1, k_2, \ldots, k_M\}, \\ &\forall K_s = [k_{si}]_{1\times M} \in F(\bar{K}), \\ &K_m = [k_{mi} = \min(k_{si}, k_{s(i+1)}, \ldots, k_{sM})]_{1\times M} \end{aligned} \tag{33}$$

The decision variable in the above optimization problem is $\boldsymbol{K_m}$ generated by a specified execution sequence. $F(\bar{K})$ is the search space that represents all possible execution sequences. If the phase duration is affected by the load and component capacity, we set τ_i in (8) to the maximum duration of each phase:

$$\tau_i = \frac{L_i}{(n_i - \Delta k_i)\mu} \tag{34}$$

where L_i is the load in the i_{th} phase, μ is the component capacity, n_i is the number of surviving components at the beginning of the i_{th} phase, and Δk_i is the number of newly failed components in the i_{th} phase. As a result, the optimized reliability in (33) is a lower bound.

4.3. A genetic algorithm for the optimization problem

Many researchers have studied similar optimal problems, such as the standby element sequencing problem (SESP) [22], the redundancy allocation problem (RAP) [6] and the reliability-redundancy allocation problem (RRAP) [13]. Lad *et al.* [17] provided the latest review of optimal reliability design problems. The genetic algorithm (GA) is an effective optimization tool for these problems. The detailed information on development of GA theory and practice can be found in the works of Goldberg [14] and Back [5]. The GA used in this paper is named GENITOR, which was proposed by Whitley [32]. GENITOR outperforms the basic "generational" GA [28]. A successful application of GENITOR has been reported for optimal system operation scheduling problems by Levitin *et al.* [21].

The following algorithm is from the method of Levitin *et al.* [21]. Each solution is represented by a string of M integer numbers, each of which ranges from 1 to M. The crossover procedure is suggested in [27].

Algorithm 2 [21], **GA for the optimization problem**:

1. Generate an initial population that consists of N_s randomly constructed solutions and evaluate their fitness. We apply **Algorithm 1** to every solution. (33) is the objective function.
2. Randomly select two solutions and perform a crossover procedure to produce a new solution (offspring). A rank-based parent selection scheme is adopted in which all solutions in the population are ranked in increasing order of their fitness; the probability of selecting a solution as a parent is proportional to its rank.
3. Apply a mutation operation to the offspring. The mutation procedure exchanges the positions of two randomly chosen components of the string.
4. Decode the offspring to obtain the objective function value (fitness).
5. Apply a selection procedure that compares the offspring with the worst solution in the current population, and then selects the better solution and discards the worse one. Eliminate redundant equivalent solutions to decrease the population size.
6. Repeat step 2-5 N_{rep} times or until the population contains only a single solution or solutions with equal quality. Generate new random solutions to replenish the population and return to step 2 to run a new genetic cycle.
7. Terminate the GA after N_c genetic cycles.

5. Numerical examples

In this section, practical applications of the method are illustrated with four examples. The first example demonstrates the calculation of the phased-mission reliability, the second example studies the computation time of the method and the other two examples are related to the operation scheduling problem of phased-mission systems with independent submissions.

Example 1. The phased-mission reliability calculation

The following example is a k-out-of-n phased-mission system with 8 phases and 16 components. The failure rate of each surviving component is directly proportional to the load, which indicates $\delta(L) \propto L$; therefore, (22) is used. The parameters of the system are listed in Table 1.

Table 1. Parameters of Example 1

Phase	k	Duration	α
No.1	4	20	0.005
No.2	8	30	0.01
No.3	10	40	0.015
No.4	12	50	0.02
No.5	4	20	0.02
No.6	8	30	0.015
No.7	10	40	0.01
No.8	12	50	0.005

With (7) and (22), the phased-mission reliability is 0.7787.

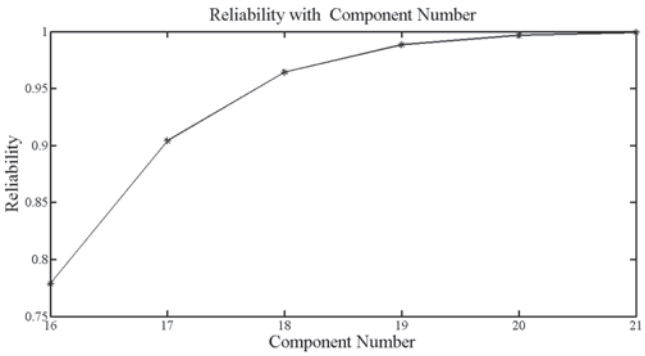

Fig. 1. Reliability with Component Number

The system is more reliable and robust if the number of components increases; however, the system cost also increases. Fig. 1 shows the reliability varies with the number of components. The reliability of a system with 16 or 17 components is more sensitive to the number of components. By adding only one component, the reliability increases from 0.7787 to 0.9041 for a system with 16 components

and from 0.9041 to 0.9643 for a system with 17 components. In this example, the system with 20 or 21 components is a good choice because of the high reliability (0.9967 or 0.9991), good robustness and relatively low cost.

Example 2. Computation time vs. system size and the number of missions

The second example investigates the computation time of the reliability evaluation of the system as a function of the number of components and missions. We suppose that all missions have the same duration (= 40) and value of α (= 0.015). Table 2 shows four systems with different numbers of components and missions. For each system, we add one mission to the system each time and evaluate the reliability.

Fig. 2 shows that the computation time varies with the number of missions for each system. We find that the computation time is mainly affected by the number of missions, increasing exponentially as the number of missions increases. The same conclusion can be drawn from (16).

Table 2. Four Systems for Studying the Computation Time

	k_1	k_2	k_3	k_4	k_5	k_6	k_7	k_8
12-component system	3	4	5	6	7	8	9	10
16-component system	3	4	5	6	7	8	10	12
20-component system	3	4	5	6	7	10	12	14
24-component system	3	4	5	6	10	12	14	16

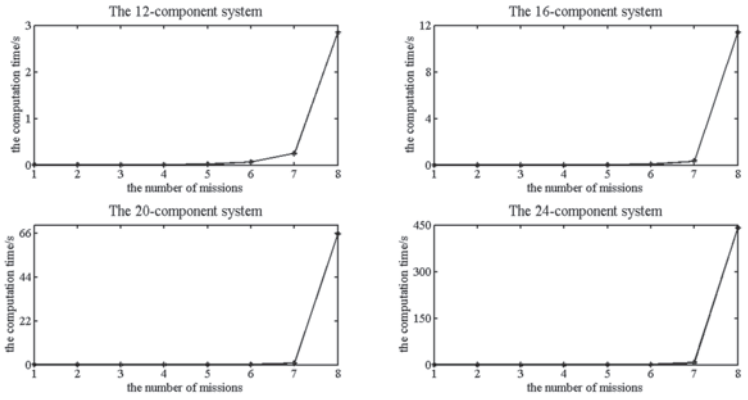

Fig. 2. Computation time for each system

Example 3. Reliability optimization

A. The durations of phases are constant.

We use the system in Example 1 but assume that the phase durations are constant. The parameters of GENITOR are listed in Table 3.

Table 3. Parameters of GENITOR for Example 3-A

N_s	10
N_{rep}	30
N_c	10
Mutation Probability	0.2

Fig. 3 shows the fast convergence of the algorithm, and the reliability increases from 0.8891 to 0.9732 after rescheduling. The best phase arrangement is [No. 1, No. 5, No. 6, No. 2, No. 3, No. 7, No. 4, No. 8]. Hence, a phase with higher required reliability is assigned an earlier execution time, which is consistent with the conclusion of the method (sorting all *k*-values in ascending order) of **Theorem 4.1**.

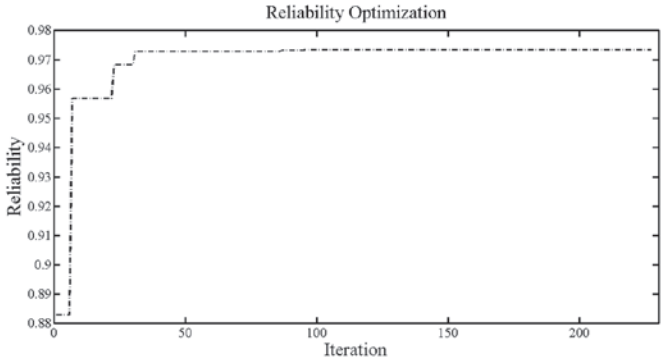

Fig. 3. Reliability Optimization (Constant Duration)

B. The durations of phases are affected by the load and component capacity.

Here, we present a system with 20 components in which the component capacity is 1 (μ=1). The system parameters are provided in Tables 4 and 5.

Table 4. Parameters of Example 3-B

Phase	*K*	α	Load
No. 1	4	0.01	40
No. 2	6	0.0225	90
No. 3	8	0.015	50
No. 4	10	0.0125	100
No. 5	11	0.0125	50
No. 6	13	0.025	100
No. 7	15	0.01	40
No. 8	17	0.0225	90

Table 5. Parameters of GENITOR for Example 3-B

N_s	10
N_{rep}	50
N_c	3
Mutation Probability	0.15

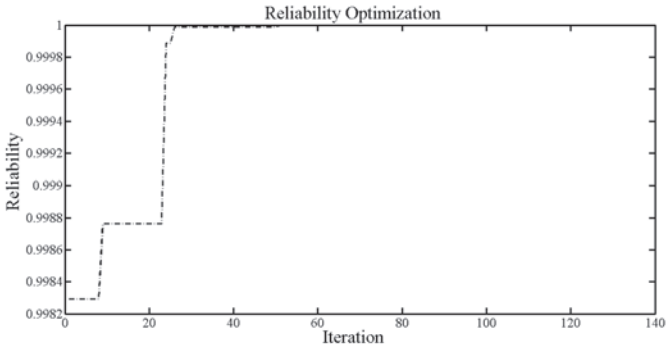

Fig. 4. Reliability Optimization (Non-Constant Duration)

Fig. 4 shows that the reliability increases from 0.998293718927419 to 0.999999568373216, and the best arrangement is [No. 1, No. 5, No. 3, No. 2, No. 7, No. 4, No. 6, No. 8]. Because the load varies in different phases, the result is different from the conclusion of Theorem 4.2, which is only suitable for all phases with similar loads. Fig. 5 shows the correctness of Theorem 4.2. The load is 100 in all phases.

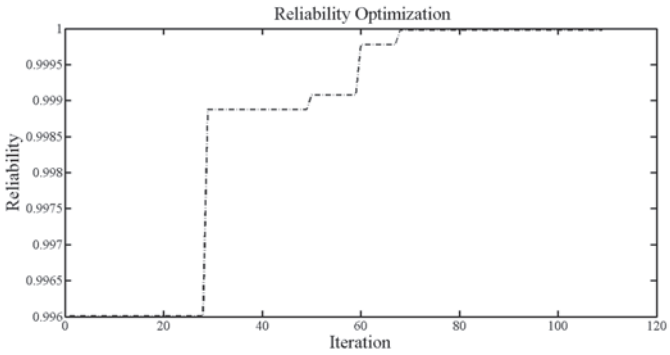

Fig. 5. Reliability Optimization (Load is 100 in All Phases)

The reliability increases from 0.996008009997850 to 0.999981789542223 in Fig. 5, and the best arrangement is [No. 1, No. 2, No. 3, No. 4, No. 6, No. 5, No. 7, No. 8], which is very close to the conclusion of **Theorem 4.2**, from which the best reliability is 0.999981905093990 by sorting all *k*-values in ascending order.

6. Conclusions

An AFP-based method is proposed for the phased-mission reliability analysis of equal load-sharing *k*-out-of-*n* phase-mission systems with identical components. Because the TRF load-sharing model for exactly *k*-out-*n* systems is introduced, the method can analyze systems having components with any type of baseline failure distributions. According to the time and space complexity analysis, this method is particularly suitable for systems with small *k*-values. Finally, the GENITOR algorithm, which integrates the method, is proposed to solve the operational scheduling problem of systems with independent submissions. If all phase durations and loads are equal, according to the theorems in section 4, the maximum reliability can be obtained by sorting all *k*-values in ascending order without using the GENTIOR algorithm. Moreover, an example in section 5 illustrates another application to select the optimal number of components to make the system reliable and robust. Our future work will consider the presented system with non-identical components and use the effective age to solve the system with dependence across phases.

Acknowledgment

This paper was supported by the National High Technology Research and Development Program of China (863 Program) under Grant No. 2011AA11A101

References

1. Amari S V, Bergman R. Reliability analysis of k-out-of-n load-sharing systems. Reliability and Maintainability Symposium, 2008. RAMS 2008. Annual. IEEE, 2008.
2. Amari S V, Krishna M B, Hoang P. Tampered failure rate load-sharing systems: status and perspectives. Handbook of Performability Engineering. Springer London. 2008; 291-308.
3. Amari S V, Misra K B, Pham H. Reliability analysis of tampered failure rate load-sharing k-out-of-n: G systems. Proc. 12th ISSAT Int. Conf. on Reliability and Quality in Design, Honolulu, Hawaii. 2006: 30-35.
4. Amari S V, Xing L. Reliability analysis of k-out-of-n systems with phased-mission requirements. International Journal of Performability Engineering, 2011; 7(6): 604 -609.
5. Back T. Evolutionary algorithms in theory and practice. Oxford University Press, New York.1996.
6. Bai D S, Yun W Y, Chung S W. Redundancy optimization of k-out-of-n systems with common-cause failures. Reliability, IEEE Transactions on, 1991; 40(1): 56-59, http://dx.doi.org/10.1109/24.75334.
7. Bhattacharyya G K, Soejoeti Z. A tampered failure rate model for step-stress accelerated life test. Communications in Statistics- Theory and Methods, 1989; 18(5): 1627-1643, http://dx.doi.org/10.1080/03610928908829990.
8. Birnbaum Z W, Esary J D, Saunders S C. Multi-component systems and structures and their reliability. Technometrics, 1961; 3(1): 55-77. http://dx.doi.org/10.1080/00401706.1961.1048992.
9. Cha J H, Yamamoto H, Yun W Y. Optimal Workload for a Multi-Tasking k-out-of-n: G Load Sharing System. IEICE Transactions on Fundamentals of Electronics, Communications and Computer Sciences, 2006; 89(1): 288-296, http://dx.doi.org/10.1093/ietfec/e89-a.1.288
10. Cha J H, Yamamoto H, Yun W Y. Optimal Workload for a Multi-Tasking k-out-of-n: G Load Sharing System. IEICE Transactions on Fundamentals of Electronics, Communications and Computer Sciences, 2006; 89(1): 288-296, http://dx.doi.org/10.1093/ietfec/e89-a.1.288.
11. Dai J. A delay system approach to networked control systems with limited communication capacity. Journal of the Franklin Institute, 2010; 347(7): 1334-1352, http://dx.doi.org/10.1016/j.jfranklin.2010.06.00.
12. Destercke S, Sallak M.An extension of universal generating function in multi-state systems considering epistemic uncertainties. Reliability, IEEE Transactions on, 2013; 62(2): 504–514, http://dx.doi.org/10.1109/TR.2013.2259206.
13. Dhingra A K. Optimal apportionment of reliability and redundancy in series systems under multiple objectives. Reliability, IEEE Transactions on, 1992; 41(4): 576-582, http://dx.doi.org/10.1109/24.249589.
14. Goldberg D E. Genetic algorithms in search, optimization and machine learning. Addison Wesley, 1989.
15. Goyal P, Vin H M, Chen H. Start-time fair queueing: a scheduling algorithm for integrated services packet switching networks. ACM SIGCOMM Computer Communication Review. ACM, 1996, 26(4): 157-168.
16. Grigoriu M. Reliability analysis of dynamic Daniels systems with local load-sharing rule. Journal of engineering mechanics, 1990; 116(12): 2625-2642, http://dx.doi.org/10.1061/(ASCE)0733-9399(1990)116:12(2625).
17. Lad B K, Kulkarni M S, Misra K B. Optimal reliability design of a system. Handbook of Performability Engineering. Springer London. 2008; 499-519, http://dx.doi.org/10.1007/978-1-84800-131-2_32.
18. Levitin G. A universal generating function approach for the analysis of multi-state systems with dependent elements. Reliability Engineering & System Safety, 2004; 84(3): 285-292, http://dx.doi.org/10.1016/j.ress.2003.12.002.

19. Levitin G. The Universal Generating Function in Reliability Analysis and Optimization. Berlin, Germany: Springer-Verlag. 2005.
20. Levitin G, Xing L, Amari S V. Recursive algorithm for reliability evaluation of non-repairable phased mission systems with binary elements. Reliability, IEEE Transactions on, 2012; 61(2): 533-542, http://dx.doi.org/10.1109/TR.2012.2192060.
21. Levitin G, Xing L, Dai Y, 2013. Optimal Sequencing of Warm Standby Elements. Computers & Industrial Engineering, 65 (4): 570–576, http://dx.doi.org/10.1016/j.cie.2013.05.001.
22. Levitin G, Xing L, Dai Y. Cold-standby sequencing optimization considering mission cost. Reliability Engineering & System Safety, 2013; 118: 28–34, http://dx.doi.org/10.1016/j.ress.2013.04.010.
23. Liu H. Reliability of a load-sharing k-out-of-n: G system: non-iid components with arbitrary distributions. Reliability, IEEE Transactions on, 1998; 47(3): 279-284, http://dx.doi.org/10.1109/24.740502.
24. Mohammad R, Kalam A, Amari S V. Reliability evaluation of Phased-Mission Systems with load-sharing components. Reliability and Maintainability Symposium (RAMS), 2012 Proceedings-Annual. IEEE, 2012: 1-6.
25. Myers F A. k-out-of-n: G system reliability with imperfect fault coverage. Reliability, IEEE Transactions on, 2007; 56(3): 464- 473, http://dx.doi.org/10.1109/TR.2007.90322.
26. Pham H, Amari S, Misra R B. Reliability and MTTF prediction of k-out-of-n complex systems with components subjected to multiple stages of degradation. International journal of systems science, 1996; 27(10): 995-1000, http://dx.doi.org/10.1080/00207729608929304.
27. Rubinovitz J, Levitin G. Genetic algorithm for assembly line balancing. International Journal of Production Economics, 1995, 41(1): 343-354, http://dx.doi.org/10.1016/0925-5273(95)00059-3.
28. Syswerda G. A study of reproduction in generational and steady-state genetic algorithms. Foundations of genetic algorithms. Morgan Kaufmann. 1991.
29. Ushakov I A. A universal generating function. Soviet Journal of Computer and Systems Sciences, 1986, 24(5): 118-129.
30. Wang K S, Huang J J, Tsai Y T, Hsu F S. Study of loading policies for unequal strength shared-load system. Reliability Engineering & System Safety, 2002; 67(2): 119-128, http://dx.doi.org/10.1016/S0951-8320(99)00057-5.
31. Wang R, Fei H. Conditions for the coincidence of the TFR, TRV and CE models. Statistical papers, 2004; 45(3): 393- 412, http://dx.doi.org/10.1007/BF02777579.
32. Whitley L D. The GENITOR algorithm and selective pressure: why rank-based allocation of reproductive trials is best. ICGA. 1989, 89: 116-123.
33. Wu X, Yan H, Li L. Numerical Method for Reliability Analysis of Phased-Mission System Using Markov Chains. Communications in Statistics-Theory and Method, 2012; 41(21): 3960-3973, http://dx.doi.org/10.1080/03610926.2012.697969.
34. Xing L, Amari S V. Reliability of phased-mission systems. Handbook of Performability Engineering. Springer London.2008; 349-368, http://dx.doi.org/10.1007/978-1-84800-131-2_2.
35. Xing L, Amari S V, Wang C. Reliability of k-out-of-n systems with phased-mission requirements and imperfect fault coverage. Reliability Engineering & System Safety, 2012; 103: 45-50, http://dx.doi.org/10.1016/j.ress.2012.03.018.
36. Xing L, Levitin G. BDD-based reliability evaluation of phased-mission systems with internal/external common-cause failures. Reliability Engineering & System Safety 2012;112: 145-153, http://dx.doi.org/10.1016/j.ress.2012.12.003.
37. Yun W Y, Kim G R, Yamamoto H. Economic design of a load-sharing consecutive k-out-of-n: F system. IIE Transactions, 2012; 44(1): 55-67, http://dx.doi.org/10.1080/0740817X.2011.590442.
38. Zang X, Sun H, Trivedi K S. A BDD-based algorithm for reliability analysis of phased-mission systems. Reliability, IEEE Transactions, 1999, 48(1): 50-60. http://dx.doi.org/10.1109/24.765927.

Chen JIAKAI
He YAN
Wei WEI
College of Electrical Engineering
Jiaoer 321, Yuquan Campus
Zhejiang University
Hangzhou, Zhejiang, China
Email: cjkkaze@zju.edu.cn, heyan@zju.edu.cn, wwei@zju.edu.cn

Article citation info:
JUREVICIUS M, TURLA V, BUREIKA G, KILIKEVICIUS A. Effect of external excitation on dynamic characteristics of vibration isolating table. Eksploatacja i Niezawodnosc – Maintenance and Reliability 2015; 17 (2): 260–265, http://dx.doi.org/10.17531/ein.2015.2.13.

Mindaugas JUREVICIUS
Vytautas TURLA
Gintautas BUREIKA
Arturas KILIKEVICIUS

EFFECT OF EXTERNAL EXCITATION ON DYNAMIC CHARACTERISTICS OF VIBRATION ISOLATING TABLE

WPŁYW WZBUDZANIA ZEWNĘTRZNEGO NA WŁAŚCIWOŚCI DYNAMICZNE STOŁU WIBROIZOLACYJNEGO

Scientific publications available on sandwich panels in evaluating fundamental frequency with a non-dimensional parameter have been discussed in this article. Effectiveness of optical table with pneumatic vibration insulation supports have been analysed in low (1-50) Hz and higher (500-1200) Hz frequency range. Experiments of vibration transmissibility performed using vibration excitation apparatus and other special test equipment. The dynamics characteristics and application ranges of a table as low frequency vibration damper have been defined. Theoretical and experimental modal analysis of the main part of the system – top surface of table – has been performed. This analysis enabled to determine four resonant eigen-frequencies at higher frequency range. Research results show the reliability of vibration table usage and the dangerous zones of its exploitation.

Keywords: *vibro-isolator, low and higher frequency, optical table, honeycomb core.*

W artykule omówiono dostępne publikacje naukowe dotyczące oceny częstotliwości podstawowej paneli przekładkowych z wykorzystaniem parametru bezwymiarowego. Analizowano wydajność stołu optycznego wyposażonego w podpory wibroizolacyjne w niskim (1-50 Hz) i wyższym (500-1200 Hz) zakresie częstotliwości. Doświadczenia dotyczące charaketrystyk przenoszenia drgań prowadzono z zastosowaniem aparatury do wzbudzania drgań i innych specjalnych urządzeń badawczych. Określono właściwości dynamiczne i zakres wykorzystania stołu jako tłumika drgań o niskiej częstotliwości. Dokonano teoretycznej i eksperymentalnej analizy modalnej głównej części systemu – górnej powierzchni stołu. Analiza ta pozwoliła wyodrębnić cztery częstości drgań własnych z wyższego zakresu częstotliwości. Wyniki badań potwierdzają niezawodność stołu wibracyjnego oraz określają strefy jego eksploatacji wykazujące niekorzystne właściwości.

Słowa kluczowe*: wibroizolator, niskie i wysokie częstotliwości, stół optyczny, rdzeń o strukturze plastra miodu.*

1. Introduction

Most of metrological instruments are sensitive to low-frequency mechanical vibrations and higher frequency – acoustic noise. These oscillations can occur from both outside and inside of the building, i.e. from passing automobiles, wind, heating, ventilation and air-conditioning equipment, and these building vibrations effect on laboratory equipment operation as well. The possibility and method of time varying vibration decomposition are discussed in the scientific workof professor Radkowski [11].

Honeycomb sandwich structures are currently being used in various engineering solutions, both within and outside of aerospace engineering. Lightweight honeycomb materials can be used in the construction of composite panels, shells, and tubes with high structural efficiency. The dynamic characteristics of Multilayer Polyurethane foam glass/fiber composite sandwich panels have been determined through Experimental Investigations by Havaldar and others [4].

Sandwich shell structures including metal alloys and composites are being increasingly applied to many aircraft, automobile and construction industries due to their lightweight and highly load carrying capacities. Furthermore, the use of cellular cores for panels and shells not only can further reduce the structural weight, but also potentially possess superior heat dissipation, vibration control and energy dissipation characteristics. Filament winding and twice co-curing processes were proposed to make a carbon fiber reinforced composite (CFRC) sandwich cylinder with Kagome cores. Axial compression was carried out to reveal the stiffness and load capacity of the fabricated sandwich cylinder. Compared with the stiffened cylinder with similar dimensions and mass, the sandwich cylinder is shown to be stiffer and stronger by several times [3]. Linear and nonlinear analysis using the ABAQUS finite element is described in paper [15]. Some mechanical properties such as compression, bending, impacting and vibration have been reported by many scientists worldwide. Analytical calculation methods have a clear advantage when designing multi-layered composite cylindrical shells. Compared to Finite Element Methods (FEM) they enable more precise physical interpretations and weighting of the different design variables to be made and, hence, significantly facilitate problem-specified parameter studies and sensitivity analysis [5]. Sandwich cylindrical shells are the major components of aerospace apparatus structures [17]. Nevertheless, an analytical investigation was carried out to examine the response of CFRC sandwich cylinders with lattice cores.

Researchers Xiong et al [20] manufactured sandwich-walled cylindrical shells with aluminium pyramidal truss core of constant curva-

ture employing an interlocking fabrication technique for the metallic core. Thereafter is carried out axial compression tests on some representative samples to investigate the failure modes of these structures and compared with an analytical failure map developed to account for Euler buckling, shell buckling, local buckling between reinforcements and face-crushing. A combined experimental and numerical study is conducted to assess the effects of impact energy, impact site and core density on the compression-after-impact (CAI) strength of pyramidal truss core sandwich structures [24]. It is found that the severity of impact damage highly depends on the impact site. The CAI tests show that the local buckling occurs for both the un-impact specimens and the specimens impacted under lower energy, while debonding is observed for the specimens impacted under higher energy. In addition to experimental tests, the numerical simulation performs well in capturing the failure modes for impact-damaged specimens under compressive load. Composite pyramidal lattice structures with hollow trusses afford a convenient means to enable functionality by inserting elements into free volumes within or between trusses are presented by researchers Yin, Wu and others [23]. In this study, vibration and low-velocity impact tests were carried out to investigate the dynamic behaviour of hollow composite pyramidal lattice structures filled with silicone rubber. Frequencies and the corresponding damping ratios were obtained, which revealed that the damping ratios of space-filled composite pyramidal lattices increased by two times but those of hybrid composite pyramidal lattices decreased by 2% for the first three orders compared with hollow composite pyramidal lattices.

FEM has been used to predict the modal properties of free-free FRP plates, and the predictions were verified experimentally by scientists Maheri, Adams and Hugon [8, 9]. Results are presented for materials for which little dynamic data have yet been available, including the thermoplastic matrix material PEEK. Also, it is shown how using improved experimental techniques can lead to closer theoretical and experimental damping results. In the paper [10] laminated composite shells are frequently used in various engineering applications in the aerospace, mechanical, marine, and automotive industries. This article follows a previous book and review articles published by the leading author. It reviews most of the research done in recent years (2000–2009) on the dynamic behaviour (including vibration) of composite shells. This review is conducted with emphasis on the type of testing or analysis performed (free vibration, impact, transient, shock, etc.), complicating effects in material (damping, piezoelectric, etc.) and structure (stiffened shells, etc.), and the various shell geometries that are subjected to dynamic research (cylindrical, conical, spherical and others). A general discussion of the various theories (classical, shear deformation, 3D, non-linear etc.) is also given. The main aim of this review article is to collate the research performed in the area of dynamic analysis of composite shells during the last 10 years, thereby giving a broad perspective of the state of art in this field. The paper [12] deals with the free vibration analysis of composite sandwich cylindrical shell with a flexible core using a higher order sandwich panel theory. The formulation uses the classical shell theory for the face sheets and an elasticity theory for the core and includes derivation of the governing equations along with the appropriate boundary conditions. The model consists of a systematic approach for the analysis of sandwich shells with a flexible core, having high-order effects caused by the nonlinearity of the in-plane and the vertical displacements of the core. The behaviour is presented in terms of internal resultants and displacements in the faces, peeling and shear stresses in the face–core interface and stress and displacement field in the core.

The paper [13] explores the partial coverage of cylindrical shells with a constrained viscoelastic damping layer, with emphasis on examining the minimum area of coverage that will yield optimal damping. The distribution of damping patches on the structure is based on strain energy intensity distribution maps derived for the purpose. The analysis uses the FEM, and a suitable curved shell element is formulated for the add-on damping treatment. Numerical studies show that a partial coating procedure can be a viable approach in optimal damping designs. A semi-analytical finite element for doubly curved, multi-layered shells of revolution, based on an extension of the displacement field proposed by Wilkins et al, is proposed in paper [14]. Numerical analysis is done to study the vibration and damping characteristics of multi-layered fluid filled shells with alternating elastic and viscoelastic layers. The effect of varying the number of viscoelastic layers on the vibration and damping characteristics is also studied. The effect of the fluid is incorporated by the added mass concept. The effect of shear parameter on natural frequency and modal loss factor is studied for various circumferential and axial modes. The vibration and damping characteristics of free–free composite sandwich cylindrical shell with pyramidal truss-like cores have been conducted using the Rayleigh-Ritz model and FEM is presented in paper [22]. The predictions for the modal properties of composite sandwich cylindrical shell with pyramidal truss-like cores showed good agreement with the experimental tests. The influences of fiber ply angles on the natural frequency and damping loss factor were investigated. Three types of such composite sandwich cylindrical shells were manufactured using a hot press moulding method and the relevant modal characteristics of various sandwich cylindrical shells could be obtained by modal tests. The natural frequencies of composite sandwich cylindrical shell increased with the increasing of the ply angle of the inner and outer curve face sheets, whereas the damping loss factors of present shells did not increase monotonically. The natural frequencies of composite sandwich beams with lattice truss core are investigated by combining the Bernoulli–Euler beam theory and Timoshenko beam theory were analysed by Xu and Qiu [21].

Latterly, the scientists concerning honeycomb sandwich structures have been focused on effective numerical modelling methods, vibration properties, crash- worthiness, damage, and failure and impact response. Researchers Adams and Maheri[1] investigated the damping of composite honeycomb sandwich beams in steady-state flexural vibration using the method extended from that for monolithic beams.

The material properties such as elastic modules and strengths are various in different directions, and even the compressive and tensile properties are different in the thickness-direction, primarily due to the initial deflection of cell walls. Vibration frequencies and mode shapes of honeycomb sandwich panels with various structural parameters were studied by Qunli Liu and Yi Zhao [7] using computational and experimental methods. Two computational models were used to predict the mode shapes and frequencies of honeycomb sandwich panels. Plate elements were used for honeycomb cell walls to reflect the geometric nature of the hexagonal cells.

Optical table vibrations typically are between 2 Hz and 7 Hz, because it is eigen-frequency at which the optical table resonates. However, especially for low (from 0.7 Hz) frequencies a better insulator, working with scanning probe microscopy and interferometry is required. Existing quasi-zero (negative) stiffness isolators resonates from 0.5 Hz [6].This frequency has almost no power, because it would be very unusual to find large oscillations at 0.5 Hz[18]. Optical tables and active systems do not work very well when placed in a vacuum, especially at high or low temperature and radiation. Such an environment occurs during specific investigations of semiconductors. Quasi-zero stiffness system can work in vacuum, high and low temperatures and under radiation [6].

Optical tables with pneumatic vibration isolators are suitable for laser centres. Theoretical analysis of vibration parameters and analysis of experimental results allows to assess of honeycomb systems reliability. Comprehensive analysis of vibration theoretical methods are described by scientists Cveticanin, Mester and Biro [2], Siljak, Subasi [16] and Wicher, Więckowski [19].

A lot of studies presented in bibliographic sources are related to one of the attributes (high strength/weight or increased energy absorp-

tion) mentioned above. With regard to the development of a honeycomb panels, one issue that has been overlooked is the scaling of honeycomb properties with respect to cell size. The variation in cell size may have a large influence on the dynamic properties of honeycomb panels. The goal of this study was to reveal the effect of cell size on the fundamental frequency of honeycomb panels. The results of the experimental investigation are presented and discussed. Nevertheless, authors described the determination of mechanical passive isolation systems ability to isolate low (from 0.7 to 50 Hz) and higher (from 500 to 1200 Hz) frequency oscillations.

2. Research objects, instruments and equipment

The experimental research combination of optical table with pneumatic vibration insulators is shown in Fig. 1.

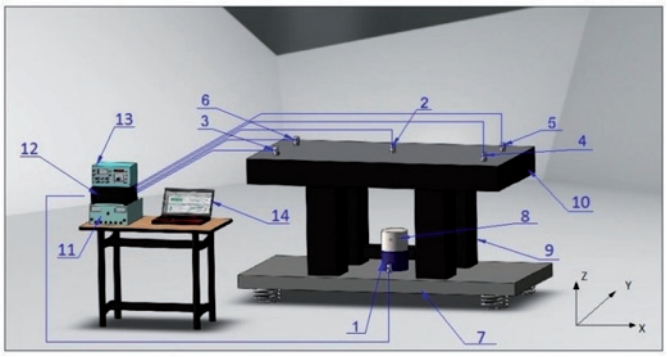

Fig. 1. Research scheme of optical table dynamic characteristic: 1, 2, 3, 4, 5, 6 – vibration transducers; 7 – platform (base); 8 – vibrator; 9 – supports of vibration isolation; 10 – optical table with experimental of vibration isolation; 11 – impulse generator; 12 – amplifier; 13 – generator; 14 – computer with analyser

Top and bottom countertop surfaces of analysed optical table are made of cold-rolled ferro-magnetic steel sheets, which combine lightweight structure made of corrosion resistant cellular steel, giving the table exceptional toughness. The optical table is usually mounted on special vibration isolating supports. The optical table structures resist to static and dynamic forces not only vertically, but also horizontally considered being highly important defining quality factors.

Idealized "seismic" mounting system of optical tables is a rigid table, mounted on a massive foundation or on the supports that inhibit vibrations. Various types of vibration isolation bearings with compressed air dampers are used in world practice. These supports must ensure the stability of the table in vertical and horizontal directions. Horizontal environmental vibration effect is particularly striking when the laboratories are installed on the upper floors of the buildings.

The lightweight honeycomb structures for manufacture objects that are resistant to the dynamic and static forces are widely used. Honeycomb cells are characterized by the size, wall thickness, the material from which they are made, etc. Typical features of honeycomb structures are lightness and resistance to compression and bending. These qualities are especially important when it is required for optimal characteristics ratio of mass and stiffness. Therefore cellular structures are used in aircraft, helicopters, and other plant production.

This type of structures is widely used for optical laboratory tables also. Cellular tables have good vibration damping properties, they are much lighter than the massive tables made of granite. In most cases not resistant for mechanical loads heavy granite table, but lightweight cellular structure have been chosen.

The most important quality criteria of insulating pillars is characteristics of mechanical vibration transmission from a base supports the table top. These characteristics determine the applicability of various experimental techniques. The specific method is selected according to a number of factors, among which the more important one is dominant frequency range.

Study includes analysis and measurement of vibration and other dynamic properties by using "Brüel&Kjær" firm equipment. The portable measurement results processing device connected with computer, and vibration sensors (type 8341 and 8306) with vibration meter 2511 were used as well. An experimental part of modal analysis was carried out by using this equipment as well.

The vibration excitation platform with a vibrator and other special test equipment were used in and tested for research of dynamic parameters of pneumatic isolator of vibrations. Easily tuned vibration excitation platform has been built, allowing the test subject to excite vibrations of (1–50) Hz frequency range in any of three directions: vertical transverse, horizontal transverse and horizontal longitudinal directions.

Using aforementioned equipment modal analysis of top plate of table was performed. This analysis was done with purpose to obtain eigen-frequencies of top plate which are unwelcome in precise measuring process. During experiment top plate of vibro-isolating table was treated as single deformable body instead of construction with supports.

3. Results of theoretical and experimental modal analysis

The results of typical damping (Fig. 1) of vibration isolation supports excited by harmonic vibrations, impulse and white noise, shown in Fig. 2. (a, b, c, d, e).Oscillations are not isolated when there is a harmonic excitation at 2 Hz; isolation starts with 4 Hz. Thus, optical tables are not effective for frequencies up to 4 Hz.

Following are presented the most important results of vibration isolating supports at 1–50 Hz frequency range at different sizes of load (transmission dependence on frequency curves T_v, corresponding resonant frequency of the f_{vr} and transmissibility coefficient values at resonance 5 Hz to 10 Hz frequencies). Maximum value of transmissibility coefficient at different loads varies from 3 to 4 Hz: without load – 2.9 Hz; 100 kg – 2.7 Hz; 250 kg – 2.4 Hz; 500 kg – 2.1 Hz. This shows that the vibration isolating supports with the load forms an elementary single mass vibrating system. Resonance frequency decreases by increasing the load of vibration isolating supports. With increasing frequency above the resonance transmissibility steadily decreases, and at frequencies of 50 Hz is less than 0.01.

Further results of modal analysis are provided.The experimental results were compared with the analytical model of the vibro-isolating table; approximate simplified model of vibro-isolating table built. This analytical model is thoroughly described in paper [6]. In current paper mathematical model of vibro-isolating table was built in ANSYS environment and modal analysis was performed. The table top was modelled using SHELL63 finite element; mesh of 25x25 elements, which gave converged results of eigen-frequencies (see Fig. 3).

Table was measured in 16 points using same equipment as in previous experiments. As top plate of the vibro-isolating table is permitted to freely bend, there are many different shapes in which the top plate can bend. An eigen-mode describes the shape of bended top plate; an eigen-frequency describes how fast bending occurs. Eigen-mode vibrates at its eigen-frequency and the total bending and frequency of the top plate is their sum. Eigen-modes depend on the support configuration of the vibro-isolating table, and the natural frequencies depend on the stiffness and mass components of the top plate and its shape. Natural modes with the highest frequencies are usually not very important because their amplitude is relatively small. Only four lowest eigen-frequencies of the vibro-isolating table are considered to be significant.

Eigen-mode shapes of experiment match ones of mathematical model. Results of mathematical model showed good corresponding

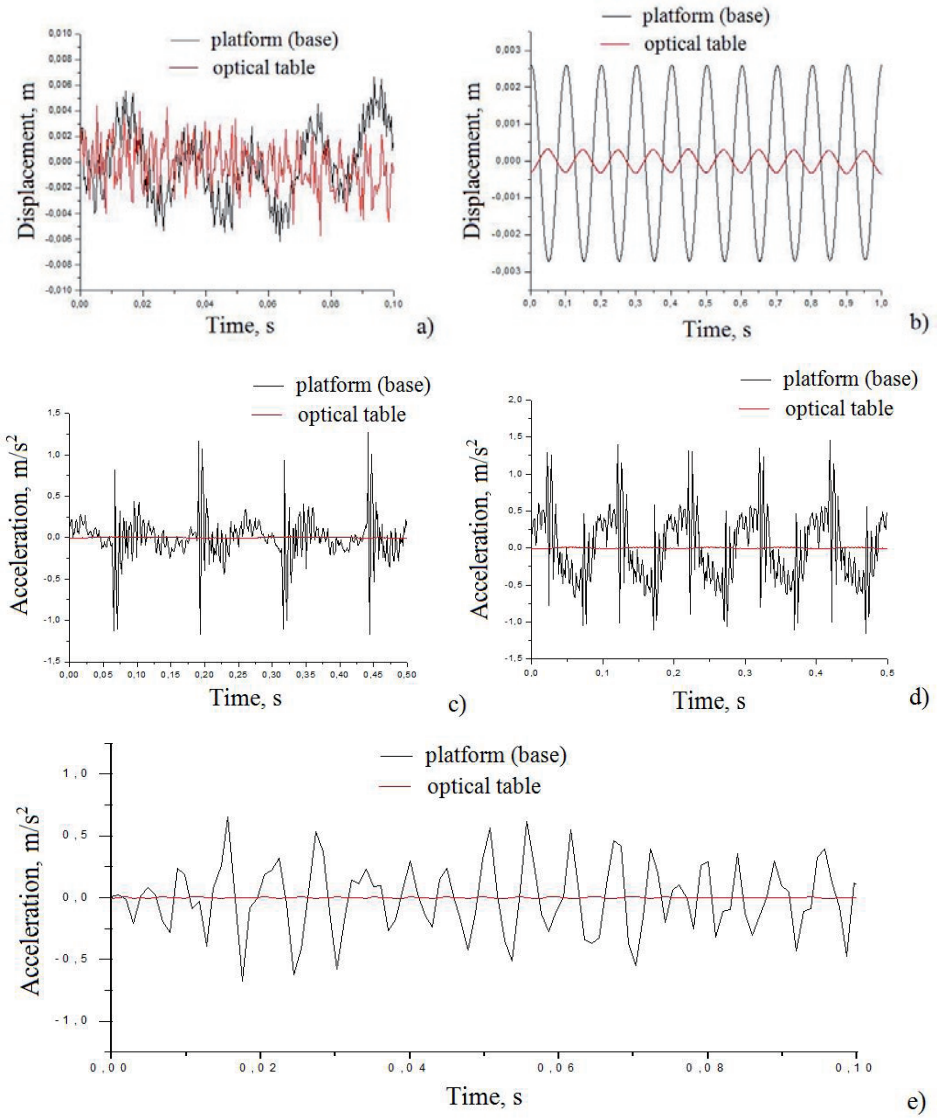

Fig. 2. Damping characteristics of vibration isolation supports (black signal – of platform, red – of optical table): a – 2Hz harmonic excitation frequency; b – 10 Hz harmonic excitation frequency; c – 4 Hz impulse excitation; d – 10 Hz impulse excitation; e – excitation by white noise

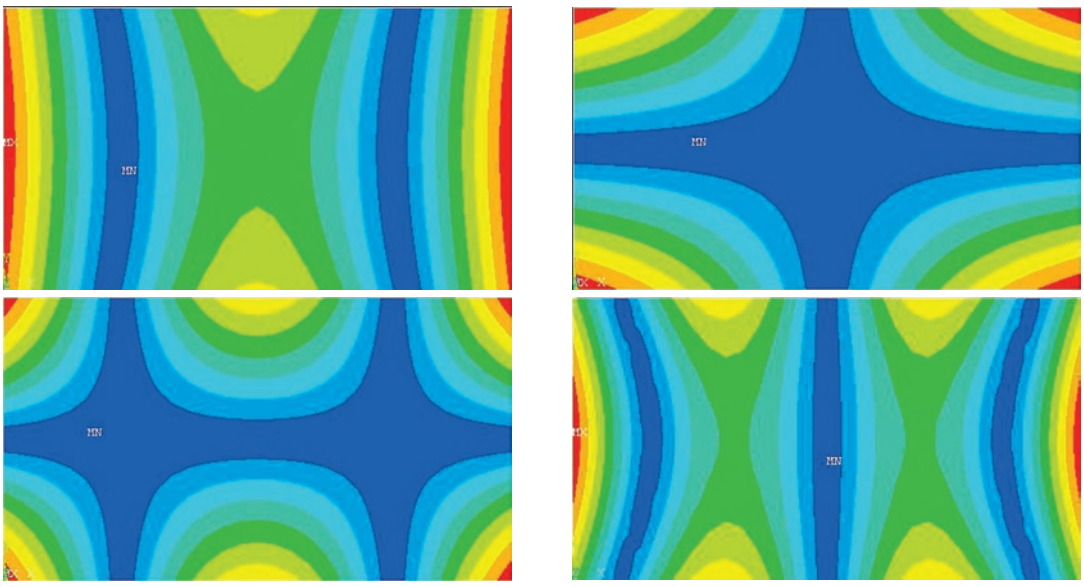

Fig. 3. Lowest four natural modes of the top plate

Table 1. Comparison of modelling and experiment results

Mode	Experimental, f_E, Hz	Theoretical, (using ANSYS) f_T, Hz	Discrepancy, Δ, %
1	504.4	495.8	1.7
2	535.8	551.2	2.8
3	1012.8	989.7	2.3
4	1172.0	1205.6	2.9

with experiment;i.e. discrepancy does not exceed 2.9% between results of experimental and mathematical tests (Table 1).

As seen in Table 1, the discrepancy of theoretical and experimental results varies from 1.7 % up to 2.9 %. This shows enough high reliability of above mentioned modelling method.

4. Conclusions

1. Designated vibration excitation test equipment intended for identification of dynamic characteristics of the investigated objects was designed by authors and tested. The following pneumatic vibration isolator dynamic parameters identified: coefficient of transmissibility in vertical direction – oscillation characteristics at 50 Hz frequency range is less than 0.01; resonant frequency in vertical direction – 3–4 Hz depending on load; and damping efficiency at 5 Hz to 10 Hz depending on optical table load was derived. It was proved, that optical table has less than unitary transmissibility coefficient (vibration isolating properties) in analysed frequency range.
2. Performed modal theoretical and experimental analysis of upper share of the table enable to define four resonant eigenfrequencies at higher frequency diapason: 504.4 Hz, 535.8 Hz, 1012.8 Hz and 1172.0 Hz.
3. The results of this study show thatduring forthcoming experiments with this equipment fixed on the table it is required to avoid these four dangerous resonant eigen-frequecies of the table and table top surface.

References

1. Adams RD, Maheri MR. Dynamic Shear Properties of Structural Honeycomb Materials. Composites Science and Technology. 1993. 47(1): 15–23, http://dx.doi.org/10.1016/0266-3538(93)90091-T.
2. Cveticanin L., Mester G., Biro I. Parameter Influence on the Harmonically Excited Duffing Oscillator. Acta polytechnica Hungarica. 2014.11(5): 145–160.
3. Fan HL, Fang DN, Chen LM, Dai Z and Yang W. Manufacturing and testing of a CFRC sandwich cylinder with Kagome cores. Compos Sci Technol. 2009. 69: 2695–700, http://dx.doi.org/10.1016/j.compscitech.2009.08.012.
4. Havaldar SS, Sharma RS, Antony AP and Bangaru M. Effect of cell size on the fundamental natural frequency of FRP honeycomb sandwich panels. Journal of Minerals and Materials Characterization and Engineering. 2012. 11: 653–660.
5. Hufenbach W, Holste C, Kroll L. Vibration and damping behaviour of multilayered composite cylindrical shells. Compos Struct. 2002;58:165–74, http://dx.doi.org/10.1016/S0263-8223(02)00025-9.
6. Jurevicius M, Kilikevicius A, Berba M. Impact of external excitations on the dynamic properties of negative-stiffness vibration isolation table, Journal of Vibroengineering. 2011. 13(2): 352–357.
7. Liu QL, Zhao Y. Role of Anisotropic Core in Vibration Properties of Honeycomb Sandwich Panels, Journal of Thermoplastic Composite Materials. 2002. 15 (1): 944–952, http://dx.doi.org/10.1106/089270502022860.
8. Maheri MR, Adams RD. Finite-element prediction of modal response of damped layered composite panels. Compos Sci Technol. 1995. 55:13–23, http://dx.doi.org/10.1016/0266-3538(95)00074-7.
9. Maheri MR, Adams RD, Hugon J. Vibration damping in sandwich panels. J Mater Sci. 2008. 43: 6604–6618, http://dx.doi.org/10.1007/s10853-008-2694-y.
10. Qatu MS, Sullivan RW, Wang W. Recent research advances on the dynamic analysis of composite shells: 2000–2009. Compos Struct. 2010. 93: 14–31, http://dx.doi.org/10.1016/j.compstruct.2010.05.014.
11. Radkowski S. Use of vibroacoustical signal in detecting early stages of failures. Eksploatacja i Niezawodnosc – Maintenance and Reliability. 2007. 35(3): 11–18.
12. Rahmani O, Khalili SMR, Malekzadeh K. Free vibration response of composite sandwich cylindrical shell with flexible core. Compos Struct. 2010. 92:1269–81, http://dx.doi.org/10.1016/j.compstruct.2009.10.021.
13. Sainsbury MG, Masti RS. Vibration damping of cylindrical shells using strain energy-based distribution of an add-on viscoelastic treatment. Finite Elem Anal Des. 2007. 43:175–92, http://dx.doi.org/10.1016/j.finel.2006.09.003.
14. Saravanan C, Ganesan N, Ramamurti V. Vibration and damping analysis of multilayered fluid filled cylindrical shells with constrained viscoelastic damping using modal strain energy method. Comput Struct. 2000. 75: 395–417, http://dx.doi.org/10.1016/S0045-7949(99)00099-1.
15. Shariati MSM, Saemi J, Eipakchi HR and Allahbakhsh HR. Numerical and experimental investigation on ultimate strength of cracked cylindrical shells subjected to combined loading. Mechanika. 2010. 4:12–9.
16. Siljak H, Subasi A. Fourier spectrum related properties of vibration signals in accelerated motor aging applicable for age determination. Eksploatacja i Niezawodnosc – Maintenance and Reliability. 2014. 16 (4): 616–621.
17. Sun FF, Fan HL, Zhou CW, et al. Equivalent analysis and failure prediction of quasi-isotropic composite sandwich cylinder with lattice core under uniaxial compression. Compos Struct. 2013. 101:180–90, http://dx.doi.org/10.1016/j.compstruct.2013.02.005.
18. Vijayan V, Karthikeyan T. Design and Analysis of Compliant Mechanism for Active Vibration Isolation Using FEA Technique. Int. Journal of Recent Trends in Engineering. 2009. 1(5): 77-81.
19. Wicher J, Więckowski D. Influence of vibrations of the child seat on the comfort of child's ride in a car. Eksploatacja i Niezawodnosc – Maintenance and Reliability. 2010. 4(48): 102-110.
20. Xiong J, Ghosh R, Ma L, Vaziri A, Wang YL, Wu LZ. Sandwich-walled cylindrical shells with lightweight metallic lattice truss cores and

carbon fiber-reinforced composite face sheets. Compos: Part A. 2014. 6: 226–238, http://dx.doi.org/10.1016/j.compositesa.2013.10.008.
21. Xu MH, Qiu ZP. Free vibration analysis and optimization of composite lattice truss core sandwich beams with interval parameters. Compos Struct. 2013. 106: 85–95, http://dx.doi.org/10.1016/j.compstruct.2013.05.048.
22. Yang J, Xiong J, Ma L, Zhang G, Wang X and Wu L. Study on vibration damping of composite sandwich cylindrical shell with pyramidal truss-like cores. Composite Structures 2014. 117: 362–372, http://dx.doi.org/10.1016/j.compstruct.2014.06.042.
23. Yin S, Wu LZ, Yang JS, Ma L, Nutt S. Damping and low-velocity impact behavior of filled composite pyramidal lattice structures. J Compos Mater. 2013. 1–12.
24. Zhang GQ, Wang B, Ma L, Xiong J, Yang JS and Wu LZ. The residual compressive strength of impact-damaged sandwich structures with pyramidal truss cores. Compos Struct. 2013. 105: 188–98, http://dx.doi.org/10.1016/j.compstruct.2013.05.016.

Mindaugas JUREVICIUS
Arturas KILIKEVICIUS
Department of Mechanical Engineering, Vilnius Gediminas Technical University
J. Basanavičiaus str. 28, LT-03224 Vilnius, Lithuania

Vytautas TURLA
Department of Printing Machines, Vilnius Gediminas Technical University
J. Basanavičiaus str. 28, LT-03224 Vilnius, Lithuania

Gintautas BUREIKA
Department of Railway Transport,Vilnius Gediminas Technical University
J. Basanavičiaus str. 28, LT-03224 Vilnius, Lithuania

E-mails: mindaugas.jurevicius@vgtu.lt, arturas.kilikevicius@vgtu.lt;
vytautas.turla@vgtu.lt; gintautas.bureika@vgtu.lt

Article citation info:
KUSZ A, MARCINIAK A, SKWARCZ J. Implementation of computation process in a bayesian network on the example of unit operating costs determination. Eksploatacja i Niezawodnosc – Maintenance and Reliability 2015; 17 (2): 266–272, http://dx.doi.org/10.17531/ein.2015.2.14.

Andrzej KUSZ
Andrzej MARCINIAK
Jacek SKWARCZ

IMPLEMENTATION OF COMPUTATION PROCESS IN A BAYESIAN NETWORK ON THE EXAMPLE OF UNIT OPERATING COSTS DETERMINATION

IMPLEMENTACJA PROCEDURY OBLICZENIOWEJ W SIECI BAYESOWSKIEJ NA PRZYKŁADZIE WYZNACZANIA JEDNOSTKOWYCH KOSZTÓW EKSPLOATACJI*

In technical systems understood in terms of Agile Systems, the important elements are information flows between all phases of an object existence. Among these information streams computation processes play an important role and can be done automatically and also in a natural way should include consideration of uncertainty. This article presents a model of such a process implemented in a Bayesian network technology. The model allows the prediction of the unit costs of operation of a combine harvester based on the monitoring of dependent variables. The values of the decision variables representing the parameters of the machine's operation and the intensity and the conditions for its operation, are known to an accuracy, which is defined by a probability distribution. The study shows, using inference mechanisms built into the network, how cost simulation studies of various situational options can be carried out.

***Keywords**: agricultural machinery operation, computing processes, unit operating costs, Bayesian networks.*

W systemach technicznych rozumianych w kategoriach Agile Systems istotnym elementem są przepływy informacyjne pomiędzy wszystkimi fazami istnienia obiektu. Pośród tych strumieni informacyjnych istotną rolę odgrywają procesy obliczeniowe, które mogą być realizowane automatycznie a ponadto w naturalny sposób powinny umożliwiać uwzględnienie niepewności. W artykule przedstawiono przykład takiego procesu realizowanego w technologii sieci bayesowskiej. Model umożliwia predykcję jednostkowych kosztów eksploatacji kombajnu zbożowego na podstawie monitorowania wielkości zmiennych od których one zależą. Wartości zmiennych decyzyjnych reprezentujących parametry pracy maszyny oraz intensywność i warunki jej eksploatacji są znane z dokładnością do rozkładu prawdopodobieństwa. W pracy pokazano w jaki sposób wykorzystując mechanizmy wnioskowania wbudowane w sieci można prowadzić symulacyjne badania kosztów w różnych wariantach sytuacyjnych.

***Słowa kluczowe**: eksploatacja maszyn rolniczych, procesy obliczeniowe, jednostkowe koszty eksploatacji, sieci bayesowskie.*

1. Introduction

The technical systems of today can be understood in terms of Agile Systems. This means that their existence is not a series of separate phases: design, manufacturing, operation and recycling. The "agile paradigm" assumes the simultaneous presence of all these phases. For example, the design works are carried out all the time and are aimed at continuous adaptations of technical systems to changing requirements [1, 22, 23]. The manufacturing process implements these adaptations and translates them into the operating features.

In such a system, an important role is played by intensive information flows manageable in Big Data information technology. The process of this data collection and its processing is automatic and takes place in a semantic data network technology [6,7,10]. Computational processes are performed automatically using advanced systems of cognitive modeling [8.22]. This modeling should take into account uncertainty factors. The states of processes and objects used in specific processes are known with an accuracy of the probability distribution. Cognitive modeling can therefore be based on probabilistic network technology.

In engineering of technical systems, in particular bio-agrotechnical [15], one of the important computational processes that must be embedded in the system is the ability to monitor operating costs. This is a multidimensional process of entire systems, their components (subsystems), and finally specific groups and types of machines. Optimization of operating costs forms the basis of the effective use of technical systems in agriculture. In the literature, and increasingly in the databases one can find information about the cost of the actions that make operational processes for the selected category of objects. Determining unit operating costs, being the cost of one hour of operation of a tractor or other machine, which is the sum of the unit costs of maintenance and use [24], based on information obtained from databases, allows for comparison of a particular technical object with other objects having the same purpose. This is essential during selection and purchase of a particular object. The possibility of feedback information from a particular class of objects allows designers to estimate the critical unit operating costs that cannot be exceeded if the designed object is to be competitive with the current market offer.

A wide commercial range of tractors and other machinery makes the rational selection of specific technical solutions, depending on the size of the farm and production profile, a difficult task from the point of view of their effective use. Principles of analysis and operational evaluation of an object [29] are defined by the methodological frameworks of determining the cost, depending on the intensity of use. The

(*) Tekst artykułu w polskiej wersji językowej dostępny w elektronicznym wydaniu kwartalnika na stronie ***www.ein.org.pl***

proposed computational procedures are based on the deterministic approach [28], with consideration of the indicative methods [24].

An alternative approach to the methods described above is an approach based on the Bayesian network. The use of the network is justified by the uncertainty factor integrally associated with the operation process of technical objects. The essence of the proposed approach is predicated on the fact that the individual cost elements and factors determining their size, such as the operating parameters of technical objects, conditions and intensity of using the equipment, and other factors such as maintenance costs, loan interest rates, etc. are represented as random variables.

Bayesian networks have been widely used in situations where in the explicit way the factor of uncertainty and inference in non-deterministic categories of cause–effect relationships should be encoded [13, 14, 27]. They are a useful tool for modeling uncertainty in agricultural production processes [18, 19], the prediction of the technical condition of the object in order to plan preventive measures [3, 4], computer-supported decision making processes [14, 21], and representation of the reliability knowledge, both in practical terms [4 , 8.15] and for the purpose of theoretical analysis [2.30].

Another application of Bayesian networks is the problem of managing complex networks of activities [17]. This approach makes possible the inclusion in the model of the relationship between the time of carrying out a particular activity and the conditions of its implementation and currently available production resources.

This study aims to provide a method of conceptualization in the language of Bayesian networks of the computation process on the example of determining the unit operating costs of agricultural machinery. The unit operating cost is determined as the average value of the cost per unit of measure of the work done in the lifetime of an object [24,29]. An important element of the methodology is the consistency with the demands of knowledge engineering, which assumes the possibility of using machine-learning methods to build a network. The possible scenarios for the functioning of the model are based on inference methods typical for Bayesian networks [27].

2. Conceptualization of determining the operating costs of agricultural machinery

Substantive knowledge of the operation of technical object, including the computation process, provides qualitative knowledge that is necessary to build the correct semantics of process models. In the case of Bayesian networks, this knowledge is used to establish the topology and thus the factorization of the total probability distribution, or presenting it as the product of the conditional probability distributions. At the stage of network usage, substantive knowledge is essential for choosing the significant paths of inference and interpretation of outcomes of the inference process.

As a basis of reference for the calculation of unit operation costs, one hour of the machine's operation was chosen [24]. The general rule is to calculate the cost of machines operation based on the reconstruction price regardless of whether the calculations concern a new machine or the one already used. In addition, this approach allows for consideration of the situation when, while planning the purchase of a particular machine, the limited time of its operation can be taken into account, assuming that after a certain time the machine can be sold off. Such an interpretation of the price is justified by the fact of its representation as a random variable, and the range of variation of this variable should be determined based on the difference between the purchase price and the expected selling price. Similarly, the lifetime of the machine (i.e. the normative, or pre-determined amount of "work" that it can perform from the purchase to its cassation or resale) and the hourly use of the machine per year (h/year) in the specific conditions of use, are represented as continuous random variables with a determined probability distribution established on the basis of learning data.

The adoption of these assumptions means that the individual components of the operating costs will be represented in the model as conditional random variables and the determination of unit operating costs in a particular case boils down to using these variables.

Graphical form of this conceptualization and simultaneously the structure of the network enabling the determination of operating costs in Bayesian network technology, is shown in Fig. 1 [11]. Network topology results from the structure of the calculation process. The network can be divided into nodes representing the raw input data, nodes representing the operations on these data and, finally, the final node that represents the unit operating costs. The nodes, which collect data from the data stream, represent the values of the data. Probability distributions on the set of values of these nodes are determined automatically based on the data obtained from the history of operation of the machine. The values assigned to nodes representing operations on random variables are also random variables. The value of the final variable is also determined with an accuracy of the probability distribution.

The parameters of the machine operation and the individual cost components adopted for the calculations are represented by the variables having the same name.

A machine's lifetime is represented by the variable Z. This variable represents the assumed time of use of the machine. The model assumes that this variable is expressed in hours of operation. It can

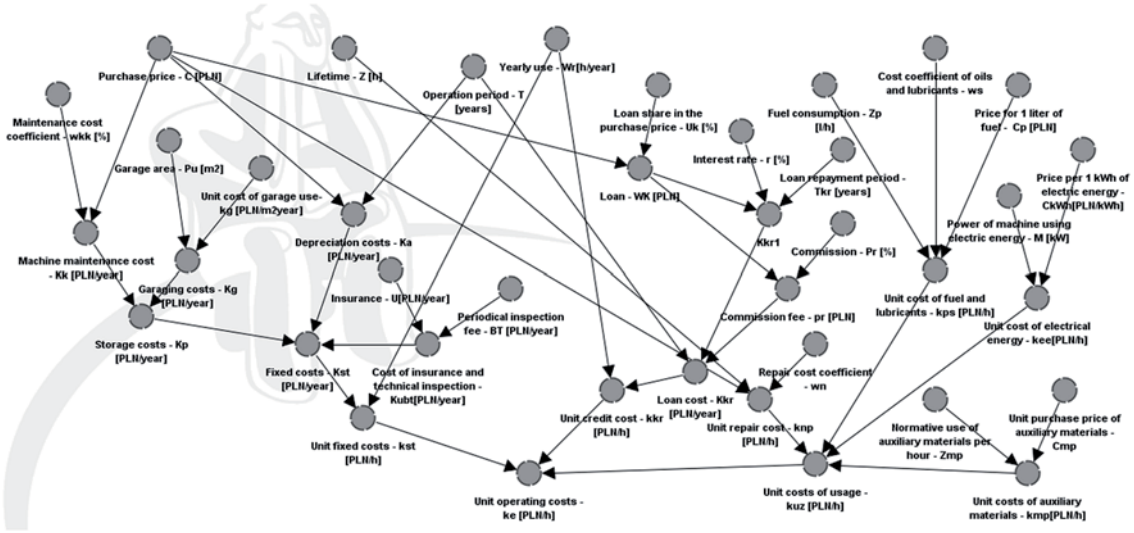

Fig. 1. Structure of the network for determining unit operating costs (own analysis)

also be expressed in other units such as the amount of work done. The hourly use of the machine per year W_r (h / year) is a random variable depending on the intensity of machine's operation in the specific conditions of its use. Another variable T represents the machine's operational time in years. The maximum value of this variable can be estimated by dividing the machine 's life time Z by the assumed time of its use per year W_r.

Amortization cost K_a is the expression of financial reduction in value of machines per year:

$$K_a = \frac{C}{T}, \tag{1}$$

where: C- purchase price in PLN
T- operation time in years

The cost of storing the machine K_P (PLN / year) is calculated as the sum of the garaging cost K_g and maintenance cost K_k. The garaging cost K_g (PLN / year) is calculated as the product of usable area P_u (m^2) of the garage or shed, and the unit cost of operation of the object i.e. the garage or the shed k_g (PLN / m^2year):

$$K_g = P_u \cdot k_g. \tag{2}$$

The maintenance cost of the machine K_k (PLN / year) includes the value of non-cash outlay and labor costs that are associated with post-season cleaning of the machine and securing it for the time of storage. This cost can be determined on the assumption that there is known distribution of working time, depending on the type of machine, the method and extent of maintenance, and the type of machine; or by using the simplified method as the product of the purchase price and the coefficient of maintenance cost w_{kk}. It is assumed that the w_{kk} coefficient, depending on the complexity level, is 0.5% – 1% of the machine's price. In the current procedure, the second method has been implemented.

The distribution of the variable representing the costs of insurance and technical inspections (if obligatory) K_{ubt} is estimated based on the current tariffs of insurance companies and the applicable rates.

The above cost components are independent of the intensity of operation of the machine. The total cost of this group K_{st} is the sum of the costs K_a, K_g, K_{ubt}. The sum of these components divided by the time of the operation of the machine per year W_r determines the unit fixed costs k_{st} per 1 hour of operation:

$$k_{st} = \frac{K_a + K_g + K_{ubt}}{W_r}. \tag{3}$$

When the purchase of the machine is associated with taking a loan, the user incurs additional costs. They include the interest on the loan, including additional charges, (although it does not apply to the loan's capital repayments, which are part of the depreciation costs). This cost is known in advance, but may vary due to conditions for granting loans for investments (e.g. interest, commission, repayment period and the grace period) by individual banks, the type of credit line, or the credit-worthiness of a borrower and loan collateral. Assuming that the cost of the loan K_{kr} (PLN / year) is spread over the period of the machine's use T, this cost can be determined on the basis of a simplified formula:

$$K_{kr} = \frac{1}{T}\left[\frac{U_k \cdot C \cdot r \cdot (T_{kr}+1)}{2} + pr\right], \tag{4}$$

where: T- machine's operation time (years)
U_k - loan share in the purchase price (%/100),
T_{kr} - loan repayment period (years),
r - interest rate (% / 100),
pr - commission and other fees associated with the loan facility (PLN)
C – price (PLN).

In the above considerations, the cost of interest on capital as an alternative method of gaining revenues in cases when the cost of the investment is financed from one's own resources, has been omitted. Currently, there is a prevailing opinion that the value of the cost of interest on capital is compensated by calculating the depreciation cost each time from the current price.

The loan cost K_{kr} divided by the time of the machine use per year W_r determines the unit cost component k_{kr} (in PLN / h)of work resulting from servicing the loan:

$$k_{kr} = \frac{K_{kr}}{W_r}. \tag{5}$$

The next category of cost includes the costs directly related to the machine's use. These costs include the cost of repairs, fuel and lubricants, the cost of electricity and any additional materials. The total value of these costs in a year depends on the amount of work done. In the model, the average values of these costs over the entire operation period are represented, because in principle, with the increase in machine wear, the unit cost of its use, especially repairs, will be higher than in the first year of its operation.

There are two alternative approaches to determine the cost of repairs. The first one is used when we have reliable statistics of operating history on the basis of which the actual distributions of normative cost of repairs, emergency repairs, maintenance and other tasks for the whole operation period can be estimated. The second approach (implemented in this model) assumes that the cost of repairs over the total operation period is from 0.4 to 1.5 of the purchase price, depending on the machine, and then the unit cost of repairs k_{np} in PLN per hour of operation is calculated as:

$$k_{np} = \frac{w_n \cdot C}{Z}, \tag{6}$$

where: w_n - repair cost coefficient,
Z- lifetime in hours
C- price.

Depending on the conditions of the machine's use, skills of technicians and quality of repairs and maintenance, repair costs k_{np} can vary considerably and this is taken into account by the fact that the coefficient w_n is represented as a random variable.

The unit cost of fuel and lubricants k_{ps} (PLN / h of work) is the product of unit fuel consumption Z_p (l / h of operation), of the engine and the price of 1 liter of fuel C_p, while the value of oils and lubricants used is determined in relation to the value of fuel consumed by an indicative method. The total unit cost of fuel and lubricants is:

$$k_{ps} = w_s \cdot Z_p \cdot C_p, \tag{7}$$

where: w_s – coefficient of lubricants cost to fuel cost.

The unit cost of electricity k_{ee} consumed by the devices is estimated as the product of the nominal capacity of the machine (M) and the price (C_{kWh}) of 1 kWh of electricity:

$$k_{ee} = M \cdot C_{kWh}. \tag{8}$$

The unit cost of auxiliary materials k_{mp} (PLN / h of work) is only present in the case of some machines, such as string or mesh for binding bales of straw in harvesting press, film for wrapping bales or silage etc. This cost is the product of the normative consumption of these materials Z_{mp} for 1 hour of the operation of the machine and the unit purchase price C_{mp}.

$$k_{mp} = Z_{mp} \cdot C_{mp}. \tag{9}$$

The total unit costs of machine use k_{uz} per 1 hour of operation are:

$$k_{uz} = k_{np} + k_{ps} + k_{ee} + k_{mp}. \tag{10}$$

The unit cost of operation k_e (PLN / h), (i.e. the cost of one hour of work of the tractor or machine) is the sum of unit costs independent of the amount of work, loan costs and operating costs:

$$k_e = k_{ST} + k_{kr} + k_{uz}. \tag{11}$$

Unit cost of operation of a set comprising tractor and machines is the sum of unit costs of operation of the machine and the associated tractor. This cost can also be expressed per unit of work performed (e.g. for 1 hour of work per 1 hectare) as the ratio of the cost per hour of operational performance of the tractor-machine set or the self-propelled machinery.

The above algorithm for determining unit operating costs based on Bayesian network technology is general in nature. The terminal node represents the unit cost of operation. The value of this variable in accordance with the methodology set out above is determined as the sum of unit costs (fixed, loan and the cost of use). These costs are represented in the network as three basic modules. The application of this model to assess a specific machine requires its "concretization". This concretization takes place in two stages. In the first stage, the network topology should be matched to a particular situation. Network topology takes into account the form of purchase of the machine (cash or credit) and energy sources (self-propelled machine, trailed or stationary electric- motor driven). Matching of the network involves activation of its respective modules. If the purchase is financed by a loan, the module for determining the *unit cost of loan* is activated. Similarly, depending on the energy source, a module for determination of the *unit cost of fuel* is activated (in the case of self-propelled or trailed machinery) or a *unit cost of electricity* module (in the case of stationary machines driven by electric energy). The second step of problem concretization involves assigning prior-conditional probability distributions to network nodes and specifying domains of nodes variability values.

3. Determination of unit operation costs of a combine harvester

In order to verify the model, calculations were carried out concerning combine harvesters with a working width of 4.5 – 5.0 meters. Network topology takes into account the possibility of buying the machine for cash or with part credit. A priori probability distributions were estimated using catalog data and the literature [24]. The purchase price was assumed at C = 322 500 PLN, lifetime Z = 2440 h, the operation time T = 15 years, the annual use W_r = 158 h / year; fuel costs and insurance and other components correspond to currently applicable prices. The first example analyzed assumes that the purchase was covered by one's own funds.

The typical mechanism of operation of the network (i.e. prediction of the decision effects) enables determination of the unit costs depending on the form of purchase, the assumed parameters of a combine harvester, projected costs of service and projected intensity of its use.

Calculations were performed for two scenarios of cost: optimistic and pessimistic. The optimistic variant (Fig. 2) implies that the components of the cost determined by an indicative method adopt minimum values. The pessimistic scenario assumes that these costs are maximised.

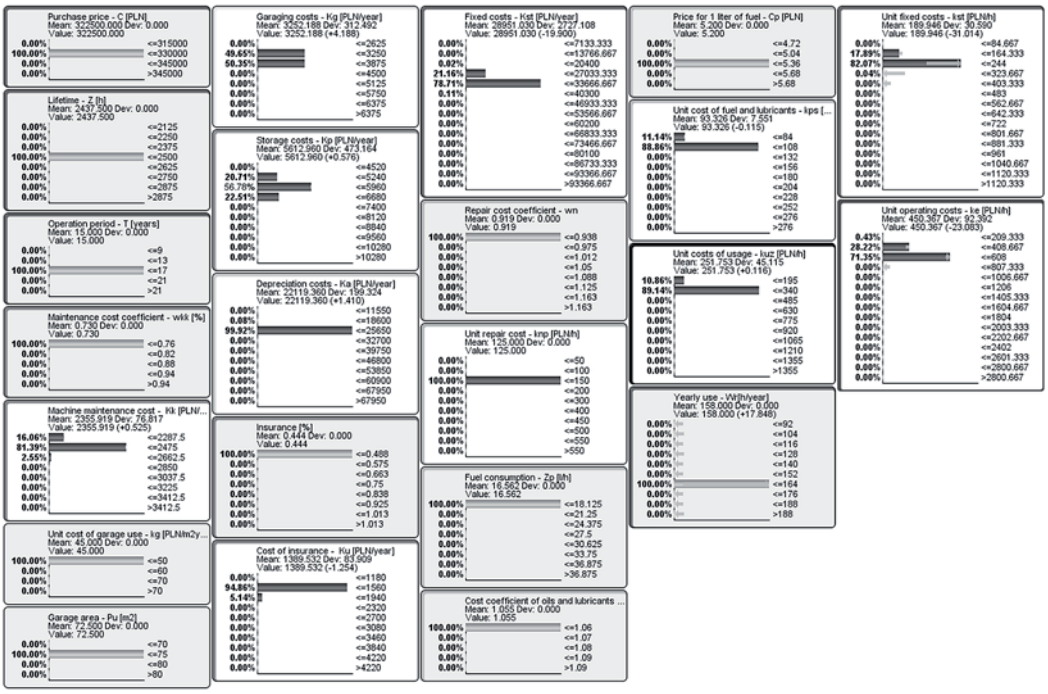

Fig. 2. Predictive inference optimistic scenario (own analysis)

If the variable is known to an accuracy of probability distribution (i.e. soft evidence) our knowledge of the terminal variable is fuzzy. As shown by the calculations, the expected values of variables representing the unit cost of operation, fixed costs and the use, amount to (in PLN per hours of operation) respectively: 456.1 (standard deviation 89.4), 191.3 (standard deviation 29.4), 254.3 (standard deviation 41.8).

In the case of a pessimistic scenario (Fig. 3), the unit cost of operation is a random variable with an expected value of 636.3. The expected values of the individual components are as follows (in PLN per hours of operation: the unit fixed cost 214.3 (standard deviation 28.6), and the unit cost of operation 411.0 (standard deviation 14.6).

Fig. 3 shows the probability distributions over a set of variables representing the unit operating costs, in the optimistic (W_1) and the pessimistic scenario (W_2).

Fig. 4 shows the relationship between unit cost of operation k_e (PLN/h) and the time of use of combine harvester per year (W_r) determined by using the network for both variants analyzed.

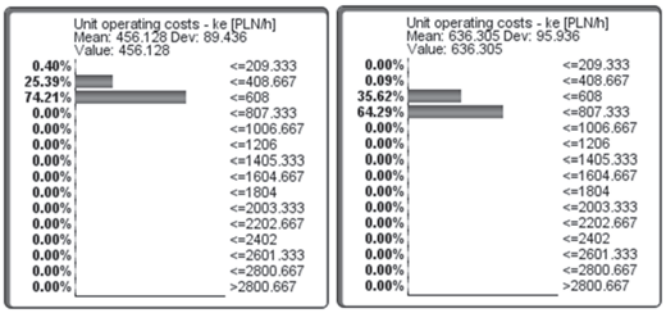

Fig. 3. Probability distributions for unit operating costs (own analysis)

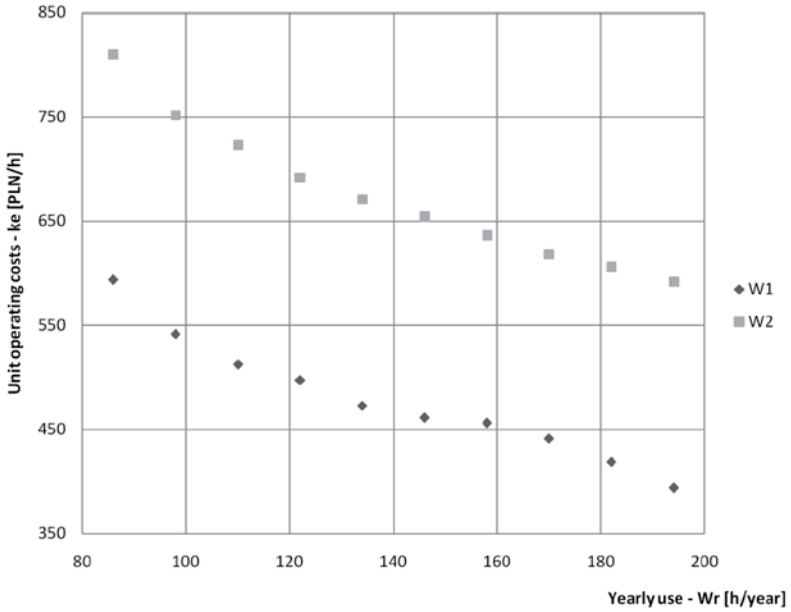

Fig. 4. Unit operating costs depending on the use of combine harvester per year

Similar calculations were performed when the purchase was half-financed by a loan, assuming optimistic scenario of the individual cost components. The adopted loan repayment period was T_{kr} = 3.5 years. In the variants analyzed the following interest rates and commissions were assumed: r = 11.4 (W_1) and r = 14.2 (W_2). Commission was assumed to be 0.7% (W_1) and 1.9% (W_2) of the loan amount. Based on the calculations, the unit operation cost depending on the use of the combine harvester per year for both analyzed variants was determined (Fig. 5).

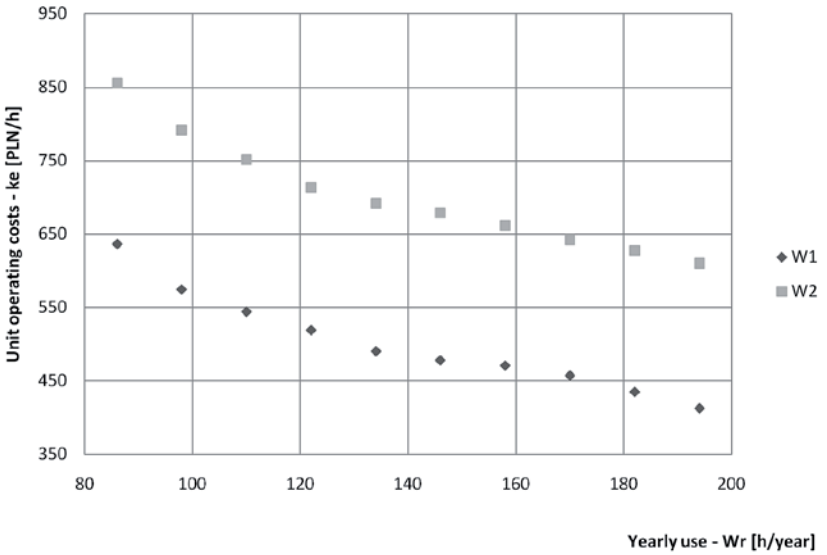

Fig. 5. Unit operating costs depending on the use of combine harvester per year (the purchase with 50% loan)

The diagnostic inference mechanism available in the networks (i.e. time projection backwards) is useful when we want to specify conditions that must be met in order to achieve a particular level of unit costs. Fig. 6 shows the points corresponding to the fixed costs per unit, depending on the lifetime and yearly use of the object with no credit for investment and two analyzed variants, the optimistic and pessimistic scenarios.

The above scenarios of the model's operation, by analogy, can be used for determining other cost components. Information that is possible to achieve with the model have great practical significance and can be used in the operational management process.

Summary

The implemented in Bayesian network procedure of calculating the unit operation costs is an example of the computation process, which due to the built-in inference mechanisms, can be completely automated. Easy changes of input data depending on the available financial resources and the expected conditions of use means that the proposed method can be of great significance in the design, planning, monitoring and analysis of the operational process of a specific object in its specific conditions of use.

Predictive inference allows for analyzing all possible solutions depending on the operating environment. With the accuracy of probability distribution, a set of mutually acceptable solutions can be determined. Hypothetical-deductive inference (time projection backwards) allows for the preset terminal variable value (in this case, the unit costs operation) determining the requirements for the variables representing the individual components of the cost, and the variables characterizing the machine parameters and its conditions of use.

The machine learning mechanisms available in the system [12] ensure adaptability of the model at both the level of topology (adaptation of the model to a particular type of object) and at the level of determining ,a priori, the probability distributions of individual variables.

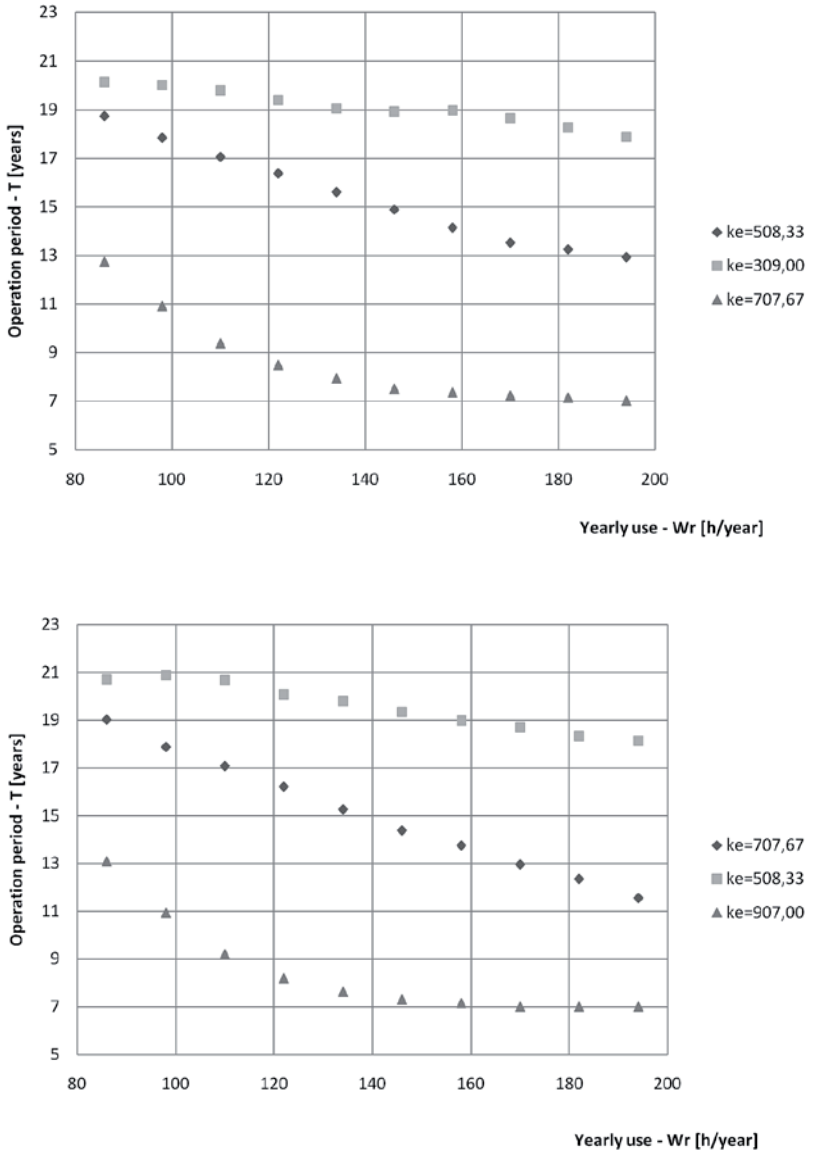

Fig. 6. The points corresponding to fixed unit operation costs, depending on the operation period (T) and the yearly use of W_r (optimistic scenario: upper graph, pessimistic scenario: bottom graph)

References

1. Andrzejczak K. Metody prognozowania w modelowaniu eksploatacji środków transportu. Rozprawy, Wydawnictwo Politechniki Poznańskiej 2013; nr 496.
2. Barlow R.E. Using influence diagrams. In: Clarotti CA, Lindley DV, editors. Accelerated life testing and experts' opinions in reliability 1988; 145–57.
3. Bartnik G., Kalbarczyk G. and Marciniak A. W. Application of the operational reliability model to the risk analysis in medical device production. Teka 2011;Vol. XIC: 366-370.
4. Bartnik G., Kusz A. and Marciniak A. Dynamiczne sieci bayesowskie w modelowaniu procesu eksploatacji obiektów technicznych. Inżynieria Wiedzy i Systemy Ekspertowe, Oficyna Wydawnicza Politechniki Wrocławskiej 2006; t. II: 201-208.
5. Bartnik G. and Marciniak A. W. Operational reliability model of the production line. Teka 2011; Vol. XIC: 361-365.
6. Berners-Lee T., Karger D.R., Stein L.A., Swick R.R., Weitzner D.J. Proposal: Semantic Web Development Retrieved from W3C 2000.
7. Berners-Lee, Hendler J., Lassila O. The Semantic Web. Scientific American 2001.
8. Chmielecki A. Konceptualne podstawy kognitywistyki – krytyka i propozycje własne. Szczecin: VII Zjazd Filozoficzny 2004.
9. Chun Su, Ye-qun Fu.:Reliability Assessment for Wind Turbines Considering the Influence of Wind Speed Using Bayesian Network. Eksploatacja i Niezawodnosc – Maintenance and Reliability 2014; 16 (1): 1–8.
10. Cost S., Finin T., Joshi A. A Case Study in the Semantic Web and DAML+OIL. IEEE Intelligent Systems 2002, http://dx.doi.org/10.1109/5254.988447.
11. Dokumentacja programu BayesiaLab. http://www.bayesia.com, 10.06.2014.
12. Doguc O. and Ramirez-Marquez J.E. A generic method for estimating system reliability using Bayesian networks. Reliability Engineering and System Safety 2009; 94: 542-550, http://dx.doi.org/10.1016/j.ress.2008.06.009.

13. Halpern J., Y. Reasoning about uncertainty. The MIT Press Cambridge, Massachusetts, London, 2005.
14. Hołaj H., Kusz A., Maksym P., Marciniak A. W. Modelowanie problemów decyzyjnych w integrowanym systemie produkcji rolniczej. Inżynieria Rolnicza 2011; 6 (131): 53-60.
15. Kocira S., Kuboń M. The operating costs machines and general type of farming. Roczniki Naukowe Stowarzyszenia Ekonomistów Rolnictwa i Agrobiznesu SERiA 2011;Tom XIII, Zeszyt 6: 103-107.
16. Kusz A., Maksym P., Marciniak A. W. Bayesian networks as knowledge representation system in domain of reliability engineering. Teka 2011; Vol. XIC: 173-180.
17. Kusz A., Maksym P., Skwarcz, J. Grudziński J. The representation of actions in probabilistic networks. Teka 2013; Vol. XII: 41-47.
18. Kusz A., Marciniak A.W. Modelowanie niezawodności złożonych systemów bioagrotechnicznych. Inżynieria Rolnicza 2010; 5 (114): 147-154.
19. Maksym P. Podstawowe zasady modelowania procesu produkcji rolniczej. Inżynieria rolnicza 2011; 1 (126): 155-162.
20. Maksym P., Marciniak A. W., Kostecki R. Zastosowanie sieci bayesowskich do modelowania rolniczego procesu produkcyjnego. Inżynieria Rolnicza 2006; 12 (87): 321-330.
21. Maksym P., Marciniak A. W., Kusz A. Modelowanie syntezy działań ochronnych w rolniczym procesie produkcyjnym. Inżynieria Rolnicza 2011; 4 (129): 213-220.
22. Marciniak A. Projektowanie systemu reprezentacji wiedzy o rolniczym procesie produkcyjnym. Rozprawy naukowe Akademii Rolniczej w Lublinie, Wydział Inżynierii Produkcji 2005; zeszyt 298.
23. Młyńczak M. Metodyka badań eksploatacyjnych obiektów mechanicznych. Oficyna Wydawnicza Politechniki Wrocławskiej, 2012.
24. Muzalewski A. Koszty eksploatacji maszyn. Wydawnictwo ITP, 2010; 25.
25. Oniśko A., Marek J. Druzdzel M. J., Wasyluk H. Learning Bayesian network parameters from small data sets: Application of noisy-or gates. International Journal of Approximate Reasoning 2001; 27(2): 165–182, http://dx.doi.org/10.1016/S0888-613X(01)00039-1.
26. Pearl J. Fusion, Propagation, and Structuring in Belief Networks. Artificial Intelligence. 1986; 29(3): 241-288, http://dx.doi.org/10.1016/0004-3702(86)90072-X.
27. Pearl J. Probabilistic Reasoning in Intelligent Systems: Network of Plausible Inference. Morgan Kaufmann, 1988.
28. Piasecki S. Eksploatacyjna ocena wyrobu na przykładzie maszyn roboczych. Eksploatacja i Niezawodnosc – Maintenance and Reliability 2001; 1(8): 3-8.
29. Piasecki S. Zasady analizy i oceny obiektu technicznego. Eksploatacja i Niezawodnosc – Maintenance and Reliability 2001; 1(8): 50-51.
30. Tchangani A.P. Reliability analysis using Bayesian networks. Stud. Inform. Control 2001; 10(3): 181–188.

Andrzej KUSZ
Department of Technology Fundamentals
University of Life Sciences
ul. Doświadczalna 50A, 20-680 Lublin, Poland
E-mail:

Andrzej MARCINIAK
University of Economics and Innovation in Lublin, Poland
ul. Projektowa 4. 20-209 Lublin
E-mail: andrzej.marciniak@wsei.lublin.pl

Jacek SKWARCZ
Department of Technology Fundamentals
University of Life Sciences
ul. Doświadczalna 50A, 20-680 Lublin, Poland

E-mails: andrzej.kusz@up.lublin.pl,
andrzej.marciniak@wsei.lublin.pl, jacek.skwarcz@up.lublin.pl

Article citation info:
LI X-T, TAO L-M, JIA M. A Bayesian networks approach for event tree time-dependency analysis on phased-mission system. Eksploatacja i Niezawodnosc – Maintenance and Reliability 2015; 17 (2): 273–281, http://dx.doi.org/10.17531/ein.2015.2.15.

Xiao-tao LI
Li-min TAO
Mu JIA

A BAYESIAN NETWORKS APPROACH FOR EVENT TREE TIME-DEPENDENCY ANALYSIS ON PHASED-MISSION SYSTEM

OPARTE NA SIECIACH BAYESOWSKICH PODEJŚCIE DO ANALIZY ZALEŻNOŚCI CZASOWYCHW SYSTEMACH O ZADANIACH OKRESOWYCH WYKORZYSTUJĄCE METODĘ DRZEWA ZDARZEŃ

Abstract: Event tree/ fault tree (E/FT) method is the most recognized probabilistic risk assessment tool for complex large engineering systems, while its classical formalism most often only considers pivotal events (PEs) being independent or time-independent. However, the practical difficulty regarding phased-mission system (PMS) is that the PEs always modelled by fault trees (FTs) are explicit dependent caused by shared basic events, and phase-dependent when the time interval between PEs is not negligible. In this paper, we combine the Bayesian networks (BN) with the E/FT analysis to figure such types of PMS based on the conditional probability to give expression of the phase-dependency, and further expand it by the dynamic Bayesian networks (DBN) to cope with more complex time-dependency such as functional dependency and spares. Then, two detailed examples are used to demonstrate the application of the proposed approach in complex event tree time-dependency analysis.

Keywords: *time-dependency, Bayesian networks, event tree, fault tree, phased-mission system; reliability; risk analysis*

Metoda drzewa zdarzeń/drzewa błędów jest najbardziej znanym narzędziem probabilistycznej oceny ryzyka w złożonych, dużych systemach inżynieryjnych; jednak jej klasyczny formalizm najczęściej uwzględnia jedynie niezależne lub niezależne od czasu zdarzenia kluczowe. Praktyczną trudnością występującą w systemach o zadaniach okresowych jest to, że zdarzenia kluczowe, które zazwyczaj przedstawiane są w modelach drzewa błędów jako powiązane zależnościami jawnymi, mającymi związek ze wspólnym zdarzeniem podstawowym, tutaj powiązane są zależnościami czasowymi, jako że przedział czasowy pomiędzy pojedynczymi zdarzeniami kluczowymi nie jest bez znaczenia. W niniejszej pracy, połączyliśmy metodologie sieci Bayesa i analizy drzewa zdarzeń/ błędów aby opisać za pomocą pojęcia prawdopodobieństwa warunkowego, zależności czasowe w systemach o zadaniach okresowych, a następnie rozwinęliśmy tę metodę, wykorzystując dynamiczne sieci Bayesa, które pozwalają na analizę bardziej złożonych zależności czasowych, takich jak zależności funkcjonalne i związane z użyciem części zamiennych. W końcowej części pracy przedstawiliśmy dwa szczegółowe przykłady zastosowania proponowanej metody do analizy złożonych zależności czasowych w drzewach zdarzeń.

Słowa kluczowe: *zależność czasowa, sieć bayesowska, drzewo błędów, system o zadaniach okresowych, niezawodność, analiza ryzyka.*

1. Introduction

Among several techniques available to model sequence and quantify the failure probability in probabilistic risk assessment (PRA), event trees (ETs) are the most recognized methods that develop logical relationship among the events leading to the possible consequences, while fault trees (FTs) best represent the logic corresponding to pivotal events (PEs) and estimate the probabilities [16].

Dependencies in event tree/ fault tree (E/FT) model are frequently encountered, and, if neglected, may result in an error estimation. Hosseini and Takahashi [4] classify dependencies into two categories—implicit and explicit. Explicit dependencies are due to shared basic events (SBEs) such as shared utilities or shared components which appear in more than one corresponding FTs, while the expression of implicit dependencies is a bit vague. Nývlt and Rausand [13] expanded the before-mentioned division to cover more types of dependencies such as common cause failures and cascading effect, and further classified the explicit dependencies with static and dynamic behaviour. Many of the classical methods, such as Binary Decision Diagram (BDD) [1], Markov Chain (MC) [23] and Petri net [13] have been exploited and developed, in order to deal with different kinds of dependencies in E/FT analysis.

However, in practice of aerospace PRA, such as lunar exploration which has the characteristics of the phased-mission system (PMS), ETs are typically used to portray progressions of phase mission over time, and the time interval between pivotal events (PEs) is not negligible, dependencies therefore become phase-dependency (as a subset of time-dependency in this context), and make the E/FT based reliability and risk analysis more difficult [1, 13].

In ET analysis, not so much work has been done with time-dependency analysis, and the papers cited above are mainly based on the hypothesis about static or time-independent behaviour [1, 4, 13, 23]. PMS reliability attracts substantial attentions, and various techniques have been developed to deal with the phase-dependency. The analytical techniques for the PMS can be classified into two categories: combinatorial models (e.g., mini-components, sum of disjoint phase products, BDD) and state-space transition models (e.g., Markov models, Petri nets) [19, 21]. The combinatorial method is based on the

static PMS, whose assumption is that all the states of all the system components are s-independent. Esary and Ziehams [3] used a set of independent mini-components to replace the component in each phase to deal with the phase-dependency. Over the past decade, researchers have proposed a new algorithms based on BDD for fault tree analysis of PMS by incorporating phase algebra into the generation and traversal of the BDD to deal with phase-dependency [17, 21, 24]. The other method solves the dependency across the phases using state-based approaches, which are flexible and powerful in modelling complex dynamic systems [12, 15].

The above PMS reliability theory is gradually perfecting, but there are still some inadequacies in its application. For the BDD-based fault tree analysis of PMS, the ordering of variables is critical, and, it is not capable of treating other kinds of dependencies of system dynamic behaviour [22]. For MC-based method, it is unreasonable to construct a single Markov model due to the obvious disadvantage that the size would face a state-space explosion problem when modelling large-scale systems [17].

To address the above-mentioned problems, this paper proposes a recently developed methodology based on Bayesian networks (BN). The whole ET with all related FTs is mapped into BNs, and all the FTs resulted BNs are combined by connecting the nodes that represent the same component but belong to different PEs. Thus, the purpose is to demonstrate an alternative perspective on the problem of complex time-dependencies and offer a basis for safety and reliability analysis of PMS.

This paper consists of 5 sections. In the rest sections, we first discuss the dependencies by a demonstrative E/FT model of PMS in Section 2. Section 3 introduces our BN-based approach for E/FT time-dependency analysis. Section 4 describes two examples to demonstrate our proposed approach. Section 5 concludes the paper.

2. Problem statement: time-dependencies in PMS-E/FT model

PMS is subject to multiple, consecutive and non-overlapping phases (time periods) of operation, in which the system configuration, success criteria and component behaviour may vary from phase to phase[19]. To demonstrate the complex dependencies in E/FT model when performing PMS reliability and risk analysis, a simple E/FT model with *n* phases is discussed as shown in Fig. 1. There are three PEs (means ternate consecutive phases) represented by three fault trees FT_{i-1}, FT_i and FT_{i+1} respectively. Because some basic events (e.g. "*C*") occur in more than one FT, there is an explicit dependency between PEs.

A problem related to solving explicit dependencies is that the behaviour such as time-independency and time-dependency should be distinguished. The former is a behaviour assumed in most of the papers within a basic assumption is the occurrence/ nonoccurrence of the SBE is the same in every associated FT [1, 4, 13, 23], which means that $C \cdot \overline{C}$ and $\overline{C} \cdot C$ are always impossible to occur and should be neglected.

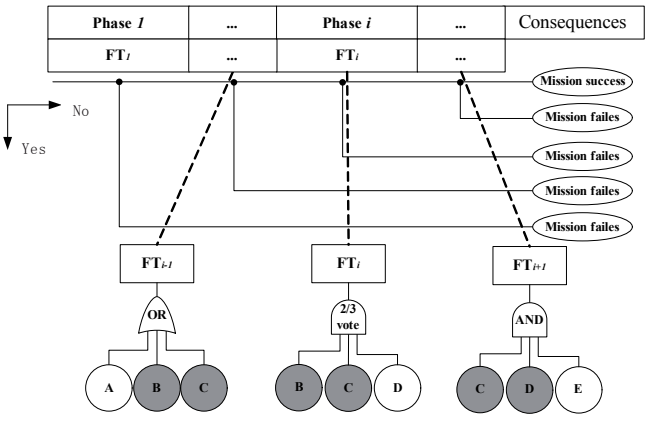

Fig. 1. E/FT synthetical *model of phased-mission system*

However, it is not realistic especially when E/FT are typically used to portray the phases' evolvation over time. The time and the order of events are critical for the occurrence or not of consequences. The sequences such as $C \cdot \overline{C}$ and $\overline{C} \cdot C$ always occur in these situations as follow:

(1) When an event tree has been done regarding PMS such as space exploration, the component "*C*" may work in the previous phase, but fail in the subsequent phase. Therefore, the sequence $C \cdot \overline{C}$ should be taken into account.

(2) If components are repairable, they can be repaired once the failure occurs during test or work. It means that the sequence $\overline{C} \cdot C$ comes true and should be taken into account.

This dynamic behaviour is closer to reality, but it is also more complicated to model, and the painful aspect is that the basic event probability may change with time. The BDD-based method and state-based method use phase algebra and time dependent rate respectively to deal with the dependency across phases. However, these methods have to confront various degrees of problem with the increase of phases number. In the next section, we will introduce a new approach based on Bayesian networks to model the PMS, and show how to use conditional probability to give expression of the phase-dependency, and further expand the model by the dynamic Bayesian networks (DBN) to cope with more complex time-dependency.

3. Method Description: Modelling time-dependencies in E/FT

3.1. Introduction of BN and DBN

A BN is a graphical inference technique and it's defined by two components: qualitative structure and quantitative parameters. The qualitative part is a directed acyclic graph comprised of nodes and arcs in which the nodes represent Random Variables (RVs) and the arcs symbolize dependencies or cause effect relationships among the RVs. The quantitative part is the conditional probabilistic table (CPT), which presents the quantitative relations between each node and its parents [25].

Benefiting from the modelling advantages, BN is a powerful tool for global systems estimation and can better address some aspects such as multi-state, failures' dependencies, coverage factors, etc. [9], and the unique bidirectional inference mechanism which can be used either to predict the probability or to update the probability of known variables as well as diagnostic [8]. In recent years, BNs have become popular as a robust alternative to most classical methods such as FT [2, 5], ET [10], Bow-tie(BT) [6] etc. In order to represent temporal dependencies, the time-dependency of some random variables that follows a Markov process can be integrated into a dynamic BN. Montani et al.[11] developed the RADYBAN software for converting dynamic FT into a 2-time-slice dynamic BN. Their work was further developed by Portinale et al. [14], enabling the modelling of repair systems by introducing the repair box gate. Weber et al. [20] gave an exhaustive review of BN application and showed its obvious superiority over classical methods in terms of modelling and analysis capabilities. However, details of proposed combination of E/FT with BN for the PMS reliability and risk analysis are not given.

3.2. Translating E/FT to a single BN

3.2.1. Translating PMS-ET into PMS-BN

In practice of a simple PMS, ET is used to model the mission using ordinal linked phase-PEs with a single entry point. Since the system mission will fail if any phase fails, the success of the current mission is conditioned on that of the previous mission and the system survival of current individual phase supporting subsystem (IPSS), which is always represented by a corresponding FT in E/FT model. The logical relationships of the overall mission success criteria are easily presented by the conditional probability as shown in Eq.(1).

$$\begin{aligned} &P(PMS(i)=0 \mid PMS(i-1)=0, IPSS(i)=0)=1 \\ &P(PMS(i)=0 \mid else)=0 \end{aligned} \tag{1}$$

Where, PMS_i and $IPSS_i$ respectively symbolize the state of *i'th* PMS and IPSS. The number 0 represents the success, and number 1 represents the failure. Different from the mapping rules of ET according to [10], the PMS-ET is translated into corresponding BN as shown in Fig. 2.

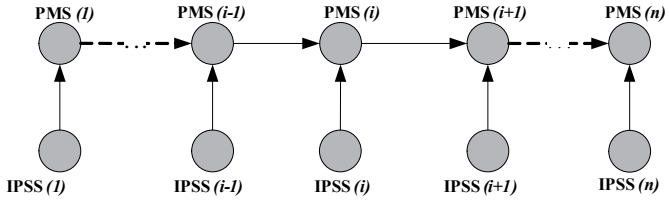

Fig. 2. A Bayesian network representing the Event Tree

3.2.2. Translating FT into corresponding BN

The IPSS is modelled by the corresponding FT, and Fig. 3 illustrates a simplified process of FT 2/3vote gate being converted to the BN, the primary events, intermediate events, and the top event of FT are represented as IPSS node, intermediate node, and leaf node in the corresponding BN, and the CPTs of the IPSS nodes is developed according to the type of logic gate. More basic gates mapping cases and mapping rules can be seen in the work of Bobbio et.al. [2] and Khakzad et.al. [5].

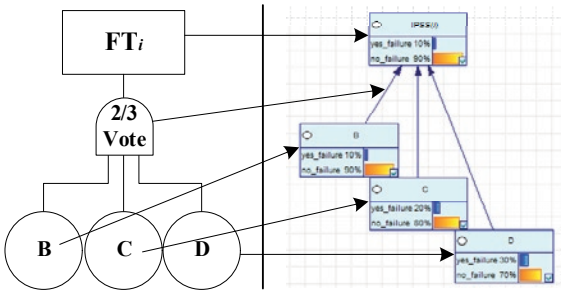

Fig. 3. The 2/3vote-gate converted to BN represented by GeNIe

3.2.3. Incorporating BN

After the equivalent the corresponding BNs of the FTs are developed, they are added into Fig. 2 to construct an integrated BN model via the following two steps: first, incorporate IPSS nodes in Fig.2 with corresponding nodes of the phase-FTs top events; second, add the direct arc to connect the SBE-nodes that represent the same components but belong to different IPSS-BNs.

A three-level hierarchical PMS-BN model which can be equivalent to the PMS-E/FT in Fig.1 is developed and illustrated in Fig.4.

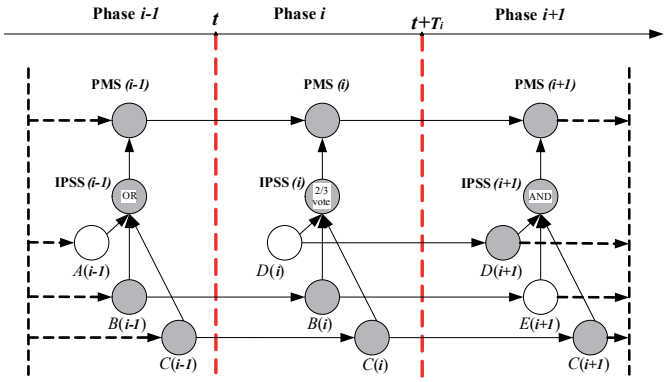

Fig. 4. BN of Fig. 1 representing the PMS-E/FT with phase-dependent

The three levels respectively represent the entire mission states, the reliability of IPSS and the component states. The phase-dependency is defined by the connection of the nodes in the first level and shared nodes of adjacent phases in the third level. The CPTs of the basic events nodes can be computed as follows.

The basic event "C" is taken as as a example and supposed to have functioned in all the previous phases. According to the total probability law, the failure function of "C" in the end of phase i is given by

$$P(C_i=1)=\sum_{j=0,1} P(C_{i-1}=j)P(C_i=1 \mid C_{i-1}=j) \tag{2}$$

Where, C_{i-1} and C_i respectively symbolize the random states of "*C*" at the end of *i-1'th* and *i'th* phase, and *j* denotes the states of the component. Considering the component is non-repairable, once "*C*" fails in phase *i-1*, it will maintain its status in phase *i*, which means

$$P(C_i=1 \mid C_{i-1}=1)=1 \tag{3}$$

$$P(C_i=0 \mid C_{i-1}=1)=0 \tag{4}$$

Substituting Eq.(3) and (4) into (2), thus,

$$P(C_i=1 \mid C_{i-1}=0)=\frac{P(C_i=1)-P(C_{i-1}=1)}{P(C_{i-1}=0)}=\frac{\int_t^{t+T_i} f_{C_i}(\tau)d\tau}{1-\int_{t-T_{i-1}}^{t} f_{C_i}(\tau)d\tau}=F_{C_i} \tag{5}$$

$$P(C_i=0 \mid C_{i-1}=0)=\frac{P(C_i=0)}{P(C_{i-1}=0)}=\frac{1-\int_t^{t+T_i} f(\tau)d\tau}{1-\int_{t-T_{i-1}}^{t} f(\tau)d\tau}=1-F_{C_i} \tag{6}$$

Where, $f_{C_i}(t)$ is the failure density function of *"C"* in the phase *i*; T_i is the duration of phase *i*; F_{C_i} presents the component cumulative failure probabilities at the end of phase *i*, which equals to the conditional failure probability of mini-component given by [3, 24].

If the failure rate of *"C"* is exponentially distributed, Eq. (5) and (6) can be calculated as:

$$P(C_i=1 \mid C_{i-1}=0)=1-e^{-\lambda(T_i)} \tag{7}$$

$$P(C_i=0 \mid C_{i-1}=0)=e^{-\lambda(T_i)} \tag{8}$$

3.3. Extending more complex time dependencies by dynamic BN

If the IPSS exhibits dynamic interactions between components and is modelled by a dynamic fault tree (DFT), it makes the PMS analysis more complex. In this section, we introduce the DBN with further expansion to consider more complex time-dependency.

3.3.1. Translating DFT into corresponding DBN

Dynamic BN extend the BN formalism by providing an explicit discrete temporal dimension. Fig. 5 illustrates a DFT functional dependency (FDEP) gate converted to the IPSS-DBN, the CPTs of the IPSS node is developed according to the type of gate. More basic dynamic gates mapping cases and mapping rules can be seen in the work of Montani et.al. [11].

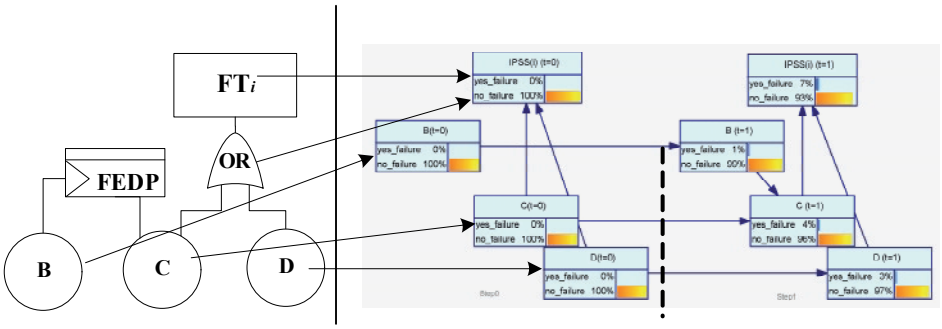

Fig. 5. The FEDP–gate converted to DBN represented by GeNIe

3.3.2. Incorporating DBN

The adjacent phases (e.g. phase *i-1* and phase *i*) are two consecutive and non-overlapping phases, therefore the initial probability in phase i should be equal to the end probability in phase *i-1* for each state. The PMS time line is partitioned into a finite number of time instants (e.g. t-1, t, t+1), and, the *n* mission phases can be treated as $\sum N_i (i = 1,2,...n)$ smaller phases. The difference is that identical BN structures are generated for each time instantly during an individual phase merely, while different BN structureS occur across the phase. The PMS-DBN model which can be equivalent to the PMS-E/FT in Fig. 1 is developed and illustrated in Fig. 6.

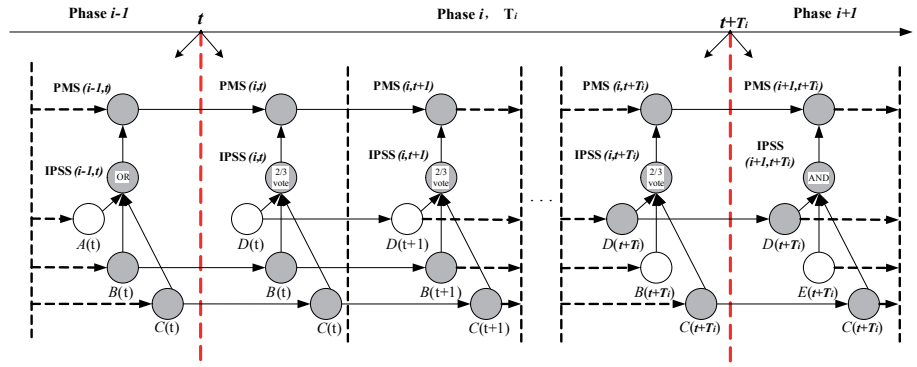

Fig. 6. DBN of Fig. 1 show the PMS-E/FT with time-dependent behaviour

The relationships between basic events in an individual phase at successive time steps are represented by inter-slice arcs, $C_i(t) \to C_i(t + \Delta t)$, and the relationships of SBEs between adjacent phases are represent by cross-phase arcs, $C_{i-1}(t) \to C_i(t)$. The same procedure in section 3.2.3 may be easily adapted to obtain the CPTs in PMS-DBN model, as shown in Table 1.

Table1. Conditional probability table for node "C"

$P\{C_i(t) \mid C_{i-1}(t)\}$		$C_{i-1}(t)$	
		0	1
$C_i(t)$	0	1	0
	1	0	1
$P\{C_i(t+1) \mid C_i(t)\}$		$C_i(t)$	
		0	1
$C_i(t+1)$	0	$e^{-\lambda\Delta t}$	0
	1	$1-e^{-\lambda\Delta t}$	1

3.4. Algorithm summary

Based on the above discussion, we depict our approach of combination of E/FT with BN for modelling and analysing the time-dependency with a 5-step procedure as follows:

1) Build the E/FT or E/DFT model to express the PMS for reliability or risk analysis.
2) Transform ET into the BN mainly based on the work of section 3.2.1.
3) Transform FT/DFT into the corresponding BN/DBN according the work of section 3.2.1 and 3.3.1.
4) Incorporate IPSS nodes with the top nodes of corresponding BN, and add the direct arc to connect the shared nodes of adjacent phases that represent the phase-dependency, and The CPTs between two time slices are subsequently established.
5) Finally, the whole BNs are equally able to analyse the reliability and safety of the PMS system based on the mature reasoning arithmetic of commercial software.

4. Method application

4.1. Case 1: A simple static PMS

In this section, we apply our approach to a simple example with 2 phases and 3 components (A, B, C), and the E/FT model of system configurations in two phases are shown in Fig. 7. The system parameters are given in table2.

Fig.8 is the PMS-BN model of the example system shown in Fig.7 using GeNIe 2.0 (http://genie.sis.pitt.edu), then the nodes conditional probabilities can be calculated using Eq. (1)~(8). The whole PMS reliability is 0.775584, which is consistent with that using of the BDD-based method according to the reference[18].

4.2. Case 2: Auxiliary Power Unit (APU)

4.2.1. Example description and preliminary analysis

The APU as a safety-critical system is used to generate power to drive hydraulic pumps that produce pressure for the orbiter's hydraulic system [22]. The orbiter is equipped with three hydraulic systems to supply redundant power to all hydraulically driven components. Each

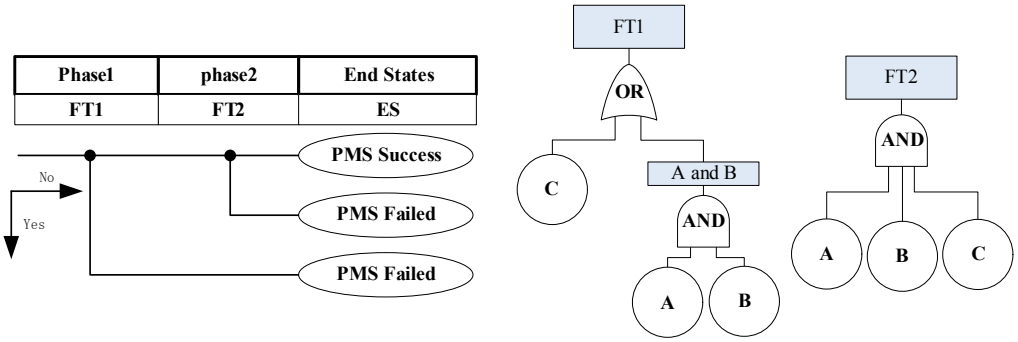

Fig. 7. A simple PMS-E/FT model

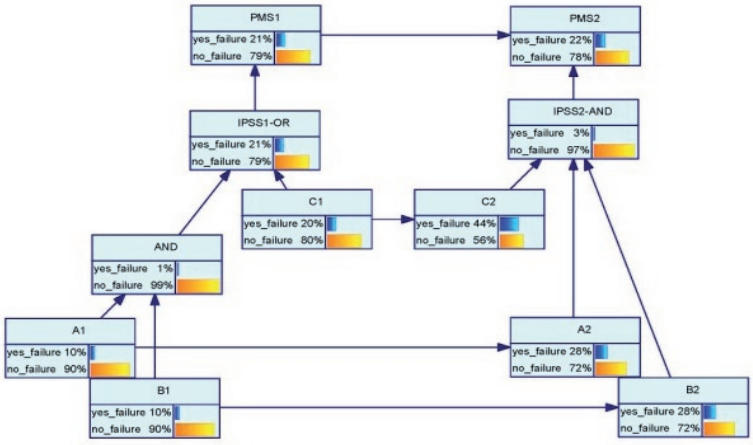

Fig. 8. BN of the PMS-E/FT shown in Fig. 7 by GeNIe

Table 2. Component failure probabilityes in each phase

Component probability	A	B	C
phase1	0.1	0.1	0.2
phase2	0.2	0.2	0.3

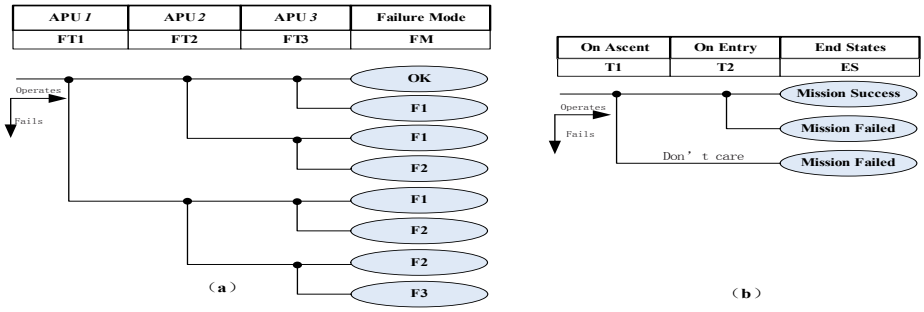

Fig. 9. Scenario model of APU by Two event trees

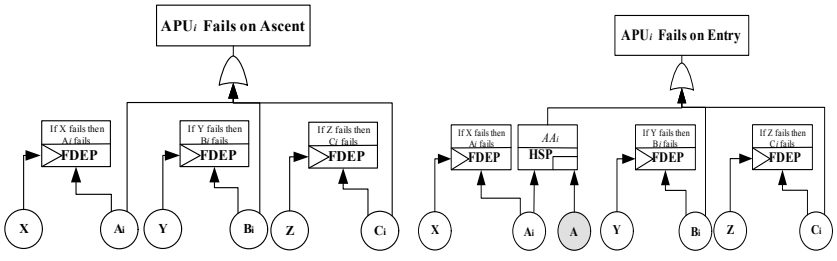

(a) On Ascent (b) On Entry

Fig. 10. DFTs of APUi in two phases

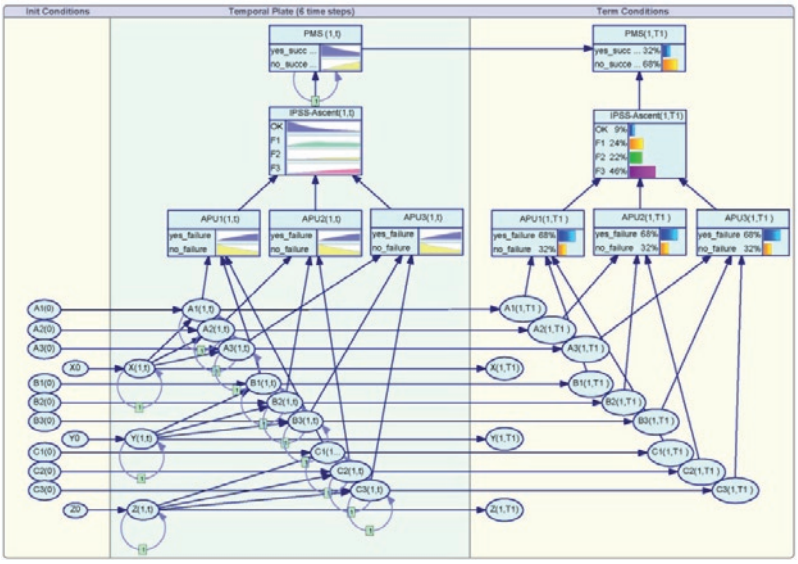

(a). On Ascent phase

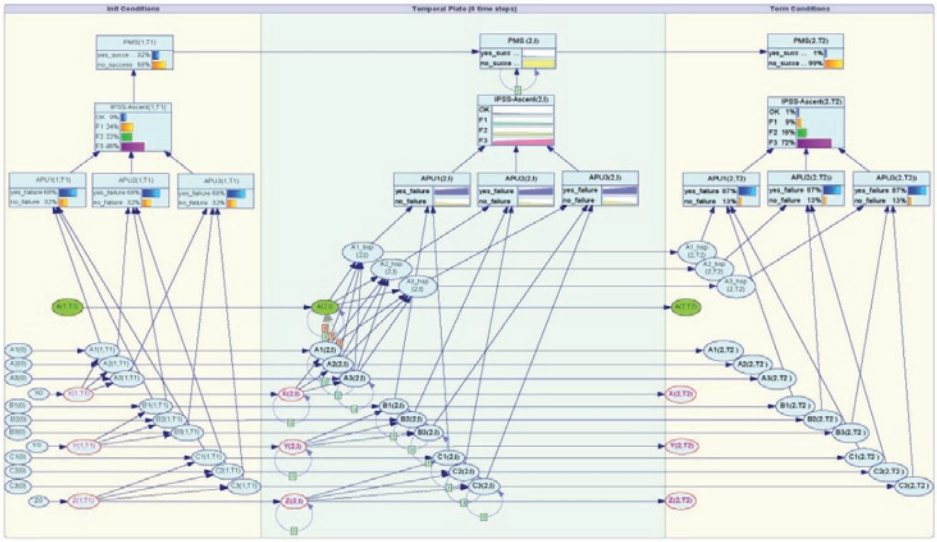

(b). On Entry phase

Fig. 11. DBN for both phases of APU using GeNIe

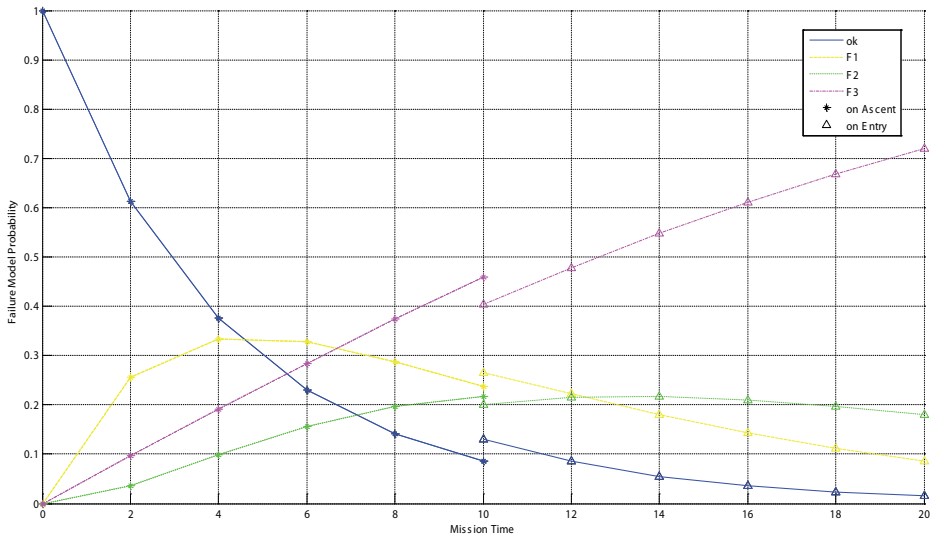

Fig. 12. The failure mode probability of APU system for both phases vs. mission time

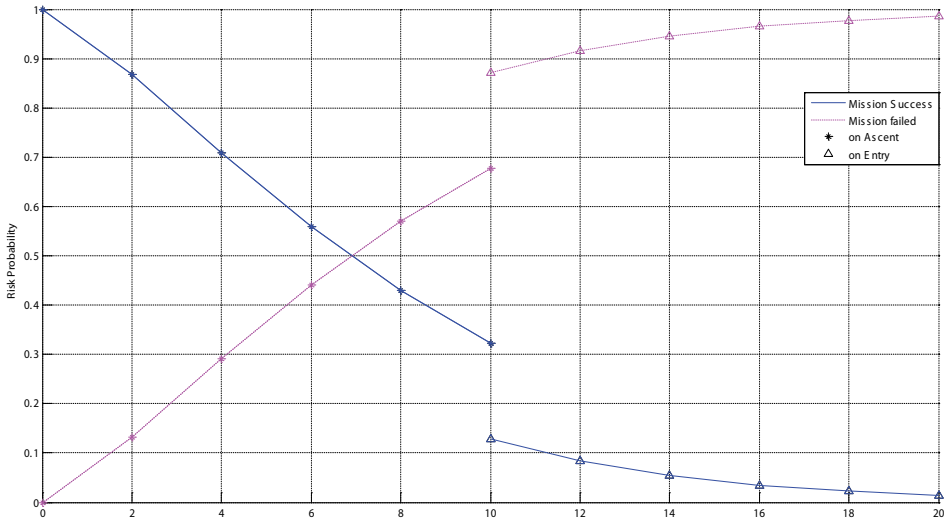

Fig. 13. The risk probability of mission for both phases vs. mission time

system is divided into three subsystems. Since the APU is to serve as an integrating platform for the other two subsystems, the single hydraulic system can be modeled as an APU for ease of presentation.

The system failure mode criteria is defined as such that (1) no loss of any APU unit is regarded as mode OK, (2) loss of any single APU is considered as failure mode Fl, (3) loss of any two APUs is failure mode F2, and the worst case (4) loss of all three APUs is failure mode F3. Such accident scenario can be modelled using an ET, as shown in Fig. 9(a).

In this case study, the mission of APU system was simplified into two phases for operation: on Ascent and on Entry. The difference between these two phases is that the APU control spare, denoted by "A", is only available during the entry phase. Fig. 9(b) and Fig. 10 give the scenario model of APU launch mission by ET and DFTs in two phases for a better comparison. Symbols in the Fig. 10 are explained in [22].

The following assumptions are made for this example.

(1) The time of failure of all components is exponentially distributed. The failure rates of all given basic events and the mission duration of both phases are represented in [22].
(2) All components are non-repairable. Once a component fails, it will maintain its status for the remainder of the mission.

Based on the above-mentioned presentation, the combining E/DFTs are presented along with application to the APU system including multi-type dependencies (Shared APUi, external common cause failure modelled by FDEP gate, hot spare, and phase-dependency).

4.2.2. Construction of PMS-DBN

In the first phase, APU system can be treated as a single system, and the DBN model of ascent phase is easily constructed as shown in Fig. 11(a). In the second phase, because phase 1 and phase 2 are consecutive and non-overlapped, the end net (as seen in right hand of Fig.11 (a)) in phase 1 at time T1 is the initial conditions of the phase 2 at time T1, and the initial probabilities in phase 2 at time T1 are equal to the end probabilities in phase 1 for each state. The PMS temporal behaviour in phase 2 is the same as phase 1 other than the APU control spare, denoted by "A", activated in phase2. Finally we obtain the established model of DBN using GeNIe, as seen in Fig. 11 (b).

4.2.3. Quantitative analysis results

Based on the exact reasoning algorithm of the GeNIe software platform, the complete failure probability during the mission time with all the four failure modes can be calculated as shown in Fig.12.

Fig. 12 presents that the failure mode curves in the conversion time of first phase and second phase are jumping, and the probabilities of mode OK and mode F1 increase in different degrees. Therefore,

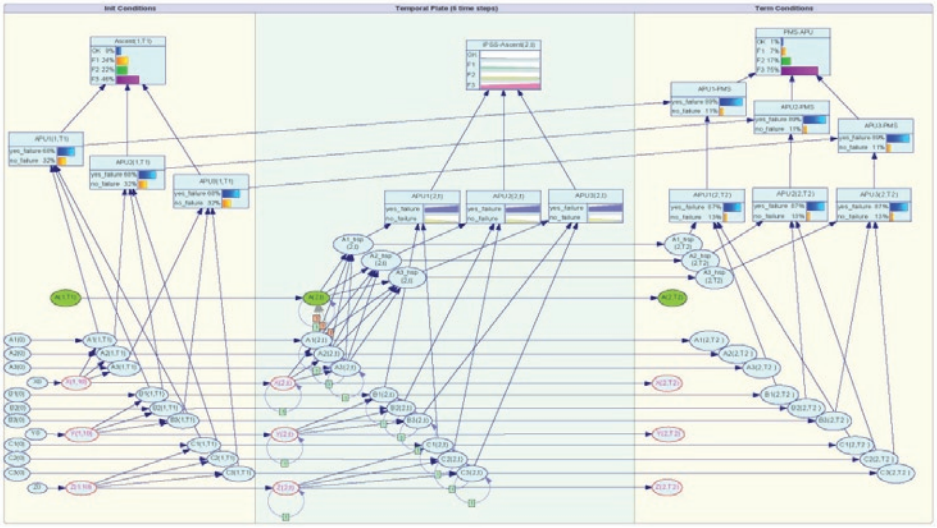

Fig. 14. Modified DBN to account four outcome modes using GeNIe

the redundancy of "A" can reduce the failure probability greatly to improve the system reliability.

To assess the risk of catastrophic failure in the mission, we define the mission success criteria as follow: (1) On Ascent: mode OK and failure mode F_1 are considered as success, and failure mode F_2 and F_3 are considered as failure; (2) On Entry: mode OK is considered as mission success, and once any APU fails, lunch mission will fail.

Fig. 13 is the risk curve of mission loss, because the second mission success criterion is more rigorous than the previous phase, there is a remarkable jump in the conversion time of the first and second phase. Considering different configuration and mission phase success criteria, it is observed that DBN produces a more explicit measure of the system reliability and risk level over time.

4.2.4. Validation of the method

Xu and Dugan[22] introduced MC-based E/DFT for APU reliability analysis, and proposed a modularization method to improve efficiency due to the problem of building a single MC for the whole system. Results of four ET outcome mode probabilities obtained from the Xu and Dugan's work are shown in column 2 of Table 3.

Compared to the MC model, the modified DBN to account four outcome modes is easily constructed by adding several nodes and corresponding arcs to obtain different combinations of APUi status (as shown in Fig. 14), and all the outcome mode probabilities are given in column 3 of Table 3.

Table 3. Probabilities comparison of outcome modes under DBN and MC

Outcome Mode	MC results	DBN results	error
OK	0.01056	0.01072	1.52%
F_1	0.06858	0.07118	3.80%
F_2	0.16517	0.16876	2.17%
F_3	0.75569	0.74934	0.84%

This result shows that small percentage errors exist between DBN-based method and MC-based method even in this complex system, besides that, DBN can construct a more integrative system scenarios model relative to Markov method.

5. Conclusion

This study has presented a new method to analyze time-dependencies in E/FT model when performing PMS reliability and risk analysis by using Bayesian networks. Various types of dependencies especially time-dependency in event trees are discussed. The proposed method shows how to use conditional probability to give expression of the phase-dependency, and further expands by the dynamic BN to cope with more complex time-dependency. The results obtained from a real auxiliary power unit system have shown this method's engineering applicability on large and complex engineering systems.

The advantage of the BN-based approach is that it is easy to understand and use in practice owe to the flexible modeling ability and mature inference algorithm of Bayesian networks. And yet for all that, it is just the beginning of our work. One challenge is related to the unnecessarily large networks due to the DBN repeating the same structure for each time instance, but may find its solution within the any time horizon of 2-time-slice BN structures. Future works may be devoted to extensions of the proposed approach, such as modeling the units with the reparable function, and more complex mission success logical relationships, so that the model can be closer to the reality of the system.

References

1. Andrews J, Dunnett SJ. Event-tree analysis using binary decision diagrams. IEEE Transactions on Reliability 2000; 49(2): 230–238, http://dx.doi.org/10.1109/24.877343.
2. Bobbio A, Portinale L, Minichino M, Ciancamerla E. Improving the analysis of dependable systems by mapping FTs into Bayesian networks. Journal of Reliability Engineering and System Safety2001; 71: 249–260, http://dx.doi.org/10.1016/S0951-8320(00)00077-6.
3. Esary JD, Ziehms H. Reliability analysis of phased missions. In: Barlow RE, Fussell JB, Singpurwalla ND, editors. Reliability and fault tree analysis: theoretical and applied aspects of system reliability and safety assessment. Philadelphia, PA: SIAM; 1975: 213–236.
4. Hadi Hosseini, SM, Takahashi M. Combining Static/Dynamic Fault Trees and Event Trees Using Bayesian Networks. SAFECOMP; 2007: 93–99.
5. Khakzad N, Khan F, Amyotte P. Safety analysis in process facilities: Comparison of fault tree and Bayesian network approaches. Reliability Engineering and System Safety2011; 96: 925-932, http://dx.doi.org/10.1016/j.ress.2011.03.012.
6. Khakzad N, Khan F, Amyotte P. Dynamic safety analysis of process systems by mapping bow-tie into Bayesian network. Process Safety and Environmental Protection 2013; 91:46–53, http://dx.doi.org/10.1016/j.psep.2012.01.005.
7. Kim K, Park KS. Phased-mission system reliability under Markov environment. IEEE Transactions on Reliability1994, 43(2): 301-309, http://dx.doi.org/10.1109/24.295013.
8. Lampis M, Andrews D. Bayesian belief networks for system fault diagnostics. International Journal of Quality and Reliability Engineering 2009; 25: 409–426, http://dx.doi.org/10.1002/qre.978.
9. Langseth H, Portinale L. Bayesian networks in reliability. Reliability Engineering and System Safety2007; 92(1):92-108, http://dx.doi.org/10.1016/j.ress.2005.11.037.
10. Marsh DWR, Bearfield G. Generalizing event trees using Bayesian networks. Proceedings of the Institution of Mechanical Engineers, Part O: Journal of Risk and Reliability2008; 222: 105-114, http://dx.doi.org/10.1243/1748006XJRR131.
11. Montani S, Portinale L, Bobbio A, Codetta-Raiteri D. RADYBAN: a tool for reliability analysis of dynamic FTs through conversion into dynamic Bayesian networks. Reliability Engineering and System Safety2008;93:922-932, http://dx.doi.org/10.1016/j.ress.2007.03.013.
12. Mura I, Bondavalli A. Markov regenerative stochastic Petri nets to model and evaluate phased mission systems dependability. IEEE Transactions on Computers2001; 50(12): 1337–1351, http://dx.doi.org/10.1109/TC.2001.970572.
13. Nývlt O, Rausand M. Dependencies in event trees analyzed by Petri nets. Reliability Engineering and System Safety2012;104: 45–47, http://dx.doi.org/10.1016/j.ress.2012.03.013.

14. Portinale L, Raiteri DC, Montani S. Supporting reliability engineers in exploiting the power of dynamic Bayesian networks. International Journal of Approximate Reasoning2010; 51: 179-195, http://dx.doi.org/10.1016/j.ijar.2009.05.009.
15. Dugan JB. Automated Analysis of Phased-Mission Reliability. IEEE Transaction on Reliability1991; 10(1): 45-53, http://dx.doi.org/10.1109/24.75332.
16. Stamatelatos M. Probabilistic Risk Assessment Procedures Guide for NASA Managers and Practitioners. Technical report. US NASA, Office of Safety and Mission Assurance, NASA Headquarters, Washington, DC; 2011. NASA/SP-2011-3421.
17. Tang ZH, Dugan JB. BDD-Based Reliability Analysis of Phased-Mission Systems With Multimode Failures. IEEE transactions on Reliability2006; 55(2): 350-360, http://dx.doi.org/10.1109/TR.2006.874941.
18. Tang ZH, Xu H, Dugan JB. Reliability Analysis of Phased Mission Systems with Common Cause Failures. In: Reliability and Maintainability Symposium, 2005 annual symposium-RAMS; 2005: 313–318.
19. Wang CN, Xing LD, Levitin G. Competing failure analysis in phased-mission systems with functional dependence in one of phases. Reliability Engineering and System Safety2012; 108 : 90-99, http://dx.doi.org/10.1016/j.ress.2012.07.004.
20. Weber P, Medina-Oliva G, Simon C, Iung B. Overview on Bayesian networks applications for dependability, risk analysis and maintenance areas. Engineering Applications of Artificial Intelligence2012; 25: 671-682, http://dx.doi.org/10.1016/j.engappai.2010.06.002.
21. Xing LD, Levitin G. BDD-based reliability evaluation of phased-mission systems with internal/external common-cause failures. Reliability Engineering and System Safety 2013; 112: 145–153, http://dx.doi.org/10.1016/j.ress.2012.12.003.
22. Xu H. Dynamic event fault tree(DEFT): a methodology for probabilistic risk assessment of computer-based systems. Ph.D. Dissertation. Charlottesville: University of Virginia, 2008
23. Xu H, Dugan JB. Combining dynamic fault trees and event trees for probabilistic risk assessment. In: Reliability and Maintainability Symposium, 2004 annual symposium-RAMS; 2004: 214–219.
24. Zang XY, Sun HR, Trivedi KS. A BDD-Based Algorithm for Reliability Analysis of Phased-Mission Systems. IEEE Transactions on Reliability1999; 48(1): 50–60, http://dx.doi.org/10.1109/24.765927.
25. Zhang LW, Guo HP. Introduction to Bayesian networks [M]. Beijing: Science Press, 2006.

Xiao-Tao LI
Li-min TAO
Mu JIA
Laboratory of Science and Technology on Integrated Logistics Support
School of Mechatronics Engineering and Automation
National University of Defense Technology
De Ya Road., 109, Changsha, Hunan 410073, P. R. China

E-mails: lixt8866@163.com, tlm1964@sina.com, jiamufight@126.com,

Article citation info:
GILL A, KADZIŃSKI A. The determination procedure of the onset of the object wear-out period based on monitoring of the empirical failure intensity function. Eksploatacja i Niezawodnosc – Maintenance and Reliability 2015; 17 (2): 282–287, http://dx.doi.org/10.17531/ein.2015.2.16.

Adrian GILL
Adam KADZIŃSKI

THE DETERMINATION PROCEDURE OF THE ONSET OF THE OBJECT WEAR-OUT PERIOD BASED ON MONITORING OF THE EMPIRICAL FAILURE INTENSITY FUNCTION

PROCEDURA WYZNACZANIA POCZĄTKU STARZENIA SIĘ OBIEKTÓW NA PODSTAWIE MONITOROWANIA EMPIRYCZNEJ FUNKCJI INTENSYWNOŚCI USZKODZEŃ*

The estimation of the number of failures of technical objects is of key importance throughout the object life cycle, particularly in the wear-out period when the number of failures begins to grow significantly. In the literature related to this problem, examples exist of solutions (mathematical models) that can assist the estimation of the number of failures. For the description of the life cycles of objects, functions are usually used of known forms of probability distribution of the number of object failures. The procedure presented in this paper assumes the use of statistical data related to the failures of uniform population of nonrenewable technical objects, recorded in the form of empirical function of failure intensity. It specifically serves the purpose of determining the characteristic point of life of these objects i.e. the onset of the wear-out period. Within the procedure, a model of fuzzy inference has been applied that reflects the human reasoning (expert of the system) observing/investigating the objects. The results of the developed procedure may constitute a basis for forecasting of failures of mechanical nonrenewable technical objects.

***Keywords**: failure intensity function, aging, nonrenewable objects, failure forecasting.*

Oszacowanie liczby uszkodzeń obiektów technicznych ma kluczowe znaczenie we wszystkich okresach cyklu życia obiektów, szczególnie w okresie uszkodzeń starzeniowych, kiedy to liczba uszkodzeń zaczyna znacząco rosnąć. W bibliografii tego zagadnienia przytoczone są przykłady rozwiązań (modeli matematycznych), którymi można wspomagać m.in. szacowanie liczby uszkodzeń. Do opisu cyklu życia obiektów technicznych wykorzystuje się zwykle funkcje o znanych postaciach rozkładów prawdopodobieństwa liczb uszkodzeń tych obiektów. Przedstawiona w niniejszym artykule procedura, zakłada korzystanie ze statystycznych danych o uszkodzeniach jednorodnej zbiorowości nieodnawianych obiektów technicznych, zapisanych w postaci empirycznej funkcji intensywności uszkodzeń. Służy ona w szczególności do wyznaczenia charakterystycznego punktu życia tych obiektów tj. chwili rozpoczynania się okresu uszkodzeń starzeniowych. W ramach procedury zastosowano model wnioskowania rozmytego, który odwzorowuje rozumowanie człowieka (eksperta systemu) obserwującego/badającego obiekty. Wyniki opracowanej procedury mogą stać się podstawą prognozowania uszkodzeń nieodnawianych obiektów technicznych typu mechanicznego.

***Słowa kluczowe**: funkcja intensywności uszkodzeń, starzenie, obiekty nieodnawiane, prognozowanie liczby uszkodzeń.*

1. Introduction

In all periods of the object life cycle the number of failures needs to be forecasted. It is required by the demand estimation processes related to renewable objects, the need to configure maintenance systems that allow for the number of renewals as well as object proactive behavior, the lack of which may generate unacceptable hazard.

This problem is particularly conspicuous when analyzing the wear-out period and the usually surging number of failures in that period (assuming that the investigated population is sufficiently large). Relevant literature presents mathematical models that assist the process of reaction to object failure e.g. [2, 3, 10, 12], procedures that describe and compare classes of forecast models (e.g. [4, 17]) or assist in the forecasting of failures of nonrenewable technical objects in the wear-out period (e.g. [10, 12]). In [2] a method is proposed of detecting the onset of the object wear-out period and determining the maintenance efficiency based on, as the authors of [2] would call it, a step model of aging and the Bayes techniques. In [3] a new reliability model is presented of complex repaired technical objects/systems based on the bathtub curve.

The procedure presented in this paper is dedicated to uniform nonrenewable mechanical objects. As a starting point, reference to the forecasting tool of the failure of nonrenewable technical objects was assumed. These tools were developed by one of the authors of this paper (*i.a.* [10, 11, 12]). The basis for the failure forecasting models is the estimation of the parameters of object operating time distribution until wear-out failure occurs. It was assumed that the parameters of this distribution are estimated based on statistical data related to:

- number of object failures occurring in the period between the onset of the wear-out period and the end of the observation time,
- number of objects that are forecasted to fail due to aging.

A troublesome point of the said models is the determination of the onset of the wear-out period that is necessary for the estimation of the

(*) Tekst artykułu w polskiej wersji językowej dostępny w elektronicznym wydaniu kwartalnika na stronie ***www.ein.org.pl***

parameters of the operating time distribution until failure. The significance of this issue is also supported by other authors ([1]) by mentioning the return point of the failure intensity function as useful in terms of maintenance and risk analysis related to failures. They present a certain way of solving problems basing on the modified function of Weibull distribution.

In relevant literature it is difficult to indicate formal algorithms allowing the determination of the onset of wear-out periods. Few publications in this matter pertain mainly to the attempts to find new forms of functions describing the processes of object operation [6, 9] or focus on modeling of the entire course of the function of failure intensity ([19]). A reliable solution is proposed by the authors of [2], but only for known continuous distributions. What is missing is the solution to the problem if the failure intensity function is a non-continuous characteristics and its form as a function is unknown.

The intention of the authors of this paper is to present the procedure of estimation of the onset of the wear-out period of objects based on the empirical function of failure intensity without having information on the reliability function.

2. Formal description of the procedure

2.1. Concept and main assumptions

The solution to the problem is the analysis of the data on the number of failures in subsequent periods of time of their investigation/observation and then selection of the moment when the number of failures begins to grow significantly. If information in the form of non-continuous functions is used, the top or bottom limit of a given interval group is assumed (interval in which the number of failures grows significantly and its growth continues in further intervals).

The simplest but least accurate and informal method to solve the problem is intuitive choice of the onset of the wear-out period by the researcher (expert) based on the analysis of the course of selected reliability functions. It is advantageous in the case of functions of untypical courses and allows (due to lack of other tools) a quick obtainment of a satisfactory result.

This enabled an adoption of the following concept of the procedure: a man well acquainted with the modeled system/object, i.e. system expert, may correctly indicate the onset of the wear-out period of objects even if he infers having limited (partial) information on the object failures. Such a subjective choice is usually made because of experience and knowledge about the object. From the observations conducted by the authors we know that a man who is not a system expert but has all the necessary needed information related to the time of the loss of object worthiness (data in the form of courses of functions of failure intensity) is also capable of deciding about the onset of the wear-out period.

This paper reproduces (through fuzzy inference models) the system expert's reasoning that leads to the indication of the onset of the wear-out period based on observations of the course of the empirical function of failure intensity. Literature mentions applications of elements of fuzzy inference to solve a variety of problems related to reliability of objects. For example [18] presents the application of fuzzy sets in the problem of matching curves to the reliability data, [20] describes its use in reliability analysis of elements while [7, 13] discuss the application of fuzzy inference in methods designed to determine the measures of reliability.

The concept of the procedure consists in determining moment t_p – the onset of the wear-out period of technical objects through mathematical models that reproduce (simulate) the reasoning of the system expert. The mathematical model was developed based on the following main assumptions:

– Uniform population of technical objects is analyzed,
– The number of failures of technical objects in time is known (observation time intervals) and the statistical data on the failures are stored in the form of stemplot,
– The type of probability distribution of the operating time of objects until failure is unknown,
– Fuzzy inference is possible based on the results of monitoring of the empirical value of the function of failure intensity $\lambda_N(t)$,
– The onset of the wear-out period t_p falls between moment t_{p0} of the first increase of function $\lambda_N(t)$ and moment t_k – the end of object observation,
– The failure intensity function is a constant interval non-decreasing function in the wear-out period.

2.2. General mathematical model

The structure of the inference models is formed by properly written rules of inference i.e. fuzzy implications R_k ($k = 1,2,\ldots,l$) [8, 14, 15]. These are the if-then type of rules that in a general form can be written as follows:

$$R_k: \text{If } x_{(1)} \text{ is } A_{1j} \text{ and } x_{(2)} \text{ is } A_{2j} \text{ and} \ldots \text{and } x_{(m)} \text{ is } A_{mj} \text{ then } y \text{ is } B_j \quad (1)$$

where:

$x_{(i)}$ – input variables of the inference model forming the m-dimensional input vector $\mathbf{x}$. It has been assumed that at the first stage of the calculations, variables $x_{(i)}$ assume the values of the empirical function of failure intensity of objects $\lambda(t_i)$ in subsequent i-th *intervals* (t_{i-1},t_i) *of the function monitoring* $\lambda_N(t)$ i.e. $x_{(i)} = \lambda_N(t_i)$, ($i = 1,2,\ldots, m$);

A_{ij} – ($i = 1,2,\ldots, m$; $j = 1,2,\ldots, n$) denote the linguistic values (parameters of the inference model) defined in a fuzzy manner by appropriate functions of membership $\mu_{A_{ij}}$ determined in spaces X_i. If A_{ij} is a fuzzy set in a given space X_i then value $\mu_{A_{ij}}(x_{(i)})$ will denote the degree of membership $x_{(i)} \in X_i$ in set A_{ij};

y – output variables of the inference model;

B_j – fuzzy sets of the conclusion of the inference rules.

Graphic interpretations of the assumptions and the understanding of some of the elements of the presented procedure have been shown in Figure 1.

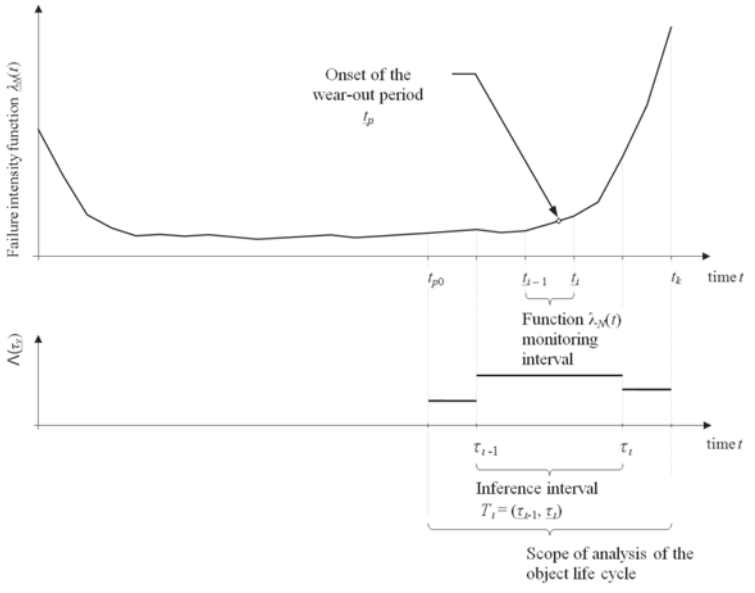

Fig. 1. Graphic interpretation of the assumptions of the determination procedure of the onset of the wear-out period based on the monitoring of the failure intensity function

In further considerations, the constructive model of inference was applied [8]. In models of this type the value of $\mu_A(\mathbf{x})$ of the function of membership related to the degree of rule activation, is interpreted in the form of a logical product of fuzzy sets. In the fuzzy sets the product operation (as well as the sum of these sets) can be performed in different ways. In the literature, many different relations for each of these operations have been presented. For a logical sum of the fuzzy sets there is a group of relations referred to as the s-norm operators and for the logical products - a group of t-norm operators. For example, to calculate the logical product of fuzzy sets a minimum (*MIN)* operator can be used – relation (2):

$$\mu_A(\mathbf{x}) = \mu_{A_{1j} \cap A_{2j} \cap \ldots \cap A_{mj}}(\mathbf{x}) = \min\{\mu_{A_{1j}}(x_{(1)}), \mu_{A_{2j}}(x_{(2)}), \ldots, \mu_{A_{mj}}(x_{(m)})\}, \quad (2)$$

The *MIN* operator has many disadvantages (as described in detail in [15]), which is why the product operator is more frequently used. The calculation of the function of membership of the product of fuzzy sets with the use of this operator is done according to the following formula:

$$\mu_A(\mathbf{x}) = \mu_{A_{1j} \cap A_{2j} \cap \ldots \cap A_{mj}}(\mathbf{x}) = \mu_{A_{1j}}(x_{(1)}) \cdot \mu_{A_{2j}}(x_{(2)}) \cdot \ldots \cdot \mu_{A_{mj}}(x_{(m)}) \quad (3)$$

It was assumed that the aggregation on the implication level is realized as an algebraic product of the degrees of membership of the fuzzy sets (relation (3)) for both the implication premise and the consequent.

The output of the inference models is made by the superposition of the outputs of individual inference rules. It consists (based on the R_k rules) in the reproduction of the realization of the input variables $x_{(i)}$ into a certain output quantity y representing moment $\hat{t}_p$.

The first step of this procedure consists in combining (for certain input data) the premises (antecedents) of the k-th fuzzy rule. We may use the operation of the product of sets – relation (2) or (3). In this way we determine ζ – degree of rule activation (activity) of the rule. Since, the inputs are non-fuzzy values the degree of rule activation ζ of each of the rules forming the database of inference rules can be determined as follows:

$$\zeta = \mu_A(\mathbf{x}). \quad (4)$$

Assuming that the database of inference rules is composed of l-th number of inference rules, another step of the procedure is the determination of the fuzzy sets C_k (k = 1, 2,…, l) derived by the k-th rule. Let sets C_k be determined in certain space y in the following way:

$$\mu_{C_k}(y) = \zeta_k \cdot \mu_{B_j}(y) \quad (5)$$

where:

ζ_k – denotes degree of rule activation (activity) of the k-th inference rule determined according to relation (4).

By performing the aggregation of sets C_k we may obtain value C for the output value y as a relation:

$$y \text{ is } C \quad (6)$$

wheras C is a fuzzy subset determined in space y.

The aggregation of fuzzy sets C_k can be performed in many ways [8, 15, 16]. For example, one may use the operation of logical sum of the fuzzy sets i.e.:

$$C = \bigcup_{k=1}^{l} C_k, \quad (7)$$

$$\mu_C(y) = \mu_{C_1 \cup C_2 \cup \ldots \cup C_l}(y) = \max[\mu_{C_1}(y), \mu_{C_2}(y), \ldots, \mu_{C_l}(y)] \quad (8)$$

2.3. Detailed mathematical model and the method algorithm

The first stage of determining of moment t_p is evaluating the input value $x_{(i)}$ of the inference models. It was assumed that this evaluation can be done by a minimum number (two) linguistic terms (w = 2). A finite set Φ of these terms takes the form:

$$\Phi = \{small, large\}. \quad (9)$$

Linguistic terms are written in the form of fuzzy sets A_j (j = 1, 2) of polygonal [8, 15] (triangular and trapezoidal) functions of membership. These sets are regular convex fuzzy sets [16] of the support limited with values a, b, c, d.

The database of inference rules, with a relatively large number of $\lambda_N(t)$ function monitoring intervals may have an excess number of rules. In order to reduce this number, it is proposed to search for moment t_p in a limited range. This is referred to as the *life cycle analysis range* (marked in Fig. 1). The range covers the period between moment t_{p0} – of the first increase of function $\lambda_N(t)$ and moment t_k – end of object observation. It was assumed that moment t_{p0} equals the onset of the monitoring interval where the first positive increment of function $\lambda_N(t)$ takes place.

In the range of analysis (t_{p0}, t_k) *four inference intervals* are then introduced $T_\iota = (\tau_{\iota-1}; \tau_\iota)$, ($\iota$ = 1, 2, 3, 4). They are created by a combination (Fig. 1) of the subsequent *monitoring intervals* (t_{i-1}; t_i) (i = 1,2,…, m). In such a case number s must be determined i.e. the number of monitoring intervals that compose a single inference interval ($\tau_{\iota-1}$; τ_ι). The preliminary number s of monitoring intervals is obtained from relation:

$$s = \text{ent}\left(\frac{t_k - t_{p0}}{4 \cdot \Delta t_{i-1,i}} + \frac{1}{2}\right), \quad (10)$$

where:

$\Delta t_{i-1,i}$ – length of the $\lambda_N(t)$ function monitoring interval.

Such a method of creating inference intervals results in a situation when, in some cases, the sum of the lengths of these intervals $\Delta\tau_{\iota-1,\iota}$ exceeds the end of the *range of life cycle analysis*. If such a situation occurs, a shortening of each of intervals T_ι is admissible by length $\Delta t_{i-1,i}$, i.e. by the length of one monitoring interval. It is also proposed that the shortening be realized starting from the last (ι = 4) of intervals T_ι. As a result of such an operation, lengths $\Delta\tau_{\iota-1,\iota}$ of intervals T_ι that will eventually be used in the inference model, may differ from one another. Number s (relation (10)) will thus be dependent on the T_ι interval number, which is further marked as $s^{(\iota)}$.

In further calculations, the values of functions $\Lambda(\tau_\iota)$ obtained according to relation (11) were assumed as input variables of the inference model:

$$\Lambda(\tau_\iota) = \frac{1}{s^{(\iota)}} \cdot \sum_{i=p0-s^{(\iota)}+S}^{p0+S-1} \lambda_n(t_i), \text{ oraz } S = \sum_{j=1}^{\iota} s^{(j)} \ (\iota = 1, 2, 3, 4), \quad (11)$$

where $p0$ is the subsequent number of interval $(t_{i-1}; t_i)$ in which the first increase of function $\lambda_N(t)$ was observed (monitoring).

Moment t_p was described with fuzzy numbers $L_{t\,w}$ related to individual inference intervals T_t. Fuzzy numbers $L_{t\,w}$ were written as follows:

$$"after\ T_t" = L_{t1} \quad \text{and} \quad "near\ T_t" = L_{t2}\,, \tag{12}$$

and expressed through appropriate fuzzy sets $B_j(y)$, $(j = 1, 2,\ldots, 8)$:

$$\underset{t=1,2,3,4}{\forall} L_{t1} \to B_j(y) \quad \text{and} \quad L_{t2} \to B_{j+1}(y)\,. \tag{13}$$

To describe fuzzy sets $B_j(y)$, $j = 1, 2,\ldots, 8$, triangular forms of the membership function were used. The sets support points (a, b, c) are within the limits of relevant monitoring intervals, which, using earlier adopted symbols, can be written as follows:

$$a = \begin{cases} t_{p0-s^{(t)}+S} & \text{dla} \quad L_{t1} \\ t_{p0-s^{(t)}+S} + \dfrac{\Delta\tau_{t-1,t}}{2} & \text{dla} \quad L_{t2} \end{cases},$$

$$b = \begin{cases} t_{p0-s^{(t)}+S} + \dfrac{\Delta\tau_{t-1,t}}{2} & \text{dla} \quad L_{t1}\,, \\ t_{p0-1+S} & \text{dla} \quad L_{t2} \end{cases} \tag{14}$$

$$c = \begin{cases} t_{p0-1+S} & \text{dla} \quad L_{t1} \\ t_{p0-1+S} + \dfrac{\Delta\tau_{t,t+1}}{2} & \text{dla} \quad L_{v2} \end{cases},$$

In the case of the fuzzy number „near T_t" = L_{12}, trapezoidal extreme function of membership was applied.

The general algorithm of the procedure in a graphical form has been shown in Figure 2.

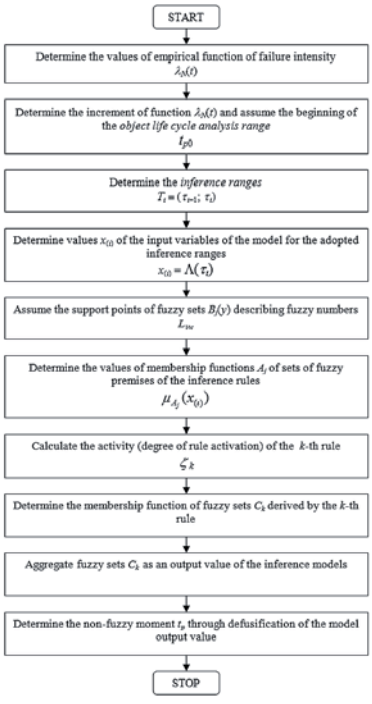

Fig. 2. General algorithm of the determination procedure of the onset of the wear-out period based on the monitoring of the failure intensity function

3. Example of procedure realization

The example of the monitoring of the course of the function of object failure intensity was performed for 100 nonrenewable railroad objects (locomotives). The objects were observed for the time corresponding to the mileage of 600.000 km. During the investigations, in the subsequent intervals $\Delta l_{i-1,i} = 50000$ km of the locomotive mileage, the number of failures was recorded. The results (number of failures and the value of the empirical function of failure intensity) have been shown in Table 1.

Table 1. Record of failure information of nonrenewable railroad objects

Interval i	Bottom interval limit t_{i-1}	Top interval limit t_i	Number of failures $n(\Delta t_{i-1,i})$	Accumulated number of failures $n_{sk}(t_i)$	Values of the empirical function of object failure intensity $\lambda_N(t_i)$
1	0	50	17	17	0.0000034
2	50	100	11	28	0.0000027
3	100	150	9	37	0.0000025
4	150	200	7	44	0.0000022
5	200	250	6	50	0.0000021
6	250	300	5	55	0.0000020
7	300	350	5	60	0.0000022
8	350	400	4	64	0.0000020
9	400	450	3	67	0.0000017
10	450	500	4	71	0.0000024
11	500	550	6	77	0.0000041
12	550	600	8	85	0.0000070

Source: based on [5]

In further part of the paper the results of the realization of selected steps of the procedure algorithm have been presented. Figure 3 shows the course of the function of object failure intensity.

In the initial stage of the calculations the life cycle analysis range is determined based on the value of function $\lambda_N(t)$. To this end, the increment of the function must be determined. Its first increase was recorded in the intervals from 300000 to 350000 km of the object operation i.e. 7th (p0 = 7) failure record interval. For this interval the increment of function $\lambda_N(t)$ was 2.22222E-07. The subsequent increments of the function were: 7.57576E-07 (for the 10th interval), 1.71369E-06 (for the 11th interval) and 2.81859E-06 (for the 12th interval). The beginning of the life cycle analysis range was thus assumed to be 300000 km.

Based on the assumed beginning of the analysis range, numbers $s^{(t)}$ of the combined intervals $(t_{i-1}:t_i)$ were determined following relation (10). Numbers $s^{(t)}$ were: $s^{(1)} = 2$, $s^{(2)} = 2$, $s^{(3)} = 1$, $s^{(4)} = 1$. The values of the input variable of the inference model $\Lambda(\tau_t)$ were also determined (relation (11)). Some of the results have been shown in Table 2.

The output value of the inference model (fuzzy onset of the wear-out period of nonrenewable railroad vehicle objects that were subjected to analysis) has been shown in figure 4 in a graphical form.

In order to determine the non-fuzzy $\hat{t}_p$, an operation of defusification of the model output value by the COA (*Center Of Area*) method was performed. The non-fuzzy onset of the wear-out period obtained according to the said procedure is 428215 km.

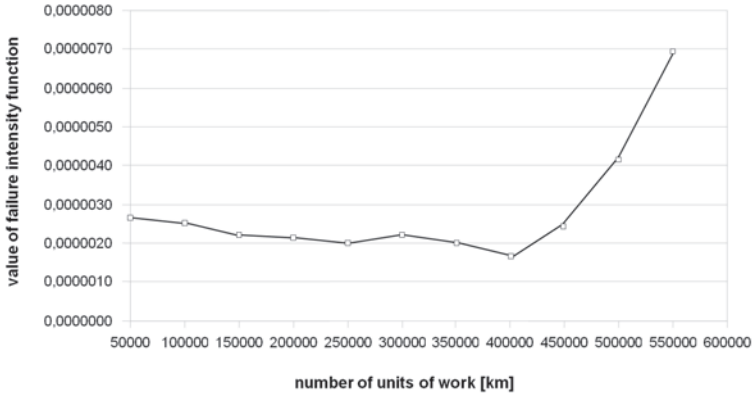

Fig. 3. Course of the function of failure intensity of example nonrenewable rail vehicles

Table 2. Values of the membership function of the fuzzy sets related to the premises of the inference rules in the example problem of determination of the onset of wear-out period of nonrenewable railroad objects

Subsequent number of the inference interval i	Bottom and top values of the inference interval $T_i = (\tau_{i-1};\tau_i)$		Values of the input variable of the inference model $\Lambda(\tau_i)$	Values of the membership function of the fuzzy sets	
	τ_{i-1}	τ_i		$\mu_{A_1}(x_{(i)})$	$\mu_{A_2}(x_{(i)})$
1	300000	400000	1.1111E-07	0.754	0.246
2	400000	500000	3.7879E-07	0.160	0.840
3	500000	550000	1.7137E-06	0.000	1.000
4	550000	600000	2.8186E-06	0.000	1.000

Source: Own findings

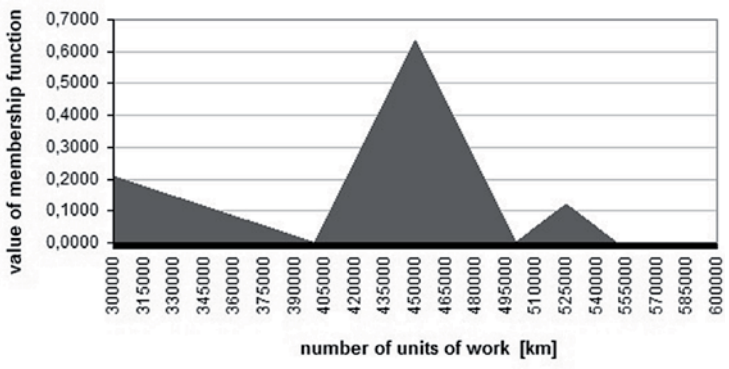

Fig. 4. Fuzzy onset of the example wear-out period of nonrenewable railroad objects

4. Conclusions

The authors attempted to present a concept of determination of the onset of the wear-out period of uniform nonrenewable technical mechanical objects. According to the analyses conducted, *inter alia,* by the authors of this paper, the determination of this moment is a major issue in forecasting of the number of failures of a variety of objects.

The presented concept of the procedure assumes the application of statistical data related to the time of object operation until failure, recorded in the form of empirical function of failure intensity. Usually, during observations/investigations, this sort of information about the failures (number of failures) is recorded in subsequent time intervals and then characteristics in the form of empirical reliability function are created.

According to the presented procedure, it is not necessary to explore the distribution of probability of the operating time until failure (and/or parameters) that characterizes the failures of the investigated objects. There is no need to use the continuous characteristics and known mathematical models reflecting the stage of wear-out period either. It has been confirmed that the determination of this moment is possible through the application of fuzzy inference model that reflects the reasoning of the human observing/investigating the objects (system expert) and does not require the information indicated herein.

The procedure has been designed to forecast failures of nonrenewable technical objects. It is particularly useful in determining the characteristics point in time of the object operation when the wear-out period begins. The presented approach constitutes a new, unique way of solving the problem. The versatility of the applied modeling originates in the possibility of utilization of the empirical equivalent of the theoretical function of failure intensity (rather than its estimation) as well as the method of fuzzy inference as input information on the observed objects. This, however, requires appropriate database of inference rules that accumulates the knowledge of the system expert.

References

1. Bebbington M, Lai Chin-Diew, Zitikis R. Estimating the turning point of a bathtub-shaped failure distribution. Journal of Statistical Planning and Inference 2008; 138(4): 1157–1166, http://dx.doi.org/10.1016/j.jspi.2007.04.031.
2. Clarotti C, Lannoy A, Odin S, Procaccia H. Detection of equipment aging and determination of the efficiency of a corrective measure. Reliability Engineering and System Safety 2004; 84(1): 57–64, http://dx.doi.org/10.1016/j.ress.2004.01.005.
3. Dijoux Y. A virtual age model based on a bathtub shaped initial intensity. Reliability Engineering and System Safety 2009; 94(5): 982–989, http://dx.doi.org/10.1016/j.ress.2008.11.004.
4. Domma F, Condino F. A new class of distribution functions for lifetime data. Reliability Engineering and System Safety 2014; 129: 36–45, http://dx.doi.org/10.1016/j.ress.2014.04.026.
5. Golovatyj A T, Borcov P I. Èlektropodvižnoj sostav. Èkspluatacija, nadežnost' i remont. Moskva: Izdatel'stvo Transport, 1983.
6. Hemmati F, Khorram E, Rezakhah S. A new three-parameter ageing distribution. Journal of Statistical Planning and Inference 2011; 141(7):

2266–2275, http://dx.doi.org/10.1016/j.jspi.2011.01.007.
7. Huang H Z. Structural reliability analysis using fuzzy sets theory. Eksploatacja i Niezawodnosc – Maintenance and Reliability 2012; 14 (4): 284–294.
8. Jager R, Filev D. Podstawy modelowania i sterowania rozmytego. Warszawa: Wydawnictwa Naukowo-Techniczne, 1995.
9. Jiang R. A new bathtub curve model with a finite support. Reliability Engineering and System Safety 2013; 119: 44–51, http://dx.doi.org/10.1016/j.ress.2013.05.019.
10. Kadziński A. Modele prognozowania uszkodzeń nieodnawialnych obiektów typu mechanicznego w okresie uszkodzeń starzeniowych. Zeszyty Naukowe Wyższej Szkoły Morskiej w Szczecinie 2002; 66: 195–205.
11. Kadziński A. O komputerowym modelu do prognozowania uszkodzeń nieodnawianych obiektów typu mechanicznego na przykładzie obiektów pojazdów szynowych. Materiały XV Konferencji Pojazdy Szynowe 2002; 1: 313–320.
12. Kadziński A. Studium wybranych aspektów niezawodności systemów oraz obiektów pojazdów szynowych. Poznań: Wydawnictwo Politechniki Poznańskiej, 2013.
13. Li Y F, Huang H Z, Liu Y, Xiao N, Li H. A new fault tree analysis method: fuzzy dynamic fault tree analysis. Eksploatacja i Niezawodnosc – Maintenance and Reliability 2012; 14 (3): 208-214.
14. Osowski S. Sieci neuronowe do przetwarzania informacji. Warszawa: Oficyna Wydawnicza Politechniki Warszawskiej, 2000.
15. Piegat A. Modelowanie i sterowanie rozmyte. Warszawa: Akademicka Oficyna Wydawnicza EXIT, 2003.
16. Rutkowska D, Piliński M, Rutkowski L. Sieci neuronowe, algorytmy genetyczne i systemy rozmyte. Warszawa–Łódź: PWN, 1997.
17. Sikorska J Z, Hodkiewicz M, Ma L. Prognostic modeling options for remaining useful life estimation by industry. Mechanical Systems and Signal Processing 2011; 25: 1803–1836, http://dx.doi.org/10.1016/j.ymssp.2010.11.018.
18. Sun R, Peng WW, Huang HZ, Ling D, Yang J. Improved reliability data curve fitting method by considering samples distinction. Eksploatacja i Niezawodnosc – Maintenance and Reliability 2012; 14 (1): 62–71.
19. Wong K S, Hsu F S, Liu P P. Modeling the bathtub shape hazard rate function in terms of reliability. Reliability Engineering and System Safety 2002; 75(3): 397–406, http://dx.doi.org/10.1016/S0951-8320(01)00124-7.
20. Wu W, Huang HZ, Wang ZL, Li YF, Pang Y. Reliability analysis of mechanical vibration component using fuzzy sets theory. Eksploatacja i Niezawodnosc – Maintenance and Reliability 2012; 14 (2): 130–134.

Adrian GILL
Adam KADZIŃSKI
Institute of Combustion Engines and Transport
Poznan University of Technology
Piotrowo 3, 60-965 Poznan, Poland
E-mails: adrian.gill@put.poznan.pl, adam.kadzinski@put.poznan.pl

Article citation info:
WU Z, HUANG N, LI R, ZHANG Y. A delay reliability estimation method for Avionics Full Duplex Switched Ethernet based on stochastic network calculus. Eksploatacja i Niezawodnosc – Maintenance and Reliability 2015; 17 (2): 288–296, http://dx.doi.org/10.17531/ein.2015.2.17.

Zhitao WU
Ning HUANG
Ruiying LI
Yue ZHANG

A DELAY RELIABILITY ESTIMATION METHOD FOR AVIONICS FULL DUPLEX SWITCHED ETHERNET BASED ON STOCHASTIC NETWORK CALCULUS

OPARTA NA STOCHASTYCZNYM RACHUNKU SIECIOWYM METODA ESTYMACJI NIEZAWODNOŚCI CZASU TRANSMISJI DLA PRZEŁĄCZANEJ POKŁADOWEJ SIECI ETHERNETOWEJ TYPU AFDX UMOŻLIWIAJĄCEJ RÓWNOCZESNĄ TRANSMISJĘ DWUKIERUNKOWĄ

The delay reliability estimation is required in order to guarantee the real-time communication for avionics full duplex switched Ethernet (AFDX). Stochastic network calculus (SNC) can be applied to estimate the reliability with a delay upper bound. However, only linear deterministic traffic envelope function is used to bound its traffic, which cannot represent the traffic randomness and is far from practice. In this paper, a stochastic traffic envelope function, which randomizes the input of SNC, is proposed to solve the problem. A new probabilistic algorithm is derived to estimate the delay reliability based on stochastic envelope functions. A test was conducted to demonstrate our method on an AFDX testbed, and the test results verify that the estimation of delay reliability via our algorithm is much closer to the empirical estimation.

Keywords: *reliability estimation, delay upper bound, stochastic network calculus, traffic envelope function.*

Ocena niezawodności czasu transmisji (czasu opóźnienia) jest niezbędną procedurą gwarantującą komunikację w czasie rzeczywistym za pośrednictwem przełączanej pokładowej sieci ethernetowej typu AFDX (Avionics Full Duplex Switched Ethernet), która umożliwia równoczesną transmisję dwukierunkową. Stochastyczny rachunek sieciowy (SNC) można stosować do oceny niezawodności przy zadanej górnej granicy opóźnienia. Do tej pory jednak, do ograniczania ruchu telekomunikacyjnego stosowano tylko liniową deterministyczną funkcję obwiedni (traffic envelope), która nie oddaje losowości ruchu telekomunikacyjnego i odbiega dalece od rzeczywistości. W niniejszej pracy zaproponowano rozwiązanie tego problemu wykorzystujące stochastyczną funkcję obwiedni ruchu telekomunikacyjnego. Wyprowadzono nowy algorytm probabilistyczny, który pozwala ocenić niezawodność czasu transmisji na podstawie funkcji obwiedni. Przeprowadzono badanie, w ramach którego testowano zaproponowaną metodę w środowisku testowym AFDX; wyniki testu pokazują, że ocena niezawodności czasu transmisji z wykorzystaniem zaproponowanego przez nas algorytmu jest znacznie bardziej zbliżona do estymacji empirycznej.

Słowa kluczowe: *ocena niezawodności, górna granica opóźnienia, stochastyczny rachunek sieciowy, funkcja obwiedni ruchu telekomunikacyjnego.*

1. Introduction

Airborne network plays a key role in the integration of modern airplanes. Avionics full duplex switched Ethernet (AFDX) [4] was developed by Airbus aiming to provide 100Mbps bandwidth with deterministic quality of service, and has been successfully applied in several advanced aircrafts, such as A380, Boeing 787, etc. For avionics applications, the real-time requirement is essential, so the delay reliability needs to be estimated to ensure that the network configuration satisfies the customer requirement. Customers define maximum allowed frame delay (i.e., delay upper bound) on AFDX. If a frame delay exceeds the upper bound, the frame transmission is considered as a transmission failure. If not, it is regarded as a successful transmission. The occurrence probability of successful transmission is the delay reliability, which is also named as transmission time reliability [22], delay-oriented reliability [34], and reliability with delay [18].

Network delay reliability was first introduced by Asakura and Kashiwadani [5] for road networks where it is named as transportation time reliability, and was then expanded by Li et al. [22] to computer networks. Similar studies are referred to [1, 14, 25, 28, 33], which investigate factors that affect delay reliability, and provide the corresponding estimation methods. However, traffic randomness, which has large effects on delay reliability as Meyer [26] and Ball [6] stated, was neglected in the above research, and traffic with high burst usually causes network performance degradation. Stochastic network calculus (SNC) was proposed to provide an elegant framework that can be used to evaluate the delay reliability with traffic randomness [15, 16, 24]. Traffic envelope and service envelope are used to bound traffic arrivals and the services offered at network nodes, respectively, and the delay reliability can be estimated based on the mathematical foundation of min-plus algebra.

When Ridouard et al. [29] first proposed SNC to evaluate the delay reliability which uses the maximum allowable delay as the delay upper bound in AFDX in 2008, only pessimistic linear traffic envelopes were used to bound AFDX traffic. Moreover, Yao [38] and Liu [23] summarized the current AFDX traffic models used to derive deterministic traffic envelopes, and found that the linear expression is the only form. In [17], Jiang summarized that there were two ways to estimate the delay reliability via SNC: (i) randomize the input of SNC, i.e., traffic and service envelope functions; (ii) randomize the

reliability derivation based on deterministic traffic and service envelopes (which are not randomized). The former one is an intrinsic stochastic process, which randomizes the calculation source. However, as it is difficult to build stochastic traffic and service envelope functions, to the best of our knowledge, only the latter idea has been applied in computing the delay reliability in AFDX [32]. However, since Lelend [21] discovered the self-similar property of Ethernet traffic, in which AFDX is a special case, linear traffic models cannot reflect the long range dependence and burstiness (i.e., self-similarity) of AFDX traffic [7, 19]. Therefore, the traffic self-similarity needs to be incorporated into the traffic envelope to improve the accuracy of the delay reliability estimation.

In this paper, we build a stochastic traffic envelope function, which randomizes the input of SNC, to reflect the self-similarity of AFDX traffic, and propose a new probabilistic algorithm to estimate the delay reliability based on the stochastic envelope functions, which gives a better approximation. This remainder of the paper is organized as follows. Section 2 details some basic knowledge about the AFDX. Based on a brief introduction of SNC theory, the stochastic envelope functions are analyzed for AFDX in Section 3. Particularly, the fractional Brownian motion (FBM), which is commonly used to model the self-similar traffic of Ethernet, is introduced to model the non-linear aggregate traffic in AFDX. Section 4 derives the delay reliability according to the SNC theory. Case study is presented in Section 5, and it verifies that our proposed method can provide more accurate delay reliability estimation compared to the previous SNC methods. Finally, concluding remarks are provided in Section 6.

2. AFDX context

AFDX, originating from mature Ethernet technology, is a real-time system. As shown in Fig. 1, an AFDX system comprises avionics subsystems, end systems (ES) and a redundant switched system. Avionics subsystems, such as flight control system, global positioning system, etc., are designed to accomplish multiple avionics tasks. Avionics computer systems are used to provide a computational environment for these avionics subsystems. Each avionics computer system contains an embedded ES that connects the avionics subsystems to an AFDX interconnect. The ES is generally referred to as network interface cards (NIC). The traffic between avionics subsystems is transmitted through ESs and the switched system. All frames copied at the ES are sent on both networks in the redundant switched system, and are finally received by the destination ES. Moreover, a gateway provides interconnection between AFDX and Internet.

In AFDX, the deterministic end-to-end transmission is guaranteed by the virtual link (VL) mechanism [23]. VL can be seen as a unidirectional logical channel from one source ES to one or more destinations, which defines a deterministic communication path. All the data transmission between ESs are accomplished through VLs in the AFDX. To guarantee the deterministic data exchange, each VL is assigned to a maximum allowed frame size (L_m), a maximum allowed jitter (J_m), a bandwidth allocation gap (BAG) and a maximum bandwidth, where BAG is the minimum time interval between the start of consecutive frames. Normally, S_m is denoted as the maximum frame size with interframe gap, i.e., S_m=L_m+20 Bytes, where interframe gap is a minimum idle period between transmission of frames.

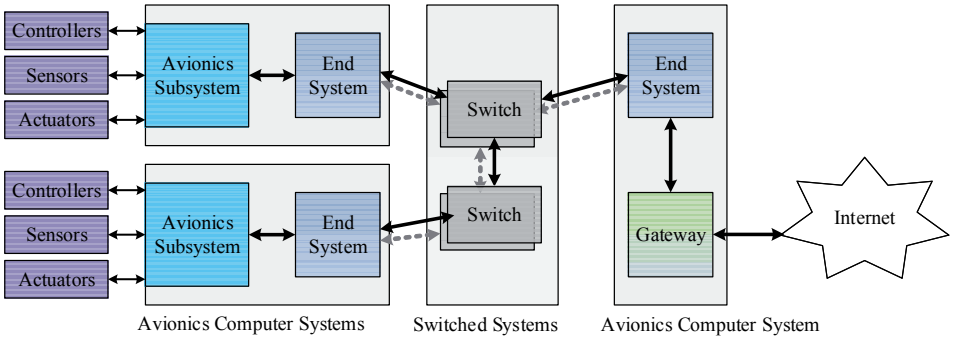

Fig. 1. AFDX context

The end-to-end delay of a certain frame F transmitted on a VL can be described as the sum of transmission delays on links and latencies in switches between source and destination. According to [32], it can be defined as:

$$D_F = LD_F + TD_F + BD_F \tag{1}$$

where LD_F is the transmission delay over the link, TD_F is the technical processing delay, and BD_F is the delay in switch buffer. In particular, LD_F is determined by $LD_F = m_L \times S_m(F)/R$, where m_L is the number of links in the VL, $S_m(F)$ is the frame size with interframe gap, and R is the link bandwidth; TD_F is caused by the protocol process in switches, such as frame policing and filtering. According to AFDX specification [4], the processing delay at one switch does not exceed 16 μs. As the number of swithes in the AFDX is not large, hence TD_F can be regarded as a fixed value, i.e., $TD_F = m_s \times 16$ μs, where m_s is the number of switches in the VL; BD_F is determined by the frame queuing process, which highly depends on the traffic load of each switch port [32]. As LD_F and TD_F are fixed values for a deterministic AFDX configuration, we focus on how to model delay reliability with BD_F consideration in our study.

3. Envelope functions for stochastic network calculus

Section 3.1 introduces the basic knowledge of the SNC theory, and the envelope functions for AFDX, i.e., STP and SSP, are derived based on the characteristics of AFDX traffic in Section 3.2 and 3.3, respectively.

3.1. Stochastic network calculus

SNC provides an analytical framework of the probabilistic upper bound estimation for BD (i.e., the delay in the switch buffer) [16], and its analytical expression is as follows:

$$\Pr(BD \geq BD_U) \leq f(BD_U), \tag{2}$$

where BD_U is the delay upper bound requirement of BD, and f is the violable function.

Eq. (2) can be used to calculate the conservative end-to-end delay reliability as:

$$\begin{aligned} R_D &= \Pr(\mathrm{D} \leq \mathrm{D}_U) \\ &= 1 - \Pr(\mathrm{D} \geq \mathrm{D}_U) \\ &= 1 - \Pr(LD + TD + BD \geq \mathrm{D}_U) \\ &\geq 1 - f(\mathrm{D}_U - LD - TD), \end{aligned} \tag{3}$$

where R_D is delay reliability with the end-to-end delay upper bound D_U.

In the SNC algorithm, left-continuous stochastic processes $A(t)$ and $A^*(t)$ are used to quantify cumulative arrivals and departures of a traffic flow in the time period

[0,*t*). Intuitively, we use $A(s,t):=A(t)-A(s)$ to denote the accumulative arriving traffic in the time period [*s*,*t*).

***Definition* 1:** A non-random function $\alpha(t)$ is a *stochastic traffic envelope* (STP) for an arrival process *A* if it bounds arrivals over a time interval by the following equation, for all $t \geq s \geq 0$ and for all $\sigma \geq 0$,

$$\Pr(A(s,t) > \alpha(t-s)+\sigma) \leq f_A(\sigma), \tag{4}$$

where $f_A(\sigma)$ is a non-negative, non-increasing function known as the violable probability function of $\alpha(t)$, and satisfies $f_A(\sigma) \to 0$ as $\sigma \to \infty$.

***Definition* 2:** A *stochastic service envelope*(SSP) for a network system with arrival traffic *A* is a function $\beta(t)$, if for all δ>0,

$$\Pr(A \otimes \beta(t) - A^*(t) > \delta) \leq g_A(\delta), \tag{5}$$

where symbol $\otimes$ is the min-plus convolution: $a \otimes b(x) = \inf_{0 \leq y \leq x}[a(y)+b(x-y)]$, $g_A(\delta)$ is the violable function of $\beta(t)$.

The delay in the network switch buffer at time *t* can be defined as:

$$BD(t) = \inf_{0 \leq \tau \leq t}\{\tau, A(t-\tau) \leq A^*(t)\}. \tag{6}$$

As is shown in Fig. 2, the delay at time t_1 in the network switch buffer actually is the horizontal distance of STP and SSP. With STP and SSP, SNC can be applied to derive the delay reliability via Eq. (6). Note that $f(\cdot)$ in Eq. (6) is a compound function of $f_A(\sigma)$ and $g_A(\delta)$.

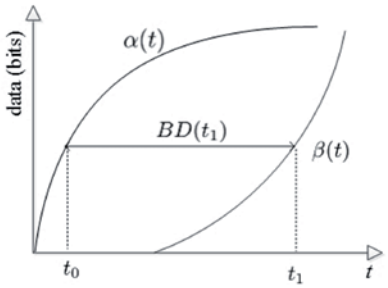

Fig. 2. Transmission delay bound

When there are multiple flows competing for service resources in a system, the following theorem presented in [16] provides a useful technique to construct SSP for a single flow.

Theorem 1 (*Left-over service characterization*): Consider the case where two traffic flows A_1 and A_2 compete for resources in a switch system under the scheduling policy. Assume the SSP of the network system is $\beta(t)$, the STP of A_i is $\alpha_i(t)$, and the SSP $\beta(t)$ provided by the system for A_i can be expressed as $\beta_i(t) = \max\{\beta(t) - \alpha_{A_j}(t), 0\}$ (*i*=1,2, and *j*=3–*i*), and its violable function can be calculated as $g_{A_i}(x) = g \otimes f_{A_j}(x)$.

3.2. Stochastic traffic envelope

In the switched network of AFDX, the traffic arrival process is determined by its departural process at the source ES, as the frame transmission on link dose not change the frame interval. To guarantee the *BAG* for each VL, the traffic at ES outports are regulated by traffic regulator, and no more than one frame can be sent out in each interval of *BAG*. When multiple VLs exist, the VL scheduler will introduce jitter for the frame if it arrives at a non-empty virtual link queue. The frame transmitting process at the ES outport is illustrated in Fig. 3. Therefore, in the i^{th} VL, the frame intervals are between $BAG_i - J_m^i$ and $BAG_i + J_m^i$, where J_m^i is the jitter of the i^{th} VL.

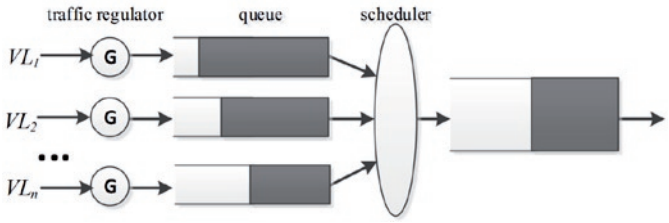

Fig. 3. Frame transmitting process in multiple VLs at an ES outport

In a switch, the queuing is occured at the outport. In one outport (see Fig. 4), except the VL_i traffic under estimation, other traffic of VLs, i.e., background traffic, is also transmitted through the same outport. Note that, background traffic is actually a superposition of frames from all VLs in the outport except the i^{th} VL. Let $A_i(t)$ and $A_B(t)$ be the cumulative arrivals of VL_i and background traffic flow in the time period [0, *t*), respectively.

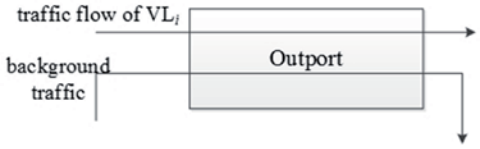

Fig. 4. VL_i traffic under estimation and its background traffic at the switch

3.2.1. The stochastic traffic envelope for VLi

In the previous study [23], as seen in Fig. 5, a series of frames are transmitted through VL_i, and the linear traffic envelope (LTP) is built for the worst-case situation, i.e., transmitting maximum-size frames with the minimum transmission intervals. Hence, LTP $\alpha_i(t)$ (in bits) for A_i can be expressed as:

$$\alpha_i(t) = 8S_m^i + \frac{8S_m^i}{BAG_i}t. \tag{7}$$

From Eq. (4), the STP of VL_i can be written as:

$$\Pr\left(A_i(s,t) > \alpha_i(t-s)+\sigma\right) \leq f_i(\sigma), \tag{8}$$

and the corresponding $f_i(\sigma) = 0$, as the LTP $\alpha_i(t)$ can surely bound the traffic.

3.2.2. The stochastic traffic envelope for the background traffic

When multiple VLs exist in a physical link, the aggregate traffic LTP $\alpha_B(t)$ can be obtained as:

$$\alpha_B(t) = 8\sum_i S_m^i + 8\sum_i \frac{S_m^i}{BAG_i}t. \tag{9}$$

In [23, 32, 38], the above LTP is applied to estimate the delay reliability using SNC. Obviously, Eq. (7) provides a rough bound of the cumulative traffic in a single VL, and Eq. (9) supposes that the traffic statistical characteristics do not change after the traffic is aggregated from different VLs at switches. However, it is not the real situation, as aggregating process in AFDX may lead to a non-linear statistical property, i.e., self-similarity appears.

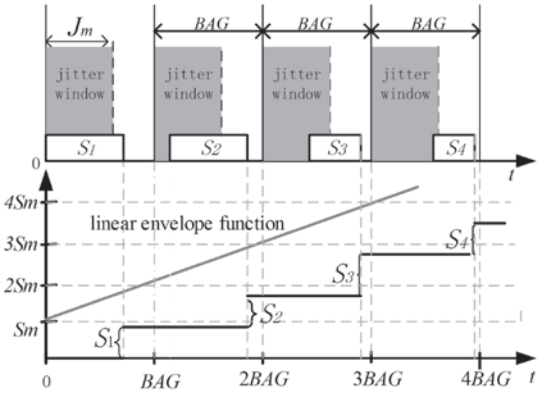

Fig. 5. Cumulative process of frames and linear envelope function in VL_i

In order to illustrate the statistical characteristics of the AFDX aggregate traffic, we collected time intervals between frames from four AFDX traffic, as shown in Fig. 6. One can see that some large traffic occurs with a small probability, which shows the traffic burstiness. Moreover, the traffic self-similarity property can be verified by the Hurst parameter (H). Using the absolute value method with the tool designed by Karagiannis [20], the H values of the collected data can be calculated as follows: 0.820, 0.763, 0.693 and 0.778, respectively, which show typical self-similar characteristics (Clegg [7] stated that the traffic self-similarity exsits if H>0.5). This is consistent with the traffic feature of Ethernet, in which the self-similarity has been widely recognized [9, 36].

Willinger [35] first applied fractal brown motion(FBM) to model self-similar aggregate traffic in 1998. Nowadays, FBM is widely used to model the aggregate traffic (see [7, 9, 19] for details). Rizk and Fidler [30, 31] analyzed the envelope function of FBM, and their result has been applied to derive performance bound in Internet. Hence, in this paper, we adopt FBM to model AFDX aggregate traffic, i.e., the aggregate traffic $\alpha_B(t)$ can be computed as:

$$\alpha_B(t) = \sum_{i=1}^{n} \alpha_i(t) = \rho t + \sqrt{\rho\omega^2}\, B_H(t), \tag{10}$$

where n is the number of VLs of the background traffic, ρ is the mean arrival rate, ω^2 is the variance of traffic flow, and $B_H(t)$ is a trace of FBM with the Hurst parameter $H \in (0.5,1)$, which depends on n. FBM is used to model the traffic deviations from its mean value, and the self-similarity is characterized by H in FBM. According to the property of FBM presented by Duffield et al. [8], for $\forall \sigma, c \geq 0$, $\alpha_B(t)$ satisfies:

$$\ln\left\{\Pr\left[A_B(s,t) - \alpha_B(t-s) \geq \sigma\right]\right\} \leq -\sigma^{2(1-H)} \inf_c \left\{c^{-2(1-H)}(c+\rho)^2 / 2\right\}. \tag{11}$$

In order to simplify Eq. (11), the minimum value of $c^{-2(1-H)}(c+\rho)^2 / 2$ over c>0 can be obtained at c=(1–H)ρ/H by derivation. Substituting the value of c into Eq. (11) yields:

$$\Pr\left[A_B(s,t) - \alpha_B(t-s) \geq \sigma\right] \leq \min\left\{1, \exp\left\{-0.5\left(\frac{\sigma}{1-H}\right)^{2(1-H)}\left(\frac{\rho}{H}\right)^{2H}\right\}\right\}. \tag{12}$$

Therefore, the right part of Eq. (12) can be viewed as the violable probability function, i.e.,

$$f_B(\sigma) = \min\left\{1, \exp\left\{-0.5\left(\frac{\sigma}{1-H}\right)^{2(1-H)}\left(\frac{\rho}{H}\right)^{2H}\right\}\right\}.$$

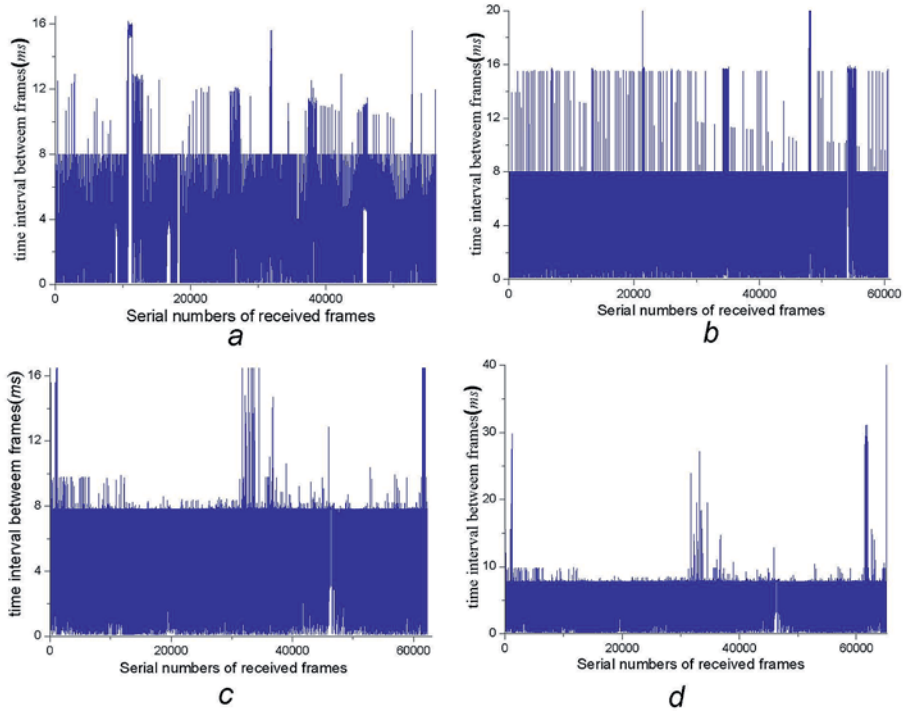

Fig. 6 Time interval between frames

3.3. Stochastic service envelope

As shown in Fig. 4, the service resource competition between traffic in the i^{th} VL and background traffic widely exists at the switch outports. Suppose that the switches are in the work-conserving manner, then the SSP $\beta(t)$ for the aggregate traffic at a switch outport can be obtained as [32]:

$$\Pr(A \otimes \beta(t) - A^*(t) > \delta) \leq g(\delta), \tag{13}$$

where $A(t)$ and $A^*(t)$ are the cumulative arrivals and departures of the aggregate traffic at the switch outport, $\beta(t) = Ct$ and $g(\delta)$=0, C is the bandwidth of the switch outport. According to the left-over service theorem (Theorem 1), we can derive the SSP $\beta_i(t)$ for VL_i as:

$$\Pr(A_i \otimes \beta_i(t) - A_i^*(t) > \delta) \leq g_i(\delta), \tag{14}$$

where $\beta_i(t)=\max\{\beta(t)-\alpha_B(t),0\}$, and $g_i(\delta)=g\otimes f_B(\delta)=f_B(\delta)$ as $g(\delta)=0$.

4. Reliability estimation with the given delay upper bound

With the basic knowledge of SNC theory, we can derive the following theorem to estimate the end-to-end delay reliability for a VL:

Theorem 2: Assume that a switch k whose SSP $\beta(t)$ satisfies Eq. (13), provides service for multiple VLs in AFDX as shown in Fig. 4. If the STPs for A_i and background traffic follow Eq. (8) and (12), respectively. We have:

$$\Pr(BD_k \geq BD_{U,k}) \leq f_B((C-\rho_k)BD_{U,k}), \tag{15}$$

where BD_k is the delay of a frame in the outport buffer at switch k, and $BD_{U,k}$ is the given upper bound requirement of k. For a VL with m_s switches, the end-to-end delay reliability R_D with the given delay upper bound BD_U is given by:

$$R_D \geq 1-f_B\left(\frac{D_U-LD-TD}{\sum_{k=1}^{m_s}\frac{1}{C-\rho_k}}\right). \tag{16}$$

Proof: According to Eq. (6), the delay in the outpor buffer at switch k can be computed as:

$$BD_k = \inf_{0\leq\tau\leq t}\left\{\tau, A_i(t-\tau)\leq A_i^*(t)\right\}.$$

Hence, for any $t>0$, $\Pr(BD_k>d)\leq\Pr\left\{A_i(t-d)\leq A_i^*(t)\right\}$ holds.

In order to compute the probability, for all $y\in[0,t]$, we have:

$$\begin{aligned}
&A_i(t-y)-A_i^*(t)=A_i(t-y)-\inf_{0\leq s\leq t-y}\{A_i(s)+\beta_i(t-s)\}+\inf_{0\leq s\leq t-y}\{A_i(s)+\beta_i(t-s)\}-A_i^*(t)\\
&\leq \sup_{0\leq s\leq t-y}[A_i(t-y)-A_i(s)-\beta_i(t-s)]+A_i\otimes\beta_i(t)-A_i^*(t)\\
&=\sup_{0\leq s\leq t-y}[A_i(s,t-y)-\alpha_i(t-y-s)+\alpha_i(t-y-s)-\beta_i(t-s)]+A_i\otimes\beta_i(t)-A_i^*(t)\\
&\leq \sup_{0\leq s\leq t-y}[A_i(s,t-y)-\alpha_i(t-y-s)]+\sup_{0\leq s\leq t-y}[\alpha_i(t-y-s)-\beta_i(t-s)]+A_i\otimes\beta_i(t)-A_i^*(t)\\
&\triangleq \sup_{0\leq s\leq t-y}[\alpha_i(t-y-s)-\beta_i(t-s)]+A_i\otimes\beta_i(t)-A_i^*(t)\\
&=\sup_{0\leq s\leq t-y}\left[\frac{8S_m}{BAG}(t-y-s)-(C-\rho_k)(t-s)+\sqrt{\rho_k\omega^2}B_H(t-s)\right]+A_i\otimes\beta_i(t)-A_i^*(t)\\
&\triangleq -(C-\rho_k)y+A_i\otimes\beta_i(t)-A_i^*(t).
\end{aligned}$$

The equation $\triangleq$ of the above inference holds as Eq. (8) shows $\Pr(A_i(s,t)>\alpha_i(t-s)+\sigma)\leq 0$ for all $\sigma>0$. Since $B_H(t)$ is used as a deviation and has expectation zero, $\sqrt{\rho_k\omega^2}B_H(t-s)$ is assigned to 0 in statistical sense, in addition, the bandwidth C of the outport is larger than $8S_m/BAG+\rho_k$, and hence the maximum value of

$$\left[\frac{8S_m}{BAG}(t-y-s)-(C-\rho_k)(t-s)+\sqrt{\rho_k\omega^2}B_H(t-s)\right]$$

over $s\in[0,t-y]$ is obtained at $s=t-y$, which yields the equation $\triangleq$. Therefore, we have

$$A_i(t-d)-A_i^*(t)\leq A_i\otimes\beta_i(t)-A_i^*(t)-(C-\rho_k)d.$$

Based on the above analysis, we can obtain,

$$\begin{aligned}
\Pr(BD_k\geq d)&=\inf_t\Pr\{A_i(t-d)\leq A_i^*(t)\}\\
&\leq\inf_t\Pr\{A_i\otimes\beta_i(t)-A_i^*(t)\geq(C-\rho_k)d\}\\
&=f_B\otimes g((C-\rho_k)d)=f_B((C-\rho_k)d),
\end{aligned}$$

where f_B is given in Eq. (12).

In a VL (with m_s switches) whose end-to-end delay upper bound is D_U, for each switch, we have $\Pr(BD_k\leq BD_{U,k})\geq 1-f_B((C-\rho_k)BD_{U,k})$. Solving:

$$\begin{cases}\sum_{k=1}^{m_s}BD_{U,k}=D_U-LD-TD,\\ (C-\rho_1)BD_{U,1}=(C-\rho_2)BD_{U,2}=\cdots=(C-\rho_{m_s})BD_{U,m_s},\end{cases}$$

where the second equation holds as the traffic of the same VL is identical. We have:

$$\begin{cases}BD_{U,1}=\dfrac{D_U-LD-TD}{(C-\rho_1)\sum_{S=1}^{m_s}\frac{1}{C-\rho_S}},\\ BD_{U,k}=\dfrac{C-\rho_1}{C-\rho_k}BD_{U,1},\qquad k=1,2,\ldots,m_S.\end{cases}$$

Hence, the end-to-end delay reliability can be written as:

$$\begin{aligned}
R_D&=\Pr(D\leq D_U)\\
&=1-\Pr(\sum_{S=1}^{m_s}BD_S\geq D_U-LD-TD)\\
&\text{(Accorrding to the min-plus convolution)}\\
&\geq 1-f_B((C-\rho_1)BD_{U,1})\otimes\cdots\otimes f_B((C-\rho_{m_S})BD_{U,2})\\
&=1-f_B\left(\frac{D_U-LD-TD}{\sum_{S=1}^{m_s}\frac{1}{C-\rho_S}}\right).
\end{aligned}$$

According to Theorem 2, the delay reliability with a given delay upper bound can be obtained. The proposed method makes a distinct contribution to estimate the delay reliability for a certain VL: (1) the non-linear FBM aggregate traffic envelope is randomized, which represents the self-similarity of the AFDX background traffic; and (2) the compact algrithom for the delay reliability with a given delay upper bound is derived using STP and SSP, which is an intrinsic stochastic process.

5. Case study

In this section, a case study is provided to illustrate the effectiveness of the proposed method. We consider an AFDX with the topology and parameters shown in Fig. 7 and Table 1. Messages are transmitted from ES1, ES2 and ES3 to ES4 through SW1 and SW2. In this case, messages of all VLs are generated according to Pareto and exponential distributions, which form a typical self-similar traffic and is frequently used in network traffic analysis (see Addie et al. [2], Field et al. [10], Nadarajah [27], Yamkhin [37], and Fras et al. [11, 12] for details). Our proposed algorithm is applicable to other heavy-tailed traffic distributions only if its background traffic is self-similar. Moreover, this idea can also be applied in non-heavy-tailed traffic distribution based on similar derivation. In this case study, the delay reliability of VL_{11} is measured with a delay upper bound.

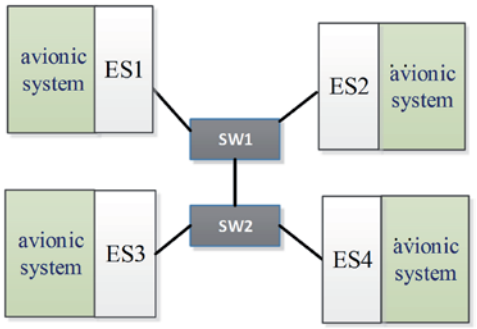

Fig. 7. AFDX Topology

Table 1. AFDX configuration

VL Number	Source ES	Message generation parameters① (λ, α, X_{min})	Destination ES	*BAG* (ms)	L_m (byte)	R (Mbps)
VL_{11}-VL_{16}	ES1	0.2,1.1, 3MB	ES4	8,32,2,4,8,16	1518	100
VL_{21}-VL_{27}	ES2	0.4, 1.1, 1MB	ES4	8,1,64,16,16,128,64		
VL_{31}-VL_{38}	ES3	0.6, 1.1, 133KB	ES4	1,32,16,1,128,32,8,2		

① *The size X of avionics message generated by source ES is supposed to follow Pareto distribution:* $F_X(X \le x) = 1 - (X_{\min}/x)^{\alpha}$, *and the time interval Y between message generation follows exponential distribution with parameter λ:* $F_Y(Y \le y) = 1 - \exp\{-\lambda y\}$. *All parameters are adopted according to the statistical results presented in [13].*

We conducted a test on an AFDX testbed to compute the empirical estimate of delay reliability, and the estimation results obtained by our method is much closer to the empirical estimate compared a previous method.

5.1. AFDX testbed

Our AFDX testbed is shown in Fig. 8. In the testbed, there are three types of nodes as follows,

(1) Three personal computers (PC) embedded with ES peripheral component interconnect (PCI) cards, which are used as substitutions of avionic subsystems.
(2) Two switches, which are used to forward frames to the destination.
(3) A test equipment, which is served as both test device and destination ES.

Both ES PCI cards and switches, ACTRI-FDX-ES-PMC and ACTRI-FDX-SW-24, are designed and manufactured by an avionics institution in China. The test equipment [3], AFDX/ARINC664P7 (AIM), is an advanced avionics test apparatus designed by AIM GmbH of Germany with nanosecond resolution. As a test device, it can capture transmission data to calculate the delay. As a destination ES, it can receive data transmitted from ES1, ES2 and ES3 via VLs. Traffic can be generated by the software installed in the three source ES, and transmitted to the destination, i.e., the AIM test equipment, via different VLs. Timestamps of each frame can be recorded at the outport of either source ES or switch by the AIM test equipment. The red dotted lines in Fig. 8 show an example of the timestamp capture, and the delay between the time that the frame departures the outports of ES1 and SW2 can be calculated using PBA.pro Databus Analyser & Analysis Software embedded in AIM.

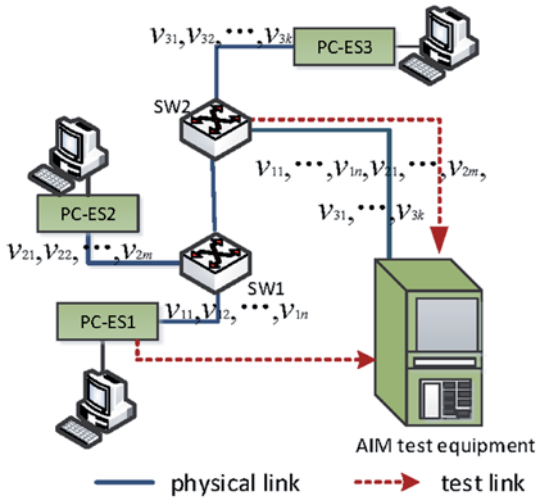

Fig. 8. AFDX testbed

5.2. Test result and discussion

5.2.1. Empirical estimation from test

We conducted a test according to the configuration shown in Table 1, and millions of frames were collected by AIM. According to the data collected from the test, the Hurst parameter was estimated by the absolute value method as 0.778, which well satisfies the typical non-linear self-similar characteristics of the aggregate traffic.

As shown in Fig. 9, the delay obtained by AIM is in a range from 251 μs to 507 μs, and the empirical estimate of the delay reliability can be obtained by:

$$\hat{R}(D_U) = \frac{k_{D_U}}{n}, \tag{17}$$

where k_{D_U} is the number of frames whose delay does not exceed the delay upper bound D_U, and n is the total number collected. The test result is recorded using the green solid curve in Fig. 9.

5.2.2. Estimation by the new method

With the parameter presented in Table 1, we can calculate the transmission delay of frames in VL_{11} as:

$$LD = m_L \times S_m / R = 2 \times 8 \times (1518 + 20) / 100 \times 10^6 \ \mu s = 246 \ \mu s,$$

According to AFDX specification, the processing delay can be calculated as:

$$TD = m_s \times 16\ \mu s = 2 \times 16\ \mu s = 32\ \mu s.$$

From the test, ρ_1 and ρ_2, the mean arrival rate in outport buffer of SW1 and SW2, are measured as ρ_1=1.935 Mbps and ρ_2=2.469 Mbps by AIM. According to Theorem 2, the delay reliability can be estimated under the given delay upper bounds. For example, if D_U=500 μs, then $BD_U = D_U - LD - TD$=222 μs, and the delay reliability can be calculated as:

$$\begin{aligned} R_{D_U} &= \Pr(BD_{SW1} + BD_{SW2} \le BD_U) \\ &= 1 - f_B\left(\frac{D_U - LD - TD}{\frac{1}{C-\rho_1}+\frac{1}{C-\rho_2}}\right) \\ &= 1 - f_B\left(\frac{222\times10^{-6}}{\frac{1}{100-1.935}+\frac{1}{100-2.469}}\right) \\ &\cong 0.8125. \end{aligned}$$

As the sum of *LD* and *TD* is deterministic in the new method, i.e., 278μs, the delay reliability keeps 0 when D_U is smaller than 278μs. It is larger than the test result (251 μs), because fixed *TD* used in this method is actually an upper bound. When D_U varies, the estimation results can be seen in the black dotted line in Fig. 9.

5.2.3. Estimation by SNC proposed by [32]

Similarly, the delay reliability can also be estimated using SNC method from [32] with LTP (Eq. (9)),

$$R_D = 1 - \Pr(D > D_U) \ge 1 - \frac{C}{\rho}\sum_{k=1}^{K-1} \exp(-A(s_k, s_{k+1}, BD_U)),$$

where $A(s_k, s_{k+1}, d)$ can be found in Theorem 1 of [32], and $0 = s_0 \le s_1 \le \cdots \le s_K = \tau$ for any $K \in \mathbb{Z}^+$ and $\tau = \lim_{u\ge 0}\{\alpha_i(u) \le \beta_i(u)\}$.

If *d*=4 ms, the delay reliability can be calculated as 0.96. When *d* varies, the estimation results can be seen in the blue dashed line in Fig. 9.

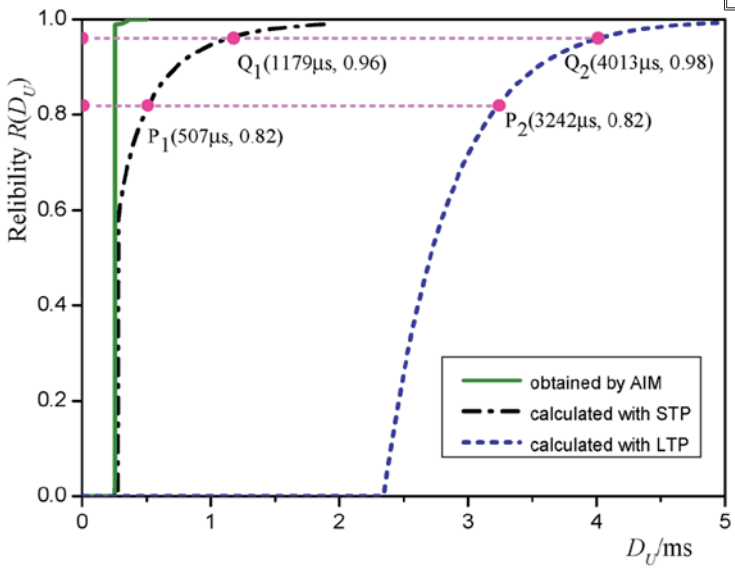

Fig. 9. Reliability with given delay upper bounds

5.2.4. Discussion

From Fig. 9, one can see that both estimates obtained by SNC methods are conservative estimates, as they exceed the empirical estimate from test for any given delay upper bound, as well as the delay upper bounds are larger than the test results for any given delay reliability requirement. It is obvious that the black dotted curve (calculated by our SNC method) is much closer to the blue solid one (the test result) compared to the blue dashed one (calculated by SNC proposed by [32]). The major reason for the error is that LTP analyzes the worst-case situation, i.e., each frame experiences the maximum queue as all frames from different VLs arrive at the switch together. STP captures a more realistic statistical feature of AFDX traffic by considering the traffic randomness, while LTP uses the worst-case situation. It means that the SNC method from [32] with LTP (Eq. (9)) is over conservative which may cause design waste.

Moreover, if the delay reliability is given, one can calculate the delay upper bound. For example, if the given reliability requirement *R*=0.82, the delay upper bounds for the two SNC methods are 507μs and 3242 μs (see P_1 and P_2 in Fig. 9). If the reliability requirement increases to *R*=0.96, the delay upper bounds are relaxed to 1179 μs and 4013 μs, respectively. More discussions can be seen in Table 2. The results show our method is more accurate.

Table 2. Delay upper bound of the three methods with different delay reliability

method \ R		0.82	0.88	0.96	0.99
AIM	D_u(ms)	0.253	0.254	0.255	0.279
SNC with STP		0.507	0.660	1.179	1.877
SNC with LTP		3.242	3.450	4.013	4.740

Table 3. Comparison of the three methods

methods	traffic envelope	service envelope	estimation
SNC with STP	statistical multiplexing	statistical multiplexing	Both traffic and service envelope are randomized, and the derivation is not randomized.
SNC with LTP	worst-case	worst-case	The reliability derivation is randomized with deterministic traffic and service envelope.
AIM	--	--	empirical estimation.

Further analysis reveals that: 1) compared to worst-case LTP, STP captures a more realistic statistical feature of AFDX traffic; 2) SNC with STP and SSP randomizes the calculation source, i.e., traffic envelope and service envelope, which derives more accuracy result than the one with LTP. Table 3 is listed to compare the three methods.

6. Conclusion

The current SNC algorithm based on linear deterministic traffic envelop function cannot represent the traffic self-similarity (which has already been verified in the real situation) of AFDX. To solve the problem, a stochastic traffic envelope is proposed based on FBM model, a common analytical model of Ethernet aggregate traffic, to model the background aggregate traffic in AFDX. A closed form expression of reliability with the end-to-end delay considerations is derived according to the framework of SNC theory, in which the traffic randomness is taken into account. The test result from a high-precision testbed verifies that our proposed method can obtain a better estimation result compared to

the previous algorithm. To the best of our knowledge, this work is among the first that uses SNC with stochastic FBM envelope to derive the reliability with the given delay upper bound in a deterministic AFDX configuration.

Since different scheduling algorithms are used in the outport buffers at the switch, an exploration of the effect caused by different scheduling algorithms will be studied in our future research.

Acknowledgement

This work was supported by the National Natural Science Foundation of China (61304220) and the Beijing Natural Science Foundation (4143064). (Corresponding author: Li R.)

References

1. Abdrabou A, Liang B, Zhuang W H. Delay Analysis for Sparse Vehicular Sensor Networks with Reliability Considerations. IEEE Transactions on Wireless Communications 2013; 12: 4402-4413, http://dx.doi.org/10.1109/TW.2013.072313.121397.
2. Addie, R G, Neame T D, Zukerman M. Performance evaluation of a queue fed by a Poisson Pareto burst process', Computer Networks-the International Journal Of Computer And Telecommunications Networking 2002; 40(3): 377-397.
3. AIM GmbH. The AIM's AFDX/ ARINC664P7. http://www.aim-online.com/index.aspx (accessed 10 Dec 2013).
4. ARINC. ARINC 664 Part 7:Aircraft Data Network-Deterministic Networks. 2003.
5. Asakura Y, Kashiwadani M. Road network reliability caused by daily fluctuation of traffc flow. in: Proceedings of Seminar G Held at the PTRC Transport, Highways and Planning Summer Annual Meeting, University of Sussex, United Kingdom, 1991:73–84.
6. Ball M O, Colbourn C J, Provan J S. Network reliability. Handbooks in operations research and management science. 1995; 7: 673-762, http://dx.doi.org/10.1016/S0927-0507(05)80128-8.
7. Clegg R G, Di Cairano-Gilfedder C, Zhou S. A critical look at power law modelling of the Internet. Computer Communications 2010; 33: 259-268, http://dx.doi.org/10.1016/j.comcom.2009.09.009.
8. Duffield N G, O'connell N. Large deviations and overflow probabilities for the general single-server queue. Mathematical Proceedings of the Cambridge Philosophical Society with applications, Cambridge Univ Press, 1995:363-374.
9. Erramilli A, Roughan M, Veitch D, Willinger W. Self-similar traffic and network dynamics. Proceedings of the IEEE 2002; 90: 800-819, http://dx.doi.org/10.1109/JPROC.2002.1015008.
10. Field T, Harder U, Harrison P. Network traffic behaviour in switched Ethernet systems. Performance Evaluation 2004; 58(2-3): 243-260, http://dx.doi.org/10.1016/j.peva.2004.07.017.
11. Fras M, Mohorko J, Cucej Z. Modeling of measured self-similar network traffic in OPNET simulation tool. Informacije Midem-Journal Of Microelectronics Electronic Components And Materials 2010; 40(3): 224-231.
12. Fras M, Mohorko J, Cucej Z. Limitations of a Mapping Algorithm with Fragmentation Mimics (MAFM) when modeling statistical data sources based on measured packet network traffic. Computer Networks 2013; 57(17): 3686-3700, http://dx.doi.org/10.1016/j.comnet.2013.07.032.
13. Ha S, Le L, Rhee I, Xu L. Impact of background traffic on performance of high-speed TCP variant protocols. Computer Networks 2007; 51: 1748-1762, http://dx.doi.org/10.1016/j.comnet.2006.11.005.
14. Huang N, Hou D, Chen Y, Xing L D, Kang R. A network reliability evaluation method based on applications and topological structure. Eksploatacja I Niezawodnosc-Maintenance and Reliability 2011; 3: 77-83.
15. Jiang Y M. A basic Stochastic network calculus. Computer Communication Review 2006; 36: 123-134, http://dx.doi.org/10.1145/1151659.1159929.
16. Jiang Y M, Liu Y. Stochastic network calculus, Springer, 2008.
17. Jiang Y M, Yin Q, Liu Y, Jiang S. Fundamental calculus on generalized stochastically bounded bursty traffic for communication networks. Computer Networks 2009; 53: 2011-2021, http://dx.doi.org/10.1016/j.comnet.2009.03.004.
18. Jin P Y, Tanaka S. Reliability Evaluation of a Network with Delay. IEEE Transactions on Reliability 1979; R-28:320-324, http://dx.doi.org/10.1109/TR.1979.5220618.
19. Karagiannis T, Molle M, Faloutsos. Long-range dependence ten years of Internet traffic modeling. IEEE on Internet Computing 2004; 8: 57-64, http://dx.doi.org/10.1109/MIC.2004.46.
20. Karagiannis T. The SELFIS Tool, 2002. http://alumni.cs.ucr.edu/tkarag/Selfis/Selfis.html(accessed10Dec2013).
21. Leland W E, Taqqu M S, Willinger W, Wilson D V. On the self-similar nature of Ethernet traffic. ACM SIGCOMM Computer Communication Review 1993: 183-193, http://dx.doi.org/10.1145/167954.166255.
22. Li R Y, Huang N, Kang R. Modeling and simulation for network transmission time reliability. Reliability and Maintainability Symposium (RAMS) 2010: 1-6.
23. Liu C, Wang T, Zhao C, Xiong H G. Worst-case flow model of VL for worst-case delay analysis of AFDX. Electronics Letters 2012; 48: 327-328, http://dx.doi.org/10.1049/el.2011.4028.
24. Liu Y, Tham C K, Jiang Y M. A calculus for stochastic QoS analysis. Performance Evaluation 2007; 64: 547-572, http://dx.doi.org/10.1016/j.peva.2006.07.003.
25. Ma X M. On the reliability and performance of real-time one-hop broadcast MANETs. Wireless Networks 2011; 17: 1323-1337, http://dx.doi.org/10.1007/s11276-011-0351-x.
26. Meyer J F. Performability evaluation: Where it is and what lies ahead. Computer Performance and Dependability Symposium 1995:334-343.
27. Nadarajah S. Comment on "A general model for long-tailed network traffic approximation". Journal Of Supercomputing 2008; 44(1): 98-101, http://dx.doi.org/10.1007/s11227-007-0150-4.
28. Ramirez-Marquez J E, Coit D W. A Monte-Carlo simulation approach for approximating multi-state two-terminal reliability. Reliability Engineering & System Safety 2005; 87: 253-264, http://dx.doi.org/10.1016/j.ress.2004.05.002.
29. Ridouard F, Scharbarg J L, Fraboul C. Probabilistic upper bounds for heterogeneous flows using a static priority queuing on an AFDX network. IEEE International Conference on Emerging Technologies and Factory Automation(ETFA) 2008: 1220-1227.
30. Rizk A, Fidler M. Non-asymptotic end-to-end performance bounds for networks with long range dependent fBm cross traffic. Computer

Networks 2012; 56: 127-141, http://dx.doi.org/10.1016/j.comnet.2011.07.027.
31. Rizk A, Fidler M. Sample path bounds for long memory FBM traffic. Proceedings IEEE INFOCOM 2010:1-5.
32. Scharbarg J L, Ridouard F, Fraboul C. A probabilistic analysis of end-to-end delays on an AFDX avionic network. IEEE Transactions on Industrial Informatics 2009; 5: 38-49, http://dx.doi.org/10.1109/TII.2009.2016085
33. Vaze R. Throughput-delay-reliability tradeoff in ad hoc networks. Proceedings of the 8th International Symposium on Modeling and Optimization in Mobile, Ad Hoc and Wireless Networks (WiOpt) 2010: 459-464.
34. Wang S P, Sun D, Shi J, Tomovic M. Time delay oriented reliability analysis of Avionics Full Duplex Switched Ethernet. 8th IEEE Conference on Industrial Electronics and Applications (ICIEA) 2013: 982-987.
35. Willinger W, Paxson V, Taqqu M S. Self-similarity and heavy tails: Structural modeling of network traffic. A practical guide to heavy tails: statistical techniques and applications 1998; 23: 27-53.
36. Willinger W, Taqqu M S, Sherman R, Wilson D V. Self-similarity through high-variability: statistical analysis of Ethernet LAN traffic at the source level. ACM SIGCOMM Computer Communication Review 1995; 25: 100-113, http://dx.doi.org/10.1145/217391.217418.
37. Yamkhin D, Won Y. Modeling and Analysis of Wireless LAN Traffic. Journal Of Information Science And Engineering 2009; 25(6): 1783-1801.
38. Yao M, Qiu Z, Kwak K. Leaky bucket algorithms in AFDX. Electronics Letters 2009; 45: 543-545, http://dx.doi.org/10.1049/el.2009.1043.
39. Zeng X, Song D. The research on end-to-end delay calculation method for real-time network AFDX. International Conference on Computational Intelligence and Software Engineering(CiSE) 2009:1-4.

Zhitao WU
Ning HUANG
Ruiying LI
Yue ZHANG
School of Reliability and Systems Engineering, Beihang University
No.37, Xueyuan Road, Haidian District, Beijing, 100191, China
Science and Technology on Reliability and Environmental Engineering Laboratory
No. 37, Xueyuan Road, Haidian District
Beijing, 100191, China
E-mails: wuzt2010@gmail.com, hn@buaa.edu.cn, liruiying@buaa.edu.cn, zybuaa2013@163.com

Article citation info:
TU J, SUN C, ZHANG X, PAN H, CHENG R. Maintenance strategy decision for avionics system based on cognitive uncertainty information processing. Eksploatacja i Niezawodnosc – Maintenance and Reliability 2015; 17 (2): 297–305, http://dx.doi.org/10.17531/ein.2015.2.18.

Jiliang TU
Chengli SUN
Xiangyang ZHANG
Hongliang PAN
Ruofa CHENG

MAINTENANCE STRATEGY DECISION FOR AVIONICS SYSTEM BASED ON COGNITIVE UNCERTAINTY INFORMATION PROCESSING

DECYZJA W ZAKRESIE STRATEGII UTRZYMANIA RUCHU UKŁADU ELEKTRONIKI LOTNICZEJ W OPARCIU O PRZETWARZANIE INFORMACJI ZWIĄZANYCH Z NIEPEWNOŚCIĄ KOGNITYWNĄ

Proper maintenance schedule is required to improve avionics systems reliability and safety. A decision approach to maintenance strategy remains a longstanding challenge in avionics system. With regard to fault diagnosis and equipment maintenance of avionics system, in which the equipment fault information are complex and uncertainty, a multi criteria of decision making method for avionics system based on cognitive uncertainty information processing is proposed to be used in the maintenance strategy decision. Firstly, vague set with three-parameters is introduced to make up for the shortage of the original vague set in expressing fuzzy information, a linguistic variables describing the qualitative indexes into three parameter vague of interval number is proposed. At the same time, due to risk psychological factors of maintenance policymakers that cause cognitive uncertainty are introduced into the maintenance decision process, and a prospect value function of three parameters vague interval value is defined based on prospect theory and the formula for measuring the distance between vague interval value, and a non-linear model of equipment maintenance policies can be established. The implementing process of maintenance policy decision for avionics system based on cognitive uncertainty information processing is given in this paper, and a ranking of the maintenance alternatives is determined. Finally, A specific example of decision of maintenance strategies in avionics system with the application of the proposed method is given, showing that the reliability centered maintenance strategy is the most suitable for avionics system.

Keywords: *The avionics system, Vague sets, Prospect theory, Maintenance strategy, multi criteria decision making*

Doskonalenie niezawodności i bezpieczeństwa układów elektroniki lotniczej wymaga odpowiedniego harmonogramu działań obsługowych. Podejście decyzyjne do strategii utrzymania ruchu od dawna pozostaje wyzwaniem w systemach awioniki. W odniesieniu do diagnozy uszkodzeń i konserwacji urządzeń systemów elektroniki lotniczej, w których informacje o usterkach urządzeń są złożone i obarczone niepewnością, zaproponowano metodę wielokryterialnego podejmowania decyzji opartą na przetwarzaniu informacji związanych z niepewnością kognitywną, którą można stosować przy podejmowaniu decyzji dotyczących strategii utrzymania ruchu. Po pierwsze, wprowadzono nieostry zbiór trzech parametrów, które pozwalają na wyrażenie wartości liczbowej zaproponowanych zmiennych lingwistycznych opisujących wskaźniki jakościowe, jako wartości z przedziału nieostrego. Jednocześnie, do pojęcia procesu decyzyjnego dotyczącego utrzymania ruchu wprowadzono pojęcie ryzyka związanego z powodującymi niepewność poznawczą czynnikami psychologicznymi kierującymi osobami podejmującymi decyzje obsługowe. Zdefiniowano także funkcję oceny dla wartości z przedziału nieostrego trzech parametrów na podstawie teorii perspektywy i wzór do pomiaru odległości między wartościami z przedziału nieostrego, oraz ustalono nieliniowy tryb polityki konserwacji sprzętu. W artykule zaprezentowano proces implementacji decyzji w zakresie polityki konserwacji układów elektroniki lotniczej w oparciu o przetwarzanie informacji związanych z niepewnością kognitywną, stworzono też ranking dostępnych alternatyw w zakresie utrzymania ruchu. Na koniec, zaprezentowano konkretny przykład decyzji w zakresie strategii konserwacji układów elektroniki lotniczej z zastosowaniem proponowanej metody, pokazując, że strategia utrzymania ruchu oparta na niezawodności jest najbardziej odpowiednia dla układów awioniki.

Słowa kluczowe: *układ elektroniki lotniczej, zbiory nieostre, teoria perspektywy, strategia utrzymania ruchu, wielokryterialne podejmowanie decyzji*

1. Introduction

Avionics system is an important part of aircraft, being safe, fast and environmentally friendly, whose failures are among the top five reasons that caused aircraft on ground (AOG) as Seidenman and Spanovich stated [20]. Air Wisconsin and Jet Age Airline claimed that nearly 50% and 30% of AOG (Aircraft On Ground) incidents were related to avionics (particularly to interconnected equipments). Maintenance-related failures have been associated with up to 15% of major aircraft accidents [19]. Despite this seemingly small percentage, but Vassilis Tsagkas [25] found that maintenance related failures are the second leading cause of fatal accidents in aviation exceeded

only by pilot error. In that sense, the importance of maintenance activity has increased due to its key role on improving system availability, performance efficiency, safety and reliability, etc. Thus in order to improve avionics considerations in general, maintenance managers (MM) should take decisions about the maintenance strategies to be implemented as well as the necessary resources to satisfy avionics system performances and requirements.

Satisfactory performance of an aircraft depends up on the continued reliability, security, features enhancements of avionics system. Reliability is proportional to amount of maintenance received and knowledge of men who performed such maintenance [13, 17]. Now, an avionics system may comprise a large number of components, and efficient maintenance strategy is required to improve the reliability of relevant functions and to reduce high maintenance cost. For a long time, both home and abroad have to take preventive tests and routine maintenance to ensure the safe operation of avionics system [7]]. According to Tan & Kramer et al. study, the high cost of maintenance is an important factor in business operations, accounting for approximately 20-50% of the total operating budget of process systems [22]. Thus cost-effective maintenance strategies for avionics system equipment are required. Avionics system maintenance work includes pre-flight checks, post-flight inspection and scheduled maintenance. According to statistics, only 60% of the aircraft total failure can be found with ground inspection, while 40% of the fault is exposed during flight [5]. It is obvious that the integrity of the aircraft with a high rate is difficult to guarantee only with the ground inspection, but due to bad maintenance such as frequent power-on check or ineffective removal of equipment will cause the equipment to reduce the inherent reliability and waste the human and financial resources.

Recent literature in aircraft maintenance safety tends to accept that deviations, uncertainties and surprises are inherent and to a large extent inevitable in maintenance operations [10,23,4]. In the process of avionics systems equipment maintenance, some judgments from maintenance experts or engineers may not be (fully) compatible due to lack of knowledge of the actual use and maintenance of the equipment. In fact, the factors of maintenance strategy are also related to maintenance economic, environmental, social influence and other human factors, there are different degrees of cognitive uncertainty, so the avionics communications systems equipment maintenance program is actually a complex decision problems, involving many factors based on uncertain information processing multiple attribute decision making problems (MADM) [27]. For example, Bevilacqua M. describes an application of the Analytic Hierarchy Process (AHP) for decision the best maintenance strategy for an important Italian oil refinery (an Integrated Gasification and Combined Cycle plant)[23]. In this decision model, when the number of experts on the different levels of equipment maintenance program to make decisions, often difficult to avoid the qualitative, imprecise, incomplete and uncertain information. Over the past years, there have been a number of researchers tempted to develop techniques involving fuzzy set theory to complement conventional system maintenance decision-making [21, 2, 18, 1], where uncertain and imprecise judgments of decision makers are translated into fuzzy numbers. However, in the existing methods, it is seldom considered that attribute value and aspiration-level are in the form of interval numbers. In the real world, the attribute values of alternatives are often uncertain due to estimation inaccuracies and errors in measurement and it is also difficult for the MM to provide a clear aspiration-level. Interval numbers can usually be used to describe uncertain and inaccurate attribute values or aspiration-levels in practical MADM problems [6]. Solve the above problems are in need of repair or engineering technician expert judgment, MM are often at risk for a maintenance program on subjective preferences, then mostly also showed varying degrees of knowledge based on experience and knowledge uncertainty, but the existing methods sufficiently consider the important role of the aspiration-level in decision analysis.

Fortunately, a powerful tool, vague sets theory [8] is available and it has been extensively adopted in the fields of decision making. It is emerging as an efficient tool in managing uncertainty, incomplete and imprecise information. For the sake of characteristic with the vague set of membership have the two aspects of information, which makes the vague set have more advantages than traditional fuzzy sets in the treatment of cognitive uncertainty information. Jue Wang and Wei Xu [14] provides a soft and expansive way to help the decision maker in NSFC to make his decision based on vague set theory. They also introduced a family of intersection and union aggregation operators for vague values. In choosing a maintenance plan of engineering practice, maintenance experts often base on different decision criteria for maintenance scheme judgment when using language form to give its personal preference information. The use of vague sets and the concept of interval numbers can well express the MM's fuzzy decision-making process. Because of the decision-making problems for maintenance strategy are usually risky and uncertain, it is necessary to consider the MM's psychological behavior in decision analysis. Therefore, it is urgent to investigate the risk decision analysis methods considering human behavior for the purpose of providing effective decision support to the MM in maintenance strategy. Tversky and Kahneman [24] put forward the prospect theory, which can more accurately reflect the risk when facing maintenance plan decision preference psychological characteristics, through the value function and the decision weighting function to calculate the comprehensive prospects of different maintenance schemes under different criteria values to prioritize. Each maintenance scheme allows the theory to a more scientific description of uncertainty in the actual circumstances experts or engineering technical personnel in the maintenance scheme decision-making behavior. The objective of this paper is to develop a method based on the research of vague set and prospect theory to solve the MADM problem considering aspiration-levels. The paper combines the two theories in cognitive uncertainty information processing advantages, and builds a kind of based on Vague language variables of three parameter sets to describe the maintenance decision makers in the criteria weights information incomplete solution under the circumstance of the fuzzy interval value.

The rest of this paper is arranged as follows. Section 2 gives a brief introduction to vague set and prospect theory. Section 3 provides a brief introduction on avionics and its hierarchy structure. Section 4 describes the formulation and the resolution procedure of the maintenance strategy decision problem considering aspiration-levels based on vague set. In Section 5, a decision making example is given to illustrate the specific implementation process of the proposed method for verify its validity and rationality. The outcomes of the research and future research recommendations are presented in the final section.

2. Concept of Vague Sets and Prospective Theory

In practice, interval number is often used to present uncertainty information. The basic concept of vague set theory is as follows [8]. Let a set X be a finite universe of discourse, then a fuzzy set A $A = \{< x, \mu_A(x) > | x \in X\}$ defined by Zadeh is characterized by a membership function $\mu_A : X \to [0,1]$,where μ_A denotes the membership degree of the element x to the set A.

Definition 1. Concerning the domain $X = \{x_1, x_2, ..., x_n\}$, Vague set A by true membership function and false membership function is described. $t_A : X \to [0,1]$, $f_A : X \to [0,1]$, which is the recognition by the evidence of $x_i \in X$ membership degree lower bound, by against $x_i \in X$ negative membership degree and lower bounds of the evidence, and $0 \le t_A + f_A \le 1$. Elements x_i in Vague set A of membership degree by the interval $[0,1]$ show as follows: $A = \{< x, t_A(x), 1 - f_A(x) > | x \in X\}$.

Definition 2. (three parameters of Vague set)) $\forall x \in X$, $\tilde{t}_A = \frac{1-f_A+t_A}{2} + \gamma \bullet (1-f_A-t_A)$ is called for x relative to A maximum likelihood measurement, known as the nucleus of Vague set, where $|\gamma| \le 0.2$. By the known, x relative to A subordinate situation should adopt three-dimensional parameter interval $[t_A, \tilde{t}_A, 1-f_A]$.

Definition 3. $\forall x,y \in X$, if $x=[t_A, \tilde{t}_A, t_A^*]$, $y=[t_B, \tilde{t}_B, t_B^*]$, where $t_A^*=1-f_A$, $t_B^*=1-f_B$. Now we consider the distance measure between Vague A and vague B is given as follows:

$$d_\lambda(A,B) = \lambda|t_A - t_B| + \lambda|t_A^* - t_B^*| + (1-2\lambda)|\tilde{t}_A - \tilde{t}_B| \quad (1)$$

The parameter λ representing the weight of decision interval value, namely the importance of three parameters interval Vague left and right endpoint and the maximum degree of membership. In this paper, the three parameter importance degree are the same equal, where $\lambda = 1/3$.

Due to human thinking is fuzzy, the cognitive uncertainty and complexity of the decision-making problem, experts in maintenance of maintenance schemes under different decision criteria to determine the language form is given preference information is universal and convenient. Experts in maintenance give their judgments on criteria of alternatives in linguistic terms. Therefore, the linguistic variables of judgments on criteria are inconsistent, and the complexity of this issue will be increased. In order to simplify the treatment of judgments expression, a unified set of linguistic variables is predetermined in this paper, which can be used to evaluate every criterion from the satisfaction perspective. The general linguistic term set used in the questionnaires consists of the following seven terms, i.e. very low (VL), low (L), relatively low (RL), medium (M), relatively high (RH), high (H), and very high (VH).To get the quantitative evaluation of value, the linguistic term can be quantified with three parameters interval numbers in definition (2). The way to determine the vague values of linguistic variables are various, but all of these methods basically ignore the impact of possible degree [26].

Table 1. The scale of linguistic variables and the corresponding vague interval numbers

linguistic variables	t_A	f_A	$\tilde{t}_A$	1- f_A	Three parameters interval Vague $\gamma = 0.1$
(VL)	0	0.9	0.06	0.1	[0, 0.06, 0.1]
(L)	0.1	0.75	0.19	0.25	[0.1, 0.19, 0.25]
(RL)	0.25	0.55	0.37	0.45	[0.25, 0.37, 0.45]
(M)	0.45	0.45	0.51	0.55	[0.45, 0.51, 0.55]
(RH)	0.55	0.25	0.67	0.75	[0.55, 0.67, 0.75]
(H)	0.75	0.1	0.84	0.9	[0.75, 0.84, 0.9]
(VH)	0.9	0	0.96	1	[0.9, 0.96, 1]

In this paper, a linguistic assessment set of ideas for quantitative is provided, the reference value of truth-membership t_A of each linguistic variable is per-determined, and the false-membership degree f_A is given with linguistic judgment. In the end, the membership of maximum possible degrees $\tilde{t}_A$ is also determined by the definition (2). So the three parameters interval Vague of seven level language variables in this paper is established, the process is seen in Table 1.

2.2. Concept of prospect theory

According to prospect theory, a decision process consists of two phases: the editing phase and the evaluation phase. In the editing phase, outcomes of alternatives are coded as gains or losses relative to a reference point. In the evaluation phase, the edited prospects are evaluated by a value function and a weighting function, and the prospect of highest value is chosen.

We suppose a gamble is composed of n potential monetary outcomes $x_1, x_2, ..., x_n$ with probabilities $p_1, p_2, ..., p_n$, where x_i is potential outcome and p_i is the probability of potential outcome , Thus, the prospect is defined as the ordered pair f and the prospect value of the gamble is given by [28].

$$V(f) = \sum_{i=1}^{n} \pi(p_i) v(x_i) \quad (2)$$

where $v(x_i)$ is the value of potential outcome x_i, $\pi(p_i)$ is the decision weight for the value of potential gain or loss x_i. $v(x_i)$ can be represented by [28]:

$$v(x_i) = \begin{cases} x^\alpha, x \ge 0; \\ -\theta(-x)^\beta, x < 0. \end{cases} \quad (3)$$

Where α and β quantify the degree of diminishing sensitivity for gain and loss, θ quantifies the degree of loss aversion. It has been widely recognized that loss-aversion factor θ should be greater than 1, which indicates that individuals are more sensitive to losses than gains [15].

Definition 4. Suppose $v_A = [t_A, \tilde{t}_A, t_A^*]$ and $v_B = [t_B, \tilde{t}_B, t_B^*]$ denote the two Vague set by use of three parameter interval number respectively, if the interval number as a reference point, then the prospect value with interval number is given below:

$$V(d_\lambda(v_A, v_B)) = \begin{cases} (d_\lambda(v_A, v_B))^\alpha, v_A \ge v_B; \\ -\theta(d_\lambda(v_A, v_B))^\beta, v_A < v_B. \end{cases} \quad (4)$$

3. Hierarchy of Avionics System

To clearly describe the avionics maintenance strategy decision problem, we first define avionics system hierarchy structure. Avionics System can be divided into three system levels, system, subsystem and component, which are involved in this paper. The three system levels can be defined as follows [19]: (1) a system is a combination of subsystems that complete a task together, (2) a subsystem consists of components, which can perform a specific function of the system, and (3) a component is an operating part of the subsystem. Taken a domestic avionics as an example(see Fig.1),the avionics system can be divided into seven subsystems according to their functions and operational characteristics, which is made up of subsystems including flight control subsystem, engine control subsystem, cockpit control-display subsystem, energy control subsystem, fuel and LG(landing gear) control subsystem, cabin control subsystem and airborne network subsystem. These subsystems can be further broken down to components. For example, the flight control subsystem contains three FCGC (flight control and guidance computer) and three FCSC (flight control secondary computer), and the airborne network subsystem involves ES

(end system) and switches. The others abbreviations note: AC–Air Conditioning; ACR–Avionics Communication Router; ADIRU–Air Data Inertial Reference Unit; CDIS–Cabin Data Intercommunication System; EEC–Engine Electronic Control; ELM–Electrical Load Management; FM–Flight Management; IPCU–Ice Protection Control Unit; IRDC–Intelligent Remote Data Concentrator. Due to the complexity, the avionics contractor usually subcontracts the avionic subsystems and even components to several subcontractors for further design and manufacturing.

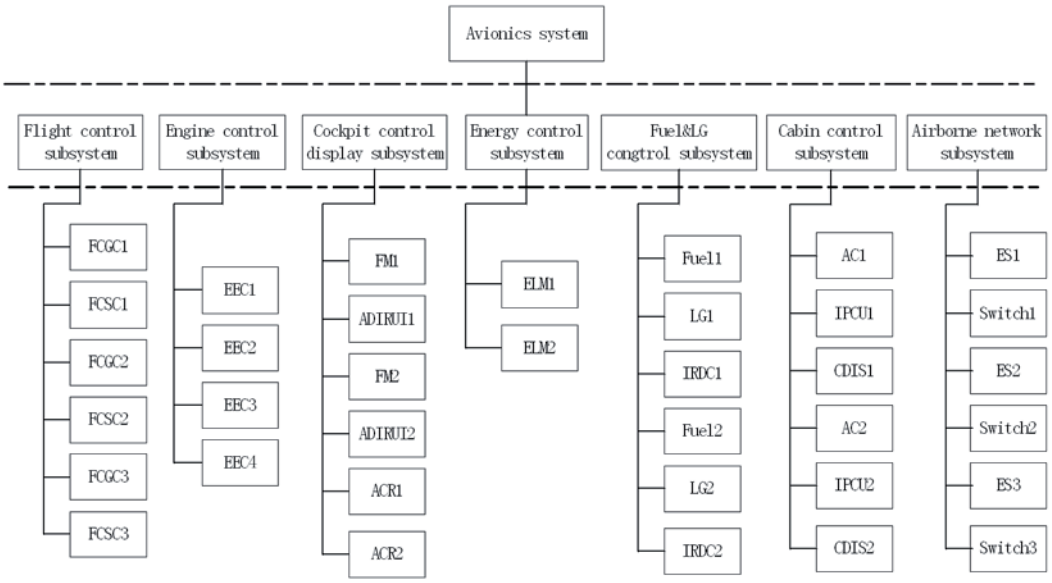

Fig. 1. The hierarchy of Avionics system

On the original organic basis, the system expands the scope of monitoring to improve the data collection, storage, distribution, and uses the data link to send the data package to data processing terminal in the ground station. Nowadays, avionic subsystems and components are interconnected through an airborne network consist of the air-ground access devices and the air-ground communication transmission system, via which both the information and the function integrations are realized. The air-ground access devices are responsible for information acquisition, information composition, information decomposition, information encoding, information decoding, and information transmission security mechanism. For example, the engine data captured by the engine control subsystem must be transmitted to the cockpit control-display subsystem, and then the pilot can receive the engine information for further decision making. The data transmission plays a key role in the avionic system, and one or more data transmission used to complete a specified function (e.g. reception of the engine data, display the atmospheric pressure) is defined as a mission. This can guarantee a safe, reliable and real-time information transmission. It is obvious that the maintenance strategy decision of avionics is a multi-mission problem.

4. The implementing process of the proposed approach

4.1. Prepare the maintenance plan and decision attribute

Subsystems with unacceptable risks are identified after risk evaluation. Equipment in these subsystems is regarded as high risk equipment. Proper maintenance plans should be performed to reduce the equipment failure probability. In this paper, a general maintenance decision-making strategy is proposed by considering both avionics systems degradation and hierarchy structure. The maintenance effect in the follows was considered to be perfect, though it is always imperfect in practice [11]. Periodic preventive maintenance (PM) is applied to some key equipment. Corrective maintenance (CM) and PM are considered to be imperfect maintenance, since they generally only repair failed or faulty components; Condition-based maintenance (CBM), shortly described, is maintenance when need arises. This maintenance is performed after one or more indicators show that equipment is going to fail or that equipment performance is deteriorating [16]. This concept is applicable to mission critical systems that incorporate active redundancy and fault reporting. First and most important of all, the initial cost of CBM can be high. It requires improved instrumentation of the equipment. To reduce the economic risk due to unexpected failures, the risk-based maintenance (RBM) strategy is applied to determine the proper interval of periodic PM for each piece of equipment at a cost of probably low maintenance expenditure. According to the reliability limits, the interval of periodic PM for key equipment was obtained under the condition that the default maintenance effect is perfect. Reliability Centered Maintenance (RCM) analysis provides a structured framework for analyzing the functions and potential failures for a physical asset (such as an airplane, a manufacturing production line, etc.) with a focus on preserving system functions, rather than preserving equipment. RCM is used to develop scheduled maintenance plans that will provide an acceptable level of operability, with an acceptable level of risk, in an efficient and cost-effective manner.

Probabilistic approaches constitute the most reasonable way to deal with the various uncertainties inherent to this task. Several indicators have been proposed during recent years to represent the time dependent structural performance of deteriorating structures [9].Once the future condition of the device estimated effectively applying probability forecasting model, the equipment failure rate at a certain time, reliability function, or residual life distribution function has been obtained. A maintenance decision model can be established in accordance with the economy, equipment availability, risk and other criteria, and the optimal strategy [12].

4.2. Flowchart of maintenance strategy decision

According to the above research content in this paper, the maintenance policy decision for avionics system based on cognitive uncertainty information processing can be description as follows, the implementing process of this proposed approach in this paper is shown by flow chart in Fig. 2 and details process are given here after.

Step 1: Collected the maintenance records and historic failure data

First step of the technique is the information extraction phase in which information is extracted from various sources. Information in the form of system components' failure rates and repair times are extracted from various sources such as historical maintenance records, reliability databases, system reliability expert opinion, etc. In decision-making process, based on the fault information provided by the

diagnosis and prediction program, the decision is made according to if the faulty equipment is needed to be repaired and when to be repaired, and analysis accounting about maintenance costs and repair working time calculation.

Step 2: ascertain the range of attribute weights

Decision making problem in avionics system equipment maintenance, maintenance experts often according to their own maintenance experience and skills, for maintenance scheme under different criteria values are formed certain risk forecast, such expectations can be considered as maintenance decision makers with reference to the risk behavior characteristics of the formation of the reference point, so the maintenance plan is called a reference. According to the reference service solutions can measure the maintenance of gains and losses. Because 5 set of evaluation index are efficiency index, which requires the bigger is the better. Each attribute weight is not entirely sure, but its range of decision attribute weights for avionics system be set as follows :

$$H:\{0.25 \le w_1 \le 0.32, 0.25 \le w_2 \le 0.3, 0.15 \le w_3 \le 0.2, \\ 0.18 \le w_4 \le 0.22, 0.06 \le w_1 \le 0.15\} \tag{5}$$

And all weight must be meet the requirement: $w_1 + w_2 + w_3 + w_4 + w_5 = 1$. Under the condition of above-mentioned cognitive uncertainty information to determine each strategy of the equipment maintenance plan set A sorting, which choice satisfies the requirement of decision-making of maintenance plan.

Step 3 : Express the corresponding vague interval numbers of each maintenance policy

MMs give their judgments on criteria of alternatives in linguistic terms. Vague set theory is used to give styles of judgments and transform linguistic judgments into vague numbers. The original judgment information is in the form of linguistic variable. In general, linguistic variables are pre-determined. We can set to equipment maintenance plan, as norm constraint set, and assumes that plan under rule constraint set values are given in the form of language variable, by maintenance specialist again by definition vague converts it to three parameters interval number 2, can be represented as:

$$a_i = \{a_{i1},...,a_{i5}\} = \left\{(c_1,[t_{i1},\tilde{t}_{i1},t_{i1}^{*}]),(c_2,[t_{i2},\tilde{t}_{i2},t_{i2}^{*}]),...,(c_5,[t_{i5},\tilde{t}_{i5},t_{i5}^{*}])\right\} \tag{6}$$

When choosing positive and negative ideal solution maintenance, relatively Vague interval number nuclear first, think scheme is optimal, the greater the second comparison, two Vague interval number and the same, if you have more scoring function, also value the bigger the better. Based on the positive ideal solution (PIS) and negative ideal solution (NIS) as a reference for maintenance plan, get:

$$\left.\begin{aligned} G = (G_1,...,G_5) &= ([t_1^{+},\tilde{t}_1^{+},t_1^{*+}],[t_2^{+},\tilde{t}_2^{+},t_2^{*+}],...,[t_5^{+},\tilde{t}_5^{+},t_5^{*+}]) \\ B = (B_1,...,B_5) &= ([t_1^{-},\tilde{t}_1^{-},t_1^{*-}],[t_2^{-},\tilde{t}_2^{-},t_2^{*-}],...,[t_5^{-},\tilde{t}_5^{-},t_5^{*-}]) \end{aligned}\right\} \tag{7}$$

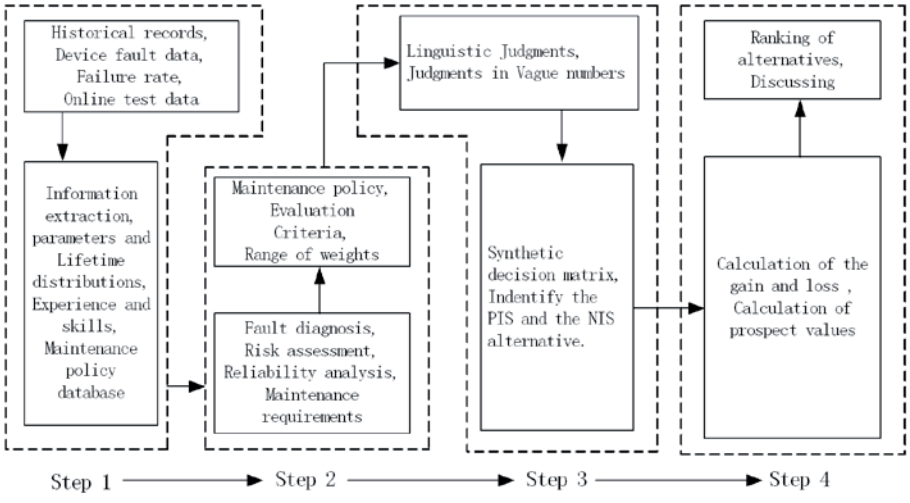

Fig. 2. The flowchart of the proposed approach

Step 4: Maintenance plan decision based on Prospect theory

(1) Calculation of the gain and loss for maintenance policy

According to the definition of Vague distance calculation formula for each maintenance scheme for degree to the positive and negative ideal solution (distance),

$$d(a_i,G) = \{d(a_{i1},G_1),d(a_{i2},G_2),...,d(a_{i5},G_5)\},$$

$$d(a_i,B) = \{d(a_{i1},B_1),d(a_{i2},B_2),...,d(a_{i5},B_5)\}$$

According to definition (4), maintenance solution can be got under the rule of the value of future utility value function:

$$v(a_{ij}) = \begin{cases} (d(a_{ij},B_j))^{\alpha}, B_j \in B \\ -\theta(d(a_{ij},G_j))^{\beta}, G_j \in G \end{cases} \tag{8}$$

(2) Calculation of the prospect values of each maintenance plan

To maintenance scheme for the reference point is ideal, the maintenance plan is inferior to ideal solution, maintenance for decision makers, is facing losses, the policy makers to pursue risk right now, will plug in formula (3), can get it:

$$v^{-}(d(a_{ij},G_j)) = -\theta(d(a_{ij},G_j))^{\beta} \tag{9}$$

Take Negative ideal maintenance plan as a reference point in this paper, because of the repair scheme a_i is better than negative ideal repair scheme, so the decision makers are faced with profit, MMs will avoid the risk at this time according to prospect theory. For the situation that attribute value and aspiration-level are in the form of interval numbers, we give the following formula:

$$v^{+}(d(a_{ij},B_j)) = (d(a_{ij},B_j))^{\alpha} \tag{10}$$

In summary, by Equation (8) and (9), the calculation formula of gain for Positive V^{+} and negative V^{-} prospect matrix is expressed by:

$$V_i = \sum_{j=1}^{5} v(a_{ij})^{+}\pi^{+}(w_j) + \sum_{j=1}^{5} v(a_{ij})^{-}\pi^{-}(w_j) \tag{11}$$

Where, $\pi^+(w_j)$, $\pi^-(w_j)$ denote the weighting functions of maintenance strategy for gains and losses, respectively, and they are given by formula (11) and (12).

$$\pi^+(w_j)=\frac{{w_j}^{\gamma^+}}{({w_j}^{\gamma^+}+(1-w_j)^{\gamma+})^{1/\gamma^+}} \tag{12}$$

$$\pi^-(w_j)=\frac{{w_j}^{\gamma^-}}{({w_j}^{\gamma^-}+(1-w_j)^{\gamma^-})^{1/\gamma^-}} \tag{13}$$

where, γ^+, γ^- are model parameters, $\pi^+(w_j)$ and $\pi^-(w_j)$ are monotonic and exhibit inverse S-shapes for γ^+>0.27, γ^->1. They are adequate for average decision-making behavior (i.e., overweight the outcomes with low probabilities and underweight the outcomes with moderate and high probabilities)

(3) Ranking alternatives and discussion

In order to more accurately determine the advantages and disadvantages of various maintenance scheme of quantitative evaluation, decided in the comprehensive prospect calculate each maintenance plan value, must come from the same criteria weight vector set $W=\{w_1,w_2,w_3,w_4,w_5\}$ .The weight of each criterion maintenance schemes decision value can be selected according to expert experience or through the analytic hierarchy process. In this paper, combined with the calculation process in prospect theory value show that calculation criterion weight should guarantee comprehensive prospect value of all maintenance scheme sets is optimal. Therefore, based on this point, based on the above theoretical analysis process, the maintenance scheme decision optimization model is established in this paper as follows:

$$\begin{aligned}&\max V=\sum_{i=1}^{5}\sum_{j=1}^{5}v(a_{ij})^+\pi^+(w_j)+\sum_{i=1}^{5}\sum_{j=1}^{5}v(a_{ij})^-\pi^-(w_j)\\&S.T.\quad\sum_{i=1}^{5}w_i=1,w_i\geq 0,w\in H.\end{aligned} \tag{14}$$

According to the maintenance decision-making model, criterion weights of the optimal solution $w^*=\{w_1^*,w_2^*,w_3^*,w_4^*,w_5^*\}$ can be got. Then according to the formula (10) – formula (12), the maintenance scheme a_i can be got comprehensive value outlook. Then according to the size of the prospect of comprehensive value, and can carry on the order maintenance plan of all set, to determine the optimal maintenance plan. Obviously, the greater overall prospect value V is, the better Maintenance scheme A will be. Therefore, based on the overall prospect values, we can determine the ranking of response actions and select the most desirable action for reducing the consequent negative effect of maintenance scheme.

5. Case Analysis

In order to validate the proposed based on the cognition of uncertain information processing Aeronautical wireless communication system decision making method, the feasibility and effectiveness of equipment maintenance in front of the parking preventive test for the maintenance scheme decision-making system equipment. In order to guarantee the correctness of the decision, before the decision by the engineering and maintenance personnel for each equipment testing and reliability evaluation system, check the equipment operation records report, again through the laboratory test data of the equipment operation, field testing and other testing methods, the results were not found abnormal, can be used after the maintenance strategy. The decision-making process is as follows:

Step 1: Parameters of the failure distribution and maintenance effect are estimated from maintenance records. The two-parameter Weibull distribution is a general distribution widely used to model processes such as failure due to aging and wear. Maintenance records from different observation periods are collected together to obtain more accurate estimation. Parameter uncertainty often implies that maintenance should be performed more frequently, especially if the parameter uncertainty constitutes a large fraction of the total uncertainty and if preventive maintenance costs are low. The more frequent maintenance actions ensure that costly failures are unlikely to occur. An immediate consequence, however, is that hardly any failure data will be collected, sustaining the uncertainty. If one aims to reduce this uncertainty, maintenance actions should be postponed or, if this is undesirable, tests should be performed in a controlled setting.

Step 2: By the on-line monitoring at any time of avionics system, through equipment fault diagnosis system and state trend forecasting system, we can diagnose the avionics system facilities of latent fault and its development trend. From a macro point of view, based on the implementation of the avionics system at home and abroad widely used to CBM, PM, CM, RBM and RCM, 5 kinds of maintenance policy can be referred to as follows:

$$A=\{a_1,a_2,a_3,a_4,a_5\} \tag{15}$$

where, a_1 is CBM, a_2 is PM, a_3 is CM, a_4 is RBM, a_5 is RCM.

Avionics systems equipments of safety indicators characterizing the influence of the equipment fault on the person, other related equipment and operating environment adversely; Reliability can measure the ability of the equipment to accomplish the required task in conditions within the prescribed time and under the provisions; Maintainability said occurred in the time of equipment failure, the provisions ability which can back to the specified function within the time specified under the maintenance condition equipment, while maintenance cost is considered as another indicators related to the economy (e.g. spare parts' costs, external party services, financial penalties) and the availability is considered as a local objective related to the maintenance efficiency, reinstall the removed and inspect it. (Restart the task).So, a multi-attribute maintenance decision-making model based on multiple attribute value theory is proposed to give an overall objective to determine the optimal maintenance policy. The attribute set are shown as follows:

$$C=\{c_1,c_2,c_3,c_4,c_5\} \tag{16}$$

where, c_1 is indicator of system safety, c_2 is Reliability, c_3 is Maintainability, c_4 is maintenance economy, c_5 is availability.

Step 3: maintenance organization are maintenance countermeasures of each set of linguistic variables set, get the corresponding evaluation index of language variable, then in turn according to Table 1 for conversion method due to Vague language variables set with corresponding three parameters interval number. According to the reference solution definition, determine the positive and negative ideal scheme, the data are shown in Table 2.

Step 4*:* According to prospect theory, we firstly regard aspiration-levels as reference points. Then, gains and losses of alternatives are calculated by measuring perceived differences of attribute values from reference points (aspiration-levels).

Table 2. The corresponding vague interval numbers of each maintenance policy

Alternatives	c_1	c_2	c_3	c_4	c_5
a_1	[0.55,0.67, 0.75]	[0.1, 0.19, 0.25]	[0.25,0.37, 0.45]	[0.25,0.37, 0.45]	[0.1, 0.19, 0.25]
a_2	[0.75, 0.84, 0.9]	[0.45,0.51, 0.55]	[0.25,0.37, 0.45]	[0.25,0.37, 0.45]	[0.45,0.51, 0.55]
a_3	[0.75, 0.84, 0.9]	[0.55,0.67, 0.75]	[0.45,0.51, 0.55]	[0.55,0.67, 0.75]	[0.45,0.51, 0.55]
a_4	[0.55,0.67, 0.75]	[0.55,0.67, 0.75]	[0.25,0.37, 0.45]	[0.25,0.37, 0.45]	[0.55,0.67, 0.75]
a_5	[0.9, 0.96, 1]	[0.55,0.67, 0.75]	[0.55,0.67, 0.75]	[0.55,0.67, 0.75]	[0.55,0.67, 0.75]
G	[0.9, 0.96, 1]	[0.55,0.67, 0.75]	[0.45,0.51, 0.55]	[0.55,0.67, 0.75]	[0.55,0.67, 0.75]
B	[0.55,0.67, 0.75]	[0.1, 0.19, 0.25]	[0.25,0.37, 0.45]	[0.25,0.37, 0.45]	[0.1, 0.19, 0.25]

(1) To determine the maintenance plan and the distance of the positive and negative ideal solution (degree), calculated value function as follows:

$$d(a_1,G)=\{d(a_{11},G_1),d(a_{12},G_2),...,d(a_{15},G_5)\}=\{0.297,0.477,0.147,0.3,0.477\},$$

$$d(a_2,G)=\{d(a_{21},G_1),d(a_{22},G_2),...,d(a_{25},G_5)\}=\{0.123,0.153,0.147,0.3,0.153\},$$

$$d(a_3,G)=\{d(a_{31},G_1),d(a_{32},G_2),...,d(a_{35},G_5)\}=\{0.123,0,0,0,0.153\},$$

$$d(a_4,G)=\{d(a_{41},G_1),d(a_{42},G_2),...,d(a_{45},G_5)\}=\{0.297,0,0.147,0.3,0\},$$

$$d(a_5,G)=\{d(a_{51},G_1),d(a_{52},G_2),...,d(a_{55},G_5)\}=\{0,0,0.153,0,0\},$$

$$d(a_1,B)=\{d(a_{11},B_1),d(a_{12},B_2),...,d(a_{15},B_5)\}=\{0,0,0,0,0\},$$

$$d(a_2,B)=\{d(a_{21},B_1),d(a_{22},B_2),...,d(a_{25},B_5)\}=\{0.173,0.323,0,0,0.323\},$$

$$d(a_3,B)=\{d(a_{31},B_1),d(a_{32},B_2),...,d(a_{35},B_5)\}=\{0.173,0.477,0.147,0.3,0.323\},$$

$$d(a_4,B)=\{d(a_{41},B_1),d(a_{42},B_2),...,d(a_{45},B_5)\}=\{0,0.477,0,0,0.477\},$$

$$d(a_5,B)=\{d(a_{51},B_1),d(a_{52},B_2),...,d(a_{55},B_5)\}=\{0.297,0.477,0.3,0.3,0.477\}.$$

The above calculation results fed into formula (9) and formula (10) to obtain the prospects of each maintenance scheme under different criterion utility value. According to the experimental results given by Tversky and Kahneman [15], the value of the function of each parameter is given as follows:

$\alpha=\beta=0.88$, $\theta=2.25$, therefore:

$$v^{-}(d(a_{ij},G_j))=\text{-}2.25(d(a_{ij},G_j))^{0.88}$$

$$v^{+}(d(a_{ij},B_j))=(d(a_{ij},B_j))^{0.88}$$

(2) According to the above results, by the calculation formula (9) and (10), gain matrix V^{+} and loss matrix V^{-} are constructed, respectively, i.e.,

$$V^{-}=\begin{bmatrix} -0.773 & -1.173 & -0.416 & -0.779 & -1.173 \\ -0.356 & -0.192 & -0.416 & -0.779 & -0.192 \\ -0.356 & 0.0000 & 0.0000 & 0.0000 & -0.192 \\ -0.773 & 0.0000 & -0.146 & -0.779 & 0.0000 \\ 0.0000 & 0.0000 & -0.192 & 0.0000 & 0.0000 \end{bmatrix}$$

$$V^{+}=\begin{bmatrix} 0.000 & 0.000 & 0.000 & 0.000 & 0.000 \\ 0.214 & 0.370 & 0.000 & 0.000 & 0.370 \\ 0.214 & 0.521 & 0.185 & 0.347 & 0.370 \\ 0.000 & 0.521 & 0.000 & 0.000 & 0.521 \\ 0.344 & 0.521 & 0.347 & 0.347 & 0.521 \end{bmatrix}$$

(3) Calculate the overall prospect value of each alternative and confirm the ranking order of alternatives according to the obtained overall prospect values. The prospect of plus or minus value matrix into the horizon optimization model (14), at the same time, according to the formula (12) and formula (13).Many scholars had paid great attention to the parameter estimation of weighting function. Tversky and Kahneman estimated parameters using median data which suggested the median values of $\gamma^{+}=0.61$, $\gamma^{-}=0.69$ [15]. Their estimation results were reasonably close to each other. The essential characteristics of weighting function (i.e., underweighting of high probabilities and inflation of small probabilities) were the same, and the degrees of distortion were almost the same.

The optimal criteria weight vector $w^{*}=\{0.28,0.25,0.16,0.2,0.11\}$ can be convenient deprived from the nonlinear optimization programming by using matlab 7.0 software. According to the formula (12) and formula (13), the each decision maintenance policy of the profit and loss probability weighting function can be obtained:

$$\pi^{+}(w_j)=\{0.308,\ 0.291,\ 0.234,\ 0.261,\ 0.195\},$$

$$\pi^{-}(w_j)=\{0.314,\ 0.293,\ 0.225,\ 0.257,\ 0.18\ \}.$$

Further, using the formula (11), The overall prospect value of each maintenance policy can be obtained, i.e.,

$V(a_1)=-1.091$, $V(a_2)=-0.4964+0.2457=-0.251$,
$V(a_3)=-0.1463+0.4235=0.277$, $V(a_4)=-0.4758+0.2532=-0.223$,
$V(a_5)=-0.0432+0.5309=0.488$.

Finally, MM select the maintenance strategy with the highest prospect value in evaluation phase. Therefore, according to the overall prospect value of maintenance strategy, a ranking order of the five alternatives is $a_5>a_3>a_4>a_2>a_1$, obviously, RCM policy can be as the basis of schedule avionic system equipment maintenance, the decision results conform to the avionic system in maintenance of actual engineering standards. With this information managers could easily focus where to put efforts: on the implementation of a maintenance strategy, on the implementation of redundancy, in optimizing the spare of stocks, etc.

Conclusions

Maintenance strategy plays a key role in reducing cost, minimizing equipment downtime, improving quality, increasing safety and providing reliable equipment and as a result achieving organizational goals and objectives for avionic system. The purpose of this paper is to present an approach for deciding on an appropriate maintenance strategy decision for avionics system. The issue of avionic system maintenance strategy decision is not just a cost-oriented issue, and it should be consider safety, reliability, cost, and other quality aspects. This paper has presented a method based on vague sets and prospect theory to solve maintenance strategy decision problems considering aspiration-levels under cognitive uncertainty information circumstance. It can deal with DM's vague and uncertain judgment where uncertain and imprecise judgments of decision makers are translated into vague interval numbers with three parameters. From definition in Section 2, it can be concluded that vague set theory is superior to fuzzy set theory in dealing with cognitive uncertain and vague information in decision-making. Compared with the traditional behavioral economics theories, prospect theory is more conform to the characteristics of human behavior, providing an appealing way to understand individual attitudes under risk and uncertainty. The parameterized prospect theory, involved the MM's risk attitudes of maintenance policy choice behavior, was simple and effective to evaluate alternative policy under dynamic maintenance information. According to prospect theory, MM's aspiration-levels are regarded as the reference points. By measuring the perceived difference between the attribute value and the reference point, gain and loss of each alternative are assessed, and the prospect value of each alternative is calculated. Ranking result of alternatives can be determined according to the prospect values. In the proposed method, it is a valuable attempt to incorporate prospect theory and vague set into maintenance policy decision analysis.

As demonstrated by this case study, our method proposed in this paper is a simple and effective tool for tackling the uncertainty and imprecision associated with MADM problems of maintenance decision for avionics system, which might prove beneficial for plant maintenance managers to define the optimum maintenance strategy for each piece of system or subsystem equipment.

Acknowledgements

Authors gratefully acknowledge the financial support provided by the National Natural Science Foundation of China (Grant No. 51167013),Natural Science Foundation of Jiangxi Province(Grant No. 20142BAB207002) and Aeronautical Science Foundation of China (Grant No.20142056005), especially the research fund for the doctoral program of higher education of NCHU, Jiang Xi, China (Project No.EA201304348).The authors would also like to express their grateful appreciation to the anonymous referees for their helpful comments to improve the quality of this paper.

References

1. Al-Najjar B, Alsyouf I. Selecting the most efficient maintenance approach using fuzzy multiple criteria decision making. International Journal of Production Economics 2003;84:85-100, http://dx.doi.org/10.1016/S0925-5273(02)00380-8.
2. Azizollah Jafari, Mehdi Jafarian, Abalfazl Zareei. Using Fuzzy Delphi Method in Maintenance Strategy Selection Problem. Jouranl of Uncertain system 2008; 2(4): 289-298.
3. Bevilacqua M., Braglia M.. The analytic hierarchy process applied to maintenance strategy selection. Reliability Engineering and System Safety 2000;70(1):71-83, http://dx.doi.org/10.1016/S0951-8320(00)00047-8.
4. Bram de Jonge, Warse Klingenberg, Ruud Teunter, Tiedo Tinga. Optimum maintenance strategy under uncertainty in the lifetime distribution. Reliability Engineering and System Safety, 2015;133(2):59–67, http://dx.doi.org/10.1016/j.ress.2014.09.013.
5. Dehuang Chen, Xiaowei Wang, Jing Zhao. Aircraft Maintenance Decision System Based on Real-time Condition Monitoring. Procedia Engineering 2012;29 (1): 765 – 769, http://dx.doi.org/10.1016/j.proeng.2012.01.038.
6. Echefske Chris K, Wang Zheng. Using fuzzy linguistics to select optimum maintenance and condition monitoring strategies. Mechanical Systems and Signal Processing 2003;17(2): 305-316, http://dx.doi.org/10.1006/mssp.2001.1395.
7. Elix C Go'mez de Leo'n Hijes, JOSE´ Javier Ruiz Cartagena. Maintenance strategy based on a multicriterion classification of equipments. Reliability Engineering and System Safety 2006, 91:444-451, http://dx.doi.org/10.1016/j.ress.2005.03.001.
8. Gau, W.L., Buehrer, D.J. Vague sets. IEEE Transactions on Systems, Man and Cybernetics 1993; 23 (2): 610–614, http://dx.doi.org/10.1109/21.229476.
9. Giorgio Barone, Dan M.Frangopol. Life-cycle maintenance of deteriorating structures by multi-objective optimization involving reliability, risk, availability, hazard and cost. Structural Safety 2014;48 (3): 40-50, http://dx.doi.org/10.1016/j.strusafe.2014.02.002.
10. G. Medina-Oliva,P.Weber, B.Iung.Industrial system knowledge formalization to aid decision making in maintenance strategies assessment. Engineering Applications of Artificial Intelligence 2015;37(1):343–360, http://dx.doi.org/10.1016/j.engappai.2014.09.006.
11. Haijun Hua, Guangxu Cheng, Yun Li, Yiping Tang. Risk-based maintenance strategy and its applications in a petrochemical reforming reaction system. Journal of Loss Prevention in the Process Industries 2009;22 (2): 392–397, http://dx.doi.org/10.1016/j.jlp.2009.02.001.
12. Hai Canh Vu, Phuc Do, Anne Barros, Christophe Bérenguer. Maintenance grouping strategy for multi-component systems with dynamic contexts. Reliability Engineering and System Safety 2014;132(1):233–249, http://dx.doi.org/10.1016/j.ress.2014.08.002.
13. Hobbs A. An overview of human factors in aviation maintenance. ATSB safety report, aviation research and analysis report AR 2008;55(1):234-242.
14. Jue Wang, Wei Xu, Jian Ma, Shouyang Wang. A vague set based decision support approach for evaluating research funding programs. European Journal of Operational Research 2013; 230 (1): 656-665, http://dx.doi.org/10.1016/j.ejor.2013.04.045.
15. Kahneman D,Tversky A. Prospect theory: An analysis of decision under risk. Economic 1979; 47(2): 263-291, http://dx.doi.org/10.2307/1914185.
16. Lee J, Ramji A, Andrews KSJ, Darning L, and Dragan B. An integrated platform for diagnostics, prognostics and maintenance optimization. In Proceedings of Intelligent Maintenance System, Arles, France 2004;15-17.
17. Nicolai RP, Dekker R. Optimal maintenance of multi-component systems: a review In: Complex system maintenance handbook. London: Springer 2008:263–86, http://dx.doi.org/10.1007/978-1-84800-011-7_11.
18. R.R. Yager. Uncertainty representation using fuzzy measures. IEEE Trans Systems, Man, and Cybernetics, Part B, 2002;32 (1):13–20, http://dx.doi.org/10.1109/3477.979955.

19. Ruiying Li, Jingfu Wang, Haitao Liao, Ning Huang. A new method for reliability allocation of avionics connected via an airborne network. Journal of Network and Computer Applications 2013;34(2):678-682.
20. Seidenman P,Spanovich DJ. Avionics integrity. Aircraft Technology Engineering & Maintenance 2011;6:29–31.
21. Sharma,R.K.,D.Kumar, and P. Kumar.FLM to select suitable maintenance strategy in process industries using MISO model, Journal of Quality in Maintenance Engineering 2005;1 1(2):359-374.
22. Tan, J. S., Kramer, M. A. A general framework for preventive maintenance optimization in chemical process operations. Computers Chemical Engineering 1997;21(12):1451-1469, http://dx.doi.org/10.1016/S0098-1354(97)88493-1
23. Tangbin Xia, Lifeng Xi, Xiaojun Zhou, Jay Lee. Dynamic maintenance decision-making for series parallel manufacturing system based on MAM-MTW methodology. European Journal of Operational Research 2012;221 (1) 231-240, http://dx.doi.org/10.1016/j.ejor.2012.03.027.
24. Tversky, A., Kahneman, D.. Advances in prospect theory: Cumulative representation of uncertainty. Journal of Risk and Uncertainty, 1992;5(4):297–323, http://dx.doi.org/10.1007/BF00122574.
25. Vassilis Tsagkas, Dimitris Nathanael,Nicolas Marmaras. A pragmatic mapping of factors behind deviating acts in aircraft maintenance. Reliability Engineering and System Safety 2014;130(1);106–11, http://dx.doi.org/10.1016/j.ress.2014.05.011.
26. Xiuli Geng,Xuening Chu,Zaifang Zhang.A new integrated design concept evaluation approach based on vague sets. Expert Systems with Applications 2010;37 (3): 6629–6638, http://dx.doi.org/10.1016/j.eswa.2010.03.058.
27. Y. Liu. H. Z. Huang. Optimal selective maintenance strategy for multi-state systems under imperfect maintenance. IEEE Transactions on Reliability 2010;59(2): 356-367, http://dx.doi.org/10.1109/TR.2010.2046798.
28. Zhi-Ping Fan, Xiao Zhang, Fa-Dong Chen, Yang Liu. Multiple attribute decision making considering aspiration-levels: A method based on prospect theory. Computers & Industrial Engineering 2013; 65 (1) 341–350, http://dx.doi.org/10.1016/j.cie.2013.02.013.

Jiliang TU
Chengli SUN
Xiangyang ZHANG
Ruofa CHENG
School of Information Engineering
Nanchang Hangkong University
No. 696, Fenghenan Avenue, Honggutan New Zone
Nanchang, Jiangxi, 330063, China

Hongliang PAN
Magnetic Suspension Traffic Engineering Technology Research Center of Tongji University
Shanghai, 201804, China

E-mails: tjl1980@nchu.edu.cn, 395229630@qq.com

Article citation info:
PENG W, LIU Y, ZHANG X, HUANG H-Z. Sequential preventive maintenance policies with consideration of random adjustment-reduction features. Eksploatacja i Niezawodnosc – Maintenance and Reliability 2015; 17 (2): 306–313, http://dx.doi.org/10.17531/ein.2015.2.19.

Wei PENG
Yu LIU
Xiaoling ZHANG
Hong-Zhong HUANG

SEQUENTIAL PREVENTIVE MAINTENANCE POLICIES WITH CONSIDERATION OF RANDOM ADJUSTMENT-REDUCTION FEATURES

STRATEGIA SEKWENCYJNEJ KONSERWACJI ZAPOBIEGAWCZEJ Z UWZGLĘDNIENIEM CECH LOSOWEJ KOREKCJI I LOSOWEJ REDUKCJI WIEKU

In existing literature, imperfect maintenance has been widely studied and many studies treat the effectiveness of imperfect maintenance as a fixed constant. In reality, it is more realistic to regard the maintenance efficiency as a random quantity as it may not be precise value due to the lack of sufficient data and/or the variation from system to system. In this paper, a hybrid imperfect maintenance model with random adjustment-reduction parameters is proposed, and a maintenance policy, namely the sequential preventive maintenance in periodic leisure interval, is studied based on the proposed hybrid random imperfect maintenance model, and the corresponding maintenance strategy is optimized by the genetic algorithm (GA). A numerical example and an example of the fuel injection pump of diesel engines are presented to illustrate the proposed method.

Keywords: *Maintenance policy; Imperfect maintenance; Preventive maintenance; Random maintenance efficiency.*

W literaturze, temat konserwacji niepełnej został szeroko zbadany i wiele z opisywanych badań traktuje wydajność konserwacji niepełnej jako wartość stałą. W rzeczywistości jednak wydajność konserwacji należy traktować jako wielkość losową, ponieważ nie można jej dokładnie określić ze względu na brak wystarczających danych i / lub różnice między poszczególnymi systemami. W niniejszej pracy zaproponowano model hybrydowy konserwacji niepełnej łączący pojęcia parametrów losowej korekcji i losowej redukcji wieku. Na podstawie proponowanego modelu hybrydowego losowej konserwacji niepełnej przebadano strategię sekwencyjnej konserwacji zapobiegawczej przeprowadzanej okresowo w czasie wolnym od pracy; omawianą strategię konserwacji zoptymalizowano za pomocą algorytmu genetycznego (GA). Proponowaną metodę zilustrowano przykładem liczbowym oraz omówiono na przykładzie pompy wtryskowej paliwa do silników wysokoprężnych.

Słowa kluczowe: *polityka konserwacji, konserwacja niepełna, konserwacja zapobiegawcza, losowa wydajność konserwacji.*

1. Introduction

Systems are suffering deterioration due to aging and unexpected shock damages after launched. Maintenance is executed to retain a system in or restore it to an acceptable operating condition for the fulfillment of requirement. Generally, it involves two major maintenance categories: corrective (unplanned) or preventive (planned). Corrective maintenance (CM) is any maintenance activity performed when the system is failed or breakdown. Preventive maintenance (PM) is all activities performed in an attempt to retain a system in specified condition by providing systematic inspection, detection, and prevention of incipient failure. Commonly, preventive maintenances are undertaken regularly at pre-selected intervals to reduce or eliminate the accumulated deterioration, and corrective maintenances are carried out whenever shocked and unexpected failure happens. Obviously, CM is performed at unpredictable time points because the failure time of products is unknown. CM is typically carried out in three steps: (1) Diagnosis of the problem, (2) Repair and/or replacement of faulty component(s), and (3) Verification of the repair action. Preventive maintenance (PM) is the maintenance that occurs when the system is still in operating condition.

According to the efficiency, maintenance can be generally classified into five categories as: perfect, minimal, imperfect, worse, and worst [21]. A prefect maintenance action restores the system to "as good as new" condition. In most cases, a replacement can be viewed as a perfect maintenance. A minimal maintenance activity restores a system back to the functioning state without changing its failure intensity. After minimal repair, it has the same failure intensity with when it failed, and it seems "as bad as old". Imperfect maintenance does not restore the system "as good as new" or "as bad as old" conditions. It assumes the maintenance efficiency is somewhere between the two extreme cases, i.e. perfect and minimal. The imperfect maintenance broadly exists and be more realistic and in practical engineering. The worse maintenance is a negative maintenance action making a system

worse after repair (increases failure intensity) but not break down. Worst maintenance will lead a system to failure or breakdown.

Imperfect maintenance models have been extensively studied in the past decades as many maintenance actions may realistically not resulting in perfect and minimal situations but in an intermediate one. Many imperfect models have been proposed, for example, Pham et al. [21], Nakagawa [17], Block et al. [3], Kijima [6, 7], Wang [26], Lam [9], Zhao [33], Pham and Wang [22], Wang and Pham [27]. Pham et al. [21] summarize various treatments of imperfect maintenance of binary-state systems. Wu and Zuo [31] studied the commonality and interrelationship between some commonly used imperfect maintenance, and categorized the existing models into two groups, i.e. linear and nonlinear models. Liu et al. [15] proposed a new approach to selecting the most adequate imperfect maintenance model among several candidates based on the collected failure data. The uncertainty associated with imperfect maintenance model selection is also considered in maintenance decision-makings. In most recently, the imperfect maintenance model has been extended to the context of multi-state systems. For example, Liu et al. [14] proposed a new imperfect maintenance model for multi-state components, and jointly optimized the redundancy levels and maintenance strategy for multi-state systems.

According to Brown and Proschan [4], maintenance policies based on planned inspections are "periodic inspection", and "inspection interval dependent on age". By periodic inspections, a failed unit is identified (*e.g.*, spare battery, a fire detection device, *etc.*). With aging of units, the inspection interval may be shortened [23, 28]. These inspection methods are subject to imperfect maintenance caused by randomness in the actual time of inspection in spite of the schedule, imperfect inspection, and cost structure. Therefore, realistic and valid maintenance models must incorporate random features of the inspection and maintenance policy [29].

In this paper, we develop a hybrid PM model considering the random features of both the adjustment factor and age reduction factor, called the random adjustment-reduction maintenance (RAM) model. Throughout this paper, we will call the RAM model for short. This model is an extension to the study by Wu and Clemets-Croome [30] in which we will discuss in details the RAM including the failure rate PM, the age reduction PM, the hybrid PM addressing the random adjustment-reduction factors. It is more realistic to describe the imperfect maintenance efficiency through a random variable and a hybrid model. Later on, a finite-horizon PM decision model is proposed with considering sequential PM policy under the random PM efficiency. We then optimize the sequential PM policy by using the genetic algorithm.

The remainder of this paper is organized as follows: Section 2 derives reliability metrics including the failure intensity function and the reliability function for the RAM model. Section 3 introduces the proposed PM policy model under the features of random maintenance strategy. Section 4 presents the genetic algorithm to obtain the optimal PM sequence T_P^* and PM times N^*. Two studied cases are given to illustrate the proposed maintenance policy in Section 5. A brief conclusion is given in Section 6.

2. Imperfect PM Model

The earliest preventive maintenance models consider that a system after a PM activity is "as good as new" and this kind of PM is called the perfect PM. The replacement of component or system with a new one can be considered to be a perfect one. Sometimes, the system after PM activities cannot be "as good as new". Barlow et al. [1] introduced a minimal repair model in which PM activities do not change the failure intensity of the system. Later on, Nakagawa [17] studied a failure rate PM model, Malik [16] proposed an age reduction PM model, and Kijima [6, 7] proposed and discussed type I and type II imperfect repair models. Lin et al. [13] introduced a hybrid PM model by combining the failure rate PM model and the age reduction PM model. Random maintenance quality was studied by Wu et al. [30] and random variables were implemented in failure rate and age reduction models respectively.

In the failure rate model, Nakagawa [17] assumed that when a repairable system launches, its failure intensity will continuously increase if no PM activity intervenes, otherwise its failure intensity will be changed by a PM, that is, after the i^{th} PM action, the failure intensity function can be written as $A_i\lambda_{i-1}(t)$ where $t \in (0, t_{i+1} - t_i)$ and $\lambda_{i-1}(t)$ is the failure intensity function at $t \in (0, t_i - t_{i-1})$. A_i should satisfy $A_i > 1$, and it is considered as a adjustment factor or improvement factor which illuminate although the failure intensity is reset to the value at t=0, after PM, its slope will increase in the next repair cycle. The larger A_i is, the higher slope its failure intensity has after a PM.

In age reduction model, Malik [16] suggested that a system's failure intensity is $\lambda_0(t)$ where $t \in (0, t_1)$, and it will monotonously increase without maintenance activity. When PM is taken at t_1, the failure intensity will be formulated as $\lambda_1(t) = \lambda_0(t + \alpha_0 t_1)$ for $t \in (0, t_2 - t_1)$ and $\alpha_0 \in (0,1)$. α_0 is defined as the virtual age reduction factor. It means that before performing a PM action, the actual age and virtual age are both equal to T_{P1}, and after the PM action, the actual age is $t + t_1$ while the virtual age $(t + \alpha_0 t_1)$, where virtual age is less than actual age and the health condition becomes better after a PM. Then, the failure intensity of the system is a function with respect to the virtual age, and each PM action reduces the virtual age of the system to a certain extent. Kijima et al. [6] [7] introduced two types of virtual age PM model. In the Kijima's type I model, it assumes that PMs serve only to remove damage created in the last sojourn, the virtual age at the start of working after PM is $v_k = t_{k-1} + \xi_k(t_k - t_{k-1})$, and in the Kijima's type II model, it assumes that the PM actions could remove all damage accumulated up to that point in time and virtual age can be expressed as $v_k = \xi_k(v_{k-1} + (t_k - t_{k-1}))$ where $\xi_k \in (0,1)$ in both I and II models. Actually, the Kijima's type I model is similar to Malik's model, and type I and II models are both practical in different kinds of system and maintenance activity.

Lin et al. [13] introduced a hybrid PM model with combining the failure rate model and the age reduction model. The failure intensity $\lambda_k(t)$ after the k^{th} PM becomes to $a_k\lambda_{k-1}(b_k t_k + t)$, where t_k is the interval between $(k-1)^{\text{th}}$ and k^{th} PM activities.

Actually, in previous literature, adjustment factor and age reduction factor directly affect system's failure intensity when PM actions are performed and they represent the maintenance efficiency. Gasmi et al. [5] proposed a statistical method to estimate the maintenance efficiency according to failure data, and unknown parameters were estimated using the maximum likelihood estimate (MLE) method with 1% and 5% lower and upper *s*-confidence bounds. It is, however, impossible to obtain a fixed precise value unless sufficient data can be collected. Liu et al. [15] found that the uncertainty associate parameters estimation and model selection cannot ignored in decision-making, especially in the case of lack of sufficient data. Wu et al. [30] introduced random maintenance quality in both the failure rate model and the age reduction model respectively and in which adjustment factor A_i and age reduction factor α_i were considered as random variables respectively, then two maintenance policies model were discussed separately. It is obviously more realistic than previous models which treat parameters in maintenance models as fixed constants corresponding to operational time.

As an extension of Wu's model, we consider the hybrid PM model with random PM efficiency. It is of course more useful and applicable to practical analysis and modeling. The recursive relationship of failure intensity $\lambda_i(t)$ at time t, before the i^{th} PM can be expressed as follows:

$$\lambda_1(t)=\lambda(t)$$
$$\lambda_2(t)=\int_0^{\infty}A_1\int_{-\infty}^{+\infty}\lambda_1(t+\alpha_1T_{P1})dF_1(\alpha_1)dG_1(A_1)$$
$$\lambda_3(t)=\int_0^{\infty}A_2\int_{-\infty}^{+\infty}\lambda_2(t+\alpha_2T_{P2})dF_2(\alpha_2)dG_2(A_2)$$
$$\vdots$$
$$\lambda_i(t)=\int_0^{\infty}A_{i-1}\int_{-\infty}^{+\infty}\lambda_{i-1}(t+\alpha_{i-1}T_{P(i-1)})dF_i(\alpha_{i-1})dG_{i-1}(A_{i-1})$$

where A_i is the adjustment factor and α_i is the age reduction factor of i th PM activity, and they are both random quantities with distribution functions $G_i(A_i)$ and $F_i(\alpha_i)$ respectively. $T_{P(i-1)}$ represents the interval time between $(i-1)$th and i th PM activities, and there are N PM cycles. The failure intensity function can be rewritten using iterative operation as:

$$\lambda_i(t)=\prod_{k=1}^{i-1}\left(\int_0^{\infty}A_kdG_k(A_k)\right)\int_{-\infty}^{+\infty}\cdots\int_{-\infty}^{+\infty}\lambda\left(t+\sum_{j=1}^{j=i-1}(\alpha_jT_{Pj})\right)dF_j(\alpha_{i-1})\ldots dF_1(\alpha_1) \quad (1)$$

$$\lambda_{N+1}(t)=\prod_{k=1}^{N}\left(\int_0^{\infty}A_kdG_k(A_k)\right)\int_{-\infty}^{+\infty}\cdots\int_{-\infty}^{+\infty}\lambda\left(t+\sum_{j=1}^{j=i-1}(\alpha_jT_{Pj})\right)dF_j(\alpha_{i-1})\ldots dF_1(\alpha_1) \quad (2)$$

It is worth noting that if $\int_0^{\infty}A_i\lambda_i(t)dG_i(A_i)<\lambda_i(t)$, then random variable A_i should satisfy $0<\int_0^{\infty}A_idG_i(A_i)<1$, it means the slope of failure intensity function will decrease after PM actions. On the other hand, when $\int_0^{\infty}A_i\lambda_i(t)dG_i(A_i)>\lambda_i(t)$, $\int_0^{\infty}A_idG_i(A_i)>1$ should be satisfied, and the slope will increase. $\int_0^{\infty}A_idG_i(A_i)=1$ denoting no change to the slope after PMs. Meanwhile, the increment of the virtual age is $\int_{-\infty}^{+\infty}\alpha_{i-1}T_{P(i-1)}dF_{i-1}(\alpha_{i-1})$ after PM actions.

The system reliability in the i th PM cycle can be expressed as:

$$R_i(t)=\mathrm{e}^{-\int_0^{t+T_v}\lambda_i(t)dt} \quad (3)$$

where $T_v=\sum_{j=1}^{j=i-1}(\int_{-\infty}^{+\infty}\alpha_jT_{Pj}dF_j(\alpha_{i-1}))$.

The random maintenance efficiency could be more reasonable to meet realistic system requirements in practice due to many uncertainties in the field environments. Based on this random PM efficiency, a random sequential maintenance policy model will be discussed in the next section.

3. Sequential Maintenance Policy and Formulation

Optimal maintenance policies have been investigated in the past several decades with the purpose of providing maximum system reliability and/or availability and safety performance with the lowest maintenance costs and the highest profit per unit time. Barlow et al. [1] and Osaki et al. [20] proposed the basic age replacement model from the renewal reward theorem, and the expected cost per unit time in the steady state was discussed. Barlow et al. [2] studied block replacement model and compared it with age replacement model. The models extended from these two basic models were proposed in later literature [16, 30]. Furthermore, some models studied in recently years are worth mentioning. Nakagawa [18] introduced two kinds of imperfect PM models and computed the optimal PM sequences for Weibull distribution. Policy N, based on the failure number of the system for multi-state repairable system was studied to maximize the long-run expected profit per unit time and geometric process had been employed by Zhang et al. [32]. Lam [8] studied a maintenance model for two-unit redundant system with one repairman, and the long-run average cost per unit time for each kind of replacement policy was derived. Satow et al. [24] represented a two-component system of which components suffer shock damage interaction, and the minimum expected cost per unit of time for infinite time operation was expressed and optimized. Zhou et al. [34] integrated sequential imperfect maintenance policy into condition-based predictive maintenance, and a reliability-centered predictive maintenance policy was proposed for a continuously monitored system subjected to degradation due to the imperfect maintenance. The preventive maintenance strategy has been applied to a vehicle fleet [19].

In this section, we consider such a maintenance policy that a system is suffering deterioration process with operation aging and the time for the system to be replaced by a new one in a finite time. PM activities need to be performed in replacement cycle in order to reduce the system deterioration [12] and restore it to a better state. According to the practical requirement and convenience, PM actions are usually scheduled at the weekend or leisure periods since such actions would not interrupt producing and working in these periods. During each PM cycle, failures may occur which will make the system breakdown, and minimal repairs will be done immediately to restore the system to working state. The possible replacement cycle is illustrated in Fig. 1. In this figure, there are N PM cycles in finite operational time T_o with the intervals T_{Pi} respectively, and T_{Pi} has different interval according to the system state, but must be in the leisure periods such as weekend and shut down time. This policy can be considered as "sequence maintenance in periodical leisure intervals". Failures are corrected by minimal repairs during each PM cycle.

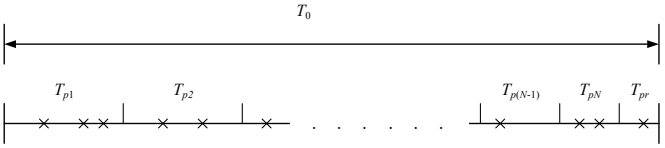

Fig. 1. Finite time replacement under PM policies

The hazard function in each PM cycle can be written as:

$$H_i(t)=\int_0^{T_{Pi}}\lambda_i(t)dt \quad (4)$$

where $\lambda_i(t)$ is the failure intensity function during the i th PM cycle, and T_{Pi} is the pre-specified interval between i th and $(i+1)$th PM actions. From Eq.(1), the hazard function is given by:

$$H_i(t)=\int_0^{T_{Pi}}\lambda_i(t)dt$$
$$=\int_0^{T_{Pi}}\left(\prod_{k=1}^{i-1}\left(\int_0^{\infty}A_kdG_k(A_k)\right)\right)\left(\int_{-\infty}^{+\infty}\cdots\int_{-\infty}^{+\infty}\lambda(t+\sum_{j=1}^{j=i-1}(\alpha_jT_{Pj}))dF_j(\alpha_{i-1})\ldots dF_1(\alpha_1)\right)dt \quad (5)$$

where $\overline{T}_P=[T_{P1},T_{P2},T_{P3},\ldots,T_{Pi},\ldots,T_{PN}]$ is a vector of PM sequential intervals, and N is the PM times.

After the last PM action, the hazard function between N th PM and replacement is given by:

$$H_{N+1}(t)=\int_0^{T_o-\sum T_{Pi}}\left(\prod_{k=1}^{N}\int_0^{\infty}A_k dG_k(A_k)\right)\left(\int_{-\infty}^{+\infty}\cdots\int_{-\infty}^{+\infty}\lambda(t+\sum_{j=1}^{j=N}(\alpha_j T_{Pj}))dF_j(\alpha_{i-1})\ldots dF_1(\alpha_1)\right)dt \tag{6}$$

The expected total maintenance cost in one replacement cycle is given by:

$$\begin{aligned}C_{Total}(N,\overline{T}_P)&=c_r\sum_{k=1}^{N+1}H_i(t)+Nc_p+c_{new}\\&=c_r\sum_{k=1}^{N+1}\int_0^{T_{Pi}}\left(\prod_{k=1}^{i-1}\int_0^{\infty}A_k dG_k(A_k)\right)\left(\int_{-\infty}^{+\infty}\cdots\int_{-\infty}^{+\infty}\lambda(t+\sum_{j=1}^{j=i-1}(\alpha_j T_{Pj}))dF_j(\alpha_{i-1})\ldots dF_1(\alpha_1)\right)dt\\&\quad+Nc_p+c_{new}\end{aligned} \tag{7}$$

where c_r, c_p and c_{new} are the minimal repair cost, preventive maintenance cost, and replacement cost respectively with $c_{new}>c_r>c_p$, and $C_{Total}(N,\overline{T}_P)$ denotes the expected total maintenance cost under N and $\overline{T}_P$ policies. The optimal N^* and $\overline{T}_P^*$ can be obtained by solving the optimization cost function $C_{Total}(N,\overline{T}_P)$. That is:

$$C_{Total}(N^*,\overline{T}_P^*)=\min C_{Total}(N,\overline{T}_P) \tag{8}$$

The existence of optimum N^* and $\overline{T}_P^*$ is discussed as follows: Assuming that when $N\to 0$, there is no PM actions during the replacement cycle, then PM cost tends to be zero:

$$\lim_{N\to 0}C_{Total}(N,\overline{T}_P)=c_r H_1(T_o)+c_{new}=c_r\int_0^{T_o}\lambda(t)dt+c_{new} \tag{9}$$

when $N\to\infty$, PM can be regarded to be continuously performed, and then, the hazard rate could be considered as zero, and we can conclude:

$$\lim_{N\to\infty}C_{Total}(N,\overline{T}_P)=Nc_p+c_{new}\to\infty \tag{10}$$

If we arrange one PM in life time, the expected total maintenance cost could be reduced if and only if

$$c_r(H_0(T_o)-H_0(0))+c_{new}<c_r(H_0(T_{P1})-H_0(0))+c_p+c_r(H_1(T_o-T_{P1})-H_1(0))+c_{new} \tag{11}$$

then

$$c_r\left(\left(H_0(T_o)-H_0(T_{P1})\right)-\left(H_1(T_o)-H_1(T_{P1})\right)\right)>c_p \tag{12}$$

$$c_r\left(\int_{T_{P1}}^{T_o}\lambda_0(t)dt-\int_{T_{P1}}^{T_o}\lambda_1(t)dt\right)>c_p \tag{13}$$

$$c_r\left(\int_{T_{P1}}^{T_o}\lambda_0(t)dt-\int_0^{T_o-T_{P1}}\int_0^{\infty}\int_{-\infty}^{+\infty}A_1\lambda_0(t+\alpha_1T_{P1})dF_1(\alpha_1)dG_1(A_1)\right)>c_p \tag{14}$$

$$\int_{T_{P1}}^{T_o}\lambda_0(t)dt-\int_0^{T_o-T_{P1}}\int_0^{\infty}\int_{-\infty}^{+\infty}A_1\lambda_0(t+\alpha_1T_{P1})dF_1(\alpha_1)dG_1(A_1)>\frac{c_p}{c_r} \tag{15}$$

$$\int_{T_{P1}}^{T_o}\left(\lambda_0(t)-\int_0^{\infty}\int_{-\infty}^{+\infty}A_1\lambda_0(t+(\alpha_1-1)T_{P1})dF_1(\alpha_1)dG_1(A_1)\right)dt>\frac{c_p}{c_r} \tag{16}$$

As we know $c_p/c_r<1$, then if $\lambda_0(t)-\int_0^{\infty}\int_{-\infty}^{+\infty}A_1\lambda_0(t+(\alpha_1-1)T_{P1})dF_1(\alpha_1)dG_1(A_1)$ is less than zero during $[T_{P1},T_o]$, there is no suitable T_{P1} that satisfies Eq. (16). When $\lambda_0(t)=c$ where c is a constant, and if $\int_0^{\infty}A_1dG_1(A_1)\geq 1$, it is obvious that in equation (16) is invalid, and PM action will increase the maintenance cost with no effect on the state of system. When $\lambda_0(t)$ is monotonous decrease with time, where $\int_0^{\infty}A_1dG_1(A_1)\geq 1$ and

$$\lambda_0(t)<\int_{-\infty}^{+\infty}\lambda_0(t+(\alpha_1-1)T_{P1})dF_1(\alpha_1) \tag{17}$$

Then, PM action should also not to be performed. When

$$\lambda_0(t)>\int_{-\infty}^{+\infty}\lambda_0(t+(\alpha_1-1)T_{P1})dF_1(\alpha_1) \tag{18}$$

there may be a suitable T_{P1} to obtain $C_{Total}(1,T_{P1})<C_{Total}(0,0)$. If $\lambda_0(t)$ is monotonous increasing and Eq.(18) is satisfied, there may exist some T_{P1} values that could reduce the expected maintenance cost.

It seems that the problem becomes even more complicated with the increase of N, and it is more difficult to obtain the optimum $\overline{T}_P^*=[T_{P1}^*,T_{P2}^*,\ldots,T_{PN^*}^*]$. In the next section, we will use the genetic algorithm (GA) approach to solve the resulting optimization problem.

4. GA Optimization method

Numerous optimization methods have been used to solve the optimization problems and combinatorial optimization problems in reliability engineering. The most popular methods are dynamic programmings and heuristic search algorithms which are strongly problem-oriented. They are designed to solving certain problem and can not adapt to other problem.

The genetic algorithm (GA) is one of the most widely used evolutionary searching methods and it was inspired by the optimization procedure that exists in nature and biological phenomenon. The GA has become the popular universal tool for solving various optimization problems because of its advantage and successful applications of GA to maintenance optimization problems [10, 11]. The GA starts the optimization process from a random generated initial population. The fitness will be calculated for each individual. Then natural selection, crossover and mutation are operated in each population, and terminate criterion is used to determine whether to stop or to continue the GA process.

Solution encoding and decoding procedure must be defined before applying the GA to a specific problem. As we mentioned in section 3, PM action should only be performed in the leisure time such as the weekend, end of month or year. We use a fix length binary string to represent the time table where PM could takes place. The length of the binary string is given by:

$$L=\left[\frac{T_0}{T_{\min}}+1\right] \tag{19}$$

where T_o is finite operation/replacement time, $T_{\min}$ is minimal leisure interval when PM could be performed, and $[\bullet]$ is the least integer upper bound. If some bits of the string are equal to one, it means PM actions are performed in these leisure times. For example, $T_o = 1\ year$ and $T_{\min} = 1\ week$ means PM can only perform in weekend and there are only 53 opportunities to do it. Then we use a binary string $s = [0010....00]$ with 53 bits to represent the variable to be optimized, where bit 1 means a PM activity should perform in the 2nd weekend after it be installed. Another example is given as: $T_o = 1\ year$ and $T_{\min} = 1\ month$, and $s = [000100100101]$ represents that PM should be performed at end of the 3rd month, the 6th month, the 9th month and the 11th month. Then $N = 4$ and $\overline{T}_P = [3,3,3,2]$ is a certain solution to maintenance problem.

After encoding the variables, crossover and mutation procedures are used to generate individuals of next population. Then GA continues process until distance of the individuals in each population is less than limit threshold $d_{\min}$ or populations are produced N_{rep} times. Finally, the individual with the minimal fitness could be considered as the global optimum result.

5. Case studies

5.1. Case 1: An illustrative example

We consider the failure distribution of a system follows a two-parameter Weibull distribution as:

$$f(t) = \frac{\beta}{\eta}\left(\frac{t}{\eta}\right)^{\beta-1} \exp\left(-\left(\frac{t}{\eta}\right)^{\beta}\right) \tag{20}$$

where $\beta = 1.2$, $\eta = 300$ and its corresponding failure intensity function is given by:

$$\lambda(t) = \frac{\beta}{\eta}\left(\frac{t}{\eta}\right)^{\beta-1} \tag{21}$$

where the failure intensity is monotonously increasing with time if there is no PM activity.

For convenience, we assume that $G_1(A_1), G_2(A_2), ..., G_N(A_N)$ have the same uniform distribution $G(A)$ which is given by:

$$G(A) = \begin{cases} 0 & A < 0.90 \\ \dfrac{A - 0.90}{1.20 - 0.90} & 0.90 \le A < 1.20 \\ 1 & 1.20 \le A \end{cases} \tag{22}$$

and similarly, $F_1(\alpha_1), F_2(\alpha_1), ..., F_N(\alpha_N)$ have the same uniform distribution $F(\alpha)$ which is given by:

$$F(\alpha) = \begin{cases} 0 & \alpha < 0.0 \\ \dfrac{\alpha}{0.6 - 0.0} & 0.0 \le \alpha < 0.6 \\ 1 & 0.6 \le \alpha \end{cases} \tag{23}$$

Without lose of generality, we assume $c_r = 400$, $c_p = 10$, $c_r = 200$, where c_r is much larger than c_p because sudden breakdown caused by random failure will lead to the loss of producing and serious delay to original plan. Beside that, it is suggested that the system replacement cycle is $T_o = 1\ year$, and PM activities should be arranged at the end of each month. Then, there are 12 possible opportunities to perform preventive maintenance. The decision variable s is a 12 bits binary string. We start GA process with initial population selected from feasible region from $[000000000000]$ to $[111111111111]$, two-point crossover method with rate 0.6 and mutation rate 0.05. Finally the optimum variable is $s^* = [000001000100]$ and the optimum PM sequence is $T_P^* = [T_{P1}^*, T_{P2}^*] = [5,4]$, $N^* = 2$.

Table 1 also presents the sensitivity analysis for various shape parameter β of the failure distribution from 1.0 to 1.5 while the other parameters are fixed. From Table 1, we observe that when β equals to zero which means the failure intensity is constant, PM is not needed. This conclusion is consistent with analysis in section 3. Furthermore, when the β increases, the N^* becomes larger and the first PM activity is more close to launch time. It is because that a larger β denotes the system has more rapidly deterioration process, and the more random failure would happen during replacement cycle while repair cost increases swiftly. PM activity can decrease the large failure intensity back to certain level and reduce the possibility of random failure. Therefore, more PM activities is needed when β increases.

Table 1. Optimum PM sequence and expected maintenance cost when changing β

β	1.0	1.1	1.2	1.3	1.4	1.5
T_P^*	–	[8]	[5,4]	[4,3,3,1]	[3,3,3,2]	[3,3,2,2,1]
C_{total}^*	1930.0	2391.0	2863.4	3370.8	3922.7	4539.8

Table 2 illustrates the optimum PM sequences and minimal expected maintenance costs while the scale parameter η of the system failure distribution changes. It shows that with the η decreasing, the less random failure would happen during the replacement cycle, therefore reducing the frequency of PM is necessary. Meanwhile, the expected cost will lower.

Table 2. Optimum PM Sequence and expected maintenance cost when changing η

η	$\eta = 1000.0$	$\eta = 400.0$	$\eta = 150.0$	$\eta = 10.0$
T_P^*	[4,4]	[3,3,3]	[3,3,3,2]	[3,3,2,2,1]
C_{total}^*	679.6	1970.0	2286.0	2606.4

The optimum T_P^* sequences are listed in Table 3 while changing the ratio of c_p / c_r, where the other parameters are fixed. It is shown that with the c_p / c_r decreasing, PM cost becomes cheaper, and more PM actions could be performed to lower failure intensity without increase too much preventive maintenance cost. When c_p / c_r equal to one, it shows no PM is needed. It can be explained that although PM can reduce the virtual age of system, it increase the slope of failure intensity. When c_p equals c_r, the extra PM cost is much more that random failure repair cost lowered by PM. Then no PM is more economical.

The optimum results by changing the distribution of α_i are listed in Table 4 and shown in Fig. 2. It indicates that more PM actions should be performed while the PM effectiveness increases, and the

Table 3. Different optimum PM Sequence by changing ratio of c_p / c_r

c_p / c_r	1/100	1/25	1/20	1/10	1/5	1/1
T_P^*	[5,4,2]	[5,4]	[5,4]	[5,4]	[7]	–

expected maintenance cost also decreases because of the higher effectual PM actions.

Table 4. T_P^* and C_{total}^* by changing α_i distribution as $U(0,x)$

x	1.0	0.9	0.8	0.7	0.6	0.5	0.4	0.3	0.2	0.1
T_P^*	[7]	[7]	[6,4]	[6,4]	[5,4]	[5,4]	[4,4,3]	[4,3,3]	[4,3,2,2]	[3,3,2,2,1]
C_{total}^*	2955.9	2940.0	2919.5	2893.6	2863.4	2830.0	2789.2	2736.7	2668.7	2573.6

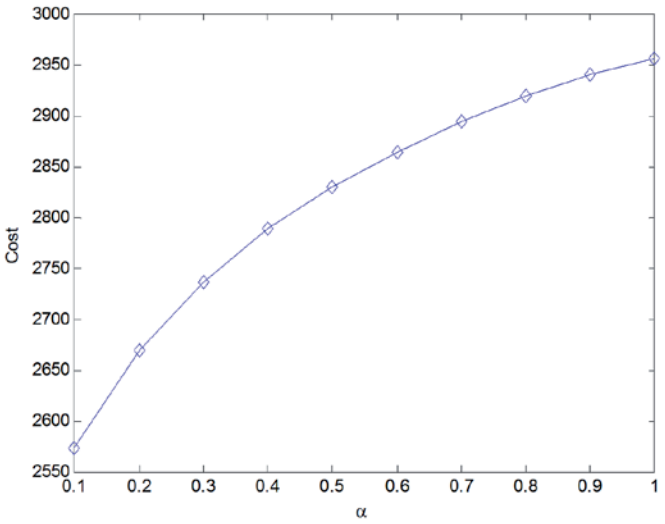

Fig. 2. Optimum cost with different α_i distribution

Table 5 and Table 6 show the optimal expected maintenance cost with periodical interval from 5 to 1 and optimal PM sequential policies and relative cost with fixed PM times respectively, and these comparisons are illustrated in Fig. 3.

As observed in Fig. 3, with the same PM times N, the sequential PM policy is much more economically efficiency than periodic one. With N increasing, the economic advantage of sequential policy is becoming dramatically. Therefore, in manufactory production, sequential policies have been widely accepted and applied because it is more reasonable and economical.

Table 5. Expected maintenance cost with periodic PM actions

Interval	5	4	3	2	1
T_P^*	[5,5]	[4,4]	[3,3,3]	[2,2,2,2,2]	[1,1,1,1,1,1,1,1,1,1,1]
C_{total}^*	2888.00	2873.1	2898.6	3002.6	3491.7

Table 6. Optimal PM sequence and expected maintenance cost with fixed PM times N

N	1	2	3	4	5
T_P^*	[7]	[5,4]	[5,4,2]	[4,4,2,1]	[4,3,2,1,1]
C_{total}^*	2886.2	2863.4	2869.7	2891.1	2926.1

5.2. Case 2: Fuel injection pump

The purpose of the fuel injection pump is to deliver an exact metered amount of fuel, under high pressure, at the right time to the injector. It is one of the most important components of diesel engines.

The parameters of the RAM model listed in Table 7 are estimated through the methodology proposed in [5, 15, 25].

According to the system requirements, oil should be refresh every 5000 miles while the fuel injection pump could be censored and do some preventive maintenance.

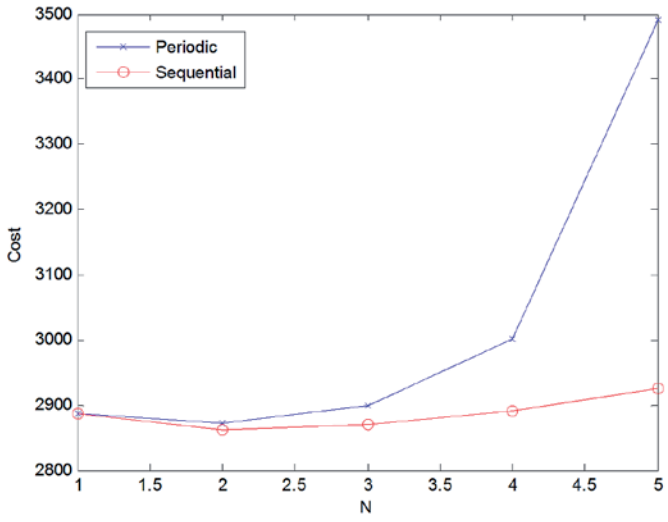

Fig. 3. Comparison between sequential and periodic PM

Table 7. The estimated parameters of fuel injection pump

	Mean	Std
$\hat{\beta}$	2.00	0.15
$\hat{\eta}$	20914.01	121.50
$\hat{A}_i$	1.05	0.02
$\hat{\alpha}_i$	0.50	0.10

Under the warranty period-50000 miles, the optimal PM policy is obtained based on our proposed models with parameters $\beta = 2.00$ $\eta = 20914.01$ $A_i \sim N(1.05, 0.02)$, $\alpha_i \sim N(0.50, 0.10)$, $c_r = \$18.75$ and $c_p = \$3.75$. The optimal PM sequences are [20000, 15000] miles with the minimal expected maintenance cost equal to $\$87.5$.

6. Conclusions

In this paper, we consider the random maintenance features of imperfect PM. This is more reasonable to many practical applications because the efficiency of maintenance action is evaluated from statis-

tical failure data of repairable systems. It could be not precise and always have confidence intervals when estimating the unknown parameters of an imperfect maintenance model. The random degree hybrid imperfect maintenance model is proposed in this paper and a "sequential PM in periodic leisure interval" policy is proposed and solved by using the GA approach. A numerical example and a fuel injection pump are presented to illustrate and implement our proposed model. As in the numerical example, it shows how the expected maintenance cost and PM sequences change with respect to the settings of model parameters. In addition, the periodic and sequential maintenance policies are compared, and it concludes that a sequential policy is dramatically more economically efficiency than periodic policy with the PM times increasing. In the second case, a practical PM policy in diesel engine is discussed under the proposed models, and it is very useful to manufactories and enterprises to plan optimum maintenance strategy and warranty policy.

Acknowledgements

This research was supported by the National Natural Science Foundation of China under contract number 71101017.

References

1. Barlow R.E, Hunter L.C. Reliability analysis of a one-unit system. Operational Research, 1961; 9: 200-8, http://dx.doi.org/10.1287/opre.9.2.200.
2. Barlow R.E, Hunter L.C. Optimum preventive maintenance policies. European Journal of Operational Research, 1960; 8: 90-100, http://dx.doi.org/10.1287/opre.8.1.90.
3. Block H.W, Borges W.S, Savits T.H. Age dependent minimal repair. Journal of Application Probability, 1985; 22: 370-85, http://dx.doi.org/10.2307/3213780.
4. Brown M, Proschan F. Imperfect maintenance. In: IMS Lecture Notes-Monograph Ser. 2: Survival analysis. Inst. Math. Statist, Hayward., Calif., 1982, 179-188.
5. Gasmi S, Love C.E, Kahle W. A general repair, proportional-hazards, framework to model complex repairable systems. IEEE Transactions on Reliability, 2003; 52(1): 26-32, http://dx.doi.org/10.1109/TR.2002.807850.
6. Kijima M. Some results for repairable systems with general repair. Journal of Application Probability, 1989; 26: 89-102, http://dx.doi.org/10.2307/3214319.
7. Kijima M, Morimura H, Suzuki Y. Periodical replacement problem without assuming minimal repair. European Journal of Operational Research, 1988; 37: 194-203, http://dx.doi.org/10.1016/0377-2217(88)90329-3.
8. Lam Y. A maintenance model for two-unit redundant system. Microelectronics Reliability, 1997; 37(3): 497-504, http://dx.doi.org/10.1016/0026-2714(95)00184-0.
9. Lam Y, Zhang Y.L, Zheng Y.H. A geometric process equivalent model for a multistate degenerative system. European Journal of Operational Research, 2002; 142(1): 21-9, http://dx.doi.org/10.1016/S0377-2217(01)00164-3.
10. Levitin G. Genetic algorithms in reliability engineering. Reliability Engineering & System Safety, 2006; 91(9): 975-6, http://dx.doi.org/10.1016/j.ress.2005.11.007.
11. Levitin G, Lisnianski A. Optimization of imperfect preventive maintenance for multi-state systems. Reliability Engineering & System Safety, 2000; 67(2): 193-203, http://dx.doi.org/10.1016/S0951-8320(99)00067-8.
12. Li W.J, Pham H. An inspection-maintenance model for systems with multiple competing processes. IEEE Transactions on Reliability, 2005, 54(2): 318-327, http://dx.doi.org/10.1109/TR.2005.847264.
13. Lin D, Zuo M.J, Yam R.C.M. General sequential imperfect preventive maintenance models. International Journal of Reliability, Quality & Safety Engineering, 2000; 7(3): 253-66, http://dx.doi.org/10.1142/S0218539300000213.
14. Liu Y, Huang H.Z, Wang Z.L. A joint redundancy and imperfect maintenance strategy optimization for multi-state systems. IEEE Transactions on Reliability, 2013; 62(2): 368-378, http://dx.doi.org/10.1109/TR.2013.2259193.
15. Liu Y, Huang H.Z, Zhang X.L. A data-driven approach to selecting imperfect maintenance models. IEEE Transactions on Reliability, 2012; 61(1): 101-112, http://dx.doi.org/10.1109/TR.2011.2170252.
16. Malik M.A.K. Reliable preventive maintenance policy. AIIE Transaction, 1979; 11: 221-8, http://dx.doi.org/10.1080/05695557908974463.
17. Nakagawa T. Imperfect preventive maintenance. IEEE Transactions on Reliability, 1979; 28(5): 402, http://dx.doi.org/10.1109/TR.1979.522065.
18. Nakagawa T. Sequential imperfect preventive maintenance policies. IEEE Transactions on Reliability, 1988; 37(3): 295-7, http://dx.doi.org/10.1109/24.3758,
19. Okulewicz J, Salamonowicz T. Modelling preventive maintenance for a vehicle fleet. Eksploatacja i Niezawodnosc-Maintenance and Reliability, 2008; 1(37):67-71.
20. Osaki S, Nakagawa T. A note on age replacement. IEEE Transactions Reliability, 1975; 24: 92-4, http://dx.doi.org/10.1109/TR.1975.5215347.
21. Pham H, Wang H. Imperfect maintenance. European Journal of Operational Research, 1996; 94: 425-38, http://dx.doi.org/10.1016/S0377-2217(96)00099-9.
22. Pham H, Wang H. Optimal opportunistic maintenance of a k-out-of-n:G system with imperfect PM and partial failure. Naval Research Logistics, 2000, 47(3): 223-239, http://dx.doi.org/10.1002/(SICI)1520-6750(200004)47:3<223::AID-NAV3>3.0.CO;2-A.
23. Pham H, Wang H. A quasi-renewal process for software reliability and testing costs. IEEE Transactions on Systems, Man and Cybernetic, Part A: Systems and Humans, 2001, 31(6): 623-631, http://dx.doi.org/10.1109/3468.983418.
24. Satom T, Osaki S. Optimal replacement policies for a two-unit system with shock damage interaction. Computers & Mathematics with Applications, 2003; 46(7): 1129-38, http://dx.doi.org/10.1016/S0898-1221(03)90128-3.
25. Shin I, Lim T.J, Lie C.H. Estimating parameters of intensity function and maintenance effect for repairable unit. Reliability Engineering & System Safety, 1996; 54(1): 1-10, http://dx.doi.org/10.1016/S0951-8320(96)00097-X.
26. Wang H. A survey of maintenance policies of deteriorating system. European Journal of Operational Research, 2002; 139(3): 469-89, http://dx.doi.org/10.1016/S0377-2217(01)00197-7.
27. Wang H, Pham H. Availability and maintenance of series systems subject to imperfect repair and correlated failure and repair. European

Journal of Operational Research, 2006; 174(3): 1706-22, http://dx.doi.org/10.1016/j.ejor.2005.03.030.
28. Wang H, Pham H. A quasi renewal process and its application in the imperfect maintenance. International Journal of Systems Science, 1996, 27: 1055-1062, http://dx.doi.org/10.1080/00207729608929311.
29. Wang H, Pham H, Reliability and Optimal Maintenance. Springer, 2006.
30. Wu S, Clemets-Croome D. Preventive maintenance models with random maintenance quality. Reliability Engineering & System Safety, 2005; 90(1): 99-105, http://dx.doi.org/10.1016/j.ress.2005.03.012.
31. Wu S, Zuo M.J. Linear and nonlinear preventive maintenance models. IEEE Transactions on Reliability, 2010; 59(1): 242-249, http://dx.doi.org/10.1109/TR.2010.2041972.
32. Zhang Y.L, Yam R.C.M, Zuo M.J, Optimal replacement policy for a multistate repairable system. Journal of Operational Research Society, 2002; 53(3): 336-41, http://dx.doi.org/10.1057/palgrave.jors.2601277.
33. Zhao X.F, Nakagawa T, Qian C.H. Optimal imperfect preventive maintenance policies for a used system. International Journal of Systems Science, 2012; 43(9): 1632-41, http://dx.doi.org/10.1080/00207721.2010.549583.
34. Zhou X, Xi L, Lee J. Reliability-centered predictive maintenance scheduling for a continuously monitored system subject to degradation. Reliability Engineering & System Safety, 2007; 92(4):530-4, http://dx.doi.org/10.1016/j.ress.2006.01.006.

Wei Peng
Institute of Reliability Engineering,
School of Mechanical, Electronic and Industrial Engineering,
University of Electronic Science and Technology of China,
No. 2006, Xiyuan Avenue, West Hi-Tech Zone
Chengdu, Sichuan, 611731, P. R. China

Zhongshan Institute
University of Electronic Science and Technology of China,
No. 1, Xueyuan Road, Shiqi District
Zhongshan, Guangdong, 528402, P. R. China

Yu LIU
Xiaoling ZHANG
Hong-Zhong HUANG
Institute of Reliability Engineering,
School of Mechanical, Electronic, and Industrial Engineering,
University of Electronic Science and Technology of China,
No. 2006, Xiyuan Avenue, West Hi-Tech Zone, Chengdu,
Sichuan, 611731, P. R. China

E-mails: yuliu@uestc.edu.cn; hzhuang@uestc.edu.cn

Article citation info:
ZHOU Y, ZHANG Z. Optimal maintenance of a series production system with two multi-component subsystems and an intermediate buffer. Eksploatacja i Niezawodnosc – Maintenance and Reliability 2015; 17 (2): 314–325, http://dx.doi.org/10.17531/ein.2015.2.20.

Yifan ZHOU
Zhisheng ZHANG

OPTIMAL MAINTENANCE OF A SERIES PRODUCTION SYSTEM WITH TWO MULTI-COMPONENT SUBSYSTEMS AND AN INTERMEDIATE BUFFER

OPTYMALNA STRATEGIA UTRZYMANIA RUCHU DLA SERYJNEGO SYSTEMU PRODUKCJI ZŁOŻONEGO Z DWÓCH PODSYSTEMÓW WIELOSKŁADNIKOWYCH ORAZ BUFORU POŚREDNIEGO

Intermediate buffers often exist in practical production systems to reduce the influence of the breakdown and maintenance ef subsystems on system production. At the same time, the effects of intermediate buffers also make the degradation process of the system more difficult to model. Some existing papers investigate the performance evaluation and maintenance optimisation of a production system with intermediate buffers under a predetermined maintenance strategy structure. However, only few papers pay attention to the property of the optimal maintenance strategy structure. This paper develops a method based on the Markov decision process to identify the optimal maintenance strategy for a series-parallel system with two multi-component subsystems and an intermediate buffer. The structure of the obtained optimal maintenance strategy is analysed, which shows that the optimal strategy structure cannot be modelled by a limited number of parameters. However, some useful properties of the strategy structure are obtained, which can simplify the maintenance optimisation. Another interesting finding is that a large buffer capacity cannot always bring about high average revenue even through the cost of holding an item in the buffer is much smaller than the production revenue per item.

Keywords: *series-parallel systems,intermediate buffers, Markov decision process,policy iteration,generalized minimum residual method.*

W systemach produkcyjnych często stosuje się bufory pośrednie w celu zmniejszenia wpływu awarii i konserwacji podsystemów na system produkcji. Jednocześnie, oddziaływanie buforów pośrednich utrudnia modelowanie procesu degradacji systemu. Istnieją badania dotyczące oceny funkcjonowania i optymalizacji utrzymania systemów produkcyjnych wykorzystujących bufory pośrednie przy założeniu wcześniej określonej struktury strategii utrzymania ruchy. Jednak tylko nieliczne prace zwracają uwagę na własności optymalnej struktury strategii utrzymania ruchu. W przedstawionej pracy opracowano opartą na procesie decyzyjnym Markowa metodę określania optymalnej strategii utrzymania ruchu dla układu szeregowo-równoległego z dwoma podsystemami wieloskładnikowymi oraz buforem pośrednim. Przeanalizowano strukturę otrzymanej optymalnej strategii utrzymania i wykazano, że struktury takiej nie można zamodelować przy użyciu ograniczonej liczby parametrów. Jednak odkryto pewne przydatne właściwości struktury strategii, które mogą ułatwić optymalizację utrzymania ruchu. Innym interesującym odkryciem było to, że duża pojemność bufora nie zawsze daje wysoką średnią przychodów mimo iż koszty przechowywania obiektu w buforze są znacznie mniejsze niż przychody z produkcji w przeliczeniu na jeden obiekt.

Słowa kluczowe: *układ szeregowo-równoległy, bufor pośredni, proces decyzyjny Markowa, iteracja strategii, uogólniona metoda najmniejszego residuum*

1. Introduction

Series-parallel systems with intermediate buffers widely exist in reality. For example, a production line can have multiple production phases connected in series. Each phase can have several production units organised in parallel to enhance the performance of the system. Between these phases, some intermediate buffers are allocated to store work in process (WIP). These buffers can reduce the influence of the breakdown and maintenance of a subsystem on the production rate of the whole system. However, the effects of intermediate buffers also make the degradation process of the system more difficult to model.

Some existing papers developed methods to evaluate the performance of the series-parallel or series system with intermediate buffers. Tan and Gershwin [20] investigated the steady-state of a general Markovian two-stage continuous-flow system by solving a system of differential equations that describes the dynamics of the system. After that, Tan and Gershwin [19] further applied their model to the steady-state analysis of more general situations, e.g. systems with multiple components in series or parallel in each subsystem. Alexandros and Chrissoleon[1] analysed the steady-state of a two-workstation one-buffer follow line by using the Markovian property of the system. Liu et al. [13] investigated a system similar to that in Ref. [1], which considers the asynchronous operations of independent parallel units. The system was modelled by a Quasi-Birth-Death (QBD) process that can be solved efficiently. When there are more than two subsystems (components) in a series-parallel (series) system, the above-mentioned performance evaluation approaches based on steady-state analysis become impractical. Besides methods using the Monte Carlo simulation [9], some approximate approaches e.g., the aggregation method [4, 8, 21] and the decomposition method [5, 12], are developed to evaluate the performance of the system analytically. Although the above papers addressed the performance evaluation of a series-parallel system, these papers assumed a predetermined maintenance strategy, while the maintenance strategy optimisation is not considered.

Some other research focused on the maintenance optimisation of a production system with intermediate buffers. Zhou et al. [25] developed an opportunistic preventive maintenance policy for a multiunit series systems with intermediate buffers based on the dynamic programming. The cumulative opportunistic maintenance cost savings was adopted as the objective function. Ribeiro et al. [17] proposed a mixed integer linear programming model to jointly optimise the maintenance strategy and the buffer size. Dehayem Nodem et al. [6] simultaneously optimised the production and maintenance of a system with a production unit and a buffer-inventory. Murino et al. [16] applied three thresholds (i.e. warning threshold, opportune threshold, and preventive threshold) on the condition of the components in a series system with intermediate buffers. Both the thresholds and the buffer size were optimised through a simulation approach. Zequeira et al. [23] optimised the maintenance strategy and the buffer size of a production system, where the opportunities to carry out a maintenance action were assumed to be random. Arab et al. [2] optimised the maintenance of a production system with intermediate buffers incorporating dynamics of the production system and real-time information from workstations. The maintenance optimisation was performed on a simulation optimisation platform. The degradation and failures of the units were not discussed in that paper.The above papers preliminarily addressed the maintenance optimisation problem of production systems with intermediate buffers. However, these papers adopted predetermined maintenance strategy structures that are not proved optimal. Some papers did not consider the relationship among the maintenance action to a component, the states of other components, and the buffer level. Other papers obtained a short-term optimal maintenance strategy.

Only few papers investigated the property of the optimal maintenance strategy structure of a production system with intermediate buffers. Kyriakidis and Dimitrakos [11] optimised the maintenance of a two-unit series system with an intermediate buffer, in which only the upstream unit suffered from degradation. The optimal maintenance policy of the upstream unit was proved to be a control-limit type for a fixed buffer level. Later, Dimitrakos and Kyriakidis [7] extended their research in Ref. [11] by using continuous distributions to model the repair time. During the numerical study, Dimitrakos and Kyriakidis found that the optimal strategy structure is also of a control-limit type. In Ref. [10], Karamatsoukis and Kyriakidis assumed a more general situation that both the upstream and downstream units deteriorate with time. It was proved that the optimal maintenance strategy of the two units both have a control-limit property. The above-mentioned papers largely focus on a two-unit series system. However, in practice, the buffer can often exist in a series-parallel system. To address this issue, this paper further investigates the situation that both the upstream and downstream subsystems contain multiple parallel-connected components. When multiple components are included in a subsystem, the degradation process of the subsystem becomes difficult to model and the maintenance strategy structure becomes more complex. In a previous paper of the authors [24], the optimal maintenance strategy structure of a two-unit series system without intermediate buffers was investigated by a Markov decision process (MDP). In this paper, the MDP is also adopted to model the system degradation and repairing process; similar to Ref. [24],the policy iteration is used to solve the MDP to obtain the optimal maintenance strategy. Because the transition matrix of the system states is sparse, the sparse incomplete LU factorization and the generalized minimum residual (GMRES) method are used in this paper to solve the system of linear equations during the policy iteration. Thus, the policy iteration method in this paper is more efficient than that in Ref. [24].The structure of the obtained optimal maintenance strategy is investigated, which privies a reference for other maintenance optimisation approaches (e.g., the embedded MDP and the method based on steady-state analysis). Furthermore, the influence of the buffer capacity on the optimal average revenue is analysed. The result shows that large buffer capacity can bring down the average revenue even when the inventory holding cost rate per item is considerably smaller than the production revenue per item. This counter-intuitive result indicates that the buffer capacity should be optimised according to system parameters.

The remaining parts of this paper are organised as follows. Section 2 introduces the mathematical formulation and assumptions of the maintenance optimisation problem. Then, an approach to identifying the optimal maintenance strategy is developed in Section 3. After that, numerical studies are performed in Section 4 to evaluate the performance of the proposed maintenance optimisation method. Section 4 also investigates the properties of the derived optimal maintenance strategy structure. Finally, Section 5 gives the conclusion of the whole paper.

Nomenclature

c_{pu}: the cost rate of the preventive maintenance to a component in the upstream subsystem in one unit time

c_{pd}: the cost rate of the preventive maintenance to a component in the downstream subsystem in one unit time

c_{cu}: the cost rate of the corrective maintenance to a component in the upstream subsystem in one unit time

c_{cd}: the cost rate of the corrective maintenance to a component in the downstream subsystem in one unit time

$c_{ou}(i, q)$: the operating cost of a component in the upstream subsystem when the component is in state I and under production rate q

$c_{od}(i, q)$: the operating cost of a component in the downstream subsystem when the component is in state iand under production rate q

c_h: the cost of holding an item in the buffer per unit time

$K(t)$: the buffer level at time t

N_k: the buffer capacity

N_u: the failure state of a component in the upstream subsystem

N_d: the failure state of a component in the downstream subsystem

p_{pu}: the probability of successfully performing the preventive maintenance to a component in the upstream subsystem in one unit time

p_{pd}: the probability of successfully performing the preventive maintenance to a component in the downstream subsystem in one unit time

p_{cu}: the probability of successfully performing the corrective maintenance to a component in the upstream subsystem in one unit time

p_{cd}: the probability of successfully performing the corrective maintenance to a component in the downstream subsystem in one unit time

$\mathbf{P_u}(q)$: the transition matrix of a component in the upstream subsystem under production rate q

$\mathbf{P}_\mathrm{d}(q)$: the transition matrix of a component in the downstream subsystem under production rate q

$\mathbf{P_u}$: the transition matrix of a component in the upstream subsystem under the nominal production rate q_u

$\mathbf{P_u^{idel}}$: the transition matrix of a component in the upstream subsystem when its production rate is zero

$\mathbf{P_d}$: the transition matrix of a component in the downstream subsystem under the nominal production rate q_u

$\mathbf{P_d^{idel}}$: the transition matrix of a component in the downstream subsystem when its production rate is zero

$P_{s,w}(\boldsymbol{\theta})$: the probability that the system is in state **w** after one unit time when the current state of the system is **s** and the adopted maintenance action is **θ**

q_u: the nominal production rates of a component in the upstream subsystem

q_d: the nominal production rates of a component in the downstream subsystem

$Q_{u,m}(k,\theta_u)$: the production rate of component m in the upstream subsystem when the buffer level is k and the maintenance action is θ_u

$Q_{d,m}(k,\theta_d)$: the production rate of component m in the downstream subsystem when the buffer level is k and the maintenance action is θ_d

r_p: the production revenue gained by an item processed by the downstream subsystem

$R(\mathbf{s}, \boldsymbol{\theta})$: the immediate revenue incurred during the next unit time when system state is **s** and the adopted maintenance action is **θ**

$\mathbf{S}(t)$: the state of the system at time t

$V(\mathbf{w})$: the relative cost function when the system is in state **w**

$X_{um}(t)$: the state of component m in the upstream subsystem at time t

$X_{dm}(t)$: the state of component m in the downstream subsystem at time t

θ: the maintenance action of the system

θ_u: the maintenance action of the upstream subsystem

θ_d: the maintenance action of the downstream subsystem

2. Problem formulation and assumptions

2.1. Problem formulation

The investigated system is illustrated in Figure 1, which contains an upstream subsystem, a downstream subsystem, and an intermediate buffer. Both the upstream and downstream subsystems consist of two identical parallel components. The upstream subsystem delivers products to the buffer, while the downstream subsystem consumes items in the buffer and processes them into final products. The nominal production rates of a component in the upstream and downstream subsystems are q_u and q_d, respectively. The buffer level at time t is denoted as $K(t)=0,1,\ldots,N_k$, where N_k is the buffer capacity. The components in the upstream and downstream subsystems all suffer from degradation, and the degradation processes follow the discrete-time discrete-state Markov process. The states of the components in the upstream and downstream subsystems at time t are $X_{um}(t)=1,2,\ldots,N_u$,PM and $X_{d,m}(t)=1,2,\ldots,N_d$,PM($m$=1,2), respectively. Here, state one is the faultless state, and state $N_u(N_d)$ is the failure state. The additional state PM indicates that the component is under preventive maintenance. The production rate of a component is zero when it fails or is under maintenance; otherwise, the component can work at the nominal production rate q_u (q_d). However, the actual production rate of a component also depends on the current buffer level $K(t)$. For example, when the buffer is full, i.e., $K(t)=N_k$, the upstream subsystem is blocked, and the production rate of its two components is zero. On the other hand, when $K(t)=0$, the downstream subsystem is starved, and the production rate of the downstream subsystem is zero. The calculation of the production rates is discussed in Section 3. In reality, the production load of a component can affect its degradation process. Therefore, this research assumes that the transition matrix of the state of a component is the function of its production rate. The transition matrix of a component in the upstream subsystem is denoted as $\mathbf{P_u}(q)$,where q is the current production rate of the component. In the same way, the transition matrix of a component in the downstream subsystem is described as $\mathbf{P_d}(q)$.

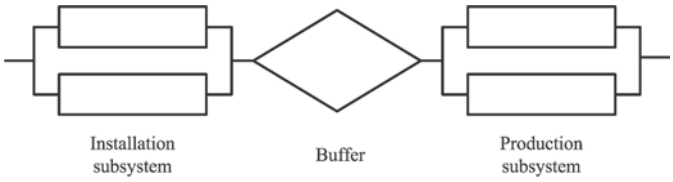

Fig. 1. The system structure

Two types of maintenance activities are applied to the components, i.e. the preventive maintenance and the corrective maintenance. The duration of the two types of maintenance activities follows the Geometric distribution. The probability of successfully performing the preventive and corrective maintenance to a component in the upstream (downstream) subsystem in one unit time is p_{pu} (p_{pd}) and $p_{cu}(p_{cd})$, respectively. The cost rate of the preventive and corrective maintenance to a component in the upstream (downstream) subsystem is c_{pu} (c_{pd}) and $c_{cu}(c_{cd})$, respectively. In practice, both the state and the production rate of a component affect its operation cost. Therefore, the operating cost of a component in the upstream subsystem is $c_{ou}(i,q)$,where i is the state of the component and the q is the current production rate of the component. This paper assumes that $c_{ou}(i, q)$ is a non-decrease function of i and q. The cost of holding an item in the buffer per unit time is c_h, and an item processed by the downstream subsystem can gain a production revenue r_p. The objective function used in maintenance optimisation is the expected revenue per unit time, which is given by:

$$\overline{R} = \overline{R}_P - \overline{C}_M - \overline{C}_O - \overline{C}_H , \tag{1}$$

where, $\overline{R}_P$ is the average production revenue per unit time; $\overline{C}_M$, $\overline{C}_O$, and $\overline{C}_H$ are the average costs per unit time incurred by maintenance, operation, and inventory.

2.2. Assumptions

- All the components have a non-decreasing degradation rate: For fixed values of q and j', the quantities $\sum_{j=j'}^{N_u}\left(\mathbf{P_u}(q)\right)_{i,j}$ and $\sum_{j=j'}^{N_d}\left(\mathbf{P_d}(q)\right)_{i,j}$ are non-decreasing in i.
- The number of products processed by the system is discrete.
- The downstream subsystem can only process the product in the buffer; an item cannot be processed by both the upstream and downstream subsystems in the same unit time.
- Both the preventive and corrective maintenance activities bring a component to a brand new state; the imperfect maintenance is not considered in this research.
- When a component is under preventive or corrective maintenance, the degradation process of the component stops, and the production rate of the component drops to zero.
- When a component fails, the corrective maintenance of the component is compulsory.
- The maintenance or failure of a component does not affect the production and maintenance of the other components.

3. Maintenance strategy optimisation

3.1. System modelling

The change of buffer level and the degradation of the components are interrelated. Therefore, the state of the system at time t is given by a vector $\mathbf{S}(t) = [X_{u1}(t)\ X_{u2}(t)\ X_{d1}(t)\ X_{d2}(t)\ K(t)]$. Because the components in a subsystem are assumed to be identical, the state space of the system can be reduced by setting $X_{u1}(t)\geq X_{u2}(t)$ and $X_{d1}(t)\geq X_{d2}(t)$.

Each system state has an optimal maintenance activity that is given by a vector $\boldsymbol{\theta}=[\theta_u\theta_d]$, where θ_u and θ_d are the maintenance actions of the upstream and downstream subsystems, respectively. The value of θ_u (θ_d) is defined as:

$$\theta_u(\theta_d)=\begin{cases}0 & \text{no maintenance is performed}\\ 1 & \text{the component in a better state is preventively maintained}\\ 2 & \text{the component in a worse state is preventively maintained}\\ 3 & \text{both the two components are preventively maintained}\\ 4 & \text{one component is correctively maintained}\\ 5 & \text{one component is correctively maintained and the other is preventively maintained}\\ 6 & \text{both the two components are correctively maintained}\end{cases} \tag{2}$$

According to the assumption in this paper, the production rate of a component is a function of the maintenance action and the buffer level k. The production rates of the two components in the upstream subsystem are given by:

$$Q_{u,1}(k,\theta_u)=\begin{cases}\min(N_k-k,2q_u)/2 & \theta_u=0\\ \min(N_k-k,q_u) & \theta_u=1\\ 0 & \theta_u=2,3,4,5,6\end{cases} \tag{3}$$

and:

$$Q_{u,2}(k,\theta_u)=\begin{cases}\min(N_k-k,2q_u)/2 & \theta_u=0\\ \min(N_k-k,q_u) & \theta_u=2,4\\ 0 & \theta_u=1,3,5,6\end{cases}. \tag{4}$$

Similarly, the production rates of the two components in the downstream subsystem can be calculated as:

$$Q_{d,1}(k,\theta_d)=\begin{cases}\min(k,2q_d)/2 & \theta_d=0\\ \min(k,q_d) & \theta_d=1\\ 0 & \theta_d=2,3,4,5,6\end{cases} \tag{5}$$

and

$$Q_{d,2}(k,\theta_d)=\begin{cases}\min(k,2q_d)/2 & \theta_d=0\\ \min(k,q_d) & \theta_d=2,4\\ 0 & \theta_d=1,3,5,6\end{cases}. \tag{6}$$

To simplify the formulation, this research assumes that the transition probabilities of a component are linear functions of its production rate q. The elements in the transition matrix $\mathbf{P_u}(q)$ of a component in the upstream subsystem can be calculated as:

$$\left(\mathbf{P_u}(q)\right)_{i,j}=\left((q_u-q)\cdot\left(\mathbf{P_u^{idel}}\right)_{i,j}+q\cdot(\mathbf{P_u})_{i,j}\right)\Big/q_u. \tag{7}$$

Here, $\mathbf{P_u}$ is the state transition matrix of a component under the nominal production rate q_u, and $\mathbf{P_u^{idel}}$ is the state transition matrix of a component when its production rate is zero. The state transition matrix of a component in the downstream subsystem can be calculated in the same way using the two transition matrices $\mathbf{P_d}$ and $\mathbf{P_d^{idel}}$. The operation cost of a component is a function of the component state i and production rate q. The operation cost of a component in the upstream subsystem is assumed as:

$$c_{ou}(i,q)=c_{ou,i}\cdot q/q_u, \tag{8}$$

where, $c_{ou,i}$ is the operation cost of a component in the upstream subsystem when its state is i and its production rate is the nominal production rate q_u. Similarly, the operation cost of a component in the downstream subsystem is:

$$c_{od}(i,q)=c_{od,i}\cdot q/q_d. \tag{9}$$

Other formulations of transition probabilities and operation costs can be also processed by the maintenance optimisation method developed in this paper.

3.2. Markov decision process model

The MDP is a useful tool to identify the optimal maintenance strategy when the optimal strategy structure is unknown [24]. Consequently, this research adopts the MDP to investigate the properties of the optimal maintenance strategy for a series-parallel system with an intermediate buffer.

A crucial part of the MDP model is the relative cost function that formulates the relative cost of a single step in the long-run decision process [14]. For the investigated maintenance optimisation problem, the relative cost function is given by:

$$V_{\boldsymbol{\theta}}(\mathbf{s})=R(\mathbf{s},\boldsymbol{\theta})-g+\sum_{\mathbf{w}\in\mathbf{S}}P_{\mathbf{s},\mathbf{w}}(\boldsymbol{\theta})V(\mathbf{w}). \tag{10}$$

Here, $\mathbf{s}=[x_{u1}x_{u2}x_{d1}x_{d2}k]$ is the system state vector, while $\mathbf{w}=[x'_{u1}x'_{u2}x'_{d1}x'_{d2}k']$ is another state in the system state space $\mathbf{S}$. The notations g and $\boldsymbol{\theta}$ are the average revenue per unit time and the adopted maintenance action, respectively. $R(\mathbf{s}, \boldsymbol{\theta})$ is the immediate revenue incurred during the next unit time when the system is in state $\mathbf{s}$ and under maintenance action $\boldsymbol{\theta}$. $P_{s,w}(\boldsymbol{\theta})$ is the probability that the system is in state $\mathbf{w}$ after one unit time when the current state of the system is $\mathbf{s}$ and the adopted maintenance action is $\boldsymbol{\theta}$. The function $V(\mathbf{w})$ is the relative cost function when the system is in state $\mathbf{w}$, which is given by:

$$V(\mathbf{w})=\min_{\boldsymbol{\theta}\in\boldsymbol{\Theta}}V_{\boldsymbol{\theta}}(\mathbf{w}), \tag{11}$$

where, $\boldsymbol{\Theta}$ is the maintenance action space.

The immediate revenue $R(\mathbf{s}, \boldsymbol{\theta})$ incurred during the next unit time is calculated as:

$$\begin{aligned}R(\mathbf{s},\boldsymbol{\theta})=r_p\sum_{m=1}^{2}Q_{d,m}(k,\theta_d)-\sum_{m=1}^{2}c_{ou}\left(x_{u,m},Q_{u,m}(k,\theta_u)\right)\\ -\sum_{m=1}^{2}c_{od}\left(x_{d,m},Q_{d,m}(k,\theta_d)\right)-C_{M,u}(\theta_u)-C_{M,d}(\theta_d)-c_hk\end{aligned}, \tag{12}$$

where, $C_{M,u}(\theta_u)$ and $C_{M,d}(\theta_d)$ are the maintenance costs of the upstream and downstream subsystems under strategies θ_u and θ_d. The two can be calculated as:

$$C_{M,u}(\theta_u)=\begin{cases}0 & \theta_u=0\\ c_{pu} & \theta_u=1,2\\ 2c_{pu} & \theta_u=3\\ c_{cu} & \theta_u=4\\ c_{pu}+c_{cu} & \theta_u=5\\ 2c_{cu} & \theta_u=6\end{cases} \quad (13)$$

and

$$C_{M,d}(\theta_d)=\begin{cases}0 & \theta_d=0\\ c_{pd} & \theta_d=1,2\\ 2c_{pd} & \theta_d=3\\ c_{cd} & \theta_d=4\\ c_{pd}+c_{cd} & \theta_d=5\\ 2c_{cd} & \theta_d=6\end{cases}. \quad (14)$$

The buffer level after one unit time can be calculated according to the adopted maintenance action and the current buffer level as:

$$k'=k+\sum_{m=1}^{2}Q_{u,m}(k,\theta_u)-\sum_{m=1}^{2}Q_{d,m}(k,\theta_d). \quad (15)$$

The degradation processes of the upstream and downstream subsystems do not depend on each other. Consequently, the transition probability of the system can be simplified as:

$$\begin{aligned}P_{\mathbf{s},\mathbf{w}}(\boldsymbol{\theta})&=\Pr\left(x'_{u1},x'_{u2},x'_{d1},x'_{d2},k'\middle|x_{u1},x_{u2},x_{d1},x_{d2},k,\theta_u,\theta_d\right)\\&=\Pr\left(x'_{u1},x'_{u2}\middle|x_{u1},x_{u2},k,\theta_u\right)\Pr\left(x'_{d1},x'_{d2}\middle|x_{d1},x_{d2},k,\theta_d\right)\\&\quad\cdot I\left(k'=k+\sum_{m=1}^{2}Q_{u,m}(k,\theta_u)-\sum_{m=1}^{2}Q_{d,m}(k,\theta_d)\right)\end{aligned} \quad (16)$$

Here, $I(A)$ is the indicator function given by:

$$I(A)=\begin{cases}1 & A \text{ is trure}\\ 0 & A \text{ is false}\end{cases}. \quad (17)$$

Because the derivation processes of the probabilities $\Pr\left(x'_{u1},x'_{u2}\middle|x_{u1},x_{u2},k,\theta_u\right)$ and $\Pr\left(x'_{d1},x'_{d2}\middle|x_{d1},x_{d2},k,\theta_d\right)$ are quite similar, only the calculation of $\Pr\left(x'_{u1},x'_{u2}\middle|x_{u1},x_{u2},k,\theta_u\right)$ is introduced as follows:

When θ_u=0, no maintenance activities are applied to the two components. The transition probability is given by:

$$\begin{aligned}\Pr\left(x'_{u1},x'_{u2}\middle|x_{u1},x_{u2},k,0\right)&=\left(\mathbf{P_u}\left(Q_{u,1}(k,0)\right)\right)_{x_{u1},x'_{u1}}\left(\mathbf{P_u}\left(Q_{u,2}(k,0)\right)\right)_{x_{u2},x'_{u2}}\\&\quad+\left(\mathbf{P_u}\left(Q_{u,1}(k,0)\right)\right)_{x_{u1},x'_{u2}}\left(\mathbf{P_u}\left(Q_{u,2}(k,0)\right)\right)_{x_{u2},x'_{u1}}\end{aligned} \quad (18)$$

When θ_u=1, only the component in a better state is maintained. After one unit time, the component can be still under preventive maintenance or in a brand new state. The transition probability is calculated as:

$$\Pr\left(x'_{u1},x'_{u2}\middle|x_{u1},x_{u2},k,1\right)=\begin{cases}\left(1-p_{pu}\right)\left(\mathbf{P_u}\left(Q_{u,1}(k,1)\right)\right)_{x_{u1},x'_{u2}} & x'_{u1}=PM\\ p_{pu}\left(\mathbf{P_u}\left(Q_{u,1}(k,1)\right)\right)_{x_{u1},x'_{u1}} & otherwise\end{cases} \quad (19)$$

Similarly, when θ_u=2, only the component in a worse state is maintained, and the transition probability is as follows:

$$\Pr\left(x'_{u1},x'_{u2}\middle|x_{u1},x_{u2},k,2\right)=\begin{cases}\left(1-p_{pu}\right)\left(\mathbf{P_u}\left(Q_{u,2}(k,2)\right)\right)_{x_{u2},x'_{u2}} & x'_{u1}=PM\\ p_{pu}\left(\mathbf{P_u}\left(Q_{u,2}(k,2)\right)\right)_{x_{u2},x'_{u1}} & otherwise\end{cases}. \quad (20)$$

When both the two components are preventively maintained, i.e. θ_u=3, the transition probability can be computed as:

$$\Pr\left(x'_{u1},x'_{u2}\middle|x_{u1},x_{u2},k,3\right)=\begin{cases}\left(1-p_{pu}\right)\left(1-p_{pu}\right) & x'_{u1}=PM,x'_{u2}=PM\\ 2p_{pu}\left(1-p_{pu}\right) & x'_{u1}=PM,x'_{u2}=1\\ p_{pu}p_{pu} & otherwise\end{cases}. \quad (21)$$

When θ_u=4,a component is failed and correctively maintained. The corresponding transition probability is given by:

$$\Pr\left(x'_{u1},x'_{u2}\middle|x_{u1},x_{u2},k,4\right)=\begin{cases}\left(1-p_{cu}\right)\left(\mathbf{P_u}\left(Q_{u,2}(k,4)\right)\right)_{x_{u2},x'_{u2}} & x'_{u1}=N_u\\ p_{cu}\left(\mathbf{P_u}\left(Q_{u,2}(k,4)\right)\right)_{x_{u2},x'_{u1}} & otherwise\end{cases}. \quad (22)$$

When θ_u=5, a component is correctively maintained and the other one is under preventive maintenance. The transition probability is calculated as:

$$\Pr\left(x'_{u1},x'_{u2}\middle|x_{u1},x_{u2},k,5\right)=\begin{cases}\left(1-p_{pu}\right)\left(1-p_{cu}\right) & x'_{u1}=PM,x'_{u2}=N_u\\ \left(1-p_{pu}\right)p_{cu} & x'_{u1}=PM,x'_{u2}=1\\ \left(1-p_{cu}\right)p_{pu} & x'_{u1}=N_u,x'_{u2}=1\\ p_{pu}p_{cu} & otherwise\end{cases}. \quad (23)$$

When both the two components are correctively maintained, i.e. θ_u=6, the transition probability can be computed as:

$$\Pr\left(x'_{u1},x'_{u2}\middle|x_{u1},x_{u2},k,6\right)=\begin{cases}\left(1-p_{cu}\right)\left(1-p_{cu}\right) & x'_{u1}=N_u,x'_{u2}=N_u\\ 2p_{cu}\left(1-p_{cu}\right) & x'_{u1}=N_u,x'_{u2}=1\\ p_{cu}p_{cu} & otherwise\end{cases}. \quad (24)$$

After different components in the relative cost function (10) are calculated, the policy iteration modified from that in Ref. [24] is used to find the optimal maintenance strategy. In policy iteration, the relationship between the maintenance action and the system state is formulated as a policy function denoted as $\delta(\mathbf{s})=\boldsymbol{\theta}$, where $\mathbf{s}$is the system state and $\boldsymbol{\theta}$ is the corresponding maintenance action. The policy iteration is used to obtain the policy function $\delta^*(\cdot)$ that incurs the largest average revenue per unit time. The process of the policy iteration is shown in Table 1. For a more detailed introduction of the policy iteration, readers can refer to [15, 22].

Table 1. The process of policy iteration

Step 1: An initial policy function $\delta_0(\mathbf{s})$ is selected by the rule of thumb, and any maintenance policy that satisfies the assumptions of this research can be adopted as the initial policy.
Step 2: Obtain the relative costs $\{V(\mathbf{s}); \mathbf{s} \in \mathbf{S}\}$ and the expected revenue per unit time g by solving the following system of linear equations that is constructed according to the current maintenance policy function $\delta_k(\mathbf{s})$: $$V(\mathbf{s}) = R(\mathbf{s}, \delta_k(\mathbf{s})) - g + \sum_{\mathbf{w} \in \mathbf{S}} P_{\mathbf{s},\mathbf{w}}(\delta_k(\mathbf{s}))V(\mathbf{w}) \quad \mathbf{s} \in \mathbf{S}$$ The size of the state space $\mathbf{S}$ is $(N_u+1)(N_u+2)/2\times(N_d+1)(N_d+2)/2\times(N_k+1)$, which is also the number of equations in the system of linear equations. It is assumed that the relative cost function is zero when the system is brand new and the buffer in empty, i.e., $V([x_{u1}, x_{u2}, x_{d1}, x_{d2}, k])=0$ if $x_{u1}=x_{u2}=x_{d1}=x_{d2}=1$ and $k=0$.
Step 3: Calculate the relative costs under different maintenance actions using the relative costs $\{V(\mathbf{s}); \mathbf{s} \in \mathbf{S}\}$ and the expected revenue per unit time g that are obtained in Step 2: $$V_{\boldsymbol{\theta}}(\mathbf{s}) = R(\mathbf{s}, \boldsymbol{\theta}) - g + \sum_{\mathbf{w} \in \mathbf{S}} P_{\mathbf{s},\mathbf{w}}(\boldsymbol{\theta})V(\mathbf{w}).$$
Step 4: Obtain the improved policy function $\delta_{k+1}(\mathbf{s})$ using the relative costs $\{V_{\boldsymbol{\theta}}(\mathbf{s}); \boldsymbol{\theta} \in \Theta, \mathbf{s} \in \mathbf{S}\}$ calculated in Step 3. The $\delta_{k+1}(\mathbf{s})$ is identified as: $$\delta_{k+1}(\mathbf{s}) = \arg\max_{\boldsymbol{\theta} \in \Theta} V_{\boldsymbol{\theta}}(\mathbf{s})$$
Step 5: If $\delta_{k+1}(\cdot) = \delta_k(\cdot)$, the optimal maintenance policy $\delta^*(\cdot)$ is obtained as $\delta_k(\cdot)$. Otherwise, go to Step 2 and start a new iteration.

In this paper, the system state is the combination of the four component states and the buffer level. Consequently, the size of the transition matrix increases quickly with the number of component states and buffer levels. For example, in the numerical study of this paper, the total number of elements in the transition matrices corresponding to different actions is 771895089. When the MATLAB is used to realise this algorithm, more than 5G memory is required to store the sevariables of type double. Fortunately, the total number of nonzero elements in these matrices is only 1121481, which requires just about 8M memory on the MATLAB platform. Another problem is that a system of linear equations that contains a large number of equations should be solved duration the policy iteration in this paper, which is computationally expensive. Fortunately, the coefficient matrix of the system of linear equations is also sparse. Subsequently, the generalized minimum residual (GMRES)method[3]that can process the large and sparse coefficient matrix efficiently is adopted. The incomplete LU factorization [18] is used to provide preconditioners for the GMRES method. The simulation study shows that the developed approach can identify the optimal maintenance strategy efficiently.

4. Numerical study

A numerical study is conducted to evaluate the performance of the proposed maintenance optimisation algorithm. Furthermore, the obtained optimal maintenance strategy is investigated to analyse the properties of the optimal strategy structure. Finally, the influence of system parameters on the result of maintenance optimisation is studied through sensitivity analysis. This numerical study is executed using MATLAB 7.14 on a desktop computer with an Intel i7 3770 CPU and eight Gigabytes of RAM.

4.1. System introduction

The structure of the system investigated in this numerical study is shown in Figure 1. The transition matrices of a component in the upstream subsystem when it is under nominal production rate and is idle are:

$$\mathbf{P_u} = \begin{bmatrix} 0.5 & 0.2 & 0.15 & 0.1 & 0.05 \\ 0 & 0.4 & 0.3 & 0.2 & 0.1 \\ 0 & 0 & 0.5 & 0.3 & 0.2 \\ 0 & 0 & 0 & 0.6 & 0.4 \\ 0 & 0 & 0 & 0 & 1 \end{bmatrix} \text{ and}$$

$$\mathbf{P_u^{idle}} = \begin{bmatrix} 0.93 & 0.03 & 0.02 & 0.01 & 0.01 \\ 0 & 0.94 & 0.03 & 0.02 & 0.01 \\ 0 & 0 & 0.95 & 0.03 & 0.02 \\ 0 & 0 & 0 & 0.96 & 0.04 \\ 0 & 0 & 0 & 0 & 1 \end{bmatrix}, \text{ respectively.}$$

On the other hand, the transition matrices of a component in the downstream subsystem are:

$$\mathbf{P_d} = \begin{bmatrix} 0.6 & 0.18 & 0.1 & 0.07 & 0.05 \\ 0 & 0.5 & 0.3 & 0.15 & 0.05 \\ 0 & 0 & 0.6 & 0.2 & 0.2 \\ 0 & 0 & 0 & 0.5 & 0.5 \\ 0 & 0 & 0 & 0 & 1 \end{bmatrix} \text{ and}$$

$$\mathbf{P}_{\mathbf{d}}^{\mathbf{idle}} = \begin{bmatrix} 0.9 & 0.04 & 0.03 & 0.02 & 0.01 \\ 0 & 0.93 & 0.03 & 0.02 & 0.02 \\ 0 & 0 & 0.93 & 0.04 & 0.03 \\ 0 & 0 & 0 & 0.96 & 0.04 \\ 0 & 0 & 0 & 0 & 1 \end{bmatrix}.$$

The probabilities of successful preventive and corrective maintenance in a unit time are assumed as:p_{pu}=0.8,p_{pd}=0.7,p_{cu}=0.2, andp_{cd}=0.15. The costs of maintenance activities are c_{pu}=50, c_{pd}=60, c_{cu}=100, and c_{cd}=110. The nominal production rates of a component in the upstream and downstream subsystems are q_u=3 and q_d=2, respectively. The operation costs of a component in different states under the nominal production rate are listedin Table 2. The buffer capacity is N_k=8, and the cost of holding an item in the buffer for a unit time is c_h=1. The production revenue brought about by a product processed by the downstream subsystem is r_p=150.

Table 2. operation costs of a component in different states under the nominal production rate

i	1	2	3	4
$c_{ou,i}$	5	10	12	15
$c_{od,i}$	4	8	10	13

4.2. Maintenance optimisation and results analysis

Before the policy iteration, the transition matrices of the system under different maintenance actions and the immediate revenue should be calculated. There are 49 transition matrices of size 3969×3969 according to different maintenance actions, while the number of immediate revenue values under different combinations of system states and maintenance actions is 3969×49=194481. The computing time of the transition matrices and the immediate revenue values is about 47 second. Then, the policy iteration is performed and the optimal revenue is finally obtained as g*=200.929 after five iterations, which takes 40 seconds. During the policy iteration, the GMRES method is used to solve the system of linear equations that contains 3969 equations, which takes only about eight seconds during each iteration.

Some parts of the obtained maintenance strategies are demonstrated in Tables 3 to 6. The notation $\mathbf{x_u}$ ($\mathbf{x_d}$) is the state vector of the upstream (downstream) subsystem before the possible maintenance action, while $\mathbf{x^+_u}$($\mathbf{x^+_d}$) is the state vector after the beginning of the maintenance action. Here, the state of the subsystems after the beginning of the maintenance action is introduced to simplify the demonstration of the maintenance actions. For example, if the maintenance action is a_d=2, the two states $\mathbf{x_d}$=[3,1] and [4,1] can be combined to a single state $\mathbf{x^+_d}$=[PM,1].

Some conclusions can be drawn from the result of this particular maintenance optimisation problem:

1. The optimal maintenance activity of a subsystem is affected by the buffer level. Here, the situation that $\mathbf{x^+_d}$=[1 1] and $\mathbf{x_u}$=[22] is considered as an example. As shown in Table 3, when the buffer is empty, preventive maintenance activity on the upstream subsystem is not required. Conversely, Table 5 shows that both the two components in the upstream subsystem should be preventively maintained when the buffer is full.
2. The optimal maintenance activity of a subsystem depends on the state of the other subsystem. However, this dependence is not straightforward to explain. E.g. as shown in Table 3, when the downstream subsystem is in state $\mathbf{x^+_d}$=[2 1] or [2 2] and the upstream subsystem is in state $\mathbf{x_u}$=[3 1], both the two components in the upstream subsystem are not maintained. On the other hand, when the downstream subsystem is in the other states and $\mathbf{x_u}$=[3 1], the component in state 3 in the upstream subsystem will be preventively maintained. Therefore, it cannot be concluded that a worse health state of the downstream

Table 3. The optimal maintenance actions of the upstream subsystem when k=0

$\mathbf{x_u}$	$\mathbf{x^+_d}$									
	1,1	2,1	2,2	PM,1	PM,2	PM,PM	D,1	D,2	D,PM	D,D
1,1	N,N	N,N	N,N	N,N	N,N	N,N	N,N	-	N,N	N,N
2,1	N,N	N,N	N,N	N,N	N,N	N,N	N,N	N,N	N,N	N,N
2,2	N,N	N,N	N,N	N,N	N,N	N,N	N,N	N,N	N,N	N,N
3,1	P,N	N,N	N,N	P,N	-	P,N	P,N	-	P,N	P,N
3,2	P,N	N,N	N,N	P,N	P,N	P,N	P,N	P,N	P,N	P,N
3,3	P,P	-	N,N	P,P	-	P,P	P,N	P,N	P,N	P,P
4,1	P,N	-	-	P,N	-	P,N	P,N	-	P,N	P,N
4,2	P,N	-	-	P,N	P,N	P,N	P,N	P,N	P,N	P,N
4,3	P,P	-	-	P,P	-	P,P	P,N	P,N	P,N	P,P
4,4	P,P	-	-	P,P	-	P,P	P,P	-	P,P	P,P
PM,1	P,N	-	-	P,N	-	P,N	P,N	-	P,N	P,N
PM,2	P,N	-	-	P,N	P,N	P,N	P,N	P,N	P,N	P,N
PM,3	P,P	-	-	P,P	-	P,P	P,N	P,N	P,N	P,P
PM,4	P,P	-	-	P,P	-	P,P	P,P	-	P,P	P,P
D,1	C,N	C,N	C,N	C,N	C,N	C,N	C,N	C,N	C,N	C,N
D,2	C,N	C,N	C,N	C,N	C,N	C,N	C,N	C,N	C,N	C,N
D,3	C,P	-	-	C,P	-	C,P	C,N	C,N	C,P	C,P
D,4	C,P	-	-	C,P	-	C,P	C,P	-	C,P	C,P

The character N means that the component is not under maintenance; P denotes preventive maintenance; C standards for corrective maintenance; D is the breakdown state. The first character is the maintenance action or the state of the first component, while the second one is that of the second component. When the optimal maintenance action of a subsystem depends on the state of the other subsystem, the background of the row is grey.

Table 4. The optimal maintenance actions of the upstream subsystem when k=4

x_u	x^+_d									
	1,1	2,1	2,2	PM,1	PM,2	PM,PM	D,1	D,2	D,PM	D,D
1,1	N,N	N,N	N,N	N,N	N,N	N,N	N,N	N,N	N,N	N,N
2,1	N,N	N,N	N,N	N,N	N,N	N,N	N,N	N,N	P,N	N,N
2,2	N,N	N,N	N,N	N,N	N,N	N,N	N,N	N,N	N,N	N,N
3,1	P,N	P,N	P,N	P,N	P,N	P,N	P,N	P,N	P,N	P,N
3,2	P,N	P,N	P,N	P,N	P,N	P,N	P,N	P,N	P,N	P,N
3,3	P,N	P,N	P,N	P,P	P,P	P,P	P,P	P,P	P,P	P,P
4,1	P,N	P,N	P,N	P,N	P,N	P,N	P,N	P,N	P,N	P,N
4,2	P,N	P,N	P,N	P,N	P,N	P,N	P,N	P,N	P,N	P,N
4,3	P,N	P,N	P,N	P,P	P,P	P,P	P,P	P,P	P,P	P,P
4,4	P,P	P,P	P,P	P,P	P,P	P,P	P,P	P,P	P,P	P,P
PM,1	P,N	P,N	P,N	P,N	P,N	P,N	P,N	P,N	P,N	P,N
PM,2	P,N	P,N	P,N	P,N	P,N	P,N	P,N	P,N	P,N	P,N
PM,3	P,N	P,N	P,N	P,P	P,P	P,P	P,P	P,P	P,P	P,P
PM,4	P,P	P,P	P,P	P,P	P,P	P,P	P,P	P,P	P,P	P,P
D,1	C,N	C,N	C,N	C,N	C,N	C,N	C,N	C,N	C,N	C,N
D,2	C,N	C,N	C,N	C,N	C,N	C,N	C,N	C,N	C,N	C,N
D,3	C,P	C,P	C,P	C,P	C,P	C,P	C,P	C,P	C,P	C,P
D,4	C,P	C,P	C,P	C,P	C,P	C,P	C,P	C,P	C,P	C,P

Table 5. The optimal maintenance actions of the upstream subsystem when k=8

x_u	x^+_d									
	1,1	2,1	2,2	PM,1	PM,2	PM,PM	D,1	D,2	D,PM	D,D
1,1	N,N	N,N	N,N	N,N	N,N	N,N	N,N	N,N	N,N	N,N
2,1	P,N	P,N	P,N	P,N	P,N	P,N	N,N	N,N	N,N	N,N
2,2	P,P	P,P	P,P	P,P	P,P	P,P	P,N	P,N	N,N	N,N
3,1	P,N	P,N	P,N	P,N	P,N	P,N	P,N	P,N	P,N	P,N
3,2	P,P	P,P	P,P	P,P	P,P	P,P	P,N	P,N	P,N	P,N
3,3	P,P	P,P	P,P	P,P	P,P	P,P	P,P	P,P	P,P	P,P
4,1	P,N	P,N	P,N	P,N	P,N	P,N	P,N	P,N	P,N	P,N
4,2	P,P	P,P	P,P	P,P	P,P	P,P	P,N	P,N	P,N	P,N
4,3	P,P	P,P	P,P	P,P	P,P	P,P	P,P	P,P	P,P	P,P
4,4	P,P	P,P	P,P	P,P	P,P	P,P	P,P	P,P	P,P	P,P
PM,1	P,N	P,N	P,N	P,N	P,N	P,N	P,N	P,N	P,N	P,N
PM,2	P,P	P,P	P,P	P,P	P,P	P,P	P,N	P,N	P,N	P,N
PM,3	P,P	P,P	P,P	P,P	P,P	P,P	P,P	P,P	P,P	P,P
PM,4	P,P	P,P	P,P	P,P	P,P	P,P	P,P	P,P	P,P	P,P
D,1	C,N	C,N	C,N	C,N	C,N	C,N	C,N	C,N	C,N	C,N
D,2	C,P	C,P	C,P	C,P	C,P	C,P	C,P	C,P	C,P	C,N
D,3	C,P	C,P	C,P	C,P	C,P	C,P	C,P	C,P	C,P	C,P
D,4	C,P	C,P	C,P	C,P	C,P	C,P	C,P	C,P	C,P	C,P

subsystem requires a more conservative or speculative maintenance strategy of the upstream subsystem.

3. The state of the downstream subsystem has a more significant effect on the maintenance strategy of the upstream subsystem. On the other hand, according to the result of this maintenance optimisation, when the buffer level is four and eight, the optimal maintenance activity of the downstream subsystem does not depend on the state of the upstream subsystem.
4. The maintenance strategy of a component depends on the state of the other component in the same subsystem. As shown in Table 4, when $\mathbf{x}^+_d$=[1 1] and a component in the upstream subsystem is in state one, the preventive maintenance threshold of the other component is state three. Conversely, when

Table 6. The optimal maintenance actions of the downstream subsystem when k=0

x_d	x^+_u														
	1,1	2,1	2,2	3,1	3,2	3,3	PM,1	PM,2	PM,3	PM,PM	D,1	D,2	D,3	D,PM	D,D
1,1	N,N	N,N	N,N	-	-	-	N,N	N,N	-	N,N	N,N	N,N	-	N,N	N,N
2,1	N,N	N,N	N,N	N,N	N,N	-	P,N	P,N	-	P,N	N,N	N,N	-	P,N	P,N
2,2	N,N	N,N	N,N	N,N	N,N	N,N	P,P	P,N	-	P,P	N,N	N,N	-	P,P	P,P
3,1	P,N	P,N	P,N	-	-	-	P,N	P,N	-	P,N	P,N	P,N	-	P,N	P,N
3,2	P,N	P,N	P,N	-	-	-	P,P	P,N	-	P,P	P,N	P,N	-	P,P	P,P
3,3	P,P	P,P	P,P	-	-	-	P,P	P,P	-	P,P	P,P	P,P	-	P,P	P,P
4,1	P,N	P,N	P,N	-	-	-	P,N	P,N	-	P,N	P,N	P,N	-	P,N	P,N
4,2	P,N	P,N	P,N	-	-	-	P,P	P,N	-	P,P	P,N	P,N	-	P,P	P,P
4,3	P,P	P,P	P,P	-	-	-	P,P	P,P	-	P,P	P,P	P,P	-	P,P	P,P
4,4	P,P	P,P	P,P	-	-	-	P,P	P,P	-	P,P	P,P	P,P	-	P,P	P,P
PM,1	P,N	P,N	P,N	-	-	-	P,N	P,N	-	P,N	P,N	P,N	-	P,N	P,N
PM,2	P,N	P,N	P,N	-	-	-	P,P	P,N	-	P,P	P,N	P,N	-	P,P	P,P
PM,3	P,P	P,P	P,P	-	-	-	P,P	P,P	-	P,P	P,P	P,P	-	P,P	P,P
PM,4	P,P	P,P	P,P	-	-	-	P,P	P,P	-	P,P	P,P	P,P	-	P,P	P,P
D,1	C,N	C,N	C,N	-	-	-	C,N	C,N	C,N	C,N	C,N	C,N	C,N	C,N	C,N
D,2	C,P	C,N	C,N	-	-	-	C,P	C,N	C,N	C,P	C,N	C,N	C,N	C,P	C,P
D,3	C,P	C,P	C,P	-	-	-	C,P	C,P	C,P	C,P	C,P	C,P	-	C,P	C,P
D,4	C,P	C,P	C,P	-	-	-	C,P	C,P	C,P	C,P	C,P	C,P	-	C,P	C,P

*Table 7. The optimal average revenue g*under different system parameters*

r_p	c_h	N_k								
		2	4	6	8	10	12	14	16	18
50	0	-24.785	-15.093	-10.633	-8.698	-7.947	-7.467	-7.122	-6.856	-6.642
50	1	-25.804	-17.195	-13.895	-13.156	-13.663	-14.438	-15.278	-16.202	-17.192
50	2	-26.823	-19.297	-17.157	-17.599	-19.137	-20.880	-22.796	-24.833	-26.961
50	5	-29.879	-25.596	-26.803	-30.454	-34.947	-39.807	-42.302	-42.378	-42.378
50	10	-34.972	-36.002	-42.647	-51.337	-55.788	-55.788	-55.788	-55.788	-55.788
100	0	23.043	68.436	89.396	98.214	101.504	103.612	105.138	106.321	107.277
100	1	22.022	66.312	86.088	93.703	95.722	96.511	96.689	96.532	96.184
100	2	21.001	64.190	82.790	89.216	89.983	89.565	88.677	87.469	86.014
100	5	17.939	57.848	72.936	75.948	73.463	70.059	66.043	63.681	63.667
100	10	12.835	47.337	56.676	54.434	47.231	45.873	45.873	45.873	45.873
150	0	70.987	153.527	190.293	205.436	211.157	214.846	217.529	219.622	221.318
150	1	69.969	151.397	186.966	200.929	205.371	207.736	209.071	209.781	210.066
150	2	68.951	149.268	183.647	196.437	199.624	200.709	200.768	200.274	199.444
150	5	65.897	142.882	173.711	183.075	182.701	180.486	177.453	173.797	172.091
150	10	60.807	132.285	157.269	161.227	155.738	151.820	151.808	151.808	151.808
200	0	119.029	239.189	291.700	312.932	320.967	326.200	330.017	332.987	335.394
200	1	118.010	237.060	288.377	308.442	315.203	319.108	321.562	323.144	324.144
200	2	116.992	234.930	285.059	303.961	309.463	312.059	313.190	313.470	313.200
200	5	113.936	228.544	275.121	290.604	292.406	291.443	289.295	286.392	282.941
200	10	108.844	217.920	258.597	268.520	264.836	259.304	258.861	258.861	258.861
400	0	311.268	582.482	699.267	745.413	761.702	772.598	780.678	787.035	792.220
400	1	310.249	580.362	695.958	740.939	755.991	765.581	772.310	777.276	781.031
400	2	309.231	578.242	692.651	736.470	750.284	758.583	763.969	767.551	769.900
400	5	306.177	571.883	682.730	723.086	733.243	737.696	739.201	739.006	737.692
400	10	301.086	561.288	666.197	700.908	705.081	703.682	699.790	697.243	697.236

The highest optimal average revenue value in each row is marked with a grey background colour

$\mathbf{x}^{+}_{\mathbf{d}}$=[1 1] and a component in the upstream subsystem is in state four, the preventive maintenance threshold of the other component becomes state four.

5. In this particular maintenance optimisation problem, the control-limit structure is always optimal for a component when the buffer level and the states of the other three components are fixed. In other words, there is always an optimal preventive maintenance threshold for a component when the states of the other components and the buffer level are determined.
6. In this simulation study, the maintenance activities a_u=1 or a_d=1 are not the optimal for all the system states. Therefore, if only one component is to be preventively maintained, it will not be the one in a better state.

Conclusions one to four show that the optimal maintenance strategy cannot be described by a small number of parameters. Consequently, the MDP is an appropriate approach to optimising the maintenance strategy. Conclusions five and six can be used to simplify the MDP model. The prerequisites of conclusions five and six will be further discussed in another paper. When the number of system states is intractably large, some factors can be ignored during the maintenance optimisation to obtain an approximate optimal strategy. For example, the maintenance activity of a component can be assumed to be independent from the other in the same subsystem.

4.3. The influence of the buffer capacity on the optimal average revenue

A large capacity of the intermediate buffer can reduce the influence of the failure and maintenance of the upstream subsystem, and can thus enhance the system production rate. However, holding products in a buffer also incurs cost in some practical applications. Under these situations, the large capacity of the buffer can increase the holding cost of work in process. Therefore, it is necessary to investigate the relationship between the optimal average revenue per unit time and the buffer capacity. This section changes the production revenue per item r_p, the storage cost rate per item c_h, and the buffer capacity N_k; other system parameters are the same as those used in Section 4.2. The optimal average revenue g^*under different system parameters is demonstrated in Table 7.

Table 7 shows that a large buffer capacity does not necessarily bring about high average revenue per unit time. When the storage cost rate c_h is not ignorable compared with the production revenue per item r_p, there exists an optimal buffer capacity that can result in the largest optimal average revenue per unit time. The optimal buffer capacity decreases with the storage cost rate per item and increases with the production revenue per item. As shown in Table 7, even when the storage cost rate per item c_h is only 1 and the production revenue per item r_p is as large as 100, the buffer capacity larger than 14 can still bring down the optimal average revenue. This counterintuitive phenomenon indicates that optimising the buffer capacity is necessary, when the holding cost of products in the buffer is not ignorable. An alternative approach to controlling the buffer level is scheduling the production according to the system state.

4.4. Sensitivity analysis of parameters of maintenance activities

The parameters of maintenance activities of the upstream and downstream subsystems can have different effects on the optimal average revenue. This section modifies the system parameters used in section 4.2. The parameters of the maintenance activities are assumed as p_{pu}= p_{pd} =0.7, p_{cu}= p_{cd}=0.175, c_{pu}= c_{pd} =50, and c_{cu}= c_{cd}=100, while the other parameters remain the same as those in section 4.2. Firstly, the sensitivity analysis about the maintenance cost rate is performed. The cost rates of preventive and corrective maintenance activities are assumed to follow the relationship c_{cu}=2c_{pu} and c_{cd}=2c_{pd}. The average revenue values under different c_{pu} and c_{pd} are plotted in Figure 2. Similar sensitivity analysis is conducted to the probability of successful maintenance activity. The average revenue values under different p_{pu} and p_{pd} are displayed in Figure 3, where p_{cu}=0.25p_{pu} and p_{cd}=0.25p_{pd}. The two figures show that the average revenue is more sensitive to the parameters of the downstream subsystem.

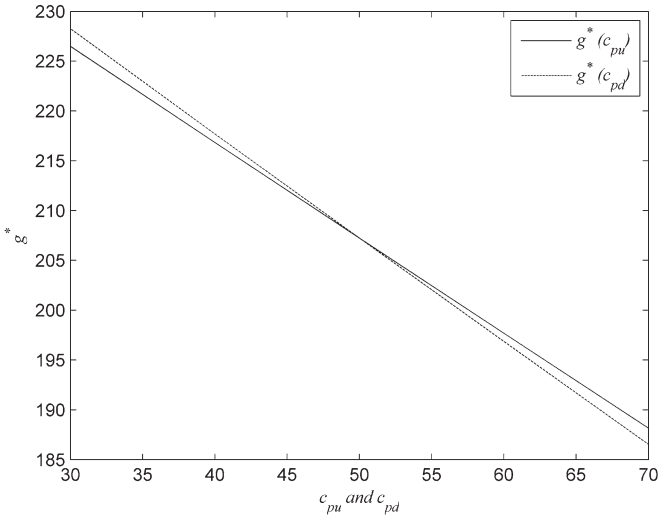

Fig. 2. The average revenue per unit time under different maintenance cost rates

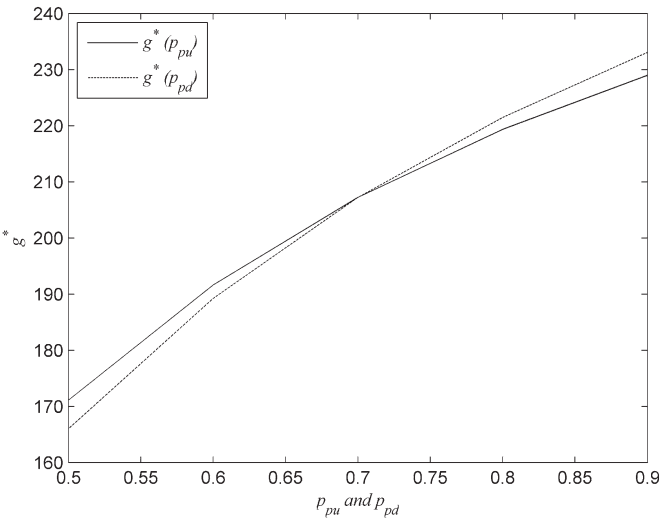

Fig. 3. The average revenue per unit time under different probability of successful maintenance in a unit time

5. Conclusion

This paper formulates the degradation process of a series-parallel system with an intermediate buffer using the MDP model. The policy iteration is used to identify the optimal maintenance strategy. The GMRES method is used to solve the system of linear equations with a sparse coefficient matrix during the policy iteration to enhance the efficiency of the algorithm. A numerical study is conducted to evaluate the performance of the developed method. The result shows that the developed method can identify the optimal maintenance strategy efficiently. The numerical study also shows that the optimal maintenance activity of a component depends on the state of the other three components and the buffer level. Therefore, the optimal maintenance

strategy structure cannot be modelled accurately with a small number of parameters, and the MDP is an appropriate tool to identify the optimal maintenance strategy. However, this research finds strong numeric evidence of several useful properties of the optimal maintenance strategy structure. These properties can simplify the maintenance optimisation process and provide reference to developing cost-effective maintenance strategy that is easy to implement in practice. Another interesting finding is that increasing the buffer capacity does not always enhance the average revenue when the cost of holding products in the buffer is not ignorable. Consequently, the buffer capacity should be optimised, or the production rates of the components should be controlled according to the system state. Finally, this research also finds that changing the repair rates and maintenance cost rates of the upstream and downstream subsystems can have different effects on the optimal average revenue. The outcome of this research is expected to provide foundation for more efficient maintenance optimisation methods for series-parallel systems with intermediate buffers.

Acknowledgements: *The research work is supported by the National Natural Science Foundation of China (Grant Nos. 71201025), the Research Fund for the Doctoral Program of Higher Education of China (Grant Nos. 20110092120007), and the opening topic fund of Jiangsu key laboratory of large engineering equipment detection and control (Grant Nos.JSKLEDC201209).*

References

1. Alexandros, D.C. and Chrissoleon, P.T. Exact analysis of a two-workstation one-buffer flow line with parallel unreliable machines. European Journal of Operational Research 2009;197(2):572-580, http://dx.doi.org/10.1016/j.ejor.2008.07.004.
2. Arab, A., Ismail, N. and Lee, L.S. Maintenance scheduling incorporating dynamics of production system and real-time information from workstations. Journal of Intelligent Manufacturing 2013;24(4):695-705, http://dx.doi.org/10.1007/s10845-011-0616-3.
3. Barrett, R., Berry, M., Chan, T.F. and Demmel, J. Templates for the Solution of Linear Systems: Building Blocks for Iterative Methods. Philadelphia: SIAM; 1994, http://dx.doi.org/10.1137/1.9781611971538.
4. Belmansour, A.-T. and Nourelfath, M. An aggregation method for performance evaluation of a tandem homogenous production line with machines having multiple failure modes. Reliability Engineering & System Safety 2010;95(11):1193-1201, http://dx.doi.org/10.1016/j.ress.2010.05.002.
5. Dallery, Y., David, R. and Xie, X.L. Approximate analysis of transfer lines with unreliable machines and finite buffers. Automatic Control, IEEE Transactions on 1989;34(9):943-953, http://dx.doi.org/10.1109/9.35807.
6. Dehayem Nodem, F.I., Kenné, J.P. and Gharbi, A. Simultaneous control of production, repair/replacement and preventive maintenance of deteriorating manufacturing systems. International Journal of Production Economics 2011;134(1):271-282, http://dx.doi.org/10.1016/j.ijpe.2011.07.011.
7. Dimitrakos, T.D. and Kyriakidis, E.G. A semi-Markov decision algorithm for the maintenance of a production system with buffer capacity and continuous repair times. International Journal of Production Economics 2008;111(2):752-762, http://dx.doi.org/10.1016/j.ijpe.2007.03.010.
8. Gu, X., Lee, S., Liang, X., Garcellano, M., Diederichs, M. and Ni, J. Hidden maintenance opportunities in discrete and complex production lines. Expert Systems with Applications 2013;40(11):4353-4361, http://dx.doi.org/10.1016/j.eswa.2013.01.016.
9. Hamada, M., Martz, H.F., Berg, E.C. and Koehler, A.J. Optimizing the product-based availability of a buffered industrial process. Reliability Engineering & System Safety 2006;91(9):1039-1048, http://dx.doi.org/10.1016/j.ress.2005.11.059.
10. Karamatsoukis, C.C. and Kyriakidis, E.G. Optimal maintenance of two stochastically deteriorating machines with an intermediate buffer. European Journal of Operational Research 2010;207(1):297-308, http://dx.doi.org/10.1016/j.ejor.2010.04.022.
11. Kyriakidis, E.G. and Dimitrakos, T.D. Optimal preventive maintenance of a production system with an intermediate buffer. European Journal of Operational Research 2006;168(1):86-99, http://dx.doi.org/10.1016/j.ejor.2004.01.052.
12. Levantesi, R., Matta, A. and Tolio, T. Performance evaluation of continuous production lines with machines having different processing times and multiple failure modes. Performance Evaluation 2003;51(2–4):247-268, http://dx.doi.org/10.1016/S0166-5316(02)00098-6.
13. Liu, J., Yang, S., Wu, A. and Hu, S.J. Multi-state throughput analysis of a two-stage manufacturing system with parallel unreliable machines and a finite buffer. European Journal of Operational Research 2012;219(2):296-304, http://dx.doi.org/10.1016/j.ejor.2011.12.025.
14. Maillart, L.M. Maintenance Policies for Systems with Condition Monitoring and Obvious Failures. IIE Transactions 2006; 38463-475.
15. Moustafa, M.S., Maksoud, E.Y.A. and Sadek, S. Optimal major and minimal maintenance policies for deteriorating systems. Reliability Engineering & System Safety 2004; 83(3): 363-368, http://dx.doi.org/10.1016/j.ress.2003.10.011.
16. Murino, T., Romano, E. and Zoppoli, P. Maintenance policies and buffer sizing: an optimization model. WSEAS TRANSACTIONS on BUSINESS and ECONOMICS 2009; 6(1): 21-30.
17. Ribeiro, M.A., Silveira, J.L. and Qassim, R.Y. Joint optimisation of maintenance and buffer size in a manufacturing system. European Journal of Operational Research 2007; 176(1): 405-413, http://dx.doi.org/10.1016/j.ejor.2005.08.007.
18. Saad, Y. Preconditioning Techniques. Iterative Methods for Sparse Linear Systems: PWS Publishing Company; 1996.
19. Tan, B. and Gershwin, S. Modelling and analysis of Markovian continuous flow systems with a finite buffer. Annals of Operations Research 2011; 182(1): 5-30, http://dx.doi.org/10.1007/s10479-009-0612-6.
20. Tan, B. and Gershwin, S.B. Analysis of a general Markovian two-stage continuous-flow production system with a finite buffer. International Journal of Production Economics 2009;120(2):327-339, http://dx.doi.org/10.1016/j.ijpe.2008.05.022.
21. Terracol, C. and David, R. An aggregation method for performance evaluation of transfer lines with unreliable machines and finite buffers. Robotics and Automation. Proceedings. 1987 IEEE International Conference on1987: 1333-1338.
22. Tijms, H.C. and van der Duyn Schouten, F.A. A Markov decision algorithm for optimal inspections and revisions in a maintenance system with partial information. European Journal of Operational Research 1985;21(2):245-253, http://dx.doi.org/10.1016/0377-2217(85)90036-0.

23. Zequeira, R.I., Valdes, J.E. and Berenguer, C. Optimal buffer inventory and opportunistic preventive maintenance under random production capacity availability. International Journal of Production Economics 2008; 111(2):686-696, http://dx.doi.org/10.1016/j.ijpe.2007.02.037.
24. Zhang, Z., Zhou, Y., Sun, Y. and Ma, L. Condition-based Maintenance Optimisation without a Predetermined Strategy Structure for a Two-component Series System. Eksploatacja i Niezawodnosc – Maintenance and Reliability 2012; 14(2):120–129.
25. Zhou, X., Lu, Z. and Xi, L. A dynamic opportunistic preventive maintenance policy for multi-unit series systems with intermediate buffers. Int. J. Industrial and Systems Engineering 2010;6(3): 276-288, http://dx.doi.org/10.1504/IJISE.2010.035012.

Yifan ZHOU
School of Mechanical Engineering
Southeast University
Nanjing, China, 211189

Jiangsu Key Laboratory of Large Engineering Equipment Detection and Control Xuzhou Institute of Technology
Xuzhou, China, 221018

Zhisheng ZHANG
School of Mechanical Engineering
Southeast University
Nanjing, China, 211189

E-mails: yifan.zhou@seu.edu.cn, oldbc@seu.edu.cn

INFORMATION FOR AUTHORS

Eksploatacja i Niezawodnosc – Maintenance and Reliability – the journal of the Polish Maintenance Society, under the scientific supervision of the Polish Academy of Sciences (Branch in Lublin), published four times a year.

The scope of the Quarterly

The quarterly *Eksploatacja i Niezawodnosc – Maintenance and Reliability* publishes articles containing original results of experimental research on the durability and reliability of technical objects. We also accept papers presenting theoretical analyses supported by physical interpretation of causes or ones that have been verified empirically. *Eksploatacja i Niezawodność – Maintenance and Reliability* also publishes articles on innovative modeling approaches and research methods regarding the durability and reliability of objects.

The following research areas are particularly relevant to the journal:

1. degradation processes of mechanical and biomechanical systems,
2. diagnosis and prognosis of operational malfunctions and failures.
3. analysis of failure risk/wear,
4. reliability-and-environmental-safety engineering in the design, manufacturing and maintenance of objects,
5. management and rationalization of object maintenance,
6. risk management in the processes of operation and maintenance,
7. the human factor and human reliability in operation and maintenance systems.

Terms and Conditions of Publication

The quarterly *Eksploatacja i Niezawodnosc – Maintenance and Reliability* publishes only original papers written in English or in Polish with an English translation. Translation into English is done by the Authors after they have received information from the Editorial Office about the outcome of the review process and have introduced the necessary modifications in accordance with the suggestions of the referees! Acceptance of papers for publication is based on two independent reviews commissioned by the Editor.

The quarterly *Eksploatacja i Niezawodnosc – Maintenance and Reliability* proceeds entirely online at submission.ein.org.pl

Technical requirements

- After receiving positive reviews and after acceptance of the paper for publication, the text must be submitted in a Microsoft Word document format.
- Drawings and photos should be additionally submitted in the form of high resolution separate graphical files in the TIFF, SVG, AI or JPG formats.
- A manuscript should include: names of authors, title, abstract, and key words that should complement the title and abstract (in Polish and in English), the text in Polish and in English with a clear division into sections (please, do not divide words in the text); tables, drawings, graphs, and photos included in the text should have descriptive two-language captions, if this can be avoided, no formulae and symbols should be inserted into text paragraphs by means of a formula editor; references (written in accordance with the required reference format); author data – first names and surnames along with scientific titles, affiliation, address, phone number, fax, and e-mail address.

The Editor reserves the right to abridge and adjust the manuscripts. All submissions should be accompanied by a submission form.

Detailed instructions to Authors, including evaluation criteria can be found on the journal's website: www.ein.org.pl

Editor contact info

Editorial Office of „Eksploatacja i Niezawodnosc - Maintenance and Reliability"
Nadbystrzycka 36, 20-618 Lublin, Poland
e-mail: office@ein.org.pl

INFORMATION FOR SUBSCRIBERS

Fees

Yearly subscription fee (four issues) is 100 zloty and includes delivery costs. Subscribers receive any additional special issues published during their year of subscription free of charge.

Orders

Subscription orders along with authorization to issue a VAT invoice without receiver's signature should be sent to the Editor's address.

Note

In accordance with the requirements of citation databases, proper citation of publications appearing in our Quarterly should include the full name of the journal in Polish and English without Polish diacritical marks, i.e.,

Eksploatacja i Niezawodnosc – Maintenance and Reliability.

Wydawca:
Polskie Naukowo Techniczne
Towarzystwo Eksploatacyjne
Warszawa

Publisher:
Polish Maintenance Society
Warsaw

Członek:
Europejskiej Federacji
Narodowych Towarzystw
Eksploatacyjnych

Member of:
European Federation of National
Maintenance Societies

Patronat naukowy:
Polska Akademia Nauk
Oddział Lublin

Scientific Supervision:
Polish Academy of Sciences
Branch in Lublin